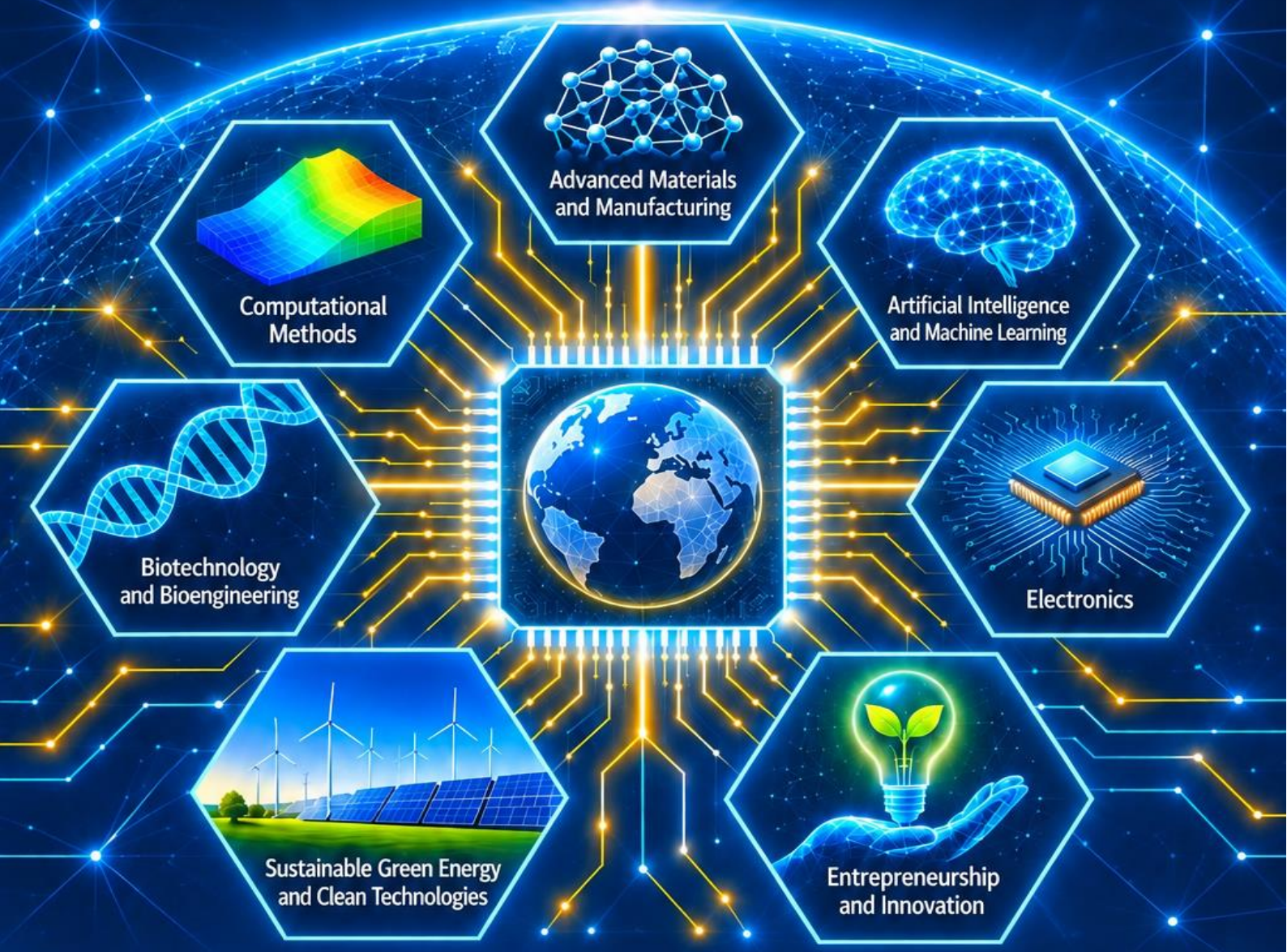
A-SIDE

DeepTech Connect 2026

INTERNATIONAL CONFERENCE



CONFERENCE PROCEEDINGS



Kragujevac, Serbia | Dublin, Ireland | Ioannina, Greece | Tours, France
Bergamo, Italy | Mondragon, Spain | Zvornik, Bosnia & Herzegovina | Gebze, Turkey

April 24, 2026

DEEPTECH CONNECT 2026

The First DeepTech Connect International Conference 2026

April 24, 2026

Kragujevac, Serbia, Dublin, Ireland, Ioannina, Greece, Tours, France, Bergamo, Italy, Mondragon, Spain, Zvornik, Bosnia and Herzegovina, Gebze, Turkey

CONFERENCE PROCEEDINGS

Editor: Fatima Zivic

The First DeepTech Connect International Conference 2026

ISBN 978-86-6335-134-9

https://doi.org/10.46793/IDeepTechConnect

Editor: Fatima Živić, Faculty of Engineering, University of Kragujevac

Publisher: Faculty of Engineering, University of Kragujevac

Sestre Janjić 6, 34000 Kragujevac, Serbia

For the Publisher: Slobodan Savić

Faculty of Engineering, University of Kragujevac

Technical editors: Marija Brankovic, Institute for Information Technologies Kragujevac, Faculty of Engineering, University of Kragujevac

Strahinja Milenkovic, Institute for Information Technologies Kragujevac, Faculty of Engineering, University of Kragujevac

Nikola Kotorcevic, Faculty of Engineering, University of Kragujevac

Dusan Milojevic, Faculty of Engineering, University of Kragujevac

Printed by: Faculty of Engineering, University of Kragujevac

Sestre Janjic 6, 34000 Kragujevac, Serbia

Circulation: 100 copies (electronic publication on CDs) and online

Copyright © 2026 by Faculty of Engineering, University of Kragujevac

The publication of this Conference Proceedings was funded through the EIT's HEI Initiative A-SIDE project, https://a-side-project.eu "Alliance for Sustainable Product Innovation in a Data Driven Economy", supported by EIT RawMaterials, funded by the European Union.

Organizing Committee

General Chair

Prof. Fatima Zivic	Faculty of Engineering, University of Kragujevac, Serbia

Co-location Chairs

Prof. Dermot Brabazon	Dublin City University, Ireland
Prof. Ana Kaplarevic-Malisic	Faculty of Science, University of Kragujevac, Serbia
Prof. Caroline Richard	University of Tours, France
Dr Maite Couto Ortega	Mondragon University, Spain
Prof. Yorgos Goletsis	University of Ioannina, Greece
Prof. Svetlana Pelemis	Faculty of Technology Zvornik, University of East Sarajevo, Bosnia and Herzegovina
Prof. Özgün Yücel	Gebze Technical University, Turkey
Prof. Giovanna Campopiano	University of Bergamo, Italy

Conference secretary

Marija Brankovic	Institute for Information Technologies Kragujevac, Faculty of Engineering, University of Kragujevac, Serbia
Strahinja Milenkovic	Institute for Information Technologies Kragujevac, Faculty of Engineering, University of Kragujevac, Serbia

Members

Joan Kelly	Dublin City University, Ireland
Dr. Neha Agarwal	Dublin City University, Ireland
Prof. Boban Stojanovic	Faculty of Science, University of Kragujevac, Serbia
Prof. Milos Ivanovic	Faculty of Science, University of Kragujevac, Serbia
Prof. Visnja Simic	Faculty of Science, University of Kragujevac, Serbia
Prof. Marina Svicevic	Faculty of Science, University of Kragujevac, Serbia
Prof. Nenad Stojanovic	Faculty of Science, University of Kragujevac, Serbia
Prof. Tatjana Stojanovic	Faculty of Science, University of Kragujevac, Serbia
Prof. Marko Milosevic	Faculty of Science, University of Kragujevac, Serbia
Prof. Milena Milutinovic	Faculty of Science, University of Kragujevac, Serbia
Prof. Sladjana Djordjevic	Faculty of Science, University of Kragujevac, Serbia
Prof. Nenad Grujovic	Faculty of Engineering, University of Kragujevac, Serbia
Nikola Kotorcevic	Faculty of Engineering, University of Kragujevac, Serbia
Dusan Milojevic	Faculty of Engineering, University of Kragujevac, Serbia
Isidora Grujic	Faculty of Engineering, University of Kragujevac, Serbia

Aleksandar Bodic	Faculty of Engineering, University of Kragujevac, Serbia
Zivana Jovanovic Pesic	Faculty of Engineering, University of Kragujevac, Serbia
Prof. Nenad Petrovic	Faculty of Medical Sciences, University of Kragujevac
Prof. François Tran Van	University of Tours, France
Prof. Isabelle Laffez	University of Tours, France
Maider Beitialarrangoita	Mondragon University, Spain
Iker Egizabal	Mondragon University, Spain
Dr Nikolaos Alexandros Theodorou	University of Ioannina, Greece
Prof. Mitar Perusic	Faculty of Technology Zvornik, University of East Sarajevo, Bosnia and Herzegovina
Prof. Milan Vukic	Faculty of Technology Zvornik, University of East Sarajevo, Bosnia and Herzegovina
Prof. Sanja Milic	Faculty of Education, University of East Sarajevo, Bosnia and Herzegovina
Prof. Dragan Vujadinovic	Faculty of Technology Zvornik, University of East Sarajevo, Bosnia and Herzegovina
Dr Ranka Sudžum	Faculty of Mechanical Engineering, University of East Sarajevo, Bosnia and Herzegovina
Dr Aleksija Djuric	Faculty of Mechanical Engineering, University of East Sarajevo, Bosnia and Herzegovina
Srdjan Vukovic	Faculty of Technology Zvornik, University of East Sarajevo, Bosnia and Herzegovina
Dr Mirjana Šipovac	Faculty of Technology Zvornik, University of East Sarajevo, Bosnia and Herzegovina
Prof. Muhammed Uzuntarla	Gebze Technical University, Turkey
Dr Daniela Acerbis	University of Bergamo, Italy
Dr Alessio Ardenghi	University of Bergamo, Italy
Dr Nadia Fabrizio	University of Bergamo, Italy
Dr Samuel Ashong	University of Bergamo, Italy

Scientific Committee

President

Fatima Zivic	Faculty of Engineering, University of Kragujevac, Serbia

Vice presidents

Dermot Brabazon	Dublin City University, Ireland
Ana Kaplarevic-Malisic	Faculty of Science, University of Kragujevac, Serbia
Caroline Richard	University of Tours, France
Maite Couto Ortega	Mondragon University, Spain
Yorgos Goletsis	University of Ioannina, Greece
Svetlana Pelemis	Faculty of Technology Zvornik, University of East Sarajevo, Bosnia and Herzegovina
Özgün Yücel	Gebze Technical University, Turkey
Giovanna Campopiano	University of Bergamo, Italy

Members

Neha Agarwal	Dublin City University, Ireland
Marija Stanic	Faculty of Science, University of Kragujevac, Serbia
Boban Stojanovic	Faculty of Science, University of Kragujevac, Serbia
Milos Ivanovic	Faculty of Science, University of Kragujevac, Serbia
Milan Stankovic	Faculty of Science, University of Kragujevac, Serbia
Visnja Simic	Faculty of Science, University of Kragujevac, Serbia
Marina Svicevic	Faculty of Science, University of Kragujevac, Serbia
Nenad Stojanovic	Faculty of Science, University of Kragujevac, Serbia
Tatjana Stojanovic	Faculty of Science, University of Kragujevac, Serbia
Sasa Simic	Faculty of Science, University of Kragujevac, Serbia
Slavko Radenkovic	Faculty of Science, University of Kragujevac, Serbia
Slobodan Savic	Faculty of Engineering, University of Kragujevac, Serbia
Nenad Grujovic	Faculty of Engineering, University of Kragujevac, Serbia
Velibor Isailovic	Faculty of Engineering, University of Kragujevac, Serbia
Vladimir Dunic	Faculty of Engineering, University of Kragujevac, Serbia
Nikola Vitković	Mechanical Engineering Faculty, University of Niš, Serbia
Dan Stan	Technical University of Cluj-Napoca, Romania
Zoran Levnajić	Faculty of Information Studies Novo mesto, Slovenia
Srđan Škrbić	Faculty of Information Studies Novo mesto, Slovenia
François Tran Van	University of Tours, France
Isabelle Laffez	University of Tours, France
Sain Milena López Perez	Mondragon University, Spain
Maria Vivar Simón	Mondragon University, Spain
Nikolaos Alexandros Theodorou	University of Ioannina, Greece

Dragan Vujadinovc	Faculty of Technology Zvornik, University of East Sarajevo, Bosnia and Herzegovina
Mitar Perusic	Faculty of Technology Zvornik, University of East Sarajevo, Bosnia and Herzegovina
Slavko Smiljanic	Faculty of Technology Zvornik, University of East Sarajevo, Bosnia and Herzegovina
Vladan Micic	Faculty of Technology Zvornik, University of East Sarajevo, Bosnia and Herzegovina
Aleksandar Dosic	Faculty of Technology Zvornik, University of East Sarajevo, Bosnia and Herzegovina
Milija Kraisnik	Faculty of Mechanical Engineering, University of East Sarajevo, Bosnia and Herzegovina
Aleksandra Mitrovic	University of Criminal Investigation and Police Studies Belgrade, Department of Forensic Engineering, Serbia
Hakan Yilmazer	Yıldız Technical University, Turkey
Peyman Mahouti	Yıldız Technical University, Turkey
Emrah Kirtil	Gebze Technical University, Turkey
Cristina Bettinelli	University of Bergamo, Italy
Tommaso Minola	University of Bergamo, Italy
Elisabetta Palumbo	University of Bergamo, Italy
Giacomo Copani	University of Bergamo, Italy
Giuseppe Rosace	University of Bergamo, Italy
Sergii Shelpuk	Shelpuk & Company, Poland
Mohamed Elbadawi	Queen Mary University of London, UK

Supported by

EIT Higher Education Initiative
European Institute of Innovation & Technology
Funded by the European Union

A-SIDE

УНИВЕРЗИТЕТ У КРАГУЈЕВЦУ
UNIVERSITY OF KRAGUJEVAC

DCU Ollscoil Chathair Bhaile Átha Cliath Dublin City University

University of Ioannina

université de TOURS

Mondragon Unibertsitatea

UNIVERSITÀ DEGLI STUDI DI BERGAMO

УНИВЕРЗИТЕТ У ИСТОЧНОМ САРАЈЕВУ
University of East Sarajevo

GEBZE TEKNİK ÜNİVERSİTESİ

DeepTech CONNECT

A-SIDE

PREFACE

The **FIRST DEEPTECH CONNECT INTERNATIONAL CONFERENCE 2026** was established as an international platform for presenting scientific research, showcasing technological innovations, connecting academia with industry, and promoting the transformation of research results into practical applications and market-oriented innovations. Building on the concept of research fairs and scientific exhibitions, the Conference provides an opportunity for researchers, students, companies, entrepreneurs and other innovation ecosystem stakeholders to exchange knowledge, demonstrate new technologies, establish partnerships and explore opportunities for scientific and technological cooperation.

Deep Tech encompasses advanced scientific and technological developments with the potential to generate significant breakthroughs and address major societal, environmental and industrial challenges. The Conference brings together interdisciplinary research and innovation across seven major thematic areas:

- **Advanced Materials and Manufacturing**, covering advanced and functional materials, additive manufacturing, architected materials, smart materials, mechanical behaviour, manufacturing processes, tribology, surface engineering, structural monitoring and sustainable manufacturing.
- **Artificial Intelligence and Machine Learning**, including machine learning algorithms, explainable AI, deep learning, computer vision, image processing, natural language processing, speech recognition, generative AI and AI applications in healthcare, engineering, manufacturing, energy and environmental systems.
- **Computational Methods**, encompassing numerical modelling, finite element analysis, computational simulation, engineering design optimization, manufacturing process modelling, structural and biomechanical simulation, virtual twins and advanced mathematical methods.
- **Biotechnology and Bioengineering**, including biological resources, food biotechnology, biomaterials, polymeric scaffolds, tissue engineering, engineered living materials, molecular and cellular research, biomedical instrumentation, healthcare technologies and rehabilitation.
- **Electronics**, addressing electronic circuit design, antennas, embedded systems, sensors, digital communications, wireless networking, Internet of Things (IoT), vehicle-to-everything (V2X) communications and cybersecurity.
- **Sustainable Green Energy and Clean Technologies**, covering waste management, circular economy, resource recovery, bioenergy, hydrogen production, energy efficiency, sustainable buildings, environmental monitoring, renewable energy, solar technologies, sustainable materials and digital energy systems.
- **Entrepreneurship and Innovation**, focusing on deep-tech entrepreneurship, start-up development, innovation ecosystems, technology transfer, knowledge valorisation, university–industry cooperation, management, education and skills development, green and social innovation, and digital and cultural innovation.

The scientific programme reflects the increasingly interdisciplinary nature of contemporary research, where advanced materials, computational methods, artificial intelligence, biotechnology, electronics and sustainable technologies contribute to the development of new products, processes and services.

Particular attention is given to the connections between scientific discovery, technological development, industrial applications and the commercialisation of research results.

The **First DeepTech Connect International Conference 2026** was held on **April 24, 2026**, simultaneously at eight university locations across Europe: University of Kragujevac (Serbia), Dublin City University (Ireland), University of Tours (France), Mondragon University (Spain), University of Ioannina (Greece), University of East Sarajevo (Bosnia and Herzegovina), Gebze Technical University (Türkiye) and University of Bergamo (Italy). This multi-location concept enabled participants to attend in person at their respective universities while connecting with researchers, students, companies and other participants across all locations through online networking. The simultaneous organisation of the Conference created an international environment for exchanging research capacities, identifying complementary expertise and initiating cross-border academic and industrial cooperation.

A distinctive feature of DeepTech Connect 2026 was its **research fair and exhibition format**. Instead of relying exclusively on conventional oral presentations, the Conference encouraged the presentation of scientific and technological contributions through physical exhibits, prototypes, experimental models, posters, computer simulations and interactive demonstrations. This approach provided opportunities for direct engagement with research results, enabling visitors to discuss scientific challenges, explore practical applications and interact with the researchers behind the innovations.

The Conference proceedings bring together contributions covering a broad spectrum of scientific disciplines and innovation activities. The **Advanced Materials and Manufacturing** section presents research on additive manufacturing, shape-memory materials, functional ceramics, structural design, manufacturing processes, tribology, coatings, sensing and monitoring, and engineering applications. The **Artificial Intelligence and Machine Learning** section demonstrates the growing role of intelligent computational approaches in prediction, image analysis, speech and language processing, healthcare, industrial systems, environmental monitoring and smart applications. Complementing these developments, the **Computational Methods** section addresses numerical and analytical modelling, finite element analysis, manufacturing simulation, engineering optimization, structural dynamics and virtual twin technologies. The proceedings also highlight the contribution of biological and medical sciences to technological innovation. The **Biotechnology and Bioengineering** section includes research on natural biological resources, food applications, biomaterials, polymeric scaffolds for bone regeneration, tissue engineering, engineered living materials, molecular biomarkers, biomedical instrumentation, cancer care and rehabilitation. The **Electronics** section presents developments in antennas, electronic circuits, embedded sensing, digital communications, wireless positioning, connected vehicles and automotive cybersecurity. In response to the increasing importance of environmental responsibility and the transition towards sustainable economic and industrial systems, the **Sustainable Green Energy and Clean Technologies** section addresses waste management, circular resource utilisation, bioenergy, hydrogen production, energy-efficient buildings, geothermal systems, environmental monitoring, solar energy, protective coatings and digitally enabled energy

communities. These contributions demonstrate how technological innovation, resource efficiency and digital solutions can support the development of more sustainable energy and environmental systems.
Beyond scientific and technological developments, the Conference recognises the importance of creating effective pathways for translating research into innovation and economic and societal value. The **Entrepreneurship and Innovation** section therefore addresses deep-tech enterprise development, entrepreneurial opportunities, prototyping, technology transfer offices, university–industry cooperation, innovation ecosystems, business competitiveness, project management, education and workforce development, green entrepreneurship, ESG approaches and user-driven, digital and cultural innovation. This section reinforces the importance of connecting research excellence with entrepreneurial capabilities, industrial needs and the wider innovation ecosystem.

An important objective of the Conference was to promote research careers and doctoral education by bringing students and young researchers into direct contact with experienced scientists, research groups, companies and innovation ecosystem representatives. The event provided opportunities to explore research topics, identify potential PhD supervisors and collaborators, learn about emerging technologies and better understand the opportunities associated with scientific and technological development.

International networking was an integral part of the Conference concept. Participants were encouraged to use the dedicated Conference web application, https://dtc.lineupr.com/dtc/ to connect with other attendees before and during the event, exchange information about their research interests and identify potential partners across the participating universities. This digital networking dimension complemented the physical exhibitions and enabled interaction beyond geographical and institutional boundaries.

The Conference was organised within the framework of the **A-SIDE project**, supported by the European Institute of Innovation and Technology (EIT) Higher Education Initiative. It contributed to the broader objectives of strengthening innovation and entrepreneurial capacity in higher education institutions, promoting knowledge valorisation, fostering university–industry cooperation and supporting the development of regional and international innovation ecosystems.

The **Conference Proceedings** provide a multidisciplinary overview of the research, technological developments and innovation activities presented at DeepTech Connect 2026. The contributions demonstrate the diversity of contemporary research, from fundamental scientific investigations and computational approaches to experimental developments, engineering applications, biomedical solutions, sustainable technologies and innovation-oriented business and educational models. Their thematic organisation also highlights important connections between the different fields, demonstrating how advanced materials and manufacturing, computational methods and artificial intelligence can support technological development, while biotechnology, electronics and sustainable energy provide pathways towards practical applications and solutions to societal challenges.

The First DeepTech Connect International Conference 2026 represents an important step towards establishing a sustainable international platform for connecting science, technology, education, entrepreneurship and industry. Its distinctive multi-university format and exhibition-oriented approach demonstrate the value of bringing research closer to students, companies and society, while creating opportunities for new partnerships, interdisciplinary cooperation and the commercialisation of deep-tech innovations.

The Conference was highly successful, attracting a large number of young people, early-career researchers, aspiring researchers, and PhD students. The scientific research fair format demonstrated that this innovative approach to presenting scientific work was very well received by young participants, who remained actively engaged throughout the Conference.

We hope that this publication will inspire further scientific research, encourage international and interdisciplinary collaborations, strengthen connections between academia and industry, and contribute to transforming scientific knowledge into innovative solutions with meaningful economic, environmental and societal impact.

Kragujevac, Serbia, 2026

Conference General Chair
Prof. Dr. Fatima Zivic
Faculty of Engineering
University of Kragujevac, Serbia

Contents

ADVANCED MATERIALS AND MANUFACTURING 27

Additive Manufacturing and Architected Materials 28

Design of Lattice Based Nitinol Actuators for Optimal Displacement and Load Bearing Capability 29

Yvonne Omowunmi-Kayode[1, 2] , Deeksha Hota[1,3] , Andrea Villano[1,3], Ajai Sankar[1,3], Ian Kiernan[1,2], Mehran Bahramyan[1,2,*] and Dermot Brabazon [1, 2] 29

Inducing the Two-Way Shape Memory Effect in Additively Manufactured NiTi Wires 37

Gavin Chapman[*a,1,2], Thomas Gillick[b,1,2], Ankur Majumdar[c,1,2], Meris Ikiz[d,1,2], Merve Nur Dogu[e,1,2], Neha Agarwal[f,1,2], Dermot Brabazon[g,1,2] 37

Review of Phase Transformation Behaviour in NiTi Lattice Structures Fabricated via Wire-Based Directed Energy Deposition 45

Terence Bowden[1,2,*], Ronan McCann[1,2], Dermot Brabazon[1,2] 45

Forensic Challenges in Additively Manufactured Materials: Reliability of 3D-Printed Evidence 49

Aleksandra Mitrovic[1], Nenad Mitrovic[2], Svetlana Pelemis[3] 49

3D Printed Porous Filters for Sustainable Water Treatment Applications 53

Nikola Kotorčević[1], Dušan Milojević[1], Fatima Živić[1] 53

Comparing 3D-printed Part Mesh Design Techniques for Thermoforming 57

Živana Jovanović Pešić[1], Strahinja Milenković[2], Nenad Petrović[3], Nenad Marjanović[3], Vesna Marjanović[3] 57

Advanced Materials, Microstructure, and Functional Materials 62

Microstructural Engineering and Mechanical Behavior of KNN and KNN-Ta Ceramics Sintered by Spark Plasma Sintering 63

Jade Clément[1], Isabelle Monot-Laffez[1], Micka Bah[1], Caroline Richard[1] 63

Solid lubricant coatings based on chromium nitride and metal sulfide deposited by reactive magnetron sputtering 67

Rubenson Mareus[1,2], Amaël Caillard[2], Caroline Richard[1], Anne-Lise Thomann[2], Loïc Gimenez[2] 67

Electromagnetic Shielding of Biochar-Coated Drywall Panels: a Performance Overview from 1 to 27 GHz 72

Isabella Natali Sora[1], Giuseppe Ruscica[1], Patrizia Savi[2] 72

Orientation Dependent EMI Shielding Performance of CFRP Laminates ... 76
Maria Vlacha[1], Angelos Voudouris Itskaras[1], Christos Vazouras [2], Alkiviadis S. Paipetis[1] ... 76
Mechanical Behavior, Structural Design, and Joining ... 80
Dimensional Optimization of a Cantilever Structure with Stress–Strain Analysis ... 81
Nebojša Arsić[1*], Nenad Kostić[1], Nenad Marjanović[1], Vesna Marjanović[1] ... 81
Shear Strength Testing of Adhesively Bonded Joints: Experimental and Numerical Analysis ... 85
Vladimir Milovanović[1], Veljko Kanjevac[1], Miloš Pešić[2], Gordana Jovičić[1] ... 85
Graphical representation of adhesive joints in technical drawings for railway industry ... 89
Srdjan Samardzic[1], Aleksija Djuric[1] ... 89
Investigation of the bond strength of laser-textured interference-fit joints ... 94
Meris Ikiz [*1,2], Merve Nur Dogu [1,2], Muhannad Obeidi[2,3], Dermot Brabazon[1,2] ... 94
Improvement of thin-walled semi-rigid beam-to-column connections in rack structures ... 101
Mirjana Piskulic[1], Rodoljub Vujanac[1*], Snezana Vulovic[2] ... 101
Microvoid nucleation mechanisms in cold forming metal components ... 106
Milija Kraišnik[1], Mladomir Milutinović[2], Jelica Anić[1] ... 106
Manufacturing Processes and Process Optimization ... 111
Force analysis for incremental forming of metal sheets ... 112
Jelica Anić[1], Mladomir Milutinović[2], Milija Kraišnik[1] ... 112
Laser Engraving of Submillimeter Text ... 117
Petar Todorović[1] ... 117
Radiotracers as Advanced Tools for Industrial Process Diagnostics and Optimization ... 122
Srđan Vuković[1*], Danijela Vuković[1], Aleksandar Vuković[2], Vesna Gojković Cvjetković[1], Svetlana Pelemiš[1] ... 122
Closing the Loop of the EURO-TITAN Process: Residue Valorisation, Wastewater Recycling and Development of Functional Materials ... 126
Mitar Perušić[1], Duško Kostić[1], Nebojša Vasiljević[1], Jelena Vuković[1], Srećko Stopić[2], Maria Teresa Bellver Baca[3], Radislav Filipović[1,4], Vladimir Damjanović[4], Bengi Yagmurlu[5], Konstantinos Sakkas[6] ... 126
Tribology, Wear, Lubrication, and Surface Engineering ... 131
An Enhanced Pin-on-Disc Tribometer with Integrated Lubrication and Digital Positioning System ... 132

Stefan Čukić[1], Anđela Perović[1], Slavica Miladinović[1], Miloš Matejić[1], Blaža Stojanović[1] ... 132

Influence of intermittent friction cycles on tribocorrosion behavior of 316L stainless steel in 5% $NaHCO_3$ ... 136

Kaouthar Bouguerra[1], Yan-Ming Chen[2], Alexandre Romaine[3], Nadege Ducommun[3], Pierre François Cardey[4], Alexis Fontaine[5], Caroline Richard[1] ... 136

Influence of Linear Reciprocating and Rotational Modes on Wear Track Width of Brass ... 142

Dragan Dzunic[1], Milan Eric[1], Vladimir Kocovic[1], Jelena Djusic[1], Zivana Jovanovic Pesic[1], Slobodan Mitrovic[1], ... 142

Influence of Organic and Inorganic Based Lubricating Greases on the Tribological Characteristics of Contact Pairs ... 146

Stefan Miletić[1], Dragan Džunić[1], Milan Ivković[1], Slobodan Mitrović[1] ... 146

Manufacturing Quality, Inspection, and Structural Monitoring ... 150

Visual Inspection Systems for Tool Wear Monitoring in Machining ... 151

Milan Ivković[1], Julija Bošković[1], Nadica Stojanovic[1], Strahinja Đurović[2], Stefan Miletić[1], Goran Devedzic[1], Suzana Petrović Savić[1], ... 151

Benchmarking a wireless strain gauge monitoring system against DFOS in CFRP ... 156

Maria Xenidou[1], Andreas Kalogirou[1], Kyriaki Tsirka[1], Dimitrios Fakis[1], Alkiviadis S. Paipetis[1] ... 156

Flexible Sensor Development for Smart Packaging via CeraPrinter F-Series System Technologies 160

D. A. Exarchos, P. T. Dalla, P. Pantazis, I. Angelopoulos and T. Matikas ... 160

Engineering Applications and Human-Centered Design ... 164

The Impact of Seatback Angle on Driver Discomfort: A Systematic Review ... 165

Slavica Macuzic Saveljic[1], Igor Saveljic[2] ... 165

When it comes to silence, it is necessary to face the opposite concept: noise insulation ... 169

Dragutin Tijanić[1], Tamara Dimitrijević[2] ... 169

ARTIFICIAL INTELLIGENCE AND MACHINE LEARNING ... 172

Foundations, Methods, and AI/ML Algorithms ... 173

The Predictive Power of Genomic Damage: A Machine Learning Approach to Endometrial Cancer Biomarkers ... 174

Aleksandra Marković[1], Bogdan Milićević[1], Marija Živković Radojević[2,3] ... 174

Data-Driven Prediction of Master's Degree Enrolment Using Explainable Machine Learning ... 178

[1]University of East Sarajevo, Faculty of Education, Bosnia and Herzegovina, 0000-0002-8119-5190 178

The importance of k-fold cross-validation in evaluating machine learning models for biomass gasifier output prediction. 183

Kadriye Deniz Olca[1], Özgün Yücel[1] 183

Stylistic Adaptation of a Pre-trained Language Model via Fine-tuning on a Slavic Literary Corpus 188

Aleksandr Uchaev and Vladimir Milovanović 188

Methodological framework for automated solving of mathematics competition problems in Serbia using LLMs 192

Marina Svičević[1], Aleksandar Milutinović[1], Nemanja Vučićević[1], Aleksandar Milenković[1], Miloš Pavković[2] 192

Implementation of an 8-bit Floating-Point Coprocessor for Deep Learning Applications 196

Isidora Grujić[1], Marija Božilov[1], Aleksandar Kondić[1], Vladimir M. Milovanović[1] 196

Decision-Making Algorithm for Intuitionistic Fuzzy Soft Sets 203

Nemanja Vučićević[1], Nenad Stojanović[1], Marina Svičević[1] 203

Clustering of the Zeros of Orthogonal Polynomials on the Semicircle 207

Marija P. Stanić[1], Tatjana V. Tomović Mladenović[1], Aleksandra S. Milosavljević[1] 207

Turning the Sky into a Tool for Peace 210

Mikel Espiga 210

Computer Vision, Image Analysis, and Pattern Recognition 214

Few-Shot Approach for Mouse Lung Segmentation in Synchrotron X-Ray Tomography 215

Andjela Blagojevic[1,2], Tijana Geroski[1,2], Nenad Filipović[1,2] 215

Development of a YOLOv11-Based Desktop Application for Concrete Crack Detection 220

Jovana Nikolic[1], Velibor Isailovic[1] 220

An affordable webcam-based real-time hand gesture recognition system using simple multilayer perceptron deep learning models 225

Ana Jovanović and Vladimir Milovanović 225

Di<Au>logues: Gesture-Based Navigation in Archaeological Museum of Thessaloniki. A Case Study using MediaPipe and p5.js. 230

Nikolaos Konstantinou[1], Nikolaos Papadimitriou[1], Michail Semoglou[2], Dimitrios Traperas[1] 230

Graph and Recurrent Neural Networks for MRI-Based Parkinson's Disease Analysis: A Short Review and Confidence-Driven Pruning Framework 234

Vasileios Stergiou[1], Angelos Giotis[1], Michail Vrigkas[2], Loukas Astakas[3], Spyridon Konitsiotis [3], Christophoros Nikou[1] 234

Speech, Language, and Human–AI Interaction 238

Real-Time Speech Analysis and Vowel Classification Using Linear Predictive Coding 239

Sava Todorović 239

Speech Emotion Recognition with LSTM: Cross-Lingual Transfer to Serbian 243

Nikola Radovanovic[1], Velibor Isailovic[1] 243

Automated Detection of Business Email Compromise Attacks in Serbian Language Using Linear Probabilistic Models 248

Miljan Koturović[†], Uroš Deljanin[†] and Vladimir Milovanović 248

Semestrify: A Cross-Platform System for Intelligent Academic Schedule Extraction and Calendar Integration 252

George Tzanopoulos[1], Vasileios Ralis[1], Christos Gogos[1] 252

How Do Translators Learn to Use AI? A Constructivist Approach 257

Airidas Kairys 257

Friendly Foes: Metaphorical conceptualization of AI based on the source domain of PERSON in English 263

Tatjana Grujić[1] 263

AI for Healthcare, Medicine, and Assistive Technologies 268

Building a Transnational AI-Health Innovation Network for Predictive Medicine and Health Crisis Preparedness: the HERACLES Project 269

Yorgos Goletsis[1], Konstantina Christogeorgou[1], Nikolaos Alexandros Theodorou[1] 269

AI-Guided 3D-Printed Meander-Line Antenna for Non-Invasive Bone-Tumor Detection 273

Tarlan Mahouti[1], Hakan Yılmazer[1], Mehmet Ali Belen[2] 273

Virtual Reality and Haptic Simulation in Dental Clinical Skills Development 277

Andrija Brkić[1], Marija Branković[2], Jelena Popović[3] 277

WellPet.ai: Edge AI-Powered Smart Collar for Real-Time Canine Health and Behavior Monitoring 281

Aleksandar Milutinović[1], Nikola Milanović[1], Branko Ilić[1] 281

Assistive app for BVI people BegIA 286

Oier Arano Urrutia and Alain Ordoñez Alvaro[1] 286

AI for Engineering, Manufacturing, and Industrial Systems 288

Decision-Boundary Instrumentation: Deployer-Side AI Monitoring for European Industry 289

Dorleta Urrutia-Onate[1], Asier Perallos[2], Enrique Onieva[3] 289

Development of an AI-Supported Optimization and Decision-Support Industrial SaaS Platform for FMEA Risk Management 294

Nikola Komatina[1], Nikola Banduka[2], Pavle Rvović[2], Kristina Mojsić[2] 294

Application of AI tools in analyses of Welded Structure 298

Aleksija Đurić[1], Miodrag Milčić[2], Srđan Samardžić[1], Dragan Milčić[2], Biljana Marković[1] ... 298

Application of artificial intelligence to predict and optimize driver comfort based on anthropometric data 301

Slavica Macuzic Saveljic[1], Igor Saveljic[2] 301

Data-Driven Artificial Intelligence Applications in Energy Production Systems 305

Mert Akin INSEL[1,2,*], Hasan SADIKOGLU[1,2], Ozgun YUCEL[3] 305

Predictive Modeling of Ignition Quality in Diesel-Biodiesel-Alcohol Systems for Sustainable Fuel Design 309

Kaan YEŞİLOVA[1], Özgün YÜCEL[2], Başak TEMUR ERGAN[3], Ümran ÜNLÜ[4] 309

AI for Energy, Environment, and Smart Infrastructure 313

Empowering Industrial Cooling through Predictive Intelligence 314

Jimena Castrillo, Álvaro Enriquez, Francisco Javier Enriquez 314

VodostAI – AI-based Flood Prediction and Prevention Platform ID 53122, Innovation Fund of Serbia – GovTech Program, 2024–2025 316

Boban Stojanović[1,2], Vladimir Bačanin[1], Boško Laković[1], Tomislav Mrđa[1], Dušan Stefanović[1], Miroljub Krstić[1] 316

Vodena - Next Gen Water and Energy software solutions 320

Miroljub Krstić[1], Dušan Stefanović[1] 320

Substrate Effects on Plant Metabolism: A Machine Learning Perspective 324

Nenad Zlatić & Milan Stanković 324
AI Applications in Mobility and Smart Systems 328
HAL Mobility AI: AI-Assisted Urban Mobility Orchestration for Local Taxi Ecosystems 329
Milovan Ostojić[1], Dragutin Ostojić[2], Mihajlo Čekerevac[1], Lazar Avramović[3] 329
COMPUTATIONAL METHODS 333
Analytical and Numerical Modelling Fundamentals 334
Modeling and Simulation of Shear in Shape Memory Alloys 335
Natalija Milićević[1], Aleksandar Bodić[1], Vladimir Dunić[1]* 335
Comparative Numerical Study of Two Interface-Capturing Methods for a Rising Bubble Problem 339
Aleksandar Bodić[1], Slobodan Savić[1*], Miloš Pešić[2], Marko Topalović[2] 339
Finite Element Analysis of Geotechnical Engineering Problems 346
Jovana Minić[1], Dragan Rakić[1] 346
Computational Modeling of Manufacturing and Processing 350
Analytical Modelling of Track Formation in Laser Powder Bed Fusion of IN939 351
Sampreet Rangaswamy[1,2], Merve Nur Doğu[1,2], Dermot Brabazon[1,2] 351
Determining the influence of process parameters during ironing using FEA 355
Marko Delić[1], Vesna Mandić[2], Dušan Arsić[1], Đorđe Ivković[1], Nada Ratković[1], Anđelka Ilić[1] 355
Computational Optimization and Engineering Design 360
Geometry Optimization of a PVDF-Based Piezoelectric Impact Sensor Using a Hertz-Contact-Informed Axisymmetric Finite Element Model 361
Strahinja Milenković[1,2], Nenad Grujović[1], Fatima Živić[1], ... 361
Optimizing Titanium Hip Implant Performance Through Surface Topography and Numerical Analysis 365
Aleksandra Vulović[1], Živana Jovanović Pešić[1], Đorđe Ilić[1], Strahinja Milenković[2], Dragan Džunić[1] 365
Structural, Dynamic, and Biomechanical Simulation 369
Structural dynamic simulation of an iconic railway infrastructure under a Multiple Moving Load scenario 370
Michele Guerini[1], Rosalba Ferrari[1], Giuseppe Cocchetti[2], Egidio Rizzi[1] 370

Virtual and Digital Twin Modeling ... 374

Virtual Twin Modeling of Bio-Inspired Butterfly Wing Flapping ... 375

Julija Boskovic[1], Milan Ivkovic[1], Ivan Grujic[1], Goran Devedzic[1], Suzana Petrovic Savic[1] ... 375

Advanced Mathematical and Theoretical Methods ... 380

Molecular Nanogears as Quantum Brownian Rotators ... 381

Jasmina Jeknic-Dugic[1], Igor Petrovic[2], Momir Arenijevic[3], Miroljub Dugic[3] ... 381

On the construction of multiple orthogonal polynomials with nearly diagonal multi-indices with respect to bilinear forms ... 386

Nevena Z. Petrović[1] ... 386

BIOTECHNOLOGY AND BIOENGINEERING ... 390

Natural Resources, Food Biotechnology, and Biological Systems ... 391

Biopotential of Autochthonous Lignicolous Mushrooms for Nutraceutical Applications ... 392

Aleksandra Novaković[1], Mirjana Šipovac[2], Milan Vukić[2], Neda Gavrić[1], Maja Karaman[3], Aleksandar Marić[4], Jelena Vulinović[2], Nataša Vojnović[5], Vesna Šolaja[3], Neda Ubiparipović[2], Enisa Musić[2] ... 392

The application of herbs and spices in the food industry ... 398

Vesna Gojković Cvjetković[1], Milenko Smiljanić[1], Željka Marjanović-Balaban[2], Milan Vukić[1], Dragan Vujadinović[1] ... 398

Integrated Non-Invasive Multi-Sensor Approach for Monitoring Fish Community Dynamics: A Case Study in Gruža Reservoir ... 402

Aleksa B. Cvetković[1]*, Tijana Z. Veličković[1,2], Vladica M. Simić[1] ... 402

Host–microbiota interactions in *Drosophila*: composition, regulatory mechanisms and translational relevance ... 407

Enisa Musić[1], Mirjana Šipovac[1], Aleksandra Novaković[2], Maja Palangetić[1] ... 407

Biomaterials, Scaffolds, and Tissue Engineering ... 411

PCL vs. PLA in Bone Regenerative Scaffolds: Current Potential and Challenges ... 412

Jana Baščarević[1], Marija Branković[1], Katarina Virijević[1] ... 412

Polymeric Scaffolds Based on PCL/PEG and Chitosan/PLA for Osteogenic Applications ... 416

Katarina Virijević, Jana Baščarević[1], Nenad Filipović[1] ... 416

Engineered Living Materials: Advanced Approaches for Biomedical Engineering ... 420

Marija Branković[1], Jana Baščarević[1], Fatima Živić[2] ... 420

Molecular and Cellular Biomedical Research 424

Can ATP Citrate Synthase Be Potential Biomarker For Breast Cancer Progression? 425

Jovana Jovankić[1], Milena Milutinović[1], Stefan Blagojević[1], Danijela Nikodijević[1], Aleksandra Nikezić[1], Danijela Cvetković[2] 425

Genetic Polymorphism and CGM-Based Glucose Prediction in Type 1 Diabetes 431

Daphne N. Katsarou[1,2], Eleni I. Georga[2], Stelios Tigas[3], Costas Papaloukas[1,2] and Dimitrios I. Fotiadis, Fellow, IEEE[2,4] 431

Biomedical Instrumentation and Laboratory Automation 435

Automated Cytogenetic Chromosome Spreading Device with Real-Time Environmental Control .. 436

Seyfettin Kazanır Alanya Alaaddin Keykubat University (ALKÜ) Antalya, Türkiye
Seyfettin.kazanir@alanya.edu.tr 436

Cancer Care, Clinical Management, and Digital Health 442

Improving quality of life after breast cancer 443

Iratxe Sobera 443

An Interdisciplinary Approach for the Management of the Elderly Multimorbid Patient with Breast Cancer Therapy-Induced Cardiac Toxicity 445

Alexandros Mitsis[1], Georgia Karanasiou[1,2], Dimitrios I. Fotiadis[1] 445

Smart Mirrors supporting healthier lives of Adolescents and Young Adults after cancer 449

Alexandros Mitsis [1], Georgia Karanasiou [1,2], Dimitrios I. Fotiadis[1] 449

Reway – Restoring Mobility, Redefining Care 452

Sara Milosevic, Jana Jankovic, Marija Velickovic, Jana Cvetkovic, Marko Ilic, Nikola Nikolic[1] 452

ELECTRONICS 456

RF, Antennas, and Electronic Circuit Design 457

A Cylindrical Dielectric Lens–Loaded Microstrip Patch Antenna With Enhanced Gain for 3.5-GHz Sub-6-GHz 5G 458

Tarlan Mahouti[1], Hakan Yılmazer[1], Mehmet Ali Belen[2] 458

Mathematical Model of a Ring-Based Digitally Controlled Oscillator for Frequency Range and Resolution Prediction 462

Đorđe Gačić[1], Lazar Ilić[2], Dejan Petković[3], Vladimir Milovanović[4] 462

Embedded Electronics and Sensor Systems 466

Arduino Temperature Monitoring System 467

Luka Virijević[1], Tijana Dimitrijević[2], Milan Čabarkapa[3] 467

Digital Communication and Signal Processing 471

Equalization and Carrier Recovery for Downstream Data Over Cable Service Interface Specification (DOCSIS) 3.0 Modems 472

Dejan Rakić, Milan Čabarkapa, Vladimir Milovanović 472

Wireless Networking and Positioning 478

A hardware/software platform for precise client device positioning in IEEE 802.11-based Wi-Fi communication networks 479

Zoran Đorđević[1], Nedeljko Stefanović[1], Vladimir Milovanović[2] 479

Connected Vehicles, V2X, and Automotive Cybersecurity 484

IoT and V2X Communications in Autonomous and Electric Vehicles 485

Sandra Antanasijevic[1], Milan Čabarkapa[1], Tijana Dimitrijević[1,2] 485

Cybersecurity of IoT-Based CAN Systems in Autonomous and Electric Vehicles 489

Ema Radovanović[1], Tijana Dimitrijević[2], Milan Čabarkapa[3] 489

Robotics 493

Industrial robots: global trends in exports, dynamics, and challenges 494

Anelia Stoikova 494

Integrating Advanced Robotic Solutions into Lean Industrial Systems: A Human-Centered Approach 498

Nastasija Nikolic[1], Marko Djapan[2], Arso Vukicevic[3], Djordje Milojevic[4], Ivan Macuzic[5] 498

SUSTAINABLE GREEN ENERGY AND CLEAN TECHNOLOGIES 502

Waste Management, Circular Economy, and Resource Recovery 503

Evaluating municipal waste management efficiency in the context of sustainable development: A DEA-based analysis 504

Angelina Cvetanović[1], Goran Bošković[1], Nebojša Jovičić[1] 504

Co-Digestion Plants and Production Assessment 512

Nikola Rakić[1], Vanja Šušteršič[2] 512

Composting of Food Waste in the Hospitality Sector: Lessons from Vrnjačka Banja 517

Sonja Veljović[1], Marija Kostić[2], Milica Luković[3] 517

Sustainable Hydrogen Production from Food Waste Using Integrated Gasification and Sorption-Enhanced Reforming 521

Ali Atas[a,b,*], Nader Javani[b], Betul Colak Karadag[b,c], Ozgun Yucel[d] 521

Sustainable Buildings, Energy Efficiency, and Water Systems 526

Integrated Monitoring and Determination of Showering Parameters in Residential Buildings 527

Natalija Aleksić[1], Vanja Šušteršič[2], Strahinja Milenković[3] 527

Assessing Building Energy Efficiency in Kragujevac (Serbia): Insights from a Retrospective Research Analysis 533

Nebojša Jurišević[1], Minja Velemir[2], Natalija Aleksić[3], Dušan Gordić[4] 533

Improving the Energy Efficiency of Water Hydraulic System Components within Sustainable Energy Plant 539

Nenad Todić[1], Slobodan Savić[1], Blaža Stojanović[1], Saša Milojević[1] 539

IT-Based Feasibility Assessment of a Shallow Geothermal System in a Renovated Educational Building in Kragujevac 543

Filip Nastić, Dubravka Živković, Davor Končalović, Vladimir Vukašinović, Mladen Josijević, Dušan Gordić 543

Environmental Monitoring and Clean-Technology Assessment 548

Assessing The Potential of Citizen-Installed PM2.5 Sensors for Air Pollution Prediction and Mapping 549

Filip Nastić 549

Assessment of PVGIS Accuracy Against EnergyPlus Simulations in Europe 553

Novak Popović[1], Novak Nikolić[1], Nebojša Lukić[1], Minja Velemir Radović[1] 553

Renewable Energy and Solar Technologies 560

Performance Enhancement of $FASnI_3$ Perovskite Solar Cells with CBTS Hole Transport Layer: A SCAPS-1D Study 561

Khadija BOUGHANBOUR*[1] https://orcid.org/0009-0000-3905-4741, Mustapha SAHAL[1] http://orcid.org/0000-0003-0528-8413 561

Digital Infrastructure for Collective Solar Self-Consumption: Enabling Scalable Energy Communities through Data, Algorithms and Governance Platforms 566

Mikel Ubiria Pérez 566

Sustainable Materials, Coatings, and Corrosion Protection 569

Development and Optimization of Water-Based Acrylic Coatings for Enhanced Corrosion Resistance of Metallic Materials 570

Milorad Tomić[1,2], Nebojša Vasiljević[1], Marija Mitrović[1], Regina Fuchs-Godec[3], Jelena Bajat[4] 570

Application of Thyme Extract as a Steel Corrosion Inhibitor in HCl and NaCl Solutions 574

Marija Mitrović[1], Nebojša Vasiljević[1], Regina Fuchs-Godec[2], Milorad Tomić[1,3] 574

ENTREPRENEURSHIP AND INNOVATION 578

Entrepreneurship, Start-ups, and Entrepreneurial Development 579

Opportunities for young Entrepreneurs 580

Maider Beitialarrangoitia[1], Laida San Sebastian[2] 580

Fostering the Growth of Deep-Tech Enterprises Through Enterprise Europe Network 584

Milan Vukic[1], Vesna Gojković Cvjetković[1] 584

Prototypes in the Innovation Development 589

Saša Vasiljević[1], Jelena Domanović[1], Jasna Glišović[2] 589

A Scientific Coordinator Enabling Industry Access to Laboratory Services 593

Panagiotis Pantazis[1] 593

Innovation Ecosystems, Technology Transfer, and Competitiveness 597

Understanding Governance and Capabilities in Technology Transfer Offices: Patterns of Efficiency 598

Konstantina Christogeorgou[1], Maite Couto-Ortega[2], Nikolaos Alexandros Theodorou[1], Maider Beitialarrangotia[2], Maria Vivar-Simon[2], Giovanna Campopiano[3], Nikolaos Mylonidis[1], Yorgos Goletsis[1] 598

Competitiveness, internationalization, and innovation in the creative and cultural industries, COMP-ICC project's presentation 603

Maite Couto-Ortega[1], Maria Vivar-Simón[1] 603

Green Innovation and Innovation Ecosystem Participation on Family and Non-family SMEs Performance 607

Samuel Ashong[1], Giovanna Campopiano[1], Mara Brumana[1] 607

Identity-based Legitimacy Buffering and Organizational Attention Triggering Strategic Distinctiveness in Family Businesses 612

Qiuyang Xu[1], Tommaso Minola[1], Nadine Kammerlander[2] 612

Entrepreneurship, Teams, and Management 616

Teampreneurship for Climate Action: An Open Approach to Green Entrepreneurship Education 617

Lander Jimenez Ocio[1], Jerémy Legardeur[2], Maialen Mendizabal[1], Mar Rubio-Varas[3] 617

Beyond Time, Cost and Scope: Managerial Skills in Achieving Contemporary Dimensions of Project Success 621

Mirjana Jokanović Đajić[1], Danijela Ćirić Lalić[2], Milica Radovanović[1], Ranka Sudžum[3] 621

Adapting Quality Management Models to Local Organizations: A Literature Review on EFQM and Hybrid Decision-Making Approaches 625

Tijana Petrovic[1] 625

Innovation, Education, Skills, and Workforce Development 629

The Leaky Pipeline in STEM careers: Gender Segregation and the Shift Toward Pedagogical Careers 630

Sanja Milić[1], Svetlana Pelemiš,..... 630

AI4DLG: Establishing a Joint International Master's Programme in Artificial Intelligence for Digital Learning and Gamification and Developing Its Digital Presence 634

Jenny Pange[1], Eugenia I. Toki[2]..... 634

Integrating Digital and Green Skills in Higher Education 638

Jenny Pange[1], Dimitrios Panagiotou2, Ioannis Fudos[3] 638

Developing a European VET Model for Rural Destination Managers- A Competence-Based Approach to Sustainable Tourism 642

Soultana Demirtzioglou1, Yorgos Goletsis2, Naoum Mylonas3, Luca Reitano4 642

Green, Social, and Sustainable Innovation 645

Spontaneous Ecosystems in Rural Areas: A Case Study (*Espacio Comün*, Nalda, Spain) 646

Sofía Moreno-Domínguez[1] 646

Mara Stanojević[1], Jelena Nešić[1], Marta Jovanović[1], Mentors: Kristina Cvetković, Bojana Đurković 650

Multi-Criteria Decision Analysis for ESG measurement: A Systematic and Bibliometric Review .. 654

Yorgos Goletsis[1], Vasiliki Spyridonos[2] 654

Strengthening University Disaster Preparedness: Cross-Country Intervention Strategies from the DRU Project 658

Konstantinos Plachouras[1], Zoi Nikiforidou[2], Dimitrios Panagiotou[3], Jenny Pange[4] 658

User-Driven, Digital, and Cultural Innovation 661

Rethinking Personal Safety Through User-Driven Innovation 662

Ivan Martin[1] 662

The role of Avatar in Business – the case study of a company Priče iz Kanca 665

Jelena M. Pavlović Jovanović[1], Nataša Spasić[2], Milan Todorović[3] 665

InTransparency - Verified Talent Marketplace 669

Fabio Chefane[1] 669

DeCiTeL (Democratic Citizenship Teaching and Learning) 675

Jenny Pange[1], Zoi Nikiforidou[2] 675

#DanceMuse: A Phygital Hybrid Museum for the Multisensory and Interdisciplinary Interpretation of Traditional Dance in Epirus 678

Aikaterini Vasilaki[1], Melina Papadopoulou[1], Christina Nika[2], Dimitrios D. Vergados[2], Stavros Papapanagiotou[3], Apostolos Karalis[3], Christos Papakostas[1] 678

ADVANCED MATERIALS AND MANUFACTURING

Additive Manufacturing and Architected Materials

Design of Lattice Based Nitinol Actuators for Optimal Displacement and Load Bearing Capability

Yvonne Omowunmi-Kayode[1, 2], Deeksha Hota[1,3], Andrea Villano[1,3], Ajai Sankar[1,3], Ian Kiernan[1,2], Mehran Bahramyan[1,2,*] and Dermot Brabazon [1, 2]

[1] *I-Form Advanced Manufacturing Research Centre, Dublin City University, Glasnevin, Dublin 9, Ireland.*

[2] *DCU Institute for Advanced Processing Technology, School of Mechanical and Manufacturing Engineering, Dublin City University, Glasnevin, Dublin 9, Ireland*

[3] *UCD School of Mechanical & Materials Engineering, University College Dublin, Belfield, Dublin 4, Ireland.*

yeyetunde.omowunmikayode3@mail.dcu.ie, deeksha.hota@ucdconnect.ie (0009-0000-4044-1247), andrea.villano@ucdconnect.ie, ajai.kavunkarathadayil@ucdconnect.ie (0009-0006-2323-3909), ian.kiernan4@mail.dcu.ie, mehran.bahramyan@dcu.ie (0009-0003-6445-8651), dermot.brabazon@dcu.ie (0000-0003-3214-638). *Corresponding author: mehran.bahramyan@dcu.ie

Abstract

Nitinol is a shape memory alloy that exhibits unique functional properties such as the shape memory effect and superelasticity. When combined with lattice architectures, Nitinol actuators can achieve large reversible deformations with enhanced mechanical performance. This study investigates the influence of lattice topology on the actuation behavior of a cylindrical Nitinol actuator. Six lattice designs, including triply periodic minimal surface (TPMS) and strut-based structures, were analyzed using finite element simulations in ANSYS under thermo mechanical loading with an applied torsional moment. The results show that lattice topology significantly affects deformation, stress distribution, and recovery behavior. While the behaviour varies between designs, strut-based lattices tend to provide higher actuation capability, whereas TPMS structures often exhibit a more uniform stress distribution. These findings highlight the tradeoff between actuation output and structural reliability and provide guidance for the design of lattice-based Nitinol actuators.

Keywords: Nitinol; Actuator; Lattices; Shape memory alloy, UN SDG 7

1. Introduction

Nitinol (Nickel Titanium or NiTi) is a shape memory alloy (SMA) that exhibits unique functional properties such as the shape memory effect and superelasticity. These alloys can deform and return to their original form when heated (shape memory effect) or when relieved of mechanical loading (superelasticity), due to the reversible phase transformation between austenite (high temperature) and martensite (low temperature) [1, 2]. Due to these properties, Nitinol is a highly desirable material for a wide range of applications, including actuators, sensors, and functional coatings across fields such as aerospace, biomedical, and mechanical engineering [3, 4]. By combining Nitinol with additive manufacturing, it is possible to create complex structures

with enhanced and precise functionality [3, 5]. Among such structures, lattice structures are of particular interest due to their lightweight characteristics combined with high strength and stiffness [6]. These lattice structures can be integrated into systems to function as actuators. Achieving fast actuation and high strain recovery is critical for shape memory alloy-based actuation systems [7]. NiTi actuators, particularly when designed using lattice structures, leverage the material's superelastic properties to achieve large reversible deformations, typically up to 6–8% strain upon removal of stress [8]. Furthermore, by incorporating optimized lattice designs such as Triply Periodic Minimal Surfaces (TPMS), these actuators can overcome the limitations of traditional simple geometry NiTi components, enabling more complex and tailored deformation responses in applications such as aerospace and medical devices. In this study, six different lattice structures are investigated within a cylindrical Nitinol actuator. A torsional moment of 500 N.mm is applied, and the resulting deformation, stress distribution, and recovery behavior are evaluated to compare the performance of different lattice topologies.

2. Materials and Methods

2.1 Lattice Design

The actuator investigated in this study has a cylindrical geometry with a total height of 15 mm, consisting of solid base plates at the top and bottom and a lattice filled core. Each base plate has a thickness of 2.5 mm, while the remaining 10 mm central region is filled with lattice structures that act as the primary deformation zone. Six lattice architectures were analyzed to evaluate the influence of topology on actuator performance. These include three strut-based lattices, Face Centered Cubic (FCC), Truncated Cubohedron, and Truncated Octahedron and three TPMS structures, Schoen IWP Sheet, Schoen IWP Skeletal and Schwarz Primitive. TPMS lattices provide smooth continuous surfaces that promote more uniform stress distribution, whereas strut-based lattices consist of interconnected beam networks that transfer loads through discrete elements. All lattice configurations were designed with a relative density of approximately 0.3 (30%) and an approximate lattice volume of 160 mm³ to ensure consistent comparison. All lattice geometries and actuator models were generated using the open-source Python library MicroGen [9]. The investigated lattice architectures are shown in Figure 1.

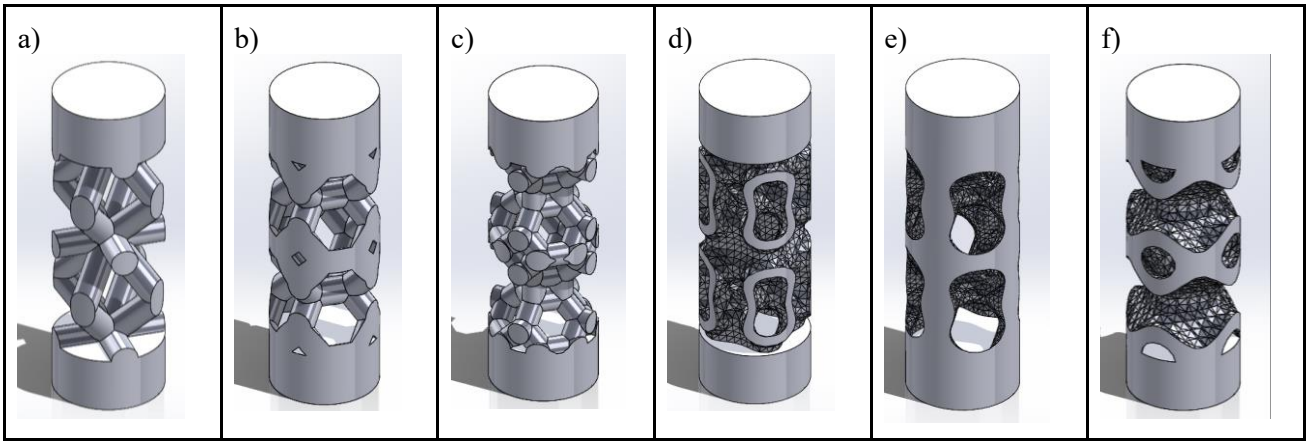


Figure 1. CAD images of the generated lattice structures a) FCC, b) Truncated Octahedron c) Truncated Cuboctahedron, d) Schoen IWP Sheet, e) Schoen IWP Skeletal and f) TPMS Schwarz Primitive

2.2 Material Model

The actuators are made of Nitinol, a nickel titanium shape memory alloy widely used for thermally driven actuation due to its ability to recover large strains during phase transformation. The material behavior was modelled using the shape memory alloy module in ANSYS Mechanical, which is based on the Auricchio constitutive model [10] and captures the thermo mechanical coupling between temperature and phase transformation. The transformation between martensite and austenite phases is defined through temperature dependent parameters. The material constants used in the simulations were taken from literature [11] and are summarized in Table 1.

Table 1. Materials model parameters used in simulations

	Young's Modulus (MPa)	Poisson's Ratio	Hardening Parameter (MPa)	Reference Temperature (C)	Elastic Limit (MPa)	Temperature Scaling Parameter (MPa/C)	Maximum Transformation Strain (mm/mm)	Load Dependency Parameter
Value	70000	0.3	500	37.85	120	8.3	0.03	0

2.3 Ansys Setup

Finite element simulations were performed using ANSYS Mechanical, where the Nitinol behavior was modelled with the shape memory alloy module to capture the thermo mechanical response during phase transformation. The actuator models were meshed using automatic tetrahedral meshing, and a mesh convergence study with different mesh sizes ensured mesh independent results. The bottom base plate was fully fixed, while a torsional moment of 500 N.mm was applied to the top plate about the y-axis of the cylindrical actuator. Large deformation effects were enabled, and the nonlinear problem was solved using the unsymmetric Newton Raphson method. Thermo mechanical actuation was simulated through a six-step temperature loading sequence with automatic time stepping. The torsional moment was applied at 23 °C in the first step and removed in the second step. The temperature was then increased from the initial 23 °C to 37 °C, 50 °C, and 51 °C to trigger the austenitic phase transformation, with 51 °C exceeding the austenite finish temperature to ensure full recovery. In the final step the temperature was reduced to 37 °C to observe the cooling response. The loading sequence is summarized in Table 2. The main outputs evaluated were total deformation, equivalent stress, equivalent elastic strain, and rotational displacement of the actuator.

Table 2. Detailed Thermo-mechanical Loading Sequence

	Step 0	Step 1	Step 2	Step 3	Step 4	Step 5	Step 6
Mechanical Loading (N.mm)	0	500	0	0	0	0	0
Thermal Loading (°C)	23	23	23	37	50	51	37

3. Results

3.1 Mesh Convergence Study

A mesh convergence study was conducted to ensure that the numerical results were independent of mesh density. Several meshes with different element sizes were generated using automatic tetrahedral meshing in ANSYS Mechanical. The convergence analysis was performed by monitoring the maximum total deformation of the actuator under the applied torsional moment. As the mesh was refined, the variation in deformation decreased and eventually stabilized, indicating convergence of the solution. The final mesh density was selected based on the point where further refinement resulted in negligible changes in the predicted deformation. The mesh convergence results are shown in Fig. 2 for different lattice types.

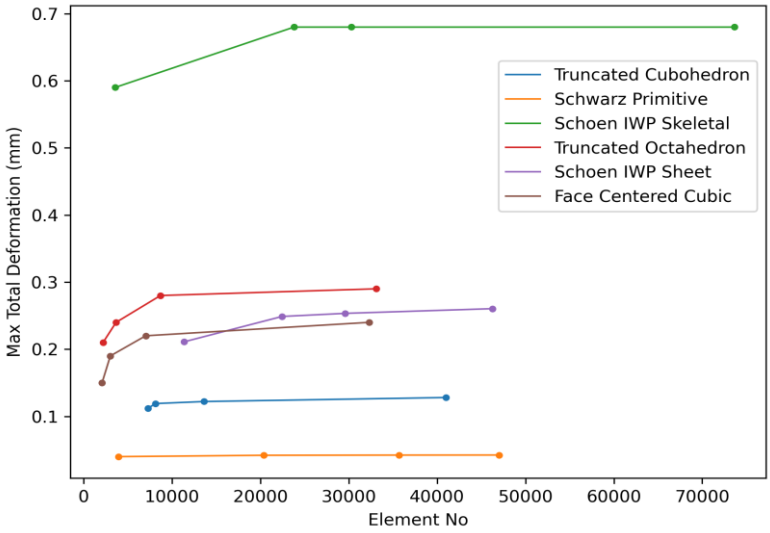


Figure 2. Mesh convergence study showing the variation of maximum total deformation with mesh density

3.2 Actuator Response

The structural response of the actuator was evaluated for the six lattice architectures under the defined thermo mechanical loading cycle. The quantities extracted from the simulations include maximum total deformation, equivalent stress, equivalent elastic strain, rotational displacement, and residual displacement after cooling. During the heating stage, the temperature increase induced the austenitic phase transformation in the Nitinol material, resulting in recovery of the deformation generated during mechanical loading. The deformation and

stress distributions indicate that most of the structural response occurs within the lattice filled core region, while the solid base plates remain relatively rigid. After the final cooling step, the residual displacement was measured to evaluate the remaining deformation in the actuator following the thermo mechanical cycle. This parameter provides insight into the recovery capability of the lattice-based actuator designs. A comparison of the main performance metrics for all lattice configurations is presented in Table 3, which summarizes the maximum deformation, maximum rotation, maximum equivalent stress, Maximum equivalent strain, and maximum residual displacement obtained from the simulations.

Table 3. Comparison of actuator performance for different lattice architectures

Type	Max Deformation (mm)	Max Rotation (deg)	Max Equivalent Stress (MPa)	Max Equivalent Strain	Max Residual Displacement (mm)	Residual Rotation (deg)	Recovery Ratio (%)
Schoen IWP Sheet	0.26	8.40	739.28	0.01	0.07	2.26	72.00
Schwarz Primitive	0.042	1.36	169.35	0.0025	0.00018	0.005	99.00
Schoen IWP Skeletal	0.68	22.04	2155.00	0.03	0.18	5.83	73.50
Face Centered Cubic	1.10	35.00	1266.80	0.02	0.28	9.07	74.00
Truncated Octahedron	0.28	9.07	539.63	0.0086	0.07	2.26	75.00
Truncated Cuboctahedron	0.63	20.42	507.70	0.0075	0.16	5.18	74.60

4. Discussion

The results demonstrate a strong dependence of actuator performance on lattice topology, particularly in terms of deformation capability, stress distribution, and recovery behavior. In terms of actuation performance, the Face Centered Cubic (FCC) lattice exhibits the highest deformation (1.10 mm) and rotation (35.0°), indicating superior compliance under torsional loading. Similarly, the Schoen IWP skeletal and Truncated Cuboctahedron lattices show relatively high deformation and rotation, making them suitable for applications requiring large actuation output. However, these structures are associated with significantly higher stress levels. In particular, the Schoen IWP skeletal lattice reaches a maximum equivalent stress of 2155 MPa, indicating an increased risk of material failure. The spatial distribution of equivalent stress for the different lattice architectures is shown in Fig. 3. The results highlight distinct stress concentration patterns depending on lattice topology. In strut-based lattices, high stress concentrations are primarily observed at node junctions and beam intersections, which are

critical regions prone to failure. In contrast, TPMS structures exhibit a more distributed stress field due to their continuous surface geometry, although localized stress concentrations can still occur in thin sections. In contrast, the Schwarz Primitive lattice demonstrates the lowest deformation (0.042 mm) and rotation (1.36°), along with the lowest stress (169 MPa) and strain values. This indicates a much stiffer structural response with improved load bearing capability and minimal risk of overstressing. It also achieves the highest recovery ratio (99%) with negligible residual displacement. However, the actuation response is very limited, which makes it less suitable for applications requiring significant rotational output. Apart from the Schwarz Primitive, all other lattice types show similar recovery ratios of approximately 75%.

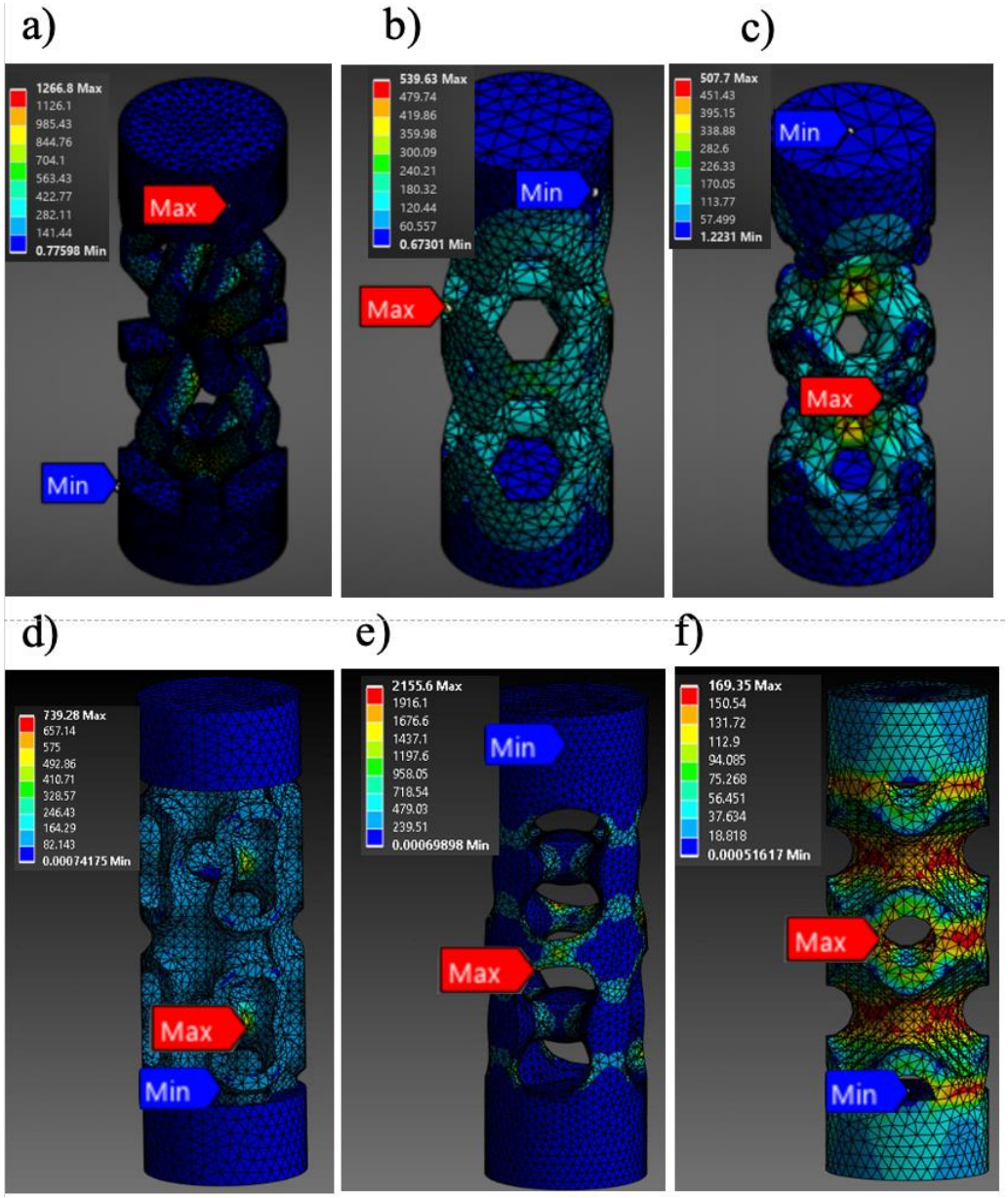


Figure 3. Equivalent Stress distribution for a) FCC, b) Truncated Octahedron c) Truncated Cuboctahedron, d) Schoen IWP Sheet, e) Schoen IWP Skeletal and f) TPMS Schwarz Primitive structures at maximum load

Among the strut-based lattices, the Truncated Octahedron and Truncated Cuboctahedron exhibit moderate deformation and stress levels, offering a balance between stiffness and actuation capability. The Truncated Cuboctahedron shows higher deformation and rotation compared to the Truncated Octahedron while maintaining relatively lower stress levels, making it a strong candidate among the investigated structures. Residual deformation results further highlight the tradeoff between actuation and recovery. Lattices with higher deformation, such as FCC and Schoen IWP skeletal, exhibit larger residual displacement and rotation, indicating incomplete recovery after the thermo mechanical cycle. In contrast, stiffer lattices such as Schwarz Primitive demonstrate near complete recovery with minimal residual deformation.
Overall, the results indicate that no single lattice topology simultaneously maximizes deformation, minimizes stress, and ensures full recovery. Highly compliant structures provide large actuation but are associated with higher stress and reduced recovery, while stiffer structures offer better load bearing capability and recovery at the cost of limited actuation. Therefore, the selection of lattice architecture should be guided by the specific requirements of the intended application.

5. Conclusions

This study investigated the effect of lattice topology on the performance of a cylindrical Nitinol actuator under thermo mechanical loading. The results show that lattice architecture strongly influences deformation, stress distribution, and recovery behavior. The Face Centered Cubic lattice exhibited the highest actuation response, while the Schwarz Primitive lattice showed superior load bearing capability and near complete recovery, but with very limited actuation. TPMS structures provided more uniform stress distribution, whereas strut-based lattices enabled greater deformation at the cost of higher stress concentrations and reduced recovery.
Overall, a clear trade off exists between actuation performance and structural reliability, and no single lattice topology optimizes all metrics. Strut based lattices are more suitable for high deformation applications, while TPMS structures are preferable when recovery and stress distribution are critical. These findings provide guidance for selecting lattice architectures based on specific application requirements.

Acknowledgements

This publication has emanated from research conducted with the financial support of Science Foundation Ireland and I-Form Advanced Manufacturing Centre under Grant number 21/RC/10295_P2.

References

1. Resnina N, Palani IA, Belyaev S, Singh S, Kumar A, Bikbaev R, et al. Functional Properties of the Multilayer NiTi Alloy Produced by Wire Arc Additive Manufacturing. Shape Mem Superelasticity. 2022 Mar 1;8(1):5–15. doi:10.1007/s40830-022-00359-0

2. Tareq S, Rahman T, Poudel B, Chung H, Kwon P. Heat treatment protocol for additively manufactured nitinol shape memory alloys in biomedical applications. Mater Sci Eng A. 2024 Apr 1;897:146274. doi:10.1016/j.msea.2024.146274

3. Kumar A, Palani IA, Yadav M. Comprehensive study of microstructure, phase transformations, and mechanical properties of nitinol alloys made of shape memory and superelastic wires and a novel approach to manufacture Belleville spring using wire arc additive manufacturing. Mater Today Commun. 2024 Mar 1;38:107881. doi:10.1016/j.mtcomm.2023.107881

4. Samal S, Tomáštík J, Václavek L, Chandra M, Kopeček J, Stachiv I, et al. Recovery of deformation surface of superelastic and shape memory NiTi alloy. Appl Surf Sci Adv. 2025 Jan 1;25:100684. doi:10.1016/j.apsadv.2024.100684

5. Tareq S, Poudel B, Nguyen H, Chung H, Kwon P. Laser powder bed fusion of nitinol shape memory alloy with superelastic characteristics on Ti substrate. J Manuf Process. 2024 Jun 15;119:964–74. doi:10.1016/j.jmapro.2024.04.005

6. Sun L, Chen K, Geng P, Zhou Y, Wen S, Shi Y. Mechanical and shape memory properties of NiTi triply periodic minimal surface structures fabricated by laser powder bed fusion. J Manuf Process. 2023 Sep 8;101:1091–100. doi:10.1016/j.jmapro.2023.06.034

7. Ryu C, Prabu SSM, Palani IA, Nguyen AP, In JB. Improving the actuation behavior of nitinol shape memory alloys by nanosecond laser surface texturing. Opt Laser Technol. 2024 Sep 1;176:110957. doi:10.1016/j.optlastec.2024.110957

8. Zhang Z, Gao J, Wei S, Song B, Yao Y, Zheng X, et al. Lattice-inspired NiTi-based metamaterials with widely tunable mechanical-superelastic synergy. Virtual Phys Prototyp. 2025 Jan 5;20(1):e2444572. doi:10.1080/17452759.2024.244457

9. Kevin Marchais, Yves Chemisky, Romain d'Esparbès, Manuel Ricardo Guevara, Yasmin Legerstee, & sudeep5511. (2025). 3MAH/microgen: v1.3.2 (v1.3.2). Zenodo. doi:10.5281/zenodo.14643858.

10. Auricchio F, Petrini L. Improvements and algorithmical considerations on a recent three-dimensional model describing stress-induced solid phase transformations. International Journal for numerical methods in engineering. 2002 Dec 20;55(11):1255-84. doi:10.1002/nme.619

11. ANSYS Learning Hub, "SHAPE MEMORY ALLOY (SMA) WITH THERMAL EFFECT" ANSYS, Inc.Available:https://innovationspace.ansys.com/courses/courses/structures-in-healthcare/lessons/using-shape-memory-alloy-sma-in-spinal-spacer-lesson-1/

Inducing the Two-Way Shape Memory Effect in Additively Manufactured NiTi Wires

Gavin Chapman[*a,1,2], Thomas Gillick[b,1,2], Ankur Majumdar[c,1,2], Meris Ikiz[d,1,2], Merve Nur Dogu[e,1,2], Neha Agarwal[f,1,2], Dermot Brabazon[g,1,2]

[1] *I-Form Advanced Manufacturing Research Centre, Dublin City University, Glasnevin, Dublin 9, Ireland*
[2] *DCU Institute for Advanced Processing Technology, School of Mechanical and Manufacturing Engineering, Dublin City University, Glasnevin, Dublin 9, Ireland*

[*] Corresponding author: [a]gavin.chapman3@mail.dcu.ie

[b]thomas.gillick3@mail.dcu.ie; [c]ankur.majumdar2@mail.dcu.ie; [d]meris.ikiz2@mail.dcu.ie; [e]mervenur.dogu@dcu.ie; [f]neha.agarwal@dcu.ie; [g]dermot.brabazon@dcu.ie

Abstract

Additive manufacturing (AM) of NiTi shape memory alloys offers unique design freedoms but presents distinct challenges in achieving the Two-Way Shape Memory Effect (TWSME). This study proposes and validates a novel training methodology specifically designed to induce TWSME in laser powder bed fusion (PBF-LB) NiTi wires. Following the proposed training protocol, the specimens were thermally cycled 15 times under manual low-stress conditions to evaluate macroscopic shape recovery. Results confirm the successful induction of TWSME, evidenced by reversible shape changes upon heating and cooling. Furthermore, the apparent hot shape loss and cold shape gain achieved through this methodology are highly comparable to existing literature for conventionally manufactured NiTi wires. These preliminary findings confirm the viability of the proposed approach for establishing the necessary internal stress fields for TWSME, providing a critical foundation for optimizing shape memory behaviour in AM NiTi components.

Keywords: Laser Powder Bed Fusion (PBF-LB); Two-Way Shape Memory Effect (TWSME); Nitinol; Shape Memory Alloys (SMA); UN SDG 9; UN SDG12

1. Introduction

Additive manufacturing (AM), commonly known as 3D printing, is a transformative industrial manufacturing process that constructs 3D objects by joining materials layer by layer from digital CAD models, fundamentally differing from traditional subtractive or formative manufacturing methods [1]. Within this scope, laser powder bed fusion (PBF-LB), also referred to as selective laser melting (SLM) serves as the most used methodology for metal part production by AM [2]. The process involves a recoating blade spreading a thin, uniform layer of metal powder across a build platform, which is then selectively fused by a high intensity laser in an inert gas environment to prevent oxidation [3]. This sequence is repeated, lowering the build platform each time to bond subsequent layers until the final geometry is realized [3]. The primary advantage of PBF-LB includes unparallel design freedom such as organic shapes and internal channels within the part which is difficult to impossible in traditional subtractive and formative manufacturing techniques [4].

Shape memory alloys (SMAs) are a unique class of smart materials capable of recovering their original shape after significant deformation through a solid-state phase transformation between a low temperature martensite phase and high temperature austenite phase. Standard SMAs exhibit a one-way shape memory effect (OWSME) requiring an external force to deform them after heating [5]. The two-way shape memory effect (TWSME) allows material to remember and spontaneously switch between two distinct shapes during both heating and cooling cycles [6]. This phenomenon is most effectively realized in Nitinol (NiTi), a nickel titanium alloy renowned for its biocompatibility and high recovery strain [7]. By undergoing a specific training process which includes setting up a hot shape and subsequently repeated cycling below martensite finish and austenite finish temperatures under stress [8]. The NiTi microstructure develops internal stress fields that guide the formation of preferred martensite variants [9]. This enables the alloy to act as a solid-state actuator, shifting predictably between shapes to perform mechanical work in applications ranging from aerospace morphing wings to self-regulating medical implants [11-12].

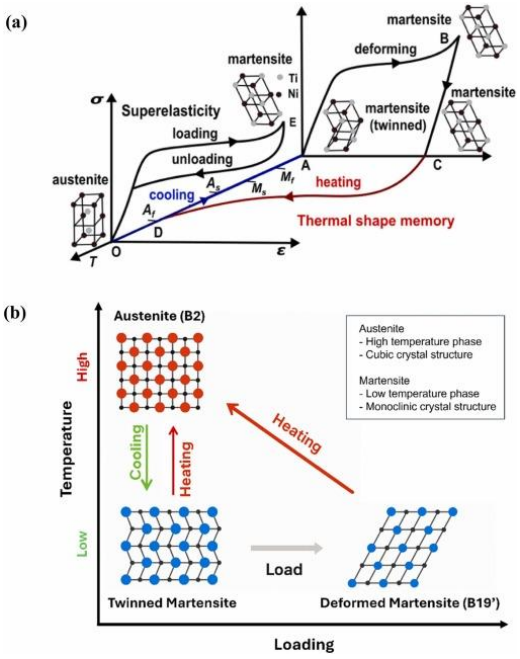


Fig. 1 *(a) Schematic diagram of Shape memory effect and super elasticity, (b) NiTi crystal structure under thermo-mechanical cycling [5].*

The shape memory effect in Nitinol (NiTi) originates from a reversible, diffusionless solid-state phase transformation between the low-temperature monoclinic martensite (B19') and the high-temperature cubic austenite (B2) crystal structures [12]. As illustrated in the Error! Reference source not found., the material in its twinned martensitic state accommodates external strain through a detwinning mechanism, resulting in a stable, deformed martensite configuration [5]. Upon heating the alloy above its specific transformation temperatures (TTs), the lattice undergoes a structural shift back to the B2 parent phase, effectively recovering the pre-trained geometry. This thermal shape memory behaviour is highly sensitive to the Ni:Ti atomic ratio, where an increased titanium content elevates the TTs for thermal actuation, while higher nickel concentrations stabilize the austenite phase at ambient temperatures to facilitate superelasticity. Consequently, precise compositional control is paramount, as even minor elemental fluctuations during processing can significantly alter the stability of the B19'and B2 phases and their associated mechanical responses [13].

Introducing TWSME in additively manufactured NiTi alloys presents a complex set of metallurgical and mechanical hurdles, primarily stemming from the extreme thermal gradient and elemental evaporation inherent in laser-based processes [14]. During PBF-LB, the high energy density often leads to the preferential evaporation of nickel, shifting the NiTi ratio and causing unpredictable fluctuations in the phase transformation temperatures [15]. Furthermore, the rapid solidification creates significant residual stresses and microstructural inhomogeneities, such as chemical segregation and unfavourable crystallographic textures, which can suppress the formation of the specific martensite variants required for TWSME [16]. Unlike OWSME, TWSME is not

an intrinsic property and requires extensive thermomechanical training to create internal stress fields [17]. In AM parts, the presence of internal defects such as porosity, cracks and brittle intermetallic precipitates such as Ti_2Ni_2 often acts as stress concentrators, leading to functional fatigue and premature structural failure during these training cycles [18]. Consequently, achieving a stable, repeatable TWSME in complex AM NiTi geometries remains a significant challenge, necessitating precise control over process parameters and specialized post-print heat treatments to homogenize the microstructure [19-20].

In this study, thin NiTi wires were fabricated via PBF-LB to establish and validate a training methodology designed specifically to induce the TWSME in additively manufactured components. To evaluate the ability of the proposed approach, the resulting macroscopic shape recovery metrics were benchmarked against established findings in literature for conventionally manufactured NiTi wires. By demonstrating comparable shape memory behaviour, this work lays a critical foundation for optimizing training protocols tailored to AM NiTi, ultimately advancing the functional integration of these complex smart materials.

2. Materials and Methods

2.1 Sample Geometry and Fabrication

Thin long wire specimens were manufactured using the Aconity MINI PBF-LB machine equipped with a 200 W, 1064 nm Yb-fiber laser. The wires had a length of 110 mm and a diameter of 0.8 mm printed parallel to the build direction. The chosen material was a near equiatomic NiTi composition of gas atomized powder. The process parameters used to manufacture the samples can be found in **Table 1**. Process parameters were selected from a preliminary study where these parameters were found to achieve the highest relative density value.

Table 1 Process parameters used for producing wire samples.

Parameter	Value
Laser power [W]	180
Scanning speed [mm/s]	1200
Hatch distance [µm]	60
Laser spot size [µm]	60
Layer thickness [µm]	50

2.2 Heat treatment

Heat treatment was carried out in a Carbolite RHF 1600 box furnace at a temperature of 500°C for two hours. The purpose of this was to train the desired shape that the samples would have at the high temperature B2 austenitic phase. Prior to heat treatment, the samples were fixed to a metallic plate in the specific shape that the austenitic phase was desired to have. For the duration of the heat treatment, the wire was fixed onto an aluminium plate and was held to have a U-shaped 180-degree bend. This was the desired shape that the wire would have in the austenitic phase. An illustration of the mounting configuration is shown in **Fig. 1**.

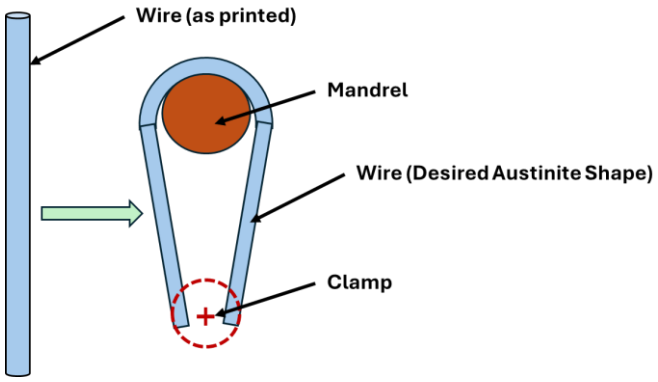


Fig. 1 *Illustration showing how the austinite shape was held during the initial high temperature heat treatment of the AM wire***.**

2.3 Two-way shape-memory effect training

To train the two-way shape-memory effect in the printed NiTi samples, a series of thermal cycles were carried out, in which the hot and cold shape, for the respective austenite and martensite phases, were trained. As was trained during the heat treatment process, the wire would have a 180-degree U-shape in the austenitic phase and would be manually deformed to be straight in the martensite phase. During training, one end of the wire was fixed, while the other end was free to deform. During heating, a heat gun was used to heat the wire, allowing it to transform into the austenite phase. Afterwards, the wire was allowed to cool in air back to the martensite phase. Thermal cycling took place on top of an aluminium block which was immersed in an ice bath, which aided cooling of the samples into the martensite phase. The change in wire shape during phase transformation was recorded with an Ash Inspex HD 1080p digital microscope. A total of fifteen thermal cycles were carried out to train the two-way shape-memory effect in the printed wire. The procedure that was adopted for the thermal cycling of the wire is described below and a flowchart is presented in **Fig. 2**.

Step 1. Martensite

The cycle begins when the wire is in its desired martensitic straight shape and is constrained at both ends. One end is fixed to the aluminium block, while the other (free) end is restrained from deforming by a pin that is also slotted into the aluminium block. This position was held for 1 minute.

Step 2. Martensite → Austenite

The pin that restricts movement of the free end of the wire is removed, and the heat gun is simultaneously turned on. As the wire heats up, it subsequently undergoes phase transformation from martensite to austenite. This phase transformation is evident by the changing of the wire shape from its straight martensitic shape to its desired austenitic U-shaped appearance.

Step 3. Austenite

To reduce shape loss in the transformation to the original heat-treated austenitic shape, the wire is manually deformed further, to reach this shape. Manual deformation is carried out twenty seconds after the last observable movement of the wire that occurred during the phase transformation from martensite to austenite.

Upon reaching the original heat-treated austenitic shape, with the aid of manual deformation, the free end of the wire is constrained with use of a pin that is slotted into the aluminium block. After constraining the wire, the heat gun is used to maintain a high temperature for one minute, to reinforce the original heat-treated austenitic shape that the wire had.

Step 4. Austenite → Martensite

The heat gun is switched off, and the sample begins to cool down. Simultaneously, the pin which constrained the sample in the trained austenite position, is removed, allowing the free edge of the sample to deform. Evidence of the two-way shape-memory effect is evident in this step. During the transformation of austenite to martensite, the wire begins to change shape and begins to deform back to its straight martensite shape. During the cooling phase, the wire is allowed to deform freely until it reaches its final martensitic shape for the given thermal cycle.

Like the austenitic phase transformation, manual deformation is subsequently carried out to deform the wire to its desired straight shape 20 seconds after the last observed deformation occurred during the phase transformation. This is carried out to reinforce the wire's desired martensitic shape. This procedure completes a single thermal cycle and is repeated for each cycle.

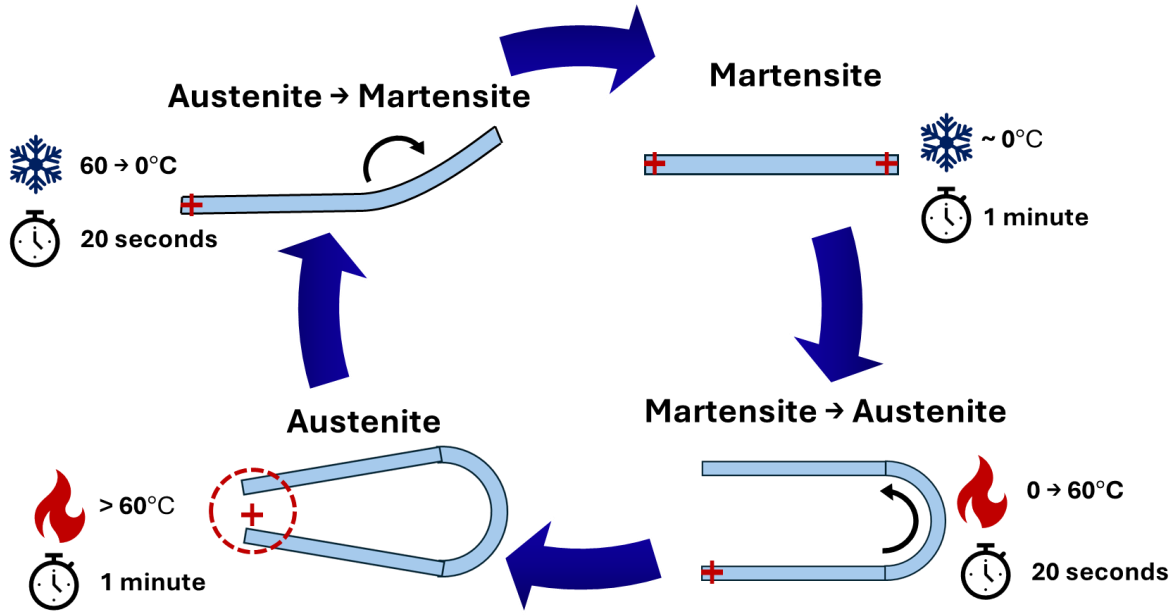


Fig. 2 Flowchart showing the proposed TWMSE training procedure.

3. Results and Discussion

The primary objective of this study was to establish and validate a methodology for inducing the TWSME PBF-LB NiTi wires. Following the proposed training protocol, macroscopic shape changes were evaluated during thermal cycling under low-stress conditions. The trained AM NiTi wires successfully demonstrated a reversible

macroscopic shape change upon heating and cooling, confirming that the methodology effectively introduces the necessary internal stress fields required for TWSME.

To assess the methodology's effectiveness and efficiency, the apparent hot shape loss and cold shape gain were evaluated. Hot shape loss indicates the accumulation of unrecoverable defects during training, while cold shape gain reflects the shape achieved upon cooling via the oriented martensitic transformation. Preliminary macroscopic evaluations show that both metrics are highly comparable to values reported in existing literature for conventionally manufactured TWSME trained NiTi wires. For instance, Luo and Abel [21] successfully induced TWSME in cold-worked NiTi wires (51 at.% Ni) targeting a 90° arc. Notably, their samples exhibited phase transformation temperatures comparable to the AM wires investigated in this study. Following 15 thermal cycles, Luo and Abel reported a hot shape loss of similar magnitude to that noted within this work. The preliminary macroscopic shape recovery achieved using our proposed AM training methodology aligns closely with these established figures. This comparison further validates that the novel approach is capable of matching the TWSME performance of traditionally cold-worked NiTi components.

5. Conclusions

In conclusion, an effective training methodology for PBF-LB manufactured NiTi wires was successfully established and validated. Thermomechanical cycling confirmed the induction of the TWSME, evidenced by reversible macroscopic shape changes. Furthermore, the apparent hot shape loss and cold shape gain resulting from this protocol are highly comparable to established literature values for conventionally manufactured wires, demonstrating the method's overall effectiveness and viability. Future work will focus on characterising the trained wire's microstructure to examine the resulting internal features, alongside comprehensive, quantitative measurements of its long-term TWSME performance.

CRediT

Gavin Chapman: Conceptualization, Investigation, Writing – original draft; **Thomas Gillick**: Conceptualization, Investigation, Writing – original draft; **Ankur Majumdar**: Investigation, Writing – original draft; **Meris Ikiz**: Investigation, Writing – review & editing; **Merve Nur Dogu**: Investigation, Writing – review & editing; **Neha Agarwal**: Investigation, Writing – review & editing; **Dermot Brabazon**: Conceptualization, Supervision, Writing – review & editing.

Acknowledgments

This publication has emanated from research supported by Research Ireland's I-Form Advanced Manufacturing Research Centre under Grant Number 21/RC/10295_P2 and is co-funded under the European Regional Development Fund.

For Open Access, the author has applied a CC BY public copyright license to any Author Accepted Manuscript version arising from this submission.

References

[1] T. D. Ngo, A. Kashani, G. Imbalzano, K. T. Q. Nguyen, and D. Hui, 'Additive manufacturing (3D printing): A review of materials, methods, applications and challenges', *Compos. Part B Eng.*, vol. 143, pp. 172–196, Jun. 2018, doi: 10.1016/j.compositesb.2018.02.012.

[2] G. M. Volpato, U. Tetzlaff, and M. C. Fredel, 'A comprehensive literature review on laser powder bed fusion of Inconel superalloys', *Addit. Manuf.*, vol. 55, p. 102871, Jul. 2022, doi: 10.1016/j.addma.2022.102871.

[3] W. Ji, R. Zhou, P. Viveganantha n, M. See Wu, H. Gao, and K. Zhou, 'Recent progress in gradient-structured metals and alloys', *Prog. Mater. Sci.*, vol. 140, p. 101194, Dec. 2023, doi: 10.1016/j.pmatsci.2023.101194.

[4] M. Mazur and PR. Selvakannan, 'Laser Powder Bed Fusion—Principles, Challenges, and Opportunities', in *Additive Manufacturing for Chemical Sciences and Engineering*, S. K. Bhargava, S. Ramakrishna, M. Brandt, and PR. Selvakannan, Eds, Singapore: Springer Nature, 2022, pp. 77–108. doi: 10.1007/978-981-19-2293-0_4.

[5] A. Ahmed, S. I. Pranto, M. H. A. Faruq, Mst. T. T. Kasfia, and A. Bin Rashid, 'A comprehensive overview of shape memory alloys: Recent advances in fabrications, properties, and applications for next-generation smart systems', *Mater.*, vol. 10, p. 101441, Jan. 2026, doi: 10.1016/j.nxmate.2025.101441.

[6] W. Huang and W. Toh, 'Training two-way shape memory alloy by reheat treatment', *J. Mater. Sci. Lett.*, vol. 19, no. 17, pp. 1549–1550, Sep. 2000, doi: 10.1023/A:1006721022185.

[7] J. Ryhänen *et al.*, 'Biocompatibility of nickel-titanium shape memory metal and its corrosion behavior in human cell cultures', *J. Biomed. Mater. Res.*, vol. 35, no. 4, pp. 451–457, 1997, doi: 10.1002/(SICI)1097-4636(19970615)35:4<451::AID-JBM5>3.0.CO;2-G.

[8] 'Effects of Predefined Thermomechanical Procedure on the Microstructure and Mechanical Properties of the Two-Way Shape Memory Effect in the NiTi Alloy - Tahaei - 2023 - Advances in Materials Science and Engineering - Wiley Online Library'. Accessed: Mar. 18, 2026. [Online]. Available: https://onlinelibrary-wiley-com.dcu.idm.oclc.org/doi/10.1155/2023/1524836

[9] O. Molnárová, O. Tyc, M. Klinger, and P. Šittner, 'Reconstruction of martensite variant microstructures in grains of deformed NiTi shape memory alloy by TEM', *Mater. Charact.*, vol. 214, p. 114084, Aug. 2024, doi: 10.1016/j.matchar.2024.114084.

[10] G. Costanza and M. E. Tata, 'Shape Memory Alloys for Aerospace, Recent Developments, and New Applications: A Short Review', *Materials*, vol. 13, no. 8, Apr. 2020, doi: 10.3390/ma13081856.

[11] N. B. Morgan, 'Medical shape memory alloy applications—the market and its products', *Mater. Sci. Eng. A*, vol. 378, no. 1, pp. 16–23, Jul. 2004, doi: 10.1016/j.msea.2003.10.326.

[12] J. C. Chekotu, R. Groarke, K. O'Toole, and D. Brabazon, 'Advances in Selective Laser Melting of Nitinol Shape Memory Alloy Part Production', *Materials*, vol. 12, no. 5, Mar. 2019, doi: 10.3390/ma12050809.

[13] J. C. Chekotu, R. Goodall, D. Kinahan, and D. Brabazon, 'Control of Ni-Ti phase structure, solid-state transformation temperatures and enthalpies via control of L-PBF process parameters', *Mater. Des.*, vol. 218, p. 110715, Jun. 2022, doi: 10.1016/j.matdes.2022.110715.

[14] T. C. da Silva *et al.*, 'Microstructure, Thermal, and Mechanical Behavior of NiTi Shape Memory Alloy Obtained by Micro Wire and Arc Direct Energy Deposition', *J. Manuf. Mater. Process.*, vol. 9, no. 2, Feb. 2025, doi: 10.3390/jmmp9020057.

[15] M. C. C. Monu, S. Kumar S., and D. Brabazon, 'Heat treatment of NiTi alloys: Influence of volumetric energy density on ageing parameters and the resulting physical properties', *J. Mater. Res. Technol.*, vol. 26, pp. 9532–9555, Sep. 2023, doi: 10.1016/j.jmrt.2023.09.251.

[16] N. Ren *et al.*, 'Solute trapping and non-equilibrium microstructure during rapid solidification of additive manufacturing', *Nat. Commun.*, vol. 14, no. 1, p. 7990, Dec. 2023, doi: 10.1038/s41467-023-43563-x.

[17] K. C. Atli, I. Karaman, R. D. Noebe, and D. Gaydosh, 'The effect of training on two-way shape memory effect of binary NiTi and NiTi based ternary high temperature shape memory alloys', *Mater. Sci. Eng. A*, vol. 560, pp. 653–666, Jan. 2013, doi: 10.1016/j.msea.2012.10.009.

[18] 'Review on Fatigue of Additive Manufactured Metallic Alloys: Microstructure, Performance, Enhancement, and Assessment Methods - Liu - 2024 - Advanced Materials - Wiley Online Library'. Accessed: Mar. 18, 2026. [Online]. Available: https://advanced-onlinelibrary-wiley-com.dcu.idm.oclc.org/doi/10.1002/adma.202306570

[19] S. Tareq, T. Rahman, B. Poudel, H. Chung, and P. Kwon, 'Heat treatment protocol for additively manufactured nitinol shape memory alloys in biomedical applications', *Mater. Sci. Eng. A*, vol. 897, p. 146274, Apr. 2024, doi: 10.1016/j.msea.2024.146274.

[20] C. Zhao, H. Liang, S. Luo, J. Yang, and Z. Wang, 'The effect of energy input on reaction, phase transition and shape memory effect of NiTi alloy by selective laser melting', *J. Alloys Compd.*, vol. 817, p. 153288, Mar. 2020, doi: 10.1016/j.jallcom.2019.153288.

[21] H. Y. Luo and E. W. Abel, 'A comparison of methods for the training of NiTi two-way shape memory alloy', *Smart Mater. Struct.*, vol. 16, no. 6, p. 2543, Oct. 2007, doi: 10.1088/0964-1726/16/6/058.

Review of Phase Transformation Behaviour in NiTi Lattice Structures Fabricated via Wire-Based Directed Energy Deposition

Terence Bowden[1,2,*], Ronan McCann[1,2], Dermot Brabazon[1,2]

[1] *I-Form Advanced Manufacturing Research Centre, Dublin City University, Glasnevin, Dublin 9, Ireland*
[2] *DCU Institute for Advanced Processing Technology, School of Mechanical and Manufacturing Engineering, Dublin City University, Glasnevin, Dublin 9, Ireland*

[*] Corresponding author: Terence.Bowden4@mail.dcu.ie

Abstract

The rapid growth of metal additive manufacturing (AM), particularly Directed Energy Deposition (DED), is being driven by industrial demand for large-scale, high-performance components with reduced material waste and increased design flexibility. Nickel–Titanium (NiTi) shape memory alloys (SMAs) offer unique thermomechanical properties, including shape memory effect and super elasticity, making them highly attractive for smart actuator applications. Three major challenges with using SMA actuators under cyclic loading are, reduced strain recovery, low working frequency and low energy efficiency (10-15%).

Current research is predominantly focused on laser powder bed fusion (LPBF), with limited exploration of wire-based DED, particularly for lattice structures. Lattice based actuators which enable enhanced strain levels, introduce additional complexity due to the interplay between geometry, thermal gradients, and phase transformation behaviour.

Keywords: *3D Printing, Additive Manufacturing, NiTi, Lattice Structure, Direct Energy Deposition, Decent work and economic growth, Industry, innovation, and infrastructure, Responsible consumption and production*

1. Introduction

Metal AM has evolved into a key enabling technology for advanced manufacturing, with DED offering distinct advantages in terms of scalability, repair capability, and material efficiency. Unlike LPBF, DED allows for higher deposition rates and the fabrication of large components, making it particularly suitable for aerospace and energy applications [1].

NiTi SMAs are of significant interest due to their reversible phase transformation between martensite and austenite, enabling shape memory and super-elastic behaviour. These properties make NiTi highly suitable for adaptive and functional structures [2].

However, integrating NiTi into DED processes presents several challenges. Small variations in nickel composition can result in significant shifts in transformation temperatures, while the cyclic thermal nature of DED introduces complex microstructural evolution[3]. Despite extensive studies on lattice structures in conventional alloys, there is limited research on NiTi lattices produced via wire-based DED.

This work is a summary of a literature review, while not fully finished it investigates where there are possible research opportunities printing lattices using NiTi in a wire based form in a DED printer. It summarises the main topic researched giving 5 possible areas for research which are also inline with the United Nations sustainable development goals UNSDG9 (industry, innovation and infrastructure) and UNSDG12 (responsible consumption and production).

2.1 NiTi in Additive Manufacturing

LPBF has been widely investigated for NiTi due to ability to produce complex geometries and potential to control the microstructures. However, it is associated with residual stress and limited scalability. Nickel evaporation during processing remains a critical issue, with reported composition shifts of up to 1–2 %wt significantly altering transformation temperatures [3].

2.2 Direct Energy Deposition (DED) Processing of NiTi

DED attracting growing interest with its ability to manufacture large, more complex parts with reduced waist when compared to PBF. However, there are drawbacks. Processing NiTi using DED can cause a loss in the Ni concentration due to preferential evaporation which alters the transformation temperature and resulting SMA properties. Repeated thermal cycling during metal additive manufacturing can lead to increased oxidation and residual stress. Thermal gradients occur within each layer as well as between layers during metal deposition [4].

2.3 Lattice Structures in AM

DED provides the ability to print these shapes at scale making it more economical due to the reduction of time and energy required to manufacture these shapes [1], when compared to traditional methods such as investment casting, plastic forming, weaving [5]. Lattices also enable high strength-to-weight ratios and tunable mechanical properties [6]. When using SMAs this can enhance functional behaviour [3]. However, research on NiTi lattices remains limited, particularly in DED systems.

2.4 Lattice Design

Lattices structures come in many variants, from the simple cubic (Truss lattice) to the Gyroid Lattice (Triply Periodic Minimal Surface) which is widely regarded as the most complex naturally occurring and engineered lattice structure [7]. Three main types of lattices are truss, plate, and TPMS.

Truss Lattices. Simple cubic (SC), Body Centre Cubic (BCC) and Face Centre Cubic (FCC) would be the most common types [8].
Plate Lattices. Is a more recent class of structure. These are identified by the plate elements added along the planes, under the cubic lattice framework (BCC, FCC).

Triply Periodic Minimal Surface (TPMS) Lattices TPMS lattices are visually very organic looking. They are a class of architected porous structures defined by mathematically continuous minimal surfaces, offering significant advantages across mechanical, mass transfer, and thermal applications [8].

3.0 Research Opportunities

From the research published to date, the following five research areas are identified as knowledge gaps requiring further research.

a. **Composition Control During Wire Deposition**
For NiTi, even a 0.1% change in nickel content can shift transformation temperatures by tens of degrees. If one cannot control the chemistry, the "smart" functionality may be lost before the part is produced.

b. **Thermal History Control for Phase Transformation**
DED involves repeated thermal cycles that act as intrinsic heat treatments. Without controlling this, the phase transformation behaviour will be inconsistent across the height of the part.

c. **DED Fabrication of NiTi Lattice Structures**
This represents a primary design target for large-scale DED of SMAs. Research here focuses on geometric accuracy and the thermomechanical response of complex, porous architectures.

d. **Functionally Graded Smart Materials (FGSMs)**
A major advantage of DED is the ability to change material properties spatially. Researching how to transition from Ni-rich to Ti-rich zones or between different alloys is a top-tier challenge for advanced engineering.

e. **AI-Based Prediction of Transformation Behaviour**
This is the most "modern" area. While critical for scaling and speed, it relies on the data generated by the foundational areas above. It is currently a high-growth research field for optimizing complex parameter windows.

4. Discussion and Conclusion

While the research is in its infant stage, several possible areas have been identified where further research needs to be investigated using NiTi wire with a DED 3D printer. NiTi produced via DED has many potential applications in space, aviation, automotive, maritime with products such as smart actuators and energy absorption systems. While the five identified areas for further investigation. There are lots of other opportunities to which will be discussed in the final literature review.

This short paper presents a summary of a literature review which is still under way. It introduces several of the materials, technologies processes involved with AM and 3D printing and some of the challenges. Discusses the research so far for investigating NiTi lattice structures fabricated via wire-based DED. By addressing challenges

related to composition control, thermal history, and structural design, this work aims to bridge a key gap in the current literature. The outcomes are expected to contribute to both fundamental understanding and industrial application of smart materials in large-scale AM systems and are in line with the UN sustainable goals.

Acknowledgements

This research is funded by Dublin City University co-fund scheme. This publication has emanated from research supported by Research Ireland's I-Form Advanced Manufacturing Research Centre under Grant Number 21/RC/10295_P2 and is co-funded under the European Regional Development Fund. For Open Access, the author has applied a CC BY public copyright license to any Author Accepted Manuscript version arising from this submission.

References

[1] T. Xu, S. Tang, C. Liu, Z. Li, H. Fan, and S. Y. Ma, "Obtaining large-size pyramidal lattice cell structures by pulse wire arc additive manufacturing," *Mater. Des.*, vol. 187, Feb. 2020, doi: 10.1016/j.matdes.2019.108401.

[2] M. Leary, S. Huang, T. Ataalla, A. Baxter, and A. Subic, "Design of shape memory alloy actuators for direct power by an automotive battery," *Mater. Des.*, vol. 43, pp. 460–466, 2013, doi: 10.1016/j.matdes.2012.07.002.

[3] C. A. Biffi, A. Tuissi, and A. G. Demir, "Martensitic transformation, microstructure and functional behavior of thin-walled Nitinol produced by micro laser metal wire deposition," *Journal of Materials Research and Technology*, vol. 12, pp. 2205–2215, 2021, doi: 10.1016/j.jmrt.2021.03.108.

[4] H. M. W. Uddin, Q. R. M. Progoti, M. C. Mondal, S. E. Arman, and S. B. Malitha, "Adaptive nickel–titanium shape memory alloy for smart systems: Mechanisms, manufacturing, and applications across biomedical, aerospace, civil, and energy," *Mater. Today Commun.*, vol. 50, Jan. 2026, doi: 10.1016/j.mtcomm.2025.114564.

[5] C. Pan, Y. Han, and J. Lu, "Design and optimization of lattice structures: A review," Sep. 02, 2020, *MDPI AG*. doi: 10.3390/APP10186374.

[6] S. Z. Ahmad, M. H. Masood, M. U. Khattab, S. S. Ahmad, S. A. A. Zaidi, and S. Z. Khan, "Recent Developments in Novel TPMS Lattice Materials: Design Optimization, Performance Control, and Applications in Biomimetic Scaffolds," Nov. 01, 2025, *Multidisciplinary Digital Publishing Institute (MDPI)*. doi: 10.3390/ma18225209.

[7] E. Goi, B. P. Cumming, and M. Gu, "Gyroid 'srs' Networks: Photonic Materials Beyond Nature," Sep. 18, 2018, *Wiley-VCH Verlag*. doi: 10.1002/adom.201800485.

[8] S. Z. Ahmad, M. H. Masood, M. U. Khattab, S. S. Ahmad, S. A. A. Zaidi, and S. Z. Khan, "Recent Developments in Novel TPMS Lattice Materials: Design Optimization, Performance Control, and Applications in Biomimetic Scaffolds," Nov. 01, 2025, *Multidisciplinary Digital Publishing Institute (MDPI)*. doi: 10.3390/ma18225209.

Forensic Challenges in Additively Manufactured Materials: Reliability of 3D-Printed Evidence

Aleksandra Mitrovic[1], Nenad Mitrovic[2], Svetlana Pelemis[3]

[1]*Department for Forensic Engineering, University of Criminal Investigation and Police Studies, Serbia, aleksandra.mitrovic@kpu.edu.rs 0000-0002-5183-6276*
[2]*University of Belgrade, Faculty of Mechanical Engineering, Center for Optical Measurement, Serbia nmitrovic@mas.bg.ac.rs 0000-0001-9296-2669*
[3]*University of East Sarajevo, Faculty of Technology Zvornik, Bosnia and Herzegovina; svetlana.pelemis@tfzv.ues.rs.ba 0000-0001-9682-5899*

Corresponding author: aleksandra.mitrovic@kpu.edu.rs

Abstract

Additive manufacturing has evolved from a rapid prototyping tool into a mature production technology capable of fabricating functional components for aerospace, medical, automotive, and consumer applications. As access to additive manufacturing technologies expands, components produced through layer-by-layer fabrication increasingly appear in forensic investigations. However, most forensic methodologies were developed for conventionally manufactured materials and implicitly assume relatively homogeneous microstructures and reproducible manufacturing conditions.

Additively manufactured materials challenge these assumptions. Their mechanical behavior is strongly influenced by building orientation, layer adhesion, thermal history, and process parameters. Consequently, components produced from the same digital model may exhibit markedly different structural properties and fracture characteristics. These variations complicate failure interpretation and raise important questions regarding the reliability of additively manufactured evidence.

This review summarizes current knowledge on structural variability, anisotropy, and fracture behavior of additively manufactured materials, drawing on findings from materials science and additive manufacturing literature. The implications of these characteristics for forensic material analysis are examined, particularly with respect to failure reconstruction and the interpretation of material evidence. The analysis highlights the need for forensic methodologies that explicitly account for manufacturing variability and emphasizes the importance of developing standardized approaches for evaluating additively manufactured components as forensic evidence.

Keywords: Additive Manufacturing; Forensic Engineering; Evidence Reliability; Structural Variability; Fracture Behavior; UN SDG 9; UN SDG 12; UN SDG 16;

1. Introduction

Additive manufacturing (AM) has fundamentally transformed the design and production of engineering components. Unlike conventional manufacturing methods, which typically rely on subtractive or formative processes, AM technologies fabricate components through the successive deposition or consolidation of material layers directly from digital models [1].

This manufacturing approach provides a high degree of geometric design flexibility and has contributed to the rapid integration of additive manufacturing technologies across a wide range of industrial sectors. Technologies such as fused filament fabrication, selective laser sintering, and selective laser melting are now widely used to produce structural components, medical implants, tooling inserts, and functional prototypes [2]. At the same time, the increasing availability of affordable desktop printers has enabled decentralized manufacturing, allowing individuals and small organizations to fabricate components without centralized production control.

These developments have important implications for forensic investigations. Additively manufactured components have been reported in contexts ranging from improvised firearm parts to customized mechanical components and consumer products involved in accidents or failures. In such cases, investigators are often confronted with components whose manufacturing history is unknown and whose material properties cannot be readily inferred from conventional standards.

Traditional forensic material analysis assumes a degree of consistency in material properties and manufacturing processes. For example, the fracture behavior of wrought metals, cast alloys, or injection-molded polymers is typically interpreted within well-established frameworks linking microstructure, processing history, and mechanical performance [3]. These assumptions become less reliable when applied to additively manufactured materials.

The layer-wise fabrication process inherent to AM introduces structural anisotropy, heterogeneous bonding between layers, and sensitivity to processing conditions. As a result, components fabricated from identical digital models may exhibit significantly different mechanical responses depending on build orientation, printing parameters, or machine characteristics. Understanding these factors is essential for evaluating the reliability of additively manufactured components in forensic investigations.

2. Structural Variability in Additive Manufacturing

Structural variability represents one of the defining characteristics of additively manufactured materials. Unlike conventional manufacturing routes, where processing parameters are typically standardized and tightly controlled, AM processes involve numerous adjustable variables that directly influence material structure and performance.

Experimental studies of polymer-based fused filament fabrication have shown that mechanical properties depend strongly on raster orientation and the quality of interlayer bonding. Ahn et al. [4] demonstrated that tensile strength and stiffness of printed ABS components vary significantly with filament orientation, reflecting the anisotropic structure created by the deposition process. Such anisotropy is an inherent feature of layer-based fabrication rather than an isolated processing artifact.

Similar observations have been reported regarding metal additive manufacturing technologies. Comprehensive reviews indicate that thermal gradients, solidification dynamics, and energy input during laser-based fabrication strongly influence microstructure, residual stress, and defect formation within printed components [2]. These process-dependent microstructures can lead to variations in mechanical properties even among components produced within the same build.

Defect formation further contributes to structural variability. Additively manufactured components may contain porosity, lack-of-fusion defects, or incomplete bonding between layers. The distribution and severity of these defects depend on processing parameters such as scanning strategy, energy density, and powder characteristics [5]. In contrast to many conventional manufacturing processes, such defects are often spatially heterogeneous and difficult to predict. For forensic investigations, this variability complicates the interpretation of material evidence. When evaluating an additively manufactured component involved in a failure or incident, investigators must consider the possibility that its structural characteristics differ significantly from those of nominally identical parts produced under different processing conditions.

3. Fracture Behavior of Additively Manufactured Materials

Fracture analysis plays a central role in forensic engineering because fracture surfaces frequently provide critical information about loading conditions, failure mechanisms, and material properties. In additively manufactured components, however, fracture behavior may deviate substantially from that observed in conventionally manufactured materials.

Research on polymer-based AM components indicates that crack initiation and propagation are often influenced by the orientation of deposited filaments and the strength of interlayer bonding. Ziemian et al. [6] reported that fracture surfaces frequently exhibit features associated with the layered structure of fused filament fabrication, including crack propagation along interlayer boundaries. This behavior reflects the anisotropic nature of additively manufactured polymers. Because bonding between adjacent layers may be weaker than bonding within individual filaments, fracture often initiates at interlayer interfaces rather than within the bulk material. Consequently, the fracture morphology may depend strongly on build orientation and printing parameters.

Metal AM components can exhibit similarly complex fracture behavior. Microstructural heterogeneity, residual stresses, and process-induced defects may influence crack initiation sites and propagation paths. Reviews of metal additive manufacturing emphasize that these factors can significantly affect mechanical performance and damage evolution [2].

Forensic interpretation of fracture surfaces in additively manufactured materials therefore requires careful consideration of manufacturing conditions. Without knowledge of build orientation or processing parameters, distinguishing between design flaws, manufacturing defects, and service-related damage may become particularly challenging.

4. Implications for Forensic Evidence

The distinctive characteristics of additively manufactured materials present significant challenges for forensic analysis. Traditional approaches to material comparison and failure interpretation often rely on assumptions of uniformity and reproducibility that may not hold for AM components.

Variations in build orientation, interlayer bonding, and process parameters can produce substantial differences in structural integrity and mechanical response. As a result, direct comparisons between questioned AM components and reference materials may be less straightforward than in the case of conventionally

manufactured parts. Forensic engineering literature emphasizes that reliable interpretation of material evidence must be grounded in a clear understanding of the underlying physical mechanisms governing material behavior [3]. In the context of additive manufacturing, this requires careful consideration of process-dependent variability and the limitations it imposes on forensic comparisons. Developing forensic methodologies tailored to additive manufacturing therefore represents an important research priority. Such methodologies must integrate knowledge from materials science, manufacturing engineering, and forensic analysis to ensure that interpretations of AM evidence remain scientifically robust and legally defensible.

5. Conclusion

Additive manufacturing introduces new complexities into forensic material analysis. The layer-wise fabrication process produces materials that are inherently anisotropic and sensitive to processing parameters, leading to structural variability and distinctive fracture behavior. These characteristics challenge assumptions commonly used in forensic investigations of conventionally manufactured materials. Differences in build orientation, interlayer bonding, and process conditions may significantly influence mechanical performance and failure patterns, even among components produced from the same digital design.

As additive manufacturing continues to expand into industrial and consumer applications, the likelihood of encountering AM components in forensic contexts will increase. Addressing this challenge requires the development of forensic methodologies that explicitly account for the variability inherent to additive manufacturing processes. Advancing the forensic interpretation of additively manufactured evidence will therefore depend on continued collaboration between materials scientists, manufacturing engineers, and forensic investigators. Such interdisciplinary efforts are essential for establishing reliable frameworks for evaluating the structural integrity and evidentiary reliability of 3D-printed components.

References

[1] Gibson I, Rosen D, Stucker B. Additive Manufacturing Technologies: 3D Printing, Rapid Prototyping, and Direct Digital Manufacturing. 3rd ed. Springer; 2021.

[2] DebRoy T, Wei HL, Zuback JS, Mukherjee T, Elmer JW, Milewski JO, Zhang W. Additive manufacturing of metallic components – Process, structure and properties. Progress in Materials Science. 2018;92:112–224.

[3] Hainsworth SV, Fitzpatrick ME. Forensic engineering: applying materials and mechanics principles to the investigation of product failures. Forensic Science, Medicine and Pathology. 2007;3(2):81-92

[4] Ahn SH, Montero M, Odell D, Roundy S, Wright PK. Anisotropic material properties of fused deposition modeling ABS. Rapid Prototyping Journal. 2002;8(4):248–257.

[5] Seifi M, Salem A, Beuth J, Harrysson O, Lewandowski JJ. Overview of materials qualification needs for metal additive manufacturing. JOM. 2016;68(3):747–764.

[6] Ziemian S, Sharma M, Ziemian C. Anisotropic mechanical properties of ABS parts fabricated by fused deposition modelling. In: Mechanical Engineering and Mechatronics. Springer; 2012.

3D Printed Porous Filters for Sustainable Water Treatment Applications

Nikola Kotorčević[1], Dušan Milojević[1], Fatima Živić[1]

[1] *Faculty of Engineering, University of Kragujevac, Serbia*

nikola.kotorcevic@uni.kg.ac.rs, ORCID: 0000-0002-5664-9832, dusanmilojevic.kg@gmail.com, ORCID: 0009-0005-0113-3918, zivic@kg.ac.rs, ORCID: 0000-0003-2509-187X

Corresponding author: nikola.kotorcevic@uni.kg.ac.rs

Abstract

This paper briefly review research on 3D printed filters for fluid filtration focusing on water treatment. Growing global demand for clean water and increasing contamination from industrial and environmental sources demands innovative, efficient, and sustainable filtration solutions. FDM 3D printing enables the fabrication of filters with complex geometries and controlled porosity, allowing optimization of flow behavior and filtration efficiency. Copper-based composites and effects on adsorption, antimicrobial, and mechanical properties are discussed, with case study of FDM 3D printed copper filters. The paper also highlights the role of computational modeling, specifically the Lattice Boltzmann Method (LBM), in simulating fluid flow through porous media to accelerate filter design and reduce experimental effort. Results indicate that 3D-printed filters offer cost-effective, customizable, and reusable solutions with significant potential for improving water purification technologies and supporting sustainable water management goals.

Keywords: Water Filter; FDM 3D printing; Lattice Boltzmann Method; UN SDG 6; UN SDG 3; UN SDG 12

1. Introduction

Fresh drinking water is rapidly becoming high-value commodity, due to increasing pollution worldwide [1], [2]. Natural contaminants (e.g., heavy metals, hydrocarbons) enter water via underground rocks, rain, or dust, while artificial ones (plastics, petrochemicals, pesticides) originate from wastewater. Water pollutants are classified as organic (pesticides, dyes, polyfluoroalkyl), inorganic (nitrate, heavy metal ions, halogens), emerging pollutants (pharmaceuticals, artificial sweeteners, surfactants), pathogens (parasites, viruses, bacteria), and radioactive pollutants [1]. Industrial sectors use around 20% of total global freshwater, of which 25% is for manufacturing processes, while 75% is used for energy production [3]. With limited water resources and a growing need for water, water treatment methods are becoming necessity.

2. Water filtration

Methods for water treatment are classified as chemical methods (ion exchange, solvent extraction, adsorption, neutralization, electrochemical oxidation, photodegradation, chemical precipitation), physical methods (sedimentation, distillation, membrane filtration) and biological treatment [1]. Two major categories of physical

separation technology are filtration and sedimentation. Filtration usually requires a pressure difference across the filter medium. Sedimentation depends on the differences in density between the suspended particle and the suspending fluid, using gravity or centrifugal force. Membrane-based methods are commonly cost-effective, including reverse osmosis (RO), ultrafiltration (UF), microfiltration (MF) and activated carbon filtration (ACF) [2]. Different filter fabrication methods exist whereas additive technologies enable complex shapes and tailored porosity for specific filtration uses.

3. Application of 3D printing in filtration

3D printing technologies have been used to create devices for various pollutant removal methods in water remediation, including photodegradation, catalysis, biocatalysis, adsorption, extraction, and bioremediation [4]. In environmental remediation, these technologies have been implemented in different water treatment processes such as desalination, separation, filtration, and heavy metal removal. 3D printing of metallic materials such as copper (Cu) has enabled cost effective solutions of filtration structures.

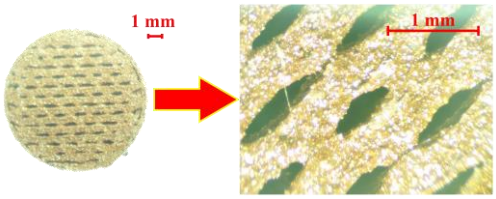


Figure 1. Cu/PLA filter fabricated by FDM 3D printing

Case example of Cu/PLA filter fabricated by FDM 3D printing is shown in Figure 1. Composite filament made of 95% copper and 5% polylactic acid (PLA) was tested in different settings of FDM 3D printing to achieve desired micro-porosity [5]. PLA/GO filters made via FDM were tested and showed that higher infill improved removal up to ~60%, after which reduced pore space limited mass transfer [6]. Studies indicate that amending porous media with copper and silver nanoparticles can create effective antimicrobial filters [7]. Silver and copper can also be used for metallic filter layers [8]. PLA scaffolds coated with Cu/Cu_2O nanoparticles effectively adsorb radioactive iodide in water across pH 3–9 [9]. Experimental design of filter structures from novel materials requires tedious trial-and-error approach where computational models, related to fluid behavior during flow through porous media, can significantly shorten the development time.

4. Simulation of Fluid Flow in Porous Structures using Lattice Boltzmann Method (LBM)

The velocity fields in porous media can be simulated using Direct Numerical Simulation (DNS), which is computationally demanding. DNS is typically implemented with the Lattice Boltzmann Method (LBM), finite volume, or finite element methods [10]. LBM is a computational fluid dynamics method well suited for simulating fluid flow in complex geometries, such as pore-scale porous media. It is effective for multiphase flows due to its simplicity and accuracy in handling irregular paths, fluid–fluid interfaces, and fluid–solid interactions. Since its introduction in 1989, LBM has been widely applied to porous media flows [11].

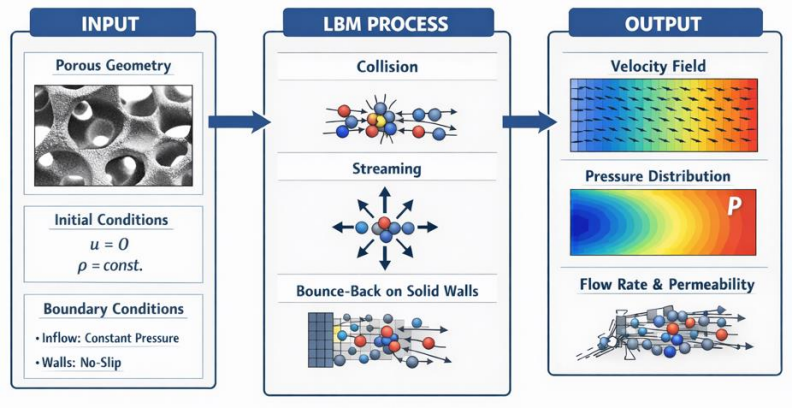


Figure 2. Schematic illustration of the Lattice Boltzmann Method (LBM) workflow

Schematic illustration of the LBM workflow for fluid flow simulation in porous media, from geometry input to velocity and pressure outputs used to estimate permeability via Darcy's law is shown in Figure 2.

5. Conclusions

Water filters are becoming a necessary part of industrial and home systems. Various technologies and materials for filter fabrication have enabled specific solutions, but additive technologies can produce low-cost filters with antibacterial properties, such as with copper-based materials for antibacterial properties. FDM 3D-printed copper-based filters offer several benefits for water filtration, including customizable design through complex geometries and controlled porosity that can be tailored to optimize flow rates and maximize surface area for filtration. Copper naturally inhibits bacterial growth, reducing biofouling and enhancing water safety. Durability is enhanced since copper is corrosion-resistant and mechanically strong, providing long-lasting filter performance. Copper surfaces can adsorb heavy metals and certain contaminants, improving water purification and enhancing adsorption. FDM printing allows fast, cost-effective production and testing of different filter designs and fluid flow behaviour. Filters can often be cleaned and reused, making them more sustainable than single-use options.

Acknowledgements

This paper is supported through the EIT's Higher Education Initiative A-SIDE projects, coordinated by EIT RawMaterials, funded by the European Union and supported by the project No. 451-03-34/2026-03/200107, Ministry of Science, Technological Development and Innovation, Republic of Serbia.

References

1. Heidari G, Kordbacheh F. Pollutants and Approaches for their Removal from Water. Mater Chem Horiz. 2023 Jul;(Online First). doi:10.22128/mch.2023.684.1039

2. Aziz S, Mazhar AR, Ubaid A, Shah SMH, Riaz Y, Talha T, Jung DW. A comprehensive review of membrane-based water filtration techniques. Appl Water Sci. 2024 Aug;14(8):169. doi:10.1007/s13201-024-02226-y

3. Norman A, Mursyid QIBMA, Chong CH, Cheah KH, Ramarad S, Yap TC, Wong VL. Pioneering clean water solutions: How cutting-edge resin-based 3D printing is driving sustainable remediation. Sustain Mater Technol. 2025 Oct;45:e01525. doi:10.1016/j.susmat.2025.e01525

4. Scaffaro R, Mistretta MC, Balsamo M. Innovative 3D-printed devices for water pollutant removal: Comprehensive review on printing parameters, composition, properties and performances of the latest 3D-systems. Polym Test. 2024 Nov;140:108627. doi:10.1016/j.polymertesting.2024.108627

5. Kotorčević N, Milenković S, Živić F, Jordović B, Adamović D, Todorović P, Grujović N. Material Extrusion 3D Printing of Micro-Porous Copper-Based Structure for Water Filters. Machines. 2024 Jul 12;12(7):470. doi:10.3390/machines12070470

6. Won G, Park SS, Park Y, Ko SO, Kim B, Hwang Y. Influence of internal structure on the adsorption performance of 3D-printed polylactic acid filters with graphene oxide for water treatment. J Mater Res Technol. 2026 Mar;41:435–43. doi:10.1016/j.jmrt.2025.12.002

7. Meegahakumbura S, Chandrasena GI, McCarthy DT, Deletic A, Li Y. Advancing biofilter resilience: Stability of copper-zeolite antimicrobial filter media under realistic stormwater and operational conditions. J Water Process Eng. 2026 Feb;82:109513. doi:10.1016/j.jwpe.2026.109513

8. Melo LGTC, De Menezes FD, Peixoto Da Costa JÂ, Silva KDM, Chiang YW, Santos RM. Fabrication of copper- and silver-coated triply periodic minimal surface structures through 3D printing, electroplating and electroless processes. Surf Interfaces. 2025 Jul;69:106771. doi:10.1016/j.surfin.2025.106771

9. Kim B, Park Y, Kim HW, Kim JA, Hwang Y. Enhanced iodide removal from aqueous solutions using 3D-printed PLA scaffold coated with Cu/Cu2O nanoparticles. Environ Res. 2025 Aug;279:121835. doi:10.1016/j.envres.2025.121835

10. Yang G, Xu R, Tian Y, Guo S, Wu J, Chu X. Data-driven methods for flow and transport in porous media: A review. Int J Heat Mass Transf. 2024 Dec;235:126149. doi:10.1016/j.ijheatmasstransfer.2024.126149

11. Ghassemi A, Pak A. Numerical study of factors influencing relative permeabilities of two immiscible fluids flowing through porous media using lattice Boltzmann method. J Pet Sci Eng. 2011 Apr;77(1):135–45. doi:10.1016/j.petrol.2011.02.007

Comparing 3D-printed Part Mesh Design Techniques for Thermoforming

Živana Jovanović Pešić[1], Strahinja Milenković[2], Nenad Petrović[3], Nenad Marjanović[3], Vesna Marjanović[3]

[1]*Department of Production Engineering, Faculty of Engineering, University of Kragujevac, Kragujevac, Serbia, zixi90@gmail.com , 0000-0002-1373-0040,*

[2]*Institute for Information Technologies Kragujevac, University of Kragujevac, Kragujevac, Serbia, strahinja.milenkovic@kg.ac.rs , 0000-0002-5822-4846,*

[3]*Department of Mechanical Constructions and Mechanization, Faculty of Engineering, University of Kragujevac, Kragujevac, Serbia, npetrovic@kg.ac.rs , 0000-0002-7563-9883, nesam@kg.ac.rs, 0000-0002-8441-4328, vmarjanovic@kg.ac.rs, 0000-0001-6266-5540*

Corresponding author: vmarjanovic@kg.ac.rs

Abstract

This research presents a comparison of mesh design techniques for thermoforming 3D-printed parts produced by fused deposition modeling (FDM). The study considers two different approaches to mesh design intended for thermoforming. The first method uses the infill option in the slicing software of a solid wafer without top and bottom layers as the basis for creating the mesh geometry, and the second method uses a mesh designed as the part with mesh features is designed to have the same geometry as the slicer-created model, which will be printed only as walls. The resulting models with two different mesh infill settings will be examined for mass, filament length used, and printing time. These results will be compared with the measured parameters of the 3D-printed parts to determine which method produces more accurate results in practice than the theoretical values calculated by the slicing software. For the purposes of the experiment, a commercially available 3D printer was used with PLA filament.

Keywords: 3D-printing; thermoforming; PLA; FDM; meshing; 'UN SDG 9';

1. Introduction

The wide adoption of 3D printing in both industry and the hobby sector has created a large community of enthusiasts willing to experiment with different 3D printing techniques to meet various design specifications and produce parts that would be impossible to create with conventional manufacturing. In recent years, researchers have developed various FDM printing techniques that have removed or significantly reduced some of the process's inherent drawbacks for specific applications. In [1], researchers further developed non-planar printing, which enables improved surface finishes on curved layers where curvature extends across the X-, Y-, and Z-axes. This is particularly useful for shapes such as aerofoils, where the surface finish directly influences part performance. Aside from surface finish, research on non-planar printing offers other benefits, such as increased printable overhangs without the need for additional supports. This has been presented in [2] with unconventional printing materials, where the authors experimented with printing clay, and in [3] by Wüthrich et al., who used PLA filaments. Other authors, such as [4–6], analyzed the practical implementation of 3D-printed geometries intended for use with off-the-shelf metal components. More recently, infill structures and

their properties have been gaining more attention in published research. Factors affecting the mechanical performance of PLA printed parts were studied in [7]. In [8], the authors tested the effects of infill on the mechanical properties of 3D printed parts. Kang et al. [9] tested various failure modes of various infill meshes.

The ability to create complex shapes with internal features has expanded the possibilities for engineers in prototyping and low-volume production. This paper aims to determine whether using infill as a mesh for thermoforming is a viable alternative to creating mesh features in the CAD model.

2. Materials and Methods

For the purposes of this research, parts intended for thermoforming of 3D-printed meshed wafers were designed in different ways to assess the physical differences expected based on the meshing method and mesh resolution. The experiment consists of two different meshing methods applied to circular wafers made according to Figure 1. The first method was to create meshed wafers from a full section. STL models using the Bambu Studio V2.5.0.66 properties to achieve a grid. For disk 1, the grid pattern infill was set to 20% infill, and for disk 2, to 40% infill, in the Ø62 segment of the wafer. The top and bottom layers were set to zero in order to expose the mesh. The second method used was to use the sliced geometry to trace the part in CAD software and convert the traced part into a .STL file with the mesh already included in the part. To preserve the complete infill of the lip around the mesh, the slicer was set to a 10-wall count for all models, ensuring the outer ring was fully filled. Print resolution was set to 0.2 mm and infill direction to 45°. The result of slicing is that both models have the same structure along the lip of the part; the only difference is that the infill method will print the mesh as infill, and the feature method will print it as walls.

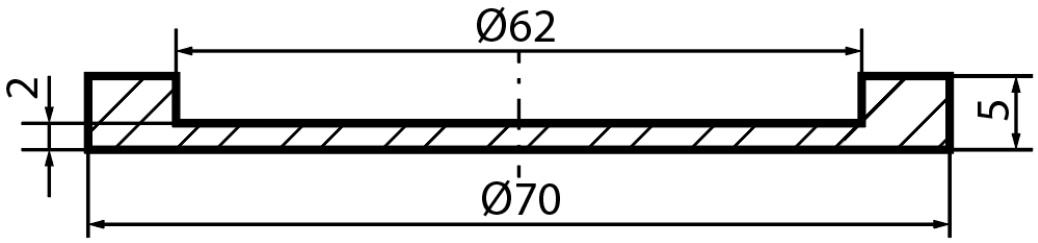
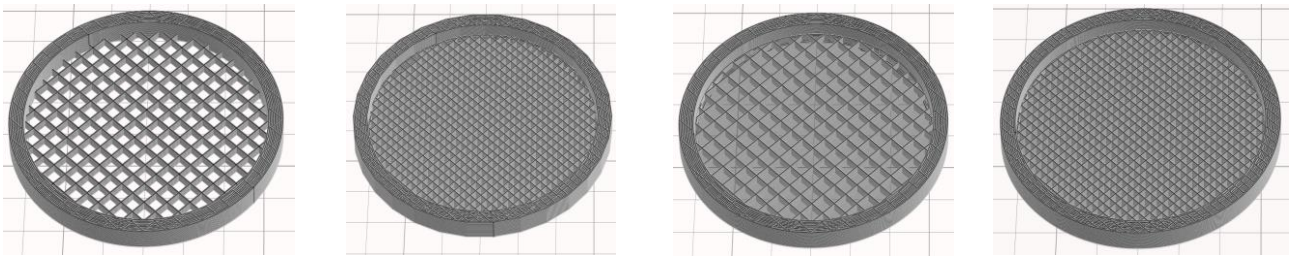


Figure 1. Wafer cross-section dimensions.

All parts were printed on a Bambu Lab H2S AMS Combo using AzureFilm white PLA filament, with the speed and acceleration settings in the Bambu Studio V2.5.0.66 slicing software set to their default values. All four models were weighed after printing using a highly precise digital analytical balance (Kern AET-200) to compare results.

3. Results

The sliced files are shown in Figure 2, where models a and b are the models meshed in CAD as features with 20% and 40% surface meshing, respectively. Models c and d are meshed in the slicer as infill with 20% and 40% infill, respectively. CAD models with mesh features were traced from sliced parts and checked to insure the same thicknesses of the mesh as in the infill generated models.



a) b) c) d)

Figure 2. Sliced models using features a) and b), and using infill c) and d)

Measurements were conducted shortly after printing, and all samples were stored in vacuum bags to reduce variation due to moisture. Figure 3 shows the measurement process on the 40% infill wafer using the digital analytical balance (Kern AET-200) and the printed samples.

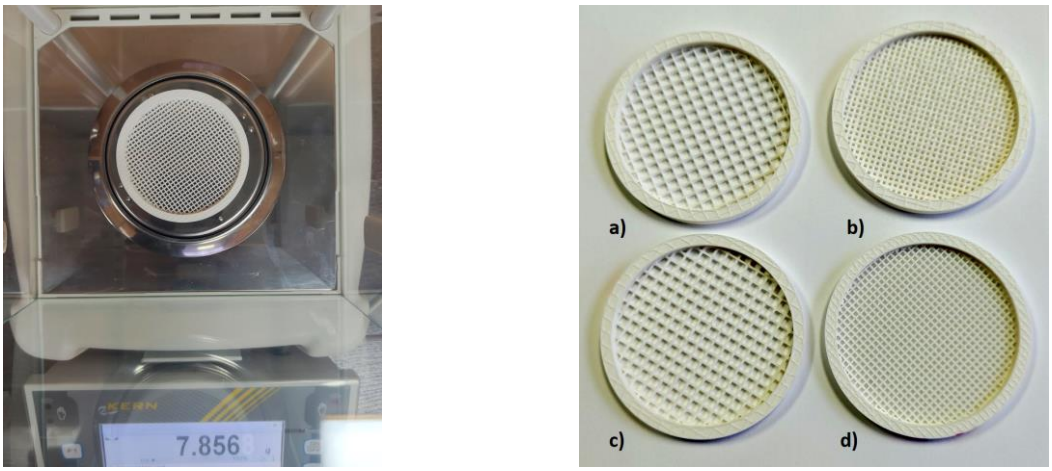


Figure 3. Weight measurement on the Kern AET-200 (left) and all the printed samples (right)

The parts were printed one at a time to measure the print time for each infill type. Table 1 shows the results of the filament length used, the estimated weight, the total print time, and the weight measured after printing. Preparation time for all prints was 6 minutes and 30 seconds, which was added to the print time to get the total print time.

Table 1. Model results

Model	Filament length	Estimated weight [g]	Total time	Measured weight [g]
a	2.55	7.60	34m20s	7.446
b	3.38	10.09	1h6m	9.819
c	2.17	6.46	17m9s	6.319
d	2.68	7.98	19m39s	7.856

4. Conclusions

The difference between the measured weights and the slicer estimates is ~1.5% to ~2.7%, with measured parts always being lighter than estimated. This could be due to slight under-extrusion or due to a slightly lower

filament density. The results show a drastic decrease in print time of 50.05% for the 20% infill model and 70.25% for the 40% infill model compared to their feature (CAD modeled mesh) counterparts. A slight decrease of 15.14% in measured weight can be seen when using the 20% infill model, and a 20% decrease using the 40% infill model compared to their feature counterparts. The increase in weight is also apparent visually, with the mesh being denser on the meshes created as features. This correlates with infill generally being printed thinner than walls. The study concludes that using infill without top and bottom layers can be a viable alternative to modeling meshes when applicable. The time saved both in the modeling and printing phases is sufficient to recommend its use over creating meshes as model features. The thinner mesh should also make thermoforming easier.

Acknowledgements

This paper is the result of research conducted under the authors' scientific research work agreement contracts no. 451-03-34/2026-03/200107, and 451-03-33/2026-03/200378.

References

[1] Maity M, Das S, Kumar R, Mondal JK. Experimental Investigation for Enhancing Surface Quality in 3D Printing Process Using Non-planar Layer Method. In: Kumar A, Zunaid M, Subramanian KA, Lim H, editors. Recent Advances in Manufacturing and Thermal Engineering, Singapore: Springer Nature Singapore; 2023, p. 191–200. https://doi.org/10.1007/978-981-19-8517-1_14.

[2] Vele J, Achten H. Clay Non-Planar Printing of Overhangs, Bialystok University of Technology, Poland: Bialystok University of Technology, Poland; 2023.

[3] Wüthrich M, Gubser M, Elspass WJ, Jaeger C. A Novel Slicing Strategy to Print Overhangs without Support Material. Applied Sciences 2021;11:8760. https://doi.org/10.3390/app11188760.

[4] INFLUENCE OF PRESS-FIT DIMENSIONS ON REPEATED ASSEMBLY OF BALL BEARINGS INTO 3D PRINTED HOUSINGS. Proceedings - 19th International Conference on Tribology - SERBIATRIB '25, Faculty of Engineering University of Kragujevac, Serbia; 2025. https://doi.org/10.24874/ST.25.205.

[5] Palic S, Petrovic N, Palic N, Milenkovic S, Pesic ZJ. Using Experimental Results to Determine Calculation Parameters for Press Fitting Ball Bearings into 3D Printed Parts. In: Rackov M, Miltenović A, Banić M, editors. Machine and Industrial Design in Mechanical Engineering, vol. 174, Cham: Springer Nature Switzerland; 2025, p. 92–101. https://doi.org/10.1007/978-3-031-80512-7_9.

[6] Petrović N, Milenković S, Pešić ŽJ, Kostić N, Marijanović N. DETERMINING 3D PRINTED HOUSING DIAMETERS FOR PRESS-FITTING STANDARD BALL BEARINGS, Kragujevac, Serbia: Faculty of Engineering University of Kragujevac, Serbia; 2024.

[7] Saefudin S, Samsudi Raharjo, Ilham Yustar Afif, Syarifudin, Purnomo, Muhammad Omar Rusydi, et al. A Review of Factors Affecting the Mechanical Performance of PLA in FDM 3D Printing. ASSET 2025;7:0250208. https://doi.org/10.26877/chs1gc62.

[8] Muhammet DAĞLI, Elif GÜDEN, Ahmet DEMİRER, Esra YUMAT. Effect of Infill Pattern on Mechanical Properties of PLA-Based Structures in 3D Printing. 7th International Conference on Engineering Technology and Applied Sciences, Afyon Kocatepe University; 2024.

[9] Kang Y, Liu T, Tian X, Li H, Zhang H, Li Y, et al. Spider web-inspired continuous fibre floating 3D printing for large lightweight mesh structures. Virtual and Physical Prototyping 2025;20:e2546676. https://doi.org/10.1080/17452759.2025.2546676.

Advanced Materials, Microstructure, and Functional Materials

Microstructural Engineering and Mechanical Behavior of KNN and KNN-Ta Ceramics Sintered by Spark Plasma Sintering

Jade Clément[1], Isabelle Monot-Laffez[1], Micka Bah[1], Caroline Richard[1]

[1] Greman UMR CNRS 7347, Université de Tours, INSA Centre-Val-de-Loire, 37200, Tours, France, jade.clement@univ-tours.fr, 0009-0003-6604-7848, isabelle.monot-laffez@univ-tours.fr, 0000-0003-0716-0827, micka.bah@univ-tours.fr, 0000-0001-6636-2854, caroline.richard@univ-tours.fr, 0000-0002-8375-8241

Corresponding author: jade.clement@univ-tours.fr

Abstract

To comply with European Union directives aiming to ban lead in electronic devices, researchers are seeking alternatives to the widely used **Lead Zirconate Titanate (PZT)**. The **$(K,Na)NbO_3$ (KNN)** system is a primary candidate, but its industrial adoption is hindered by a lack of data regarding its mechanical behavior and scaling challenges. This study specifically investigates the microstructural engineering and mechanical properties of **KNN** and tantalum-doped **KNN-Ta** ceramics.

Keywords: Microhardness, Spark plasma sintering, Lead free, KNN, UN SDG-9

1. Introduction: The Search for Lead Free Alternatives

The industrial market for piezoelectric materials—essential for sensors, actuators, and transducers—has long been dominated by **Lead Zirconate Titanate (PZT)** [1]. However, due to the toxicity of lead, European directives such as **RoHS** and **REACH** have mandated the banishment of lead-based ceramics.

Among the various candidates, the $(K,Na)NbO_3$ (**KNN**) system is the most promising due to its:

- High Curie temperature (>400°C).
- Lower theoretical density compared to PZT.
- Tunable piezoelectric properties via chemical doping (e.g., Li, Ta, Sb).

Despite its potential, KNN faces two major industrial hurdles: the **volatilization of alkali elements** during high-temperature sintering and a **significant lack of mechanical data**, which is crucial for device reliability.

2. Materials and Methods

2.1Powder Synthesis

Two types of powders were prepared using a conventional solid-state reaction:

1. **Pure KNN**: $K_{0.5}Na_{0.5}NbO_3$.
2. **KNN-Ta**: $K_{0.5}Na_{0.5}Nb_{0.85}Ta_{0.15}O_3$ (where 15% of Niobium is substituted by Tantalum). The raw materials (K_2CO_3,Na_2CO_3,Nb_2O_5,Ta_2O_5) were milled and calcined at 830°C to achieve a narrow particle size distribution centered around **0.65 µm**.

2.2 Sintering Techniques Compared

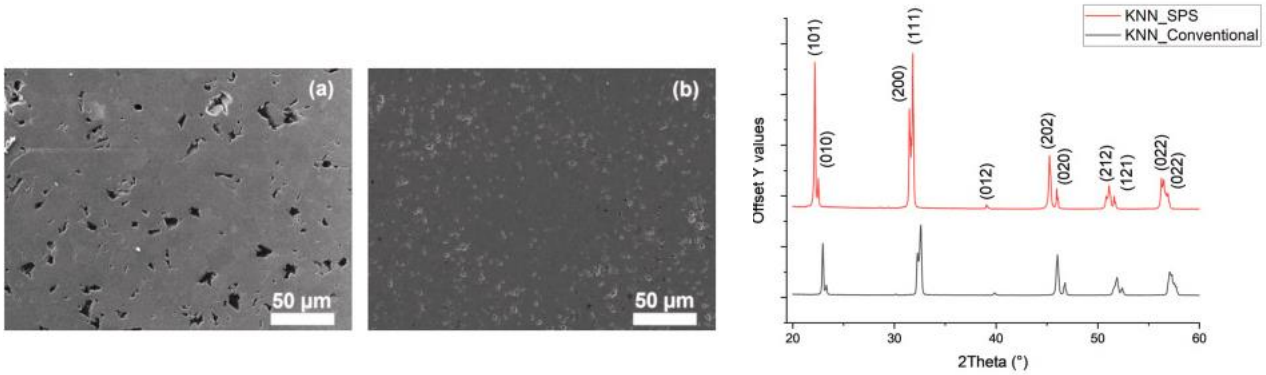
The study contrasts two primary methods:

- **Conventional Sintering (CS)**: Sintered at 1120°C–1150°C for long durations (up to 48h). This resulted in low relative densities (**75–89%**) due to the difficulty of densifying KNN without sintering aids.
- **Spark Plasma Sintering (SPS)**: Utilizes high DC pulse current and uniaxial pressure (50MPa) at lower temperatures (930°C–985°C) over very short cycles (2–5 min). This technique achieved high relative densities (**up to 98%**) and minimized alkali loss.

3. Results: Microstructural Results and Observations

3.1 The Advantage of SPS

The SPS process proves superior in managing the competition between densification and grain growth. While conventional sintering produces large grains (~7.6 µm) and significant porosity, SPS results in a dense, homogeneous microstructure with grain sizes ranging from **1 to 3.5 µm**. Figure 1 shows SEM micrographs and XRD patterns.



c)

Figure 1. SEM micrographs of KNN sintered by conventional sintering at 1120 °C/10h (a) and sintered by spark plasma sintering at 930 °C/2.5 min (b) -XRD patterns of KNN ceramics sintered by spark plasma sintering (red) and conventional route (black) (c)

3.2 The Role of Tantalum (Ta) Doping

Tantalum acts as a **grain growth inhibitor**.

- **Composite Microstructure**: KNN-Ta samples exhibit a "composite" look under Back-Scattered Electron (BSE) imaging, showing Ta-rich light inclusions within a stoichiometric matrix.

- **Grain Refinement**: The average grain size decreased from 3 µm in pure KNN to **1 µm** in KNN-Ta, further enhancing the material's density

3.3 Mechanical Characterization: Microhardness

The study evaluated microhardness (H) using instrumented indentation at a 10N load. Figure 2 shows examples of microindentation of KNN-Ta versus different conditions of sintering.

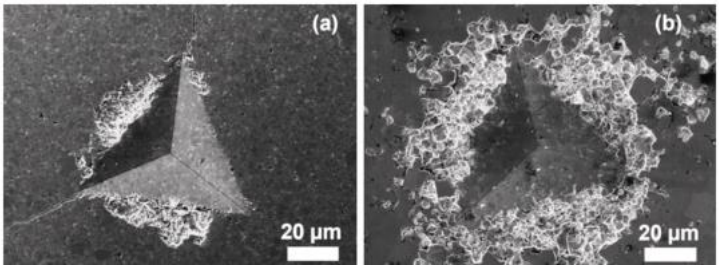


Figure 2. Indentations impressions at 10N load for KNN-Ta sintered at 985 °C/3 min (a) and KNN sintered at 930 °C/2 min (b).

The results highlight two primary "driving forces" for mechanical strength:

3.3.1. Densification and Porosity

For ceramics with relative densities below 90%, the hardness remains low (~0.7 GPa) regardless of the sintering method. However, as density exceeds 90% via SPS, hardness increases exponentially. This follows the empirical relationship: $H=H_0\exp(-bP)$ where P is porosity. Reducing pores (which act as stress concentrators) significantly strengthens the ceramic matrix [2].

3.3.2 The Hall-Petch Effect (Grain Size)

In highly dense samples (>92%), the grain size becomes the dominant factor. The relationship follows the Hall-Petch equation: $H=H_0+kd^{-1/2}$ where H is the microhardness, H_0 the intrinsic grain microhardness, k the Hall–Petch constant, that is a material-specific strengthening coefficient, and d the average grain size [3].

Smaller grains result in a higher density of grain boundaries. These boundaries act as barriers to dislocation motion (the "pile-up" effect), thereby increasing the stress required for plastic deformation and raising the hardness. Table 1 shows comparative hardness data [4].

Table 1. Comparative Hardness Data

Materials	Sintering Method	Density	Grain Size	Hardness
KNN	Conventionnal	89 %	7.6 µm	1.79 GPa
KNN	SPS	94%	2.2 µm	2.38 GPa
KNN-Ta	SPS	98%	1.0µm	3.11 GPa

4. Conclusions

The study proves that **Spark Plasma Sintering (SPS)** is an effective technique for producing high-quality, homogeneous KNN ceramics. It consistently achieves high densification (up to **98%**) while allowing precise control over grain size distribution. The improvement in the material's hardness is attributed to two main factors [5]:

- **Densification:** This is the primary driver for ceramics with relative densities up to 90%.
- **Grain Size Reduction:** In highly dense ceramics (>90%), reducing the grain size further boosts hardness.

Doping KNN with Tantalum (KNN-Ta) creates a composite microstructure that further refines grain size and increases density. This chemical modification resulted in:

- A **25% increase** in microhardness compared to pure KNN.
- A peak hardness of **3.11 GPa** in 98% dense samples.

By combining specific sintering parameters with chemical design, this study provides a roadmap for engineering high-performance **lead-free piezoelectric ceramics**. These mechanical improvements are a vital step toward replacing lead-based materials in industrial applications.

Acknowledgements

This research did not receive any specific grant from funding agencies in the public, commercial, or not-for-profit sectors

References

1. Saito Y, Takao H, Tani T, Nonoyama T, Takatori K, Homma T, Nagaya T, Nakamura M, Lead-free piezoceramics, Nature. 2004 ; 432 :84-87, 10.1038/nature03028
2. Rice R. W, Mechanical Properties of Ceramics and Composites: Grain and Particle Effects, CRC Press, New York.2000, 10.1201/9780203908471
3. Armstrong R.W, Engineering science aspects of the hall–petch relation, Acta Mech. 2014 ; 225 :1013-1028, 10.1007/s00707-013-1048-2
4. G.M. Pharr, E.G. Herbert, Y. Gao, The indentation size effect: a critical examination of experimental observations and mechanistic interprétations,Annu. Rev. Mater. Res. 2010 ;40 :271-292, 10.1146/annurev-matsci-070909-104456
5. Clément J, Richard C, Monot-Laffez I, Design and mechanical charecterization of lead-free piezoelectric ceramics, Ceramics International. (2025) ; 51 :36014-36021,10.1016/J.ceramint.2025.05.322.

Solid lubricant coatings based on chromium nitride and metal sulfide deposited by reactive magnetron sputtering

Rubenson Mareus[1,2], Amaël Caillard[2], Caroline Richard[1], Anne-Lise Thomann[2], Loïc Gimenez[2]

[1]Greman UMR CNRS 7347, University of Tours, Tours, France, mareusrubenson@yahoo.fr, caroline.richard@univ-tours.fr, 0000-0002-8375-8241
[2]Gremi UMR CNRS 7344, Université d'Orléans, Orléans, France, amael.caillard@univ-orleans.fr, 0000-0001-9540-1381, anne-lise.thomann@univ-orleans.fr, 0000-0002-8524-9694, loic.gimenez@univ-orleans.fr,

Corresponding author: mareusrubenson@yahoo.fr

Abstract

The development of solid lubricant coatings capable of operating under severe contact conditions remains a major challenge in tribological engineering. In this study, chromium nitride (CrN)-based WS_2-containing nanocomposite coatings were deposited by reactive magnetron sputtering to combine high load-bearing capacity with low shear strength. The influence of the coating architecture on the structural and tribological properties was systematically investigated.

The incorporation of WS_2 significantly reduced the coefficient of friction compared with monolithic CrN, while maintaining adequate hardness and adhesion. The tribological performance strongly depended on the coating architecture, particularly on the distribution and content of the WS_2 phase within the CrN matrix. A synergistic effect between the hard CrN and lubricious WS_2 phases led to improved wear resistance under sliding conditions. These results highlight the importance of coating architectural design in optimizing the performance of CrN-based solid lubricant coatings for demanding applications.

Keywords: ***magnetron sputtering, solid lubricant coating, sulfide, chromium nitride, mechanical and tribological,*** *UN SDG 7, UN SDG 9.*

1. Introduction

Efficient control of friction and wear remains a primary challenge in engineering, particularly in environments where conventional liquid lubricants fail [1]. This study investigates the development of chromium nitride (CrN)-based nanocomposite coatings integrated with metal sulfide solid lubricants (WS_2) to address the trade-off between mechanical durability and low-friction performance. While CrN offers superior hardness and thermal stability, its relatively high coefficient of friction limits its utility in sliding contacts. Conversely, lamellar metal sulfides provide excellent lubrication but lack sufficient load-bearing capacity.

Using reactive magnetron sputtering, this research systematically evaluates the influence of coating composition and microstructure to harness the synergistic effects of these materials. The study specifically focuses on the role of the distribution and content of the lubricating phases (WS_2) within the CrN matrix on the governing tribological mechanisms. By providing a direct comparative analysis of WS_2 within identical CrN-based systems, this work elucidates how coating architecture influences the structural, mechanical, and wear behavior of high-performance protective surfaces.

2. Materials and Methods

In this study, CrN and $CrNW_xS_y$ nanocomposite coatings were fabricated using DC reactive magnetron sputtering at room temperature. The process employed Si (100) and AISI 440A stainless steel substrates, which were prepared by ultrasonic cleaning followed by a 30-minute argon ion bombardment at −400 V at low pressure to ensure surface purity. To enhance adhesion, a pure chromium interlayer was first deposited, followed by the functional coatings obtained by co-sputtering Cr and WS_2 targets in an Ar/N_2 atmosphere. All depositions were carried by simultaneously sputtering two facing targets: 4 inches Cr target and 2 inches WS_2 target, both being powered using DC supply (200 and <100 W respectively) under a gas mixture of Ar/N2 (20/15 sccm) at a pressure of 0.5 Pa and floating potential (0 V) and room temperature to optimize stoichiometry and structural properties.

The structural and tribological properties of the resulting CrN and $CrNW_xS_y$ coatings were characterized using a multi-analytical approach. Surface morphology and cross-sectional thickness were examined by scanning electron microscope (SEM) operating at 10 kV, while elemental composition and phase identification were determined by energy dispersive X-ray spectroscopy (EDS) and X-ray diffraction (XRD, Cu Kα radiation). Surface topography and nanoscale roughness were further analyzed using atomic force microscopy (AFM) in tapping mode. Tribological performance was evaluated using a High-Frequency Reciprocating Rig (HFRR) under dry sliding conditions (24∘C, 40% relative humidity) with a 9 N load (~1.5 GPa contact pressure), a 2 mm stroke, and a frequency of 50 Hz. Continuous monitoring of the coefficient of friction (COF) combined with post-test digital microscopy and stylus profilometry enabled the identification of of the dominant wear mechanisms.

3. Results

The microstructure of pure CrN deposited by reactive magnetron sputtering is typically characterized by:

- Columnar Growth**:** CrN naturally forms a dense, columnar grain structure. These columns grow perpendicular to the substrate and are often visible in cross-sectional SEM images.
- Microstructure: it typically adopts a face-centered cubic (fcc) NaCl-type structure. Depending on the nitrogen flow, it exhibits a preferred orientation—most commonly the (200) plane (high density) or the (111) plane (higher hardness).

Even if both target is facing each other with the rotating substrate between them, sulfide does not appear in a separate layer but is dispersed within the CrN matrix.

- Microstructure: XRD analysis reveal that $CrNW_xS_y$ coatings crystallized in the same structure as CrN, as no WS_2 peaks were observed. All cubic CrN peaks shift to lower angle indicated an increase of cell parameter due to the incorporation of W_xS_y species inside cell. Increasing too much the sulfide content can cause a transition from a crystalline/amorphous mixture to a fully amorphous-like structure, which can sometimes reduce hardness but significantly lower the friction coefficient.
- Grain Refinement: The presence of the sulfide phase during growth restricts the grain growth of the CrN, leading to a "nanocomposite" effect where the material remains extremely fine-grained.

- Composition: x and y does not exceed equal to few % to maintain the mechanical properties of CrN coating. Both x and y values are equal to 0.01 and 0.02 for 40 and 100 W powers applied on WS_2 target, respectively. x/y is close to 1.

  Figures 1 and 2 show the SEM cross sections and top view of CrN reference coatings and $CrWS_xN$ coatings and XRD analysis.

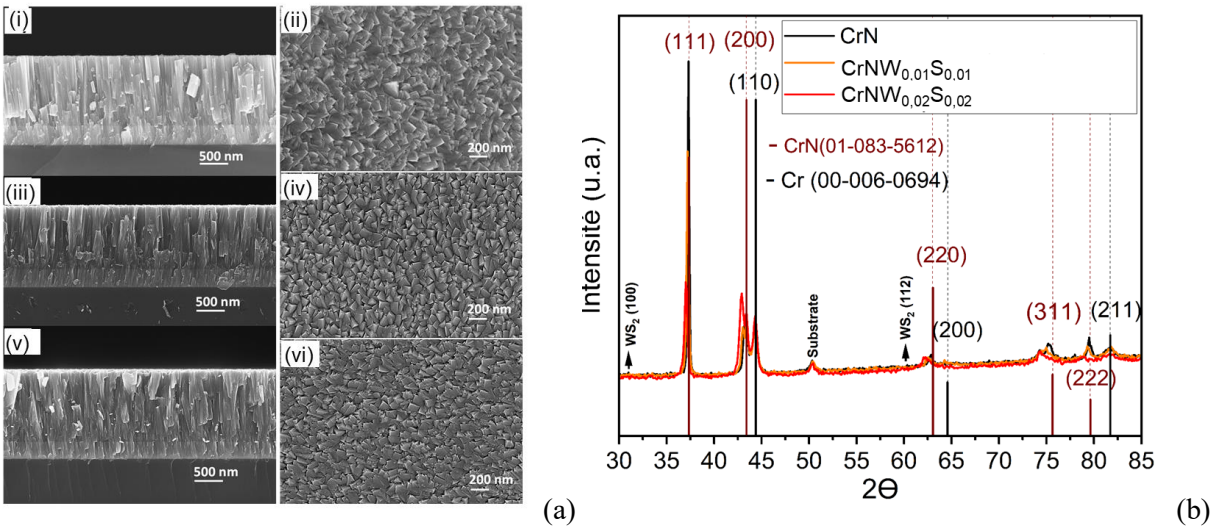
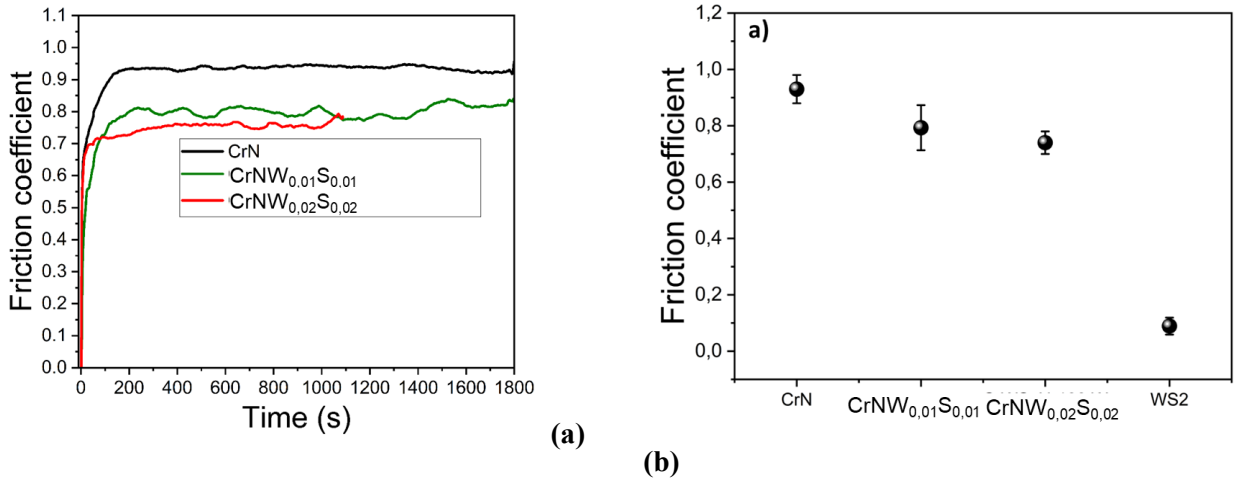


Figure 1. (a) (i, ii) Cross-section and top view of CrN reference coating; (iii, iv) of $CrNW_xS_y$ coating at 40 W on WS_2 target; (v , vi) of $CrNW_xS_y$ coating at 60 W on WS_2 target. (b) XRD patterns of CrN, $CrNW_{0.01}S_{0.01}$ (40 W) and $CrNW_{0.02}S_{0.02}$ (100 W) coatings.

The monolithic CrN served as the mechanical baseline. While it protects the substrate from deformation, its high friction leads to significant energy loss and eventual adhesive wear. By introducing WS_2, we sacrifice a small amount of absolute hardness to gain a massive reduction in the Coefficient of Friction (COF) (figure 3). The nanocomposite ($CrNW_xS_y$) approach is a "chemical/structural" solution. Because sulfide is distributed everywhere, there is no "waiting" for a layer to be exposed. This often results in a more immediate low-friction response, but if the sulfide content is too high, the CrN grains may lose their connectivity, leading to lower load-bearing capacity [2-4].



(a) (b)

Figure 3. Frictiograms of CrN and $CrNW_xS_y$ coatings (a) and average COF versus type of coatings (b).

Table 1 synthesizes the performance and structural characteristics of these three systems.

Table 1. Synthesis of Coating Architectures

Feature	Monolithic CrN	Nanocomposite $CrNW_xS_y$
Morphology and microstructure	Dense, columnar grains; cubic CrN.	Dense, columnar grains; cubic CrN with increase cell size
Load Bearing	Highest. The rigid lattice resists high contact pressures (~1.5 GPa).	Moderate/High. Depends on the volume fraction of the sulfide phase.
Friction (COF)	High (~0.9). Direct ceramic-to-metal contact leads to high shear resistance.	Lowest (Initial – 0.7-0.8). Homogeneous distribution of lubricant at the surface.
Wear Mechanism	Primarily abrasive. Hard particles or asperities cause surface gouging.	Tribofilm Formation. A continuous lubricating film forms on the wear track.

4. Conclusions

The nanocomposite design often emerges as a superior choice for tribological performance. It maintains the load-bearing capacity of CrN, while the dispersed W_xS_y phase provides effective lubrication. This type of coating is particularly well suited for precision applications where surface smoothness and a stable coefficient of friction (COF) from the very first sliding cycle are critical. The Cr interlayer and stoichiometric control act as the "glue" that enables this system to outperform monolithic CrN by preventing the premature delamination, a common limitation of solid lubricant coatings.

Acknowledgements

This work was financially supported by ARD Matex (Hycoat project) of Centre Val de Loire Region, France.

References

1. Grützmacher PG, Voevodin AA, Korényi-Both A, Righi MC, DellaCorte C, Bagcivan N, Erdemir A, Gatot C. The Promise of Solid Lubricants for a Sustainable Future. Adv Mater. 2026; 38. https://doi.org/10.1002/adma.202500867
2. Wang, G.; Jiang, Y.; Wang, X.; Guo, C. Review on the Mechanical Properties of Cr-N Coatings Prepared by Physical Vapor Deposition. *Coatings* 2026; *16*: 9. https://doi.org/10.3390/coatings16010009
3. Xiao-Ming He, N. Baker, B. A. Kehler, K. C. Walter, M. Nastasi, Y. Nakamura; Structure, hardness, and tribological properties of reactive magnetron sputtered chromium nitride films. *J. Vac. Sci. Technol. A* 1 2000; 18 (1): 30–36. https://doi.org/10.1116/1.582154
4. Semih Mahmut Aktarer, Yaşar Sert, Tevfik Küçükömeroğlu, Investigation of structural, hardness, adhesion, and tribological properties of CrN and AlCrN coatings deposited on cylinder liner. Materials & Design.2025; 253:113972 https://doi.org/10.1016/j.matdes.2025.113972

Electromagnetic Shielding of Biochar-Coated Drywall Panels: a Performance Overview from 1 to 27 GHz

Isabella Natali Sora[1], Giuseppe Ruscica[1], Patrizia Savi[2]

[1]Department of Engineering and Applied Sciences, Università degli Studi di Bergamo, 24044 Dalmine, Italy, isabella.natali-sora@unibg.it, https://orcid.org/0000-0001-8052-344X, giuseppe.ruscica@unibg.it, https://orcid.org/0000-0003-0447-9453

[2]Department of Electronic and Telecommunications, Politecnico di Torino, Torino, Italy, patrizia.savi@polito.it, https://orcid.org/0000-0001-9585-310X

Corresponding author: giuseppe.ruscica@unibg.it

Abstract

Electromagnetic pollution resulting from the proliferation of telecommunication systems requires the development of new shielding materials that can be integrated into the building envelope. This paper presents an overview of the results obtained using biochar, a sustainable and low-cost carbonaceous material, as a coating for common drywall panels. We analyze the fabrication methods and the shielding effectiveness (SE) performances tested in an anechoic chamber over a wide frequency spectrum (1-27 GHz). The results demonstrate that the application of biochar layers significantly increases the attenuation of drywall. For single-panel configurations, SE exceeds 27 dB in the frequency band 18-27 GHz, while the use of double-panel configurations allows for attenuation exceeding 46 dB. The proposed system stands out as an ecological, scalable, and easy-to-install solution for indoor electromagnetic protection.

Keywords: shielding effectiveness; biochar; sustainable building materials; drywall; electromagnetic interference; UN SDG 3; UN SDG 9; UN SDG 12.

1. Introduction

In recent years, the growing exposure to radiofrequency (RF) radiation due to modern wireless communication systems has raised the need for rigorous electromagnetic risk assessment and mitigation inside buildings [1]. With the advent of 5G and the exploration of sub-Terahertz and millimeter-wave (mmWave) networks, understanding and controlling wireless propagation and penetration in buildings has become a critical challenge for indoor environments [2]. Traditionally, shielding sensitive environments relies on metal sheets or meshes, which present disadvantages related to high weight, costs, susceptibility to corrosion, and difficulty of integration with standard building components.

Among modern alternatives, polymer and building composites reinforced with metal and carbon fillers have shown excellent electromagnetic interference (EMI) shielding properties [3]. Biochar, a solid product derived from the thermochemical conversion of biomass, stands out as an exceptional bioresource [4]. Characterized by

a high carbon content and tunable porosity, biochar emerges as a renewable, sustainable, and inexpensive material capable of replacing more costly and less eco-friendly carbon fillers. Building on these premises, this paper provides a summary of recent investigations focusing on a novel, highly practical application: the coating of commercial drywall panels with a biochar-based paste. We measured the shielding effectiveness (SE) of these eco-friendly panels at microwave frequencies (from 1 GHz up to 27 GHz) and for various structural configurations [5–7].

2. Materials and Methods

The reviewed studies utilized commercial biochar powder derived from wood and thermally treated at 750 °C [5,6]. To enable application, the biochar was mixed with a binder to create a dense paste [6,7]. This paste was overlaid on common drywall panels (1200 × 2000 × 10 mm), which were cut into tiles measuring 300 × 300 mm. The drywall panel alone is inherently transparent to microwaves. Depending on the number of applied layers (typically 2 to 5 layers), different biochar concentrations per unit area were achieved, reaching values up to 0.20 g/cm^2 [5,6]. X-ray Diffraction (XRD) analysis was performed to identify the phase composition of the biochar and to evaluate its crystallinity. Shielding Effectiveness (SE) measurements were performed at normal incidence inside a shielded anechoic chamber (4,6) by using two broadband double-ridge horn antennas connected to a Vector Network Analyzer (VNA) as shown in Fig. 2b. In addition to tests on single panels, a double-panel configuration, formed by joining two coated boards was investigated [5,6].

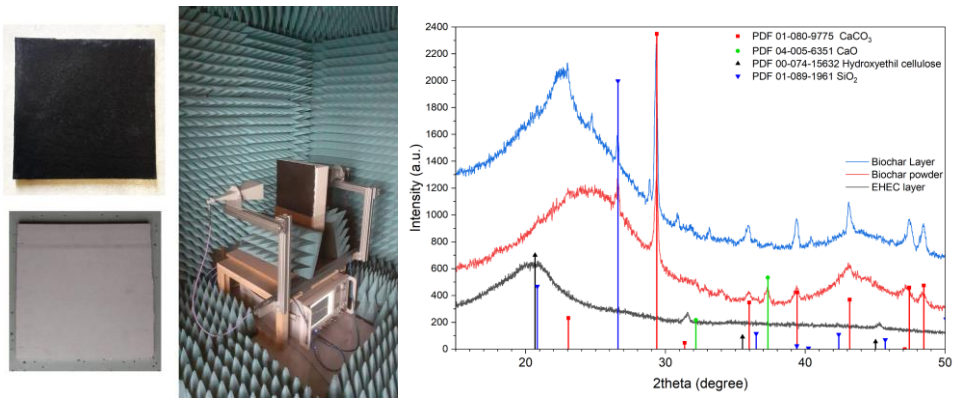


Figure 1. Left: An example of a drywall panel with and without biochar coating. Center: Measurement setup. Right: XRD pattern of EHEC, biochar powder, and biochar-containing layer [6], under CC BY 4.0 license.

3. Results

X-Ray Diffraction (XRD) is shown in Figure 1c. The powder is rather amorphous, with 65 wt% of amorphous fraction (mainly graphitic carbon). The main crystalline phases are as follows: in the biochar powder, calcite $CaCO_3$, quartz SiO_2, and lime CaO; in the EHEC powder, hydroxyethyl cellulose.

The addition of a biochar coating modifies the electromagnetic response of the drywall [5]. Initial measurement campaigns from 1 GHz to 18 GHz validated the signal attenuation capability of the biochar coating [7]. Increasing biochar density resulted in a proportional increase in SE, which remained stable [5]. At higher frequencies (18-27 GHz), the biochar coating maximizes its performance. At the highest tested load level (0.20

g/cm2), the SE on a single panel consistently exceeds 27 dB across the entire frequency band [6]. Combining two panels in a double panel configuration (see Fig. 3) yields a dramatic increase in SE, exceeding 46 dB over the band [6].

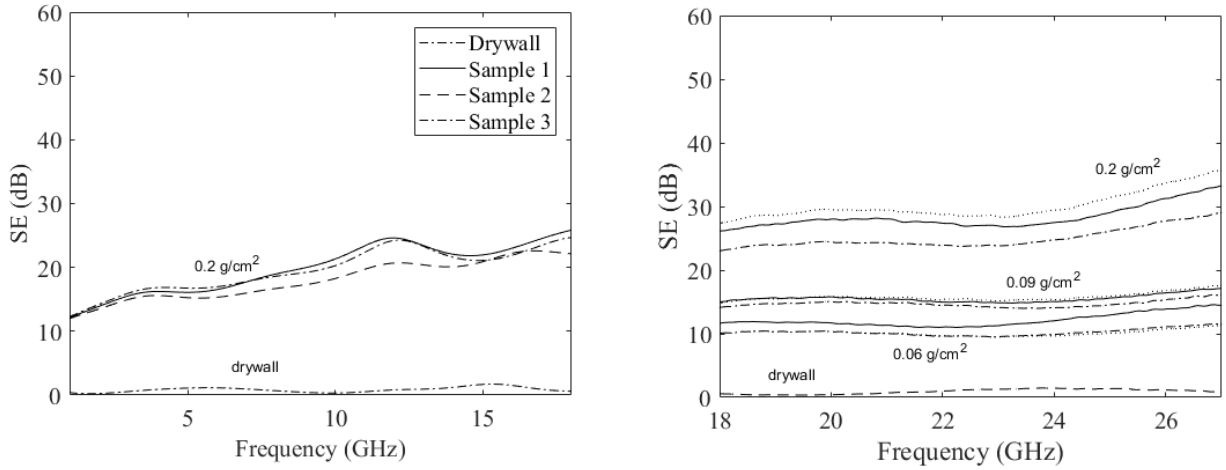


Figure 2. SE of drywall panels coated with 0.2 g/cm² of biochar in the frequency band 1-18 GHz (left). SE obtained in the case of 0.06 g/cm², 0.09 g/cm² and 0.2 g/cm² in the frequency band 18-27 GHz. (right) [5,6], under CC BY 4.0 license.

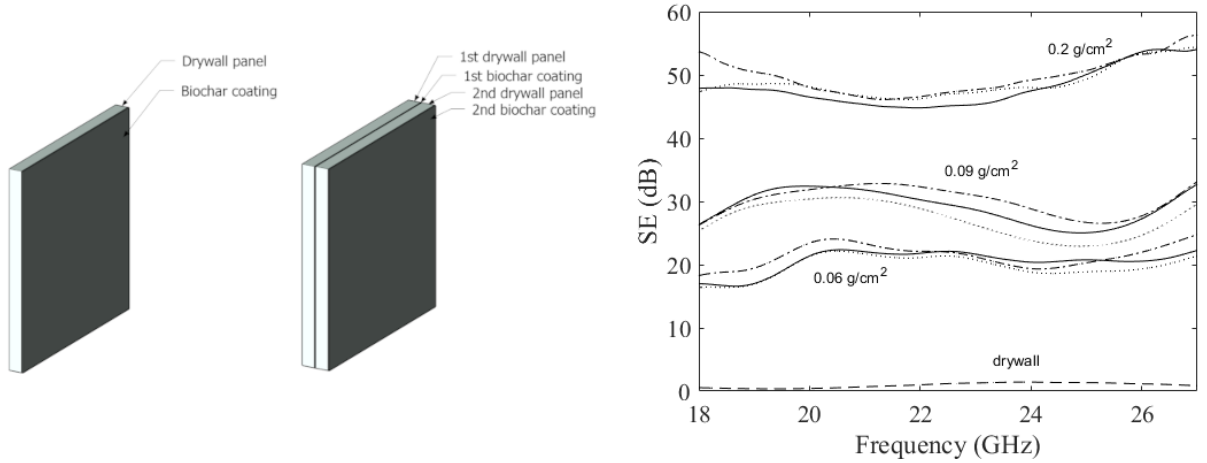


Figure 3. Single and double panel configuration (left). SE measurements with biochar 0.06 g/cm², 0.09 g/cm², and 0.20 g/cm² for double panel configuration in the frequency band 18-27 GHz (right) [6], under CC BY 4.0 license.

4. Discussion

The data confirm that biochar is a highly valid alternative for functionalizing passive elements like drywall [6]. The provided attenuation derives from combined mechanisms of reflection and absorption. The performance of

these biochar-coated panels is highly competitive when compared to other matrix-filler systems studied in the literature. The application of a coating on the drywall surface offers a much simpler, retrofittable application in construction engineering. Drywall panels coated with biochar achieves good attenuation levels especially with the double-layer configuration (SE > 46 dB), using an inexpensive recovered material without disrupting standard dry construction procedures [5,6].

5. Conclusions

Biochar-coated drywall panels represent a practical, ecological, and high-performance solution for shielding against electromagnetic interference [5,6]. Tests conducted in the 1-27 GHz range reveal effective shielding that can be modulated based on coating thickness or the use of double-panel structures. By bridging the gap between agricultural waste valorization and advanced building materials, these systems pave the way for innovative, low-environmental-impact applications to control indoor exposure to high-frequency electromagnetic fields.

References

[1] Jamshed MA, Héliot F, Brown TWC. A Survey on Electromagnetic Risk Assessment and Evaluation Mechanism for Future Wireless Communication Systems. IEEE J Electromagn RF Microw Med Biol 2020;4:24–36. https://doi.org/10.1109/JERM.2019.2917766.
[2] Du K, Ozdemir O, Erden F, Guvenc I. Sub-Terahertz and mmWave Penetration Loss Measurements for Indoor Environments. 2021 IEEE Int. Conf. Commun. Workshop ICC Workshop, 2021, p. 1–6. https://doi.org/10.1109/ICCWorkshops50388.2021.9473898.
[3] Sankaran S, Deshmukh K, Ahamed MB, Pasha SK. Recent advances in electromagnetic interference shielding properties of metal and carbon filler reinforced flexible polymer composites: A review. Compos Part Appl Sci Manuf 2018;114:49–71.
[4] Nanda S, Dalai AK, Berruti F, Kozinski JA. Biochar as an Exceptional Bioresource for Energy, Agronomy, Carbon Sequestration, Activated Carbon and Specialty Materials. Waste Biomass Valorization 2016;7:201–35. https://doi.org/10.1007/s12649-015-9459-z.
[5] Savi P, Ruscica G, di Summa D, Natali Sora I. Shielding Effectiveness Measurements of Drywall Panel Coated with Biochar Layers. Electronics 2022;11:2312. https://doi.org/10.3390/electronics11152312.
[6] Ruscica G, Savi P, Perotti M, Natali Sora I. Biochar-Coated Drywall Panels for Electromagnetic Shielding Applications in the K-Band. Electronics 2026;15:1073. https://doi.org/10.3390/electronics15051073.
[7] Savi P, di Summa D, Natali Sora I, Dassano G, Ruscica G, Pelosato R. Drywall coated with biochar as electromagnetic interference shielding material. 2021 Int. Conf. Electromagn. Adv. Appl. ICEAA, 2021, p. 403–4. https://doi.org/10.1109/ICEAA52647.2021.9539791.

Orientation Dependent EMI Shielding Performance of CFRP Laminates

Maria Vlacha[1], Angelos Voudouris Itskaras[1], Christos Vazouras [2], Alkiviadis S. Paipetis[1]

Corresponding author: Alkiviadis S. Paipetis, paipetis@uoi.gr

[1] *Composite and Smart Materials Laboratory, Department of Materials Science and Engineering, University of Ioannina, GR-45110, Ioannina, Greece, m.vlacha@uoi.gr, 0009-0001-7540-8102, a.voudouris@uoi.gr, 0009-0000-2286-2208, paipetis@uoi.gr, 0000-0001-9668-9719*

[2] *Telecommunications Laboratory, Sector of Combat Systems, Naval Operations, Electronics and Telecommunications, Hellenic Naval Academy, 18539 Piraeus, Greece, chvazour@hna.gr*

Abstract

Electromagnetic interference (EMI) shielding is a critical functionality for advanced multifunctional materials used in aerospace, electronics, and smart systems. Carbon fiber reinforced polymers (CFRPs) offer lightweight characteristics and high electrical conductivity, making them promising candidates for EMI shielding applications. However, the influence of carbon fiber orientation on EMI shielding has not been fully explored, especially under specific measurement conditions. In this study, the effect of fiber lay-up configuration on the shielding effectiveness (SE) of CFRP laminates is investigated. Three different stacking configurations ([0/0/0], [90/90/90], and [45/45/45]) and one with chopped carbon fibers were examined using a vector network analyzer (VNA) and a waveguide setup, in the 5.8-8.3 GHz frequency range. The results show the dependence of shielding performance on fiber orientation. The [90/90/90] configuration exhibited the highest shielding capability, while the [0/0/0] showed lower values of shielding effectiveness. Intermediate behavior was observed for the [45/45/45] and composites with chopped fibers. These findings highlight the importance of composites' design in controlling EMI shielding performance and demonstrate that orientation can be used as a parameter for developing multifunctional composite materials with desirable electromagnetic properties.

Keywords: EMI shielding; CFRP; Fiber orientation; Anisotropy; S-parameters; UN SDG 9

1. Introduction

Electromagnetic interference (EMI) is a recent kind of "pollution" that has become a challenge for electronic devices and systems' efficient operation in a wide range of sectors, including industrial automation, healthcare, transportation, aviation and aerospace, telecommunications [1]. Therefore, the development of materials with EMI shielding capabilities has gained significant interest. Traditionally metals have been the first choice for EMI shielding, due to high electrical conductivity. However, limitations such as corrosion and high weight, have led to polymer based composite materials as a promising alternative, combining low weight, structural integrity, and the potential for tunable electromagnetic properties [2]. Carbon fiber reinforced polymers (CFRPs) have attracted significant attention as multifunctional materials capable of simultaneously providing high durability and multiple functionalities, with electromagnetic shielding being one of them [3]. Based on the

inherent properties they have, carbon fibers and carbon based fillers are effective in EMI shielding and they facilitate interaction with electromagnetic waves through reflection and absorption mechanisms [4]. The shielding effectiveness (SE) of a composite depends on different factors, with the formation of a continuous conductive network within the polymer matrix being a fundamental one [5]. Different conductive fillers for the polymer matrix and their concentration are some of the parameters that are intensively studied, while the architecture and structural arrangement of the reinforcement is also a primary determinant for the EMI shielding performance. Recent studies have established a framework for shielding effectiveness based on fiber orientation [6]. While these models provide an understanding of how orientation angles influence shielding performance, the behavior of simple unidirectional lay-up configurations in a rectangular waveguide-based system remains an area of interest. In this study, the impact of fiber orientation on the EMI shielding effectiveness of CFRPs is investigated. Laminates with three different lay-up configurations [0/0/0], [90/90/90], [45/45/45] and a composite with randomly oriented chopped fibers are examined using S-parameter measurements in a waveguide setup. This work aims to show how fiber alignment can be used as a parameter to design smart multifunctional materials, with the goal to achieve tunability of the shielding performance. This approach is particularly relevant for next-generation applications, where components act not only as structural elements but also as tailored electromagnetic shielding materials.

2. Materials and Methods

2.1 Materials and Fabrication

CFRP laminates were fabricated using a thermoset epoxy resin system. Three unidirectional lay-up configurations were prepared, [0/0/0], [90/90/90], and [45/45/45], where the fiber orientation is defined relative to the electric field direction in the waveguide (TE_{10} mode). The [90/90/90] configuration corresponds to fibers aligned parallel to the electric field, while the [0/0/0] configuration to fibers oriented perpendicular to it. All samples were manufactured using the same resin system and curing conditions to ensure consistency. An unidirectional (UD) carbon fiber fabric consisting of stitched T700 carbon fiber tows (Toray Carbon Fibers Europe, France) was used as reinforcement. The matrix material was an epoxy system (Araldite LY5052/Aradur HY5052, Huntsman Advanced Materials, Switzerland), with a resin-to-hardener ratio of 100:38 (w/w). The chopped carbon fibers were cut to a length of 5 mm using a fiber chopper and their amount was adjusted to match the total fibers weight used in the UD laminates. The laminates were fabricated via a hand lay-up process, and a curing in a hot press, 3 MPa, for 24h at ambient temperature and subsequently post-cured at 373 K for 4 h. The final thickness of all samples was 1 mm. The cured laminates were cut into rectangular specimens compatible with the dimensions of the waveguide system.

2.2 Electromagnetic Characterization

The electromagnetic properties of the CFRP laminates were evaluated using a vector network analyzer (VNA) (P9372A, 300 kHz to 9 GHz, 2-port), with a rectangular waveguide (WR-137), operating in the frequency range of 5.8–8.3 GHz. The samples were inserted into the waveguide, fully covering the cross-section to prevent electromagnetic leakage. Scattering parameters (S11 and S21) were measured.The total shielding effectiveness was determined as [6]: $SE_{total}\,(dB) = -10\log_{10}(|S21|^2)$ where S_{21}represents the transmission coefficient.

All measurements were performed on three independent samples for each configuration to ensure reproducibility.

3. Results

Figure 1 shows the variation of SEtotal (dB) as a function of frequency for the different configurations.

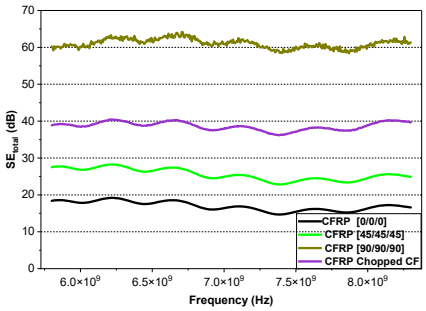


Figure 1. Total shielding effectiveness (SEtotal) as a function of frequency for CFRP laminates with different fiber orientations measured using a waveguide-based setup in the 5.8–8.3 GHz frequency range.

As shown in Figure 1, a clear dependence of EMI shielding performance on fiber orientation is observed across the investigated frequency range (5.8-8.3 GHz). Among measured configurations, the CFRP [90/90/90] exhibits the highest shielding effectiveness (values more than 60 dB), while the CFRP [0/0/0] configuration presents the lowest one (under 20db). The CFRP [45/45/45] laminate demonstrates intermediate behavior, with shielding effectiveness values around 25dB. The chopped carbon fiber composite also exhibits values around 40 dB, exceeding those of the CFRP [0/0/0] and CFRP [45/45/45] laminates but remaining lower than the CFRP [90/90/90]. Overall, the results indicate a strong dependence of shielding effectiveness on fiber orientation.

4. Discussion

The observed differences in shielding effectiveness among the investigated CFRP laminates can be primarily attributed to the anisotropic electrical behavior of carbon fibers and their interaction with the electromagnetic field. In the waveguide WR-137 used, the dominant TE_{10} mode generates an electric field perpendicular to the direction of wave propagation. As a result, the relative orientation between the electric field and the carbon fibers plays a critical role in determining the shielding performance [6]. For the CFRP [90/90/90], the electric field is aligned parallel to the fiber direction. This leads to enhanced conductivity in the direction of the electric field and increased electromagnetic attenuation. Regarding the CFRP [0/0/0], the electric field is oriented perpendicular to the fiber direction. The intermediate performance observed for the CFRP [45/45/45] can be attributed to partial alignment between the electric field and the fiber direction, allowing limited charge transport compared to CFRP [90/90/90]. It is also worth considering that the measured SE is influenced not only by the anisotropy of the composite but also by the measurement configuration and specimen geometry. Therefore, the enhanced shielding observed in the CFRP [90/90/90] is likely the result of a combined effect of material anisotropy and favorable current paths imposed by the measurement setup. The chopped fiber composite exhibits a kind of isotropic shielding response, with intermediate shielding effectiveness values, due to the

random orientation of fibers resulting in conductive pathways in multiple directions. However, due to the shorter fiber length, the overall conductivity remains lower than that of the CFRP [90/90/90], as the efficient conductive network depends highly on connectivity [3]. The observed anisotropic shielding behavior is consistent with previous studies [6], which have indicated that measurement techniques with defined electric field polarization can highlight orientation dependent electromagnetic responses. Overall, the results demonstrate that fiber orientation is a key design parameter for tailoring the EMI shielding performance of CFRP composites under controlled measurement conditions, highlighting the importance of anisotropy in electromagnetic applications.

5. Conclusions

This study investigated the effect of fiber orientation on the electromagnetic interference (EMI) shielding capability of CFRP laminates in 5.8-8.3 GHz frequency range. The results demonstrated a dependence of shielding performance on fiber orientation. The [90/90/90] configuration exhibited the highest shielding effectiveness, as the electric field is aligned with the conductive carbon fibers. In contrast, the [0/0/0] laminate showed lower performance, while the [45/45/45] and chopped fiber composites exhibited intermediate behavior. These findings highlight the important role of the anisotropic nature of CFRPs in their electromagnetic response and demonstrate that fiber orientation can be effectively used as a design parameter to tailor EMI shielding performance under controlled measurement conditions. Future work will focus on extending this approach to multifunctional composite systems including the incorporation of conductive nanomaterials and the development of tunable EMI shielding materials, as well as further investigation of the influence of material architecture and measurement conditions on shielding behavior.

References

1. Shahapurkar K, Gelaw M, Tirth V, Soudagar MEM, Shahapurkar P, Mujtaba MA, MC K, Ahmed GMS. Comprehensive review on polymer composites as electromagnetic interference shielding materials. Polymers and Polymer Composites. 2022;30:1–17.
2. Zecchi S, Cristoforo G, Bartoli M, Tagliaferro A, Torsello D, Rosso C, Boccaccio M, Acerra F. A Comprehensive Review of Electromagnetic Interference Shielding Composite Materials. Micromachines. 2024;15:187.
3. Orasugh JT, Ray SS. Functional and Structural Facts of Effective Electromagnetic Interference Shielding Materials: A Review. ACS Omega. 2023;8:8134–8158.
4. Abdelal NR. Multifunctional Carbon Fiber Composite with Improved Electromagnetic Interference Shielding and Interlaminar Fracture Toughness Characteristics. IOP Conference Series: Materials Science and Engineering. 2020;938:012001.
5. Jang D, Kim BJ, Nam IW. A Comprehensive Study on EMI Shielding Performance of Carbon Nanomaterials-Embedded CFRP or GFRP Composites. Polymers. 2022;14:5224.
6. Hong J, Xu P. Electromagnetic Interference Shielding Anisotropy of Unidirectional CFRP Composites. Materials. 2021;14:1907.

Mechanical Behavior, Structural Design, and Joining

Dimensional Optimization of a Cantilever Structure with Stress–Strain Analysis

Nebojša Arsić[1*], Nenad Kostić[1], Nenad Marjanović[1], Vesna Marjanović[1]

[1] *University of Kragujevac, Faculty of Engineering, Kragujevac, Serbia, nebojsa.arsic@kg.ac.rs , 0009-0009-2605-8108; nkostic@kg.ac.rs , 0000-0002-0157-7501; nesam@kg.ac.rs , 0000-0002-8441-4328; vmarjanovic@kg.ac.rs , 0000-0001-6266-5540*

Corresponding author: *nebojsa.arsic@kg.ac.rs*

Abstract

The paper presents dimensional optimization of a cantilever structure with an analysis of its stress–strain state. The geometric model was developed in the CAD/CAE environment CATIA V5, and the analysis was carried out using the finite element method. The objective of the optimization was to minimize volume while constraining the maximum Von Mises stress to 250 MPa. The height of the cross-section was selected as the variable parameter. Two cases were analyzed: a solid and a hollow cross-section with a wall thickness of 3 mm. The results show that the optimal height is approximately 41.273 mm for the solid and 59.709 mm for the hollow cross-section. Although it requires a greater height, the hollow profile provides a smaller volume and a more favorable mass-to-load-bearing ratio, confirming the importance of optimization in structural design.

Keywords: *structural optimization; cantilever beam; finite element analysis; Von Mises stress, 'UN SDG 9', 'UN SDG 12'.*

1. Introduction

Structural optimization represents a fundamental approach in modern mechanical design, enabling improved performance and efficient material utilization. The goal of optimization is to minimize the volume of a structure while satisfying strength constraints, most commonly defined in terms of Von Mises stress, as confirmed by numerous contemporary studies [1]. The development of CAD/CAE systems has enabled the application of advanced numerical methods for analyzing the mechanical behavior of structures. The finite element method (FEM) represents a key tool for stress–strain analysis and an essential component of the optimization process [2]. In the field of structural optimization, three main approaches are distinguished: size, shape, and topology optimization. Size optimization involves modifying geometric parameters such as the thickness, height, and width of elements to improve stress distribution and achieve more efficient material utilization, a topic of many recent studies [3].

A parametric geometric model was developed to enable systematic evaluation of the influence of cross-sectional height.

2. Materials and Methods

Within the scope of this research, a cantilever structure defined according to a reference example from the literature [4], shown in Figure 1, was analyzed.

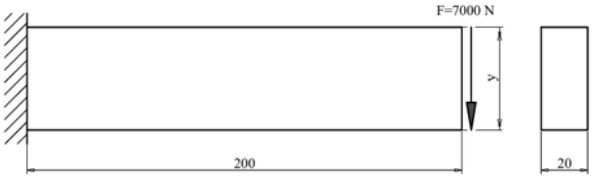


Figure 1. Cantilever dimensions, support, and loading [4].

The geometric model of the structure was recreated in the CAD environment CATIA V5, with the basic dimensions adopted in accordance with the original example from the literature. The structure was modeled as a prismatic cantilever with a length of 200 mm and a thickness of 20 mm, while the height was treated as a variable geometric parameter, denoted by y, in line with contemporary approaches to structural optimization [5]. Structural steel S235 (EN 10025) was selected due to its widespread application. The material parameters were defined as modulus of elasticity $E = 2\times10^5$ MPa, Poisson's ratio ν=0.266, material density of 7860 kg/m³, and a yield strength of approximately $\sigma_y \approx 250$ MPa. The stress–strain analysis was performed using the finite element method in the "Generative Structural Analysis" module of the CATIA V5 software package, a standard approach in structural analysis [6]. The boundary conditions were defined such that the left end of the cantilever was fixed (encastre condition), while a vertical force F = 7000 N was applied at the opposite free end.

To examine the influence of the geometric parameter, two cases were analyzed: a solid cross-section [4] and a hollow cross-section with a 3 mm wall thickness, with all other dimensions kept the same as in the first case. This approach enables comparison of the mechanical behavior of different cross-section types and assessment of the effect of material reduction on the structure's load-bearing capacity [6].

3. Results

Parabolic tetrahedral elements were used for the finite element discretization. As finite elements, parabolic tetrahedra provide high analysis accuracy, although computations are significantly slower than with planar or linear elements. The element characteristics are as follows: element size 10 mm, geometric deviation 2 mm, total number of nodes - 442, and total number of elements - 1302. In the analysis, y was chosen as the variable, and the objective function was the structure volume V, which needed to be minimized. The constraint was that the maximum Von Mises stress must not exceed 250 MPa. To solve the optimization problem, a simulated annealing algorithm with fast convergence was applied. The stopping criteria for the algorithm were a maximum of 200 iterations, 50 consecutive unsuccessful iterations, or a maximum optimization time of 5 minutes. The extreme values of the Von Mises stress indicate that the global maximum is 250.5 MPa. The computed stress value slightly exceeds the prescribed limit due to numerical approximations and the finite element mesh. The minimum value of the parameter y that satisfies the maximum-stress condition was found to be $y = 41.273$ mm. The results of the finite element analysis are shown in Figure 2. Figure 3 shows the optimization parameter as a function of the number of iterations and its variation over iterations.

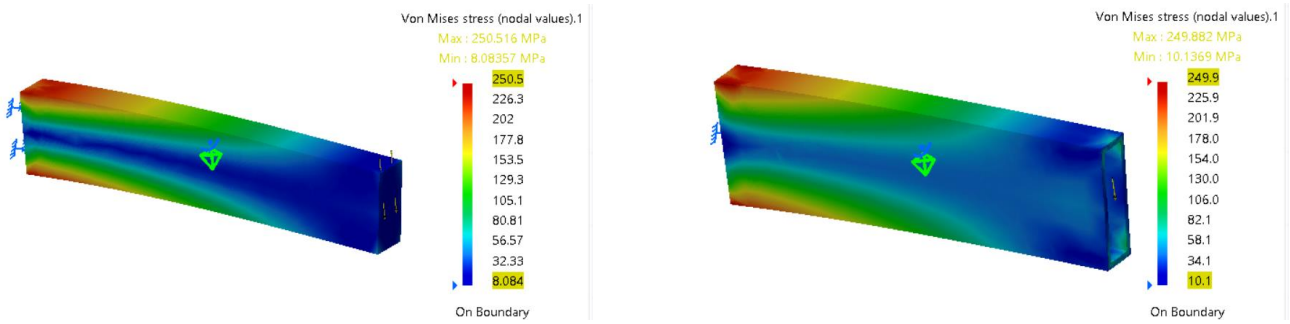


Figure 2. Stress state of the structure for Case 1 (left) and Case 2 (right)

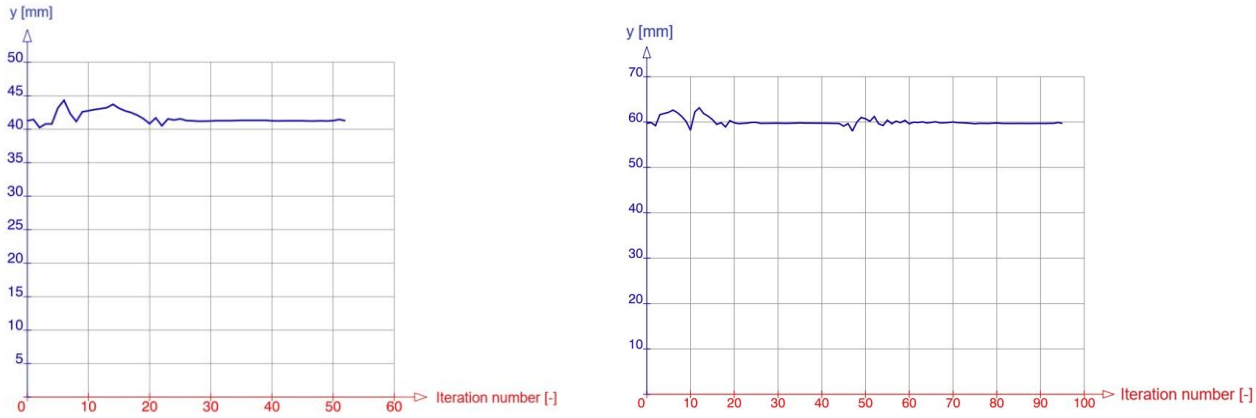


Figure 3. Optimization parameter versus iteration number for case 1 (left) and case 2 (right)

The parameter value stabilizes around 40–41 mm for case 1 and 59–60 mm for case 2, indicating convergence of the optimization process. The minimum volume of the structure, which depends on the cantilever's length, width, and height, as well as the parameter y, is $V = 1.651 \times 10^{-4}$. The same optimization process was repeated for a hollow cross-section with a 3 mm wall thickness. The hollow configuration requires a greater height due to reduced material near the neutral axis, but results in a lower overall volume while maintaining the same stress constraint. Figure 4 shows the results of the variation of the optimization parameter as a function of the number of iterations for Case 2. The minimum volume of the structure obtained is $V = 0.8845 \times 10^{-4}$.

The results were verified by strength-of-materials calculations [4], while the procedure for Case 2 is presented below:

$$\sigma_{max} = \frac{M \cdot c}{I}, \tag{1}$$

where $c = \frac{y}{2}$, M is the maximal bending moment, c is the distance to the furthest point of the cross-section, I is the moment of inertia, and the parameter y is the total height of the cross-section for the condition of $\sigma_{max} = 250$ MPa. The calculated results based on analytical calculations give 40.988 mm for Case 1, and 58.274 mm for Case 2. Numerical analysis gives 41.273 mm for Case 1 and 59.709 mm for Case 2. The values obtained through numerical analysis do not significantly deviate from those obtained analytically, which confirms the reliability of the dimensional optimization results.

4. Discussion

The results indicate a significant influence of cross-sectional geometry on the structure's load-bearing capacity and efficiency. In hollow profiles, the material is distributed farther from the neutral axis, which increases the moment of inertia and reduces stress for the same amount of material. As a result, a more favorable mass-to-load-bearing ratio is achieved compared to solid cross-sections. On the other hand, solid profiles require smaller dimensions but involve higher material consumption. A strong agreement between analytical and numerical results was observed, confirming the reliability of the finite element method for analyzing such structures.

5. Conclusion

The paper presents the dimensional optimization of a cantilever structure with both solid and hollow cross-sections using the finite element method. It was shown that the hollow profile enables more efficient material utilization compared to the solid cross-section. Comparison with analytical calculations confirmed the reliability of the obtained results. Future research may include the application of different materials and more advanced optimization methods.

Acknowledgements

This research was supported by the Ministry of Science, Technological Development and Innovation of the Republic of Serbia, Agreement No. 451-03-34/2026-03/200107.

References

1. Bendsøe MP, Sigmund O. Topology Optimization: Theory, Methods, and Applications. Berlin: Springer; 2003.
2. Liu K, Tovar A. An efficient 3D topology optimization code written in MATLAB. Structural and Multidisciplinary Optimization. 2014;50(6):1175–1196.
3. Rozvany GIN. A critical review of established methods of structural topology optimization. Structural and Multidisciplinary Optimization. 2009;37(3):217–237.
4. Isailović B. Strukturna optimizacija elemenata mašinskih konstrukcija u CAD okruženju [master's thesis]. Kragujevac: Fakultet inženjerskih nauka, Univerzitet u Kragujevcu; 2010.
5. Nikaein G, Haji Mohammadvali M, Sadeghi MH. Topology optimization of cantilever beams with non-cellular, cellular, and hybrid structures for enhanced mechanical performance. Applications in Engineering Science. 2026;25:100279.
6. Săvescu C, Comeagă D, Stoicescu A. Optimization of cantilever piezoelectric harvester to triangular shape with material reduction using finite element analysis. Heliyon. 2024;10(13):e33209.

Shear Strength Testing of Adhesively Bonded Joints: Experimental and Numerical Analysis

Vladimir Milovanović[1], Veljko Kanjevac[1], Miloš Pešić[2], Gordana Jovičić[1]

[1]*Faculty of Engineering, University of Kragujevac, Kragujevac, Serbia, vladicka@kg.ac.rs, [0000-0003-3071-4728], veljko463@gmail.com, gjovicic.kg.ac.rs@gmail.com, [0000-0002-9799-5555],*
[2] *Institute for Information Technologies, University of Kragujevac, Kragujevac, Serbia, milospesic@uni.kg.ac.rs, [0000-0002-3405-5216]*

Corresponding author: gjovicic.kg.ac.rs@gmail.com

Abstract

This paper presents an experimental and numerical investigation of adhesively bonded aluminum lap joints subjected to shear loading. The specimens were prepared and tested in accordance with EN 17460 using Sikaflex®-268 adhesive. Experimental testing was performed on a universal testing machine, while a three-dimensional FE model was developed in Femap and analyzed using NX Nastran. Good agreement was obtained between the experimental and numerical results, confirming the applicability of both approaches for evaluating bonded joints.

Keywords: adhesive bonding, lap shear strength, EN 17460, finite element method, Sikaflex®-268, aluminum joints, UN SDG 9

1. Introduction

Adhesive bonding is widely used in modern industry because it enables efficient joining of metallic and non-metallic materials while providing more uniform stress transfer than many conventional joining techniques. Compared with welding or mechanical fastening, adhesive bonding may reduce stress concentrations, preserve the integrity of the base material, and contribute to weight reduction in engineering structures. These advantages are especially important in transportation industries, including railway engineering, where structural reliability and durability are essential. Recent review literature confirms that adhesively bonded joints remain a major research topic in structural design, manufacturing, testing, and numerical modeling. [1,2].

The mechanical behavior of bonded joints depends on several factors, such as adhesive properties, adherend material, overlap geometry, adhesive thickness, surface preparation, and curing conditions. For this reason, experimental testing is necessary for evaluating joint strength and failure behavior, while numerical simulation provides additional insight into stress distribution and critical zones in the adhesive layer. Standards such as EN 17460 define the general requirements for adhesive bonding and sealing work in rail vehicles and their components. [3].

The aim of this paper is to compare the experimental and numerical results for adhesively bonded aluminum lap joints subjected to shear loading.

2. Materials and Methods

2.1 Specimen Preparation

The experimental investigation was performed on bonded aluminum lap-joint specimens prepared in accordance with EN 17460. Each specimen consisted of two aluminum adherends with a bonded region of 15 × 35 mm, a nominal overlap length of 20 mm, and an adhesive layer thickness of 5 mm. Bonding was performed using Sikaflex®-268 polyurethane adhesive [4].

Before bonding, the aluminum surfaces were prepared using a cleaning–grinding–cleaning–priming procedure to ensure proper adhesion. The specimens were positioned in a specially designed aluminum mold, which enabled controlled adhesive thickness and proper alignment of the adherends. After preparation, the joints were cured under controlled laboratory conditions for 30 days. Figure 1 shows prepared specimen for testing.

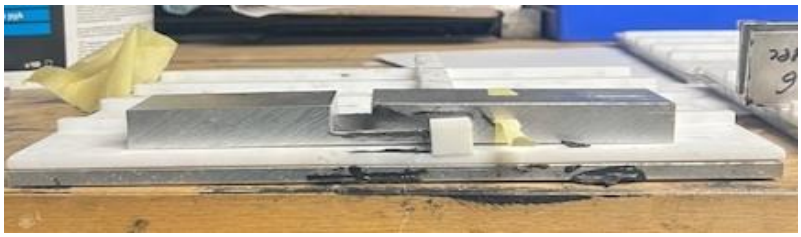


Figure 1. Bonded lap-joint specimen prepared for experimental testing

2.2 Experimental Testing

Mechanical testing was carried out on a universal testing machine equipped with grips suitable for lap shear loading. The tests were performed under controlled laboratory conditions. The crosshead speed was set to 30 mm/min, and force–displacement data were continuously recorded until specimen failure.

A total of 10 specimens were tested. The recorded curves were used to determine the maximum force, displacement at maximum force, displacement at failure, and lap shear strength.

2.3 FE Model

A FE model of the bonded specimen was created in Femap, while the numerical analysis was performed in NX Nastran. The FE model was discretized using eight-node 3D solid finite elements. The finite element mesh consisted of 5320 elements and 6975 nodes, with an average finite element size of 2.5 mm.

Both aluminum adherends and the adhesive layer were modeled as isotropic, homogeneous, and linearly elastic materials. The mechanical properties used in the analysis were: elastic modulus 70,000 MPa, Poisson's ratio 0.33, and density 2700 kg/m³ for aluminum; and elastic modulus 1.3 MPa, Poisson's ratio 0.49, and density 1300 kg/m³ for the adhesive layer. One end of the FE model was fully constrained, while a prescribed longitudinal displacement of 30 mm was applied to the opposite end, as shown in Figure 2. The numerical simulation was performed as a linear static analysis.

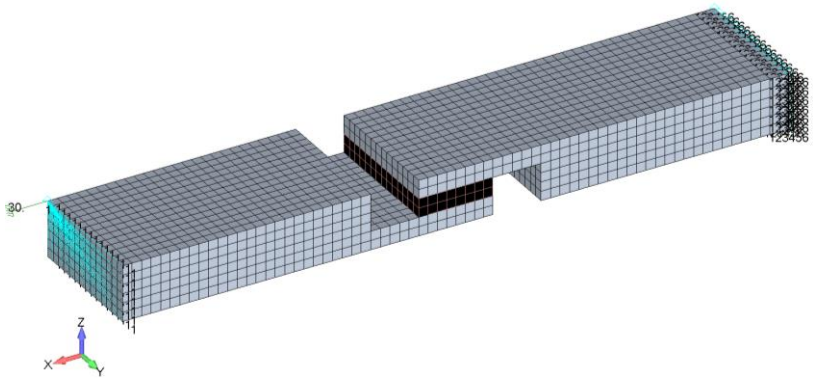


Figure 2. FE model with applied boundary and load conditions

3. Results and Discussion

The experimental results showed a relatively uniform mechanical response of all tested specimens, as shown in Figure 3. In the initial stage of loading, the force increased almost linearly with displacement, which corresponds to elastic deformation of the bonded joint. Maximum force values were reached at displacements of approximately 24–33 mm, after which a sudden drop in force indicated failure of the adhesive joint.

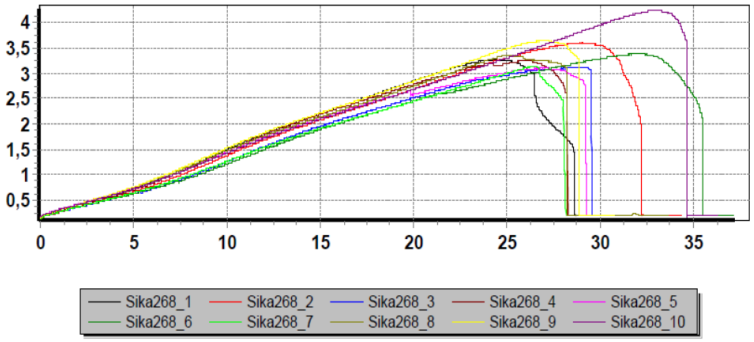


Figure 3. Force–displacement curves of the tested specimens

The measured lap shear strength values ranged from 4.41 MPa to 6.04 MPa, with an average value of 4.86 MPa. The average elongation at break was about 650%, while the average hardness was 57 Shore A. These results are in good agreement with the manufacturer's technical data sheet, which reports a nominal lap-shear strength of about 4.5 MPa and Shore A hardness of about 55 [4].

Most tested specimens showed cohesive failure, indicating that failure occurred predominantly within the adhesive layer. This suggests that the adopted surface preparation and bonding conditions provided good adhesion quality.

The numerical results were in good agreement with the experimental observations. The predicted displacement field reproduced the expected deformation pattern of the lap joint, while the stress field showed that the highest equivalent stresses were concentrated in the adhesive layer and near the ends of the overlap region, as shown in

Figure 4. This distribution is characteristic of lap-joint loading and agrees with trends commonly reported in the literature on bonded joints [1, 2].

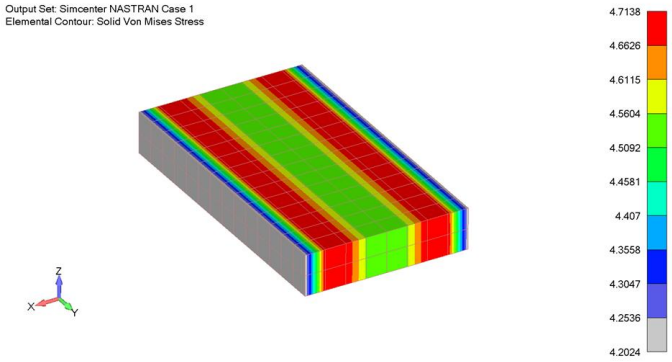


Figure 4. Equivalent Von Mises stress in the adhesive layer

The finite element analysis predicted a maximum equivalent stress in the adhesive of approximately 4.71 MPa, which is very close to the experimentally obtained average lap shear strength of 4.86 MPa. The difference between the numerical and experimental values is small, indicating that the developed FE model can adequately reproduce the global behavior of the bonded joint. Although the adhesive was modeled as a linear elastic material, the obtained agreement confirms that the FE model is suitable for preliminary strength assessment and for identifying critical stress regions in the joint.

5. Conclusions

This paper presents a comparative experimental and numerical investigation of adhesively bonded aluminum lap joints subjected to shear loading. The experimental testing showed stable behavior of the bonded specimens, with an average lap shear strength of 4.86 MPa. The dominant cohesive failure mode indicated good adhesion quality and adequate surface preparation. The numerical analysis performed in Femap with NX Nastran predicted a maximum equivalent stress of approximately 4.71 MPa in the adhesive layer, which is in good agreement with the experimental results. It can be concluded that both approaches provide reliable tools for evaluating the mechanical behavior of adhesively bonded joints.

Acknowledgements

This research was supported by the Science Fund of the Republic of Serbia, Grant No. 7475, PROMINENT.

References

1. Wei Y, Du J, Chen B, Zhang W, Li S, Liu H. *Adhesively bonded joints: A review on design, manufacturing, experiments, modeling and challenges*. Composites Part B: Engineering, 2024.
2. Maggiore S, Banea MD, Stagnaro P, Luciano G. *A Review of Structural Adhesive Joints in Hybrid Joining Processes*. Polymers, 2021, 13(22):3961.
3. EN 17460:2022. *Railway applications - Adhesive bonding of rail vehicles and their components*. European Committee for Standardization, Brussels, 2022.
4. Sika Industry. *Sikaflex®-268 Product Data Sheet*. Sika Services AG, latest available edition.

Graphical representation of adhesive joints in technical drawings for railway industry

Srdjan Samardzic[1], Aleksija Djuric[1]

[1] *Faculty of Mechanical Engineering, University of East Sarajevo, East Sarajevo, Bosnia and Herzegovina, srdjan.samardzic@ues.rs.ba, 0009-0003-4096-7523, aleksija.djuric@ues.rs.ba, 0000-0002-0251-6364*

Corresponding author: srdjan.samardzic@ues.rs.ba

Abstract

The increasing demand for lightweight structures in the railway industry has led to greater use of adhesive bonding technologies. Compared with traditional joining methods, adhesive joints offer improved stress distribution, reduced weight, and increased corrosion resistance. Despite their growing importance, adhesive joints are not adequately standardized in technical drawings. Existing standards mainly address welded and mechanical joints, while adhesive bonding is often represented by inconsistent textual notes or company-specific practices. This lack of uniformity can lead to misinterpretation, manufacturing errors, and safety concerns. This paper aims to highlight the need for improved and standardized graphical representation methods in technical documentation.

Keywords: Graphical representation; adhesive joints; railway industry, sustainable transport

1. Introduction

Currently, railways are the most widespread form of transport worldwide [1], and therefore extensively incorporate modern technological advancements such as digital twins, artificial intelligence, and IoT [2-3]. Adhesive bonding is a complex and rapidly evolving research field that has attracted significant industrial attention in recent years [3,4]. Due to ongoing advancements in materials, surface preparation techniques, and manufacturing processes, adhesive-bonded joints are increasingly recognized as a reliable and efficient alternative to conventional joining methods such as welding, riveting, and mechanical fastening [5]. Besides enabling weight reduction, these joints offer more uniform stress distribution, improved fatigue performance, and the ability to join dissimilar materials, which is particularly important in modern engineering applications [6]. In addition to adhesive joints, hybrid joints combining two or more joining processes are increasingly used in practice [7] to achieve joints with improved characteristics compared to their parent techniques [7,8].

Product Lifecycle Management (PLM) represents a strategic framework for overseeing a product throughout its entire lifecycle, from initial concept and development, through engineering, design, and manufacturing, to usage and recycling [9]. Standards constitute globally recognized documents that define requirements, specifications, guidelines, and characteristics aimed at ensuring that materials, products, processes, and services fulfill their intended purpose [10]. This paper aims to highlight the need for improved and standardized graphical representation methods of adhesive joints in technical documentation, especially as hybrid joints are already

widely used. Certain amount of information and photos are censored due to data protection obligations and to protect end customers.

2. Current standards and practices

The study [11] proposed graphic standard to represent adhesive joints, unifying and simplifying the technical design criteria to improve the exchange of information throughout the Product Lifecycle Management. The researchers also developed software for automatically generating graphic labels. Through the graphical interface, by entering and selecting data the user can automatically generate a label in accordance with the integrated graphic standard. This software can be considered a predecessor of modern macros in PLM platforms.

According to [12], the adhesive joint symbol consists of two main elements: the leader and the reference line. The reference line can be extended with a tail at the end to include additional information or requirements. Symbols for adhesive joints geometry, along with geometrical information (thickness and width of the joint), are placed above the reference line (Figure 1).

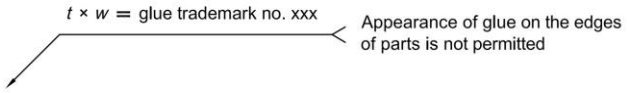


Figure 1. Graphical representation of adhesive joint according to ISO 15785 [10]

ASTM has defined a standard practice [13] for the graphical representation of adhesive joints, which is based on ISO 15785 but is significantly more detailed. The graphical representation shown in Figure 2 includes additional information such as instructions for surface preparation, curing, adhesive physical form, technology families, application method, and more. Unlike ISO 15785, the label can include a filled flag to indicate that the adhesive is to be applied in the field, while the absence of this element indicates factory application.

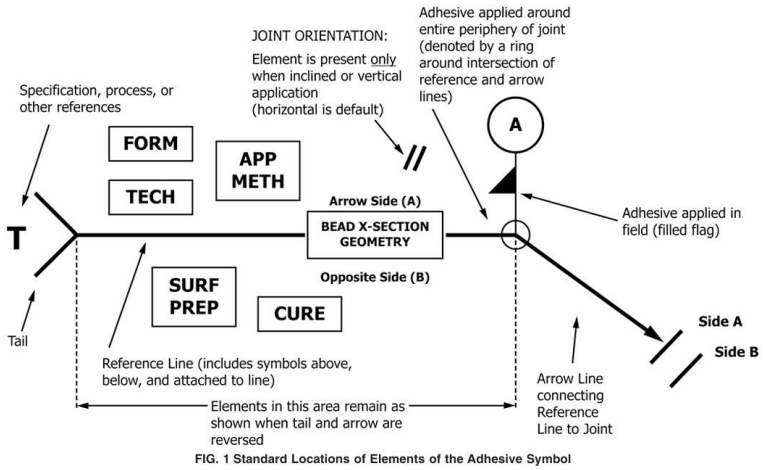
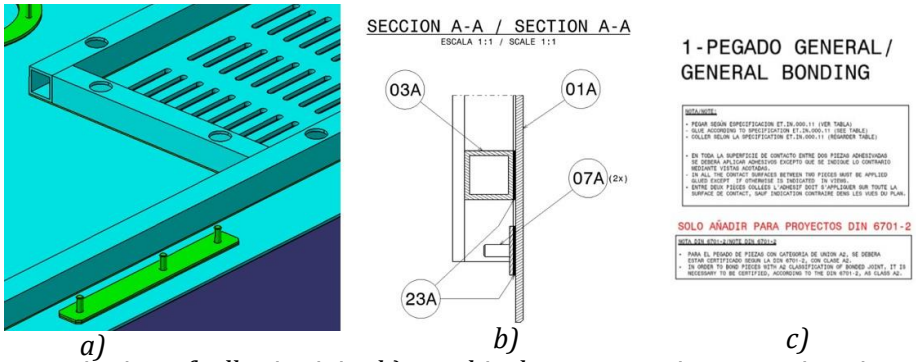


Figure 2. Graphical representation of adhesive joint according to ASTM D7447 – 08

3. Practical examples of adhesive joints symbols in railway industry

Figure 3 shows an adhesive joint between sheet metal and square tubes to increase rigidity. The development of CAD software has significantly facilitated the spatial representation of parts and assemblies in drawings (Figure 3a), as well as the depiction of specific joints between parts. Figure 3b shows the same joint in cross-section, with assigned balloons referring to the joined parts and the adhesive itself. This type of representation always requires additional notes and instructions (Figure 3c).



a) b) c)

Figure 3. a) Isometric view of adhesive joint b) graphical representation at section view c) additional notes

The graphic representation of the adhesive joint in Figure 4 is often used in organisations that actively implement the DIN 6701 standard. It consists of a leader and a reference line with a defined total joint surface and adhesive thickness. The reference line is extended with a tail containing information about the quality class of the connection, as well as balloons related to the connected parts and adhesive in the BOM.

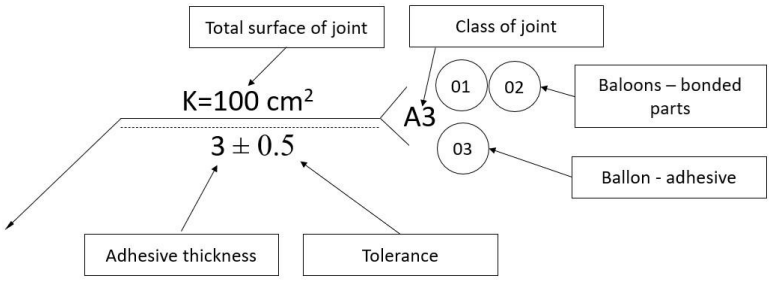


Figure 4. Adhesive joint representation corelated with implementation of DIN 6701

Figure 5 shows a representation of an adhesive joint generated using a macro. The reference line indicates the quality class based on an internal standard, as well as the code of person responsible for control. At the tail of the reference line are the balloons for the adhesive and the internal process specification.

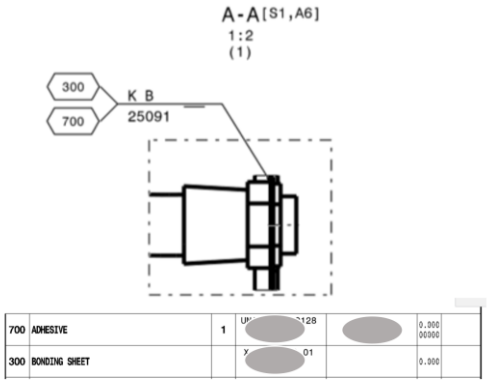


Figure 5. Adhesive joint representation generated using macro

5. Conclusions

The main goal of this paper was to present the problem of non-standardized labelling of adhesive joints on technical drawings. Examples from the technical documentation of companies that fully integrate the quality system throughout the entire product life cycle are presented. Despite this integration and the use of modern PLM platforms such as 3DExperience, problems in communication between individuals in the product life cycle chain persist. These issues can halt production and consequently increase total costs. There is clear scope and need for standardization in this area, and it should be the subject of more extensive research, including data collection from all participants in the product life cycle chain.

References

1. Kushwaha, D., Kumar, A., Harsha, S. P. Advancements and applications of digital twin in the railway industry: a literature review. International Journal of Rail Transportation. 2025; 13(5), 865-890.
2. Qi, J., Wang, J. Bridging artificial intelligence and railway cybersecurity: A comprehensive anomaly detection review. Transportation Research Record. 2025; 2679(5), 232-255.
3. Thompson, E. A., Lu, P., Alimo, P. K., Atuobi, H. B., Akoto, E. T., Abbew, C. K. Revolutionizing railway systems: A systematic review of digital twin technologies. High-speed Railway. 2025; 3(3), 238-250.
4. Cavezza, F., Boehm, M., Terryn, H., & Hauffman, T. A review on adhesively bonded aluminium joints in the automotive industry. Metals. 2020; 10(6), 730.
5. Delzendehrooy, F., Akhavan-Safar, A., Barbosa, A. Q., Beygi, R., Cardoso, D., Carbas, R. J. C., Marques, E. A. S., Da Silva, L. F. M. A comprehensive review on structural joining techniques in the marine industry. Composite Structures. 2022; 289, 115490.
6. Liu, Y., Carnegie, C., Ascroft, H., Li, W., Han, X., Guo, H., & Hughes, D. J. Investigation of adhesive joining strategies for the application of a multi-material light rail vehicle. Materials. 2021; 14(22), 6991.
7. Maggiore, S., Banea, M. D., Stagnaro, P., & Luciano, G. A review of structural adhesive joints in hybrid joining processes. Polymers. 2021; 13(22), 3961.

8. Đurić, A., Klobčar, D., Milčić, D., Marković, B., Samardžić, S., Zdravković, N., & Milčić, M. Analysis of the Possibility of Joining DP Steel and CFRP with Epoxy Adhesive and Hybrid Joining Technology. In International Conference on Machine and Industrial Design in Mechanical Engineering. Cham: Springer Nature Switzerland. 2024; 393-402.
9. Autodesk. (n.d.). PLM: Flexible and scalable data and process management. https://www.autodesk.com/industry/design-manufacturing/plm/overview
10. ISO - International Organization for Standardization. (n.d.). ISO. https://www.iso.org/standards.html
11. Arenas, J. M., & Guillamón, A. Proposal for the graphic representation of structural adhesive joints in engineering drawings and their integration in a computer-assisted designing system. International journal of adhesion and adhesives. 2007; 27(2), 122-128.
12. ISO 15785:2002, Technical drawings — Symbolic presentation and indication of adhesive, fold and pressed joints.
13. ASTM D7447 – 08 : 2023, Standard Practice for Symbolizing Adhesive Applications.

Investigation of the bond strength of laser-textured interference-fit joints

Meris Ikiz [*1,2], Merve Nur Dogu [1,2], Muhannad Obeidi[2,3], Dermot Brabazon[1,2]

[1] *I-Form Advanced Manufacturing Research Centre, Dublin City University, Glasnevin, Dublin 9, Ireland*
[2] *DCU Institute for Advanced Processing Technology, School of Mechanical and Manufacturing Engineering, Dublin City University, Glasnevin, Dublin 9, Ireland*

[3]*Nammo, Northwest Business Park, Dublin 15*

[*] Corresponding author: meris.ikiz2@mail.dcu.ie

Abstract

This project report explores the use of laser surface texturing on 316L stainless steel to develop high-performance interference-fit fasteners. The study proposes a laser-based surface modification technique designed to improve control over surface roughness and, consequently, the bonding strength in interference-fit joints. Cylindrical pins measuring 10 mm in diameter and 10 mm in length were textured using a pulsed-wave CO_2 laser, with the focal point positioned 1 mm below the surface. The primary objective was to tailor surface morphology, increase roughness, and modify the effective diameter to achieve tighter tolerances for specified insertion and removal forces. Key laser processing parameters including laser power, pulse repetition frequency, and scan track overlap were systematically investigated to determine their influence on surface characteristics and dimensional precision. The results highlight the potential of laser texturing as a controllable and effective method for optimizing interference-fit performance in precision engineering applications.

Keywords: *Laser treatment, Surface texturing, CO_2 laser, interference fit, stainless steel, surface roughness, insertion test*

Introduction

Laser Surface Texturing (LST) is a high-efficiency, non-contact engineering technique used to modify surface topography without changing a material's bulk composition Compared to conventional techniques such as etching or micro-milling, LST provides greater precision, faster processing speeds, and a more environmentally friendly approach. It typically involves three mechanisms: ablation, interference melting, or shock-induced deformation. These modifications improve tribological, anti-corrosion, and biological properties across metals, ceramics, and polymers(1–3).

The CO2 laser is a molecular gas laser widely used in industrial welding, cutting, and drilling. Its advantages include in an automation: Easy integration into CNC systems for high-precision machining in automation industries, as a thermal interaction at lower power levels (e.g., 0.1 kW), energy is dissipated as localized heat rather than freeing electrons, making it ideal for controlled surface treatments (3). High output power (up to 15 kW) and lack of physical tool wear reduce overall processing costs so that this technique is highly efficient(4,5). Laser energy is absorbed by a metal's free electrons, converting to thermal energy that triggers rapid melting or

vaporization. To optimize the quality of the textured surface, three parameters are critical which are Laser Power (P): Controls energy input; higher power increases penetration depth but risks thermal damage. Pulse Repetition Frequency (PRF): Determines the timing of energy delivery to the surface and Overlap Percentage (OV%); The degree of overlap between pulses; high overlap ensures surface uniformity but can cause overheating if excessive(6–8).

An interference (or press) fit joins components by friction and material deformation, where a pin is machined slightly larger than the receiving hole. Common in aerospace and automotive sectors for rivets, positioning pins, and shafts. Offers high load-bearing capacity, precise alignment, and simplified assembly/disassembly for maintenance (6,9,10).

Experimental Methods

Cylindrical 316L stainless steel samples (10 mm diameter, 50mm longer) were sandblasted and processed using a CNC CO2 laser (1.5 kW max). The beam was focused 1 mm below the surface with a 0.2 mm diameter. Argon gas was used during texturing to prevent oxidation and surface cracking. The samples were rotated by a DC motor and translated linearly via CNC control. Rotational and linear speeds were calculated using specific formulas to achieve three overlap scenarios: negative (-20%), zero (0%), and positive (20%).The study was conducted in three phases to refine the process shown in Table.1: DOE 1: Tested two power levels (300W, 400W) across three overlap settings at a constant 100 Hz PRF. DOE 2 & 3: Focused on repeating successful parameters from DOE 1 using longer samples (60 mm) to ensure consistency and validate results. Pre- and post-test surface morphology and roughness were analyzed using SEM (Carl-Zeiss EVO-LS15) and 3D digital microscopy (Keyence VHX-2000). For surface roughness, Bruker Contour GT profilometer was also used to quantify how laser parameters and insertion forces impacted microstructural integrity. Insertion and Pull-Out testing were conducted on a Zwick/Roell Z-050 machine at 5 mm/min by pressing textured pins into 10.05 mm 316L hub rings, followed by a 30-second hold and subsequent removal. While DOE 1 utilized a basic configuration, DOE 2 and 3 implemented a refined setup featuring a cylindrical press and specialized V-shaped jaws to ensure precise alignment and more accurate force measurements.

Results and Discussion

Surface Morphology

Laser texturing of 316L stainless steel bars (DOE 1–3 given in Table.1) resulted in distinct topographical changes and visible color shifts. A significant challenge was the ±25W power fluctuation of the Rofin DC-015 CO2 laser, which led to surface inconsistencies among samples with identical nominal parameters. Additionally, remelted material accumulated at the scan ends, forming burs that influenced subsequent mechanical interlocking.

Influence of Overlap on Diameter

The overlap percentage OV% was identified as the dominant factor affecting sample diameter, outweighing the influence of laser power.

- Positive Overlap (+20%): Caused a decrease in diameter (Samples 2, 5, 8, and 9). The lower rotational and linear speeds required for positive overlap increased heat input and pulse residence time, leading to excessive melting, evaporation, and material loss.
- Negative Overlap (-20%): Consistently resulted in diameter increments (Samples 7, 10, 11, and 12). This was attributed to material displacement and the formation of raised surface features without significant ablation.

Table. 1 Experimental design 1, 2, and 3, showing the laser process parameters that were used for sample production.

Experimental-1						
Sample no	Power(W)	PRF(Hz)	OV%	Number of replicate	Linear Speed VL	Rotational Speed ω(rpm)
1	400	100	-20	x3	11.44	47.74
2	400	100	20	x3	5.09	31.8
3	400	100	0	x3	7.63	38.197
4	300	100	0	x3	7.63	38.197
5	300	100	20	x3	5.09	31.8
6	300	100	-20	x3	11.44	47.74
Experimental-2						
Sample no	Power(W)	PRF(Hz)	OV%	Number of replicate	Linear Speed VL	Rotational Speed ω(rpm)
7	400	100	-20	x3	11.44	47.74
8	400	100	20	x3	5.09	31.8
9	300	100	20	x3	5.09	31.8
10	300	100	-20	x3	11.44	47.74
11	300	100	0	x3	7.63	38.197
Experimental-3						
Sample no	Power(W)	PRF(Hz)	OV%	Number of replicate	Linear Speed VL	Rotational Speed ω(rpm)
12	400	100	-20	x3	11.44	47.74
13	300	100	-20	x3	11.44	47.74
14	300	100	0	x3	7.63	38.197

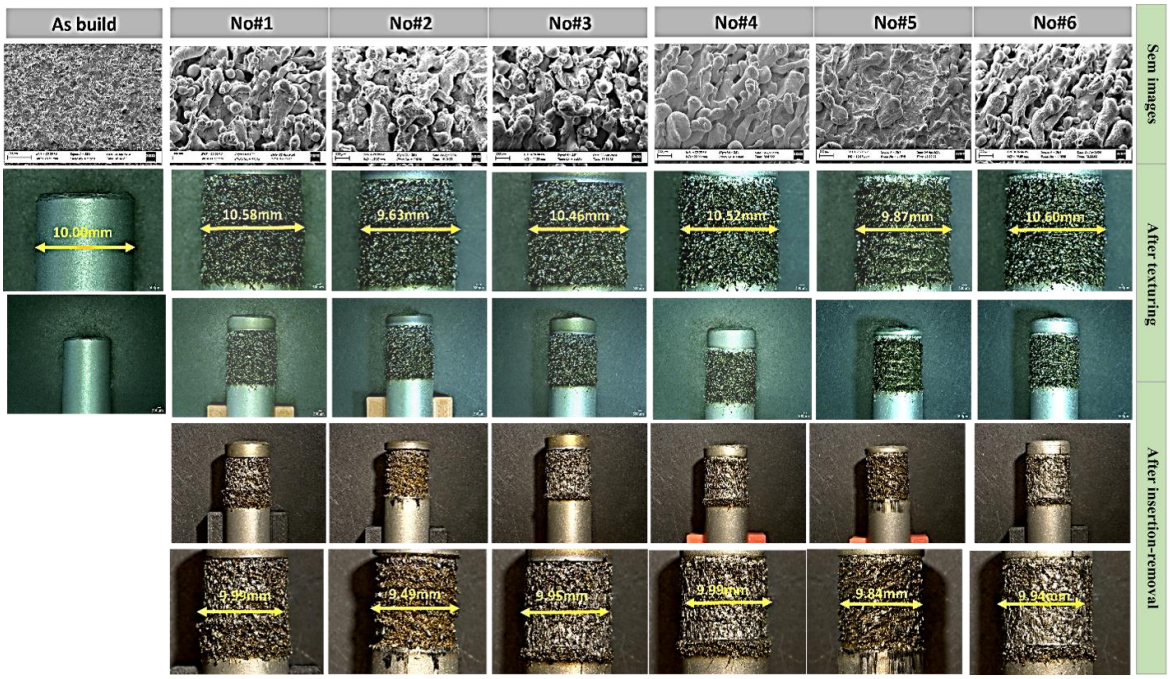
Surface Characterization

Initial roughness measurements using traditional profilometry were inadequate due to the high surface relief and the curvature of the cylindrical specimens. This was successfully addressed in DOE 3 by employing Digital Microscope, which provided reliable topographical data and 3D imaging regardless of surface geometry.

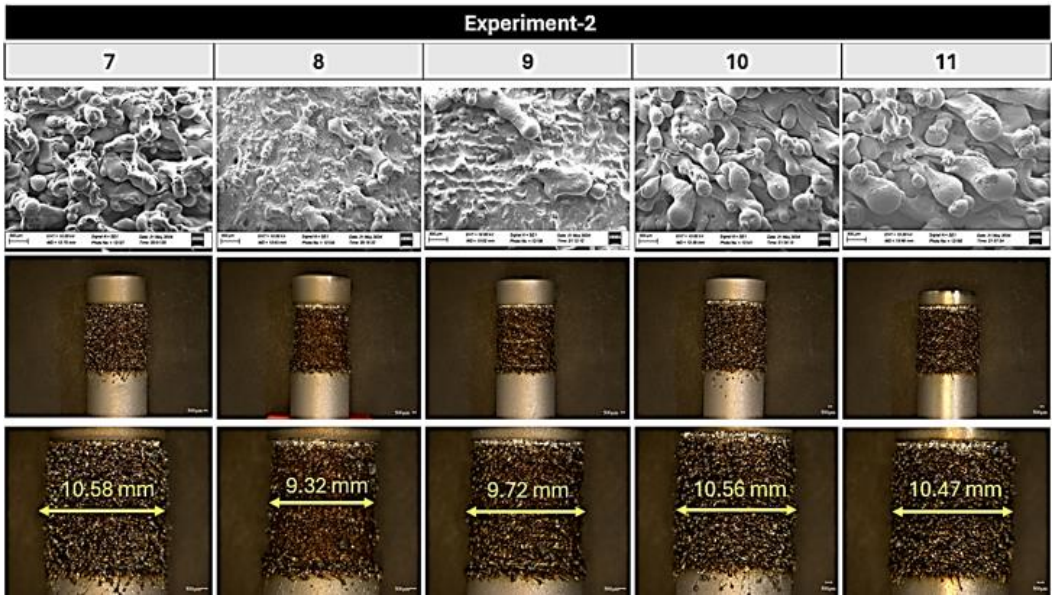
Insertion and Pull-out Tests

Refinements in gripping mechanics transitioning from standard clamps to serrated V-clamp grips were essential for data validity.

- DOE 2: Samples 10 and 11 (negative overlap) exhibited the highest insertion forces (33,419 N and 27,786 N, respectively). Conversely, samples with positive overlap (8 and 9) showed negligible pull-out resistance due to diameter reduction as shown in Figure.3b.
- DOE 3: Optimized parameters confirmed the efficacy of the process, with Sample 12 achieving the highest insertion force (32,493 N) and pull-out force (4,047 N). The results demonstrate that laser-induced surface roughening and diameter expansion significantly enhance the mechanical interlocking and bond strength of interference-fit connections.



(a)



(b)

Fig.1. SEM and optical images for design of experiments of (a) DOE-1 and (b) DOE- 2.

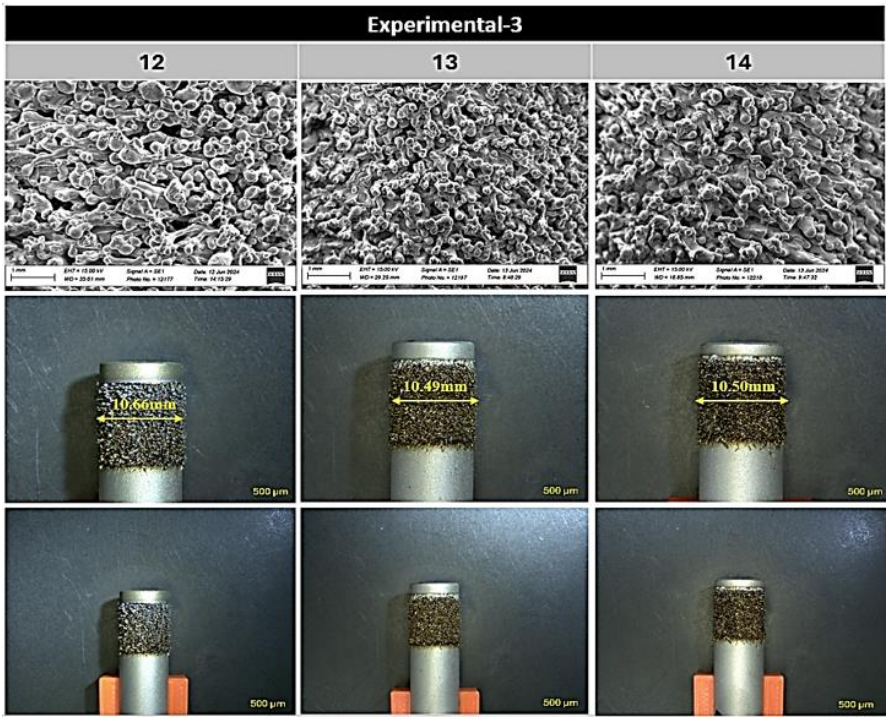


Fig.2. SEM and optical images for design of experiments 3.

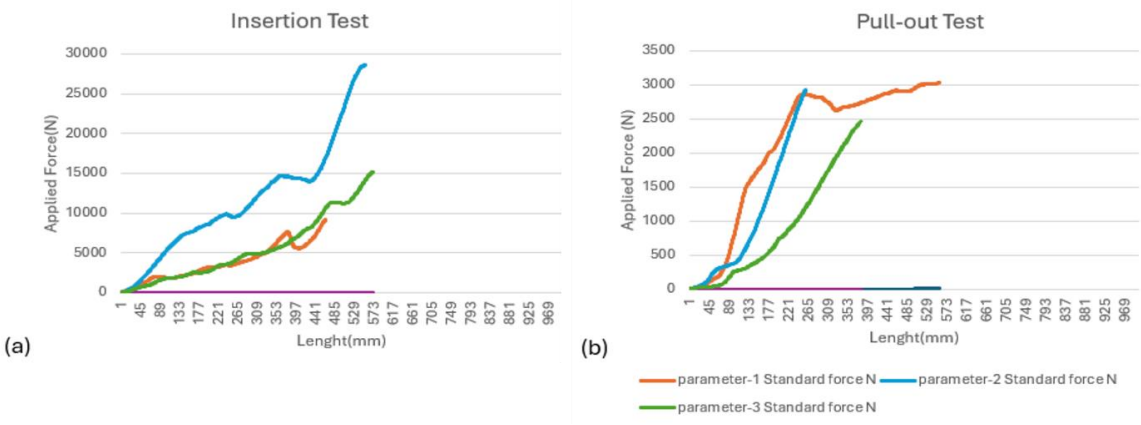


Fig. 3. Force versus displacement graphs for the (a) insertion and (b) pull-out test.

Conclusion

This investigation demonstrates that CO2 laser texturing is a viable method for modifying the mechanical performance of 316L stainless steel interference fits. The overlap percentage is the critical governing parameter: negative overlap facilitates diameter increases necessary for high-strength bonds, while positive overlap leads to material loss and reduced fit integrity. Furthermore, accurate characterization of these highly textured, cylindrical surfaces requires 3D digital microscopy rather than traditional profilometry. Future work should focus on stabilizing laser power delivery and exploring the scalability of these parameters for diverse industrial geometries.

References

[1] J. D. Majumdar and I. Manna, "1994 Fall Meeting Combines Excitement Over Research Advancements with Concern Over Future Direction," MRS Bulletin, vol. 20, no. 3, pp. 47–62, Mar. 1995, doi: https://doi.org/10.1557/s0883769400044420.

[2] B. Mao, A. Siddaiah, Y. Liao, and P. L. Menezes, 'Laser surface texturing and related techniques for enhancing tribological performance of engineering materials: A review', J. Manuf. Process., vol. 53, pp. 153–173, May 2020, doi: 10.1016/j.jmapro.2020.02.009.

[3] J. A. Wahab, M. J. Ghazali, W. M. W. Yusoff, and Z. Sajuri, 'Enhancing material performance through laser surface texturing: a review', Trans. IMF, vol. 94, no. 4, pp. 193–198, Jul. 2016, doi: 10.1080/00202967.2016.1191141.

[4] M. Yasseen, A. Obeidi, B. Eng, and S. Dermot Brabazon, "Laser processing of metallic surfaces for controlled micro-texturing and metallic bonding," 2018. Accessed: Jun. 24, 2024. [Online]. Available: https://doras.dcu.ie/22172/1/Final.pdf

[5] R. A. Alsaigh, 'Enhancement of Surface Properties Using Ultrashort-Pulsed-Laser Texturing: A Review', Crystals, vol. 14, no. 4, p. 353, Apr. 2024, doi 10.3390/cryst14040353.

[6] J. Nagpal, R. Rana, R. Lal, R. Muttanna Singari, and H. Kumar, 'A brief review on various effects of surface texturing using lasers on the tool inserts', Mater. Today Proc., vol. 56, pp. 3803–3812, 2022, doi: 10.1016/j.matpr.2022.01.272.

[7] A. Cholkar et al., 'Advances in laser-based surface texturing for developing antifouling surfaces: A comprehensive review', Appl. Surf. Sci. Adv., vol. 18, p. 100513, Dec. 2023, doi: 10.1016/j.apsadv.2023.100513.
[8] Outokumpu, Handbook of Stainless Steel, (2013) 1–89.
[9] M. A. Obeidi, E. McCarthy, L. Kailas, and D. Brabazon, 'Laser surface texturing of stainless steel 316L cylindrical pins for interference fit applications', 2018. Accessed: May 03, 2024. [Online]. Available: https://linkinghub.elsevier.com/retrieve/pii/S0924013617304156
[10] J. Madej and M. Śliwka, 'Analysis of Interference-Fit Joints', Appl. Sci., vol. 11, no. 23, p. 11428, Dec. 2021, doi: 10.3390/app112311428.

Improvement of thin-walled semi-rigid beam-to-column connections in rack structures

Mirjana Piskulic[1], Rodoljub Vujanac[1*], Snezana Vulovic[2]

[1]*Faculty of Engineering, University of Kragujevac, Kragujevac, Serbia, mirjana.piskulic@kg.ac.rs, 0009-0005-7199-1280, vujanac@kg.ac.rs, 0000-0002-8215-5668*

[2]*Institute of Information Technologies, University of Kragujevac, Kragujevac, Serbia, vsneza@kg.ac.rs, 0000-0001-5784-0906*

[*]Corresponding author: vujanac@kg.ac.rs

Abstract

In storage systems, a crucial aspect of pallet rack behavior is the structural performance of cold-formed thin-walled steel profiles, which is heavily dependent on the characteristics and load-bearing capacity of beam-to-column connections (BCCs). This research represents a starting point that evaluates a shift from a traditional high-stiffness welded joint over a weaker bolted one to a newly developed, optimized welded solution, driven by global steel and labor cost changes. The aim is to verify whether all these beam changes, achieved by an advanced welded joint and stronger beam-end connector (BEC), can compensate for weakened uprights. Using an analytical framework based on FEM regulations and EN standards, this research assesses global stability and first-order analysis in the rack structure. Results show that this optimization ensures that all parameters are within the safe limits. However, while this analysis establishes the analytical feasibility of the new connection, it requires further validation, as a necessary part of the experimental and numerical analysis, to characterize the non-linear response and local stability of the optimized connection.

Keywords: *thin-walled structures, beam-to-column connection, semi-rigid connections, UN SDG 9.*

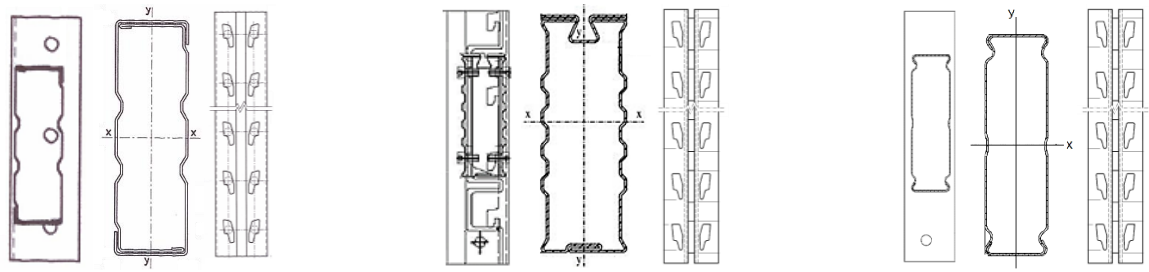
1. Introduction

In global analysis of pallet racks, connections are generally classified according to rotational stiffness and moment capacity. Therefore, European standard EN 1993-1-8 prescribes three types of connections: rigid, semi-rigid and pinned. Semi-rigid nature of BCCs governs the structural response of pallet racks. Unlike idealized rigid or pinned, semi-rigid connections exhibit moment-rotation (M-θ) behavior that significantly influence global stability, due to high nonlinearity and strong dependence on parameters such as: type of BEC, weld position on BEC, beam profile height and upright profile thickness [1]. Permanent shifts in global steel prices and production costs have required constant evaluation of connections. While earlier welded connections offered high stiffness, previously mentioned economic conditions led to attempts to use bolted solutions despite their reduced stiffness. The current optimization trend aims to restore high rotational stiffness through the reinforced BEC with a welded joint, allowing the use of lighter uprights but with a higher load capacity, without affecting structural stability. This is particularly emphasized in the down-aisle direction, where the dominant influence of BEC and BCC was analyzed per FEM 10.2.02 (Appendix B and F) [2–4]. Initially, first-order analysis is used to verify whether the recovery of connection stiffness can successfully compensate for weakened uprights while ensuring that global stability parameters remain within safe limits. Future research will focus on experimental verification of (M-θ) response for developed BCC to confirm analytical predictions,

as well as the advanced numerical modeling required to analyze connections as an alternative to expensive and time-consuming experiments.

2. Analytical approach

Considering the beam as a main part of the racking structure, bolted and welded joints are commonly used between the beam profile and the BEC. Starting from the traditional welded joint between these two parts with a weaker BEC, as shown in Figure 1 a), an attempt at development went across a stronger BEC but a weaker bolted connection and a weakened upright by additional perforation, as shown in Figure 1 b). As illustrated in Figure 1 c), further enhancement will consider keeping the changed stronger BEC but reverting to the earlier welded solution with the beam profile.



a) b) c)

Figure 1. BEC, beam profile and BCC: a) RS130-S80/140B, b) R140L-S80ML and c) RT130E-S80ML [5, 6].

This approximate analytical analysis of semi-rigid BCCs progress will be conducted in elastic zone due to complexity of these connections. BEC and beam profile parameters were modified, but beam level height and applied actions were kept constant in all analyzed models. Elastic critical value of vertical load V_{cr} was determined as the minimum among calculated for each beam level, for the purpose of calculating the amplification factor, acc. to Appendix B [4]. If it is lower than 3,33λ, although valid for this analysis, with λ as a slenderness ratio, for this purpose also normalized to unity, whereas second-order effects are treated indirectly, still requires further analyses. Since the first beam level is obtained as equivalent for V_{cr}, it is given as follows:

$$V_{cr_0} = \frac{K_{cc} \cdot h_1 + E \cdot I_{cc}}{\left[\frac{K_{cc} \cdot h_1}{2} + E \cdot I_{cc}\right] \cdot \theta_1 + \frac{\Sigma W \cdot h_1^2}{12 \cdot E \cdot I_{cc}} (K_{cc} \cdot h_1 + 4 \cdot E \cdot I_{cc})} \quad (1)$$

where: K_{cc} is total base flexibility, h_1 is height of the first beam level, E is Young's modulus, I_{cc} is total moment of area of upright, θ_1 is rotation and ΣW is total load on a rack.

To allow the elastic critical load to serve as a direct indicator of the global stability reserve for each configuration, according to Appendix F [4], the design vertical load V_{sd} was normalized to unity. Based on these values the amplification factor β is calculated as following, taking into account second-order effects:

$$\beta = \frac{V_{cr}}{V_{cr} - V_{sd}} \quad (2)$$

While the design moment in BEC M_{sd_2} for semi-rigid bases is given as follows:

$$M_{sd_2} = \frac{W_d \cdot L}{12} \cdot \frac{\beta_\theta}{1 + \frac{2 \cdot E \cdot I_b}{k_b \cdot L}} \cdot \frac{\Phi \cdot W_d \cdot h \cdot (2 \cdot n_s - 1)}{4} \cdot \beta \quad (3)$$

where: W_d is total design load on beam, L is beam span, β_θ is end rotation factor for non-uniform load, I_b is second moment of area of beam, h is beam level height, n_s is number of beam levels and Φ as global sway imperfection included because it directly accounts for second-order analysis moments that must be resisted by BCCs.

According to FEM regulations, it is necessary to compare the design moment at mid-span and the maximal deflection to their respective ultimate (ULS) and serviceability limit state (SLS), where the design moment at mid-span M_{sd}, is directly governed by the effective stiffness of BCC k_e, and given as:

$$M_{sd} = \frac{W_d \cdot L}{8} \cdot \beta_m \cdot \left[1 - \frac{{}^2/_3 \cdot \beta_\theta}{\beta_m \cdot \left[1 + \frac{2 \cdot E \cdot I_b}{k_e \cdot L}\right]}\right] \quad (4)$$

The effective stiffness k_e is as following:

$$k_e = \frac{k_b}{1 + \frac{k_b \cdot h}{3 \cdot E \cdot I_c}} \quad (5)$$

where: β_{max} is bending moment factor for non-uniform load, I_c is second moment of area of upright and rotational stiffness of BCC is k_b obtained experimentally [7]. According to Eq. (4), lower connection stiffness is, smaller is the moment at its ends, inevitably increasing the moment in the middle of the beam, therefore increasing maximum deflection δ_{max}, evaluated to verify SLS, as follows:

$$\delta_{max} = \frac{5 \cdot W_{ser} \cdot L^3}{384 \cdot E \cdot I_b} \cdot \beta_\Delta \cdot \left[1 - \frac{{}^2/_3 \cdot \beta_\theta}{\beta_\Delta \cdot \left[1 + \frac{2 \cdot E \cdot I_b}{k_e \cdot L}\right]}\right] \quad (6)$$

where: W_{ser} is the total serviceability load per beam and β_Δ is a deflection factor for non-uniform loads.
Equations (1-6) show the interaction between BCC flexibility and the structural response. Including rotational stiffness in the calculation of design moment, second-order effects inherent in semi-rigid connections are indirectly considered. This approach is significant for thin-walled profiles, where even minor variations in connection geometry and joint position can lead to an increase in the effective stiffness and, consequently, in load-bearing capacity of the entire structure. Further analysis will show how these relationships are reflected across different connection types.

3. Results

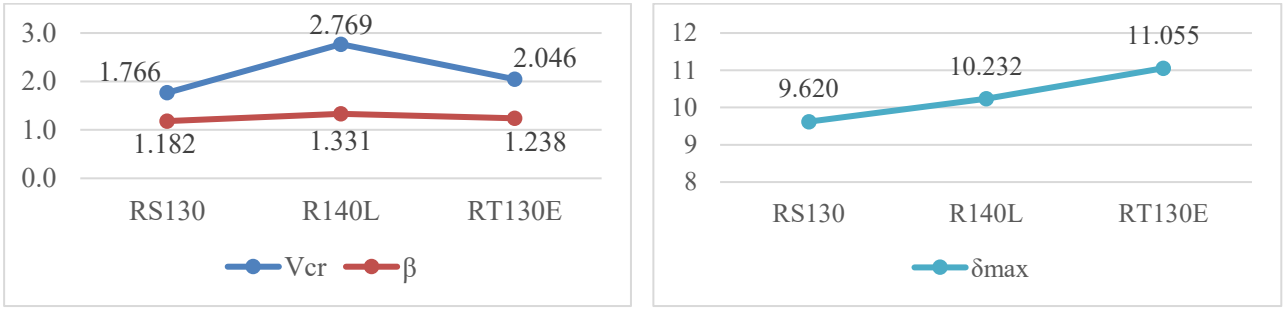
The analytical comparison of obtained results for ULS and SLS for considered connections is given in Table 1.

Table 1. Summary of characteristics and obtained results for BCC per ULS and SLS [5, 6].

	Parameter	RS130x40x1.5	R140L	RT130E
Characteristics	Connection type between beam and BCC	welded	bolted	welded
	Beam profile height, h_p [mm]	130	140	130
	Beam thickness, t [mm]	1,5	1,0	1,2
	Max. load-bearing capacity per beam, Q [kg]	3300	3000	3000
	Cross-sectional area of a beam, A [mm^2]	645	531	555
Obtained	Rotational stiffness, k_b [kNmm/rad]	122280	63420	122280 (predicted)
	Effective stiffness, k_e [kNmm/rad]	79451,423	41704,762	61019,764
	Elastic critical value of vertical load, V_{cr} [-]	1,766	2,769	2,046

Amplification factor, β [-]	1,182	1,331	1,238
Design moment at mid-span, M_{sd} [kNmm]	4213,649	4573,316	4306,614
Design moment of resistance, M_{Rd} [kNmm]	7081,378	7512,979	7192,938
Maximum deflection of a beam, δ_{max} [mm]	9,620	10,232	11,055
Limit deflection, δ_{lim} [mm]	13,5	13,5	13,5
Design moment of BEC, M_{sd_2} [kNmm]	4043,26	1833,87	3241,58

A comparison of the obtained results is given in Fig. 2, to reflect the increasing trend of the new welded joint.



a) b)

Figure 2. Comparative analysis of the obtained results for each BCC type for: a) elastic critical value of vertical load and amplification factor and b) maximum deflection.

4. Discussion and conclusions

Results presented in Table 1 confirm a direct relationship between the type of the beam, stiffness of the BCC and the corresponding parameters like elastic critical value of vertical load, amplification factor, distribution of bending moments in the beam and beam deflection. In the weakened bolted beam model, where, further, the BCC stiffness was significantly reduced even with a stronger BEC, the lowest effective stiffness was observed, inevitably increasing the moment in the mid-span of the beam to its highest value as well as beam deflection. Eliminating bolt-induced losses in beam type R140L and reverting the welded beam profile with a stronger BEC, the new type of beam, R130E, demonstrates that the welded joint with a predicted rotational stiffness, as in the first case with beam type RS130, enhances most of the considered parameters of the beam, remaining within the allowable ULS and SLS. Therefore, this analytical approach, carried out for beams in accordance with up-to-date regulations and standards, provides a reliable foundation for further analyses focusing on experimental validation and nonlinear numerical modeling as for the upright's behavior consideration.

Acknowledgements

This research is supported by the Ministry of Education, Science and Technological Development, Republic of Serbia, Grant 451-03-34/2026-03/200107.

References

1. Piskulic M, Vujanac R, Vulović S, Miloradovic N, Blagojevic M, Djordjevic Z. Structural Performance of Semi-Rigid Beam-to-Column Connections in Steel Storage Racks: A Review Focused on FEM Analysis. Metals. 2025 Dec 19;16(1):2. doi:10.3390/met16010002.

2. Lyu ZJ, Wu M, Huang Y, Song Y, Cui X. Assessment of the Dynamic Behavior of Beam-to-Column Connections in Steel Pallet Racks under Cyclic Load: Numerical Investigation. Adv. Civ. Eng. 2018 Jan; 2018(1). doi:10.1155/2018/9243216.
3. Yazici C, Gusella F, Özkal FM. Effect of beam-to-connector weld position on the flexural response of boltless rack connections. J Constr Steel Res. 2026 Feb;237. doi: 10.1016/j.jcsr.2025.110141.
4. FEM 10.2.02. The design of static steel pallet racking: racking design code. West Bromwich, England: Federation Europeene de la Manutention, Section X; 2001.
5. Dalmine Logistic Solutions. Pallet rack: RAPID-BLOC, Technical Manual. Piacenza, Italy; 2003.
6. Dalmine Logistic Solutions. Pallet rack: BI-BLOC, Technical Manual. Piacenza, Italy; 2022.
7. Vujanac R, Miloradović N, Vulović S, Pavlović A. A Comprehensive Study into the Boltless Connections of Racking Systems. Metals. 2020 Feb 20;10(2):276. doi:10.3390/met10020276.

Microvoid nucleation mechanisms in cold forming metal components

Milija Kraišnik[1], Mladomir Milutinović[2], Jelica Anić[1]

[1]University of East Sarajevo, Faculty of Mechanical Engineering, East Sarajevo, Republic of Srpska, BiH
milija.kraisnik@ues.rs.ba, 0000-0001-9672-7121, jelica.anic@ues.rs.ba, 0000-0002-1462-4637
[2]University of Novi Sad, Faculty of Technical Sciences, Novi Sad, Republic of Serbia, mladomil@uns.ac.rs, 0000-0002-2023-1215

Corresponding author: milija.kraisnik@ues.rs.ba

Abstract

Forming processes of metallic components significantly influence their service properties as well as subsequent processing stages, as they modify the material's microstructure and alter its mechanical characteristics. Conversely, during the forming process, the development and accumulation of microstructural damage are inevitable, which, upon reaching a critical threshold, lead to the initiation of cracks, fracture, or other macroscopic failures. The characterization of ductile damage evolution in metallic components can be based on both experimental and theoretical approaches. However, in both approaches, the generation of microvoids within the material's microstructure represents the initial stage. Based on reference sources, this paper analyzes various mechanisms of microvoid nucleation in metallic components during cold forming. Finally, experimental results concerning the identification of nucleation mechanisms in cylindrical specimens prepared from C45E ferrite-pearlite steel during the cold upsetting process are presented in a concise manner.

Keywords: cold metal forming, ductile damage mechanisms, micro void nucleation, SEM analysis, UN SDG 9

1. Introduction

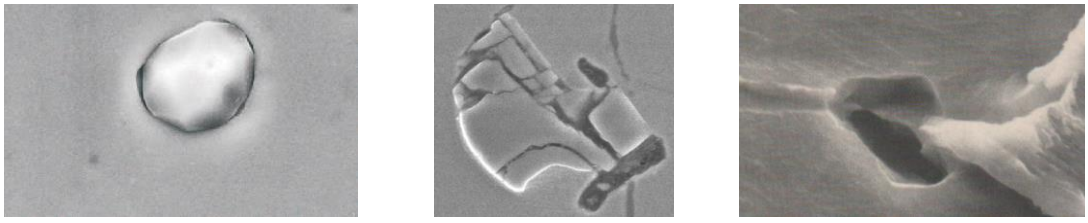
The phenomenology of material damage in forming processes has been the subject of extensive research [1], [2], [3], [4]. In this context, various methodological approaches have been employed to study the mechanisms associated with microstructural changes, which adversely affect the material's workability and can ultimately lead to crack initiation or fracture. The failure of polycrystalline metallic components is primarily associated with the evolution (nucleation, growth, and coalescence) of internal discontinuities (microvoids or microcracks), which reach macroscopic proportions at the moment of fracture. This is a progressive, irreversible, and highly complex process that occurs through the simultaneous action of multiple mechanisms across various scales. Consequently, it is quite challenging to predict material behavior during forming, including the damage accumulation level within the forming component. The level of accumulated microstructural damage depends on several factors, with the stress-strain state being the dominant one [5]. It should be emphasized that most polycrystalline metals undergo a significant amount of plastic strain prior to fracture. Researchers involved in the assessment of microstructural damage and fracture in metals and alloys during forming processes are primarily focused on nucleation mechanisms under tensile loading. However, the process of ductile damage evolution under compressive loading conditions is far less analyzed and understood. Given that compressive stress components dominate in most bulk forming processes, this fact represents a significant shortcoming.

2. Ductile damage

In a broader sense, ductile damage represents the undesirable evolution of one or more structural characteristics of a material that impairs its expected engineering performance. In the context of controlled damage evolution during forming processes, Hirt et al. [6] propose a more comprehensive definition. Ductile damage induces the degradation of physical and, specifically, mechanical properties of the material. Its evolution at the micro-scale is characterized by the creation of new surfaces. In structural materials, microvoids and microcracks are generated due to decohesion at grain or inclusion interfaces, or as a result of the brittle fracture of hard particles. The subsequent evolution of the initiated micro-damage progresses under thermo-mechanical loading, ultimately resulting in the fracture of the metallic component. This specific definition of ductile damage is based on continuum mechanics, specifically on the phenomena of microvoid nucleation and growth.

3. Nucleation of microvoids: A brief literature review

Engineering metals and alloys contain a large number of defects in their polycrystalline microstructure. Additionally, numerous materials contain hard and brittle second-phase particles. While some of these are deliberately introduced to tailor the microstructure (as in MMCs), others act as impurity phases with a detrimental effect. Each of these structural discontinuities contributes to the microvoid nucleation process to a certain extent. Nevertheless, during forming processes, microvoids are primarily generated at grain boundaries and at the interfaces between the soft metal matrix and difficult-to-deform secondary phase particles (e.g., inclusions or hard precipitate particles). Due to the heterogeneous mechanical properties of the microstructural constituents, nucleation is typically associated with strain incompatibility and local stress concentration at the micro-level [7]. Results from certain experimental studies provide a strong indication that the evolution of ductile damage is directly related to the volume fraction and type of secondary phase particles [8]. As stated by Benzerga [9], microvoid nucleation is strongly governed by several critical factors, including the matrix yield strength and work-hardening exponent, the morphology and strength of secondary phases, the loading direction, and the stress triaxiality. In materials with a soft metal matrix, microvoid nucleation predominantly occurs through the decohesion mechanism [10], [11] (Fig. 1a).



a) *b)* *c)*

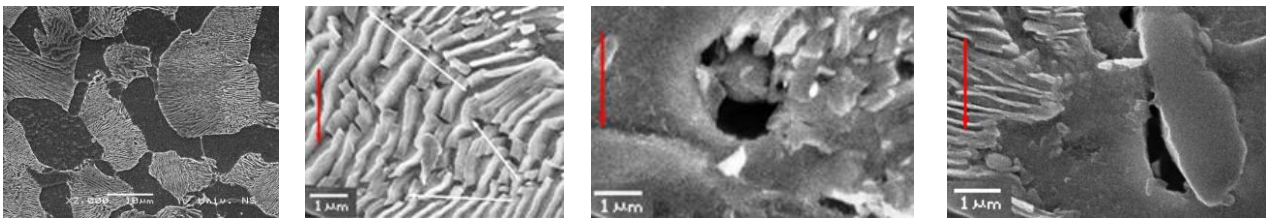
Figure 1. Microvoid nucleation mechanisms: a) decohesion [11], b) fracture of hard phases [11], c) triple junction of two grains of the metal matrix and the hard phase [12]

In contrast to the decohesion mechanism, which is attributed to the movement and coalescence of dislocation loops at the interface, fracture-induced nucleation occurs as a result of the highly restricted or non-existent local plastic strain of the secondary phase particles. This mechanism is present in many multiphase steels, where

nucleation occurs within the brittle and hard phases [11] (Fig. 1b). During the forming of dual-phase martensitic steels, microvoid nucleation can occur at the triple junctions of microconstituent interfaces, as documented in the study by Šiđanin and Miyasato [12] (Fig. 1c).

4. Experimental work

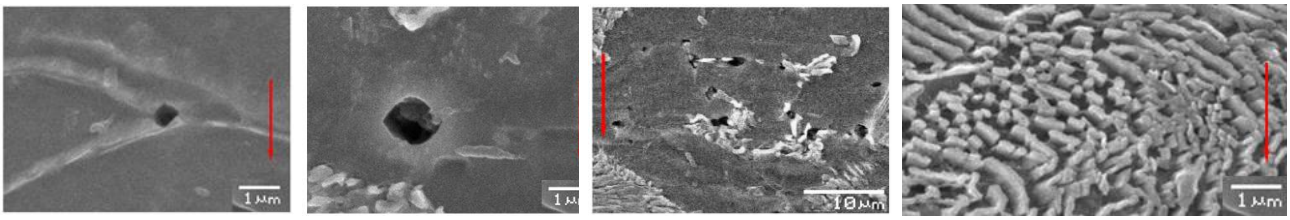
The experimental research was conducted on specimens prepared from C45E structural steel. Cylindrical specimens with initial dimensions of Ø25×20 mm were utilized to investigate the evolution of microstructural damage and identify microvoid nucleation mechanisms under high compressive loading. The specimens were upset between flat platens until a visible crack initiated on the free surface. The upsetting process was carried out incrementally at various strain levels (height reduction): ε_{h1}=0.38, ε_{h2}=0.75, ε_{h3}=1.10 and ε_{h4}=1.59.
The microstructure of the undeformed specimen is shown in Figure 2a. According to the ASTM E562 standard, it consists of ferrite grains (40%) and lamellar pearlite colonies (60%). At the first strain level (ε_{h1}=0.38), numerous microcracks were detected, resulting from the fracture of multiple adjacent cementite lamellae (Fig. 2b). Additionally, the activation of the microvoid nucleation mechanism by decohesion at the non-metallic inclusion/ferrite grain interface was observed (Fig. 2c,d).



a) ε_{h0}=0 undeformed specimen | *b) ε_{h1}=0.38; cementite lamellae cracking* | *c) ε_{h1}=0.38; decohesion spheroidal inclusion* | *d) ε_{h1}=0.38; decohesion longitudinal inclusion*

Figure 2. Undeformed microstructure and microvoid nucleation mechanisms at ε_{h1}=0.38 [1]

Upon reaching a strain level of ε_{h2}=0.75, the initiation of microvoids was detected at the triple junctions of the ferritic grain boundaries (Fig. 3a). Since the microvoids generated within the free ferrite were smaller than 1 µm, it can be concluded that a high degree of strain is required for their nucleation, subsequent growth, and coalescence. Furthermore, at a strain level of ε_{h2}=0.75, continuous nucleation and growth of microvoids were observed at the non-metallic inclusion/matrix interfaces (Fig. 3b). At a strain level of ε_{h3}=1.10, a high accumulation of microvoids was recorded, resulting from the decohesion mechanism at ferrite grain boundaries or the radial expansion of microvoids previously initiated by decohesion at the ferrite/pearlite interfaces (Fig. 3c). At the limiting strain of ε_{h4}=1.59, the cementite lamellae underwent extensive fragmentation, with many of them in certain regions of the sample undergoing transformation into sub-microscopic particles, predominantly smaller than 1 µm in size (Fig. 3d).



a) ε_{h2}=0.75; ferrite grain boundary triple junctions *b) ε_{h2}=0.75; microvoid growth* *c) ε_{h3}=1.10; decohesion and microvoid growth* *d) ε_{h4}=1.59; cementite lamellae cracking*

Figure 3. Microvoid nucleation mechanisms at higher strain levels [1]

5. Conclusions

The volume fraction of the metallic matrix and secondary phases, the morphology and distribution of inclusions, heat treatment history, stress state, mechanical properties, and loading orientation are critical factors governing the activation of various microvoid nucleation mechanisms in metallic components during cold forming. Experimental investigations, conducted via SEM analysis, revealed that the microstructural degradation in C45E steel resulted from the simultaneous activation of multiple microvoid nucleation and growth mechanisms. The cracking of cementite lamellae emerged as the dominant micro-damage mechanism. A significant extent of microstructural damage resulted from the decohesion mechanism at the interfaces between ferrite grains and pearlite colonies. Microvoid generation at the triple junctions of the microconstituents was found to be negligible. Fracture of non-metallic inclusions was not observed. Generally, microvoid nucleation is a continuous process occurring throughout all stages of the cold forming of metallic components.

References

1. Kraišnik M, Čep R, Kouřil K, Baloš S, Antić A, Milutinović M. Characterization of microstructural damage and failure mechanisms in C45E structural steel under compressive load. Crystals. 2022;12:426.
2. Qayyum F, Umar M, Elagin V, Kirschner M, Hoffmann F, Guk S, Prahl U. Influence of non-metallic inclusions on local deformation and damage behavior of modified 16MnCrS5 steel. Crystals.2022;12:281.
3. Wang X, Chen JG, Su G, Li HY, Wang C. Plastic damage evolution in structural steel and its non-destructive evaluation. Journal of materials research and technology. 2020;9,2:1189-1199.
4. Gerstein G, Besserer HB, Nürnberger F, Barrales-Mora, LA, Shvindlerman LS, Estrin Y, Maier HJ. Formation and growth of voids in dual-phase steel at microscale and nanoscale levels. Journal of materials science. 2017;52:4234–4243.
5. Kusche CF, Pütz F, Münstermann S, Al-Samman T, Korte-Kerzel S. On the effect of strain and triaxiality on void evolution in a heterogeneous microstructure-A statistical and single void study of damage in DP800 steel. Materials science and engineering A. 2021;799:140332.
6. Hirt G, Tekkaya AE, Clausmeyer T, Lohmar J. Potential and status of damage controlled forming processes. Production engineering, Research and development. 2020;14:1-4.
7. Horstemeyer MF, Gokhale AM. A void–crack nucleation model for ductile metals. International journal of solid and structures. 1999;36,33:5029–5055.
8. Dieter G, Kuhn H, Semiatin L. Handbook of workability and process design. ASM International, Materials Park Ohio. 2003.
9. Benzerga AA, Leblond JB. Ductile fracture by void growth to coalescence. Advances in applied mechanics. 2010;44:169–305.
10. Achouri M, Germain G, Dal Santo P, Saidane D. Experimental characterization and numerical modeling of micromechanical damage under different stress states. Materials & Design. 2013;50:207-222.

11. Tasan CC, Hoefnagels JPM, Ten Horn CHLJ, Geers MGD. Experimental analysis of strain path dependent ductile damage mechanics and forming limits. Mechanics of materials. 2009;41:1264-1276.
12. Šiđanin L, Miyasato S. Void nucleation and growth in dual phase steel wires. Materials science and technology. 1989;5;1200-1206.

Manufacturing Processes and Process Optimization

Force analysis for incremental forming of metal sheets

Jelica Anić[1], Mladomir Milutinović[2], Milija Kraišnik[1]

[1] *University of East Sarajevo, Faculty of Mechanical Engineering, East Sarajevo, Republic of Srpska, BiH, jelica.anic@ues.rs.ba, milija.kraisnik@ues.rs.ba*

[2]*University of Novi Sad, Faculty of Technical Sciences, Novi Sad, Republic of Serbia, mladomil@uns.ac.rs*

Corresponding author: jelica.anic@ues.rs.ba

Abstract

The paper provides a brief insight into the process of incremental forming of metal sheets. Essentially, this is a forming process that represents an unconventional processing method, primarily intended for individual production. At the beginning, the foundations of the process are presented. Then, based on reference sources, the development of the forming force was analyzed from the aspect of process parameters, material fracture indicators, modeling and prediction of its value, including various trends of change The analysis demonstrated the success of developing analytical models for force monitoring, clearly identifying the most influential process parameters on its growth during incremetal sheet forming process.

Key words: incremental sheet forming, forming force, ISF, SPIF, UN SDG 9

1. Introduction

Conventional sheet metal processing methods are applied to large production series where there are significant economic investments in the acquisition of equipment required to perform the process. For individual or small-series production, these methods are less acceptable due to cost-effectiveness. For this reason, the Incremental Sheet Forming (ISF) process was developed. Incremental sheet forming is an unconventional method of sheet metal processing, where expensive specific-shaped tools are replaced by universal, flexible shapes. The foundations of this technology were laid by Edward Leszak in 1967 with his patent for an apparatus that uses a spherical shape of the tool to forming sheet metal without the use of specially dies [1]. The process was designed to produce rotational shapes such as cones using simple tools. His work is considered the basis for the development of this process [2]. Significant application began in the 1990s in Japan with the development of CNC technology [3]. The application of automated CNC systems in processes like spin forming led to the evolution of these processes [4]. Emmens in his work provides a retrospective through an analysis of patents, where he highlights the work of Mason from 1978 as the moment of introduction of three-axis control of tool movement [1]. Reddy et al. associates point out that incremental sheet forming, due to low costs related to the necessary equipment, represents a significant technology for prototyping [5]. This technology has significant application in forming sheet metal blanks made of aluminum and other alloys in the production of automobiles, shipbuilding, pressure vessels, storage tanks, fuselages and wings of modern aircraft, etc [6]. In the continuation of the paper, the foundations of the incremental sheet forming process are given.

2. Incremental sheet forming

The forming of a workpiece in the incremental sheet metal forming process is achieved using a universal tool mounted on a CNC machine. The process itself begins with the creation of a 3D CAD model of the part to be obtained. Then, based on the obtained model, a toolpath is generated. The blank in the form of a metal sheet is placed in a rigid frame, i.e., a sheet holder. A tool of simple shape is used, with a spherical end, which is placed in the machine spindle. The tool moves along a defined path in the direction of the X and Y axes, while simultaneously penetrating along the Z axis. Z axis. The tool circles layer by layer, drawing out the material until the required part geometry is achieved. The two most common variants of the process are SPIF (Single Point Incremental Forming), where the tool acts on the free surface of the sheet, and TPIF (Two-point Incremental Forming), which includes additional support in the form of a mold or a static support, which helps in more precisely defining the internal geometry. In addition to the mentioned incremental sheet forming procedures, so-called hybrid procedures are increasingly in use. The difference compared to classic procedures is that in hybrid procedures, instead of supports, the pressure of an incompressible fluid is used. In the continuation of the paper, an analysis of the force during incremental forming of metal sheets was performed. This value is primarily significant for the safe use of machines that are not specially designed for incremental deformation processes. An example of such a machine is a CNC milling machine, which has been most commonly used in experimental research so far. Also, predicting the trend of force development is very significant so that control and optimization of the process itself can be achieved.

3. Different approaches to researching forming force in processes of incremental forming of metal sheets

Predicting forming forces is very important for successfully performing process optimization and protecting the machine on which the procedure is performed. Duflou conducted measurements showing that the axial force increases with an increase in the size of the vertical step, tool diameter or the wall angle of the workpiece. Of these parameters, the tool diameter has the greatest influence on force growth, while the vertical step has the least. It was also shown that it is possible to achieve reliable process optimization, given that the forming forces showed repeatability under the same geometric conditions [7]. The same topic was dealt with by Ambrogio, who proposed monitoring the force as an indicator of crack initiation, as there is a sharp drop in force when they appear [8]. Based on the obtained measurements, a system was developed that corrects parameters to stabilize the process before part failure occurs. Three different force trends were defined: 1. Steady-state curves: Upon reaching the maximum, the deformation force remains constant. The influence of sheet thickness reduction is compensated by material hardening. 2. Polynomial curves: After reaching the maximum force, a significant reduction in sheet thickness occurs. Then, after a few mm of depth, the force becomes stable again due to the harmony between material stretching and hardening. 3. Monotonically decreasing curves: A sharp reduction in sheet thickness occurs relative to material hardening, leading to fracture [8]. By developing an autonomous on-line system, Petek improved this concept [9]. The system is intended for analyzing the skewness of the force signal to identify a crack before it becomes visible to the naked eye. Positive values in the system indicate a healthy process, while negative values indicate the presence of cracks [9]. Aerens et al. defined practical regression formulas for predicting three force components for different materials by establishing a linear relationship between the logarithm of the force components and the sheet thickness. To enable successful estimation for new materials, proportionality was established between the forming force and tensile strength

[10]. Bagudanch showed through experimental research that a higher spindle speed reduces the force because friction causes an increase in the local temperature of the material. With an increase in tool diameter and vertical step, the force increases [11]. Li et al. [12] also worked on force prediction. The authors identified different force trends depending on the deformation mechanism. Initial force growth occurs due to the bending mechanism, while the further force trend depends on the balance between material hardening and sheet thinning. Material hardening increases the force, while sheet thinning decreases it. Also, an analytical model based on the upper bound method was implemented in MATLAB, intended for force prediction [12]. Saidi compared the incremental forming processes of workpieces made of aluminum and steel and concluded that the forming force of steel sheet is almost four times higher compared to aluminum sheet of the same thickness. Greater sheet thickness, a larger wall angle and vertical step increase the force [13]. Bansal [14] focused research on the development of a modified analytical model for the accurate prediction of the forming force. Forces are calculated based on the predicted stresses and geometry in the contact zone. It was determined that the new model reduces the maximum prediction error, giving more accurate results than Aerens' empirical model [14]. Chang et al. [15] also developed analytical models for predicting forces during incremental forming process, but also during the specific process of incremental hole flanging. The contribution of this work is based on investigating the phenomenon of periodic force fluctuation, caused by the variable elastic deflection of the deformed sheet. This analytical model also proved to be more efficient compared to Aerens' empirical model because it takes strain hardening into account [15]. The authors of the paper [16] also dealt with the influence of process parameters on the forming force. The results obtained were in agreement with previous research. A larger tool diameter, vertical step and wall angle yield higher force values. The influence of material thickness on the force value is very large. An increase from 1 mm to 2 mm in thickness leads to a fourfold increase in force [16]. The authors of work [17] also dealt with the same topic. The results confirmed that the tool diameter and the size of the vertical step have the greatest influence on the force value. An increase in the feed rate led to a decrease in force [17]. A systematic literature review related to forming force is presented in Kumar's study [18]. An analysis of the influence of temperature on the force was performed, showing that hybrid processes can lead to a significant reduction in force. Increasing the material strength affects the growth of the force. The correct choice of lubricant also significantly influences the stabilization of the force [18]. A significant contribution to researching the issue of force prediction is contained in study [19]. Namely, the authors concluded that an analytical model based on experimental research of the contact zone and deformation mechanisms allows for the reliable calculation of all components of the forming force [19].

4. Conclusions

Incremental sheet forming represents a significant technology for metal sheet processing in individual and small-series production. The application of simple tool shapes in obtaining various part shapes is extremely favorable from a commercial aspect. Analyzing the force generated in the incremental forming process is very important in preventing the occurrence of cracks on the part. Three force behavior trends are listed and their influence on the course of the forming process is described. In the past, various analytical methods and empirical formulas were developed that had high predictive potential regarding the identification of the forming force value. It was also shown that with an increase in tool diameter, vertical step and wall angle, the force increases.

An increase in feed rate, as well as the presence of temperature at the point of contact between the tool and the material, leads to a decrease in the force value.

References

1. Emmens WC, Sebastiani G, van den Boogaard AH. The technology of Incremental Sheet Forming—A brief review of the history. J Mater Process Technol. 2010;210(8):981-997. doi:10.1016/j.jmatprotec.2010.02.014.
2. Jackson K, Allwood J. The mechanics of incremental sheet forming. J Mater Process Technol. 2009;209:1158-1174. doi:10.1016/j.jmatprotec.2008.03.025.
3. Filice L, Fratini L, Micari F. Analysis of Material Formability in Incremental Forming. CIRP Ann. 2002;51(1):199-202. doi:10.1016/S0007-8506(07)61475-9.
4. Hagan E, Jeswiet J. A review of conventional and modern single-point sheet metal forming methods. Proc Inst Mech Eng Part B J Eng Manuf. 2003;217(2):213-225. doi:10.1243/095440503321148858.
5. Reddy NV, Lingam R, Cao J. Incremental Metal Forming Processes in Manufacturing. In: Nee AYC, editor. Handbook of Manufacturing Engineering and Technology. London: Springer-Verlag; 2015. p. 412-448. doi:10.1007/978-1-4471-4670-4_45.
6. Maji K, Kumar G. Inverse analysis and multi-objective optimization of single-point incremental forming of AA5083 aluminum alloy sheet. Soft Computing. 2019.
7. Duflou JR, Szekeres A, Vanherck P. Force Measurements for Single Point Incremental Forming: An Experimental Study. Adv Mater Res. 2005;6-8:441-448. doi:10.4028/www.scientific.net/AMR.6-8.441.
8. Ambrogio G, Filice L, Micari F. A force measuring based strategy for failure prevention in incremental forming. J Mater Process Technol. 2006;177(1-3):413-416. doi:10.1016/j.jmatprotec.2006.04.032.
9. Petek A, Kuzman K, Suhač B. Autonomous on-line system for fracture identification at incremental sheet forming. CIRP Ann. 2009;58(1):283-286. doi:10.1016/j.cirp.2009.03.111.
10. Aerens R, Eyckens P, Van Bael A, Duflou JR. Force prediction for single point incremental forming deduced from experimental and FEM observations. Int J Adv Manuf Technol. 2010;46(9-12):969-982. doi:10.1007/s00170-009-2160-2.
11. Bagudanch I, Centeno G, Vallellano C, Garcia-Romeu ML. Forming force in Single Point Incremental Forming under different bending conditions. Procedia Engineering. 2013;63:354–360.
12. Li Y, Liu Z, Lu H, Daniel WJT, Meehan PA. Experimental Study and Efficient Prediction on Forming Forces in Incremental Sheet Forming. Advanced Materials Research. 2014;939:313–321
13. Saidi B, Boulila A, Ayadi M, Nasri R. Experimental force measurements in single point incremental sheet forming SPIF. Mechanics & Industry. 2015;16(410).
14. Bansal A, Lingam R, Yadav SK, Reddy NV. Prediction of forming forces in single point incremental forming. Journal of Manufacturing Processes. 2017;28:486–493.
15. Chang Z, Li M, Chen J. Analytical modeling and experimental validation of the forming force in several typical incremental sheet forming processes. International Journal of Machine Tools and Manufacture. 2019;140:62–76.
16. Kumar G P, Suresh K. Experimental Study On Force Measurement For AA 1100 Sheets Formed By Incremental Forming. Materials Today: Proceedings. 2019;18:2738–2744.

17. Kumar A, Gulati V, Kumar P, Singh H, Singh V, Kumar S, Haleem A. Parametric Investigation of Forming Forces in Single Point Incremental Forming. Materials Today: Proceedings. 2020;24:611–617.
18. Kumar A, Gulati V, Kumar P, Singh H. Forming force in incremental sheet forming: a comparative analysis of the state of the art. Journal of the Brazilian Society of Mechanical Sciences and Engineering. 2019.
19. Liu F, Li Y, Cheng Z, Wang Z, Li F, Li J. Preliminary modelling of forming forces in three directions for incremental sheet forming process based on the contact area. Procedia Manufacturing. 2020;50:630–636.

Laser Engraving of Submillimeter Text

Petar Todorović[1]

[1]*Department for production engineering, Faculty of Engineering, University of Kragujevac, Serbia*
ORCID: https://orcid.org/0000-0003-3260-1655

Corresponding author: petar@kg.ac.rs

Abstract

The paper analyzes the possibility of realizing laser engraving of text with submillimeter dimensions. The experiment was performed on a redesigned 3d printer that was used as a laser engraver. The engraving text was generated using a Python script within the free CNC control software mikroCNC. A single line font was used for engraving, and the height of the text was 1.0mm, 0.75mm and 0.5mm. The experiment showed that the text is readable even for the smallest size of the engraved font.

Keywords: Text engrave, laser engrave, single line font, submillimeter engraving, UN SDG 4

1. Introduction

Laser engraving represents one of the most precise technologies for permanent marking of materials, widely used in industry, medicine, electronics, and many other fields. A particular challenge is the engraving of submillimeter text, i.e., text with a height smaller than 1 mm, typically in the range of 0.1 to 1 mm. In this domain, a number of limitations and requirements become prominent, related to font selection, process parameters, engraving technology, and the characteristics of the material being engraved.

One of the key aspects of laser text engraving is the choice of font type. Classical fonts, such as TrueType or OpenType fonts, which are predominantly used in printed and digital text display (Figure 1.a), are based on outlines (Figure 1.b). When applied in laser engraving, these outlines must either be traced as closed paths or filled (hatch engraving) (Figure 1.c), which significantly increases processing time and may lead to material overheating and loss of precision at small dimensions [1]. In submillimeter text, these effects become even more pronounced, as the laser line width may be comparable to or larger than the thickness of the characters defined by the font. This results in unclear engraving due to merging of nearby lines, making the text illegible.

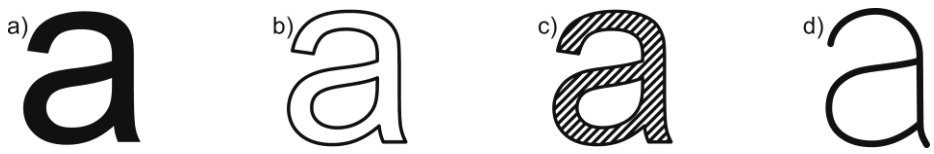


Figure 1. *TrueType font: a) original form, b) outline view, c) hatched view, and d) single line font.*

Due to these limitations, single line fonts are used for engraving (Figure 1.d), where each character is represented by a single line without defined thickness. This approach allows direct path tracing without the need for filling or contour processing, reducing engraving time and improving precision and readability. The

advantage of single line fonts is especially evident at very small text sizes, where the goal is to achieve maximum readability with minimal thermal load on the material.

When using single line fonts, the relationship between text height and the effective laser beam line width must be considered. The line width, determined by the laser spot size, depends on the laser wavelength, system optics, and focus, and typically ranges from several tens to several hundreds of micrometers (µm). For text to be readable, the character height must be several times larger than the line width. In practice, it is recommended that the ratio of character height to line width be at least 5:1 to 10:1 [3]. Otherwise, line overlap and loss of character definition may occur.

Figure 2 shows a comparison of engraved TrueType and single line fonts for different height-to-width (H/W) ratios: 20:1, 10:1, 5:1, and 3:1. It is evident that TrueType fonts remain readable for H/W ratios greater than 5:1, while single line fonts remain readable even at a ratio of 3:1 or slightly lower.

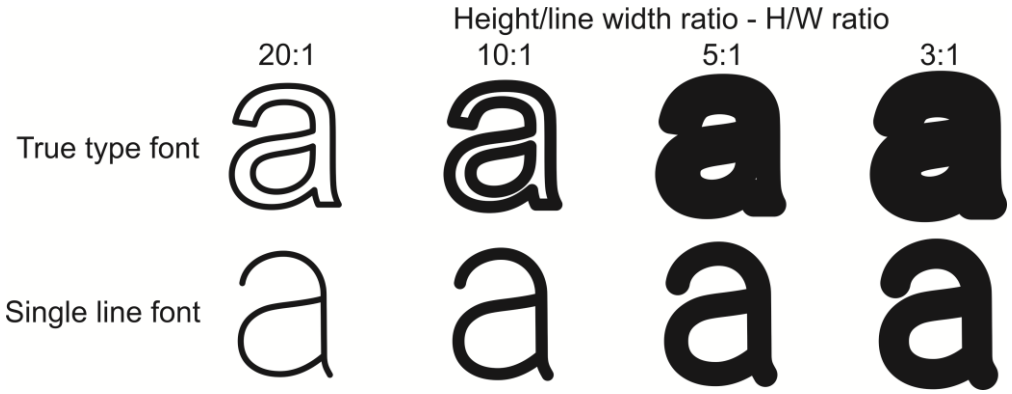


Figure 2. *Readability comparison of TrueType and single line fonts after engraving for different H/W ratios.*

Specific challenges in submillimeter laser engraving also include limitations in positioning accuracy, beam stability, and focusing quality. At font heights below 1 mm, even minimal positioning errors or mechanical vibrations can significantly degrade engraving quality. Additionally, diffraction effects and thermal expansion of the material can further affect the final result [4].

Moreover, laser–material interaction plays a crucial role. Materials with fine microstructure and good contrast after engraving (e.g., anodized aluminum, stainless steel, certain plastics, and coatings) are more suitable for submillimeter text. In contrast, materials with coarse structure or low contrast make readability more difficult [5]. Reflective materials can cause beam reflection and may require specific wavelengths or surface treatments, such as surface darkening.

Limitations of submillimeter engraving include the minimum achievable line width, limited optical and mechanical system resolution, and thermal effects such as melting, carbonization, or micro-deformations. These effects can distort characters and reduce readability, especially for complex fonts with fine details. Therefore, simple geometric character shapes with minimal detail and uniform lines are recommended.

2. Materials and Methods

A semiconductor laser Tree K20 was used as the laser source, with an optical power of 20 W and a wavelength of 450 nm ± 10 nm. The laser beam has a fixed focus at 40 mm and a spot size of approximately 0.15 mm. The laser source was mounted on a redesigned older-generation 3D printer with a robust mechanical structure. The complete control electronics of the 3D printer were replaced with an ETH-MCI motion controller based on Ethernet communication with the control computer [6], along with MST-109 microstep drivers for stepper motors [7]. After redesign, the 3D printer was transformed into a multifunctional device that can be used as a laser engraver, plotter, measuring machine, or light milling device depending on the mounted head (Figure 3.a).

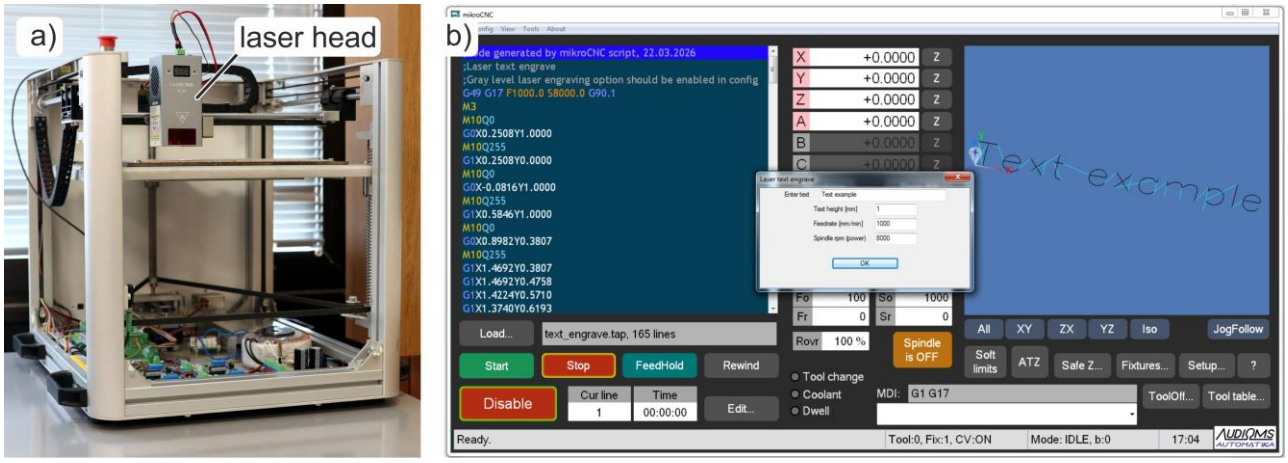


Figure 3. *a) Redesigned 3D printer as laser engraver and b) launching the wizard for generating G-code for text engraving in mikroCNC software.*

The free software mikroCNC [8], primarily intended for CNC machine control, was used to operate the laser engraver. Built-in support for Python 3.x [9] provides significant flexibility through user scripts for automation and customization. The integrated laser engraving wizard enables direct conversion of text into a single line font, generating standard G-code ready for direct control of the laser engraver (Figure 3.b).

For G-code generation, the function `gcodetext(file,text,x,y,height)` from the `textengrave` module (included in the mikroCNC Python 3.x interpreter) is used.

3. Results and discussion

Single line text engraving was performed on an MDF board with a thickness of 2.5 mm. Text heights of 1.0 mm, 0.75 mm, and 0.5 mm were engraved (Figure 5).



Figure 5. *Laser engraving of text: a) height 1.0 mm, b) height 0.75 mm, c) height 0.5 mm.*

It can be concluded that text with a height of 0.5 mm remains clearly readable (Figure 5.c). Given the laser spot size of 0.15 mm, the H/W ratio in this case is 3.33:1, confirming the readability of single line fonts even at very low H/W ratios. It should be noted that readability is negatively affected by the relatively coarse texture of the MDF material.

5. Conclusions

Laser engraving of submillimeter text represents a complex engineering challenge that requires careful font selection, optimization of process parameters, and appropriate material choice. Single line fonts represent an optimal solution for most applications in this domain, while classical outline fonts have limited applicability due to technological and physical constraints. In this study, an experiment of engraving submillimeter single line text was conducted using a redesigned 3D printer as a laser engraver with a fixed-focus 20 W laser source. The readability of engraved text with a height of 0.5 mm was confirmed at an H/W ratio of 3.33:1. This font size is very difficult to read with the naked eye, as it lies near the resolution limit of the average human eye.

Future research should include the analysis of the possibility of engraving text with dimensions below 0.5 mm, as well as the analysis of factors that can affect the accuracy of engraving: system stiffness, engraving speed, engraving power, font shape, etc. Different materials with different textures should also be considered to determine which material would be most suitable for submillimeter text engraving.

Acknowledgements

This paper is supported by the project No. 451-03-34/2026-03/200107, Ministry of Science, Technological Development and Innovation, Republic of Serbia.

References

1. Steen WM, Mazumder J. Laser material processing. London: Springer; 2010.

2. Ready JF. LIA handbook of laser materials processing. Orlando: Laser Institute of America; 2001.

3. Powell J. CO_2 laser cutting. London: Springer; 1998.

4. Ion JC. Laser processing of engineering materials. Oxford: Elsevier; 2005.

5. Dubey AK, Yadava V. Laser beam machining – a review. Int J Mach Tools Manuf. 2008;48(6):609–628.

6. ETH-MCI Ethernet CNC Motion Controller User's Manual, https://www.audiohms.com/download/eth-mci/eth-mci-en.pdf (accessed 22.3.2026.)

7. MST-109 Mikrostep Stepper Motor Drive User's Manual, https://www.audiohms.com/download/MST-109_man_en.pdf (accessed 22.3.2026.)

8. mikroCNC Software for Controlling CNC Machines – Instructions for Installation, Setup and Use, https://www.audiohms.com/download/mikrocnc/mikroCNC_en.pdf (accessed 22.3.2026.)

9. mikroCNC Scripting – User Scripting Support Documentation, https://www.audiohms.com/download/mikrocnc/mikroCNC_scripting_en.pdf (accessed 22.3.2026.)

Radiotracers as Advanced Tools for Industrial Process Diagnostics and Optimization

Srđan Vuković[1*], Danijela Vuković[1], Aleksandar Vuković[2], Vesna Gojković Cvjetković[1], Svetlana Pelemiš[1]

[1]University of East Sarajevo, Faculty of Technology Zvornik, Bosnia and Herzegovina, srdjan.vukovic92@gmail.com, 0000-0001-7573-5712, drajic1029@gmail.com, 0000-0002-1169-5755, vesna.gojkovic@yahoo.com, 0000-0003-1118-4565, alannica@gmail.com, 0000-0001-9682-5899
[2]University of Novi Sad, Faculty of Technical Sciences, Novi Sad, Serbia, sasaaco994@gmail.com, 0000-0003-0549-6183

Corresponding author: srdjan.vukovic92@gmail.com

Abstract
Radiotracers are highly reliable tools for diagnosing and optimizing complex industrial processes under real operating conditions. This short review summarizes the methodological basis and practical significance of radiotracer applications in industrial process monitoring, with emphasis on residence time distribution (RTD) analysis, flow validation, and identification of hydrodynamic anomalies. The paper is based on selected methodological sources and recent industrial case studies from mineral processing and wastewater systems. Particular attention is given to radiotracer selection, pulse injection, signal detection, and interpretation of tracer responses for estimating mean residence time, flow imbalance, bypassing, stagnant regions, and flowmeter deviations. Recent applications show that radiotracers provide highly sensitive and quantitatively reliable data for validating industrial measurements, improving water balance calculations, and supporting process optimization. The reviewed studies confirm that radiotracer techniques remain indispensable where conventional methods are insufficient or impractical. Their integration with digital monitoring, RTD-based modeling, and data-driven analysis further strengthens their relevance in contemporary industrial diagnostics and optimization.
Keywords: radiotracers; industrial process diagnostics; residence time distribution; process optimization; UN SDG 9

1. Introduction

Radiotracer techniques have been used in industrial problem-solving for more than half a century and remain among the most powerful methods for diagnosing and optimizing complex process systems. Their main advantage is the ability to provide information on plant operation under real process conditions, often without interrupting production. Because of the high sensitivity of radiation detection and the possibility of external measurements through process equipment, radiotracers are especially valuable in opaque or inaccessible systems where conventional techniques cannot provide sufficiently reliable hydrodynamic information [1,2].
Among radiotracer-based approaches, residence time distribution (RTD) analysis has become one of the most important tools for industrial diagnostics. RTD investigations are widely used to characterize flow behavior,

identify bypassing and stagnant regions, evaluate mixing performance, and support process simulation and control. According to IAEA sources, radiotracer RTD techniques have been extensively applied to optimize processes, solve operational problems, improve product quality, reduce energy consumption, and minimize pollution in petroleum, petrochemical, mineral-processing, and wastewater-treatment systems [1,2].

Recent studies confirm that radiotracer methods remain highly relevant in modern data-driven industry. In mineral processing, they have been used to detect feed flowrate imbalances, estimate mean residence times in flotation circuits, and assess particle-size segregation under industrial conditions [3]. Radiotracer transit-time measurements have also been highlighted as highly accurate reference tools for on-site validation of industrial flowmeters, with reported uncertainties around 1%, which is particularly relevant within the Mining 4.0 framework [4]. RTD-based hydrodynamic characterization has likewise been reported for large industrial flotation cells [5]. The aim of this short review is therefore to present radiotracers as advanced tools for industrial process diagnostics and optimization.

2. Methodological Basis of Radiotracer Diagnostics

Radiotracers are well suited for industrial diagnostics because they allow investigation of real process systems under operating conditions while using very small tracer quantities. In industrial practice, they are particularly useful for troubleshooting, process optimization, flow characterization, and validation of mathematical or computational models when conventional measurements are limited or unreliable [1,2].

The methodological core of many investigations is the RTD approach. In a typical RTD experiment, a tracer is introduced as a short pulse at the inlet of a system, and its concentration-time response is measured at the outlet or between selected detection points. After background correction, radioactive decay correction, and normalization, the measured signal is treated as the RTD of the traced material or, more generally, as the impulse response between selected points of the system [1,2]. The analysis commonly includes moment calculations, with the mean residence time (MRT) defined as the first moment of the RTD curve, while the spread of the distribution is described through variance or standard deviation [2]. For systems of volume V and volumetric flowrate Q, the theoretical holding time is commonly expressed as V/Q, which provides a useful reference for comparison with the experimentally determined MRT [2,6].

RTD analysis can diagnose several practically important anomalies. For normal process conditions, the experimentally determined MRT is expected to be close to the theoretical holding time; significant deviations, long tails, or irregular early responses may indicate bypassing, stagnant regions, non-ideal mixing, or exchange between flowing and poorly exchanged zones [1,2,6]. Reliable interpretation therefore depends not only on RTD moments, but also on appropriate flow modeling, knowledge of process conditions, and correct placement of injection and detection points. Recent studies further show that radiotracer diagnostics can extend beyond classical RTD interpretation to the validation of flow measurements and the identification of flow imbalance in parallel process units [3,4].

3. Representative Industrial Applications

Representative applications clearly demonstrate the diagnostic value of radiotracer techniques in systems where direct observation of hydrodynamic behavior is difficult or impossible. In mineral processing, radiotracers have proven particularly useful for flotation circuit characterization. Diaz and Barrientos showed that pulse radiotracer measurements can be used to determine feed flowrate imbalances in parallel flotation lines by

calculating mean residence times and effective flow distribution. In their industrial case study, the rougher circuit exhibited an uneven split of feed, with about 38% of the flow directed to lines 2 and 3 and only 24% to line 4, while in the scavenger stage the distribution was about 59% toward line 1 and 41% toward line 2 [3]. The same study also showed particle-size segregation, with the inlet machine of the rougher stage displaying a bias of 11.4% toward fine particles [3]. Additional work on large industrial flotation cells has likewise confirmed that RTD measurements and modeling remain valuable for full-scale hydrodynamic characterization [5].

A second important field is the validation of industrial flow measurements. Barrientos and Diaz showed that the radiotracer transit-time method can serve as a highly accurate reference tool for on-site flowmeter verification in mineral-processing systems [4]. In recirculation pumping stations, deviations between online flowmeter data and radiotracer-based measurements ranged from 6.91% to 22.55%, while only 36% of evaluated measurements in one industrial example were within an acceptable 5% error margin [4]. These findings demonstrate that significant measurement errors may remain undetected if conventional instrumentation is used without independent validation.

Radiotracer methods are also highly relevant in wastewater treatment and related multiphase process units. According to IAEA case studies, RTD experiments in wastewater treatment plants can be used to characterize bypassing, stagnant regions, and non-ideal flow structures in clarifiers, aeration tanks, and digesters [1,2]. In one documented settling-tank case, a primary clarifier of 5000 m^3 investigated with Br-82 exhibited a stagnant zone corresponding to approximately 25% of the tank volume [2]. Similarly, in packed beds and packed towers, radiotracer RTD testing has revealed liquid maldistribution that conventional gamma scanning could not resolve sufficiently, thereby supporting more accurate diagnosis of process underperformance [1,2].

4. Advantages, Limitations and Future Perspectives

Radiotracer techniques offer several major advantages for industrial diagnostics. Their principal strength is the possibility of investigating real process systems under operating conditions while using only very small tracer quantities because of the high sensitivity of radiation detection [1,2]. Gamma-emitting radiotracers can often be measured externally through pipes and vessel walls, which makes them particularly useful in opaque, large-scale, and difficult-to-access industrial installations [1,2]. In addition, radiotracer methods can provide highly reliable reference data for flow validation, hydrodynamic diagnosis, and process optimization, as illustrated by recent applications in flotation systems and Mining 4.0-related flow assessment [3–5].

At the same time, these methods have important limitations. Since radiotracers emit ionizing radiation, radiation protection measures, regulatory compliance, and trained personnel are essential in all phases of their use [1,2]. Another limitation concerns tracer selection itself: the radiotracer must behave representatively with respect to the investigated material; otherwise, adsorption, decomposition, or phase transfer may compromise the reliability of the results [2]. Accurate interpretation also depends on process knowledge, detector geometry, data treatment, and appropriate RTD or systemic modeling [1,2].

From a future perspective, radiotracer methodology is likely to gain additional relevance through integration with computational fluid dynamics, digital monitoring systems, and data-driven industrial analytics. The IAEA guidebook emphasizes the value of combining RTD tracing with model-based analysis [1]. More recent Mining 4.0-oriented studies suggest that historical radiotracer data may be combined with online flowmeters and advanced analytics to improve long-term accuracy, detect flowmeter drift, and support predictive maintenance and process optimization [4].

5. Conclusions

Radiotracer techniques remain highly valuable tools for industrial process diagnostics because they provide direct and reliable insight into flow behavior under real operating conditions. As shown in the reviewed studies, their application is particularly effective in RTD analysis, the detection of bypassing and stagnant regions, the assessment of flotation circuit performance, and the validation of industrial flow measurements [1–5]. These capabilities make radiotracers especially important in systems where conventional methods are insufficient or impractical.

The analyzed literature further confirms that the significance of radiotracer techniques extends beyond classical troubleshooting. In modern industrial environments, they support process optimization, improve data reliability, and provide a strong basis for model validation and informed engineering decisions [1,3–5]. Although their application requires radiation protection measures, regulatory compliance, and specialized expertise, radiotracers continue to represent advanced and indispensable tools for industrial diagnostics, with growing relevance in the context of digital monitoring, CFD-supported interpretation, and data-driven process optimization [1,4].

Acknowledgments: This paper is funded through the EIT's Higher Education Initiative A-SIDE project, coordinated by EIT RawMaterials, funded by the European Union

References

[1] International Atomic Energy Agency. *Radiotracer applications in industry: a guidebook*. Vienna: International Atomic Energy Agency; 2004. Technical Reports Series No. 423.

[2] International Atomic Energy Agency. *The radiotracer residence time distribution method for industrial and environmental applications: material for education and on-job training for practitioners of radiotracer technology*. Vienna: International Atomic Energy Agency; 2008. Training Course Series No. 31.

[3] Diaz F, Barrientos NA. Application of radiotracers as tools to determine feed flowrate imbalances and particle size segregation in industrial flotation circuits. *Physicochem Probl Miner Process.* 2023;59(5):174817. doi:10.37190/ppmp/174817.

[4] Barrientos N, Diaz F. Optimizing industrial flow measurements in mineral processing: Utilizing radiotracers for enhanced data reliability within Mining 4.0. *Physicochem Probl Miner Process.* 2025;61(1):200742. doi:10.37190/ppmp/200742.

[5] Vinnett L, Yianatos J, Hassanzadeh A, Diaz F, Henríquez F. Residence Time Distribution Measurements and Modeling in an Industrial-Scale Siemens Flotation Cell. Minerals. 2023;13:678.

[6] Levenspiel O. Chemical Reaction Engineering. 3rd ed. New York: John Wiley & Sons; 1998.

Closing the Loop of the EURO-TITAN Process: Residue Valorisation, Wastewater Recycling and Development of Functional Materials

Project: Decarbonized Titanium Recovery from Aluminium and Titanium Production Residues, EURO-TITAN, 101135077, Horizon Europe, (01.01.2024. - 31.12.2027.)

Mitar Perušić[1], Duško Kostić[1], Nebojša Vasiljević[1], Jelena Vuković[1], Srećko Stopić[2], Maria Teresa Bellver Baca[3], Radislav Filipović[1,4], Vladimir Damjanović[4], Bengi Yagmurlu[5], Konstantinos Sakkas[6]

[1]Department for Process Engineering, Faculty of Technology Zvornik, University of East Sarajevo, Karakaj 34A, 75400 Zvornik, Bosnia and Herzegovina; Email: mitar.perušić@tfzv.ues.rs.ba; ORCID: 0000-0001-9335-1405, Email: dusko.kostic@tfzv.ues.rs.ba; ORCID: 0000-0002-4115-8571, Email: nebojsa.vasiljevic@tfzv.ues.rs.ba; ORCID: 0000-0002-3789-9975, Email: jelena.vukovic@tfzv.ues.rs.ba; ORCID: 0000-0001-8850-1640

[2]IME Process Metallurgy and Metal Recycling, RWTH Aachen University, Intzestraße 3, 52072 Aachen, Germany; Email: SStopic@metallurgie.rwth-aachen.de; ORCID: 0000-0002-1752-5378

[3]Sika Technology AG, Corporate R&D, Tüffenwies 16, 8048 Zürich, Switzerland; Email: bellverbaca.teresa@ch.sika.com; ORCID: 0000-0002-0825-5599

[4]Nova Alumina d.o.o. Zvornik, Karakaj bb, 75400 Zvornik, Bosnia and Herzegovina; Email: radislav.filipovic@birac.ba; ORCID: 0009-0000-9938-2499, vladimir.damjanovic@birac.ba; ORCID: 0000-0002-5375-440X

[5]Institute of Metallurgy, Clausthal University of Technology (Technische Universität Clausthal), Robert-Koch-Straße 42, 38678 Clausthal-Zellerfeld, Germany; Email: bengi.yagmurlu@tu-clausthal.de; ORCID: 0000-0002-5376-1677

[6]SE&C, Michalakopoulou 169, Athens, Greece; Email: sakkasdin@yaho o.gr; ORCID: 0000-0001-8249-307X

Corresponding author: mitar.perušić@tfzv.ues.rs.ba

Abstract

Work Package 11 (WP11) of the EURO-TITAN project addresses the final and decisive step in sustainable titanium recovery, closing the material and water loops. Following the reduction of red mud and tionite, and subsequent hydrometallurgical leaching, residual slags and wastewater streams are generated. This paper presents the integrated valorisation strategy developed within EURO-TITAN project, including residue characterization, development of innovative building materials, wastewater recycling, and transformation of

slag into functional low-cost sorbents. The results demonstrate that reduction-derived slags can serve both as supplementary cementitious materials and as efficient phosphate adsorbents, achieving removal efficiencies of approximately 90% under optimized conditions. The proposed framework establishes a near-zero-waste approach aligned with circular economy principles and strengthens the environmental performance of decarbonized titanium production.

Keywords: red mud, reduction, titanium slag, circular economy, adsorption, wastewater recycling, SDG 13.

1. Project Background and Objectives

The EURO-TITAN project develops a low-carbon impact route for titanium recovery from metallurgical and chemical residues. Hydrogen-based reduction enables iron removal while preserving titanium within the slag phase. Subsequent hydrometallurgical treatment transfers titanium into solution for further purification and powder production.

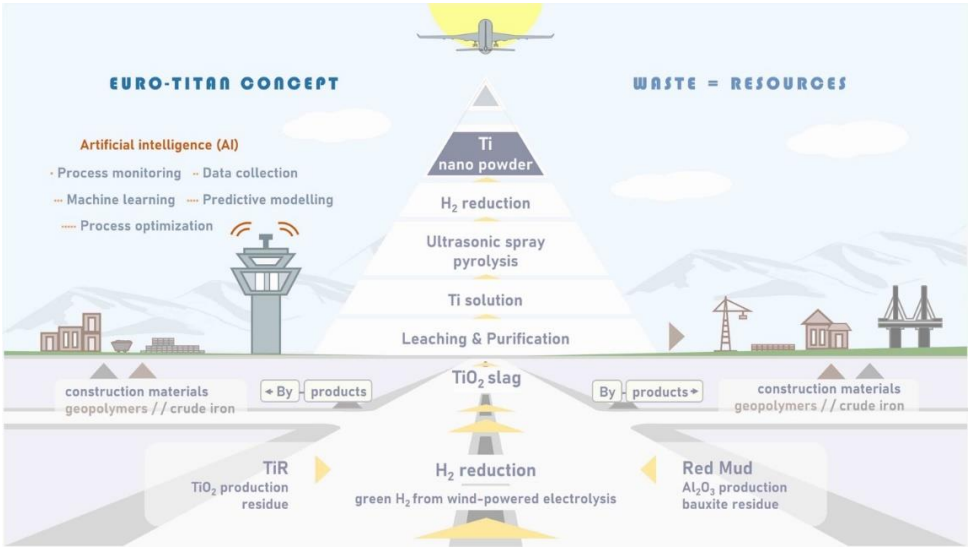


Figure 1. The EURO-TITAN project scheme [1]

However, sustainable metallurgy requires more than efficient extraction. Residual solids and process waters must be reintegrated into productive cycles. WP11 was therefore designed to close the loop of the EURO-TITAN process by converting residues into valuable materials and application by minimizing water consumption across the chain.

2. Methodology and Work Performed

Two primary feedstocks were investigated: red mud from the Bayer alumina process and tionite from TiO_2 production via the sulphate route. Both materials were subjected to reduction using carbon, hydrogen, and hydrogen plasma technologies.

Carbothermal reduction in a DC electric arc furnace successfully transformed iron oxides into metallic iron, enabling magnetic separation [2] The addition of CaO improved slag fluidity and promoted phase transformations, leading to Ti-enriched slag. Hydrogen reduction in tubular and rotary furnaces achieved

effective iron removal but produced metallic iron in powder form. Hydrogen plasma reduction proved particularly efficient, achieving deep iron reduction within short treatment times while maintaining titanium content within the slag matrix.

Subsequent high-pressure autoclave leaching under optimized conditions (150°C, elevated oxygen pressure, concentrated sulfuric acid) enabled titanium dissolution efficiencies approaching 97% for carbothermally reduced slag. Iron and aluminium were also efficiently transferred into solution, while silica largely remained in the solid residue, preventing gel formation [3,4].

These processes generated two key secondary material streams: mineral slag residues and acidic leachates, both addressed within WP11.

3. Key Results

3.1 Slag Characterization

XRD and ICP analyses confirmed complete reduction of hematite to metallic iron during hydrogen plasma treatment, while titanium remained stable in titanate or ilmenite phases. The slag obtained after reduction consisted primarily of Fe-oxides, Al_2O_3, SiO_2, and TiO_2. Leaching experiments revealed that oxygen pressure is a decisive parameter in titanium dissolution. Under optimized conditions, most Ti, Fe, and Al were dissolved, leaving $CaSO_4$ and SiO_2 as dominant crystalline phases in the residue. SEM-EDS analysis confirmed that titanium and iron were largely removed from the solid phase under intensified conditions.

3.2 Development of Building Materials

The chemical composition and partial amorphous character of the slag indicate potential suitability for use as a supplementary cementitious material. The presence of calcium (Ca), aluminium (Al), and silica (Si) containing phases suggests that the material may exhibit pozzolanic or latent hydraulic behavior under appropriate activation conditions. SIKA's future work will focus on evaluating the reactivity of the slag in cementitious systems through standardized tests, including compressive strength development, setting time, and durability assessment. Particular attention will be given to determining its influence on mechanical performance and long-term stability in mortar formulations. In parallel, alkaline activation using NaOH and sodium silicate solutions is planned to investigate the feasibility of geopolymer formation.

3.3 Wastewater Treatment

Hydrometallurgical processing generates acidic effluents containing dissolved metal ions, primarily Ti, Fe, and Al, along with residual acid. A combined treatment approach is currently under investigation, including neutralization, precipitation, filtration, and sorption steps. Particular attention is being given to the formation of calcium sulphate during neutralization, which may contribute to stabilization of dissolved species and facilitate solid-liquid separation. The objective of this treatment is to enable internal recycling of process water, thereby reducing fresh water demand and minimizing effluent discharge within the EURO-TITAN process chain.

3.4 Slag as Adsorbent for Phosphate Removal

Phosphate removal experiments demonstrate that both carbothermal red mud slag (CRMS/RMS) and hydrogen-plasma-reduced red mud slag (H2RMS) exhibit adsorption potential, with clear differences in performance

depending on material type and operating conditions. Among the tested fractions, the fine CRMS fraction (<150 µm) achieved the highest efficiency, reaching 74-86% removal, while raw slag and sieved residue showed significantly lower efficiencies (~30% and ~20%, respectively).

H2RMS exhibited enhanced adsorption behavior, achieving up to 88-89% phosphate removal under optimized process conditions. The adsorption process showed strong pH dependence, with maximum efficiency at acidic conditions (pH ≈ 2-3) and a sharp decline at higher pH values. Contact time studies indicated that equilibrium was reached after approximately 18 hours, with no significant improvement after 24 hours [5,6].

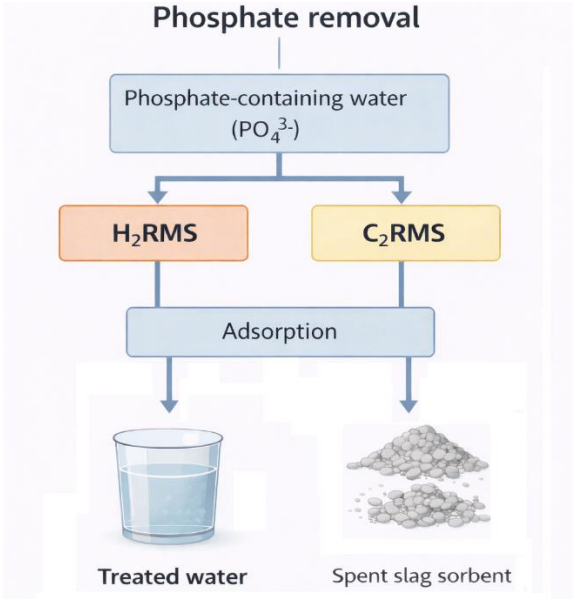


Figure 2. Phosphate removal [5]

Increasing sorbent dosage improved removal efficiency, reaching above 94% at 10 g/L and up to 96% at 20 g/L, although the improvement above 10 g/L became marginal.

4. Discussion and Impact

The integrated WP11 strategy establishes multiple valorisation pathways, including but not limited to:

- Iron is recovered during reduction, titanium is extracted through optimized leaching, residual slag is transformed into construction materials or used as adsorbent, and wastewater is treated and recycled.
- Hydrogen plasma reduction plays a central role, not only by reducing carbon emissions but also by producing a slag with favourable structural properties for secondary applications.
- This closed-loop framework has potential for reduction of landfill disposal also minimization of water consumption, and enhancement of the life-cycle performance of the overall titanium recovery chain.

5. Conclusions and Outlook

WP11 demonstrates that metallurgical residues generated during titanium production, under some conditions, can be transformed into valuable secondary products. Reduction and leaching processes enable efficient iron

removal and titanium recovery, while the remaining slag exhibits conditional technical suitability both as potential construction material precursor and as functional sorbent for phosphate removal.

By integrating residue valorisation and wastewater recycling into the titanium production chain, EURO-TITAN establishes a circular process model aligned with EU sustainability objectives and critical raw materials strategy.

Acknowledgements / Funding

This work was carried out within the framework of the EURO-TITAN project, funded by the European Union's Horizon Europe research and innovation programme under Grant Agreement No. 101135077.

The authors acknowledge the collaboration and support of the EURO-TITAN consortium partners: Géosciences Conseils (France), SEC (Greece), VIC (The Netherlands), BAM-Bundesanstalt für Materialforschung und -prüfung (Germany), RWTH Aachen University (Germany), MEAB Chemie Technik GmbH (Germany), ORANO Mining (France), LTB (Germany), NovaMecanics Ltd. (Greece), SAIS LAB (Greece), Middle East Technical University - METU (Turkey), Ferro Duo GmbH (Germany), Xtract GmbH (Germany), Venator Materials PLC (Germany), Max Planck Institute for Sustainable Materials (Germany), and EIT Raw Materials (Germany).

References

1. Home - EURO Titan Project Available online: https://www.euro-titan.eu/ (accessed on 21 February 2026).

2. Stopic, S.; Kostić, D.; Schneider, R.; Sievers, M.; Wegmann, F.; Emil Kaya, E.; Perušić, M.; Friedrich, B. Recovery of Titanium from Red Mud Using Carbothermic Reduction and High Pressure Leaching of the Slag in an Autoclave. *Minerals 2024, Vol. 14, Page 1151* **2024**, *14*, 1151, doi:10.3390/MIN14111151.

3. Stopic, S.; Kostić, D.; Emil-Kaya, E.; Uysal, E.; Gürmen, S.; Mitrašinović, A.; Perušić, M.; Friedrich, B. High-Pressure and High-Temperature Dissolution of Titanium from Titanium and Aluminum Residues: A Comparative Study. *Surfaces 2024, Vol. 7, Pages 1096-1108* **2024**, *7*, 1096–1108, doi:10.3390/SURFACES7040072.

4. Kostić, D. Innovative Approaches to the Production of Titanium(IV) Oxide Nanopowders from Secondary Raw Materials, University of East Sarajevo, Faculty of Technology: Zvornik, 2025.

5. Vuković, J.; Smiljanić, S.N.; Kostić, D.; Stopić, S.; Perušić, M.; Vasiljević, N. A Preliminary Assessment of the Use of Red Mud Slag for Phosphate Sorption from Aqueous Solutions. *Engineering Proceedings 2025, Vol. 99, Page 5* **2025**, *99*, 5, doi:10.3390/ENGPROC2025099005.

6. Stopic, S.; Schneider, R.; Kosti´ckosti´c, D.; Souza Filho, I.R.; Peruši´cperuši´c, M.; Emil-Kaya, E.; Friedrich, B. Combined Decarbonizing Technologies for Treatment of Bauxite Residues. *Waste 2025, Vol. 3, Page 11* **2025**, *3*, 11, doi:10.3390/WASTE3020011.

Tribology, Wear, Lubrication, and Surface Engineering

An Enhanced Pin-on-Disc Tribometer with Integrated Lubrication and Digital Positioning System

Stefan Čukić[1], Anđela Perović[1], Slavica Miladinović[1], Miloš Matejić[1], Blaža Stojanović[1]

[1]*University of Kragujevac, Faculty of Engineering, Kragujevac, Serbia, stefan.cukic@kg.ac.rs, 0009-0002-5765-1712, andjela.perovic@kg.ac.rs, 0009-0005-5637-9827, slavicam@kg.ac.rs, 0000-0002-4408-0634, mmatejic@kg.ac.rs,, 0000-0003-0488-0992, blaza@kg.ac.rs, 0000-0003-4790-2856*

Corresponding author: andjela.perovic@kg.ac.rs

Abstract

Tribological properties of materials, such as friction and wear, play an important role in the reliability and service life of machine elements. Their investigation requires laboratory devices capable of providing controlled and repeatable experimental conditions. This paper presents the redesign and improvement of a previously developed pin-on-disc tribometer. Initial tests using the original configuration revealed several limitations, including the absence of a lubrication system and limited accuracy in determining the distance between the disc center and the pin position. The original positioning method had an uncertainty of ±2 mm, affecting sliding distance calculations. To address these issues, an improved tribometer design was developed. The upgraded system includes an oil lubrication unit and a digital position ruler with an accuracy of ±0.1 mm for precise pin positioning. Additional structural elements were introduced to improve experimental efficiency. The developed tribometer represents a flexible and cost-effective laboratory device, while future work will include testing under lubricated conditions.

Keywords: *tribometer; Pin-on-Disc; friction; tribology; experimental device; lubrication system*

1. Introduction

Reliability and service life of machine elements are directly affected by tribological characteristics of materials. Understanding these characteristics is an essential part of product development in industry [1,2]. Experimental investigations under laboratory conditions enable the collection of reliable data on material behavior in contact under different loading conditions [3,4]. Pin-on-Disc tribometers are one of the most commonly used configurations for determining the coefficient of friction and analyzing wear of metallic surfaces [4,5]. Previous studies have shown that measurement accuracy depends on load stability, tribometer design, and the data acquisition system [6]. Furthermore, many industrial applications such as sliding bearings, machine guideways, and brake systems require tribological data under both dry and lubricated conditions, highlighting the need for flexible laboratory tribometers. This paper presents an improved Pin-on-Disc tribometer that provides more stable contact, more accurate real-time measurement of friction force, and greater flexibility in different experimental conditions. The novelty of this work is the development of a tribometer that combines reliability, cost-effectiveness, and simple adaptability to different materials and testing conditions.

The aim of this study is the development and improvement of a Pin-on-Disc tribometer, as well as the analysis of design solutions that enable higher accuracy, better control, and improved repeatability of experimental conditions.

2. Original Tribometer Design and Identified Limitations

The initial pin-on-disc tribometer consists of a rotating disc driven by a 1.5 kW electric motor and a loading system based on a lever mechanism with weights generating the normal force. The disc is mounted on a shaft, while the pin is fixed in a holder connected to a 100 N load cell for real-time friction force measurement, recorded using an Arduino R3-based data acquisition system [7]. Preliminary tribological tests were carried out under dry sliding conditions to verify system functionality. During these tests, the manual method for setting the sliding radius introduced positioning errors of ±2 mm, reducing repeatability and affecting calculated sliding distances [8]. The original design had several limitations: dry sliding only, manual pin positioning reducing accuracy, and poor experimental organization. These limitations required an upgraded tribometer with lubrication and precise positioning.

3. Improved Tribometer Design

One of the most significant improvements of the new design is the integration of an oil lubrication system. The lubrication unit consists of an oil pump connected to a reservoir and a supply line that directs the lubricant into the contact zone between the pin and the rotating disc. Figure 1a presents the lubrication system integrated with the tribometer, with clearly indicated component positions, including the oil pump, reservoir, and supply line, while Figure 1b shows the pin–disc contact with the lubricant supplied into the contact interface.

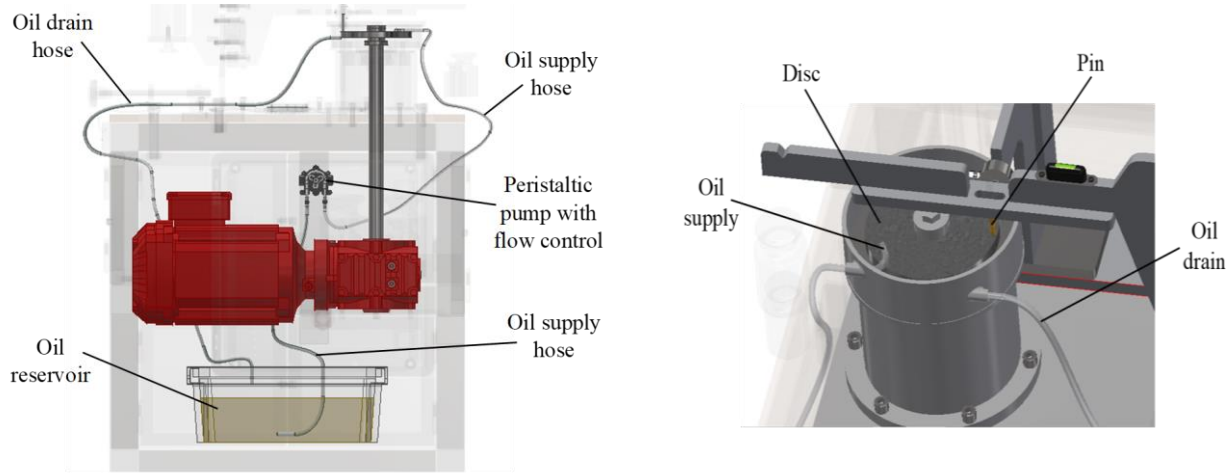
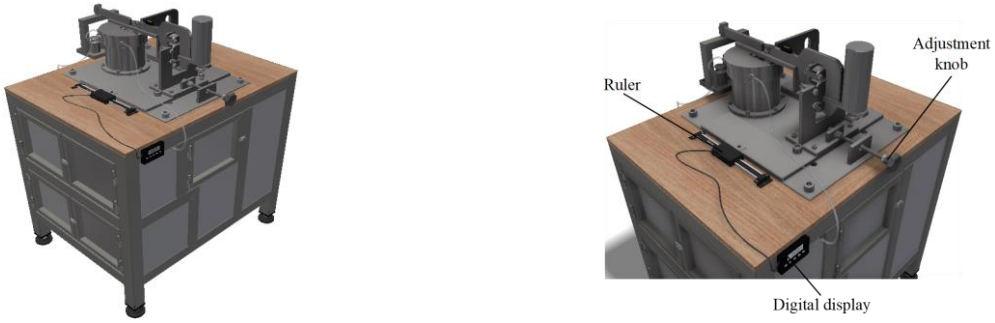


Figure 1. Pin-on-disc tribometer with integrated lubrication system: (a) layout with pump and reservoir; (b) lubricant flow to the pin–disc contact.

This solution presented on Figure 1 enables controlled lubrication during experiments and allows future investigations under lubricated sliding conditions. The integration of the lubrication system significantly

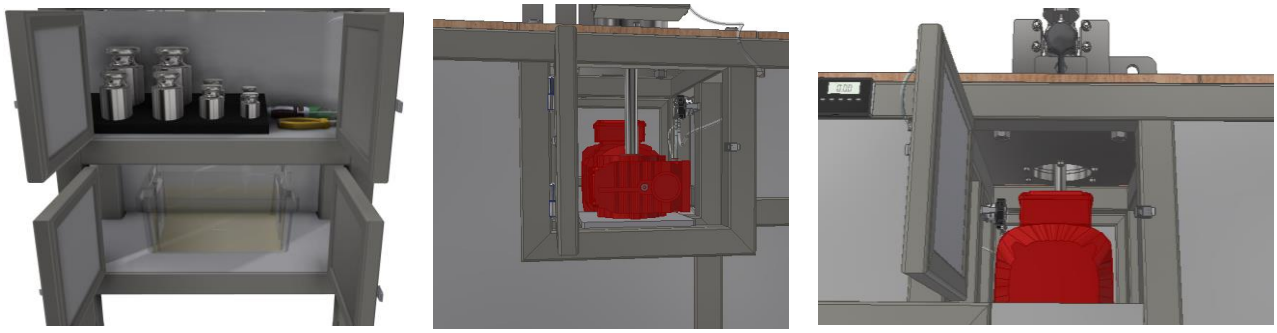
expands the experimental capabilities of the tribometer. The pump delivers a flow rate of 5 ml/min, and it is suitable for testing lubricants with viscosities ranging from 10 to 50 cSt. For precise determination of the sliding radius, a digital ruler was integrated into the system. Figure 2a shows the tribometer with the integrated ruler, while Figure 2b illustrates the measurement principle with highlighted positions. By moving the lever, the pin position is adjusted, and the scale displays the corresponding value, representing the distance between the disc center and the pin. This value is used to calculate the sliding distance and test duration. Measurement accuracy is ±0.1 mm, improving repeatability and reliability of sliding speed and distance calculations.



(a) (b)

Figure 2. Digital ruler: (a) setup; (b) sliding radius reading

Figures 3a, 3b, and 3c present additional structural elements in the form of integrated shelves within the tribometer. Their implementation aims to improve workspace organization, aesthetic appearance, and ergonomics, thereby facilitating easier operation of the device. All shelves are equipped with doors that can be opened and closed, ensuring safe operation. Figure 3a shows a shelf containing the weights used to generate the normal load, as well as the oil container. Figure 3b provides access to the electric motor and oil pump for maintenance purposes, while Figure 3c shows access to the screws used for adjusting the pin position.



(a) (b) (c)

Figure 3. Integrated shelves: (a) weights; (b) motor/pump access; (c) pin adjustment access

These elements improve the ergonomics of the experimental procedure and enable more efficient laboratory work.

4. Discussion

The redesign of the tribometer addressed several limitations identified during the operation of the original system. The integration of the lubrication unit enables experiments under lubricated conditions, which are common in many practical tribological applications. The introduction of a digital position scale significantly improves the accuracy of defining the sliding radius, which directly affects the calculation of sliding speed and sliding distance. Improved positioning accuracy also contributes to better repeatability of experimental results. In addition, the integration of shelves for weights and auxiliary tools improves the organization of the experimental setup. Compared to the original design, the improved tribometer offers measurable advantages: ±0.1 mm positioning accuracy, controlled lubrication capability, and reduced experimental setup time by 20%.

5. Conclusions

This paper presents the redesign and improvement of a laboratory Pin-on-Disc tribometer previously developed for tribological investigations. During experimental use, several limitations of the original design were identified, including the absence of a lubrication system, limited accuracy in determining the sliding radius, and insufficient organization of experimental equipment. To overcome these limitations, an improved tribometer design was developed, including an integrated oil lubrication system, a digital position scale for precise positioning of the pin, and additional structural elements such as shelves for weights and auxiliary tools. The implemented improvements significantly enhance the experimental control, and usability of the tribometer. Future work will focus on tribological testing under lubricated conditions using the upgraded system.

Acknowledgements

This research is supported by the Ministry of Education, Science and Technological Development, Republic of Serbia, Grant 451-03-34/2026-03/200107.

References

1. Chandross M, Argibay N. Friction of Metals: A Review of Microstructural Evolution and Nanoscale Phenomena in Shearing Contacts. Tribol Lett. 2021 Dec;69(4):119. doi:10.1007/s11249-021-01477-z
2. Dabas S, Kumar P. A review on tribological behaviour of steel against steel. Materials Today: Proceedings. 2021;44:4822–6. doi:10.1016/j.matpr.2020.11.690
3. Shi R, Wang B, Yan Z, Wang Z, Dong L. Effect of Surface Topography Parameters on Friction and Wear of Random Rough Surface. Materials. 2019 Aug 28;12(17):2762. doi:10.3390/ma12172762
4. Wahlström J. A pin-on-disc tribometer study of friction at low contact pressures and sliding speeds for a disc brake material combination. Results in Engineering. 2019 Dec;4:100051. doi:10.1016/j.rineng.2019.100051
5. Küçüköztaş K, Talay İ, Çalışkan F, Elsakka M, Nassar M, Kaftanoğlu B. Design and Manufacturing of a Pin on Disk Tribometer. Makina Tasarım ve İmalat Dergisi. 2024 May 30;22(1):31–42. doi:10.56193/matim.1353203
6. Li Y, Garabedian N, Schneider J, Greiner C. Waviness Affects Friction and Abrasive Wear. Tribol Lett. 2023 Jun;71(2):64. doi:10.1007/s11249-023-01736-1
7. Perović A, Piskulić M. DESIGN AND TESTING OF PIN ON DISC TRIBOMETER: FINK-POD2025.
8. Perovic A, Cukic S, Miladinovic S, Matejic M, Gajevic S, Stojanovic B. Development and Experimental Validation of a Pin-on-Disc Tribometer for Friction Testing of Different Metal Materials. Tribol Ind. 2026 Mar;48(1):188–98. doi:10.24874/ti.2135.02.26.03

Influence of intermittent friction cycles on tribocorrosion behavior of 316L stainless steel in 5% $NaHCO_3$

Kaouthar Bouguerra[1], Yan-Ming Chen[2], Alexandre Romaine[3], Nadege Ducommun[3], Pierre François Cardey[4], Alexis Fontaine[5], Caroline Richard[1]

[1] *GREMAN UMR 7347, Université de Tours, CNRS, INSA Centre Val de Loire, Tours, France, kaouthar.bouguerra@univ-tours.fr, 0009-0003-5260-2329, caroline.richard@univ-tours.fr, 0000-0002-8375-8241*

[2] *CETIM, Senlis, France, yan-ming.chen@cetim.fr, 0000-0003-4884-5582*

[3] *CETIM, Nantes, France, [c]Alexandre.Romaine@cetim.fr, 0000-0002-9668-3883 Nadege.Ducommun@cetim.fr, 0009-0003-3904-4430*

[4] *CETIM, Saint Etienne, France Pierre-Francois.Cardey@cetim.fr*

[5] *Mouvex PSG Dover, Auxerre, [f]alexis.fontaine@psgdover.com France*

Corresponding author: kaouthar.bouguerra@univ-tours.fr

Abstract

The food processing industry requires durable stainless steel equipment resistant to repeated friction and corrosion cycles. Cleaning and maintenance procedures introduce periodic interruptions that may affect the passivation and depassivation mechanisms of these materials. This study investigates the tribocorrosion behavior of 316L stainless steel under extended experimental conditions, simulating industrial interruptions. The primary objective is to assess the robustness of the passive film and its ability to sustain protective properties over time. The study follows ASTM G-133 tribological testing standards in a 5% $NaHCO_3$ solution over 14 hours, incorporating alternating friction phases and rest periods. Open circuit potential is continuously monitored, and surface characterization employs, SEM-EDS, and XPS. Results show an initial drop in the coefficient of friction due to passive film formation, with stability maintained despite intermittent rest. A transient coefficient of friciton drop occurs after overnight pauses, indicating temporary tribo-film weakening before repassivation. Wear analysis confirms passive film stability, with corrosion product characterization revealing iron-based oxides, hydroxides, and carbonates. XPS analysis highlights a multilayered passive film dominated by Fe_2O_3, Fe_3O_4, Cr_2O_3, and $Cr(OH)_3$, . The findings confirm that 316L stainless steel maintains stable tribocorrosion performance in 5% $NaHCO_3$ despite long-term cyclic friction, supporting its industrial applicability in alkaline environments

Keywords: Tribocorrosion; AISI 316L stainless steel; Passive film; Intermittent sliding; Sodium bicarbonate solution. UN SDG 9

1. Introduction

In the food processing industry, positive displacement pumps are exposed to severe mechanical and chemical constraints, particularly during cleaning cycles with acidic or alkaline agents. These environments frequently induce lubrication-deficient regimes, enhancing tribo-chemical interactions[1]. Tribocorrosion—defined as the synergistic action of wear and corrosion—is especially detrimental to stainless steel components (rotors, stators, seals, pump bodies), as the protective passive film is continuously damaged and reformed The severity of this degradation depends strongly on the passive film properties and repassivation kinetics [2–6].

Austenitic stainless steels, especially AISI 316L, are widely used due to their corrosion resistance, but their tribological behavior under repeated cleaning remains problematic [7,8]. Industrial feedback shows that $NaHCO_3$ solutions induce significantly less wear than acetic acid, though the mechanisms are not fully understood. In a previous study, we demonstrated that 316L in 5 wt.% $NaHCO_3$ forms a complex passive structure (Cr oxides/hydroxides with Fe- and Ni-rich sublayers), resulting in low wear and friction and good corrosion resistance [1].

However, the impact of cleaning cycle duration and rest periods on passive film stability and regeneration has not yet been investigated, despite their practical relevance in food-processing environments. This study therefore focuses on the influence of exposure time and intermittent operation on the tribocorrosion behavior of 316L in 5 wt.% $NaHCO_3$, combining tribo-electrochemical tests with advanced surface analyses.

2. Materials and Methods

Tribocorrosion tests were conducted using a ball-on-plate Plint TE77 tribometer coupled with a BioLogic SP50 potentiostat, following ASTM G133. The schematic setup is presented in our previous study [1]. Tests were performed with an AISI 316L ball and plate in 5 wt.% $NaHCO_3$ solution, under 5 Hz frequency, 25 N load, 10 mm stroke, and 22 °C. Each 14 h test included four sliding sequences of 1000 s separated by rest intervals (1 h, 2 h, overnight), followed by a final sliding cycle. Open circuit potential (OCP) and coefficient of friction (CoF) were continuously monitored, and each condition was repeated three times. After testing, worn surfaces were characterized by, SEM/EDS (surface morphology and chemistry), and XPS (elemental composition).

3. Results & Discussion

3.1 Results of the tribocorrosion test

Tribocorrosion tests on AISI 316L in 5 wt.% $NaHCO_3$ (5 Hz, 25 N, 22 °C, 14 h), as shown in Fig. 1, reveal a rapid drop in CoF from 0.8 to 0.4 within the first 180 s, associated with the formation of a protective passive film acting as a tribological coating [1]. This low-friction state (~0.4) remained stable during sliding and after 1–2 h rest intervals, confirming the film's durability and lubricating efficiency under intermittent conditions. After the overnight pause (>10 h), a brief decrease in CoF (from 0.7 to 0.45) indicated partial weakening of the film, followed by rapid repassivation and

stabilization. OCP variations paralleled CoF evolution, highlighting the strong correlation between depassivation during sliding and efficient repassivation during rest.

3.2 Characterizations

Surface morphology and elemental distribution

Post-tribocorrosion observations by SEM (Fig. 2) show furrows and grooves typical of abrasive wear, confirming mechanically-driven degradation [9,10]. Backscattered imaging and EDS mapping reveal heterogeneous surface chemistry, with chromium-depleted and nickel-enriched zones, characteristic of tribocorrosion processes [11]. The EDS spectrum also indicates oxygen, confirming oxide/hydroxide formation. These compositional changes, especially nickel enrichment and chromium depletion, modify the stability of the tribofilm and enhance its protective function against tribo-electrochemical degradation.

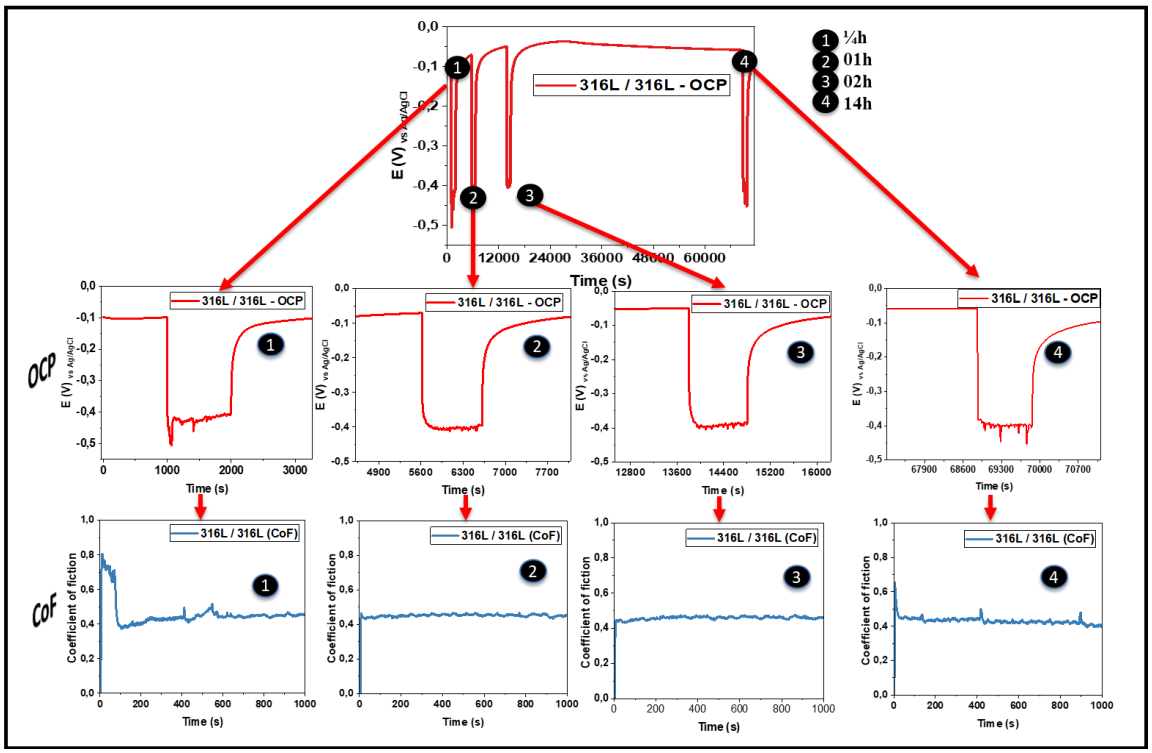


Figure 1. Electrochemical (OCP) and tribological (CoF) responses of AISI 316L stainless steel under intermittent sliding in 5 wt.% $NaHCO_3$ solution.

3.3 XPS analysis

XPS Survey spectra (Fig. 3) reveal clear compositional differences between worn and unworn regions. Inside the wear track, carbon (18.99% vs. 11.60%) and sodium (22.45% vs. 12.33%) are

enriched, indicating the accumulation of carbonaceous species and $NaHCO_3$-derived compounds. In contrast, chromium, iron, and nickel concentrations are significantly reduced, evidencing preferential dissolution under tribocorrosion. Oxygen also decreases slightly (49.6% vs. 51.0%), suggesting modifications of oxide/hydroxide species. Overall, the worn surface shows selective dissolution and higher chemical reactivity, whereas the unworn area retains a more intact passive film.

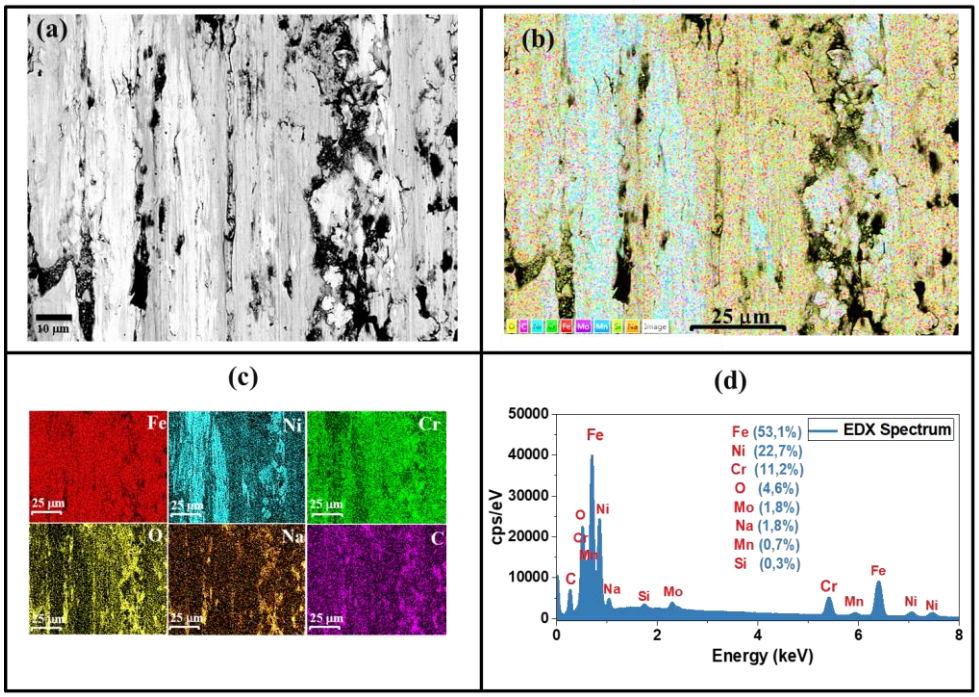


Figure 2. Wear track morphology and chemical analysis of AISI 316L after tribocorrosion. (a) (b) Secondary electron image; (c) Elemental mapping; (d) EDS spectrum.

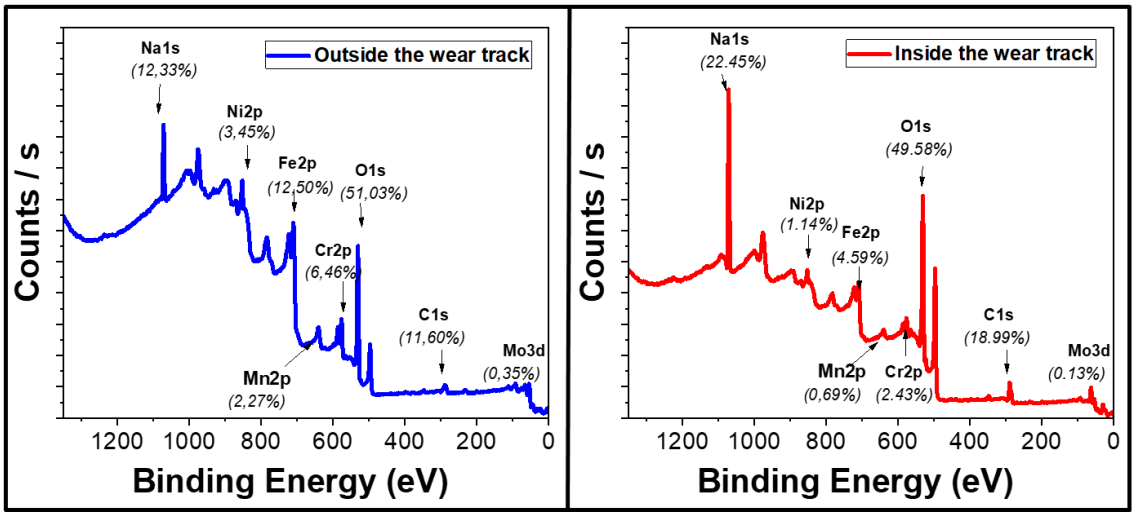


Figure 3. XPS survey spectra of AISI 316L after prolonged tribocorrosion: (a) unworn surface and (b) wear track region.

4. Conclusions

This study demonstrates that AISI 316L stainless steel exhibits robust tribocorrosion resistance in 5 wt.% $NaHCO_3$ solution, even under prolonged and intermittent sliding conditions. The rapid formation of a passive tribofilm ensures low and stable friction, with only minor and reversible weakening observed after extended rest periods. Surface analyses confirm that tribocorrosion induces both mechanical wear features and chemical heterogeneities, notably chromium depletion, nickel enrichment, and the incorporation of sodium and carbonaceous species. XPS results further reveal selective dissolution of metallic elements within the wear track, while the unworn regions preserve a relatively intact oxide/hydroxide-based passive film. Overall, the findings highlight the durability and self-regenerating capacity of the passive layer, supporting the suitability of 316L stainless steel for long-term use in alkaline cleaning environments relevant to food-processing equipment.

References

[1] Bouguerra K, Chen Y-M, Romaine A, Ducommun N, Cardey P-F, Bourhis E, et al. Improvement of tribological behavior of stainless steels in food cleaning process by sodium hydrogen carbonate. Tribol Int 2025;202:110382. https://doi.org/10.1016/j.triboint.2024.110382.

[2] De Stefano M, Ruggiero A. Tribocorrosion of couplings in seawater environment: An investigation on the positive-negative role of synergy. Tribol Int 2024;200:110143. https://doi.org/10.1016/j.triboint.2024.110143.

[3] Mary N, Ter-Ovanessian B, Normand B. Growth mechanism and repassivation kinetic determinations on stainless steel under sliding: Role of the solution pH and dissolved oxygen concentration. Wear 2020;460–461:203478. https://doi.org/10.1016/j.wear.2020.203478.

[4] Axente ER, Benea L, Bogatu N, Celis J-P. Susceptibility to tribocorrosion degradation of 304 L stainless steel from dental structures in biological solution. Tribol Int 2022;174:107769. https://doi.org/10.1016/j.triboint.2022.107769.

[5] Dalbert V, Mary N, Normand B, Verdu C, Douillard T, Saedlou S. The effects of microstructures and repassivation kinetics on the tribocorrosion resistance of ferrite and ferrite-martensite stainless steels. Wear 2019;420–421:245–56. https://doi.org/10.1016/j.wear.2018.10.023.

[6] Olsson C-OA, Landolt D. Passive films on stainless steels—chemistry, structure and growth. Electrochimica Acta 2003;48:1093–104. https://doi.org/10.1016/S0013-4686(02)00841-1.

[7] Ponthiaux P, Celis J-P, editors. Mechanical and electro-chemical interactions under tribocorrosion: from measurements to modeling for building a relevant monitoring approach. Oxford: Woodhead Publishing; 2021.

[8] McGuire MF. Stainless steels for design engineers. Materials Park, Ohio: ASM International; 2008.

[9] García-León RA, Martínez-Trinidad J, Guevara-Morales A, Campos-Silva I, Figueroa-López U. Wear Maps and Statistical Approach of AISI 316L Alloy under Dry Sliding Conditions. J Mater Eng Perform 2021;30:6175–90. https://doi.org/10.1007/s11665-021-05822-0.

[10] Jullien C, Bénézech T, Carpentier B, Lebret V, Faille C. Identification of surface characteristics relevant to the hygienic status of stainless steel for the food industry. J Food Eng 2003;56:77–87. https://doi.org/10.1016/S0260-8774(02)00150-4.

[11] Richard C, Geringer J. Tribocorrosion. Frott Usure Lubrif 2019. https://doi.org/10.51257/a-v2-cor60.

Influence of Linear Reciprocating and Rotational Modes on Wear Track Width of Brass

Dragan Dzunic[1], Milan Eric[1], Vladimir Kocovic[1], Jelena Djusic[1], Zivana Jovanovic Pesic[1], Slobodan Mitrovic[1],

[1]*Department for Production Engineering, Faculty of Engineering, University of Kragujevac, Kragujevac, Serbia, dzuna@kg.ac.rs, 0000-0002-1914-1298, ericm@kg.ac.rs, 0000-0001-8691-4863, vladimir.kocovic@kg.ac.rs, 0000-0003-1231-0041, jelenadjusic24.2009@gmail.com, 0009-0004-8630-9304, zixi90@gmail.com, 0000-0002-1373-0040, boban@kg.ac.rs, 0000-0003-3290-7873*

Corresponding author: zixi90@gmail.com

Abstract

This study investigates the influence of motion regime on the wear behavior of brass using a CSM nanotribometer. Tribological tests were conducted under two different motion conditions: rotational and linear reciprocating modes, under identical testing parameters. The wear track width was used as the primary indicator of material degradation. The results showed that the motion regime significantly affects the wear behavior of brass. In the rotational mode, a slight decrease in wear track width was observed with increasing wear track radius, indicating more stable contact conditions. In contrast, the linear reciprocating mode exhibited greater variability in wear track width, which can be attributed to the repeated reversal of motion and the resulting changes in contact conditions. Overall, the findings demonstrate that the type of motion plays a crucial role in determining wear characteristics. The results contribute to a better understanding of brass performance in tribological applications and may assist in the optimization of components operating under different motion regimes.

Keywords: Brass; Tribology; Wear track width; Rotational mode; Linear reciprocating mode; 'UN SDG 9';

1. Introduction

Brass is one of the most important copper alloys, primarily composed of copper and zinc, whose properties can be significantly modified depending on its chemical composition and microstructure [1]. By varying the zinc content, it is possible to achieve different combinations of mechanical and physical properties, including increased strength, hardness, and resistance to deformation [2]. Due to its good machinability, relatively low cost, and satisfactory corrosion resistance, brass is widely used in industry, particularly in the manufacturing of machine elements such as bearings, gears, and valves [3].

In operating conditions involving relative motion between contact surfaces, the tribological properties of materials play a crucial role in system reliability and durability. Friction and wear represent the primary mechanisms of degradation, leading to energy dissipation and material loss from contact surfaces. Experimental studies have shown that parameters such as load, sliding speed, and temperature significantly influence the coefficient of friction and wear rate in copper alloys, including brass [4, 5].

Brass exhibits relatively favorable tribological characteristics, such as stable friction behavior and the ability to form protective layers (tribofilms) on the contact surface, which can reduce wear under certain operating

conditions. However, compared to bronzes, brass may exhibit higher wear rates, particularly under higher loads or insufficient lubrication conditions [6, 7].

Recent research has focused on improving the tribological properties of brass through microstructural modification, the addition of alloying elements, and the development of composite materials. It has also been established that different wear mechanisms, such as adhesive and abrasive wear, dominate depending on operating conditions and contact parameters [8].

In this context, experimental investigations using tribometers represent an important tool for analyzing material behavior under controlled conditions. Particular attention is given to the influence of different motion regimes, such as linear reciprocating and rotational modes, as they produce distinct contact conditions and wear mechanisms. One of the key indicators of wear performance is the wear track width, which provides valuable insight into material degradation under friction. Therefore, the objective of this study is to analyze the influence of motion regime on the wear track width of brass.

2. Materials and Methods

The material used in this study was a commercially available brass alloy (Cu-Zn), with a copper content of approximately 63-65 wt.% and zinc as the main alloying element. Minor trace elements were present in negligible amounts (<1 wt.%). This composition corresponds to a typical α-brass commonly used in engineering applications due to its favorable combination of mechanical and tribological properties. A series of samples with dimensions of 10 × 15 × 6.35 mm was prepared for tribological testing. The counter-body used in all experiments was a 100Cr6 steel ball with a diameter of 1.5 mm, selected due to its high hardness and widespread use in tribological testing.

Prior to testing, all samples were mechanically ground using silicon carbide (SiC) abrasive papers with progressively finer grit sizes: P320, P600, P800, P1200, P2000, and P3000. After grinding, the samples were polished using diamond suspensions with particle sizes of 6 µm, 1 µm, and 0.4 µm to obtain a smooth and uniform surface finish. Between each preparation step, the samples were thoroughly cleaned to remove debris and contaminants, ensuring consistent surface conditions for all tests.

Tribological tests were performed using a CSM nanotribometer (Figure 1 – (a)) under two different motion regimes: rotational and linear reciprocating modes. These configurations were selected to evaluate the influence of motion type on the wear behavior of brass under controlled laboratory conditions. In the rotational mode, the tests were conducted at a sliding speed of 10 mm/s, under a normal load of 300 mN, with a total of 500 cycles. The wear track radii were set to 2 mm, 2.5 mm, and 3 mm. In the linear reciprocating mode, the tests were carried out under the same sliding speed (10 mm/s), normal load (300 mN), and number of cycles (500), with a stroke length (amplitude) of 0.5 mm.

3. Results and Discussion

The wear track width obtained under different testing conditions is presented in Figure 1 - (b), (c) . The results clearly indicate that the motion regime and contact configuration have a significant influence on the wear behavior of brass.

In the case of the rotational mode (Figure 1 - (b)), the wear track width decreases with increasing wear track radius. The highest wear track width was observed at a radius of 2 mm (approximately 167 µm), while slightly lower values were recorded at 2.5 mm and 3 mm. This trend can be attributed to the variation in contact conditions along the wear track, where larger radii correspond to longer sliding paths and potentially more stable contact conditions, resulting in reduced localized wear.

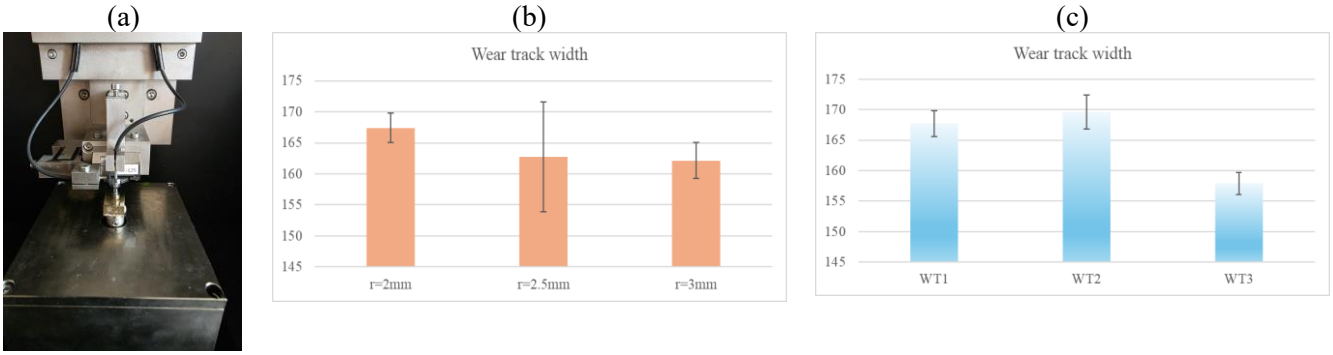


Figure 1. (a) Experimental setup of the CSM nanotribometer, (b) wear track width for rotational mode at different radii, and (c) wear track width for linear reciprocating mode

For the linear reciprocating mode (Figure (c)), the wear track width shows a different trend. The highest value was observed for sample WT2 (approximately 169 µm), while the lowest value was recorded for WT3 (approximately 158 µm). Compared to the rotational mode, the variation between measurements is more pronounced, which may be related to the nature of reciprocating motion, where repeated reversal of sliding direction leads to increased stress concentration and more complex wear mechanisms.

A comparison between the two motion regimes reveals that the rotational mode generally produces more uniform wear, while the linear reciprocating mode results in greater variability in wear track width. This difference can be explained by the continuous unidirectional motion in the rotational mode, which promotes stable friction conditions, in contrast to the reciprocating mode where frequent changes in sliding direction lead to increased frictional instability and potential material fatigue.

The error bars shown in the figures indicate the dispersion of the measured values. The larger deviation observed at a radius of 2.5 mm in the rotational mode suggests a less stable wear process under these conditions. Similarly, variations in the reciprocating mode indicate sensitivity to local contact conditions and surface interactions.

Overall, the results demonstrate that the motion regime plays a crucial role in determining the wear behavior of brass. The wear track width is influenced not only by the sliding conditions but also by the nature of motion, which affects contact stability, stress distribution, and dominant wear mechanisms. These findings are important for optimizing the application of brass in tribological systems where different motion regimes are present.

4. Conclusions

Summarize key findings and outline future work. The present study investigated the influence of motion regime on the wear behavior of brass using a CSM nanotribometer under rotational and linear reciprocating modes. The results showed that the motion regime has a significant effect on the wear track width.

In the rotational mode, a slight decrease in wear track width was observed with increasing wear track radius, indicating more stable contact conditions at larger radii. In contrast, the linear reciprocating mode exhibited greater variability in wear track width, which can be attributed to the repeated reversal of motion and the resulting changes in contact conditions.

Overall, the findings suggest that rotational motion provides more uniform wear behavior, while reciprocating motion leads to more complex and less stable wear mechanisms. These results contribute to a better understanding of the tribological performance of brass and can be useful in the design and optimization of engineering components operating under different motion regimes.

Acknowledgements

This paper is the result of research conducted under the author's contract No. 451-03-34/2026-03/200107, dated February 5, 2026, supported by the Ministry of Science, Technological Development and Innovation, Republic of Serbia.

References

1. Davis JR, ASM International, editors. Copper and copper alloys. Materials Park, Ohio: ASM International; 2001.
2. Jasper S, Subash R, Muthuneelakandan K, Vijayakumar D, Jhansi Ida S. The Mechanical Properties of Brass Alloys: A Review. ICMechD 2024, MDPI; 2025, p. 11. https://doi.org/10.3390/engproc2025093011.
3. Ribeiro BL, Monteiro J, Truta M, Santos RF, Barbosa M, Sequeiros EW. Trends and Challenges in Lead-Free Brass Alloy Development for Machining Applications: A Systematic Literature Review. J Sustain Metall 2026;12:971–93. https://doi.org/10.1007/s40831-025-01371-1.
4. Patel S, Shaikh T, Prajapati N. A Review On Dry Sliding Wear Analysis On Brass Using Taguchi Technique. International Journal of Computational Engineering Research n.d.;4.
5. Senhadji F, Belarifi F, Robbe-Valloire F. Experimental Investigation of Friction Coefficient and Wear Rate of Brass and Bronze under Lubrication Conditions. Tribology in Industry 2016;38:102–7.
6. Grandin M, Wiklund U. Friction, wear and tribofilm formation on electrical contact materials in reciprocating sliding against silver-graphite. Wear 2013;302:1481–91. https://doi.org/https://doi.org/10.1016/j.wear.2013.02.007.
7. Haque FMA. Tribofilm Formation of PTFE-Cr on Different Counterbody Materials for Dry Sliding Applications. Master's Thesis. Miami University, 2023.
8. Liu L, Yang C, Zhou J, Garmestani H, Dastan D. Study on Wear Model and Adhesive Wear Mechanism of Brass under Boundary Lubrication. Prot Met Phys Chem Surf 2021;57:367–73. https://doi.org/10.1134/S2070205121010147.

Influence of Organic and Inorganic Based Lubricating Greases on the Tribological Characteristics of Contact Pairs

Stefan Miletić[1], Dragan Džunić[1], Milan Ivković[1], Slobodan Mitrović[1]

[1] *University of Kragujevac, Faculty of Engineering, Department for Production Engineering, Kragujevac, Serbia, smiletic@kg.ac.rs, 0009-0007-0253-2819, dzuna@kg.ac.rs, 0000-0002-1914-1298, milanivkovicfin@gmail.com, 0000-0001-5176-5837, boban@kg.ac.rs, 0000-0003-3290-7873*

Corresponding author: boban@kg.ac.rs

Abstract

This paper is designed as the first in a series of studies focused on investigating the influence of animal-based lubricating greases on the tribological characteristics of materials. The research examines the effectiveness of organic and inorganic greases in terms of reducing friction and wear, while monitoring the coefficient of friction in mechanical elements to facilitate a comparative analysis of the results. Modern industrial requirements impose a necessity for environmentally friendly lubricants; therefore, the research focus is directed towards a comparative analysis of the tribological properties of biodegradable greases (animal-based) relative to conventional inorganic greases. Experimental testing was conducted using a block-on-disk tribometer, under a normal load of F_n = 200 N, a sliding speed of v = 0.5 m/s, and a test duration of t = 1800 s per wear track. For each lubricant, three experimental trials were performed, each lasting t = 1800 s. The primary monitoring parameters included the coefficient of friction and the wear track width, which served as the basis for calculating the wear area and volume of the block. Extensive further research is required to determine the optimal composition of organic lubricating greases that would satisfy a broader range of tribological operational requirements. This study contributes to a better understanding of the potential implementation of organic lubricants as substitutes for inorganic ones, aligning directly with the United Nations Sustainable Development Goals: UN SDG 7, UN SDG 9, and UN SDG 12.

Keywords: lubricating greases, bio-lubricants / organic lubricants, friction, wear, Coefficient of friction, UN SDG 7, 9 and 12

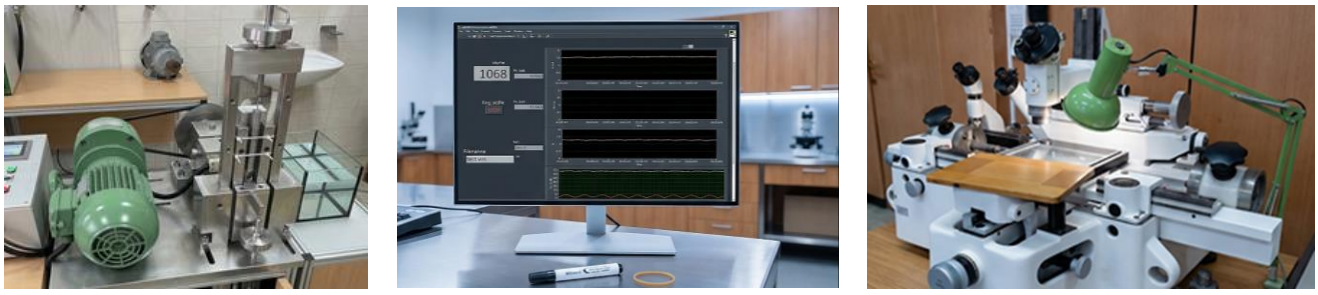
1. Introduction

Contemporary tribology is undergoing a paradigm shift toward environmental sustainability, driven by the need to replace mineral-based lubricants with biodegradable alternatives to mitigate the fact that tribological contacts account for approximately 23% of global energy consumption. In alignment with UN SDGs 9 and 12, animal-based fats such as lard and beef tallow have emerged as viable, eco-friendly feedstocks for next-generation lubricating greases. Optimizing these lubricants directly enhances energy efficiency and supports industrial decarbonization by reducing the coefficient of friction and associated greenhouse gas emissions. Furthermore, their high viscosity index and superior adhesion properties extend component service life and reduce operational costs, making them economically superior to petroleum-based products. Unlike conventional lubricants that

pose toxicological risks to soil and groundwater, animal-based greases offer high biodegradability and are non-toxic, making them ideal for ecologically sensitive sectors like agriculture and maritime transport. Transitioning to these organic alternatives eliminates reliance on carcinogenic hydrocarbons and hazardous additives inherent in outdated petrochemical technologies. At the molecular level, polar fatty acids within these greases adsorb onto metallic substrates to form robust tribofilms with low shear resistance, effectively preventing metal-to-metal contact even under extreme pressure. Ultimately, repurposing waste fats into high-performance lubricants facilitates a strategic transition toward a circular economy and energy-efficient industrial operations [1-13].

2. Materials and Methods

The following equipment was utilized for the experimental procedures. The TR-95 Universal Tribometer, shown in Figure 1a, served as the primary experimental apparatus for this study. Its fundamental function is the simulation of tribological processes to accurately quantify tribological parameters. The device operates on the block-on-disk contact principle, where the test specimen is pressed against a rotating disk with a predefined normal force. During the contact, the tribometer's integrated sensors continuously measure the frictional force, and the data is automatically transmitted to a computer for further processing. The data acquisition system includes sensors for measuring both the normal force (Fn) and the frictional force (Ft). The control software, presented in Figure 1b, is used for real-time monitoring and recording of critical parameters, including time (t), the coefficient of friction (μ), and contact forces. Finally, the UIM-21 Universal Measuring Microscope, shown in Figure 1c, was employed following the completion of the tribological tests for precise wear track width analysis and detailed visual inspection of the worn surfaces. Lubricant was applied to the contact surfaces prior to the start of each measurement cycle to ensure lubricated contact conditions. The tests were conducted through three cycles of 1800 s each for every lubricant. Aluminum blocks were used as specimens, and measurements were performed under a constant force of 200 N (20 daN) at room temperature. Within this experiment, lubricants belonging to both organic and inorganic groups were investigated.



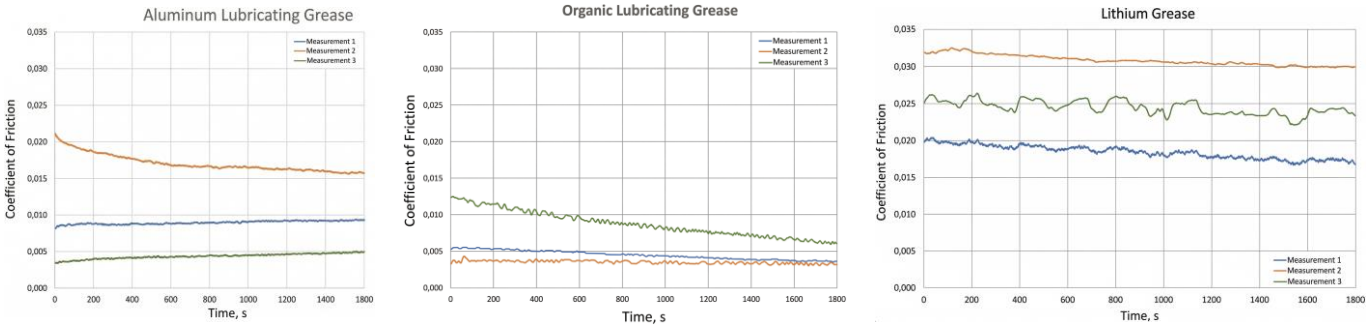
a) b) c)

Figure 1. a) TR-95 Tribometer, b) Data acquisition system, and c) UIM-21 Universal measuring microscope.

Animal-based lubricating grease was used as the organic grease, while aluminum-based and lithium-based lubricating greases were used as the inorganic lubricants for the experiment.

3. Results

Based on the experiment conducted on the tribometer, numerical data for the coefficient of friction values were obtained, which are subsequently used to generate the friction coefficient versus time diagrams shown in Figure 2. Specifically, Figure 2a presents the coefficient of friction for aluminum-based grease, Figure 2b displays the coefficient of friction for animal-based lubricating grease, and Figure 2c illustrates the coefficient of friction for lithium-based grease. In the case of aluminum-based and organic greases, the coefficient of friction generally decreases or fluctuates slightly over time, with certain exceptions noted during the initial measurements of the organic grease. Conversely, for the lithium-based grease, the coefficient remains relatively stable or shows a slight decrease following the initial running-in period.



a) b) c)

Figure 2. a)CoF for aluminum-based grease, b)CoF for animal-based lubricating grease, and c)CoF for lithium-based grease

The lithium-based grease exhibits significantly higher coefficient of friction values, ranging between 0.020 and 0.035, with a mean wear volume of approximately 0.003 mm^3. While the aluminum-based and organic greases operate at substantially lower friction levels 0.005 to 0.020 for the aluminum-based and 0.003 to 0.012 for the organic grease the wear volume of the block specimens lubricated with organic grease was the highest, reaching approximately 0.025 mm^3. In contrast, for the specimens lubricated with the aluminum-based grease, the wear tracks were too minimal to be measured.

4. Discussion and Conclusions

Among the three tested lubricants, the organic grease demonstrates superior anti-friction properties by achieving the lowest overall coefficient of friction, while the lithium-based grease shows the poorest friction reduction performance. The measurements for the lithium grease exhibit high repeatability and stability over time, whereas the organic grease displays significant discrepancies between trials, suggesting a higher sensitivity to running-in conditions or sample instability. While the organic grease possesses the potential for the lowest friction levels, the lithium and aluminum-based greases currently offer more predictable and consistent performance. However, the performance of organic greases in their base form should not be evaluated in isolation, as modern tribological trends suggest that the incorporation of eco-friendly additives can drastically enhance their stability and wear reduction. Future research should focus on animal-based bio-greases due to their high biodegradability, resource renewability, and natural affinity for metallic surfaces. By integrating these organic bases with modern "green" additives, a sustainable alternative to conventional lubricants is created, achieving a necessary balance between technical efficiency and the imperative of ecosystem preservation.

Acknowledgements

This work presents the results of research conducted within projects financially supported by the Ministry of Science, Technological Development and Innovation of the Republic of Serbia, under Contract No. 451-03 33/2026-03/200107.

References

1. Jafari A, Majdoub M, Sengottuvelu D, Ucak-Astarlioglu M. G., Al-Ostaz A., Nouranian S. Tribological Properties of Synthetic and Biosourced Lubricants Enhanced by Graphene and Its Derivatives: A Review. ACS Omega. 2024;9:50868–50893.

2. Rawat S. S., Harsha A. P., Khatri O. P. Tribological Investigations of Two-Dimensional Nanostructured Lamellar Materials as Additives to Castor-Oil-Derived Lithium Grease. Journal of Tribology. 2022;144:091902.

3. Niu M., Gao Y., Wang X., Liu Z. Tribo-synergism in titanium complex grease using micro and nano particles. PLOS ONE. 2025;20:e0323444.

4. Bartz W. J. Lubricants and the environment. Tribology International. 1998;31:35–47.

5. Shalwan A., Alajmi T., Alajmi N. Study on the tribological performance of bio-lubricant conditions- Review. Global Journal of Engineering and Technology Advances. 2023;16:1–11.

6. Opia A. C., Abdollah M. F. B., Hamid M. K. A., Veza I. A Review on Bio-Lubricants as an Alternative Green Product: Tribological Performance, Mechanism, Challenges and Future Opportunities. Tribology Online. 2023;18:18–33.

7. Holmberg K., Erdemir A. The Impact of Tribology on Energy Use and CO2 Emission Globally and in Combustion Engine and Electric Cars. Tribology International. 2019;135:389–396.

8. Holmberg K., Erdemir A. Influence of Tribology on Global Energy Consumption, Costs and Emissions. Friction. 2017;5:263–284.

9. Tamada I. S., Lopes P. R. M., Montagnolli R. N., Bidoia E. D. Biodegradation and Toxicological Evaluation of Lubricant Oils. Brazilian Archives of Biology and Technology. 2012;55:951–956.

10. Nowak P., Kucharska K., Kamiński M. Ecological and Health Effects of Lubricant Oils Emitted into the Environment. International Journal of Environmental Research and Public Health. 2019;16:3002.

11. Zhang G., Xu Y., Xiang X., Zheng G., Zeng X., Li Z, Ren T., Zhang Y. Tribological Performances of Highly Dispersed Graphene Oxide Derivatives in Vegetable Oil. Tribology International. 2018;126:39–48.

12. Ge X., Li J., Luo R., Zhang C., Luo J. Macroscale Superlubricity Enabled by the Synergy Effect of Graphene-Oxide Nanoflakes and Ethanediol. ACS Applied Materials & Interfaces. 2018;10:40863–40870.

13. Cecilia J. A, Ballesteros Plata D., Alves Saboya R. M., Tavares de Luna F. M., Cavalcante C. L., Rodríguez-Castellón E. An Overview of the Biolubricant Production Process: Challenges and Future Perspectives. Processes. 2020;8:257.

Manufacturing Quality, Inspection, and Structural Monitoring

Visual Inspection Systems for Tool Wear Monitoring in Machining

Milan Ivković[1], Julija Bošković[1], Nadica Stojanovic[1], Strahinja Đurović[2], Stefan Miletić[1], Goran Devedzic[1], Suzana Petrović Savić[1],

[1] *University of Kragujevac, Faculty of Engineering, Department for Production Engineering, Kragujevac, Serbia, milan.ivkovic@kg.ac.rs, 0000-0001-5176-5837, julijabkg@gmail.com*, 0009-0006-3031-2234, *nadica.stojanovic@kg.ac.rs , 0000-0002-4199-0587, smiletic@kg.ac.rs, 0009-0007-0253-2819, devedzic@kg.ac.rs,* 0000-0002-6589-5883, *petrovic.savic@kg.ac.rs*, 0000-0002-5629-6221

[2] *Academy of applied studies Kosovo and Metohija, Department of Manufacturing Technologies and Materials in Mechanical Engineering Leposavić, Republic of Serbia, strahinja.djurovic@akademijakm.edu.rs, 0000-0003-3971-7984*

Corresponding author: petrovic.savic@kg.ac.rs

Abstract

Tool wear significantly affects machining accuracy, surface quality, and the overall efficiency of modern manufacturing systems. Therefore, reliable tool condition monitoring is of critical importance for ensuring process stability and reducing production costs. In recent years, visual inspection systems have emerged as an effective direct approach for monitoring tool wear, enabling precise measurement of wear geometry. This paper provides an overview of visual inspection systems in machining processes, with a focus on drilling and milling. Key system components are analyzed, including image acquisition equipment, software platforms, and image processing methods, with particular emphasis on machine learning and deep learning approaches. Based on the literature review, an integrated workflow for offline visual inspection is proposed, encompassing the stages of image acquisition, preprocessing, feature extraction, wear quantification, and dataset generation. The results indicate that machine vision-based systems provide high accuracy and repeatability, along with significant potential for automation and future application of deep learning in industry.

Keywords: tool wear; machine vision; image processing; drilling; deep learning; inspection; dataset; UN SDG 9 and 12.

1. Introduction

Machining is a key technology in modern manufacturing, where tool condition directly affects accuracy, surface quality, process stability, and production costs [1]. Progressive tool wear can lead to defects, tool failure, and unplanned downtime, making tool condition monitoring (TCM) essential. Traditional monitoring methods, based on cutting forces, vibrations, and acoustic signals, enable continuous observation but do not provide direct insight into wear geometry. With the advancement of industrial cameras and image processing, visual approaches have gained importance due to their ability to directly detect tool wear and damage [2].

This paper presents machine vision-based approaches for tool wear analysis in drilling, focusing on feature extraction from images and their use in machine learning and deep learning models. Rather than experimental

results, the study proposes a methodological framework for the development of intelligent tool monitoring systems applicable in adaptive and autonomous manufacturing.

2. Materials and Methods

2.1 Visual Inspection Equipment

Visual inspection systems for tool wear are based on the integration of optical and mechanical components that enable reliable image acquisition under controlled conditions, where image quality directly affects detection accuracy.

The core component is an industrial camera, typically equipped with high-resolution sensors, while both area-scan and line-scan cameras are used depending on the application. Line-scan cameras are particularly suitable for capturing the full periphery of rotating tools, enabling complete surface inspection[3], and are widely applied in automated inspection systems requiring consistent geometry acquisition [4]. Optical elements, such as lenses, are essential for ensuring sufficient resolution and minimizing distortions, especially when measuring small wear features. Lighting is one of the most critical factors, as controlled illumination improves the visibility of wear zones and ensures measurement repeatability. Different lighting strategies are used to highlight surface defects, while variations in lighting conditions can significantly affect detection accuracy [3,5].

In this work, an offline visual inspection system is considered, consisting of an industrial camera and controlled lighting, providing stable acquisition conditions suitable for further image processing and dataset generation.

2.2 Software Platforms

The implementation of visual inspection systems relies on software tools for image acquisition, processing, and analysis, including both open-source and commercial solutions. Open-source libraries such as OpenCV and MATLAB are widely used for image processing tasks, including filtering, segmentation, and feature extraction, due to their flexibility and suitability for rapid development. In industrial environments, specialized platforms such as HALCON and Cognex VisionPro provide optimized solutions for inspection, measurement, and real-time quality control. Recent studies show that combining classical image processing with machine learning methods improves the performance of tool wear monitoring systems, especially under complex conditions [1,6]. In this work, a software environment supporting preprocessing, segmentation, feature extraction, and annotated dataset generation is considered.

2.3 Image Processing and Machine Learning Methods

Image processing methods play a key role in extracting relevant information from images of cutting tools. A typical workflow includes preprocessing, segmentation, feature extraction, and wear quantification. Preprocessing techniques, such as grayscale conversion, filtering, contrast enhancement, and normalization, are used to improve image quality and reduce noise, ensuring robustness to variations in acquisition conditions[2].

Segmentation is applied to isolate regions of interest, particularly wear zones, using methods such as thresholding, edge detection, and contour extraction[6]. Feature extraction involves quantifying key wear

parameters, including flank wear width (VB), maximum wear (VBmax), and contour irregularities, which are essential for tool condition evaluation [7].

Recently, machine learning and deep learning methods have significantly improved tool wear monitoring. Convolutional neural networks (CNNs) enable automatic feature extraction and classification, enhancing the detection of complex wear patterns[5,8]. Segmentation-based models, such as Mask R-CNN, have shown high efficiency in detecting and localizing wear regions, although their performance depends on dataset quality and annotations [3].

In this work, a structured workflow for image acquisition and processing is considered, with a focus on the preparation of annotated datasets to support future deep learning applications.

3. Results and Discussion

The application of visual inspection systems for tool wear monitoring has been widely investigated in the literature, confirming their capability for accurate and repeatable measurement of wear parameters such as flank wear width (VB) and maximum wear (VBmax). Classical image processing methods have proven effective for identifying wear zones under controlled conditions [2], while machine vision systems enable automated inspection with improved consistency and reduced inspection time [1].

Recent developments highlight the growing role of machine learning and deep learning methods, particularly CNN-based approaches, which improve the detection of complex wear patterns under varying conditions [5,8]. Hybrid approaches combining visual and process signals further enhance robustness in complex environments [9].However, several limitations remain, primarily related to sensitivity to image acquisition conditions and the dependence of learning-based models on high-quality annotated datasets [2]. In addition, existing studies often lack an integrated approach, focusing on individual system components rather than the complete workflow.

In this context, this study proposes a structured workflow for offline visual inspection, integrating all key stages from image acquisition to wear quantification and dataset generation. The use of an offline system ensures stable and repeatable conditions, improving measurement reliability and enabling the creation of high-quality datasets for future deep learning applications. The proposed workflow is illustrated in Figure 1.

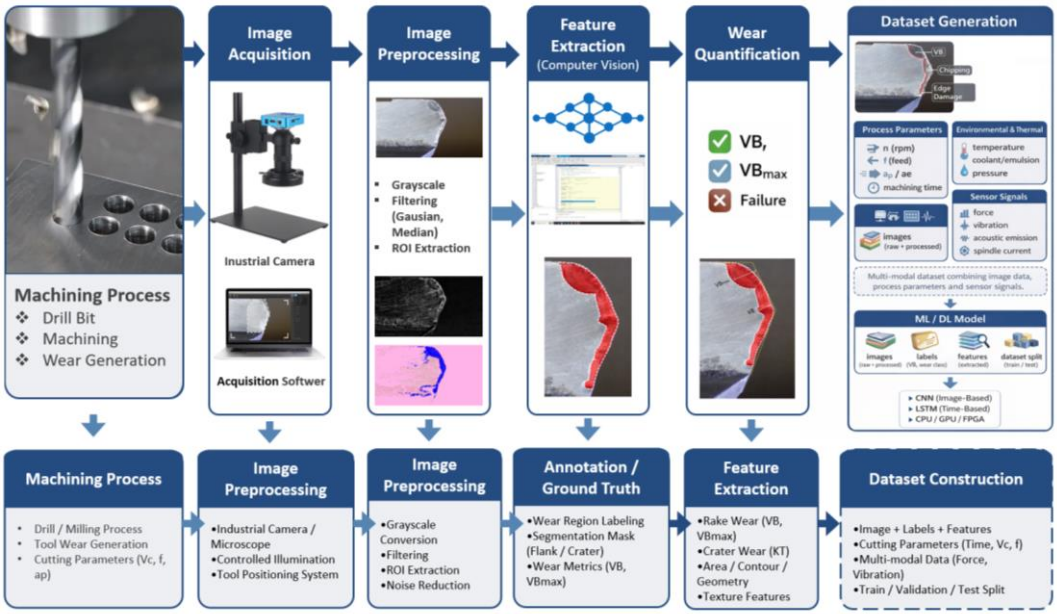


Figure 1. Structured workflow of the tool wear visual inspection system

Although modern deep learning-based approaches demonstrate high potential, their industrial application still depends on the availability of high-quality data and the robustness of models under varying conditions. Therefore, future research should focus on the integration of visual and sensor data, as well as on the development of real-time operational systems.

4. Conclusions

This paper provides a concise overview of visual inspection systems for tool wear monitoring in machining processes. The analysis confirms that machine vision-based approaches enable accurate and repeatable wear measurement, offering significant advantages over indirect monitoring methods. An integrated workflow for offline tool wear analysis is proposed, including image acquisition, preprocessing, feature extraction, wear quantification, and dataset generation. The results highlight the importance of controlled acquisition conditions and high-quality annotated datasets. The proposed approach provides a foundation for future implementation of deep learning methods and the development of real-time tool condition monitoring systems in industrial environments.

Acknowledgement

This work presents the results of research conducted within projects financially supported by the Ministry of Science, Technological Development and Innovation of the Republic of Serbia, under Contract No. 451-03-34/2026-03/200107, dated February 5, 2026.

References

[1] Zhang C, Zhang J. On-line tool wear measurement for ball-end milling cutter based on machine vision. Computers in Industry 2013;64:708–19. https://doi.org/10.1016/j.compind.2013.03.010.
[2] Ramzi R, Bakar EA, Mahmod MF. Drill Bit Flank Wear Monitoring System in Composite Drilling Process Using Image Processing. In: Zawawi MAM, Teoh SS, Abdullah NB, Mohd Sazali MIS, editors. 10th International Conference on Robotics, Vision, Signal Processing and Power Applications, vol. 547, Singapore: Springer Singapore; 2019, p. 551–7. https://doi.org/10.1007/978-981-13-6447-1_70.
[3] Andersson P. Cutting Tool Wear: Data Acquisition and Automation of Wear Measurements on End Mills n.d.
[4] Ramzi R, Bakar EA. Optical Wear Inspection of Countersink Drill Bit for Drilling Operation in Aircraft Manufacturing and Assembly Industry: A Method. IOP Conf Ser: Mater Sci Eng 2018;370:012041. https://doi.org/10.1088/1757-899X/370/1/012041.
[5] Sousa VFC, Gil J, Silva TEF, De Jesus AMP, Silva FJG, Tavares JMRS. An Image Analysis Algorithm for Measuring Flank Wear in Coated End-Mills. CMC 2025;83:177–99. https://doi.org/10.32604/cmc.2025.062133.
[6] Yu J, Cheng X, Lu L, Wu B. A machine vision method for measurement of machining tool wear. Measurement 2021;182:109683. https://doi.org/10.1016/j.measurement.2021.109683.
[7] Lee SKH, Mongan PG, Farhadi A, Hinchy EP, O'Dowd NP, McCarthy CT. In-situ evaluation of hole quality and cutting tool condition in robotic drilling of composite materials using machine learning. J Intell Manuf 2026;37:97–118. https://doi.org/10.1007/s10845-024-02528-7.
[8] Xu X, Wang J, Zhong B, Ming W, Chen M. Deep learning-based tool wear prediction and its application for machining process using multi-scale feature fusion and channel attention mechanism. Measurement 2021;177:109254. https://doi.org/10.1016/j.measurement.2021.109254.
[9] Bilal M, Podishetti R, Koval L, Gaafar MA, Grossmann D, Bregulla M. Automatized End Mill Wear Inspection Using a Novel Illumination Unit and Convolutional Neural Network. IEEE Access 2024;12:124282–97. https://doi.org/10.1109/ACCESS.2024.3454692.

Benchmarking a wireless strain gauge monitoring system against DFOS in CFRP

Maria Xenidou[1], Andreas Kalogirou[1], Kyriaki Tsirka[1], Dimitrios Fakis[1], Alkiviadis S. Paipetis[1]

[1] *Composite and Smart Materials Laboratory (CSML), Materials Science & Engineering department, School of Engineering, University of Ioannina, 45110 Ioannina, Greece, m.xenidou@uoi.gr, 0009-0006-3945-604X, akalogirou@uoi.gr, 0009-0000-2226-2173, ktsirka@uoi.gr, 0000-0001-8792-2726, fkdimitris@gmail.com, 0000-0001-5219-3607, paipetis@uoi.gr, 0000-0001-9668-9719*

Corresponding author: paipetis@uoi.gr

Abstract

In the framework of CoPropel project, this study supports the development of complementary structural health monitoring technologies for composite marine propellers. In particular, the agreement between measurements obtained from a developed wireless strain gauge acquisition system and distributed fiber optic sensing is evaluated in carbon fiber reinforced polymer specimens under three-point bending. The experimental configuration presented in this work combines a surface mounted optical fiber, an embedded optical fiber, and a surface bonded strain gauge, enabling direct comparison between the two sensing approaches while also capturing the distributed strain profile along the specimen length. Furthermore, the reliability of the embedded DFOS after integration into the composite is examined, and the difference between surface and within the laminate strain response under flexural loading is assessed. The results demonstrated that both sensing technologies successfully captured the material's response, while the optical fiber recorded higher strain values than the strain gauge. Overall, the results validate the performance of the developed strain gauge acquisition system for strain monitoring and confirm the suitability of DFOS for distributed health monitoring of composite structures.

Keywords: Structural health monitoring; Fiber optic sensors; composite materials; embedded sensors; strain measurement; sensor benchmarking; UN SDG 9

1. Introduction

Carbon fiber-reinforced polymer (CFRP) materials are increasingly used in engineering applications, creating a strong need for reliable structural health monitoring strategies capable of capturing strain evolution during operation [1,2]. Distributed fiber optic sensing (DFOS), particularly OFDR-based approaches, has attracted growing interest for composite monitoring as it provides spatially continuous, high-resolution strain information along the sensing path, in contrast to discrete measurements of point-sensing approaches. [3,4].

Previous studies have shown that DFOS can be embedded into composite laminates and provide strain measurements in good agreement with conventional reference techniques under mechanical loading [5]. Recent studies have also highlighted the importance of sensor configuration and strain transfer effects, particularly in

surface bonded optical fibers, [6], while validation studies on large FRP structures have further demonstrated the value of distributed sensing over discrete sensors for capturing full strain profiles.[2].

DFOS and a wireless strain gauge system were developed as complementary structural health monitoring approaches within Copropel, addressing sensor integration and implementation challenges for a rotating underwater propeller environment [7]. Further work focused on establishing a methodology for embedding optical fibers during manufacturing, ensuring their post manufacturing functionality, and evaluating signal reliability under bending induced strain together with the knockdown effect on the host material. [8]. In this context, the present study investigates a coupon-level benchmarking methodology for evaluating strain gauge measurements against DFOS in CFRP, using both surface mounted and embedded optical fibers under bending loading.

2. Materials and Methods

Three-point bending tests were conducted on CFRP samples employed with optical fibers (OF) and strain gauge (SG) sensors. For direct comparison, a strain gauge and a surface mounted optical fiber were bonded near the midspan, where the highest tensile strain is expected during bending. A second optical fiber was embedded on the same side of the laminate, allowing the strain measured at the surface to be compared with that within the laminate. Testing was performed over a 160 mm support span with a 3 mm loading nose to promote predominantly flexural deformation.

Distributed strain was acquired using a Rayleigh-based OFDR interrogator (LUNA ODiSI), whereas the SG response was recorded using a simplified wireless acquisition unit built around an Arduino microcontroller. To compare the two sensing techniques, a local section of the surface mounted OF was selected adjacent to the SG position so that both sensors measured the response in the same specimen region.

3. Results and Discussion

The distributed strain profiles measured by the embedded and surface mounted optical fibers showed the expected flexural response of the CFRP specimens under three-point bending, with maximum tensile strain at midspan and lower strain levels near the supports. The strain increased with increasing load for both optical fibers, indicating a consistent and response throughout the test. Under the same loading level, the surface mounted optical fiber recorded higher strain than the embedded optical fiber. This difference is consistent with the thought-thickness position of the sensors, since the surface mounted fiber was farther from the neutral axis and therefore experienced higher tensile strain, whereas the embedded fiber was closer to the neutral axis.

Comparison between the collocated strain gauge and the surface mounted optical fiber showed that both sensing techniques followed the same overall trend during loading. The optical fiber returned higher strain values than the strain gauge in general, although both signals changed monotonically with load and remained in good qualitative agreement. This behavior suggests that both systems were able to capture the mechanical response reliably, while the observed offset may be related to differences in strain transfer, gauge length, sensing principle, or calibration.

The optical fiber provided distributed strain information along the specimen length, which allowed the full bending strain profile to be observed rather than only a single local value. The strain gauge, however, remained effective up to specimen failure and provided a stable local reference measurement throughout the test. Isolated NaN values were observed in the optical fiber data over short regions of high strain gradient, while the higher-rate strain-gauge data required time averaging prior to comparison.

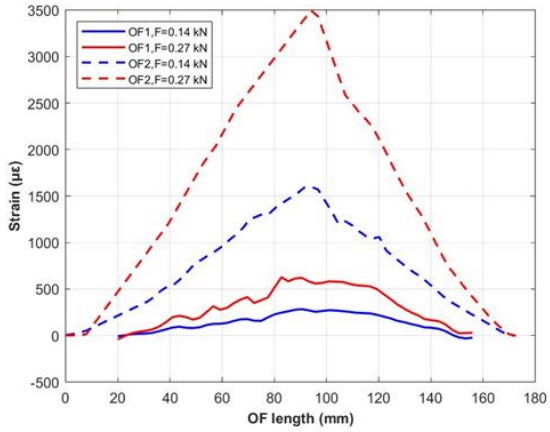


Figure 6. Strain measurements over the length of an embedded (OF1) and a surface mounted (OF2) optical fiber for two different load levels.

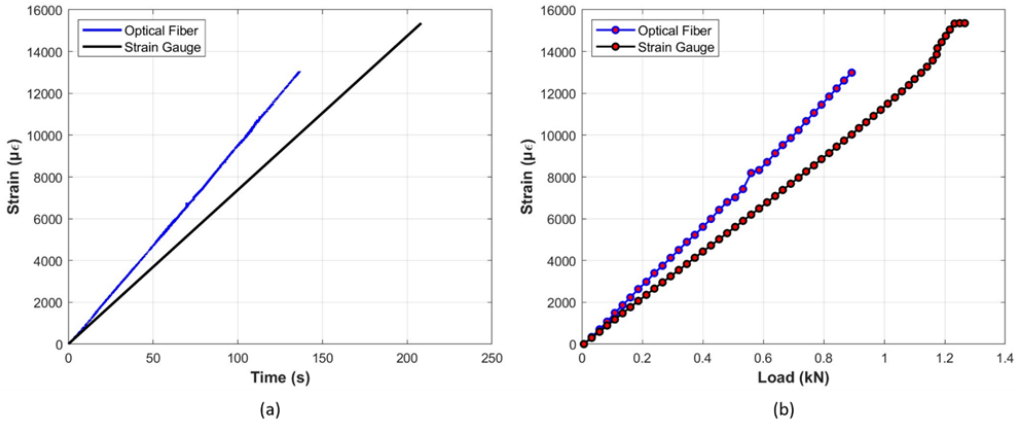


Figure 7. *Correlation of μstrain measurements acquired from a surface bonded SG and OF under three-point bending test*

4. Conclusions

This study benchmarked distributed optical fiber sensing against strain gauge measurements in CFRP specimens under three-point bending. Both sensing approaches captured the flexural response successfully, while the surface mounted optical fiber recorded higher strain than the embedded fiber because of its greater distance from the neutral axis. Good agreement in overall trend was observed between the collocated strain gauge and

the surface mounted optical fiber. The results further confirmed the post manufacturing functionality of the embedded optical fiber and demonstrated the capability of the developed wireless strain gauge acquisition system to provide reliable local strain measurements.

Overall, the study confirms that distributed optical fibers and strain gauges can operate as complementary sensing technologies, combining full field strain monitoring with local reference measurements for composite SHM.

Acknowledgements

This research has received funding from the Horizon Europe Research and Innovation Actions, under grant agreement No 101056911, project CoPropel "Composite material technology for next-generation Marine Vessel Propellers".

References

[1] Biondi A, Wu R, Cao L, Gopalan B, Ivey J, Garces C, Mitchell M, Williams JD, Wang X. Fiber Optic Sensing Textile for Strain Monitoring in Composite Substrates. Sensors 2022;22. https://doi.org/10.3390/s22239262.

[2] Siwowski T, Rajchel M, Howiacki T, Sieńko R, Bednarski Ł. Distributed fibre optic sensors in FRP composite bridge monitoring: Validation through proof load tests. Eng Struct 2021;246. https://doi.org/10.1016/j.engstruct.2021.113057.

[3] Shi J, Wang Z, Zhang Y, Chen Z, Liu E, Xian G. Full-length strain and damage monitoring for carbon fiber reinforced polymer cable based on optical frequency domain reflectometry. Mech Syst Signal Process 2024;219. https://doi.org/10.1016/j.ymssp.2024.111627.

[4] Zhan Y, Han M, Wang Z, Xu L, Song Z, Lu A, Guo X, Deng W, Huang S. Distributed strain monitoring for different composites structures with high resolution based on optical fiber sensing. Optik (Stuttg) 2021;248. https://doi.org/10.1016/j.ijleo.2021.168113.

[5] Boursier Niutta C, Tridello A, Ciardiello R, Paolino DS. Strain Measurement with Optic Fibers for Structural Health Monitoring of Woven Composites: Comparison with Strain Gauges and Digital Image Correlation Measurements. Sensors 2023;23. https://doi.org/10.3390/s23249794.

[6] Falcetelli F, Rossi L, Di Sante R, Bolognini G. Strain transfer in surface-bonded optical fiber sensors. Sensors (Switzerland) 2020;20. https://doi.org/10.3390/s20113100.

[7] Seno AH, Fakis D, Omairey S, Zitoun A, Jayasree N, Kazilas M, Xenidou M, Kalogirou A, Tsirka K, Paipetis A, Larreur M. Smart Self-sensing Composite Marine Propeller: Increased Maintenance Efficiency Through Integrated Structural Health Monitoring Systems. Lecture Notes in Mobility, vol. Part F1025, Springer; 2026, p. 61–7. https://doi.org/10.1007/978-3-032-06763-0_9.

[8] M. Xenidou, “INTEGRATION OF FIBER OPTIC SENSORS INTO CFRP FOR STRUCTURAL HEALTH MONITORING OF A MARINE COMPOSITE PROPELLER,” in Proceedings of the 21st European Conference on Composite Materials Vol 1, C. Binetriuy and F. Jasquemin, Eds., Nantes, France: The European Society for Composite Materials (ESCM) and the Ecole Centrale de Nantes., Jul. 2024, pp. 211–216.

Flexible Sensor Development for Smart Packaging via CeraPrinter F-Series System Technologies

D. A. Exarchos, P. T. Dalla, P. Pantazis, I. Angelopoulos and T. Matikas

Department of Materials Science and Engineering, University of Ioannina, Ioannina, Greece, exarchosd@gmail.com
Corresponding author: exarchosd@gmail.com

Abstract
The transition to Smart Packaging 4.0 transforms packaging from passive containment to active systems enabling real-time monitoring and traceability. This work presents the CeraPrinter F-Series as a hybrid digital deposition platform for fabricating flexible sensors on functional substrates, combining industrial inkjet and Aerosol Jet technologies for precise multi-material processing. Representative sensors include IDT biosensors for label-free bacterial detection, piezoelectric strain sensors for mechanical monitoring, and colorimetric gas sensors for oxygen detection in modified atmosphere packaging. These devices can be integrated with RFID and NFC technologies, enabling wireless data transmission and user interaction. The platform also supports the development of active packaging through printed antimicrobial coatings based on silver nanoparticles, improving product safety and shelf life. Overall, the results demonstrate the potential of hybrid additive manufacturing to produce scalable, multifunctional smart packaging systems for applications in food safety, supply chain monitoring, and sustainable product management.

Keywords: Printed Electronics, Smart Packaging, CeraPrinter F-Series, Inkjet Printing, Flexible Sensors, UN SDG 9.

1. Introduction

The change to Smart Packaging 4.0 is a radical departure from passive containment to active cyber-physical interfaces that can be autonomously monitored and traced. This development integrates sensors and communication modules into the packaging structure so that real-time data collection can be performed regarding the condition of the product and its authenticity. This transition is enabled by the underlying technology called Printed Electronics (PE), which employs additive manufacturing to transfer functional inks, such as conductive, semiconductive or dielectric inks, onto flexible substrates, such as polymer films, paper, and textiles [1]. In comparison to conventional semiconductor manufacturing, which is based on subtractive etching and lithography, hybrid digital deposition is able to masklessly pattern functional materials with picoliter precision. This additive method enables rapid prototyping of 3D electrode arrays and add electronic functionality to geometrically complex surfaces. With the help of innovative tools such as the CeraPrinter F-Series, scientists can create more intricate multi-layer architectures capable of perceiving environmental variations (temperature, oxygen, pathogens) and transmitting them wirelessly, which is one of the strategic resources of Industry 5.0 [2].

2. Technical Analysis of the CeraPrinter F-Series Platform

The CeraPrinter F-Series is an "All-in-one" state-of-the-art digital materials deposition platform designed for advanced process development in Printed Electronics and Smart 3D Printing. It is built on a modular, scalable technology that allows for quick and easy upgrades, enabling concurrent multi-user operation through a single user-friendly interface[3].

2.1 Hybrid Deposition Technology and Printhead System

The F-Series distinguishes itself as a hybrid platform combining Industrial Inkjet and Aerosol Jet® technologies, facilitating the study of hybrid processes inaccessible when using these technologies separately[3]. The system features multi-material capability, supporting up to five printheads to deposit inks and pastes up to 1000 cP. Its "Smart Door" technology allows for fast, "Plug & Play" head mounting to reduce material transition times. The platform supports various printhead types, ranging from simple single nozzles and Dimatix cartridges to industrial Konica-Minolta and Fujifilm Samba heads. Additionally, it offers flexible printing modes, including Raster-Scan, Vector, and Single Pass options.

2.2 Mechanical Precision and Substrate Management

The platform is based on a high-accuracy calibrated five-axis motion system (3 translation axes and 2 motorized rotations) to ensure precise alignment and calibration. The system handles substrate specifications up to 305 mm × 305 mm and 10 mm thick, with custom sizes available. It delivers exceptional accuracy and repeatability, featuring X/Y accuracy of ±2 µm, repeatability below ±0.5 µm, and Z accuracy within ±2 µm. High-precision substrate alignment (±2 µm) and nozzle self-calibration (<±3 µm) ensure consistent results. This high performance yields a print resolution finer than 5 µm × 5 µm at velocities reaching 500 mm/s[3].

2.3 Integrated Software and Post-Processing

The software suite enables a bottom-up approach to designing and printing complex 2D and 3D multi-material functional devices.

- CeraSlice: CAD/CAM software supporting DXF, STEP, Gerber, GDSII, and Bitmap formats.
- DropAnalyser: Automated jetting analysis software for real-time control of drop volume, velocity, and jet straightness.
- FabAnalyser: Post-printing characterization for automated measurements of distance, area, 3D reconstruction, and sheet resistance (4-point probe).
- In-line Post-Treatment: The system integrates up to 3 post-treatment modules, including Near Infrared (NIR), Ultraviolet (UV), and Vacuum Drying, synchronized with the printing job to avoid substrate manipulation[3,4].

2.4 Broad Range of Electronic Applications

The flexibility of the F-Series enables fabrication of a wide variety of components:

- IoT & Communication: HF Antennas, RFID tags, 5G/6G components[5].
- Energy: OPV photovoltaics, OLED lighting, printed batteries, supercapacitors, and fuel cells[5].
- Electronics & Sensors: Temperature and humidity sensors, piezoelectric actuators, photodetectors, printed memories, semiconductors, and LTCC/MLCC components[4,6,7].
- Flexible & 3D Electronics: Wearables, e-textiles, In-mold electronics, and stretchable/carbon electronics[5].

3. Sensor Mechanisms and Fabrication

Sensors fabricated using the CeraPrinter transduce external stimuli into measurable signals through electrochemical, piezoelectric, or optical mechanisms. The following sections present representative sensor types and their fundamental operating principles.

3.1 IDT Biosensors (University of Ioannina)

Interdigital transducer (IDT) biosensors, also referred to as interdigitated array microelectrodes (IDAM), consist of interleaved microelectrodes arranged in a comb-like geometry, where parallel conductive fingers alternate to form high-surface-area, high-sensitivity structures. The small spacing between electrodes enhances charge

transport and interaction with the analyte. Their operation is based on electrochemical impedance spectroscopy (EIS), where the total system impedance is measured in response to a low-amplitude AC sinusoidal excitation. Detection occurs through the binding of biomolecules or bacterial cells to immobilized bioreceptors on the electrode surface, inducing changes in charge transfer resistance and interfacial capacitance. Through this mechanism, IDT/IDAM sensors enable label-free detection of bacteria, such as *E. coli*, in aqueous or food samples with high sensitivity[8].

3.2 Piezoelectric Strain Sensors

Piezoelectric strain sensors fabricated via inkjet printing are implemented as multilayer structures on flexible substrates. The device consists of two printed silver (Ag) electrodes separated by an active P(VDF-TrFE) piezoelectric layer with a thickness of approximately 3 µm, deposited on a polyimide substrate. Their operation relies on the direct piezoelectric effect, where applied mechanical stress or bending generates a potential difference between the electrodes. The output voltage is proportional to the applied load, enabling real-time monitoring of dynamic mechanical variations, with typical values up to ~850 mV. These sensors operate without external power (self-powered), making them suitable for monitoring mechanical strain in flexible and integrated systems[9].

3.3 Colorimetric Gas Sensors

Colorimetric gas sensors fabricated using inkjet printing are employed for oxygen detection in smart packaging applications. The functional ink consists of toluidine blue (TB), SnO_2 nanoparticles, glycerol, and an HPMC polymer matrix, and is directly printed onto flexible substrates. The sensing mechanism is based on a photoactivated redox reaction. Upon exposure to UVC (~254 nm), TB is reduced to its colorless form (leuco-TB), while in the presence of oxygen it is re-oxidized, recovering its original blue color within approximately 55 minutes. This color change is visible to the naked eye and serves as an indicator of oxygen presence, enabling the detection of leaks in modified atmosphere packaging (MAP)[10].

4. Smart Packaging Solutions

Smart packaging technologies integrate printed sensors with functional materials, enabling real-time monitoring and protection of product integrity. The incorporation of communication mechanisms and active coatings allows both condition sensing and shelf-life extension. The following sections outline key approaches in this field.

4.1 Internet of Packaging (IoP) and RFID/NFC

The integration of sensors with communication systems is a core element of the Internet of Packaging (IoP), transforming packages into smart data nodes. Printed sensors can be combined with RFID or NFC antennas to form low-cost sensing and wireless communication units. Passive RFID tags are powered by electromagnetic fields without an internal energy source and allow reading at distances up to ~10 m, making them suitable for supply chain tracking and large-scale monitoring. This combination further enables real-time assessment of product quality parameters. NFC technologies enable direct interaction with end users via smartphones, allowing real-time access to product condition information[11].

4.2 Active Packaging and Antimicrobial Functionality

The CeraPrinter F-Series was used to deposit antimicrobial coatings based on silver nanoparticles (AgNPs) with sizes of 7–30 nm, embedded in nano-inks and deposited on polymer substrates. AgNPs exhibit strong antibacterial activity against microorganisms such as *E. coli*, achieving significant bacterial reduction and inhibition zones greater than 6 mm. The mechanism is primarily based on the release of Ag^+ ions and the generation of oxidative stress, leading to disruption of the bacterial cell membrane. The placement of the coating

on the external side of the packaging film minimizes nanoparticle migration into the food, ensuring safety while maintaining antimicrobial functionality[12,13].

5. Conclusions

The transition to Smart Packaging 4.0 transforms conventional packaging into active, cyber-physical systems. The CeraPrinter F-Series enables the direct integration of functional electronic components onto flexible substrates through hybrid digital deposition, combining inkjet precision with Aerosol Jet versatility to fabricate advanced sensors such as IDT biosensors, piezoelectric strain sensors, and colorimetric indicators. The integration of these sensors with RFID/NFC technologies converts packaging into intelligent data nodes within the Internet of Packaging (IoP), enabling real-time monitoring of product condition and traceability. In parallel, the incorporation of antimicrobial coatings enhances food safety and extends shelf life. Overall, scalable additive manufacturing approaches support the transition of smart packaging from laboratory-scale concepts to industrial applications, establishing real-time diagnostics and traceability as key features of next-generation packaging systems.

References

1. Djafar MJ, Elmatsani HM, Munarso SJ, Firdaus J, Trihadi SEY, Purwanta W, Sadikin BS, Sahlan S, Nasruddin N, Lanjar L. Smart Packaging 4.0: A bibliometric analysis of sensor integration, food safety, and sustainability in food packaging systems. ScientificWorldJournal. 2026;2026:3181510. doi:10.1155/tswj/3181510.
2. University of Ioannina, "Development of innovative biosensors for the assessment of packaged food lifespan using hybrid 3D printing techniques."
3. CERADROP, "CeraPrinter F-Serie Brochure - Hybrid Digital Materials Deposition Platform," 2022.
4. Mecca G, Bernasconi R, Zega V, Suriano R, Menegazzo M, Bussetti G, Corigliano A, Magagnin L. Inkjet-printed flexible piezoelectric sensor for large deformation applications. Technologies. 2025;13(5):206. doi:10.3390/technologies13050206.
5. Rinklin P, Tseng TM, Liu C, Li M, Terkan K, Grob L, Adly N, Zips S, Weiß L, Schlichtmann U, Wolfrum B. Flex. Print. Electron. 2019;4:045002
6. Tseng TM, Lian M, Li M, Rinklin P, Grob L, Wolfrum B et al. Manufacturing Cycle-Time Optimization Using Gaussian Drying Model for Inkjet-Printed Electronics. In 2021 40th IEEE/ACM International Conference on Computer-Aided Design, ICCAD 2021 - Proceedings. Institute of Electrical and Electronics Engineers Inc. 2021. (IEEE/ACM International Conference on Computer-Aided Design, Digest of Technical Papers, ICCAD). doi: 10.1109/ICCAD51958.2021.9643436
7. Analyst, "Inkjet-printed O2 gas sensors in intelligent packaging," Royal Society of Chemistry, 2021.
8. Varshney M, Li Y. Interdigitated array microelectrodes based impedance biosensors for detection of bacterial cells. Biosens Bioelectron. 2009;24(10):2951–2960.
9. Mecca G, Bernasconi R, Zega V, Suriano R, Menegazzo M, Bussetti G, Corigliano A, Magagnin L. Inkjet-printed flexible piezoelectric sensor for large deformation applications. Technologies. 2025;13(5):206.
10. Fernández-Ramos MD, Pageo-Cabrera M, Capitán-Vallvey LF, Pérez de Vargas-Sansalvador IM. Inkjet-printed O2 gas sensors in intelligent packaging. Analyst. 2021;146(10):3177–3184.
11. Okur EE, Eker F, Akdaşçi E, Bechelany M, Karav S. Comprehensive review of silver nanoparticles in food packaging applications. Int J Mol Sci. 2025;26(20):9842. doi:10.3390/ijms26209842.
12. Manikandan NA, McCann R, Kakavas D, Rochfort KD, Sreenilayam SP, Alkan G, Stornetta T, McGivern AR, Grintzalis K, Friedrich B, Foley G, Brabazon D, Freeland B. Production of silver nano-inks and surface coatings for antimicrobial food packaging and its ecological impact. Int J Mol Sci. 2023;24(6):5341.

Engineering Applications and Human-Centered Design

The Impact of Seatback Angle on Driver Discomfort: A Systematic Review

Slavica Macuzic Saveljic[1], Igor Saveljic[2]

[1]*Faculty of Engineering, University of Kragujevac, Kragujevac, Serbia, s.macuzic@kg.ac.rs, 0000-0003-2635-2496*

[2]*Institute for Information Technologies, University of Kragujevac, Kragujevac, Serbia, isaveljic@kg.ac.rs, 0000-0002-0707-5174*

Corresponding author: s.macuzic@kg.ac.rs

Abstract

This systematic review examines current research on the effect of seatback angle adjustments on driver discomfort and musculoskeletal health. By synthesizing findings from experimental, biomechanical, and ergonomic studies, the review highlights how seatback geometry influences pressure distribution, muscle activation, and subjective comfort during prolonged driving. Methodological trends, limitations, and gaps in knowledge are discussed, with recommendations for future research directions and design guidelines for automotive seating.

Keywords: seatback angle; driver discomfort; biomechanics; whole-body vibration

1. Introduction

The configuration of the seatback angle is a critical ergonomic factor directly influencing occupant posture and perceived comfort, especially during prolonged driving. Musculoskeletal discomfort and fatigue remain prevalent complaints among drivers, despite advances in automotive seat design. The seatback angle not only affects lumbar support but also dictates the distribution of contact pressures across the torso and lower back, potentially contributing to the onset of pain and long-term spinal issues [1]. Research suggests that certain recline angles can reduce muscle activity and delay fatigue [2], yet inconsistencies in experimental protocols and seat designs complicate the generalization of such findings [3]. This review aims to systematically synthesize the available literature on the biomechanical and subjective effects of seatback angle adjustments, identify methodological trends and limitations, and outline key considerations for future automotive seat design.

2. Review Methodology

This review is based on a structured search and analysis of scientific literature published between 2010 and 2025. Databases such as PubMed, Scopus, and Google Scholar were queried using keywords including “seatback angle,” “driver discomfort,” “automotive ergonomics,” “musculoskeletal strain,” and “vibration.” Both experimental studies and biomechanical modeling papers were included. Studies were selected based on their relevance to seatback angle, methodological rigor, and the availability of quantitative or qualitative

outcomes related to comfort, muscle activity, or pressure distribution. References were cross-checked to ensure comprehensive coverage of the topic.

3. Literature Review

3.1 Biomechanical Effects of Seatback Angle

Multiple studies have demonstrated that seatback angle directly influences musculoskeletal load and seating comfort. Increasing the recline angle from 100° to 120° can significantly reduce lumbar muscle activity, thereby delaying fatigue during prolonged seating [3]. However, the specific impact depends on seat architecture, as traditional production seats often induce unwanted shifts in lumbar support during recline adjustment [4]. Advanced laboratory studies employing seat pivots aligned with the occupant's H-point have enabled more precise assessment of these effects [5].

3.2 Pressure Distribution and Muscle Activity

Optimal seatback angles, particularly when combined with appropriate lumbar support, minimize spinal load and redistribute pressure away from the sacral region toward the thoracic and scapular areas [5]. Electromyographic (EMG) studies show that increased recline reduces lumbar paraspinal activation, but may require greater activation of the abdominal muscles to stabilize the trunk [16]. There is also evidence that excessive recline can introduce compensatory strain in the cervical region, potentially negating lumbar benefits [21].

3.3 Interaction with Other Seat Parameters

The interaction between seatback inclination and other ergonomic features, such as seat pan orientation, is crucial for achieving pelvic stability and overall comfort [7]. Adjustments in seat pitch and backrest inclination have been shown to alleviate localized discomfort, especially in the lower back and hip regions [8]. The inclusion of adjustable lumbar support and personalized seat settings further enhances comfort, with reported improvements of up to 9% in overall comfort metrics [12].

3.4 Subjective Comfort vs Objective Indicators

While biomechanical optimization can reduce physical demands, subjective reports of comfort do not always align with objective improvements. Environmental factors such as whole-body vibration can exacerbate muscle activation and discomfort regardless of seat geometry [10,11]. Studies utilizing visual analog scales and pressure mapping have revealed significant variability in individual responses, underscoring the complexity of predicting comfort solely based on mechanical design [14].

3.5 Methodological Limitations

A major limitation in the current literature is the variability in experimental setups, including differences in seat architecture, pivot points, and test populations. Many laboratory studies rely on rigid test fixtures that do not replicate the damping and pressure dissipation characteristics of production-grade automotive foams [4,7]. Furthermore, most studies fail to account for real-world variables such as dynamic driving conditions, prolonged exposure, and individual anthropometric differences.

4. Discussion and Conclusions

The reviewed studies collectively indicate that seatback inclination is a critical determinant of driver comfort and biomechanical risk. Adjusting the seatback angle can modulate muscle activation patterns, redistribute pressure, and alter the body's response to whole-body vibration and external forces [20, 22]. However, maintaining excessive recline often necessitates compensatory cervical flexion to maintain road visibility, potentially introducing new discomfort or safety risks [21]. Additionally, higher recline angles can negatively influence the biodynamic response to vibration, increasing the risk of discomfort at certain frequencies [2]. These findings highlight the need for an integrated approach that considers biomechanical, subjective, and safety factors when designing automotive seats. Despite advances in measurement technology and modeling, significant knowledge gaps remain. Future work should focus on integrating predictive models of vibration transmission, real-world ergonomic testing, and advanced materials to bridge the gap between laboratory findings and on-road comfort. Ultimately, a user-centered, multidisciplinary approach is essential to minimize long-term spinal pathologies and enhance driver well-being.

Acknowledgements

This research was supported by the Ministry of Education, Science and Technological Development of the Republic of Serbia through Projects TR35041 (Faculty of engineering, University of Kragujevac) and 451-03-33/2026-03/200378 (Institute for Information Technologies, University of Kragujevac).

References

1. Tao Q, Kang J, Sun W, Li Z, Xiao H. Digital evaluation of sitting posture comfort in human-vehicle system under industry 4.0 framework. Chinese Journal of Mechanical Engineering. 2016, 29(6):1096.
2. Rao MJ, Sivapirakasam SP, Sankaranarayanasamy K. Whole body vibration of the midibus driver with different seating condition. In: IOP Conference Series Materials Science and Engineering, IOP Publishing; 2018, 12115.
3. Reed MP. Reclined Postures in Vehicle Seats: Preferred Seatback Contours and Head Support Locations Deep Blue (University of Michigan). University of Michigan, 2023.
4. Reed MP, Ebert SM, Vallier TR. Reclined postures in vehicle seats: Preferred seatback contours and head support locations. Applied Ergonomics. 2025;125:104479.
5. Savonnet L. Development of a customizable digital tool for assessing aircraft passenger discomfort and fatigue. HAL (Le Centre pour la Communication Scientifique Directe), 2018.
6. Lecocq M, Lantoine P, Bougard C, Allègre JM, Bauvineau L, González D, et al. Perceived discomfort and neuromuscular fatigue during long-duration real driving with different car seats. PLoS ONE, 2022, 17(12).
7. Grebonval C, Beillas P, Wang X. Experimental investigation of preferred seating positions and postures in reclined seating configurations. HAL (Le Centre pour la Communication Scientifique Directe) 2021.
8. Punsongserm R. Effectiveness of Predominant Letterforms in Multi-Viewing Distances: Thai Universal Design Font Versus Familiar Thai Text Fonts. Archives of Design Research, 2023;36(4):87.

9. Sato F, MIYAZAKI Y, Morikawa S, Perez AF, Schick S, Brolin K, et al. The Effect of Seat Back Inclination on Spinal Alignment in Automotive Seating Postures. Frontiers in Bioengineering and Biotechnology, 2021, 9.
10. Arévalo MTV, Gyi D, Mansfield NJ, Picton R, Hirao A, Furuya T. Engineering movement into automotive seating: Does the driver feel more comfortable and refreshed? Applied Ergonomics, 2018, 74:214.
11. Guo LX, Dong RC, Yuan S, Feng QZ, Fan W. Influence of seat lumbar support adjustment on muscle fatigue under whole body vibration: An in vivo experimental study. Technology and Health Care, 2021, 30(2):455.
12. Min G. Analyze the physical interaction between the user and the furniture design to optimize comfort and functionality. Molecular & cellular biomechanics, 2024, 21(2):457.
13. Maradei F, Quintana L, Castellanos J. Effect of seat inclination on intradiscal pressure during simulated driving task, assessed using a biomechanical model. Ingeniare Revista chilena de ingeniería, 2016, 24(3):520.
14. Lyu J, Chen SR, Shan-shan X, Zhong Q, Chang D, Lin Y, et al. Effects of Seat Height and Backrest Inclination on Body Pressure Distribution and Subjective Comfort in Seat Design for the Elderly. Applied Sciences, 2025, 15(20):11224.
15. Cvetković D, Desai RM, Παπαϊωάννου Γ, Happee R. Kinematic body responses and perceived discomfort in a bumpy ride: Effects of sitting posture. arXiv (Cornell University), 2023.
16. Tebbache N, Hamaoui A. Effect of Seat Backrest Inclination on the Muscular Pattern and Biomechanical Parameters of the Sit-to-Stand. Frontiers in Human Neuroscience, 2021, 15.
17. Basri B, Griffin MJ. Predicting discomfort from whole-body vertical vibration when sitting with an inclined backrest. Applied Ergonomics, 2012, 44(3):423.
18. Basri B, Griffin MJ. The vibration of inclined backrests: perception and discomfort of vibration applied normal to the back in the x-axis of the body. Journal of Sound and Vibration, 2011, 330:4646.
19. Ding W, Wang L, Ao H, Chen Z, Yan H. Biodynamic response of the seated human body to a vibrating environment: Effect of seat backrest support. Research Square (Research Square), 2023.
20. Ding W, Wang L, Chen Z, Ao H, Yan H. Vibration reduction of human body biodynamic response in sitting posture under vibration environment by seat backrest support. Scientific Reports, 2024, 14(1).
21. MF MFMG, L LQ. Influencia de los movimientos lumbopélvicos en la percepción de dolor lumbar en postura sedente prolongada en conductores, realizados a partir de un dispositivo colocado sobre el asiento. Revista Ciencias de la Salud, 2014, 12(3):21.
22. Liu Z. Effects of Trunk Rotation and Backrest Activity on Lumbar sEMG Activities, Body Pressure Distribution and Sitting Discomfort during Sitting. 2019.

When it comes to silence, it is necessary to face the opposite concept: noise insulation

BECCHIS OSIRIDE DOO KRAGUJEVAC

Dragutin Tijanić[1], Tamara Dimitrijević[2]

[1]BECCHIS OSIRIDE DOO, Quality department, Kragujevac, Serbia (dragutin.tijanic@becchis.com)
[2] BECCHIS OSIRIDE DOO, HR department, Kragujevac, Serbia (tamara.dimitrijevic@becchis.com)

Contact email: info@becchis.com | Website: www.becchisosiride.it

Executive Summary

Becchis Osiride is an Italian industrial company specializing in the development and production of acoustic and thermal insulation materials. The company was founded in 1893 and is headquartered in Turin, Italy. Over more than a century of operation, it has become an important supplier of insulation components for several manufacturing industries, particularly the automotive sector.

The company focuses on designing and producing materials that reduce noise, vibration, and heat in various mechanical systems. Its main products include sound dampers, sound absorbers, heavy acoustic layers, silencers, and heat-shielding materials. These components are used to improve comfort, safety, and performance in vehicles and household appliances. In addition to acoustic solutions, Becchis Osiride also manufactures thermal insulation systems such as engine insulation, heat shields, and soft interior trims.

Production is based on specialized industrial processes that transform raw materials into advanced insulation components. The company develops both standard and customized products according to the technical requirements of its clients. Engineers and technicians work closely with manufacturers to design solutions that meet strict performance and environmental standards.

Becchis Osiride primarily supplies large industrial manufacturers, especially companies in the automotive and home appliance industries. Its products are used by global vehicle producers and other industrial partners to reduce noise levels and improve thermal protection in their products. The company operates internationally and also has production facilities outside Italy, including a factory in Kragujevac, Serbia, which manufactures insulation components for automotive applications.

Through continuous innovation and long-term industrial experience, Becchis Osiride has established itself as a reliable partner for manufacturers that require high-quality acoustic and thermal insulation solutions.

BECCHIS OSIRIDE DOO Kragujevac is a mid-sized manufacturing company located in Kragujevac, operating within the automotive supply sector as Tier 1 supplier. Founded in 2011 as a subsidiary of the Italian

company Becchis Osiride S.R.L., it focuses on producing components and materials for the automotive industry, with a strong emphasis on acoustic and thermal insulation solutions.

Keywords: flexible solutions; vibration damping; soundproofing; thermal insulation; moulding; thermoforming; die-cutting; foaming; SDG 11 – Sustainable Cities and Communities; SDG 3 – Health and Well-being.

1. Company Overview

BECCHIS OSIRIDE DOO Kragujevac is a medium-sized manufacturing company based in Kragujevac, Serbia, operating as part of the Italian Becchis Osiride Group. Established in 2011, the company specializes in the production of components and materials for the automotive industry, with a strong focus on sound, thermal, and vibration insulation solutions.

2. Technology / Product / Service Description

Company mainly uses polyurethane-based technologies and acoustic insulation technologies for automotive applications.



Figure 1. All products that are produced in Becchis Serbia

In Figure One, a group of all the parts that are produced in the company Becchis Osiride is shown. In this company, various parts are produced for cars, tractors, trucks, as well as for various household appliances. All these parts have a role in damping vibrations and noise. The company Becchis Osiride produces these parts for customers such as Fiat, Alfa Romeo, Ferrari, Maserati, and other companies in the automotive industry worldwide. The picture shows parts such as the trunk carpet, engine covers, trim seals, parts that are installed in car doors, under the hood, etc., as well as the washing machine covers.

All parts from figure 1 are parts that serve as sound insulation. Depending on the place of installation, the method of installation, and the machine into which the part is installed, the material and the method of shaping the part are chosen.

In our company, production is divided into three segments. one part of the production is pouring the sponge into molds. Chemistry consists of a mix of polyols and isocyanates which, in a mutual reaction, create foam expansion that is shaped with the help of a mold into the desired form. The second part of production consists of finalization, that is, trimming those molded sponges. The third part of production is hot molding or thermoforming of parts. Cotton is first formed into sheets called nape. The nape are later shaped into the desired form using presses on which the appropriate tools are mounted. In hot molding, we place the cold napa into an already preheated tool with which we shape the part, whereas in thermoforming we first heat the napa in ovens and then place it into a cold tool and in that way shape it. Depending on the location of the part as well as on the customers' requirements, some reinforcements can be added to the parts, mostly in the form of aluminum if the part comes into contact with hot components such as the engine.

3. Innovation and Competitive Advantage

At Becchis Osiride, we provide tailor-made acoustic and insulating components developed to the unique demands of the automotive sector. Our solutions are designed to address NVH challenges, offering vibration damping, soundproofing, and thermal insulation to enhance vehicle comfort and performance in the main four areas: Body, Interiors, ICE & BEV Engine Compartment and Powertrain & Exhaust.

4. Market Application and Impact

Becchis Osiride draws on a broad range of expertise across various industrial sectors, bringing together the best practices from multiple industries to deliver tailor-made, flexible solutions. Our compact size allows us to respond with speed and adaptability to customer needs, ensuring quick turnarounds for all the involved industrial applications.

5. Partnerships and Outlook

More than 130 years with the same name, Becchis Osiride remains a family-owned company, bringing the heritage of the past generations and the vision of ne new ones.

ARTIFICIAL INTELLIGENCE AND MACHINE LEARNING

Foundations, Methods, and AI/ML Algorithms

The Predictive Power of Genomic Damage: A Machine Learning Approach to Endometrial Cancer Biomarkers

Aleksandra Marković[1], Bogdan Milićević[1], Marija Živković Radojević[2,3]

[1]Institute for Information Technologies, University of Kragujevac, 34 000 Kragujevac, Serbia, aleksandra.markovic@uni.kg.ac.rs, 0000-0002-2276-332X, bogdan.milicevic@uni.kg.ac.rs, 0000-0002-0315-8263
[2]Centre for Radiation Oncology, University Clinical Centre, 34 000 Kragujevac, Serbia
[3]Department of Clinical Oncology, Faculty of Medical Sciences, University of Kragujevac, 34 000 Kragujevac, Serbia, makizivkovicmarija@gmail.com, 0000-0003-2146-3381

Corresponding author: aleksandra.markovic@uni.kg.ac.rs

Abstract

Genomic damage is a hallmark of cancer and plays a key role in tumor initiation, progression, and therapeutic resistance. In endometrial cancer (EC), systemic assessment of DNA strand breaks and chromosomal instability provides insight into disease biology. The micronucleus (MN) and comet assay generate complementary systemic genomic damage markers, which can be integrated with clinical and metabolic parameters to create structured datasets. These datasets are well-suited for computational analysis using machine learning (ML) approaches. ML algorithms can identify complex, nonlinear relationships among molecular, clinical, and lifestyle variables, enabling predictive modeling and theoretical patient stratification. By combining multi-level data, this framework allows exploration of interactions between genomic damage markers, tumor characteristics, and metabolic factors, highlighting patterns relevant for precision oncology. The integration of systemic genomic damage markers with ML represents a biologically grounded strategy for advancing translational research in EC. This conceptual approach supports future risk assessment, personalized clinical decision-making, and provides a framework for biomarker-driven studies in gynecological oncology.

Keywords: endometrial cancer; genetic damage; machine learning; UN SDG 3

1. Introduction

Genomic damage is a fundamental hallmark of cancer, contributing to tumor initiation, progression, and therapeutic resistance. In endometrial cancer (EC), assessment of systemic genomic damage provides valuable insight into the biological processes underlying tumor behavior [1]. The micronucleus (MN) assay provides complementary information on chromosomal instability, reflecting the frequency of chromosomal fragments or whole chromosomes that fail to be incorporated into daughter nuclei during cell division [2]. The comet assay

is a sensitive and widely used technique for quantifying DNA strand breaks and alkali-labile sites at the single-cell level. The genomic damage index (GDI) further refines this assessment by combining multiple comet assay parameters into a unified quantitative score, enhancing interpretability and comparability across samples [3,4]. Together, these assays generate systemic genomic damage markers, which can be integrated into predictive computational frameworks. Given the quantitative and multi-parametric nature of MN and comet assay data, this genomic damage markers produce structured datasets well-suited for advanced computational analysis.

2. Analytical Framework for Computational Integration

The advancement of computational analytics has revolutionized biomedical data interpretation in oncology, particularly through the implementation of structured machine learning (ML) and regression workflows [5]. By utilizing a custom Python-based pipeline, this study identifies complex relationships among molecular, clinical, and lifestyle variables that often remain obscured in traditional univariate analyses [6]. In the context of EC, systemic genomic damage markers, including DNA strand breaks and chromosomal instability assessed via MN frequency - are integrated with clinical parameters (FIGO stage, tumor grade) and metabolic factors (BMI, age, comorbidities). This approach utilizes preprocessing phase involving ordinal mapping of clinical stages and Z-score standardization of continuous biological markers, creating a multidimensional dataset optimized for supervised learning. By applying standardized Logistic Regression and point-biserial correlation analysis, the framework emphasizes integrative modeling over reliance on isolated biomarkers, demonstrating the power of computational approaches to provide a quantitative, reproducible complement to experimental data.

3. Discussion

The integration of systematic data analysis represents a sophisticated strategy within precision oncology. This methodology enables the exploration of complex datasets, uncovering subtle correlations and shifts in inter-feature dynamics, such as the differential correlation patterns observed between disease and control cohorts - that are difficult to detect via conventional methods. By employing multivariate logistic regression, we can facilitate the development of predictive scenarios capable of stratifying patients according to precise risk profiles [5,7]. Specifically, our model allows for "probability shift analysis," which quantifies how incremental changes in metabolic or genomic variables (e.g., a standard deviation increase in BMI or MN frequency) contribute to the absolute and relative probability of disease. Furthermore, this computational approach complements traditional statistical hypothesis testing by enabling multivariate interaction modeling. Because genomic damage markers are accessible through minimally invasive procedures, their inclusion in high-fidelity predictive frameworks supports scalable applications in gynecological oncology [1]. Future research may build upon this by concurrently evaluating systemic and tumor-specific markers, offering deeper insight into disease heterogeneity and therapeutic responsiveness. Ultimately, this versatile and biologically grounded approach bridges quantitative biomarker data with advanced analytics, supporting future risk assessment and personalized clinical decision-making through a multidimensional understanding of EC progression [5].

4. Conclusions

The integration of systemic genomic damage markers with a structured computational framework represents a robust and biologically grounded strategy for advancing endometrial cancer research. By bridging raw quantitative data with logistic regression modeling and standardized association metrics, this framework highlights the potential for enhanced risk assessment and data-driven clinical insights. These findings suggest that the operationalization of such predictive models - incorporating both systemic biological markers and lifestyle factors - is a vital step toward realizing the full potential of precision medicine in gynecological oncology. Further translational validation of these integrated frameworks is warranted to refine their predictive accuracy and clinical utility.

Acknowledgements

This research is funded by the Ministry of Education and Ministry of Science, Technological Development and Innovation, Republic of Serbia, (Agreement No. 451-03-33/2026-03/200378).

References

1. Marković A, Grujičić D, Živković Radojević M, Milošević-Djordjević O. Measurement of chromosomal instability and level of DNA damage in peripheral blood mononuclear cells of endometrial cancer patients. Mutagenesis 2024;39:172–80.
2. Fenech M, Knasmueller S, Knudsen LE, Kirsch-Volders M, Deo P, Franzke B, Stopper H, Andreassi M-G, Bolognesi C, Dhillon VS, Laffon B, Wagner K-H, Bonassi S. "Micronuclei and Disease" special issue: Aims, scope, and synthesis of outcomes. Mutation Research/Reviews in Mutation Research 2021;788:108384.
3. Azqueta A, Ladeira C, Giovannelli L, Boutet-Robinet E, Bonassi S, Neri M, Gajski G, Duthie S, Del Bo' C, Riso P, Koppen G, Basaran N, Collins A, Møller P. Application of the comet assay in human biomonitoring: An hCOMET perspective. Mutation Research/Reviews in Mutation Research 2020;783:108288.
4. Milić M, Ceppi M, Bruzzone M, Azqueta A, Brunborg G, Godschalk R, Koppen G, Langie S, Møller P, Teixeira JP, Alija A, Anderson D, Andrade V, Andreoli C, Asllani F, Bangkoglu EE, Barančoková M, Basaran N, Boutet-Robinet E, Buschini A, Cavallo D, Costa Pereira C, Costa C, Costa S, Da Silva J, Del Bo´ C, Dimitrijević Srećković V, Djelić N, Dobrzyńska M, Duračková Z, Dvořáková M, Gajski G, Galati S, García Lima O, Giovannelli L, Goroshinskaya IA, Grindel A, Gutzkow KB, Hernández A, Hernández C, Holven KB, Ibero-Baraibar I, Ottestad I, Kadioglu E, Kažimirová A, Kuznetsova E, Ladeira C, Laffon B, Lamonaca P, Lebailly P, Louro H, Mandina Cardoso T, Marcon F, Marcos R, Moretti M, Moretti S, Najafzadeh M, Nemeth Z, Neri M, Novotna B, Orlow I, Paduchova Z, Pastor S, Perdry H, Spremo-Potparević B, Ramadhani D, Riso P, Rohr P, Rojas E, Rossner P, Safar A, Sardas S, Silva MJ, Sirota N, Smolkova B, Staruchova M, Stetina R, Stopper H, Surikova EI, Ulven SM, Ursini CL, Valdiglesias V, Valverde M, Vodicka P, Volkovova K, Wagner K-H, Živković L, Dušinská M, Collins AR, Bonassi S. The hCOMET project: International database comparison of results with the comet assay in human biomonitoring. Baseline frequency of DNA damage and effect of main confounders. Mutation Research/Reviews in Mutation Research 2021;787:108371.

5. Bi WL, Hosny A, Schabath MB, Giger ML, Birkbak NJ, Mehrtash A, Allison T, Arnaout O, Abbosh C, Dunn IF, Mak RH, Tamimi RM, Tempany CM, Swanton C, Hoffmann U, Schwartz LH, Gillies RJ, Huang RY, Aerts HJWL. Artificial intelligence in cancer imaging: Clinical challenges and applications. CA A Cancer J Clinicians 2019;69:127–57.
6. Kourou K, Exarchos TP, Exarchos KP, Karamouzis MV, Fotiadis DI. Machine learning applications in cancer prognosis and prediction. Computational and Structural Biotechnology Journal 2015;13:8–17.
7. Lever J, Krzywinski M, Altman N. Logistic regression. Nature Methods. 2016;13:541–542.

Data-Driven Prediction of Master's Degree Enrolment Using Explainable Machine Learning

Vlado Simeunovic[1]

[1]University of East Sarajevo, Faculty of Education, Bosnia and Herzegovina, 0000-0002-8119-5190

Corresponding author: vlado.simeunovic@pfb.us.rs.ba

Abstract

Understanding the factors that influence students' decisions to pursue postgraduate education is an important challenge for higher education institutions. With the increasing availability of educational data, machine learning (ML) methods provide powerful tools for modelling complex relationships among academic, institutional, and personal factors influencing educational decisions. This study proposes a data-driven framework for predicting students' enrolment in master's studies using explainable machine learning techniques. The problem is formulated as a binary classification task distinguishing between students who enrol in master's programs and those who do not. Random Forest and XGBoost models were applied and model interpretability was analysed using SHAP. The results demonstrate excellent predictive performance, with the best-performing algorithm, XGBoost, achieving a ROC-AUC score of 0.94, indicating excellent classification capability. Feature importance and SHAP analysis reveal that personal circumstances, perceived quality of study programs, institutional conditions, and academic motivations are the most influential predictors of postgraduate enrolment. The proposed approach provides an interpretable analytical framework that can help universities better understand student decision-making processes and design policies that encourage postgraduate participation.

Keywords: *machine learning in education, higher education analytics, Random Forest, XGBoost, SHAP, XAI, SDG 4, SDG 9*

1. Introduction

Artificial intelligence (AI) and machine learning (ML) are increasingly applied in educational research to analyse student behaviour and support institutional decision-making processes. Recent developments in educational data mining and learning analytics have enabled researchers to extract meaningful insights from complex educational datasets and predict key outcomes such as academic success, student dropout, and educational progression [1-3]. Understanding the factors that influence students' decisions to continue their education at the postgraduate level represents an important challenge in higher education research. Enrolment in master's programs is influenced by a combination of academic achievement, institutional quality, career aspirations, and personal circumstances. Identifying these factors can help universities design policies that support student development and encourage postgraduate participation. Traditional statistical approaches often have limitations when modelling nonlinear relationships among multiple predictors. ML methods provide an alternative by enabling the analysis of complex interactions within educational datasets [4-6]. Ensemble algorithms such as Random Forest have demonstrated strong predictive performance in many classification

problems due to their ability to combine multiple decision trees and reduce overfitting [7]. Despite their predictive capabilities, ML models are often criticised for their limited interpretability. In educational contexts, where predictive results may influence institutional policies, understanding the reasoning behind model predictions is essential. Explainable Artificial Intelligence (XAI) methods address this challenge by providing transparent explanations of model behaviour. One widely used approach is SHAP (SHapley Additive exPlanations), which quantifies the contribution of individual predictors to the final prediction outcome based on concepts from cooperative game theory [8].

The aim of this study is to develop a ML framework for predicting students' enrolment in master's studies and to analyse the key factors influencing these decisions using explainable AI techniques. Random Forest [7] and XGBoost [9] models were applied. Both ML algorithms are consideres as widely use with strong mathematical background and practical value [10]. Finally, model interpretability was analysed using SHAP.

2. Dataset and Problem statement

The dataset used in this study consists of student responses collected through a structured questionnaire designed to examine factors influencing enrolment in master's studies Total 663 respondents. The final dataset includes several demographic, academic, and motivational variables describing students' educational experiences and perceptions. The target variable represents whether a student enrolled in master's studies. Therefore, the prediction task is formulated as a binary classification problem with two classes - Class 0: student did not enroll in master's studies; Class 1: student enrolled in master's studies. The dataset is balanced. The independent variables include the following predictors: Demographic and academic characteristics A1 – gender (A1); place of residence (A2); time required to complete undergraduate studies (A3); grade point average (A4); Institutional and motivational factors: perceived quality and applicability of study programs (A5); quality of institutional facilities and infrastructure (A6); flexibility of study organization (A7); reputation of the faculty (A8); affordability of master's program tuition (A9); Personal and career-related motivations: influence of personal circumstances (A10); motivation for scientific work (A11); perceived quality of teaching staff (A12); necessity of a master's degree for employment in the country (A13); necessity of a master's degree for employment abroad (A14); continuation of studies at another institution (A15); employment outside the educational system (A16). Prior to model training, standard preprocessing steps were applied, including data cleaning and data preparation. The dataset was divided into training and testing subsets in order to evaluate the predictive performance of the models. Two ensemble machine learning algorithms were employed: a) Random Forest, which combines multiple decision trees through bagging to improve prediction stability and reduce overfitting; b) XGBoost, an advanced gradient boosting algorithm designed to optimize predictive performance through sequential tree learning and regularization. The algorithm hyperparameters are set in accordance with the literature. To enhance model interpretability, SHAP values were used to quantify the contribution of each input variable to the model predictions. Model performance was evaluated using standard classification metrics, including accuracy, ROC AUC, etc.

3. Results and Discussion

ML models effectively predicted students' decisions to enroll in master's studies. The Random Forest model achieved an accuracy of 0.87 and ROC AUC of 0.92, while XGBoost achieved slightly higher performance with an accuracy of 0.89 and ROC AUC of 0.94 (Table 1). These results indicate that both ensemble models provide strong predictive capability for binary classification of master's enrolment.

Table 1. Model Performance Comparison

Model	**Accuracy**	**ROC AUC**
Random Forest	0.87	0.92
XGBoost	0.89	0.94

Figure 1. ROC curves comparing Random Forest and XGBoost algorithms

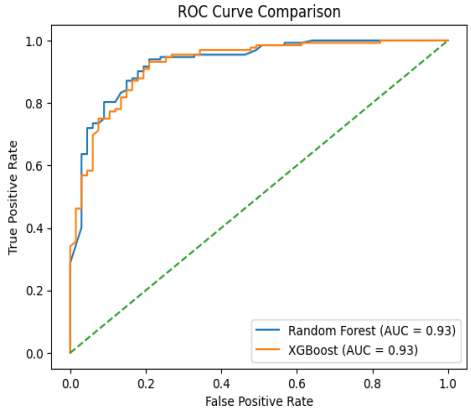


Figure 2. Feature importance plot derived from XGBoost

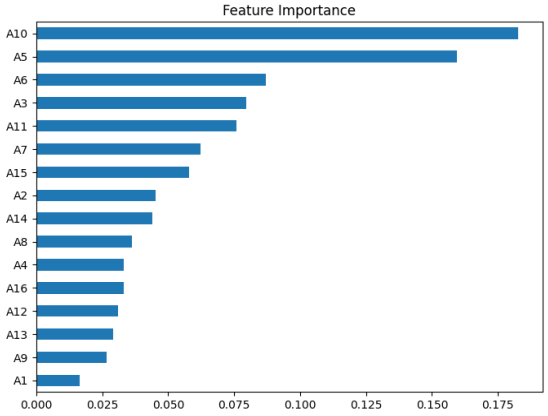


Figure 3. Title SHAP (RF)

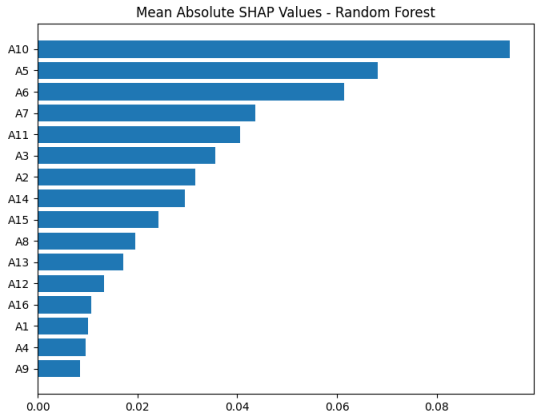
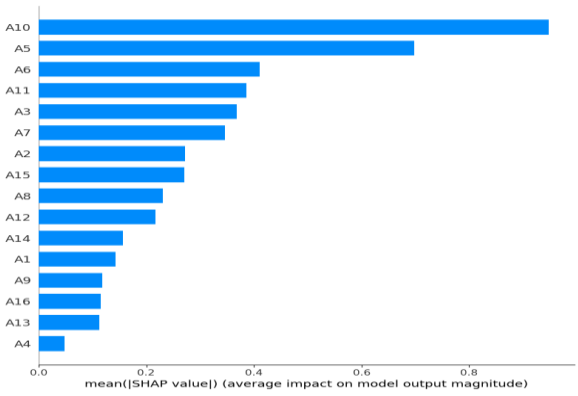


Figure4. Title SHAP (XGBoost)



Feature importance analysis, leveraging the built-in support of the tree-based algorithm, revealed the key predictors driving the model's performance analysis revealed key predictors: A10 (personal circumstances) was the most influential, followed by A5 (quality of study programs), A3 (undergraduate completion time), A6

(study conditions), A7 (study flexibility), and A11 (motivation for scientific work). SHAP analysis confirmed these results and highlighted the practical relevance of institutional quality and personal motivations. Students perceiving programs as high-quality and flexible were more likely to enroll, while personal constraints negatively impacted enrollment, emphasizing the role of socio-economic conditions in postgraduate participation. Figure 1 illustrates the ROC curves comparing Random Forest and XGBoost classifiers, highlighting the higher discriminative capability of XGBoost. Figure 2 shows the feature importance plot from XGBoost , indicating which predictors most influence enrollment decisions. Figures 3 and 4 present SHAP summary plots, demonstrating the contribution of individual features to the model predictions and providing a transparent, interpretable view of how different factors drive student enrollment decisions. The combination of predictive performance and explainability demonstrates the practical utility of ML in supporting data-driven decision-making in higher education institutions. These findings illustrate how explainable AI can bridge predictive performance with actionable insights, helping institutions design interventions that improve student engagement and support.

4. Conclusions

This study demonstrated that machine learning models can effectively predict students' enrollment in master's studies, with XGBoost achieving the highest predictive performance. The results indicate that personal circumstances, perceived program quality, and institutional conditions play a key role in shaping students' decisions to pursue postgraduate education. The use of SHAP analysis enabled transparent interpretation of model predictions, providing valuable insights into the relative importance of individual factors. These findings highlight the potential of explainable machine learning to support data-driven decision-making in higher education institutions.

References

1. Holmes W, Tuomi I. State of the art and practice in AI in education. European Journal of Education. 2022;57:542–570.

2. Molenaar I. Towards hybrid human-AI educational scenarios. European Journal of Education. v57 n4 p632-645.

3. Ayeni OO, Al Hamad NM, Chisom ON, Osawaru B, Adewusi OE. AI in education: A review of personalized learning and educational technology. GSC Advanced Research and Reviews. 2024;18:261–271.

4. Alneyadi S, Wardat Y, Alshannag Q, Abu-Al-Aish A. The effect of using smart e-learning app on the academic achievement of eighth-grade students. Eurasia Journal of Mathematics, Science and Technology Education. 2023;19:em2248.

5. Dimari A, Tyagi N, Davanageri M, Kukreti R, Yadav R, Dimari H. AI-based automated grading systems for open book examination system: Implications for assessment in higher education. In: 2024 International Conference on Knowledge Engineering and Communication Systems (ICKECS);2024:1–7.

6. Wu Q, Chang HJ, Ma L. Viability study of machine learning models to identify talented students at the early stage of their college study. Journal of Advanced Academics. 2025;36:766–787.

7. Breiman L. Random forests. Machine Learning. 2001;45:5–32.

8. Lundberg SM, Lee SI. A unified approach to interpreting model predictions. Advances in Neural Information Processing Systems. 2017;30.

9. Chen T, Guestrin C. XGBoost: A scalable tree boosting system. In: Proceedings of the 22nd ACM SIGKDD International Conference on Knowledge Discovery and Data Mining. 2016;785–794.

10. Rakićević A, Milošević P, Dragović I, Poledica A, Zukanović M, Janusz A, Ślęzak D. Predicting stock trends using common financial indicators: A summary of FedSCIS 2024 Data Science Challenge held on knowledgepit.ai platform. In: 2024 19th Conference on Computer Science and Intelligence Systems (FedCSIS);2024:731–737.

The importance of k-fold cross-validation in evaluating machine learning models for biomass gasifier output prediction.

Kadriye Deniz Olca[1], Özgün Yücel[1]

[1]Department of Chemical Engineering, Gebze Technical University, 41400, Kocaeli, Turkey

Corresponding author: *k.kose2020@gtu.edu.tr*

Abstract

This study evaluates multiple modelling approaches (LS, Kernel, GAM, RF, and ANNs) for predicting product concentrations (CO, CO_2, CH_4, H_2) and higher heating value (HHV) in biomass gasification. Model hyperparameters were optimized using Bayesian Optimization, and performance was assessed via 10-fold cross-validation using R^2, normalized RMSE, and MSLE metrics. Among the models, ANNs achieved the highest performance, with a maximum R^2 of 0.984 for HHV prediction. However, hyperparameter optimization of ANNs did not yield significant improvements; instead, it increased overfitting by enhancing training performance while reducing test accuracy. The study also demonstrates that cross-validation provides more reliable and unbiased performance estimates compared to hold-out validation, which showed high variability. Despite its advantages, the use of cross-validation in biomass gasification modelling remains limited. This work introduces a novel framework integrating cross-validation for both model evaluation and hyperparameter tuning, highlighting potential bias in prior studies relying on hold-out methods.

1. Introduction and Methods

The variability in waste quantity and composition significantly influences the outcomes of biomass gasification, a promising process for regional and small-scale green energy production. Despite this variability, machine learning methods have been widely and successfully applied in the literature to model the process. Among these, Artificial Neural Networks (ANNs) are the most extensively studied approaches [1][2][3]. In addition, other techniques such as Random Forests (RF) and Decision Trees (DT) have also been employed [4][5]. Although numerous studies exist in this field, the majority rely on hold-out validation for performance evaluation, rather than k-fold cross-validation, which has been recommended in [4][6][7]. This study aims, first, to investigate whether hyperparameter optimization improves the performance of machine learning models, and second, to examine whether the widespread use of hold-out validation provides an unbiased estimate of model performance or adequately reflects the true predictive accuracy.

A comprehensive review of the relevant literature, along with detailed explanations of k-fold cross-validation and hyperparameter optimization (used in the first part of this study where 10-fold CV is used) has been presented in our previous work [6] and is therefore not repeated here for brevity. In the second part of the study, hold-out validation is employed for comparative purposes. Hold-Out validation (70% training / 30% test) was repeated 50 times. The schematic representation of hold-out validation is given in Figure 1. The whole data set

is divided into training and test, and hyperparameter optimization is done using the training set via CV. The model is constructed based on the optimized hyperparameters and the training data defined beforehand. The procedure is repeated 50 times, and the model metrics are evaluated at each repeat. An essential feature of this method is that instances that belong to one group (e.g., training set) at one repeat can belong to the same group in the subsequent repeats as random sampling is performed compared to the nested CV approach described. The dependence of model metrics on the data set when hold-out validation is used is aimed to be demonstrated.

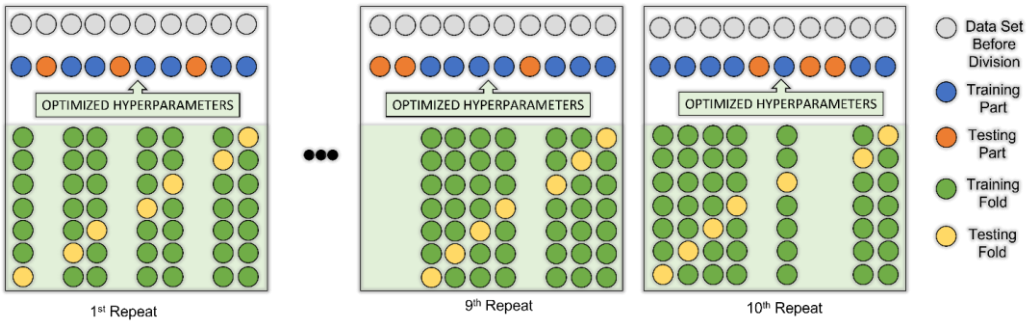


Figure 8. Schematic representation of hold-out validation with 50 Repeats (70% Training / 30% Testing) with hyperparameter optimization via CV

3. Results and Discussion

The model performances of the models studied and assessed via 10-fold CV are given (partially) in Table 1. Although the results for CO, CO_2, and CH4 are missing to fulfil the format requirements of the conference, details may be provided upon request. The best estimates are given in bold. It can be observed that Linear Regression is not able to describe the gasification system as expected based on the collinearities of the system studied. As shown in Table 1, the R^2 values vary between 0.207 and 0.518 for CO and CH_4, respectively. Artificial Neural Networks (ANN) lead to the best results. Except for specific CO and one H2 point, no significant over/ underestimation is detected for this method. Apparently, H2 (R^2 = 0.982) and HHV (R^2 = 0.984) values are the best modeled, whereas the other values are similarly well-fitted (R^2 above 0.955). RMSE is minimal, with 0.604 being their highest values, respectively. MSLE is in the order of 10-4 for all the measured outlet components, which is the lowest met among the other methods.

Hyperparameter optimization has improved prediction accuracy for most methods (Table 1). Kernel and GAM models are obviously improved when the hyperparameters are optimized. For instance, R^2 has increased from 0.627 to 0.801 and from 0.645 to 0.909 for the CO kernel and GAM models, respectively, whereas the other model performance estimates follow a similar trend. Exceptionally, LS and Kernel regression has shown slightly lower MSLE for H2. MAE of RF without hypermeter optimization is lower for CO_2, CH_4, and HHV, although the other metrics are evidently better for ANN. For the latter case, a slight worsening of the CH_4 and H_2 metrics has been observed, and the use of hyperparameter optimization is redundant. Overlearning may enhance training scores during model construction but lowers test performances. Precisely, the data fits well enough in the case

of complex models for the hyperparameter optimization to be necessary, so attempts to fit the data further may increase the model variance beyond the optimum.

Table 2. Model Performance in estimating CO, CO_2, CH_4, H_2 and HHV with 10-fold CV

		R^2		RMSE		MAE		MSLE	
		HO	**wo HO**	**HO**	**wo HO**	**HO**	**wo HO**	**HO**	**wo HO**
H_2	LS	0.373	0.303	3.281	2.896	2.665	2.159	7.51E-03	7.40E-03
	KERNEL	0.88	0.885	1.439	1.18	0.838	0.797	1.49E-03	7.97E-04
	GAM	0.954	0.854	0.894	1.32	0.616	0.973	5.50E-04	1.57E-03
	RF	0.963	0.939	0.800	0.857	0.355	0.502	3.87E-04	7.72E-04
	ANN	**0.982**	**0.986**	**0.554**	**0.411**	**0.318**	**0.238**	**2.88E-04**	**1.47E-04**
HHV	LS	0.295	0.212	1.87	3.17	1.54	2.41	6.17E-03	9.60E-03
	KERNEL	0.907	0.846	0.679	1.40	0.401	0.92	8.11E-04	1.88E-03
	GAM	0.956	0.807	0.469	1.57	0.318	1.14	4.05E-04	2.42E-03
	RF	0.960	0.939	0.447	0.882	**0.170**	0.571	3.34E-04	7.67E-04
	ANN	**0.984**	**0.979**	**0.281**	**0.516**	0.179	**0.273**	**1.46E-04**	**2.51E-04**

In order to observe the deviation of model performance metrics based on the selected fraction of the data set and hence the bias of the hold-out evaluation method, the boxplots of R^2 values of each repeated fold are provided (Figure 2). It is evident that the R^2 values are exact for RF, although there are still outliers. This may be a result of the classification nature of RF and the fact that the extensive data set available spans a wide range of the data space. So each new (not seen) instance has a representative in the modeled constructed. In short, lower performance models (as proven by CV or hold-out) are expected to perform similarly for both validation methods, although CV will most probably lead to lower mathematical performance values. However, methods (e.g., kernel, GAM) that heavily depend on the selected hyperparameters, as shown in Table 1, cannot be assessed by single (or repeated) hold-out validation. Briefly, a high-performance model, as an example RF for HHV with CV R^2 of 0.96, will provide an R^2 value very close to 1 with hold-out validation. A kernel model, the performance of which highly depends on the hyperparameters' selection, e.g., for CO with a CV R^2 value of 0.801 can demonstrate a low (R^2 = 0.3) or high (0.98) coefficient of determination with the biased selection of the validation and test data during hold-out validation. Hence, it is evident that using hold-out validation instead of CV may provide a faulty mathematical performance measure (except for RF) in cases where the model depends heavily on the data set. Hence, an extensive data set and an unbiased performance criterion are crucial for model criticism.

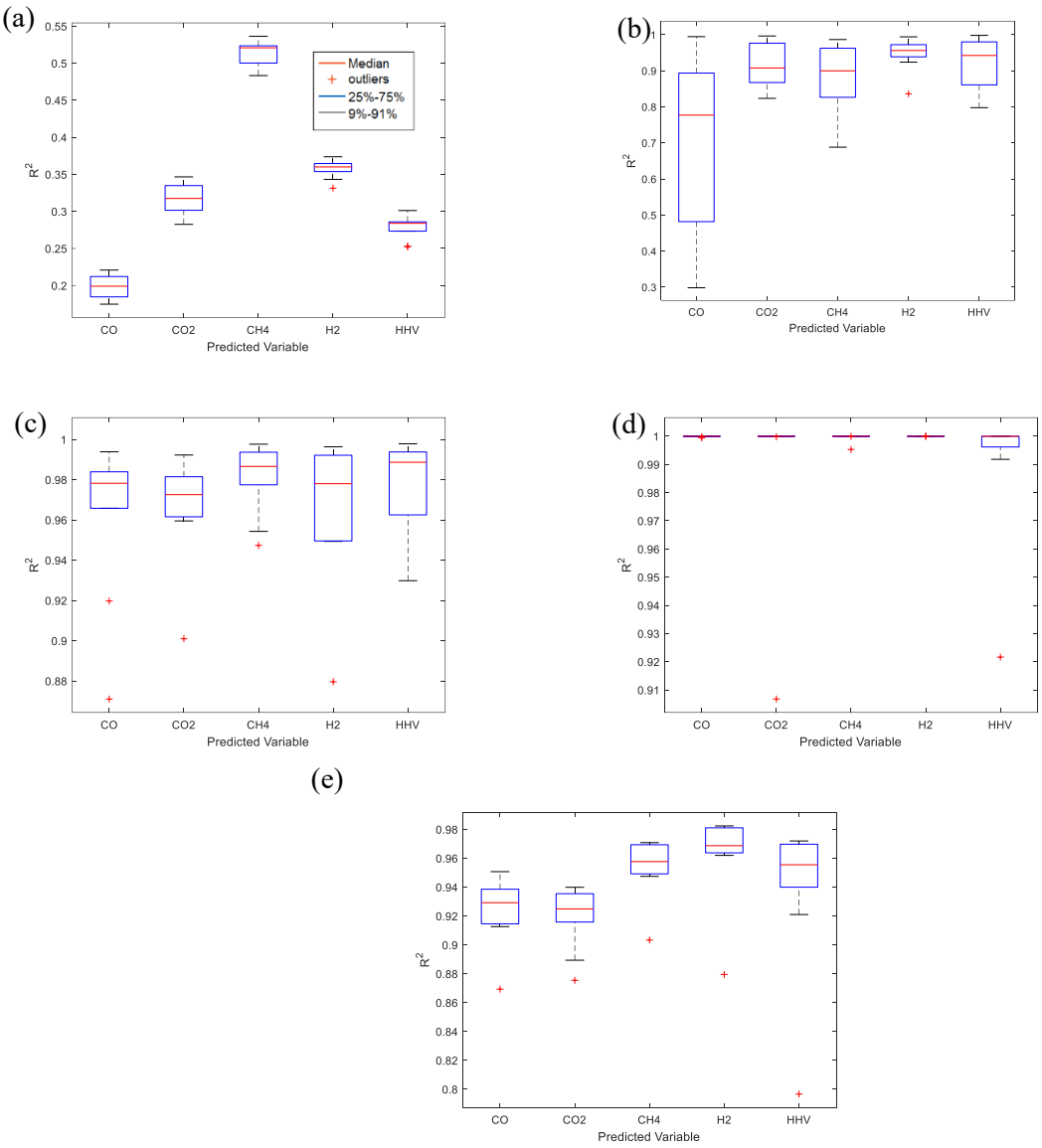


Figure 9. Coefficient of determination values boxplots for Hold-out Validation with 50 repeats (a) Least Square, (b) Gaussian Kernel, (c) Generalized Additive Model, (d) Random Forest, and (e) Artificial Neural Network

5. Conclusions

In this study, different modelling methods were used to predict the product concentrations (CO, CO_2, CH_4, H_2) and the higher heating value. The hyperparameters of each model have been optimized via Bayesian Optimization. 10-Fold cross-validation is used to obtain the model performance estimates, including R^2, Normalized RMSE, and MSLE. ANN models overpass the rest models obtained for all the predicted values with a maximum value of R^2 equal to 0.984 for HHV. It has been shown that the use of CV provides a more unbiased image of the models' predicting power, as multiple repeats of hold-out validation results vary within

a broad range. The use of CV for model evaluation in the biomass gasification literature is rare. This study provides a novel approach using CV for hyperparameter tuning and model evaluation. In this framework, the model performance estimates of previous studies where hold-out validation is preferred may be biased, and their model generalizability may not have been proven. The main point for improvement for the approach proposed is the minimization of computational time, as the large data set combined with the repeated model construction during the selection of the optimum one requires a great computational workload. Finally, underlying the unbiased nature of the validation method proposed (k-fold CV) and the high performance of the best model type (ANN w/o hyperparameter optimization) the application of this methodology to express the gasification of wastes from different origins and their mixture (municipal, plastics etc.) is recommended.

Acknowledgements

The findings of this study form part of the research conducted in partial fulfillment of the first author's PhD dissertation.

References

1. Elmaz, F., Yücel, Ö., & Mutlu, A. Y. (2020). Predictive modeling of biomass gasification with machine learning-based regression methods. *Energy*, *191*. https://doi.org/10.1016/j.energy.2019.116541
2. Lahafdoozian, M., Khoshkroudmansouri, H., Zein, S. H., & Jalil, A. A. (2024). Hydrogen production from plastic waste: A comprehensive simulation and machine learning study. *International Journal of Hydrogen Energy*, 59, 465–479. https://doi.org/10.1016/j.ijhydene.2024.01.326
3. Zhao, S., Li, J., Chen, C., Yan, B., Tao, J., & Chen, G. (2021). Interpretable machine learning for predicting and evaluating hydrogen production via supercritical water gasification of biomass. *Journal of Cleaner Production*, *316*. https://doi.org/10.1016/j.jclepro.2021.128244
4. Mutlu, A. Y., & Yucel, O. (2018). An artificial intelligence based approach to predicting syngas composition for downdraft biomass gasification. *Energy*, *165*, 895–901. https://doi.org/10.1016/j.energy.2018.09.131
5. Kardani, N., Zhou, A., Nazem, M., & Lin, X. (2021). Modeling of municipal solid waste gasification using an optimised ensemble soft computing model. Fuel, 289. https://doi.org/10.1016/j.fuel.2020.119903
6. K. D. Olca and Ö. Yücel, "Unveiling the potential of operating time in improving machine learning models' performance for waste biomass gasification systems," Renew Energy, vol. 237, Dec. 2024, doi: 10.1016/j.renene.2024.121621.
7. Ukwuoma, C. C., Cai, D., Jonathan, A. L., Chen, N., Sey, C., Ntia, N. W., Bamisile, O., & Huang, Q. (2024). Enhancing hydrogen production prediction from biomass gasification via data augmentation and explainable AI: A comparative analysis. *International Journal of Hydrogen Energy*, 68, 755–776. https://doi.org/10.1016/j.ijhydene.2024.04.283

Stylistic Adaptation of a Pre-trained Language Model via Fine-tuning on a Slavic Literary Corpus

Aleksandr Uchaev and Vladimir Milovanović

Dept. of Electrical Engineering and Computer Sciences, Faculty of Engineering – University of Kragujevac
a.uchaev97@gmail.com, *0009-0007-3950-0458, and* vlada@uni.kg.ac.rs, *0000-0002-6787-4058*

Corresponding authors: aleksandr@uni.kg.ac.rs and vlada@kg.ac.rs

Abstract

This study investigates stylistic adaptation of ruGPT-3 small (164M parameters) through fine-tuning on 373 works by 11 Slavic classical authors (~67 MB total corpus, ~38 MB training subset after stratified splitting). The fine-tuned model achieves a validation perplexity of 29.92 after 47 minutes on a consumer GPU (RTX 2060). Generated samples capture author-characteristic sentence structure and lexical patterns, and adapt out-of-domain prompts to the learned literary register.

Keywords: natural language processing; language model; fine-tuning; transfer learning; text generation; GPT-2; Slavic literature; stylistic adaptation; perplexity; transformer; UN SDG 4 (Quality Education); UN SDG 11.4 (Cultural Heritage)

1. Introduction

Generative language models based on the Transformer architecture [1] produce coherent text through autoregressive pre-training on large corpora [2]. Fine-tuning on a targeted dataset can adapt these models to specific stylistic registers. English-language models for creative generation have been studied extensively, but Slavic presents additional challenges due to its rich morphology and free word order. ruGPT-3 [3], a Slavic-language GPT-2 variant pre-trained on ~300 GB of text by Sber AI, provides a starting point for such investigation.

This study asks: can fine-tuning on a modest literary corpus capture the stylistic characteristics of Slavic classical prose, and how does corpus composition affect the result?

2. Materials and Methods

2.1 Dataset

The corpus was sourced from the Slavic Literature dataset available on Kaggle [4], containing 373 text files (~67 MB) organized into three categories: prose (269 files, 63 MB, 11 authors), poetry (78 files, 3.1 MB, 4 authors), and non-fiction (26 files, 1.2 MB, 1 author). The prose subcorpus is dominated by Dostoevsky (19

MB) and Tolstoy (16 MB), while authors such as Blok (0.08 MB) and Lermontov (0.56 MB) are significantly underrepresented.

2.2 Data Preprocessing

Preprocessing included whitespace normalization, filtering of files shorter than 500 characters, and stratified splitting into training (337 files, 38.2 MB) and validation (18 files, 0.4 MB) sets. The stratified split ensures that at least one work per author appears in the validation set (5% of each author's works, minimum 1 file). A fixed random seed (42) ensures reproducibility.

2.3 Model Architecture

The base model is ruGPT-3 small (sberbank-ai/rugpt3small_based_on_gpt2), a 164M-parameter Slavic-language GPT-2 adaptation [3] with 12 decoder layers, 768-dimensional embeddings, a 2048-token context window, and a 50,257-token BPE vocabulary.

2.4 Training Procedure

The training corpus is split into paragraphs, tokenized with BPE, concatenated into a single token sequence, and segmented into 512-token blocks. Fine-tuning used the HuggingFace Trainer API [5] with learning rate 5×10^{-5} (linear decay, 100-step warmup), effective batch size 32 (4 × 8 gradient accumulation), weight decay 0.01, AdamW optimizer, FP16 on an RTX 2060 (12 GB VRAM), and up to 10 epochs with early stopping (patience = 3, evaluated every 500 steps).

2.5 Generation and Evaluation

Text generation employs top-p (nucleus) sampling [6] with p = 0.92, temperature 0.9, and repetition penalty 1.2. Quantitative evaluation uses validation perplexity (PPL = exp(cross-entropy loss)); qualitative evaluation examines generated samples for stylistic coherence and author-characteristic features.

3. Results

3.1 Training Dynamics

Training converged after 3 epochs (1,773 steps) in 47 minutes, with early stopping triggered at the optimal checkpoint (step 1,500). Table 1 summarizes the key metrics.

Table 1. Training metrics at evaluation checkpoints.

Step	Epoch	Train Loss	Val Loss	Val PPL
500	0.85	3.476	3.419	30.53
1000	1.69	3.379	3.407	30.17
1500	2.54	3.329	3.402	29.92

The train loss decreased monotonically from 3.604 (step 50) to 3.313 (step 1,773). The train–validation loss gap remained small (~0.09), indicating no significant overfitting.

3.2 Qualitative Analysis of Generated Text

We evaluated the model on four categories of prompts: (a) prompts containing lexical cues associated with specific authors, (b) psychologically introspective prompts, (c) landscape descriptions, and (d) out-of-domain prompts.

Author-associated prompts. A prompt beginning with "The prince entered the drawing room" produced Tolstoy-characteristic elements: aristocratic titles, nested narrative with embedded letters, military-social vocabulary. A prompt with a doctor character elicited Dostoevsky-like nervous dialogue, abrupt associative transitions, and psychological tension.

Out-of-domain prompts. The prompt "Shrek returned to his native swamp" falls outside the training domain. The model adapted it into the learned register: the swamp became a Slavic village, characters wore period clothing, and the narrative adopted Gogol-like grotesque imagery with colloquial speech. This indicates learned generalization: the model applies stylistic patterns to novel content rather than reproducing memorized passages.

Observed limitations. Character name confusion within a single paragraph and factual inconsistencies (elements from different novels merged). Narrative coherence degrades beyond ~300 tokens.

4. Discussion

The low train–validation loss gap (0.09) and successful out-of-domain adaptation indicate that the model learned distributional style features rather than memorized training sequences.

Dataset imbalance surfaces in generation: Dostoevsky and Tolstoy, comprising over 50% of the corpus, dominate the output distribution. Oversampling underrepresented authors or conditional generation with author-specific prefixes could address this.

Stratified validation splitting proved important. An earlier implementation used alphabetical splitting, placing only late-alphabet authors into the validation set and yielding misleading metrics.

Coherence degrades beyond 300 tokens, consistent with known constraints of GPT-2-scale models. Larger models (760M+) or LoRA [7] could improve this within consumer hardware budgets. Perplexity of 29.92 reflects prediction accuracy on held-out text, not generation quality; human evaluation would strengthen these findings.

5. Conclusions

Fine-tuning a pre-trained Slavic-language GPT-2 model on a corpus of classical literature produces stylistically authentic text within the constraints of a 164M-parameter architecture.

1. Transfer learning achieves stylistic adaptation in 47 minutes on a single consumer GPU. Training from scratch on a corpus of this size would not yield comparable results.
2. The fine-tuned model learns author-characteristic vocabulary and sentence structure, activating them based on prompt content. Dataset composition shapes the stylistic distribution of generated text, making balanced corpora and stratified evaluation important for representative results.

Future work: conditional generation with author-specific control tokens and LoRA [7] fine-tuning for larger models. Human evaluation through blind comparison with original texts would further validate stylistic quality.

Acknowledgements

This work was conducted as part of the Advanced Machine Learning course at the Faculty of Engineering – University of Kragujevac, Serbia and is partially supported by the agreement on the funds transfer for financing the scientific research work of teaching staff in 2026, contract number: 451-03-34/2026-03/200107.

References

1. Vaswani A, Shazeer N, Parmar N, et al. Attention Is All You Need. Advances in Neural Information Processing Systems. 2017;30:5998–6008.
2. Radford A, Wu J, Child R, Luan D, Amodei D, Sutskever I. Language Models are Unsupervised Multitask Learners. OpenAI Blog. 2019.
3. Sber AI. ruGPT-3. HuggingFace Model Hub. 2021. Available from: https://huggingface.co/sberbank-ai/rugpt3small_based_on_gpt2
4. d0rj3228. Slavic Literature Dataset. Kaggle. 2022. Available from: https://www.kaggle.com/datasets/d0rj3228/russian-literature
5. Wolf T, Debut L, Sanh V, et al. Transformers: State-of-the-Art Natural Language Processing. EMNLP System Demonstrations. 2020:38–45.
6. Holtzman A, Buys J, Du L, Forbes M, Choi Y. The Curious Case of Neural Text Degeneration. ICLR. 2020.
7. Hu EJ, Shen Y, Wallis P, et al. LoRA: Low-Rank Adaptation of Large Language Models. ICLR. 2022.

Methodological framework for automated solving of mathematics competition problems in Serbia using LLMs

Marina Svičević[1], Aleksandar Milutinović[1], Nemanja Vučićević[1], Aleksandar Milenković[1], Miloš Pavković[2]

[1]Faculty of Science, University of Kragujevac, Kragujevac, Serbia, marina.svicevic@pmf.kg.ac.rs, 0000-0003-2791-3849, milutinovic.aleksandar9@gmail.com, 0009-0004-1300-3232, nemanja.vucicevic@pmf.kg.ac.rs, 0000-0002-4903-7280, aleksandar.milenkovic@pmf.kg.ac.rs, 0000-0001-6699-8772

[2]Singidunum University, Belgrade, Serbia, mpavkovic@singidunum.ac.rs, 0000-0001-7776-6045

Corresponding author: marina.svicevic@pmf.kg.ac.rs

Abstract

This paper presents a methodological framework for the automated solving of mathematics competition problems for high school students in Serbia using large language models (LLMs). The corpus includes 348 text-based problems from the municipal, regional, and national competition levels, distributed across grades and Categories A and B. The problems and their corresponding official solutions were organized in a structured format with LaTeX notation, defining prompt templates for inference and reference solutions for automatic evaluation. The study compares several models, including both general purpose and mathematically specialized LLMs. A particular contribution of the paper is a multi-aspect automatic evaluation framework based on final answer accuracy, logical flow of reasoning, and explanation quality. The results reveal a clear gap between commercial and locally executable models, as well as the importance of domain specialization for more successful solving of competition level mathematical problems.

Keywords: large language models; mathematics competitions; automated problem solving; automatic evaluation

1. Introduction

Mathematics problems that require multi step reasoning, precise interpretation of conditions, and well-argued conclusions represent a serious challenge for LLMs. As noted in [1], research on LLM-based mathematical reasoning covers diverse tasks, datasets, approaches, and evaluation settings, which makes it difficult to clearly assess the actual capabilities and limitations of these models.

Previous studies have shown that the performance of AI tools and LLMs in solving mathematical problems depends on task format, domain, and language. In [2], dedicated to problems from the Mathematical Kangaroo competition, models achieved better results on text based problems than on image based ones, and performed better in algebra and number theory than in geometry and logic. These findings also highlighted the importance of linguistic context, that is, the need to examine model performance on problems formulated in Serbian Language.

Following research focused on more complex problems from the national mathematics competition in Serbia. In [3, 4], DeepSeek-R1, o1, and o3-mini were evaluated on LaTeX-formatted problems in Serbian, with the generated solutions assessed by a member of the official competition committee using the same criteria applied to students' work. The results showed that, although the models could in some categories achieve rankings comparable to those of successful contestants, they still struggled with less standard formulations, logic problems, and tasks requiring the consistent execution of all solution steps. A similar conclusion is reported in [5], which emphasizes that competition mathematics problems remain a demanding test for LLMs and that final answer accuracy alone is insufficient for reliably assessing reasoning quality.

Based on this, the aim of this paper is to present a methodological framework for the automated solving of mathematics competition problems in Serbia. The main contribution of the paper lies in integrating data preparation, model prompting, and multi aspect automatic evaluation into a unified experimental workflow.

2. Methodology

Figure 1 presents the overall workflow used in this study, from the preparation of competition problems in LaTeX format to the automatic evaluation of generated solutions.

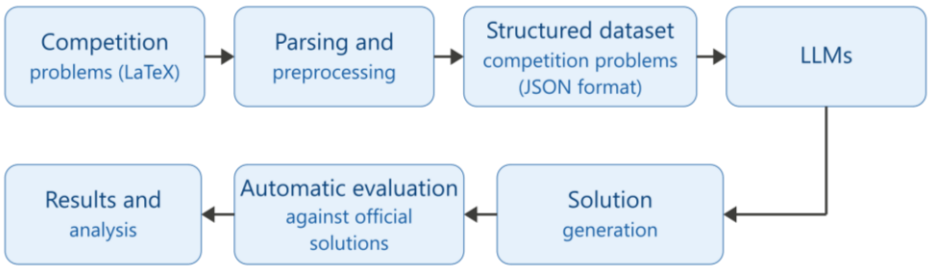


Figure 1. Workflow of the proposed methodology for automated solving of mathematics competition problems in Serbia using LLMs.

The dataset used in this study consists of mathematics competition problems for high school students in Serbia, organized by the Mathematical Society of Serbia. The corpus covers three competition levels: municipal, regional, and national. It also includes all four high school grades in Categories A and B. In the official competition structure, five problems are assigned in all grades and categories, except for Category A at the national level, where four problems are assigned. Based on the collected material, the dataset used in this paper was constructed, and its distribution by competition level and grade is shown in Table 1. For the purposes of this study, 348 problems suitable for text-based processing were selected, forming a corpus for automated solving and evaluation.

Table 1. Distribution of problems by competition level and grade.

Level	Grade 1	Grade 2	Grade 3	Grade 4
Municipal	30	30	30	30
Regional	30	30	30	30
National	27	27	27	27

Each problem was structured as a prompt reference pair: the prompt contains the task metadata (domain, grade, and competition level) together with the problem statement, while the reference represents the full official solution. Both the problem statement and the reference solution preserve LaTeX notation to maintain the precision of mathematical expressions.

For the experiments, models of different sizes and purposes were selected, including general purpose LLMs and models specialized in mathematical reasoning, enabling a comparison of their initial capabilities in solving competition level problems.

Automatic evaluation was based on three independent criteria: Answer Accuracy (A), Logical Coherence (B), and Explanation Quality (C) and was performed by an LLM judge (Claude 3.7 Sonnet). For each of the 348 problems, the generated solution, together with the problem statement and the corresponding reference solution, was submitted to LLM, with a separate system prompt defined for each criterion. Answer Accuracy (A) evaluates the correctness of the final answer and returns a binary score of 0 or 1, based entirely on a comparison with the reference solution. Logical Coherence (B) evaluates the soundness of the reasoning process on a scale from 0 to 1, independently of whether the final answer is correct. Explanation Quality (C) assesses clarity, completeness, and exactness of the presented solution, also on a scale from 0 to 1. The final score is computed as a weighted average of these three criteria as $0.30 \times A + 0.40 \times B + 0.30 \times C$.

3. Results

General results of the experiments are presented in Table 2. The table includes results for three evaluation aspects; final answer accuracy, logical coherence of reasoning, and explanation quality, as well as the weighted average, which represents an aggregated measure of overall model performance.

Table 2. General results of the experiments.

Model	A	B	C	Weighted average
Gemini 3 Flash	54.5%	74.1%	69.8%	66.9%
Claude 3.7 Sonnet	37.6%	39.6%	69.8%	48.1%
Mathstral 7B	15.6%	20.1%	19.9%	18.7%
LLaMA 3 8B	16.8%	14.3%	26.2%	18.6%
Mistral 7B Instruct	12.6%	14.2%	27.9%	17.8%
DeepSeek Math 7B	12.9%	15.1%	23.0%	16.8%
Qwen2.5 Math 7B	13.2%	4.7%	11.6%	9.3%
MAmmoTH 34B	2.6%	6.9%	11.5%	7.0%
Llemma 7B	2.4%	6.1%	10.3%	6.2%

The results reveal a clear gap between commercial models and locally executable models. Gemini 3 Flash achieved the best overall result, with a weighted average of 66.9%, while Claude 3.7 Sonnet reached 48.1%. All remaining models stayed below 20%, with Mathstral 7B achieving the best result among locally executable models, at 18.7%. The results also indicate that model size alone is not a decisive factor of success. In some cases, models specialized in mathematical reasoning outperform larger general-purpose models, highlighting the importance of domain specialization. Among local models, a particularly visible gap appears between the

logical coherence of reasoning and final answer accuracy, suggesting that models often begin solving in the right direction but fail to produce a fully correct final solution.

4. Discussion and Conclusions

This paper presented a methodological framework for the automated solving of mathematics competition problems for high school students in Serbia using LLMs. A particular contribution of the paper is the establishment of a multi aspect automatic evaluation framework, which includes final answer accuracy, logical coherence of reasoning, and explanation quality, thus enabling a more comprehensive assessment of model performance than one based solely on the final result. The obtained results indicate a clear gap between commercial and locally executable models, as well as the importance of domain specialization for better performance on competition level problems. At the same time, the differences between the values obtained in criteria A, B, and C show that model performance cannot be reliably assessed solely based on final answer accuracy, but that the quality of the reasoning process and how the solution is explained must also be considered. Future work will focus on fine-tuning selected models to improve their performance in solving problems in this domain.

Acknowledgements

The authors are supported by the Ministry of Science, Technological Development and Innovation, Republic of Serbia, Contract No. 451-03-34/2026-03/200122.

References

1. Ahn J, Verma R, Lou R, Liu D, Zhang R, Yin W. Large Language Models for Mathematical Reasoning: Progresses and Challenges. In: Proceedings of the 18th Conference of the European Chapter of the Association for Computational Linguistics: Student Research Workshop. 2024:225–237.

2. Svičević M, Milenković A, Vučićević N, Stanković M. Evaluating the Success of AI Tools in Supporting Student Performance in Mathematical Kangaroo Competition. Computer Applications in Engineering Education. 2025;33:e70063.

3. Vučićević N, Svičević M, Milenković A. Challenging DeepSeek-R1 with Serbian High School Math Competition Problems. In: Sinteza 2025 – International Scientific Conference on Information Technology, Computer Science, and Data Science. 2025:274–280.

4. Milenković A, Vučićević N, Svičević M. Evaluating Open AI Tools o1 and o3-mini in Solving High School Problems from Serbian National Mathematics Competition. The Teaching of Mathematics. 2025;28(1):14–29.

5. Mao Y, Kim Y, Zhou Y. CHAMP: A Competition-level Dataset for Fine-Grained Analyses of LLMs' Mathematical Reasoning Capabilities. In: Findings of the Association for Computational Linguistics: ACL 2024. 2024:13256–13274.

Implementation of an 8-bit Floating-Point Coprocessor for Deep Learning Applications

Isidora Grujić[1], Marija Božilov[1], Aleksandar Kondić[1], Vladimir M. Milovanović[1]

[1]*Faculty of Engineering, University of Kragujevac, Sestre Janjić 6, 34000 Kragujevac, Serbia,* isidora@uni.kg.ac.rs, *0000-0001-6474-7937,* marija@uni.kg.ac.rs, *0009-0004-8763-1434,* konda@uni.kg.ac.rs, *0009-0005-8400-271X,* vlada@uni.kg.ac.rs, *0000-0002-6787-4058*

Corresponding author: vlada@uni.kg.ac.rs

Abstract

This paper presents the design and implementation of a mathematical coprocessor for arithmetic operations on numbers represented in an 8-bit floating-point format (FP8). The motivation for this work arises from the increasing computational demands of deep learning systems and their demonstrated robustness to reduced numerical precision. The proposed coprocessor supports two FP8 encoding formats, E4M3 and E5M2, which provide different trade-offs between precision and dynamic range. The paper provides a detailed overview of floating-point representation, arithmetic algorithms, and hardware architecture. The coprocessor is implemented using hardware module generators in the Chisel programming language, enabling scalable and parameterizable design. Generated Verilog RTL is synthesized for FPGA implementation, and results demonstrate reduced hardware complexity with acceptable numerical accuracy. The proposed solution is suitable for efficient deep learning acceleration.

Keywords: FP8 floating-point format; floating-point arithmetic; E4M3 encoding, E5M2 encoding; deep learning; hardware accelerator; coprocessor design; hardware module generator; UN SDG 7.

1. Introduction

Deep learning represents a subfield of machine learning based on artificial neural networks, which consist of large numbers of interconnected processing units organized in layers [1]. These models are capable of solving complex problems in domains such as image recognition, natural language processing, and time-series analysis. Convolutional neural networks are widely used for image processing tasks [2], while recurrent neural networks are suitable for sequential data processing [3]. More recently, transformer-based architectures have become dominant in natural language processing applications [4].

A common characteristic of all deep learning models is their extremely high computational complexity. Training large neural networks requires processing vast datasets and performing billions of arithmetic operations, often on specialized hardware platforms. As model sizes continue to grow, reducing computational cost and energy consumption becomes a major challenge.

Recent research has shown that deep neural networks are robust to quantization errors and can operate effectively with reduced numerical precision. This observation has motivated the development of new numerical formats, including the FP8 floating-point format. Experimental results have demonstrated that FP8 arithmetic can achieve comparable performance to higher precision formats such as FP16, while significantly reducing memory usage and computational requirements [5].

The FP8 format has been standardized through collaborative efforts within the Open Compute Project, introducing two encoding variants: E4M3 and E5M2 [6]. These formats provide a balance between numerical precision and dynamic range, making them suitable for deep learning applications.

The objective of this paper is to present the design and implementation of an 8-bit floating-point coprocessor that supports both FP8 formats and enables efficient hardware execution of arithmetic operations.

2. Floating-Point Representation

Floating-point representation enables efficient encoding of real numbers over a wide dynamic range. A number is represented as

$$x = (-1)^s \cdot m \cdot 2^E \tag{1}$$

where s denotes the sign, m the mantissa, and E the exponent [1].

In digital systems, floating-point numbers are represented using a finite number of bits allocated to these components. The IEEE 754 standard defines widely used formats such as FP32 and FP16 [7]. These formats ensure consistent representation and arithmetic behavior across computing systems.

The FP8 format follows the same fundamental principles but reduces the total number of bits to eight. This reduction significantly decreases hardware requirements while maintaining sufficient numerical accuracy for many applications.

Two encoding formats are defined for FP8 [6]:

- E5M2, which allocates five bits to the exponent and two bits to the mantissa and
- E4M3, which allocates four bits to the exponent and three bits to the mantissa.

The E5M2 format provides a wider dynamic range, while E4M3 offers higher precision. Both formats include support for special values such as zero, infinity, and NaN, consistent with IEEE 754 rules [7,8].

3. Floating-Point Arithmetic

Floating-point arithmetic operations are significantly more complex than fixed-point operations due to the need for normalization and exponent handling.

Addition and subtraction require alignment of operands by adjusting their exponents before performing mantissa operations. After the operation, the result must be normalized and rounded to fit within the available precision.

Multiplication is performed by multiplying mantissas and adding exponents, followed by normalization. Division is more complex and is typically implemented using iterative approximation methods such as the Newton–Raphson method, which provides efficient convergence while maintaining acceptable hardware complexity [9].

In addition to arithmetic operations, the coprocessor supports comparison operations and conversion between FP8 formats. Conversion between E4M3 and E5M2 formats requires careful handling of exponent bias and mantissa truncation.

Special cases such as overflow, underflow, and undefined values must also be handled correctly. These cases are defined by IEEE 754 and are essential for ensuring reliable operation in practical systems [7,8].

4. Hardware Implementation

The proposed coprocessor is implemented using the Chisel hardware description language, which is based on Scala and enables parameterized hardware design [10]. This approach allows the creation of reusable hardware module generators that can be configured for different formats and operations.

The architecture consists of multiple functional units responsible for arithmetic operations, comparison, and format conversion. Each unit is implemented as a separate module, enabling modular design and easier verification (Figure 1).

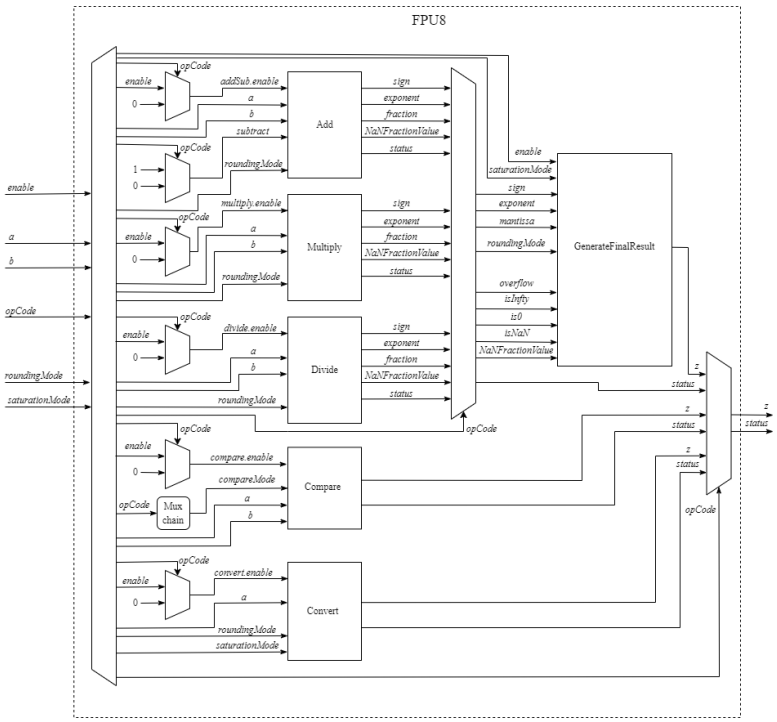


Figure 1. Block diagram of the interconnection of hardware modules for floating-point arithmetic within the FPU8 module.

Arithmetic units include floating-point adder/subtractor, floating-point multiplier, and floating-point divider. The divider is implemented using an iterative method based on Newton–Raphson approximation, which reduces hardware complexity compared to direct division.

The design supports both FP8 formats through parameterization, allowing dynamic selection of exponent and mantissa widths (Figure 2). Chisel descriptions are translated into Verilog RTL, which is then synthesized for FPGA implementation. This design flow improves productivity and enables rapid design iteration compared to traditional hardware description approaches [10].

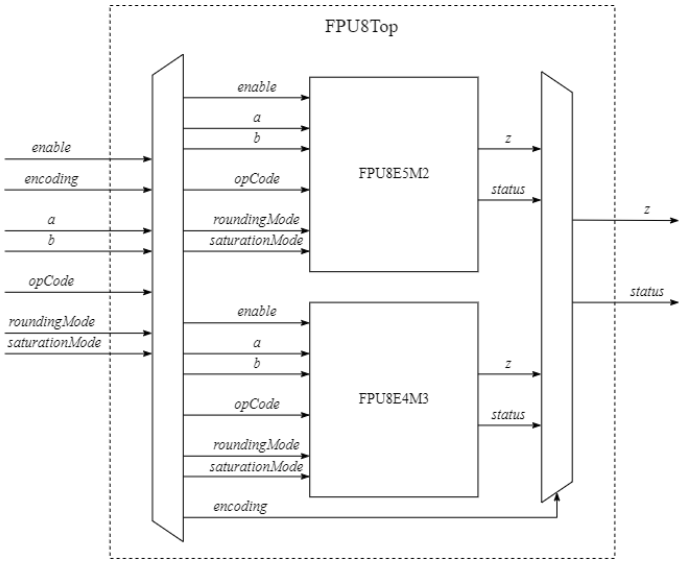


Figure 2. Block diagram of the interconnection of hardware modules for floating-point arithmetic in different FPU8 formats within the coprocessor.

5. Results

The implemented coprocessor was verified through simulation. Functional verification confirmed correct operation of all arithmetic units, including handling of edge cases such as overflow, underflow, and special values. The design was then synthesized for an FPGA platform Arty A7, which is based on the Artix-7 family of chips. After logical synthesis, detailed reports on resource utilization for the selected FPGA platform were obtained. (Table 1) summarizes the resource usage of the generated hardware modules.

The results indicate that the FPU8E4M3 module requires significantly more Slice LUT resources compared to the FPU8E5M2 module, primarily due to the wider mantissa in the E4M3 encoding format, which leads to increased logical complexity. In contrast, F7 multiplexers, which are specific to the Artix-7 architecture, are utilized only in the FPU8E5M2 module, likely due to additional logic required for handling special values such as infinity. The number of bonded I/O blocks is identical for both FPU8E4M3 and FPU8E5M2 modules, while the top-level module uses one additional I/O block due to the presence of an extra input signal for format

selection. Since the implemented design is purely combinational, the maximum operating frequency could not be directly determined; however, it can be estimated based on the critical path delay of the synthesized circuit.

Table 1. Overview of resource utilization for hardware modules generated within this project.

Generated hardware module	Slice LUTs	F7 Muxes	Bonded IOB	Critical path	Propagation delay	Estimate of the maximum operating frequency
FPU8Top	955	4	38	b[3] – z[0]	32.78 ns	30.51 MHz
FPU8E5M2	421	2	37	b[4] – status[3]	24.61 ns	40.63 MHz
FPU8E4M3	537	0	37	b[3] – z[0]	31.975 ns	31.27 MHz

The use of FP8 representation significantly reduced hardware resource utilization compared to higher precision formats. Reduced bit-width leads to lower logic usage, reduced memory requirements, and improved parallelism.

Although the estimated maximum operating frequency of 30.51 MHz for the FPU8 unit is lower than that of optimized pipelined floating-point units, this result is consistent with the combinational nature of the proposed design and confirms the feasibility of the implemented architecture.

6. Discussion

The results demonstrate that FP8 arithmetic represents a promising approach for improving efficiency in deep learning systems. The reduction in precision allows significant savings in hardware resources and power consumption while maintaining acceptable accuracy for many applications.

The choice between E4M3 and E5M2 formats depends on application requirements. E4M3 is more suitable for applications requiring higher precision, while E5M2 is preferable when a wider dynamic range is needed.

Despite its advantages, FP8 arithmetic introduces limitations in scenarios requiring high numerical accuracy, particularly in accumulation-heavy operations. However, these limitations can often be mitigated through algorithmic adjustments or mixed-precision approaches [11].

The use of Chisel enables flexible and scalable hardware design, making the proposed coprocessor suitable for integration into larger systems and future extensions.

7. Conclusions

This paper presented the design and implementation of an 8-bit floating-point coprocessor for deep learning applications. The proposed solution supports multiple encoding formats and demonstrates efficient use of hardware resources.

The results confirm that FP8 arithmetic can significantly reduce system complexity while maintaining sufficient numerical accuracy. This makes it a strong candidate for future deep learning accelerators. Recent developments in reduced-precision arithmetic have also introduced even lower bit-width formats, such as FP4 (e.g., E2M1),

as well as emerging proprietary and mixed-precision formats such as MXFP4 and NVFP4. These formats aim to further reduce hardware complexity and energy consumption while maintaining acceptable accuracy in deep learning applications, representing a promising direction for future research [12–14].

Future work includes implementing pipelining to improve the maximum operating frequency, integrating the coprocessor into complete neural network systems, evaluating its performance on real workloads, and optimizing the design for ASIC implementations.

Acknowledgements

This paper is supported by the project No. 451-03-34/2026-03/200107, Ministry of Science, Technological Development and Innovation, Republic of Serbia.

References

[1] Grujić I. Implementation of an 8-bit Mathematical Coprocessor for Floating-Point Arithmetic Intended for Deep Learning Systems. MA Thesis. University of Kragujevac, Faculty of Engineering, 2024.

[2] O'Shea K, Nash R. An Introduction to Convolutional Neural Networks 2015. https://doi.org/10.48550/arXiv.1511.08458.

[3] Schmidt RM. Recurrent Neural Networks (RNNs): A gentle Introduction and Overview 2019. https://doi.org/10.48550/arXiv.1912.05911.

[4] Han K, Xiao A, Wu E, Guo J, Xu C, Wang Y. Transformer in Transformer 2021. https://doi.org/10.48550/arXiv.2103.00112.

[5] Micikevicius P, Stosic D, Burgess N, Cornea M, Dubey P, Grisenthwaite R, Ha S, Heinecke A, Judd P, Kamalu J, Mellempudi N, Oberman S, Shoeybi M, Siu M, Wu H. FP8 Formats for Deep Learning 2022. https://doi.org/10.48550/arXiv.2209.05433.

[6] Paulius Micikevicius, Stuart Oberman, Pradeep Dubey, Marius Cornea, Andres Rodriguez, Ian Bratt, Richard Grisenthwaite, Norm Jouppi, Chiachen Chou, Amber Huffman, Michael Schulte, Ralph Wittig, Dharmesh Jani, Summer Deng. OCP 8-bit Floating Point Specification (OFP8) 2023.

[7] IEEE Standard for Floating-Point Arithmetic n.d. https://doi.org/10.1109/IEEESTD.2019.8766229.

[8] Boldo S, Jeannerod C-P, Melquiond G, Muller J-M. Floating-point arithmetic. Acta Numer 2023;32:203–90. https://doi.org/10.1017/S0962492922000101.

[9] Parhami B. Computer arithmetic: algorithms and hardware designs. 2nd ed. New York: Oxford University Press; 2010.

[10] Chisel/FIRRTL: Home n.d. https://www.chisel-lang.org (accessed April 15, 2026).

[11] Tagliavini G, Mach S, Rossi D, Marongiu A, Benini L. A transprecision floating-point platform for ultra-low power computing. 2018 Des. Autom. Test Eur. Conf. Exhib. DATE, Dresden, Germany: IEEE; 2018, p. 1051–6. https://doi.org/10.23919/DATE.2018.8342167.

[12] Chmiel B, Fishman M, Banner R, Soudry D. FP4 All the Way: Fully Quantized Training of LLMs 2025. https://doi.org/10.48550/ARXIV.2505.19115.

[13] Cim M, Topcu B, Kandemir MT. Diagnosing FP4 inference: a layer-wise and block-wise sensitivity analysis of NVFP4 and MXFP4 2026. https://doi.org/10.48550/ARXIV.2603.08747.

[14] Introducing NVFP4 for Efficient and Accurate Low-Precision Inference. NVIDIA Dev n.d. https://developer.nvidia.com/blog/introducing-nvfp4-for-efficient-and-accurate-low-precision-inference/ (accessed April 15, 2026).

Decision-Making Algorithm for Intuitionistic Fuzzy Soft Sets

Nemanja Vučićević[1], Nenad Stojanović[1], Marina Svičević[1]

[1]*Faculty of Science, University of Kragujevac, Kragujevac, Serbia, nemanja.vucicevic@pmf.kg.ac.rs, 0000-0002-4903-7280, nenad.stojanovic@pmf.kg.ac.rs, 0000-0003-3837-4043, marina.svicevic@pmf.kg.ac.rs, 0000-0003-2791-3849,*

Corresponding author: *nemanja.vucicevic@pmf.kg.ac.rs*

Abstract

This paper introduces a new numerical characteristic for intuitionistic fuzzy soft sets (IFSSs) based on the singular values of the associated membership and non-membership matrices. Using this quantity, we propose a decision-making algorithm for ranking alternatives in uncertain environments. The approach is illustrated by a case study, validated through effectiveness criteria, and complemented by a brief complexity analysis. The results indicate that the method provides a simple and informative framework for decision making with IFSSs.

Keywords: Intuitionistic fuzzy soft set, energy, singular values, decision making.

1. Introduction

Soft sets, fuzzy sets, and intuitionistic fuzzy sets ([1]) provide important tools for modeling uncertainty. Their hybridization leads to intuitionistic fuzzy soft sets (IFSSs), [2], which are suitable for decision-making problems involving several parameters and uncertain evaluations.

Many existing IFSS decision-making procedures are based on local score functions, similarity measures, or aggregation operators. In this paper, we introduce a different global numerical characteristic, called the energy of an IFSS. This characteristic is defined through the singular values of two matrices representing the membership and non-membership structure of the system ([3]). Based on it, we formulate a simple ranking procedure and illustrate its use on a practical example.

2. Materials and Methods

Definition 2.1. Let $U = \{x_1, x_2, \dots, x_n\}$ be a universe of discourse, E a set of parameters, and $A \subseteq E$. An *intuitionistic fuzzy soft set* (IFSS) over U with respect to A is a pair (F, A), where $F : A \to IF(U)$, and for each $e \in A$,

$$F(e) = \{(x, \mu_{F(e)}(x), \nu_{F(e)}(x)) \mid x \in U\}, \text{ with } 0 \leq \mu_{F(e)}(x) + \nu_{F(e)}(x) \leq 1 \text{ for all } x \in U.$$

Thus, for every parameter $e \in A$, the value $\mu_{F(e)}(x)$ describes the degree of membership of x, while $\nu_{F(e)}(x)$ describes the degree of non-membership of x.

Definition 2.2. Let (F, A) be an IFSS over $U = \{x_1, \dots, x_n\}$, where $A = \{e_1, \dots, e_m\}$. The *membership matrix* and the *non-membership matrix* of (F, A) are defined by

$$\Psi^{+}_{(F,A)} = \left[\mu_{F(e_j)(x_i)}\right]_{n\times m}, \Psi^{-}_{(F,A)} = \left[\nu_{F(e_j)(x_i)}\right]_{n\times m}.$$

These two matrices encode the complete numerical structure of the IFSS.

Definition 2.3. Let $\sigma_1{}^{+} \geq \sigma_2{}^{+} \geq \cdots \geq \sigma_n{}^{+} \geq 0$ be the singular values of $\Psi^{+}_{(F,A)}$, and let $\sigma_1{}^{-} \geq \sigma_2{}^{-} \geq \cdots \geq \sigma_n{}^{-} \geq 0$ be the singular values of $\Psi^{-}_{(F,A)}$. The *energy* of the IFSS (F, A) is defined by

$$\mathcal{E}_{(F,A)} = \sum_{i=1}^{n} (\sigma_i{}^{+} - \sigma_i{}^{-}).$$

This quantity measures the global balance between membership and non-membership information in the observed IFSS.

3. Decision-making algorithm and an estimate of the energy

The proposed decision-making rule is based on the contribution of each alternative to the total system.

Algorithm 3.1. Energy-based decision-making algorithm for IFSSs

Input: An intuitionistic fuzzy soft set (F, A) defined over the universal set $U = \{x_1, x_2, \ldots, x_n\}$.
Output: A ranking of the alternatives according to their contribution to the system, obtained by analyzing the energies of the reduced IFSSs.
Step 1. Input the intuitionistic fuzzy soft set (F, A).
Step 2. Form n new intuitionistic fuzzy soft sets, denoted by $(F, A)_i$, over $U \setminus \{x_i\}$ for each $x_i \in U$.
Step 3. For each intuitionistic fuzzy soft set from Step 2, form the corresponding membership and non-membership matrices $\Psi^{+}_{(F,A)}$ and $\Psi^{-}_{(F,A)}$.
Step 4. Determine the singular values for all matrices obtained in Step 3.
Step 5. Compute the energies $\mathcal{E}_{(F,A)_i}$ for each reduced intuitionistic fuzzy soft set $(F, A)_i$, using the singular values obtained in Step 4.
Step 6. Compare the values obtained in Step 5 and interpret the result.
The alternative whose removal gives the smallest remaining energy is the **most structurally influential**, while the alternative whose removal gives the largest remaining energy is the **least contributing** one.

The interpretation is immediate. If the energy of the remaining system is small after removing x_i, then x_i had a strong contribution to the original system. If the remaining system still has a large energy, then x_i contributed less. Therefore, $\min_i \mathcal{E}_{(F,A)_i}$ corresponds to the most contributing alternative, while $\max_i \mathcal{E}_{(F,A)_i}$ corresponds to the least contributing alternative.

Theorem 3.2. Let (F, A) be an IFSS over $U = \{x_1, \ldots, x_n\}$, where $|A| = m$. Then

$$-n\sqrt{m} \leq \mathcal{E}_{(F,A)} \leq n\sqrt{m}.$$

3. Case Study and Validation of the Energy-Based Method

We illustrate the proposed method on a team-selection problem with six candidates $U = \{x_1, x_2, x_3, x_4, x_5, x_6\}$, evaluated with respect to six parameters $A = \{e_1, e_2, e_3, e_4, e_5, e_6\}$, which represent creativity, managerial skills, intuition, research productivity, ability to work under time pressure, and knowledge. The corresponding IFSS (F, A) is given in Table 1.

Table 1. IFSS (F, A)

(F, A)	e_1	e_2	e_3	e_4	e_5	e_6
x_1	(0.8,0.1)	(0.6,0.2)	(0.4,0.4)	(0.7,0.2)	(0.6,0.1)	(0.7,0.3)
x_2	(0.6,0.2)	(0.7,0.2)	(0.4,0.5)	(0.5,0.1)	(0.6,0.2)	(0.5,0.3)
x_3	(0.7,0.3)	(0.8,0.1)	(0.6,0.3)	(0.7,0.1)	(0.2,0.5)	(0.7,0.1)
x_4	(0.8,0.1)	(0.9,0.1)	(0.6,0.2)	(0.5,0.3)	(0.7,0.2)	(0.6,0.2)
x_5	(0.5,0.4)	(0.6,0.3)	(0.7,0.2)	(0.2,0.6)	(0.7,0.1)	(0.3,0.5)
x_6	(0.6,0.1)	(0.7,0.2)	(0.5,0.3)	(0.8,0.1)	(0.6,0.3)	(0.4,0.4)

For the original system, the energy equals $\mathcal{E}_{(F,A)} = 2.306$.

Next, we remove one candidate at a time and compute the energies of the reduced systems. The obtained values are presented in Table 2.

Table 2. Energies of reduced IFSSs

	x_1	x_2	x_3	x_4	x_5	x_6
$\mathcal{E}_{(F,A)_i}$	1.883	2.230	1.986	1.950	2.380	2.045

Since $\mathcal{E}_{(F,A)_1} < \mathcal{E}_{(F,A)_4} < \mathcal{E}_{(F,A)_3} < \mathcal{E}_{(F,A)_6} < \mathcal{E}_{(F,A)_2} < \mathcal{E}_{(F,A)_5}$, the ranking of contributions is $x_1 \succ x_4 \succ x_3 \succ x_6 \succ x_2 \succ x_5$. Hence, candidate x_1 is the most influential for the structure of the system, while candidate x_5 is the least contributing one. The bar chart confirms this conclusion visually: the smallest remaining energy is obtained after removing x_1, whereas the largest remaining energy is obtained after removing x_5.

Effectiveness Test

In order to provide additional validation of the proposed energy-based method, we briefly examine the three effectiveness criteria introduced by Wang and Triantaphyllou ([4]). The considered example satisfies all three criteria.

Step 1: Verification of Criterion 1.

Criterion 1 requires that a mild deterioration of a non-optimal alternative should not change the optimal decision, nor disturb the relative order of the unaffected alternatives. Starting from the ranking $x_1 \succ x_4 \succ x_3 \succ x_6 \succ x_2 \succ x_5$, we consider the non-optimal alternative x_4 and replace its value under parameter e_1 by the corresponding inferior value of the worst-ranked alternative x_5. After applying the proposed algorithm again, the obtained ranking is $x_1 \succ x_3 \succ x_4 \succ x_6 \succ x_2 \succ x_5$. Thus, the best alternative remains unchanged, and the order of the unaffected alternatives is preserved. Therefore, Criterion 1 is satisfied.

Step 2: Verification of Criterion 2.

Criterion 2 requires consistency on subproblems. We consider the following subproblems with three alternatives each: $\{x_4, x_5, x_6\}, \{x_2, x_3, x_4\}, \{x_3, x_4, x_5\}, \{x_1, x_2, x_3\}, \{x_3, x_5, x_6\}, \{x_2, x_3, x_5\}, \{x_2, x_3, x_6\}$, and $\{x_1, x_2, x_4\}$. Applying the energy-based method to these subproblems yields the rankings $x_4 \succ x_6 \succ x_5, x_4 \succ x_3 \succ x_2$, $x_4 \succ x_3 \succ x_5$, $x_1 \succ x_3 \succ x_2$, $x_3 \succ x_6 \succ x_5$, $x_3 \succ x_2 \succ x_5$, $x_3 \succ x_6 \succ x_2$, and $x_1 \succ x_4 \succ x_2$. Each of these partial rankings is consistent with the overall order $x_1 \succ x_4 \succ x_3 \succ x_6 \succ x_2 \succ x_5$. Hence, Criterion 2 is satisfied.

Step 3: Verification of Criterion 3.

Criterion 3 requires that the aggregation of consistent subproblem rankings should reproduce the overall ranking. Since the rankings obtained in Step 2 are mutually compatible and induce the same global order $x_1 \succ$

$x_4 \succ x_3 \succ x_6 \succ x_2 \succ x_5$, Criterion 3 is also satisfied. Therefore, the proposed energy-based method passes all three effectiveness criteria.

Computational Complexity

We briefly comment on the computational complexity of the proposed algorithm. Let the IFSS contain n alternatives and m parameters. For each alternative xi, the algorithm forms a reduced IFSS $(F, A)_i$, whose membership and non-membership matrices have dimension $(n-1) \times m$. The dominant computational cost lies in computing the singular values of these matrices.

The singular value decomposition of a matrix of size $(n-1) \times m$ requires $O((n-1) \cdot m \cdot \min(n-1, m))$ operations. Since this computation is performed for all n reduced systems, the total complexity of the method is $O(n(n-1)m \cdot \min(n-1, m))$. Therefore, the proposed procedure has polynomial complexity and is computationally feasible for decision-making problems of moderate size. In practical implementations, the cost is dominated by the singular value computations, while the construction of the reduced IFSSs and their associated matrices is comparatively negligible.

5. Conclusions

In this paper, we introduced a new approach to decision making in the framework of intuitionistic fuzzy soft sets. The proposed method is based on a matrix representation of the observed system and provides a global criterion for ranking alternatives. In addition, the obtained estimate gives a general bound for the introduced numerical characteristic, while the illustrative example shows that the method is easy to apply and yields a clear ranking of alternatives. These results indicate that the proposed approach can serve as a useful tool for decision-making problems under uncertainty.

Acknowledgements

The authors are supported by the Ministry of Science, Technological Development and Innovation, Republic of Serbia, Contract No. 451-03-34/2026-03/200122.

References

1. Atanassov, K.T.: Intuitionistic fuzzy sets. Fuzzy Sets and Systems 20(1), 87–96 (1986).
2. Maji, P.K., Biswas, R., Roy, A.R.: Intuitionistic fuzzy soft sets. The Journal of Fuzzy Mathematics 9(3), 677–691 (2001).
3. Mudrić Staniškovski, Lj., Djurović, Lj., Stojanović, N.: Energy of a fuzzy soft set and its application in decision-making. Iranian Journal of Fuzzy Systems 21(2), 35–49 (2024).
4. Wang, X., Triantaphyllou, E.: Ranking irregularities when evaluating alternatives by using some electre methods. Omega 36(1), 45–63 (2008)

Clustering of the Zeros of Orthogonal Polynomials on the Semicircle

Marija P. Stanić[1], Tatjana V. Tomović Mladenović[1], Aleksandra S. Milosavljević[1]

[1]*Department of Mathematics and Informatics, Faculty of Science, University of Kragujevac, Kragujevac, Serbia, marija.stanic@pmf.kg.ac.rs, 0000-0003-4785-6730, tatjana.tomovic@pmf.kg.ac.rs, 0000-0001-9758-1515, aleksandra.milosavljevic@pmf.kg.ac.rs, 0000-0003-2483-7676*

Corresponding author: aleksandra.milosavljevic@pmf.kg.ac.rs

Abstract

In this paper, we investigate the clustering of zeros of orthogonal polynomials defined on the semicircle. Using the built-in function *FindClusters[]* in Wolfram Cloud, we perform a systematic analysis of the distribution of these zeros and identify natural groupings that emerge from their geometric and algebraic properties. The results provide insight into the structural behavior of orthogonal polynomials on the semicircle and demonstrate the effectiveness of clustering techniques in revealing hidden patterns within their zero distributions.

Keywords: orthogonality on the semicircle, clustering, zeros, UN SDG 4, UN SDG 17

1. Introduction

Weighted orthogonality on the semicircle was considered in [4] by Gautschi, Landau and Milovanović. The considered weight $w = w(z)$ was positive and integrable on the open interval $(-1,1)$, though possibly singularity at the endpoints, and which could be extended to a function $w(z)$ holomorphic in the half disc $D_+ = \{z \in \mathbb{C} \mid |z| < 1, \mathrm{Im}(z) > 0\}$. According to definition stated in [4], polynomials $\pi_k^{(S)}$, $k = 0,1, \ldots$, are orthogonal on the semicircle if the following condition is satisfied:

$$I\left(\pi_k^{(S)} \cdot \pi_l^{(S)}\right)\begin{cases} = 0, & k \neq l, \\ \neq 0, & k = l. \end{cases}$$

where $If = I(f) = \int_\Gamma f(z)(\mathrm{i}z)^{-1}w(z)\mathrm{d}z = \int_0^\pi f\left(\mathrm{e}^{\mathrm{i}\theta}\right)w\left(\mathrm{e}^{\mathrm{i}\theta}\right)\mathrm{d}\theta$. In [4] it is shown that zeros of polynomials orthogonal on the semicircle are the eigenvalues of Jacobi matrix [4, (6.1)]. One of the most notable properties of polynomials orthogonal on the semicircle is that all of their zeros lie within the semicircle D_+, except possibly a single zero when the polynomial degree is odd. For symmetric weight functions, the zeros are distributed symmetrically with respect to the imaginary axis, and as the degree increases, they tend to accumulate along the interval $[-1,1]$ (see [3], [4]).

In [6] there is an explanation of built-in function FindClusters[] that does unsupervised machine learning, where the computer just looks at data without being told anything about it. The number and composition of the clusters is influenced by the input data, the method and the evaluation criterion used. The elements can belong to a variety of data types, including numerical, textual and image, as well as dates and times.

2. Methods and Software

In this paper, we use the function FindClusters[] in Wolfram Cloud, which performs clustering of the zeros of orthogonal polynomials. We applied the well-known Golub–Welsch algorithm, as described in [5], which is available through the OrthogonalPolynomials package (see [1]) in Wolfram Mathematica 9 for calculation of zeros of polynomials orthogonal on the semicircle.

3. Results

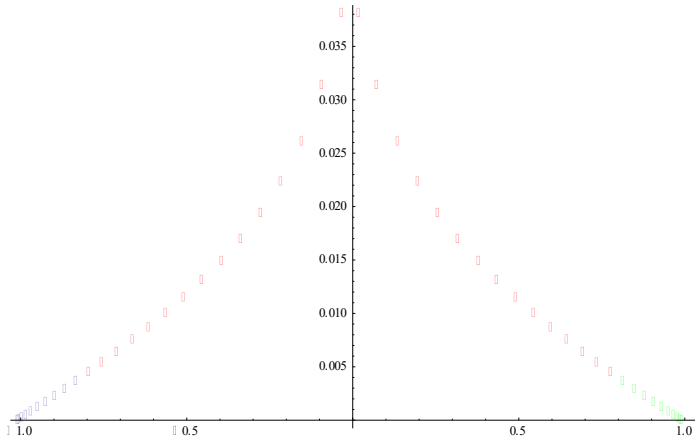


Figure 1. Clustering of zeros of $\pi_{50}^{(S)}$

The results of applying clustering to the zeros of polynomials orthogonal on the semicircle, with respect to the Chebyshev weight function of the first kind, are shown in Figures 1 and 2 for the zeros of the polynomials $\pi_{50}^{(S)}$, $\pi_{10}^{(S)}$, and $\pi_{80}^{(S)}$, respectively. The same color corresponds to the elements from the same cluster.

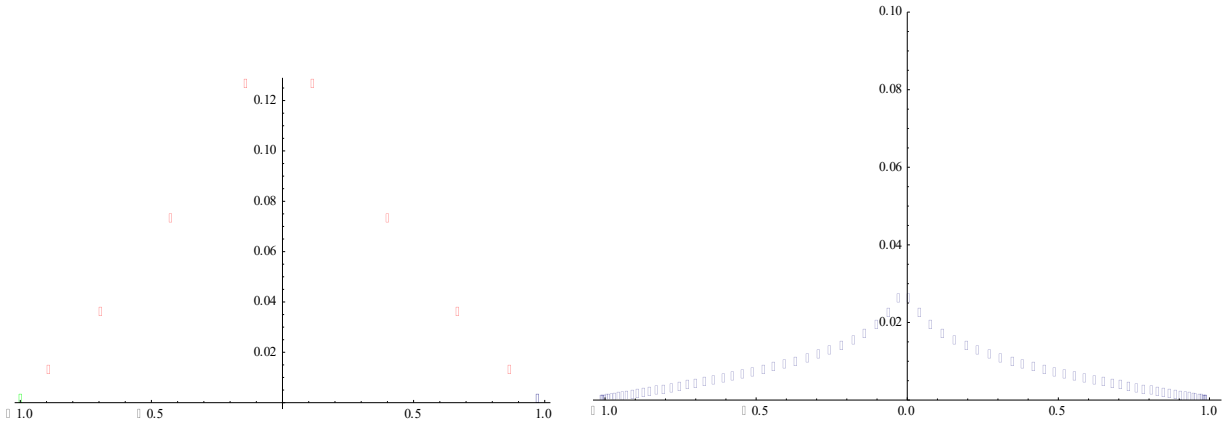


Figure 2. Clustering of zeros of $\pi_{10}^{(S)}$ *(left) and* $\pi_{80}^{(S)}$ *(right)*

4. Discussion

We observe that, in the case of polynomials orthogonal on the semicircle of lower degree, a smaller number of zeros are placed into a different cluster, specifically those located very close to the points −1 and 1 on the real axis. On the other hand, when the degree of the polynomial is significantly higher, all zeros belong to a single cluster, even to the same subcluster, which indicates that as the degree increases, the zeros of the polynomial tend to concentrate more strongly along the real interval [−1,1]. The clustering method is particularly useful when it is not easy to determine which nodes lie close to the real interval [−1,1] and which do not approach this interval, as illustrated in the case of the polynomial of degree 50 orthogonal on the semicircle.

5. Conclusions

Clustering the zeros of orthogonal polynomials on the semicircle is important because it highlights how these zeros approach the real interval [−1,1] as the polynomial degree increases. This structural insight is not only theoretical but also has practical consequences. Beyond pure mathematics, such techniques can be applied in numerical simulations of physical systems defined on circular or semicircular domains, in signal processing where orthogonal polynomials are used for spectral analysis, and in computational methods for boundary value problems where semicircle geometry naturally arises. Thus, clustering provides both a deeper theoretical understanding and a practical framework for applying semicircle orthogonal polynomials in diverse scientific and engineering contexts.

Acknowledgements

The authors were supported in part by the Serbian Ministry of Science, Technological Development and Innovation, Grant number 451-03-34/2026-03/200122.

References

1. Cvetković, A.S., Milovanović, G.V. The Mathematica package “OrthogonalPolynomials", Facta Univ. Ser. Math. Inform 2004;19:17–36
2. Milovanović G.V. On polynomials orthogonal on the semicircle and applications. J. Comput. Appl. Math. 1993;49:193–199.
3. Milovanović, G.V. Orthogonality on the semicircle: old and new results. Electron. Trans. Numer. Anal. 2023;59:99–115
4. Gautschi W., Landau H.J, Milovanović G.V. Polynomials orthogonal on the semicircle, II. Constr. Approx. 1987;3:389–404.
5. Golub, G.H., Welsch, J.H. Calculation of Gauss quadrature rules. Math. Comput. 1969;23(106):221–230.
6. Wolfram S., An Elementary Introduction to Wolfram Language, Second Edition 2017 (Section: Machine Learning)

Turning the Sky into a Tool for Peace

Aery Bizkaia

Mikel Espiga

Aery Bizkaia, Department of Engineering, Bilbao, Spain, mikel.espiga@alumni.mondragon.edu

Contact email: spinko@aerybizkaia.es | Website: www.aerybizkaia.es

Executive Summary

Aery Bizkaia is a deep-tech startup developing advanced aerial sensing systems based on Circular Synthetic Aperture Radar (CSAR) combined with artificial intelligence to address one of the most persistent global challenges: the detection of landmines and explosive remnants of war (ERW).

Our technology enables high-resolution subsurface imaging from UAV platforms, allowing safe, scalable, and efficient analysis of hazardous terrain. Current solutions rely heavily on manual processes and ground-based technologies that are slow, dangerous, and difficult to scale. Aery introduces a paradigm shift by moving detection capabilities to the air, minimizing human exposure and increasing operational efficiency. Beyond humanitarian demining, our platform has strong dual-use applications in security, infrastructure monitoring, and land intelligence. This positions Aery Bizkaia within a growing global market demanding automated, data-driven sensing solutions.

The company is embedded in the Basque innovation ecosystem and is actively building collaborations with research institutions and industry partners. With a clear roadmap toward MVP development and pilot deployments, Aery Bizkaia is preparing for its next stage of growth, including venture capital financing and international expansion.

Our mission is to unlock land, save lives, and enable economic recovery by transforming aerial sensing into actionable intelligence.

Keywords: deeptech; radar; UAV; AI; humanitarian demining; remote sensing; ERW detection; dual-use technology; UN SDG 9; UN SDG 16

1. Company Overview

Aery Bizkaia is a Spain-based deep-tech startup focused on developing advanced radar-based sensing systems for high-impact applications in humanitarian and security domains. The company's mission is to create scalable technologies that improve safety, enable land recovery, and contribute to economic development in post-conflict

regions. Aery operates at the intersection of radar engineering, artificial intelligence, and autonomous aerial systems.

Positioned within the Basque Country's strong innovation ecosystem, Aery benefits from access to research institutions, public support programs, and a growing network of industrial and academic collaborators. Strategically, the company is pursuing a technology-driven and impact-driven approach, aiming to become a leading provider of aerial sensing solutions for subsurface detection and land intelligence.

The long-term vision is to build a globally recognized deep-tech company delivering dual-use solutions that combine scientific excellence with real-world impact.

2. Technology / Product / Service Description

Aery Bizkaia is developing a UAV-integrated sensing system based on Circular Synthetic Aperture Radar (CSAR), designed to detect and classify buried objects with high precision. Core technology components are

1. CSAR Radar Payload

- Circular flight path enabling 360° data acquisition
- High-resolution imaging of subsurface structures
- Optimized for lightweight UAV integration

2. Multi-Frequency Capability

- Initial focus on L-band for subsurface penetration
- Future expansion to multi-band configurations (e.g., X-band)
- Adaptability to different terrain conditions

3. AI-Based Detection Algorithms

- Machine learning models trained on radar signatures
- Automated object detection and classification
- Continuous learning from operational data

The system builds on principles of synthetic aperture radar imaging, signal processing, and electromagnetic wave propagation. By combining circular acquisition geometry with advanced reconstruction algorithms, Aery enhances image resolution and detection reliability.

The integration of AI enables the transition from raw sensing to intelligent interpretation, significantly improving operational usability.

3. Innovation and Competitive Advantage

Aery Bizkaia introduces several key innovations that differentiate it from existing solutions:

- Unlike traditional ground-based systems, Aery enables detection from the air, improving safety (reduced human exposure), coverage (large areas scanned quickly), and operational flexibility;
- Circular SAR provides enhanced resolution compared to linear SAR, multiple angles polarization data, improved object characterization, and better detection reliability in complex environments;
- AI-Driven classification reduces a number of false positives, increases decision-making rate, and provides continuous system improvement through data acquisition;
- Scalable and Modular Architecture: adaptable to different UAV platforms, expandable to multi-drone configurations (future roadmap), suitable for multiple applications beyond demining

Dual-Use Capability

The technology can and will be applied to:

- Humanitarian demining
- Public security
- Infrastructure assessment
- Environmental monitoring

These differentiators position Aery Bizkaia at the forefront of next-generation sensing technologies.

4. Market Application and Impact

Primary Market: Humanitarian Demining

Aery addresses a global challenge affecting over 60 countries, where land contamination limits human safety, agricultural use, and infrastructure development.

Our solution enables much faster land categorization and threats detection, safer operations, and reduced operational costs. The UAV-based approach allows rapid deployment in diverse environments, coverage of large areas, and integration into existing workflows.

Secondary Markets

- Public security
- Border and perimeter monitoring
- Infrastructure and land assessment

- Environmental and geological analysis

Impact

Social impact **(**reduction in casualties, improved safety for demining personnel, restoration of land for communities), economic impact (unlocking agricultural and commercial land, enabling investment in post-conflict regions), technological impact (advancement of European deep-tech capabilities, contribution to autonomous sensing systems).

5. Partnerships and Outlook

The company is actively building a network of collaborators across research, industry, and end-user organizations to accelerate both product development and market entry.

On the technical side, Aery is engaging with leading academic and research institutions in radar signal processing, artificial intelligence, and embedded systems to strengthen its core technology and expand its intellectual property base. In parallel, Aery is establishing relationships with humanitarian demining organizations, government agencies, and international stakeholders to validate its solution in real-world conditions. From an industrial perspective, the company is exploring collaborations with UAV manufacturers, sensor integrators, and defense-sector partners to ensure seamless system integration and scalability.

The immediate focus is on delivering a fully functional MVP and initiating pilot projects that demonstrate measurable performance improvements over existing solutions. These milestones are expected to unlock early revenues and significantly increase the company's valuation.

Over the medium term, Aery aims to scale up operations, supported by a growing team and a robust partner ecosystem. The long-term vision includes the deployment of multi-drone cooperative sensing systems and expansion into adjacent dual-use markets such as infrastructure monitoring and public security.

To execute this strategy, Aery Bizkaia is preparing for a venture capital financing round to fund product development, team expansion, and initial market deployments. The company offers investors a unique opportunity to participate in a deep-tech venture addressing a global, high-impact problem with strong commercial potential and clear scalability.

Acknowledgements

This work was supported by Mondragon Unibertsitatea via the MU ISE program. The authors clarify their appreciation for the program's entrepreneurship support, particularly in startup scaling and financial development, which significantly contributed to the progress of this project.

Computer Vision, Image Analysis, and Pattern Recognition

Few-Shot Approach for Mouse Lung Segmentation in Synchrotron X-Ray Tomography

Andjela Blagojevic[1,2], Tijana Geroski[1,2], Nenad Filipović[1,2]

[1]Faculty of Engineering, University of Kragujevac, Kragujevac, Serbia
[2] Bioengineering Research and Development Center (BioIRC), Kragujevac, Serbia

andjela.blagojevic@kg.ac.rs, 0000-0002-8652-3827, tijanas@kg.ac.rs, 0000-0003-1417-0521, fica@kg.ac.rs, 0000-0001-9964-5615

Corresponding author: andjela.blagojevic@kg.ac.rs

Abstract

Accurate segmentation of mouse lung microstructures is essential for understanding lung development and disease progression. However, the small size and complex architecture of the acinus make tissue air boundaries unclear, significantly complicating this task. Additionally, traditional segmentation methods rely on large, annotated datasets, which are difficult and costly to obtain for synchrotron radiation-based X-ray tomographic microscopy (SRXTM) images. This paper proposes a few-shot learning approach using a U-Net model for segmenting mouse lungs in SRXTM images. The model pretrained on images of sections of the lungs was used as a base for segmentation of the entire lung from SRXTM images. The initial model is trained on lung section image–mask pairs, then fine-tuned on only 3 labeled full-lung pairs, with 2 used for testing. The results show that the U-Net model achieves accurate segmentation of lung sections. After transfer learning to entire lung images, few-shot segmentation results were Dice coefficient = 0.86. The proposed few-shot approach enables effective lung segmentation with significantly fewer annotated samples, demonstrating its potential for data-limited medical imaging applications.

Keywords: Few-Shot Learning; Mice Lung Segmentation; Synchrotron Radiation-based X-ray Tomographic Microscopy Imaging; U-net

1. Introduction

In recent years, advances in computer vision and machine learning have significantly improved medical image segmentation, enabling more accurate analysis of complex structures and supporting diagnostic and treatment processes [1]. However, medical images at the tissue level remain challenging to analyze due to their complexity, making traditional methods such as thresholding insufficient [2]. Segmentation of mouse lungs in synchrotron radiation-based X-ray tomographic microscopy (SRXTM) images is particularly difficult due to the small size and intricate structure of lung tissue. The pulmonary acinus, composed of fine alveolar and airway structures, exhibits subtle and often ill-defined boundaries, further complicated by imaging noise, variable contrast, and biological variability between samples [3]. These factors make both manual annotation and automated segmentation highly challenging. Traditional and unsupervised segmentation methods often fail to provide consistent results in this context, while deep learning approaches, particularly convolutional neural

networks such as U-Net and its variants, have demonstrated superior performance in medical image segmentation tasks [4, 5]. However, these methods typically require large annotated datasets, which are difficult to obtain for full mouse lung images.

Recent studies have shown that U-Net-based models can achieve high accuracy in segmenting lung sections using fully supervised learning [2, 6]. Nevertheless, these approaches rely on extensive annotated datasets and focus on simpler tasks, such as lung sections, rather than full lung structures. To address data limitations, few-shot learning has emerged as a promising approach, enabling models to achieve competitive performance with only a small number of labeled samples [7].

In this paper, we propose a methodology that combines transfer learning and few-shot learning for the segmentation of mouse lungs in SRXTM images. A U-Net model is first trained on lung section data and then adapted to full lung segmentation using a minimal number of annotated samples. The proposed approach aims to achieve accurate segmentation while significantly reducing the need for extensive manual annotation.

2. Materials and Methods

The main idea is to develop a model for whole lung segmentation, using as a base model previously trained on lung section images.

2.1 Dataset

The dataset is created using high-resolution SRXTM. Each image has the resolution of 2004x2004 but is resized to 1024x1024. Lung tissue is annotated on each image to produce a respective mask. An example of the dataset is given in Figure 1. A total of 5 image/mask pairs are contained within mice lung dataset, 3 of those pairs are utilized for training phase, and the rest 2 for the testing phases. Working with the entire lung allows us to obtain a detailed view of its structure, function, and any potential pathologies developing in different regions. Additionally, monitoring the entire lung overtime helps track the progression of diseases or the development of healthy functional units.

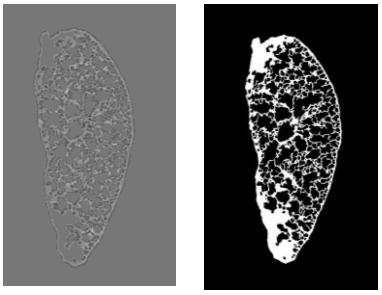


Figure 1. An example of the entire lung image-mask pair.

2.2 Methodology

To address the challenge of limited labeled data, this methodology adopts a few-shot learning approach based on the U-Net architecture. The dataset of entire lung images is divided into a small training set (3 samples) and a test set (2 samples), ensuring evaluation on unseen data. Within the training set, a support set is formed by selecting the most representative and complex samples, enabling the model to learn key patterns efficiently. A separate query set is used to evaluate the model's ability to generalize unseen examples during training. Training

is performed using an episodic strategy, where the model is first optimized on the support set and then evaluated on the query set.

3. Results and discussion

To assess the generalization ability of a U-Net model trained on images of sections of the lung, we directly applied it to the task of the entire lung segmentation without any additional fine-tuning. The pretrained model was originally optimized to segment only specific tissue regions, meaning it has not explicitly learned the full structure of the lung. By testing it on entire lung images, we aim to determine whether the learned features from segmentation of sections of the lung are sufficient for accurate segmentation of the entire lung or if additional fine-tuning is necessary. In **Error! Reference source not found.**, one test image is presented, illustrating the segmentation output of the model.

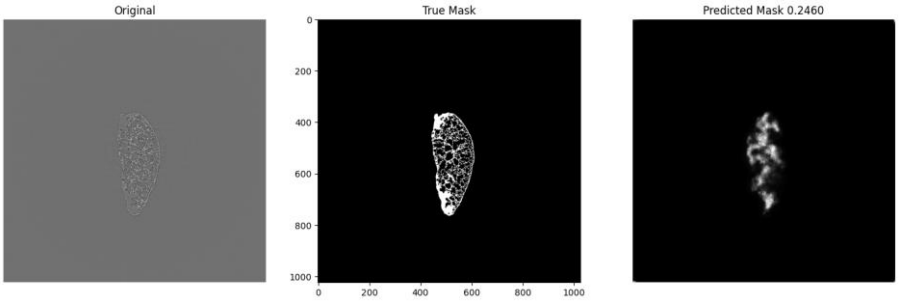


Figure 2. An example of segmentation output with calculated Dice coefficient (U-net model without fine-tuning).

In order to evaluate the few-shot approach, we experimented with different numbers of training samples in the support set. As the initial model, we used a U-Net that was already trained on images of lung sections, and then we fine-tuned this model on the entire lung images using the few-shot method. The results of the few-shot learning experiments demonstrate an improvement in segmentation accuracy as the number of samples in the support set increases. In the 1-shot scenario, where only one image was used in the support set, the mean Dice coefficient was 0.76. With three images (3-shot), accuracy improved to 0.86. An example of the 3-shot segmentation is given in Figure 3.

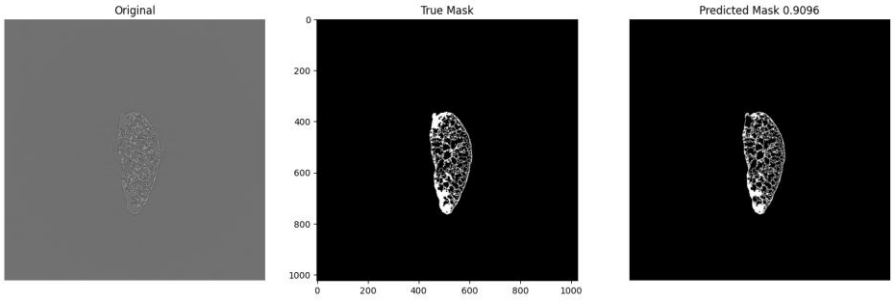


Figure 3. An example of segmentation output with calculated Dice coefficient (few shot approach).

Additionally, we compared our proposed segmentation methodology with the available approaches in literature. Fully supervised approaches, particularly U-Net and FCN, achieve strong results on lung section images, with the Dice scores up to 0.89 when data augmentation is applied [2, 6]. In contrast, traditional thresholding methods, such as Otsu, show significantly lower performance (Dice = 0.71) [6]. The proposed study extended its methodology to the entire lung segmentation using a few-shot approach with only 3 training samples. It maintains high performance (Dice coefficient = 0.86) demonstrating its effectiveness in data-limited scenarios and superiority of deep learning approaches.

5. Conclusions

This paper presents a workflow for automatic segmentation of mouse lungs in SRXTM. The proposed approach first trains a U-Net model on lung section images and then adapts it to entire lung segmentation using a few-shot learning strategy. The pretrained model is fine-tuned on a small number of entire lung images (3-shot) and evaluated using standard segmentation metrics. When applied to whole-lung segmentation using the few-shot approach, the model achieves competitive results (Dice coefficient = 0.86), demonstrating effective adaptation from a pre-trained representation to a more complex segmentation task. Overall, the results confirm that the proposed few-shot strategy is effective for segmentation in data-limited settings, enabling high performance even with only a small number of annotated whole-lung images.

Acknowledgements
This research was supported by the Ministry of Science, Technological Development and Innovation of the Republic of Serbia, contract numbers [451-03-33/2026-03/200107 (Faculty of Engineering, University of Kragujevac)].

References

[1] Zhang W, Li R, Deng H, Wang L, Lin W, Ji S, Shen D. Deep convolutional neural networks for multi-modality isointense infant brain image segmentation. NeuroImage. 2015;108:214-224.

[2] Arsic B, Saveljic I, Henry F, Filipovic N, Tsuda A. Application of Machine Learning for Segmentation of the Pulmonary Acinus Imaged by Synchrotron X-Ray Tomography. Journal of aerosol medicine and pulmonary drug delivery. 2023;36:27-33.

[3] Xiao L, Sera T, Koshiyama K, Wada S. Morphological characterization of acinar cluster in mouse lung using a multiscale-based segmentation algorithm on synchrotron micro-CT images. The Anatomical Record. 2016;299:1424-1434.

[4] Ronneberger O, Fischer P, Brox T. U-net: Convolutional networks for biomedical image segmentation. International Conference on Medical image computing and computer-assisted intervention. 2015.

[5] Zhou Z, Rahman Siddiquee M, Tajbakhsh N, Liang J. Unet++: A nested u-net architecture for medical image segmentation. Deep learning in medical image analysis and multimodal learning for clinical decision support: 4th international workshop, DLMIA 2018, and 8th international workshop, ML-CDS 2018. 2018.

[6] Arsic B, Obrenovic M, Anic M, Tsuda A, Filipovic N. Image segmentation of the pulmonary acinus imaged by synchrotron X-ray tomography. 2019 IEEE 19th International Conference on Bioinformatics and Bioengineering (BIBE). 2019.

[7] Parnami A, Lee M. Learning from few examples: A summary of approaches to few-shot learning. arXiv preprint arXiv:2203.04291 2022.

Development of a YOLOv11-Based Desktop Application for Concrete Crack Detection

Jovana Nikolic[1], Velibor Isailovic[1]

[1]*Faculty of Engineering, University of Kragujevac, Kragujevac, Serbia, joxikg@gmail.com, 0009-0003-1464-5977, velibor@kg.ac.rs, 0000-0002-1417-9633*

Corresponding author: joxikg@gmail.com

Abstract

The detection of cracks in concrete structures is a critical task in civil engineering, as it directly impacts structural safety and maintenance planning. Traditional inspection methods are time-consuming, subjective, and often inefficient for large-scale infrastructure. This paper presents the development of a desktop application for automated crack detection using the YOLOv11 deep learning model. The objective is to demonstrate how modern computer vision techniques can improve the accuracy and efficiency of structural inspections. The model was trained on the CrackSeg dataset, which contains annotated images of cracks under various real-world conditions. Training was performed using optimized parameters on a GPU environment to ensure efficient learning. The results show strong performance, with a mean Average Precision (mAP@0.5) of 0.765 and an F1-score of 0.75, indicating a good balance between precision and recall. The developed application enables users to upload images, perform detection, and save results through an intuitive interface. The proposed approach significantly enhances reliability, reduces manual effort, and demonstrates strong potential for real-world applications in infrastructure monitoring and maintenance.

Keywords: crack detection; structural health monitoring; deep learning; YOLOv11; computer vision; concrete structures; image segmentation; infrastructure inspection; UN SDG 9; UN SDG 11

1. Introduction

The rapid development of artificial intelligence and computer vision has significantly influenced modern engineering practices, particularly in the field of structural inspection. In civil engineering, the detection of damage in infrastructure systems represents a critical task, as it directly impacts safety, maintenance planning, and operational costs. Among various types of structural defects, cracks in concrete structures are one of the most common indicators of degradation and potential failure. Early detection and accurate assessment of such defects are essential for preventing serious structural issues and ensuring long-term durability. Traditional inspection methods rely primarily on manual visual assessment, which is time-consuming, subjective, and often inconsistent. These limitations become more pronounced when dealing with large-scale infrastructure or inaccessible areas. As a result, there is a growing need for automated, reliable, and scalable solutions. Early approaches to crack detection were based on classical image processing techniques such as edge detection and filtering methods [1],[2]. While effective in controlled conditions, these methods showed limited robustness in

real-world scenarios. Later developments introduced handcrafted features combined with machine learning algorithms [3], which improved performance but still required significant manual effort and domain expertise. In recent years, deep learning models, particularly convolutional neural networks (CNNs), have achieved substantial improvements by enabling automatic feature extraction and better generalization [4],[5]. Modern object detection models such as YOLO have further enhanced real-time detection capabilities with high accuracy [6]. In this context, this paper proposes the development of a desktop application for automated crack detection using the YOLOv11 model. The novelty of the proposed approach lies in the integration of a state-of-the-art deep learning model with a user-friendly software solution designed for practical engineering use. The main objective is to demonstrate how advanced computer vision techniques can be effectively applied to improve the efficiency, accuracy, and reliability of structural inspection processes.

2. Materials and Methods

2.1 Dataset

The CrackSeg dataset was used for training and evaluation of the proposed model [7]. This dataset contains 4029 images of cracks on various infrastructure surfaces, including concrete, asphalt, and bridges. The images are captured under diverse real-world conditions, such as varying lighting, shadows, and surface textures, which contributes to the robustness of the trained model. The dataset is divided into three subsets: 3717 images for training, 200 for validation, and 117 for testing. All images are provided in .jpg format with varying resolutions (approximately 680×480 pixels on average). Annotations are provided in YOLO segmentation format, where each image is associated with a corresponding .txt file. Each annotation contains a single class (crack) and polygon coordinates that define the precise contour of the crack. These coordinates are normalized relative to the image dimensions, allowing consistent processing across different resolutions.

2.2 Model Architecture

The proposed approach is based on the YOLOv11 model, a modern single-stage object detection architecture designed for real-time performance and high accuracy [6],[8]. The model consists of three main components: backbone, neck, and head. The backbone is responsible for feature extraction and utilizes convolutional layers combined with C3K2 blocks, which improve efficiency while maintaining strong feature representation. The neck incorporates the SPPF (Spatial Pyramid Pooling Fast) module, which aggregates multi-scale features and enhances detection of objects of different sizes. Additionally, the architecture includes attention mechanisms such as the C2PSA block, which enables the model to focus on spatially relevant regions of the image. This is particularly important for detecting small or low-contrast cracks. The detection head performs multi-scale predictions using feature maps at different resolutions, allowing accurate localization of cracks regardless of their size.

2.3 Training Procedure

The model was trained using the Ultralytics YOLO framework in a GPU-enabled environment [8]. Training was performed with an image size of 640 × 640 pixels, a batch size of 16, and for a total of 50 epochs. Stochastic Gradient Descent (SGD) was used as the optimization algorithm, while data augmentation techniques were

enabled to improve generalization and model robustness. The training process was executed on a Tesla T4 GPU within a cloud-based platform, ensuring efficient computation. On average, each epoch required approximately 2-3 minutes of training time.

2.4 Experimental Setup and Application Implementation

A desktop application was developed to demonstrate the practical application of the trained model. It was implemented in Python using *tkinter* and *ttkbootstrap* for the GUI, *Pillow* for image processing, *Ultralytics YOLO* for inference, and *threading* to ensure responsive performance. The application enables users to upload images, perform crack detection, and save the results. To maintain usability, the detection process runs in a separate thread, preventing the interface from freezing. Input images are validated, resized while preserving aspect ratio, and limited to standard formats (.jpg, .jpeg, .png). The processed output is displayed to the user and can be saved locally.

2.5 Evaluation Metrics

The performance of the model was evaluated using standard object detection metrics, including precision, recall, F1-score, and mean Average Precision (mAP). Precision measures the proportion of correctly predicted crack instances among all detections, while recall evaluates the model's ability to identify all actual cracks present in the dataset. The F1-score represents the harmonic mean of precision and recall, providing a balanced evaluation of overall performance. In addition, mAP@0.5 measures the average detection accuracy at an Intersection over Union (IoU) threshold of 0.5. These metrics together provide a comprehensive assessment of the model's effectiveness and enable comparison with other object detection approaches [9].

3. Results

The performance of the trained YOLOv11 model was evaluated on the test dataset using standard object detection metrics. The obtained results demonstrate strong performance in crack detection tasks in terms of both accuracy and reliability. A mean Average Precision (mAP@0.5) of 0.765 was achieved, indicating robust detection performance at a moderate Intersection over Union (IoU) threshold. In addition, the model reached a maximum precision of 1.00 at a high confidence threshold (0.940), demonstrating highly accurate predictions under strict confidence settings. The F1-score peaked at 0.75 at a confidence threshold of 0.433, reflecting a good balance between precision and recall. This indicates that the model effectively detects the majority of cracks while maintaining a relatively low false positive rate (Table 1). Furthermore, visual inspection comparing predicted crack regions with ground truth annotations shows strong agreement, confirming that the model generalizes well to unseen data.

Table 1. Performance metrics of the YOLOv11 model on the test dataset

Metric	Value	Confidence Threshold
mAP@0.5	0.765	-
Precision (max)	1.00	0.940

F1-score (max)	0.75	0.433

Figure 1 presents qualitative results of the proposed model on test images. The detected crack regions are marked with bounding boxes and corresponding confidence scores, demonstrating the model's ability to accurately localize cracks under varying surface conditions. The results confirm that the model performs reliably even in cases with complex textures and low contrast.

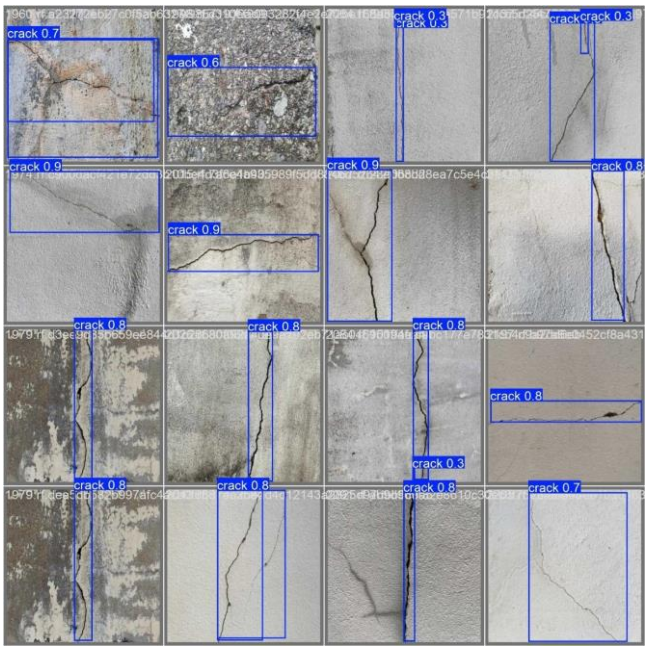


Figure 1. Examples of crack detection results using the YOLOv11 model, showing predicted bounding boxes and confidence scores across different surface conditions.

4. Discussion

The results indicate that the YOLOv11-based approach provides a reliable and efficient solution for automated crack detection. Compared to traditional image processing techniques, the proposed method demonstrates significantly improved robustness and accuracy, particularly in complex real-world conditions such as varying lighting and heterogeneous surface textures.

The achieved mAP@0.5 score of 0.765 is consistent with, or comparable to, previously reported results for YOLO-based crack detection systems [10], further confirming the effectiveness of the proposed approach. In addition, the integration of attention mechanisms and multi-scale prediction contributes to improved detection performance for small and low-contrast cracks.

However, several limitations should be acknowledged. The dataset used in this study contains only a single class (cracks), which limits the ability of the model to generalize to more complex structural damage scenarios.

Furthermore, the performance of the model may depend on image quality, resolution, and environmental conditions such as shadows or noise. Despite these limitations, the developed desktop application enhances the practical usability of the system by providing an intuitive interface and real-time processing capabilities. This makes the solution suitable for real-world applications in infrastructure inspection and maintenance.

5. Conclusions

This paper presented the development of a desktop application for automated crack detection using the YOLOv11 deep learning model. The experimental results demonstrate that the proposed approach achieves high accuracy and reliable performance, with evaluation metrics such as mAP@0.5 of 0.765 and an F1-score of 0.75. The integration of advanced computer vision techniques with a user-friendly interface enables efficient and accessible structural inspection. The proposed system reduces the need for manual inspection, improves consistency, and supports faster decision-making in engineering practice. Future work may focus on extending the model to support multi-class damage detection, improving robustness under challenging environmental conditions, and integrating the system into real-time monitoring platforms or cloud-based solutions.

References

1. Yamaguchi T, Hashimoto S. Fast crack detection method for large-size concrete surface images using percolation-based image processing. Machine Vision and Applications. 2010;21(5):797–809.
2. Abdel-Qader I, Pashaie-Rad S, Abudayyeh O, Yehia S. Automated identification of concrete cracks in digital images. NDT & E International. 2003;36(4):255–260.
3. Dorafshan S, Maguire M, Coopmans C. Comparing automated image-based crack detection techniques in concrete structures. Automation in Construction. 2018;94:92–105.
4. Feng C, Zhu X, Soibelman L. Detection of cracks in concrete structures using deep convolutional neural networks. ISARC. 2017:279–286.
5. Li S, Zhao X, Zhou G. Automatic crack detection and measurement based on convolutional neural network. Measurement. 2019;148:106816.
6. Yeum CM, Dyke SJ. Vision-based automated crack detection for bridge inspection. Computer-Aided Civil and Infrastructure Engineering. 2015;30(10):759–770.
7. Ultralytics. CrackSeg dataset for crack segmentation. 2023.
8. Ultralytics. YOLOv11 framework. 2024.
9. Sokolova M, Lapalme G. A systematic analysis of performance measures. Information Processing & Management. 2009;45(4):427–437.
10. Wu Y, Crack detection using deep learning methods. Automation in Construction. 2021;130:103844.

An affordable webcam-based real-time hand gesture recognition system using simple multilayer perceptron deep learning models

Ana Jovanović and Vladimir Milovanović

Department of Electrical Engineering and Computer Sciences, Faculty of Engineering, University of Kragujevac, Kragujevac, Serbia, e-mails: jovanovic.ana9898@gmail.com *and* vlada@kg.ac.rs

Corresponding author e-mail: vlada@kg.ac.rs and ORCID: 0000-0002-6787-4058

Abstract

A presented hand gesture recognition problem is solved using MediaPipe framework followed by multilayer perceptron fully-connected feedforward artificial neural network. Design like this facilitates training of the artificial neural network and does not require excessive amounts of training data, but only one human subject instead. Hand gesture recognition system that exploits web camera videos and employs deep learning models was implemented in Python programming language, MediaPipe and Keras libraries were used. Test results, i.e. the accuracy on the testing data obtained from a person whose hands were also used to train the neural network is 99.4%, whereas the accuracy on the testing data of another person whose hands were not used to train the neural network is 88.02%. System like this could be the basis for designing a more complex system for recognizing sign language and automatic translation of sign language into text or speech understandable to most people. This system as a foundation and mentioned possible extended version could contribute to UN SDG 10.

Keywords: hand gesture recognition; deep learning model; MediaPipe framework; web camera calibration; 'UN SDG 10'

1. Introduction

System for recognizing hand gestures has applications in the field called Human-computer interaction (HCI). Ability to recognize hand gestures can enhance experience of users from different technological domains. Hand detection, segmentation and gesture recognition enable intuitive, secure and effective interaction between people and robots in the controlled conditions, as well as in real time. This belongs to a multidisciplinary study called Human-robot interaction (HRI). Main areas of application are industrial and collaborative robotics, robotics in healthcare, social robotics, aerial and space robotics. System for recognizing hand gestures can be a base needed for understanding sign language and a base required to control devices using gestures [1].

2. Implementation of the system for recognizing hand gestures

The system for recognizing hand and hand gestures on web camera videos was implemented in Python programming language using MediaPipe and Keras libraries. System is able to recognize eight gestures including open palm, like, victory, rock and roll, ok, closed fist, pointer and dislike. Components of the system

are shown in Figure 1 and the first component is MediaPipe framework responsible for recognizing twenty-one hand landmarks. Second component is fully-connected feedforward neural network that uses hand landmark coordinates from the first component as input data and based on that coordinates neural network classifies gestures.

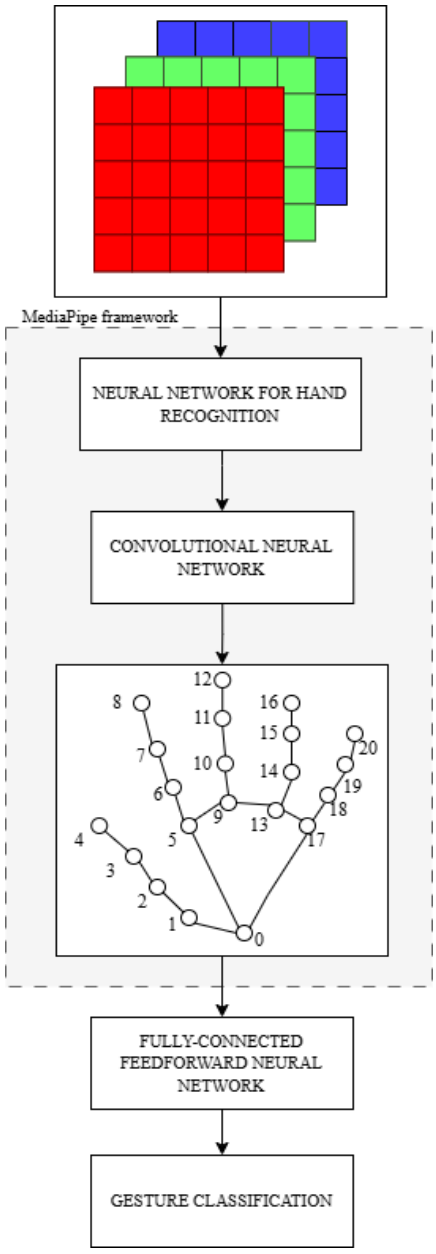


Figure 1.A two-component system for recognizing hand gestures on webcam videos.

System has two working modes. The first working mode is used for creating dataset for the system's fully-connected feedforward neural network (multilayer perceptron network) while the second working mode is used

to run the whole system in the form for end users. Implementation is partially inspired by the algorithm described in the README file of the open-source GitHub repository kinivi/hand-gesture-recognition-mediapipe.

2.1. Data preprocessing

Data preprocessing involves projecting the coordinates of each hand landmark from three-dimensional to two-dimensional space, followed by normalization of the obtained 2D coordinates. In order to project coordinates from three-dimensional to two-dimensional space calibration of the camera, used in the system for recognizing hand gestures, should be performed. Camera calibration involves determining the camera matrix, distortion coefficients, rotation and translation vectors, etc. Camera matrix consists of intrinsic (focal length and optical centers) and extrinsic parameters of the camera (rotation and translation vectors). To find mentioned parameters, images of the objects with well-defined patterns should be used, namely, images of the objects with geometry whose characteristic points can be exactly detected on the image. During the design of this system a standard eight-by-eight squares chessboard images were used. One of those images is shown in Figure 2.

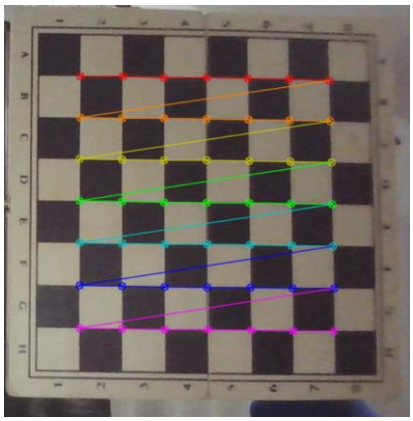


Figure 2. A chessboard used for web camera calibration.

2.2. Dataset

Dataset of the system for recognizing hand gestures is created using CSV file. File has forty-three columns. First column has labels of eight classes, i.e. eight gestures in the range from zero to seven. Other forty-two columns have normalized x and y coordinates of hand landmarks whose values are in the range from zero to one. Every row defines one sample, that is one gesture. In total, dataset has eight hundred and thirty-two samples which is a rather small amount for typical computer vision applications, but still sufficient for this application.

2.3. Gesture classification

Fully-connected feedforward neural network for gesture classification has four layers, three hidden layers and one output layer. First hidden layer has twenty neurons, second hidden layer has also twenty neurons and third hidden layer has ten neurons. The output layer has eight neurons and represents the softmax output function.

3. System testing and results

Graphs on Figure 3 show model accuracy (left inset) and loss (right inset) versus the number of training epochs. Blue and orange curves on the graph represent training and test set data, respectively.

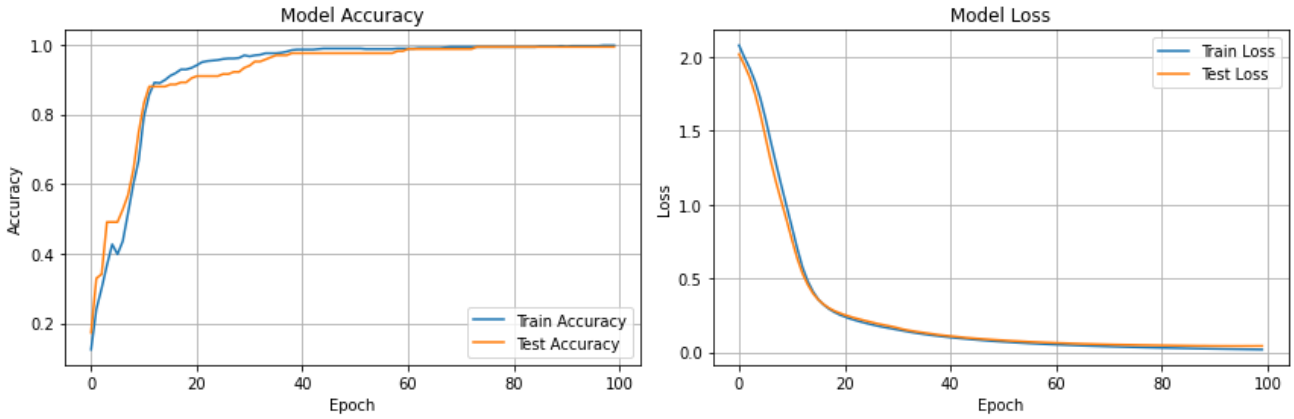


Figure 3. Model accuracy and loss on the training dataset and on the testing dataset.

Model accuracy evaluation, i.e., system for recognizing hand gestures accuracy evaluation is shown in Table 1.

Table 1. Neural network evaluation result on the training data and on the testing data.

Train accuracy	Test accuracy
99.85%	99.4%

Testing dataset on which the model achieved test accuracy 99.4% is created using hand landmarks coordinates from the person whose hands were used for model training. That testing dataset is obtained by dividing total dataset on the training dataset and on the testing dataset.

Total dataset had eight hundred and thirty-two samples. It was split so that training data was obtained using 80% of total dataset and test data was obtained using 20% of total dataset.

Another testing dataset used for evaluation of the model is obtained using hand landmarks coordinates from another person whose hands were not used for model training. Neural network model achieved test accuracy 88.02% on this second dataset.

4. Discussion

Apart from system testing using test dataset obtained by dividing total dataset on training dataset and testing dataset, samples from another person were also gathered based on which second testing dataset was created. System for recognizing hand gestures accuracy obtained using mentioned second dataset dropped to 88.02%.

Total dataset of fully-connected neural network for gesture classification has hand landmarks 2D coordinates of only one person. Number of samples per gesture was not huge. For every gesture formed with right hand

fifty-two samples were taken and for every gesture formed with left hand fifty-two samples were also taken. The number of samples mentioned can have an impact on the system's resilience on variations and changes, namely, how system works when user forms gesture slightly different and under different camera angles. During testing in real time it was noticed that the system sometimes mixes one out of eight gestures, for example instead of closed fist formed with left hand system recognizes rock and roll sign while for the same gesture formed with right hand system does not make that mistake. Mentioned accuracy 99.4% obtained on the static data shows that mistakes like this are expected in real time.

5. Conclusions

In this paper, system for recognizing eight hand gestures was implemented and accuracy achieved was 99.4% for the person whose hands were used for neural network training. The projection of the hand landmarks 3D coordinates to 2D coordinates was successfully performed using parameters obtained as a result of camera calibration. Obtained camera calibration parameters are specific for every camera and unique explicitly to the web camera used for implementation of this system. System for recognizing hand gestures could be improved by adding data gathered from more people, i.e., by adding hand landmarks coordinates from hands of different sizes, ages and genders in the dataset used for fully-connected feedforward neural network training. Recommendation for system improvement is usage of IPN HandS tool and dataset [2] proposed by researchers Gibran Benitez-Garcia et al. (2025). IPN HandS is improved version of IPN Hand dataset [3] which includes approximately seven hundred thousand samples of hand skeletons where twenty one hand landmark is defined for every sample. System proposed in this paper could be upgraded so that besides static gestures system can recognize movements. In that way system would be able to understand sign language which depends from movements. Social benefit of such a system is reflected in a fact that it would solve communication barriers between deaf and hard of hearing people and most people who do not understand sign language. System should be able to recognize sign language and to automatically translate it into text or speech. It could be designed as a mobile application on smartphones, so that deaf and hard of hearing people could use it anywhere and anytime.

Acknowledgements

Research partially funded by the grant agreement number: 451-03-34/2026-03/200107 from February 5, 2026.

References

[1] Jalayer R, Jalayer M, Orsenigo C, Tomizuka M. A review on deep learning for vision-based hand detection, hand segmentation and hand gesture recognition in human–robot interaction. Robotics and Computer-Integrated Manufacturing. 2026; vol. 97:103110, https://doi.org/10.1016/j.rcim.2025.103110

[2] Benitez-Garcia G, Olivares-Mercado J, Sanchez-Perez G, Takahashi H. IPN HandS: Efficient Annotation Tool and Dataset for Skeleton-Based Hand Gesture Recognition. Applied Sciences. 2025;15:6321.

[3] Benitez-Garcia G, Olivares-Mercado J, Sanchez-Perez G, Yanai K. IPN Hand: A Video Dataset and Benchmark for Real-Time Continuous Hand Gesture Recognition. 2020 25th International Conference on Pattern Recognition (ICPR), 2021, p. 4340–7.

Di<Au>logues: Gesture-Based Navigation in Archaeological Museum of Thessaloniki. A Case Study using MediaPipe and p5.js.

Nikolaos Konstantinou[1], Nikolaos Papadimitriou[1], Michail Semoglou[2], Dimitrios Traperas[1]

[1] School of Fine Arts, University of Ioannina, Greece, nkonstantinou@uoi.gr, n.papadim@uoi.gr, traperas@uoi.gr

[2] College of Design and Innovation, Tongji University, China, m.semoglou@tongji.edu.cn

Corresponding author: nkonstantinou@uoi.gr

Abstract

Touchless interfaces in cultural heritage sites appear to be significant both for practical reasons—such as the need for contactless interaction in the post-pandemic era—and for increasing visitor engagement. This article provides an overview of the technical implementation of a gesture-based navigation system designed for low-light museum environments (10–15 Lux). In this research, Google's MediaPipe framework was used as a p5.js rendering library for hand skeleton tracking, thus the system was designed to provide a robust method of interaction with digital artworks without the mediation of peripheral devices. This article presents the "Hybrid Tracking" methodology, which uses the center of the palm (Landmark 9) for stabilized motion and, simultaneously, the tip of the index finger (Landmark 8) for precise selection. Furthermore, the use of linear interpolation (Lerp) to mitigate high-ISO sensor noise and the use of visual progress arcs to solve the "Midas Touch" problem are analyzed. The results demonstrate high detection accuracy, allowing viewers to interact with the works to a satisfactory degree; however, in low-light conditions with light sources in the background, a certain degree of instability sometimes occurs.

Keywords: Generative Art, Natural User Interfaces, *MediaPipe, p5.js*

1. Introduction

The contemporary museum landscape is increasingly defined by the "experience economy," where passive observation is replaced by dynamic, narrated interactions. However, the physical constraints of museum halls—particularly low-light conditions required to preserve artifacts and create atmosphere—often compromise the reliability of standard computer vision systems. Since the COVID-19 pandemic, there has been a significant shift toward touchless Natural User Interfaces (NUIs) to maintain hygiene while fostering visitor agency [1]. Gesture-based interaction has been shown to improve learning outcomes and emotional engagement, but it requires a careful balance between tracking stability and interaction latency. This case study explores how web-native tools like p5.js and MediaPipe can be optimized to deliver seamless navigation without specialized, high-cost depth sensors.

2. Related Work

Public interactive displays require "walk-up-and-use" simplicity. The barrier to entry for gesture-based systems is often the complexity of the gesture set. Systems that require extensive training or specific hand orientations fail in museum settings where the user demographic is highly diverse [2].

Google's MediaPipe has revolutionized real-time hand tracking by utilizing a machine learning (ML) pipeline that predicts 21 3D hand landmarks from a single frame [3]. While highly efficient, its accuracy is significantly contingent on light intensity.[4] emphasize that MediaPipe's graph-based architecture allows for low-latency processing, but sensor noise in dark environments can lead to "landmark flipping" or jitter.

Furthermore, previous work presented in "Algorithmic Interpretations of Epirotic Silverwork" explores how generative art and computational methods can reinterpret traditional Greek silversmithing. Through a collaborative project involving fourteen artists, cultural motifs were translated into interactive digital artworks using tools such as Processing and p5.js. Emphasizing embodied interaction—via hand tracking, face detection, and audio responsiveness—the project transformed viewers into active participants. Rather than merely digitizing heritage, it proposed a model where algorithmic thinking extends traditional craftsmanship, fostering new forms of cultural expression and engagement within both physical and digitally augmented exhibition spaces [5]

3. Methodology

The core objective was the design of a peripheral-free infrastructure that effectively encapsulates and manages three distinct p5.js artworks within a unified display area. The system ensures seamless transitions and synchronous gesture tracking across diverse interactive modules, while addressing the computational overhead and GPU resource contention inherent in high-fidelity browser-based rendering. The design process for the Di<Au>logues system presented various integration challenges, such as *Noise Reduction and Low-Light Stability, Linear Interpolation (Lerp), Lux Degradation Mitigation, User Experience: Dwell-Based Selection and, Visual Progress Arcs.*

4. Implementation

The "Di<Au>logues" system in Archeological Museum of Thessaloniki utilizes a decentralized micro-frontend architecture governed by a central p5.js controller. This parent application manages the primary interaction loop (See-Think-Act) by capturing a standard 720p/1080p webcam feed and processing it via the MediaPipe Hands machine learning pipeline [6]. To ensure that heavy 3D rendering or complex generative patterns do not degrade hand-tracking performance, individual exhibition modules (e.g., "All that Shines", " Gold Adorns Bronze," "Golden Relations") are hosted within isolated HTML iframes [7]. Communication between the parent controller and these children is facilitated by the window.postMessage API, which allows for secure cross-origin data exchange. The controller broadcasts a normalized coordinate packet consisting of smoothed X, Y, and Z positions, enabling the modules to respond to user gestures without direct access to the camera hardware. For continuous operation, the system is deployed using Google Chrome in Kiosk Mode. Launch scripts include specific flags such as *--autoplay-policy=no-user-gesture-required and --kiosk* to ensure the interface occupies the full screen and starts interactive media automatically.

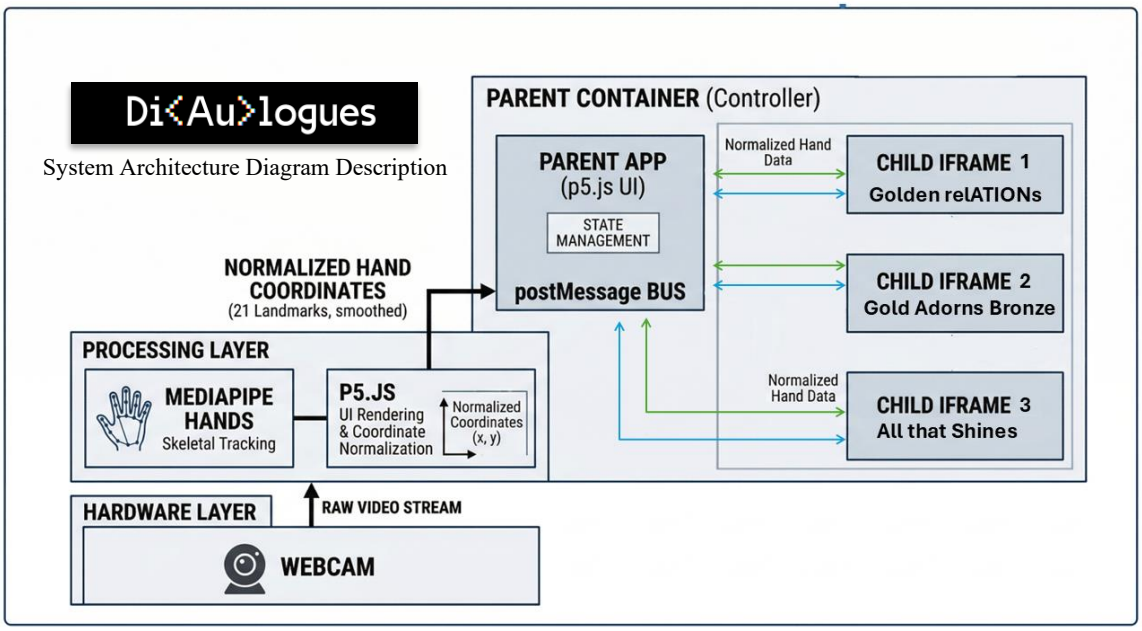


Figure 1: The hardware layer (Webcam) feeds into the processing layer (MediaPipe/p5.js). The parent container encapsulates child iframes, with a bidirectional postMessage bus distributing normalized hand coordinates and receiving module state updates. Image by the authors.



CHILD IFRAME 1 Golden relATIONs



CHILD IFRAME 2 Gold Adorns Bronze



CHILD IFRAME 3 All that Shines

Figure 2: The three distinct p5.js artworks within a unified display. Image by the authors.

5. Discussion

Empirical testing conducted by Apopei [8] during the 'Long Night of Museums' with 550 participants confirmed high levels of user engagement for similar gesture-based systems. Qualitative observations in our case study, revealed that most visitors mastered the navigation metaphors within 10–15 seconds, masterfully moving between projects like "Gold Adorns Bronze", "Golden Relations" and “All that Shines” without verbal instruction.

Reliability logs indicated high success rate in well-lit areas, with a manageable decline in the dimmest halls. The primary failure mode was "background clutter" rather than light intensity, as other visitors walking behind the active user occasionally confused the MediaPipe palm detector. To counteract the perceived latency in GPU-intensive modules, the tracking anchor was strategically shifted to the palm center (Landmark 9). This provides

a more stable data point than fingertips, ensuring that even during minor frame drops, the cursor maintains a predictable trajectory

6. Conclusions

The synergy between MediaPipe's robust skeletal tracking and p5.js's flexible visualization creates a powerful framework for touchless museum navigation. By prioritizing anatomical stability (Landmark 9) and implementing temporal smoothing (Lerp), developers can overcome the inherent limitations of high-noise, low-light environments. As digital heritage continues to move toward experience-centered curation, these scalable, hardware-independent solutions will be vital in creating accessible, hygienic and interactive landscapes.

Acknowledgements

This system was developed as part of a temporary exhibition (30.3.2026 - 30.6.2026), in collaboration with the Archaeological Museum of Thessaloniki (AMTH), drawing inspiration from its permanent collections. The authors would like to thank the Archaeological Museum of Thessaloniki for their hospitality and support during the implementation of the Di<Au>logues project. Media coverage and documentation: https://bit.ly/4szNJCB (www.ertnews.gr), https://www.youtube.com/watch?v=XDbjUlJL_RE

References

1. Baron, A. M., & Gul, L. F. (2025) Gesture-Driven Storytelling: Designing interactive experiences for cultural heritage interpretation in blended spaces. Conference: eCAADe 2025 https://doi.org/10.52842/conf.ecaade.2025.2.541

2. O'Hagan, R. G., Zelinsky, A., & Rougeaux, S. (2002). Visual gesture interfaces for virtual environments. Interacting with computers, 14(3), 231-250. https://doi.org/10.1016/S0953-5438(01)00050-9

3. Zhang, F., Bazarevsky, V., Vakunov, A., Tkachenka, A., Sung, G., Chang, C. L., & Grundmann, M. (2020). Mediapipe hands: On-device real-time hand tracking. arXiv preprint arXiv:2006.10214. https://arxiv.org/pdf/2006.10214

4. Lugaresi, C., Tang, J., Nash, H., McClanahan, C., Uboweja, E., Hays, M., ... & Grundmann, M. (2019). Mediapipe: A framework for building perception pipelines. arXiv preprint arXiv:1906.08172. https://doi.org/10.48550/arXiv.1906.08172

5. Semoglou, M, Konstantinou, N., Papadimitriou, N., (2025). Algorithmic Interpretations of Epirote Silverwork: Digital Evolution of Cultural Heritage. APARN 2025 Conference Schedule. ISBN 978-616-7901-71-8 https://doi.org/10.62788/APARN2025-paper55

6. Google. (2025). On-device, real-time hand tracking with MediaPipe. Google AI Blog. https://ai.googleblog.com/hand-tracking

7. Maliki, H. (2024). Seamless communication between parent and iframe using postMessage(). Medium. https://medium.com/@hanifmaliki/postmessage-201becfe6a75

8. Apopei, A. I. (2025). Accessible Interface for Museum Geological Exhibitions: PETRA—A Gesture-Controlled Experience of Three-Dimensional Rocks and Minerals. Minerals, 15(8), 775.

Graph and Recurrent Neural Networks for MRI-Based Parkinson's Disease Analysis: A Short Review and Confidence-Driven Pruning Framework

Vasileios Stergiou[1], Angelos Giotis[1], Michail Vrigkas[2], Loukas Astakas[3], Spyridon Konitsiotis [3], Christophoros Nikou[1]

[1]*University of Ioannina, Department of Computer Science & Engineering, Greece {v.stergiou@uoi.gr*, 0009-0009-7031-3559,*a.giotis@uoi.gr*, 0000-0001-7986-2460,*cnikou@uoi.gr, 0000-0003-1388-6915}*

[2]*University of Western Macedonia, Department of Communication and Digital Media, Greece, {mvrigkas@uowm.gr*, 0000-0001-5888-6949*}*

[3]*University of Ioannina, School of Medicine, Greece, {astrakas@uoi.gr, 0000-0002-4890-4805,skonitso@uoi.gr, 0000-0002-5217-1317}*

Corresponding author: v.stergiou@uoi.gr

Abstract

Parkinson's Disease (PD) diagnosis from MRI data remains challenging due to subtle neuroanatomical variations, inter-patient variability, and the presence of low-quality or non-informative samples. While Graph Neural Networks (GNNs) have emerged as a promising paradigm for modeling non-Euclidean brain structures, their performance is highly dependent on input data quality and consistency. In this work, we present a lightweight framework that combines a short literature overview with a confidence-driven preprocessing strategy for MRI-based PD analysis. The proposed approach operates across multiple anatomical views and filters unreliable samples prior to GNN training. Feature representations are derived from deep learning-based descriptors and transformed into a compact embedding space using unsupervised clustering with Recurrent Neural Nets. The resulting representations are used for dataset refinement and as discriminative inputs to a downstream GNN classifier, which models inter-sample relationships and enables multi-class prediction. Experimental results demonstrate that the proposed preprocessing enhances classification performance, highlighting the importance of data quality in graph-based neuroimaging pipelines.

Keywords: Parkinson's Disease; Graph Neural Networks; Neuroimaging; Deep Learning; Brain Connectomes; Multi-modal Fusion; Graph Attention Networks (GATs); Explainable AI (XAI); Medical Image Segmentation; Medical Image Classification.

1. Introduction

Parkinson's Disease (PD) is a neurodegenerative disorder characterized by dopaminergic neuron loss. While MRI is a cornerstone of diagnostic research, extracting biomarkers remains challenging due to scanner bias and data imbalance. Recent shifts in medical AI have moved from standard CNNs toward architectures that better reflect biological structures. Unlike grid-based CNNs, Graph Neural Networks (GNNs) represent the brain as a graph of nodes and edges, capturing complex, long-range dependencies. This review evaluates graph-based PD analysis, emphasizing multi-modal fusion and explainable frameworks for clinical insight.

2. Related Work

2. Methodology and Graph-Based Architectures

The selection of literature for this review focused on high-impact contributions that bridge the gap between geometric deep learning and clinical neuroimaging. Research was prioritized from prestigious venues such as CVPR, ECCV, and MICCAI to ensure technical rigor. The following subsections categorize the core GNN methodologies identified in the literature for Parkinson's Disease analysis.

2.1. Graph Convolutional Networks (GCN)

Graph Convolutional Networks represent the foundational approach for analyzing brain connectivity by generalizing convolutional operations to non-Euclidean data [3]. In PD research, GCNs are primarily utilized to analyze functional connectivity networks derived from rs-fMRI, where nodes represent brain regions and edges represent temporal correlations. These models effectively capture the global topological alterations associated with dopaminergic depletion. Furthermore, relational GCNs have been explored to model the multi-relational data inherent in patient-specific clinical metadata [5].

2.2. Graph Attention Networks (GAT)

While GCNs treat all neighboring nodes with equal importance, Graph Attention Networks (GATs) introduce an attention mechanism that allows the model to learn the relative importance of different brain regions. This is particularly relevant for PD, where certain nodes, such as the substantia nigra and basal ganglia, hold higher diagnostic weight. Recent studies have implemented geometric-weighted GATs [1] to identify functional networks specifically associated with gait impairment, providing a more granular look at motor symptom progression. Additionally, unsupervised GAT clustering has shown promise in segmenting medical images without the need for extensive manual labeling [11,12], addressing the data scarcity challenge in rare parkinsonian syndromes.

2.3. Multi-modal and Heterogeneous Graph Learning

A major advancement in the field is the shift toward omni-modal biomedical representations [2]. Unlike single-modality models, heterogeneous graph learning integrates disparate data—such as structural T1-weighted MRI, diffusion tensor imaging (DTI), and genomic profiles—into a unified structure. For instance, modality-prompted networks create comprehensive patient profiles by coupling structural and functional connectomes [6]. This integration significantly improves differential diagnosis between idiopathic PD and Parkinsonism-Plus syndromes, such as Multiple System Atrophy (MSA) [7], by leveraging adaptive fusion to capture complementary imaging biomarkers.

2.4. Explainability and Graph Pooling

To overcome the "black box" nature of deep learning, explainable graph pooling (XGNN) methods [4] highlight specific brain sub-networks driving diagnostic decisions. By employing contrastive graph pooling, researchers can visualize discriminative patterns of structural atrophy or metabolic changes [7]. These frameworks utilize

attention-guided modules to identify relevant features within the graph, ensuring outputs align with established neurological pathways [9]. Such transparency is essential for the clinical validation and ethical deployment of AI-driven systems in neurodegenerative disease management.

3. Proposed Method and Experimental Results

The proposed pipeline combines confidence-driven MRI pruning with graph-based learning, where feature representations are refined prior to graph construction to enhance data consistency. The resulting embedding space enables the GNN to operate on more discriminative graph structures, leading to improved classification performance across anatomical views.

Split	Plane	Baseline Accuracy	Baseline F1	Exp Mean Accuracy	Exp Mean F1
0	Axial	0.9931	0.9932	0.9420	0.9352
	Coronal	0.8955	0.8788	0.8827	0.8727
	Sagittal	0.8605	0.8430	0.8553	0.8249
1	Axial	0.9538	0.9310	0.9455	0.9453
	Coronal	0.9151	0.9130	0.8737	0.8627
	Sagittal	0.8623	0.8271	0.8623	0.8344
2	Axial	0.9737	0.9780	0.9554	0.9546
	Coronal	0.8913	0.8840	0.8825	0.8658
	Sagittal	0.8450	0.8273	0.8340	0.8120
3	Axial	0.9556	0.9524	0.9613	0.9579
	Coronal	0.8858	0.8280	0.8765	0.8381
	Sagittal	0.8173	0.8011	0.8595	0.8263
4	Axial	0.9383	0.9164	0.9421	0.9398
	Coronal	0.9070	0.8759	0.8827	0.8683
	Sagittal	0.7611	0.7440	0.8473	0.8144

Table 10 Preliminary Experimental Results on [1] backbone architecture with baseline and pruned versions of our MRI dataset, for K=4 pruned versions of the baseline dataset, per split.

Our results validate the GNN's efficacy in PD detection, particularly in the Axial plane, which achieved a peak mean accuracy of 0.9613. With a mean accuracy of 0.9493 across all splits, the Axial view significantly outperformed the Coronal (0.8802) and Sagittal (0.8717) planes. While not directly comparable to the 91.6% multimodal baseline in [1], our dense graph approach offers a robust framework for Axial feature extraction. The lower performance in other views suggests they require more refined feature selection. These results demonstrate that a single-view GNN effectively captures PD-related structural variations.

4. Discussion

GNNs effectively model the non-Euclidean nature of brain connectivity, facilitating the integration of GNNs effectively model the non-Euclidean structure of brain connectivity, enabling integration of heterogeneous

neuroimaging data. Our analysis indicates that the axial view yields the most discriminative *NxN* node embeddings for Parkinson's detection, highlighting the impact of anatomical perspective on graph construction. The results further suggest that input data quality and consistency play a critical role in graph-based learning performance. Despite these advantages, challenges remain regarding model generalizability across scanners and the limited interpretability of deep graph architectures. Future work should focus on explainable graph learning approaches, such as XGNN, to identify clinically meaningful substructures and improve decision-making transparency.

5. Conclusion

GNN-based approaches provide an effective framework for Parkinson's Disease analysis by capturing structural patterns in neuroimaging data. Our results highlight the importance of data quality and anatomical view selection, with the axial plane yielding the most discriminative performance. Future work should focus on multi-modal integration and explainable graph models.

6. Acknowledgements

This research was co-financed by the European Union – NextGenerationEU under the National Recovery and Resilience Plan "Greece 2.0", Action "Clusters of Research Excellence (CREs)" (Project DEVIATE, Code YP3TA-0560419

References

1. Nerrise F, et al. An explainable geometric-weighted graph attention network for identifying functional networks associated with gait impairment. MICCAI. 2023:723–733.
2. Li C, et al. Gtp-4o: Modality-prompted heterogeneous graph learning for omni-modal biomedical representation. ECCV. 2024:168–187.
3. Zhang X, et al. Analysis of Parkinson's Disease Multi-connectivity Brain Functional Networks Based on Graph Convolutional Neural Networks. SPML. 2024:202–211.
4. Xu J, et al. Contrastive graph pooling for explainable classification of brain networks. IEEE TMI. 2024;43(9):3292–3305.
5. Skaramagkas V, et al. Multi-modal deep learning diagnosis of Parkinson's disease—a systematic review. IEEE TNSRE. 2023;31:2399–2423.
6. Yang Y, et al. Multi-modal dynamic graph network: Coupling structural and functional connectome for disease diagnosis. BIBM. 2022:1343–1349.
7. Ling R, et al. Explainable graph neural network based on metabolic brain imaging for differential diagnosis of parkinsonism. Front Aging Neurosci. 2025;17:1580910.
8. Boutet A, et al. Predicting optimal deep brain stimulation parameters for Parkinson's disease using functional MRI and machine learning. Nat Commun. 2021;12(1):3043.
9. Cui H, et al. Interpretable graph neural networks for connectome-based brain disorder analysis. MICCAI. 2022:375–385.
10. Ding Y, et al. Clustering propagation for universal medical image segmentation. CVPR. 2024:3357–3369.
11. Adityaja AM, et al. UnSegMedGAT: unsupervised medical image segmentation using graph attention networks clustering. ISBI. 2025:1–4.
12. Basak H, et al. An exceedingly simple consistency regularization method for semi-supervised medical image segmentation. ISBI. 2022:1–4.

Speech, Language, and Human–AI Interaction

Real-Time Speech Analysis and Vowel Classification Using Linear Predictive Coding

Sava Todorović

School of Electrical Engineering, University of Belgrade, Belgrade, Serbia, savatodkg@gmail.com, 0009-0001-5075-5298

Corresponding author: savatodkg@gmail.com

Abstract

This paper presents a Python-based system for real-time speech analysis using live microphone input. The system visualizes (1) Linear Predictive Coding (LPC) poles in the z-plane, (2) vowel formant space (F1–F2), (3) the LPC spectral envelope, (4) an estimate of the source spectrum (harmonic comb), and (5) real-time vowel classification. The method operates on 16 kHz audio using short-time LPC analysis with robust pole-based formant selection and temporal smoothing. In addition to predefined vowel references, an interactive calibration procedure is introduced to capture user-specific vowel targets for Serbian vowels /a, e, i, o, u/. The system demonstrates how classical speech processing techniques can be combined with real-time visualization and adaptive calibration for improved vowel recognition.

Keywords: speech recognition, source-filter model, linear predictive coding, UN SDG 4

1. Introduction

The premise of human speech modeling has been a subject of numerous studies. Quatieri [1] examines the source-filter model of human speech in great detail. This paper uses this model as a foundation for analyzing and separating the source and filter components of speech in real time.

The source-filter model provides a simplified representation of the vocal system: air pressure generated by the lungs passes through the vocal cords, causing them to oscillate and produce a periodic pressure signal. The spectral representation of this signal consists of peaks at integer multiples of the fundamental frequency f_0, with amplitudes that decrease at higher frequencies.

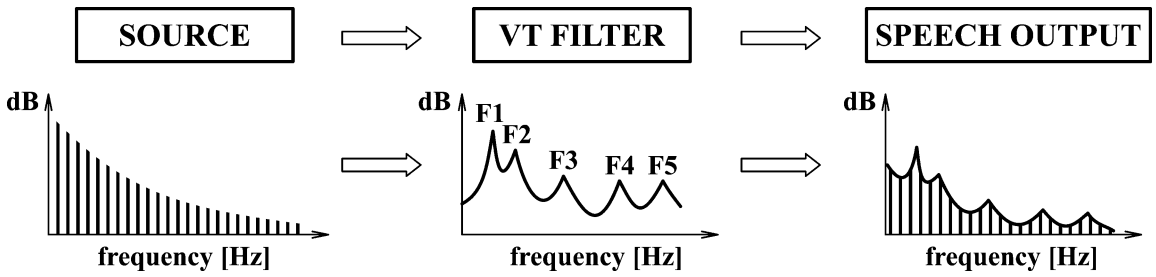


Figure 1. The source filter model, F1 to F5 represent formants.

The signal then propagates through the vocal tract and mouth before being radiated outward. This system can be modeled as a linear time-invariant filter that shapes the excitation signal. Consequently, the spectrum of the observed speech signal is the product of the excitation spectrum and the vocal tract filter response (Figure 1).

Motivated by this model, the goal of this work is to separate the source and filter components and investigate whether extracted features enable reliable differentiation between spoken vowels.

2. Materials and Methods

2.1 Signal Acquisition & Preprocessing

Speech signals were recorded in real time using a microphone via the sounddevice Python library [2]. The audio was sampled at a frequency of 16 kHz, which is sufficient to capture the relevant speech frequency range, typically below 8 kHz.

The signal was processed in short-time frames. Each frame has length of 32ms (512 samples), and every next frame starts 16ms (256 samples) after the previous, providing a 50% overlap. A circular buffer (deque) was used to store incoming samples, ensuring continuous real-time processing. Only the most recent frame was used for analysis.

Since the vocal cord signal exhibits lower energy at higher frequencies, pre-emphasis filtering is applied according to $y[n] = x[n] - \alpha x[n-1]$, where α was chosen to be 0.97 as is the standard. Naturally, windowing was applied to every frame to reduce spectral leakage, namely the Hamming window.

2.2 LPC Analysis (Filter Estimation)

The vocal tract was modeled using Linear Predictive Coding (LPC) [3]. The LPC model represents the vocal tract as an all-pole filter, meaning the transfer function has no zeroes. The filter order was set to 18, as is usual for speech analysis. The first two resonant frequencies of the vocal tract are estimated as the two poles with magnitude greater than 0.8 and the smallest angular frequencies (Figure 2.). To improve stability, an exponential moving average was used: $F_t = \alpha F_{new} + (1-\alpha)F_{t-1}$.

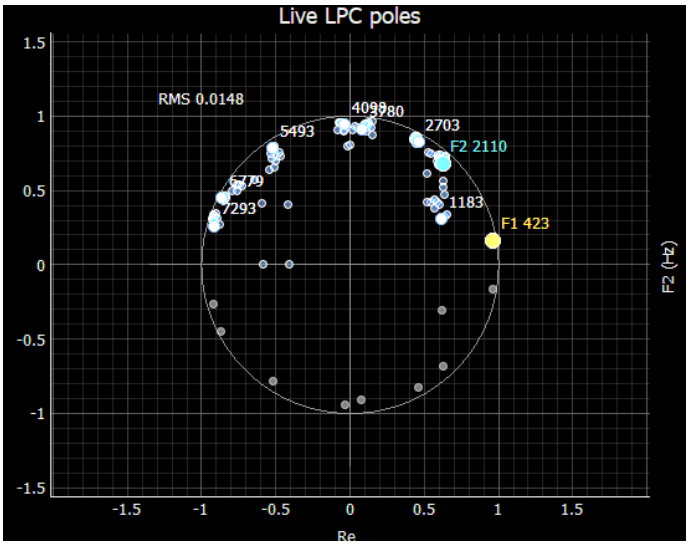


Figure 2. White dots represent the upper half-plane poles of the current frame, faint blue dots represent the upper half-plane poles of the previous frames, orange and blue dots represent the first and second formants respectively

2.3 Source Signal Estimation

To estimate the excitation i.e. the source signal, inverse filtering was applied. The spectrum of the vocal cord signal is obtained by dividing the speech spectrum by the LPC filter response. As can be seen from Figure 3, the recovered glottal signal does have strong harmonic attributes and a spectral tilt, but due to the imprecision of the LPC filtering, the spectrum is not a perfect harmonic comb.

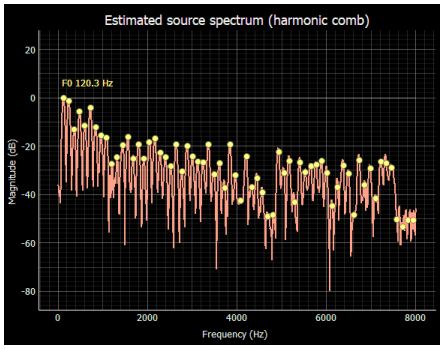


Figure 3. Recreation of the vocal cord signal with highlighted harmonics and pitch frequency F0

2.4 Vowel Classification

Directly motivated by linguistics, the current F1 and F2 formants are plotted in a plane, the "formant space" – Figure 4.a. The referent positions of the standard Serbian vowels a, e, i, o, and u are plotted. An option is provided to recalibrate the referent positions in accordance to your own speech. A simple classification criterion can be devised to estimate what vowel is currently spoken. The criterion is simply the minimum distance between the current point and all of the referent points, where distance in formant space is measured using the L_2 norm i.e. the Euclidean distance. This approach assumes isotropic variance in formant space, which may not accurately reflect perceptual vowel distances. We plot the confidence of the classification, as seen in Figure 4.b.

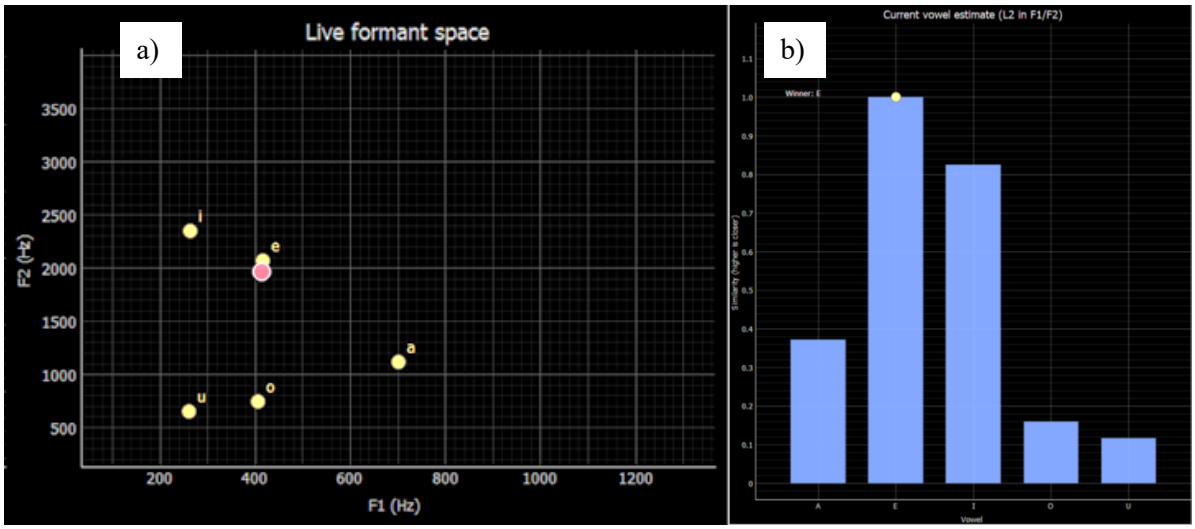


Figure 4. Formant space with a spoken vowel in red that most resembles 'e' (a) Vowel similarity scoring (b)

3. Results & Discussion

The system enables stable real-time visualization of LPC poles, spectral envelope, and formant trajectories, while the pole-based method with temporal smoothing provides reliable estimation of the first two formants (F1 and F2). Vowel classification using Euclidean distance in formant space yields satisfactory results for clearly articulated vowels and improves with user-specific calibration, although performance is affected by speaker variability, and noise. Overall, the results demonstrate that classical speech processing techniques can be effectively applied in an interactive, real-time framework.

5. Conclusions

A real-time speech analysis system based on Linear Predictive Coding was presented, capable of extracting and visualizing key speech features and performing basic vowel classification. The addition of user-specific calibration enhances adaptability and performance. Future work will focus on more advanced classification methods that utilize machine learning, and systematic evaluation on larger datasets.

6. Acknowledgements

This paper is supported by the Ministry of Science, Technological Development and Innovation, Republic of Serbia through scholarships for young researchers.

References

[1] T. F. Quatieri, Discrete-Time Speech Signal Processing: Principles and Practice. Upper Saddle River, NJ, USA: Prentice Hall, 2002.

[2] M. Geier, Sounddevice: Play and Record Sound with Python, [Online]. Available: https://python-sounddevice.readthedocs.io/, accessed Aug. 4, 2026.

[3] J. D. Markel and A. H. Gray, Linear Prediction of Speech. New York, NY, USA: Springer, 1976.

Speech Emotion Recognition with LSTM: Cross-Lingual Transfer to Serbian

Nikola Radovanovic[1], Velibor Isailovic[1]

[1]*Faculty of Engineering, University of Kragujevac, Serbia, nradovanovic@kg.ac.rs, 0009-0006-3723-6174, velibor@kg.ac.rs, 0000-0002-1417-9633*

Corresponding author: nradovanovic@kg.ac.rs

Abstract

Speech Emotion Recognition (SER) is a challenging task in affective computing aimed at inferring a speaker's emotional state from acoustic signals. This paper presents an LSTM-based SER system trained on English datasets (RAVDESS and TESS) and subsequently fine-tuned on GEES, a Serbian emotional speech corpus, to explore cross-lingual transfer learning. Mel-Frequency Cepstral Coefficients (MFCCs) are used as sequential input features, combined with RMS energy normalization to reduce inter-dataset variability. The base model achieves 88% overall accuracy on the English test set, with consistently high F1-scores across five emotion classes. After fine-tuning on the Serbian corpus, the model reaches 75% accuracy, demonstrating meaningful cross-lingual transferability despite the linguistic and phonetic differences. The results confirm that pre-training on high-quality, balanced English corpora provides a strong foundation for adapting SER systems to low-resource languages.

Keywords: speech emotion recognition; LSTM; MFCC; transfer learning; Serbian; RAVDESS; TESS; GEES; deep learning; affective computing; UN SDG 3; UN SDG 9

1. Introduction

Automatic Speech Emotion Recognition (SER) is a challenging area within audio signal processing and affective computing. The core objective is to analyze a speech signal and extract patterns indicative of the speaker's emotional state. SER systems rely on features such as pitch, energy, speech rate, and various spectral properties that vary depending on the emotion conveyed [1],[2].

Emotional expression in speech plays a critical role in human-computer interaction, with SER finding application across diverse domains including virtual assistants, driver monitoring, educational platforms, and clinical assessment [3].

SER is most modeled as a multi-class classification problem in which each speech utterance is assigned one of a predefined set of emotion categories. Key challenges include large intra- and inter-speaker variability, class imbalance in real-world datasets, phonetic and linguistic differences across languages, and cultural differences in emotional expression [4],[5]. Most of the research in this field focuses on English, using publicly available corpora such as RAVDESS [6] and TESS [7]. However, little work has been devoted to applying SER

techniques to under-represented languages such as Serbian, where the availability of emotional speech corpora and standardized benchmarks represents a significant challenge.

Prior research has shown that combinations of spectral and prosodic features, such as MFCCs, spectrograms, pitch, and energy, yield strong results in emotion classification [1],[8]. More recently, deep neural networks, particularly LSTM and CNN-LSTM hybrid models, have proven highly effective due to their ability to model the temporal structure of audio signals [9],[10]. This paper addresses the gap by developing a robust LSTM-based SER system trained on RAVDESS and TESS and subsequently fine-tuned on the Serbian GEES corpus using transfer learning, with the goal of achieving high recognition accuracy for Serbian speakers.

2. Materials and Methods

2.1 Datasets

Three emotional speech datasets were used. RAVDESS [6] is a publicly available English corpus featuring 24 professional actors (12 male, 12 female) with recordings spanning emotions including neutral, angry, happy, sad, fearful, disgusted, and surprised, captured under controlled studio conditions. TESS [7] contains recordings from two female speakers across seven basic emotions and, despite its smaller size, provides clearly articulated emotional expressions. GEES is a Serbian emotional speech dataset comprising recordings from multiple speakers across five emotion categories: angry, neutral, happy, fearful, and sad. Not all speakers contributed recordings for every emotion, introducing realistic variability.

2.2 Feature Extraction

Mel-Frequency Cepstral Coefficients (MFCCs) were selected as the sole feature type, in their sequential form suitable for LSTM processing. MFCCs are among the most widely used features in speech processing, as they approximate the acoustic properties perceived by the human auditory system [13]. The extraction pipeline divides the audio signal into short time windows, computes spectral energy across frequency bands mapped onto the Mel scale [14], and applies a Discrete Cosine Transform to decorrelate the resulting values. Forty MFCC coefficients were extracted per time frame, yielding a fine-grained frequency resolution.

All sequences were normalized to a maximum length of 300 time steps via zero-padding or truncation, yielding input tensors of shape (samples, 300, 40). Each recording was additionally subjected to Root Mean Square (RMS) energy normalization to reduce loudness variability across speakers and datasets [15], enabling the LSTM to learn dynamic temporal patterns rather than relying on a single aggregated feature vector.

2.3 Model Architecture

A Long Short-Term Memory (LSTM) recurrent neural network was selected for emotion classification. Speech is inherently sequential, and LSTM networks are well-suited to model temporal dependencies through their memory cell and gating mechanisms (forget, input, and output gates), effectively capturing long-range patterns in intonation and prosody [16]. Standard RNNs suffer from vanishing gradients; LSTM addresses this through its gating mechanism.

The architecture comprises a Masking layer to ignore zero-padded steps [17], an LSTM layer with 128 units, two Dropout layers (rate 0.3) for regularization [18], a Dense layer with 64 units and ReLU activation, and a

softmax output layer. The model was trained with the Adam optimizer, categorical cross-entropy loss, over 30 epochs with batch size 32.

3. Results

Model performance was evaluated using precision, recall, F1-score, and overall accuracy on held-out test sets. Two models were evaluated: the base model trained on the combined RAVDESS and TESS corpus, and the fine-tuned model adapted to the Serbian GEES dataset.

The RAVDESS+TESS model achieved an overall accuracy of 88% on 573 test samples (Table 1). All five emotion classes showed high F1-scores (0.82-0.91), with "angry" reaching the highest score (0.91) and "sad" the lowest (0.82). Macro-averaged precision, recall, and F1-score were all 0.88, indicating balanced performance across classes.

Table 1. Classification report for the RAVDESS+TESS model (573 test samples).

Class	Precision	Recall	F1-score	Samples
angry	0.87	0.96	0.91	119
fearful	0.92	0.87	0.90	118
happy	0.87	0.89	0.88	119
neutral	0.94	0.82	0.88	99
sad	0.81	0.84	0.82	118
accuracy			**0.88**	573

The GEES fine-tuned model was evaluated on 1,521 test samples and achieved an overall accuracy of 75% (Table 2). Performance varied more across classes: "sad" achieved the highest F1-score (0.89), while "angry" was the most difficult class to classify (F1 = 0.65). The macro-averaged F1-score was 0.74.

Table 2. Classification report for the GEES fine-tuned model (1521 test samples).

Class	Precision	Recall	F1-score	Samples
angry	0.67	0.63	0.65	293
fearful	0.75	0.64	0.69	309
happy	0.69	0.70	0.69	300
neutral	0.75	0.85	0.80	308
sad	0.87	0.92	0.89	311
accuracy			**0.75**	1521

4. Discussion

The base model trained on RAVDESS and TESS achieved 88% accuracy, consistent with recent LSTM-based SER studies on comparable English corpora [9],[10]. The high performance reflects the quality and balance of these datasets: both are professionally recorded under controlled conditions, with clearly acted emotional expressions. The consistently high F1-scores across all five classes indicate the model learned well-generalizable representations of emotional patterns.

The 13-percentage-point reduction in accuracy after fine-tuning on GEES is expected and aligns with findings in cross-lingual transfer learning [12]. The GEES corpus reflects natural, more variable emotional expressions in Serbian, a language phonetically distinct from English. Greater class confusion was observed, particularly between “angry” and “fearful”, two emotionally and acoustically proximal categories. Notably, “sad” reached an F1-score of 0.89 in the Serbian model, suggesting that the acoustic profile of sadness may be more language-invariant. The importance of data balance and speaker adaptation through transfer learning highlighted in prior literature [11],[12] is clearly reflected in these results.

A limitation of the current approach is the exclusive use of MFCC features. Supplementing with pitch-based or energy-based prosodic features could potentially further improve cross-lingual generalization. Additionally, the GEES corpus presents variability in speaker coverage across emotion categories, which may have introduced class imbalance effects during fine-tuning.

5. Conclusions

This paper presented an end-to-end Speech Emotion Recognition system based on LSTM networks, with MFCC sequential features and RMS energy normalization. Pre-training on RAVDESS and TESS yielded 88% accuracy on English speech, while transfer learning via fine-tuning on the Serbian GEES corpus achieved 75% accuracy, demonstrating meaningful cross-lingual adaptability.

Future work will focus on incorporating additional feature modalities (pitch, energy, spectrograms), exploring CNN-LSTM hybrid architectures, and expanding the GEES corpus to improve coverage across speakers and emotion categories. Investigating multilingual pre-training strategies may further bridge the performance gap between English and Serbian emotion recognition.

References

1. El Ayadi M, Kamel M, Karray F. Survey on speech emotion recognition: Features, classification schemes, and databases. Pattern Recognition;44(3):572-587.
2. Schuller B, Steidl S, Batliner A. The INTERSPEECH 2009 Emotion Challenge. Interspeech. 2009.
3. Poria S, Cambria E, Bajpai R, Hussain A. A review of affective computing: From unimodal analysis to multimodal fusion. Information Fusion. 2017;37:98-125.
4. Ververidis D, Kotropoulos C. Emotional speech recognition: Resources, features, and methods. Speech Communication. 2006;48(9):1162-1181.

5. Schuller B, Batliner A, Steidl S, Seppi D. Recognising realistic emotions and affect in speech: State of the art and lessons learnt from the first challenge. Speech Communication. 2011;53(9-10):1062-1087.
6. Livingstone SR, Russo FA. The Ryerson Audio-Visual Database of Emotional Speech and Song (RAVDESS). PLOS ONE. 2018;13(5).
7. Dupuis K, Pichora-Fuller MK. Toronto Emotional Speech Set (TESS). University of Toronto, Psychology Department. 2010.
8. Eyben F, Wöllmer M, Schuller B. openSMILE - The Munich versatile and fast open-source audio feature extractor. Proceedings of ACM Multimedia. 2010:1459-1462.
9. Zhang S, Zhang S, Huang T, Gao W, Tian Q. Learning affective features with a hybrid deep model for audio–visual emotion recognition. IEEE Transactions on Circuits and Systems for Video Technology. 2018;28(10):3030-3043.
10. Zhao Y, Zhang W, Zou Y, Yu Z. Learning emotional representations from speech using deep neural networks. Neurocomputing. 2019;333:429-442.
11. Mirsamadi S, Barsoum E, Zhang C. Automatic speech emotion recognition using recurrent neural networks with local attention. Proceedings of ICASSP. 2017.
12. Gideon J, Khorram S, Aldeneh Z, Dimitriadis D, Provost EM. Progressive Neural Networks for Transfer Learning in Emotion Recognition. Proceedings of Interspeech. 2017.
13. Rabiner L, Schafer R. Introduction to digital speech processing. Foundations and Trends in Signal Processing. 2007;1(1-2):1-194.
14. Davis SB, Mermelstein P. Comparison of parametric representations for monosyllabic word recognition in continuously spoken sentences. IEEE Transactions on Acoustics, Speech, and Signal Processing. 1980;28(4):357-366.
15. Logan B. Mel Frequency Cepstral Coefficients for Music Modeling. Proceedings of the International Symposium on Music Information Retrieval (ISMIR). 2000.
16. Hochreiter S, Schmidhuber J. Long short-term memory. Neural Computation. 1997;9(8):1735-1780.
17. Goodfellow I, Bengio Y, Courville A. Deep Learning. MIT Press. 2016.
18. Srivastava N, Hinton G, Krizhevsky A, Sutskever I, Salakhutdinov R. Dropout: A Simple Way to Prevent Neural Networks from Overfitting. Journal of Machine Learning Research. 2014;15(56):1929-1958.

Automated Detection of Business Email Compromise Attacks in Serbian Language Using Linear Probabilistic Models

Miljan Koturović†, Uroš Deljanin† and Vladimir Milovanović

Department of Electrical Engineering and Computer Sciences, Faculty of Engineering, University of Kragujevac, Kragujevac, Serbia, m.kotur2003@gmail.com, 0009-0009-9242-9456, urosdeljanin1@gmail.com, 0009-0003-1582-8556, vlada@kg.ac.rs, 0000-0002-6787-4058

Corresponding author: *vlada@kg.ac.rs*

Abstract

Phishing remains a critical threat to organizations worldwide, but detection systems often neglect the Slavic language landscape. This study presents a machine learning approach to identify phishing emails in the Serbian language, combining a custom-implemented logistic regression with TF-IDF vectorization using bigram features. We constructed a balanced dataset of 20,000 synthetic, authentic email messages in the Serbian language, with careful attention to phrasal patterns. We achieved 100% accuracy from our model's predictions on the classification of some test data. By examining the precision and recall metrics from our test set sample of the synthetic dataset, we were able to extend the capabilities of our classifier as an accurate predictor of phishing emails that will be used in practice. This includes installing our trained model into a Firefox extension, which will enable users to scan emails and decide if an email is phishing or not. The results indicate that, compared to traditional statistical approaches, the specific and complex representation of linguistic data found in many different languages can significantly enhance the ability to detect threats in those languages that are not English and therefore not represented in many cybersecurity tools.

Keywords: email security; phishing detection; machine learning; logistic regression; Serbian language; bigrams; business email compromise; TF-IDF; cybersecurity; UN SDG 9; UN SDG 16

1. Introduction

So-called "phishing" has been defined as "a type of computer attack that communicates socially engineered messages to humans via electronic communication channels in order to persuade them to perform certain actions for the attacker's benefit" [1]. However, since phishing emails written in Slavic and other non-dominant languages have different linguistic and structural features than those written in English, they are often misclassified by generic or English-trained classifiers. An example of this is the Serbian language, which has approximately 8 to 12 million speakers across the world. Existing email filtering software (commercial) does not perform effectively for emails written in the Serbian language.

† † These authors contributed equally to this work

This work addresses two interconnected challenges:

1. The absence of robust, language-aware phishing detection specifically optimized for Serbian language communication patterns
2. Second, the gap between academic classifiers and deployable security tools accessible to end users.

We developed a machine learning pipeline combining manual feature engineering via TF-IDF vectorization with a logistic regression model.

Our objectives are threefold:

1. To establish baseline performance metrics for phishing classification in the Serbian language.
2. To evaluate the effectiveness of bigram-level linguistic features in capturing phrasal red flags characteristic of phishing emails.
3. To demonstrate practical deployment of the classifier as a user-facing browser extension.

2. Materials and Methods

2.1 Dataset Construction

We generated a balanced dataset containing 20,000 email messages in the Serbian language: 10,000 labeled as phishing and 10,000 as legitimate. Phishing messages contained established social engineering tactics, including urgency signaling ("Rok ističe u roku od 2 sata"), authority impersonation ("Sektor za bezbednost"), and a request for sensitive information ("unesite podatke kartice"). Legitimate messages contained typical organizational communication: project updates, meeting confirmations, status reports, and administrative notifications. No personally identifiable information was retained.

The dataset was partitioned into training (80%) and test (20%) subsets using stratified random sampling to maintain class balance.

2.2 Feature Extraction and Preprocessing

Text preprocessing was done using standard NLP conventions: lowercasing, whitespace normalization, and removal of non-word characters. We applied TF-IDF vectorization [2] using scikit-learn's TfidfVectorizer. We enabled bigram features using ngram_range=(1,2), capturing two-word sequences that encode phrasal patterns, characteristic of phishing. The maximum feature dimensionality was set to 15,000. Bigrams proved particularly valuable for detecting stock phrases like "bezbednosni alarm" and "promenite lozinku" that frequently appear in malicious messages.

2.3 Model Implementation and Training

We implemented logistic regression from first principles using stochastic gradient descent with L2 regularization ($\lambda = 0.1$). The implementation was custom, written in Python using only NumPy and basic linear algebra. Hyperparameters that were used in training: learning rate (0.01), number of iterations (100,000), and regularization strength(0.1). The model was trained on the X_train matrix (16,000 samples × 15,000 features) over 100,000 iterations with mini-batch SGD.

2.4 Evaluation Metrics

Performance was measured using classification accuracy, precision, and recall per class, and F1 scores.

3. Results

The trained model achieved 100% overall classification accuracy on the test set containing 4,000 samples (20% of the generated dataset). Analysis revealed precision of 1.0 for phishing detection and 1.0 for legitimate messages, with corresponding recall values of 1.0 and 1.0. The weighted F1 score was 1.0, indicating balanced performance. The confusion matrix showed 1,896 true positives out of 1,896 phishing samples. Among legitimate messages, 2014 were correctly classified.

The trained classifier was successfully integrated into a Firefox browser extension, enabling analysis of displayed email text (HTML body of an email). The extension returns instant classification with confidence percentage, allowing users to make informed decisions about message authenticity.

4. Discussion

Our results demonstrate that machine learning models remain competitive for phishing detection despite recent deep learning advances.

The synthetic dataset approach enables rapid prototyping and eliminates privacy concerns associated with real email collection. However, this introduces potential risk: synthetic messages, despite linguistic authenticity, may not capture emergent attack patterns or new social engineering techniques. Future work should contain controlled samples from real phishing campaigns (with appropriate anonymization) for better generalization.

Operational deployment using Firefox extension demonstrates practical accessibility, but integration with email servers (Office 365, Gmail) requires API-level access, currently restricted for privacy reasons.

The model's decision transparent weight-based reasoning in logistic regression offers advantages over neural network approaches. Security analysts can audit individual classification decisions, understanding precisely which features triggered alerts. This interpretability can be crucial when phishing detection errors carry organizational consequences.

Limitations include:

1. Reliance on synthetic data, lacking adversarial evolution of phishing tactics.
2. Focus on the Serbian language without cross-linguistic transfer analysis.

3. Focus on content-based signals while ignoring metadata (sender reputation, SPF/DKIM headers).
4. Small validation set (4,000 test samples), limiting statistical power for rare edge cases.

5. Conclusions

We have presented a complete pipeline for Serbian language phishing detection combining custom logistic regression, TF-IDF bigram features, and practical browser-based deployment.

This paper demonstrates how interpretable machine learning methods that have been developed with regard to the linguistic context can contribute to solving security problems in underrepresented languages. The resulting open-source Firefox extension and reproducible training pipeline enable community engagement and adaptation for related Slavic languages (such as Croatian, Bulgarian, and Russian) by utilizing similar feature engineering methodologies.

Going forward, we could carry out the following:

1. Provide a temporal evaluation to track phishing changes over time.
2. Use zero-shot transfer to related Slavic languages that share linguistic features.
3. Create ensemble methods that combine logistic regression and gradient boosting to achieve superior performance.

References

1. M. Khonji, Y. Iraqi, and A. Jones. Phishing detection: A literature survey. IEEE Communications Surveys Tutorials, 2013;15(4):2091–2121

2. K. S. Jones, “Document retrieval systems,” in A Statistical Interpretation of Term Specificity and Its Application in Retrieval, London, UK: Taylor Graham Publishing, 1988;123–142

Semestrify: A Cross-Platform System for Intelligent Academic Schedule Extraction and Calendar Integration

George Tzanopoulos[1], Vasileios Ralis[1], Christos Gogos[1]

[1]*Dept. of Informatics and Telecommunications, University of Ioannina, Arta, Greece, gtzan@orailab.gr, 0009-0009-8045-7249, vrallis@orailab.gr, 0009-0001-7030-5884, cgogos@uoi.gr, 0000-0003-1113-8462*
Corresponding author: *gtzan@orailab.gr*

Abstract

This paper presents Semestrify, an AI-enabled application that automates the extraction, personalization, and synchronization of university course schedules into students' digital calendars. Academic timetables are often published in heterogeneous formats (e.g., PDFs, spreadsheets, web pages), complicating accurate schedule management. The system employs natural language processing and information extraction to parse schedule data, identify course events, and produce structured representations, which are matched with student enrollments to generate personalized timetables integrated into calendar platforms. Semestrify is available as both a web and mobile application, supporting real-time updates by continuously monitoring schedule changes. Key challenges include handling ambiguous data and format variability. Evaluation results indicate improved schedule accuracy, demonstrating the effectiveness of AI-driven timetable management in higher education.

Keywords: course schedules; personalized timetables; AI workflow

1. Introduction

University course schedules constitute a critical operational artifact for both students and administrative staff [1]. Despite their importance, timetables are typically disseminated in heterogeneous, semi-structured formats (e.g., web pages, PDFs, spreadsheets), often lacking machine-readable semantics. This fragmentation imposes a non-trivial cognitive and operational burden on students, who must manually interpret, consolidate, and maintain their personal schedules across multiple sources. The problem is exacerbated by frequent updates (room changes, cancellations, rescheduling), leading to inconsistencies, missed sessions, and reduced academic efficiency. While digital calendars (e.g., Google Calendar, Apple Calendar) are widely adopted, the integration of institutional schedules into personalized calendar environments remains largely manual and error-prone. This creates a clear need for automated, robust, and adaptive solutions that bridge institutional data and user-centric scheduling.

Prior work in timetable management has primarily focused on timetabling optimization (e.g., course and exam scheduling using combinatorial optimization, constraint programming, and metaheuristics) [2], rather than downstream consumption and personalization of schedules. In parallel, research in information extraction and natural language processing has addressed the transformation of semi-structured documents into structured data, including applications to event extraction and document understanding. More recently, intelligent personal assistants and calendar management systems have explored event detection from emails or messages (e.g., meeting extraction), but these systems typically operate on user-generated content rather than institutional academic schedules. Existing commercial or institutional tools often assume structured input or require manual configuration, limiting their applicability in real-world academic environments with high variability in data

formats. The proposed system introduces a unified pipeline that integrates AI-driven information extraction with personalized schedule generation and real-time synchronization. Its novelty lies in: (i) robust parsing of heterogeneous academic schedule sources without requiring standardized input formats, (ii) tight coupling between extracted events and individual student enrollment data for automatic personalization, and (iii) continuous monitoring and propagation of schedule updates to external calendar systems. Unlike traditional approaches that treat scheduling as an optimization problem or rely on structured inputs, this work addresses the underexplored problem of automated schedule consumption and synchronization in dynamic, real-world settings. Recent advances in LLMs have demonstrated strong capabilities in few-shot generalization and document understanding, enabling robust extraction of structured information from heterogeneous and semi-structured sources [3].

2. Materials and Methods

The system that has been developed to address the problem of automated updates of course schedules for all students at a University department was called Semestrify and it is built upon a high-performance, decoupled architecture. The backend is implemented with FastAPI (Python), leveraging its asynchronous capabilities to handle concurrent user sessions and heavy I/O operations. Data persistence is managed by DuckDB, an in-process analytical database that allows for efficient querying of course-related metadata and student enrollments. For cross-platform accessibility, the frontend utilizes the Flutter framework, providing a unified codebase for Android, iOS, and Web. Communication between the client and server is facilitated through a RESTful API with JSON as the primary data exchange format, while Google OAuth 2.0 (OpenID Connect) provides a secure authentication layer for institutional account integration.

The information flow that is followed by the system is illustrated in Figure 1 and consists of the following 5 subsystems: (i) AI-First Ingestion: Raw, unstructured timetable sources (PDFs or Excel sheets) are processed by the ingestion engine, (ii) LLM-Driven Extraction: A specialized parser translates these sources into structured course entities, (iii) Normalization & Storage: Extracted data is normalized and stored in the DuckDB database, (iv) Client Interaction: Users select their courses through the Flutter interface, which interacts with the FastAPI backend to retrieve and personalize schedules, (v) External Synchronization: The system generates dynamic iCalendar (.ics) feeds, allowing students to integrate their academic timetable into personal calendar applications like Google Calendar or Apple Calendar.

A technical challenge that Semestrify had to overcome was the robust parsing of heterogeneous looking schedules as they are published at the web pages of the university departments (e.g. Figure 12). We utilized Gemini 3 Flash (i.e., the gemini-3-flash-preview model) to handle the reasoning needed for interpreting university timetables. Our prompting strategy instructs the model to process data column-by-column (Room-by-Room), specifically identifying continuation markers (e.g., the » symbol) to correctly merge multi-hour sessions. Furthermore, the synchronization logic implements a consecutive course merging step. It identifies classes with the same instructor and location that occur in back-to-back slots, merging them into a single calendar event. Each event in the generated `.ics` feed includes a recurrence rule (RRULE) for weekly repetition and a pre-configured VALARM for push notifications, ensuring students receive timely reminders before each session. The system is deployed using a containerized approach to ensure environment parity and ease of maintenance. The FastAPI backend and DuckDB database are bundled into Docker containers, which are

managed as persistent system services on a Linux-based server. This setup facilitates rapid updates and consistent performance under varying loads. Distribution of the user interface follows a hybrid model to maximize reach while minimizing development overhead. For Android users, the application is packaged as a native APK, while for iOS and desktop users, it is served as a Progressive Web App (PWA). This strategy utilizes web manifest configurations and service workers to provide a mobile-like experience, including home-screen installation and offline capabilities, without requiring a traditional App Store release.

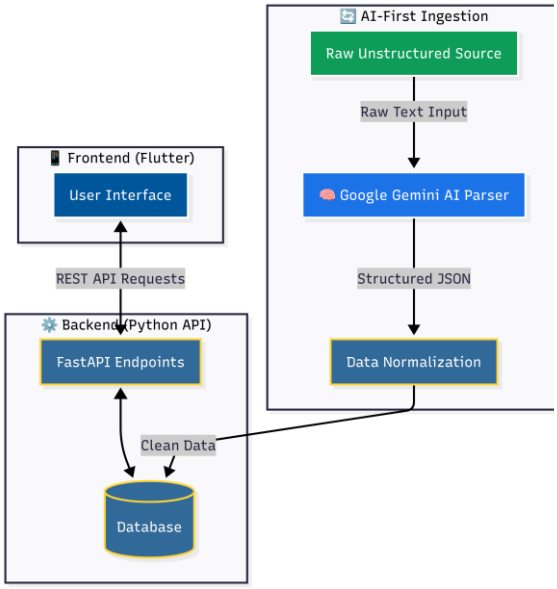
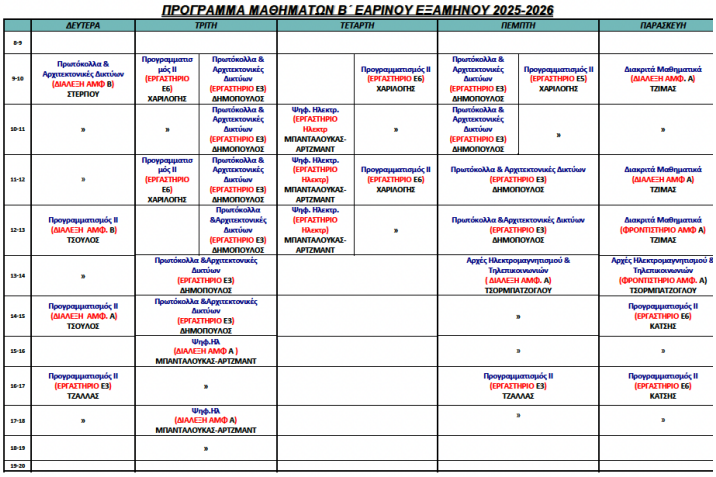


Figure 11 Semestrify – a high-level view.



ΠΡΟΓΡΑΜΜΑ ΜΑΘΗΜΑΤΩΝ Β΄ ΕΑΡΙΝΟΥ ΕΞΑΜΗΝΟΥ 2025-2026

	ΔΕΥΤΕΡΑ	ΤΡΙΤΗ		ΤΕΤΑΡΤΗ		ΠΕΜΠΤΗ		ΠΑΡΑΣΚΕΥΗ
8-9								
9-10	Πρωτόκολλα & Αρχιτεκτονικές Δικτύων (ΔΙΑΛΕΞΗ ΑΜΦ Β) ΣΤΕΡΓΙΟΥ	Προγραμματισμός II (ΕΡΓΑΣΤΗΡΙΟ Ε6) ΧΑΡΙΑΟΠΗΣ	Πρωτόκολλα & Αρχιτεκτονικές Δικτύων (ΕΡΓΑΣΤΗΡΙΟ Ε3) ΔΗΜΟΠΟΥΛΟΣ		Προγραμματισμός II (ΕΡΓΑΣΤΗΡΙΟ Ε6) ΧΑΡΙΑΟΠΗΣ	Πρωτόκολλα & Αρχιτεκτονικές Δικτύων (ΕΡΓΑΣΤΗΡΙΟ Ε3) ΔΗΜΟΠΟΥΛΟΣ	Προγραμματισμός II (ΕΡΓΑΣΤΗΡΙΟ Ε5) ΧΑΡΙΑΟΠΗΣ	Διακριτά Μαθηματικά (ΔΙΑΛΕΞΗ ΑΜΦ. Α) ΤΖΙΜΑΣ
10-11	»	»	Πρωτόκολλα & Αρχιτεκτονικές Δικτύων (ΕΡΓΑΣΤΗΡΙΟ Ε3) ΔΗΜΟΠΟΥΛΟΣ	Ψηφ. Ηλεκτρ. (ΕΡΓΑΣΤΗΡΙΟ Ηλεκτρ) ΜΠΑΝΤΑΛΟΥΚΑΣ-ΑΡΤΖΜΑΝΤ	»	Πρωτόκολλα & Αρχιτεκτονικές Δικτύων (ΕΡΓΑΣΤΗΡΙΟ Ε3) ΔΗΜΟΠΟΥΛΟΣ	»	»
11-12	»	Προγραμματισμός II (ΕΡΓΑΣΤΗΡΙΟ Ε6) ΧΑΡΙΑΟΠΗΣ	Πρωτόκολλα & Αρχιτεκτονικές Δικτύων (ΕΡΓΑΣΤΗΡΙΟ Ε3) ΔΗΜΟΠΟΥΛΟΣ	Ψηφ. Ηλεκτρ. (ΕΡΓΑΣΤΗΡΙΟ Ηλεκτρ) ΜΠΑΝΤΑΛΟΥΚΑΣ-ΑΡΤΖΜΑΝΤ	Προγραμματισμός II (ΕΡΓΑΣΤΗΡΙΟ Ε6) ΧΑΡΙΑΟΠΗΣ	Πρωτόκολλα & Αρχιτεκτονικές Δικτύων (ΕΡΓΑΣΤΗΡΙΟ Ε3) ΔΗΜΟΠΟΥΛΟΣ		Διακριτά Μαθηματικά (ΔΙΑΛΕΞΗ ΑΜΦ. Α) ΤΖΙΜΑΣ
12-13	Προγραμματισμός II (ΔΙΑΛΕΞΗ ΑΜΦ. Β) ΤΣΟΥΛΟΣ	Πρωτόκολλα &Αρχιτεκτονικές Δικτύων (ΕΡΓΑΣΤΗΡΙΟ Ε3) ΔΗΜΟΠΟΥΛΟΣ	Ψηφ. Ηλεκτρ. (ΕΡΓΑΣΤΗΡΙΟ Ηλεκτρ) ΜΠΑΝΤΑΛΟΥΚΑΣ-ΑΡΤΖΜΑΝΤ	»	Πρωτόκολλα &Αρχιτεκτονικές Δικτύων (ΕΡΓΑΣΤΗΡΙΟ Ε3) ΔΗΜΟΠΟΥΛΟΣ		Διακριτά Μαθηματικά (ΦΡΟΝΤΙΣΤΗΡΙΟ ΑΜΦ Α) ΤΖΙΜΑΣ
13-14	»	Πρωτόκολλα &Αρχιτεκτονικές Δικτύων (ΕΡΓΑΣΤΗΡΙΟ Ε3) ΔΗΜΟΠΟΥΛΟΣ			Αρχές Ηλεκτρομαγνητισμού & Τηλεπικοινωνιών (ΔΙΑΛΕΞΗ ΑΜΦ. Α) ΤΣΟΡΜΠΑΤΖΟΓΛΟΥ		Αρχές Ηλεκτρομαγνητισμού & Τηλεπικοινωνιών (ΦΡΟΝΤΙΣΤΗΡΙΟ ΑΜΦ. Α) ΤΣΟΡΜΠΑΤΖΟΓΛΟΥ
14-15	Προγραμματισμός II (ΔΙΑΛΕΞΗ ΑΜΦ. Α) ΤΣΟΥΛΟΣ	Πρωτόκολλα &Αρχιτεκτονικές Δικτύων (ΕΡΓΑΣΤΗΡΙΟ Ε3) ΔΗΜΟΠΟΥΛΟΣ			»		Προγραμματισμός II (ΕΡΓΑΣΤΗΡΙΟ Ε6) ΚΑΤΣΗΣ
15-16		Ψηφ.Ηλ. (ΔΙΑΛΕΞΗ ΑΜΦ Α) ΜΠΑΝΤΑΛΟΥΚΑΣ-ΑΡΤΖΜΑΝΤ			»		»
16-17	Προγραμματισμός II (ΕΡΓΑΣΤΗΡΙΟ Ε3) ΤΖΑΛΑΣ	»			Προγραμματισμός II (ΕΡΓΑΣΤΗΡΙΟ Ε3) ΤΖΑΛΑΣ		Προγραμματισμός II (ΕΡΓΑΣΤΗΡΙΟ Ε6) ΚΑΤΣΗΣ
17-18	»	Ψηφ.Ηλ. (ΔΙΑΛΕΞΗ ΑΜΦ Α) ΜΠΑΝΤΑΛΟΥΚΑΣ-ΑΡΤΖΜΑΝΤ			»		»
18-19		»					
19-20							

Figure 12 An example of a course schedule that Semestrify must parse (Course Schedule for the spring semester 2025-2026 for the 1st year of Dept. of Informatics and Telecommunications, Univ. of Ioannina).

3. A Typical Workflow

A typical workflow from the user/student perspective is depicted in Figure 13. The user first logs to the system (https://semestrify.orailab.gr), then selects courses and lectures and finally exports the schedule to an .ics file, which is easy to import into popular calendar systems.

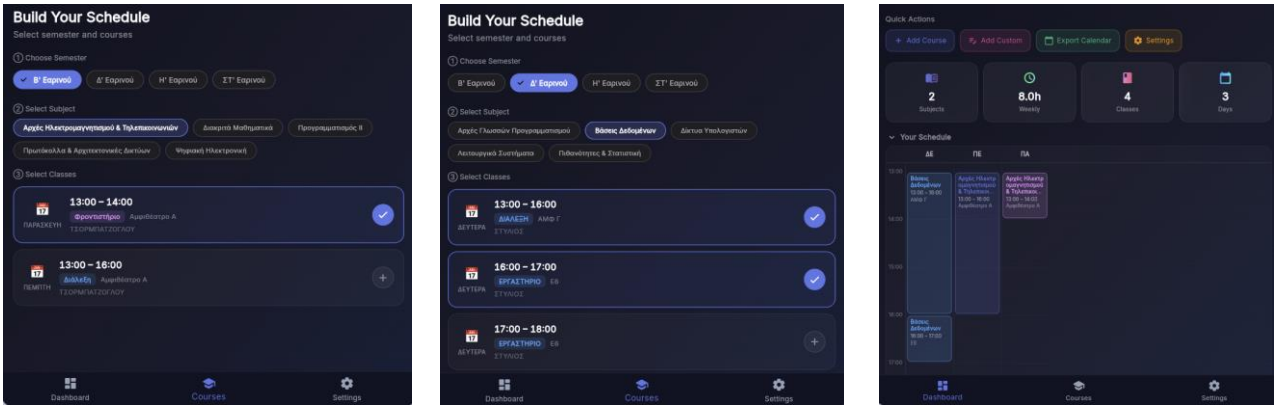


Figure 13 Screenshots of the application, the user selects courses and adds them to his/her personal calendar.

Based on usage logs, Semestrify was used at the spring semester of the 2025-2026 academic year by about 40% of the students of the Department of Informatics and Telecommunications of the University of Ioannina.

4. Discussion

The primary motivation for Semestrify was the lack of an existing solution for easily generating personalized timetables for university students. University timetables are frequently distributed as static PDF documents or complex HTML tables, requiring students to manually transcribe information into their personal calendars. This manual process is not only time-consuming but also prone to errors, especially when schedules are updated mid-semester. Semestrify addresses this gap by transforming these isolated files into dynamic, synchronized streams. Traditional rule-based parsers (e.g., using regular expressions or layout-fixed scrapers) often fail when confronted with the high variability of university document formats. A minor change in column widths or font styles can render a hard-coded parser obsolete. In contrast, our transition to an LLM-assisted approach using Gemini 3 Flash demonstrated significant resilience. The model's ability to "understand" the semantic context of a grid, even when visual markers are ambiguous, allows the system to adapt to different department formats without manual code changes. While manual parsing requires hours of developer time for each new template, the AI-driven pipeline can be tuned via prompt engineering within minutes. Despite the advantages of generative AI, data accuracy remains a critical concern. LLMs can occasionally "hallucinate" or misinterpret overlapping text in dense PDF layouts. To mitigate this, Semestrify employs a multi-step verification process where the model's JSON output is validated against expected temporal ranges and normalized against a known list of subjects and instructors. A current limitation is the reliance on external LLM APIs, which introduces latency and dependency on third-party service availability. The successful deployment of Semestrify indicates a clear demand for more integrated academic tools. Future enhancements will focus on localization, extending support to multiple languages and international university formats, and the implementation of conflict detection to alert students when elective courses overlap.

5. Conclusions

Semestrify demonstrates the potential of applying AI solutions to everyday academic administrative challenges. By automating the transition from unstructured institutional documents to personalized, synchronized calendar events, the system removes a significant operational hurdle for students. The use of Gemini 3 Flash proves that lightweight, high-speed LLMs can achieve high accuracy in complex data extraction tasks when paired with specialized prompt engineering. Future iterations will focus on expanding the platform's support for more diverse academic formats and integrating location-based services for campus-wide navigation.

References

[1] Chen MC, Sze SN, Goh SL, Sabar NR, Kendall G. A Survey of University Course Timetabling Problem: Perspectives, Trends and Opportunities. IEEE Access 2021;9:106515–29. https://doi.org/10.1109/ACCESS.2021.3100613.

[2] Dimitsas A, Nastos V, Gogos C, Valouxis C. An exact based approach for the Post Enrollment Course Timetabling Problem. Proceedings of the 26th Pan-Hellenic Conference on Informatics, Athens Greece: ACM; 2022, p. 77–82. https://doi.org/10.1145/3575879.3575970.

[3] Brown TB, Mann B, Ryder N, Subbiah M, Kaplan J, Dhariwal P, et al. Language Models are Few-Shot Learners; NeurIPS Proceedings, 2020, p. 1877-1901. https://proceedings.neurips.cc/paper_files/paper/2020/file/1457c0d6bfcb4967418bfb8ac142f64a-Paper.pdf

How Do Translators Learn to Use AI? A Constructivist Approach Based on a PhD dissertation: The Learning of Translators to Use Artificial Intelligence

(Programme ID: MIS: 5162213, Funding Resource: European Social Fund-ESF, Period (2023 – 2026)

Airidas Kairys

Department of Early Childhood Education, University of Ioannina, Greece, airidas971@gmail.com, ORCID:0009-0008-8886-9208.
Corresponding author: airidas971@gmail.com

Abstract

The aim of this study is to reveal how translators learn to integrate AI into their everyday translation work tasks. The theoretical foundation of this research is based on Berger and Luckmann's social constructivist philosophy, which maintains that individuals actively construct the social reality in which they exist. The employed research methodology is Charmaz's constructivist grounded theory, an approach that centres on participants subjective experiences and personal interpretations rather than purely objective phenomena. The study involved 19 translators based in Lithuania, working either as freelancers or within translation agencies. Data collection was carried out through semi-structured interviews. The analytical process was interpretive in its nature and followed Charmaz's methodological guidelines. Data analysis followed Charmaz's three-stage coding process: initial coding, focused coding, and theoretical coding, conducted using the MAXQDA qualitative data analysis software. Theoretical coding yielded the core category: Becoming an AI-literate translator through self-directed practice, indicating that translators are continuously engaged in lifelong learning processes. The findings demonstrate that translators predominantly utilise tools such as DeepL, Google Translate, and ChatGPT, acquiring proficiency through self-directed practice. The preliminary study concludes that formal education, particularly university-level translation study programmes, should incorporate dedicated AI modules, while additional non-formal learning opportunities should also be expanded.

Keywords: *translators, AI, self-directed practice, Charmaz, 'UN SDG 4'.*

1. Project Background and Objectives

Contemporary developments in artificial intelligence (AI), including machine translation engines and generative AI large language models used for translation, are transforming the landscape of professional translation by enabling faster and more efficient processing of large amounts of text. Consequently, translators are increasingly expected to acquire competences in AI within their professional practice. Due to the emergence of AI, it is not clear if generative AI will replace human translation, but AI should be integrated into translation education studies. Soysal [20] comments that by merging the advantages of generative artificial intelligence and human

translators, translation studies can progress and improve translation practice in the age of technology. The author believes that moral and societal factors are equally important when implementing generative AI into translation. Even if generative AI chatbots are sometimes capable of accurate and precise translations, that does not stop the necessity for human intervention and assurance of ethical concerns. It could be concluded that human translators' expertise that comes from translation studies can be used to complement the development of generative AI chatbots, thus enhancing their translation abilities. Soysal [20] thinks that the application of AI technologies into translation studies has had a profound impact on the subject. The scholar states that the constraints of AI systems emphasise the value of human knowledge and the necessity for human-AI cooperation. He notes that translation studies can help to create, evaluate, and enhance AI systems for translation tasks. He pinpoints that moral and societal concerns need to be addressed as well to guarantee generative AI's fair and balanced inclusion into translation.

The intersection between artificial intelligence and translation has been explored in past literature. For instance, Siu [19] investigated various benefits ChatGPT generative AI model had on translation. Bulut & Alimen [3] gave the students an assignment where they had to identify mistakes in machine translation output and post-edit the said text. This research concluded that it will be necessary for translators to use artificial intelligence in the upcoming times. Also, in this research, the students had the most difficulties when they had to identify the mistakes in the MT text. It is unknown if this was due to the high accuracy of the translation or, on the contrary, a high ratio of mistranslations. Whatever the case may be, machine translation is a form of AI that is already widely employed in translation. When it comes to AI itself, there was enough research done that defined it. For example, Dolanay [9] distinguished three types of artificial intelligence, and based on what he said we can put machine translation and generative AI into two separate categories. The general definition of artificial intelligence also sparked an interesting debate. Sheikh et al. [18], Minsky [16], Mahato [15], Plochberger [17] all present differing definitions, but the main point is that these researchers either view AI as some sort of calculative computer or an artificial brain or even an artificial human.

The demand for AI and new qualification requirements for translators leads to the research problem: how do translators learn to integrate AI into their everyday translation work tasks?

The objective is to disclose how translators learn to use AI in their job tasks.

2. Methodology and Work Performed

The research aim – to analyse how translators learn to use AI in their job tasks.

Grounded theory. According to Charmaz [4], [5], [6] grounded theory is an inductive process that seeks to create a theory based on actual facts. The methodology of socio-constructivist grounded theory [4], [6] was employed throughout the stages of data gathering, analysis, and theory generation. This type of grounded theory is based on the approach used by Glaser and Strauss [11], who found that theory emerged from data that was not observed by a scientific observer. Charmaz [4, p. 10] disagrees, pointing out, "I assume that neither data nor theories are discovered. Rather, we are part of the world we study and the data we collect."

Theoretical sampling. In this study, following Charmaz's advice [4], forming the empirical sample is the first step in the research process. According to Conlon et al. [7], theoretical sampling was a key component of this

investigation. Theoretical sampling, as the author points out, guided the researcher in switching back and forth between the data and the emergent theory to find empirical examples that could increase understanding of theoretical constructs that have arisen from the data or that predate the investigation.

Participants. 19 translators from Lithuania participated in this study

Data Collection Method. For a grounded theory study, semi-structured interviews work best when the investigator has tentatively defined a few areas that have been assigned the question, which interviewing can then start to expand upon [7], but in this study theorical sampling is used, thus, semi structured interview is employed for the first respondent, and further questions are changeable because after analysis of each interview and memo writing, new questions arise.

Memo writing. Memoing is a crucial part of GT (Grounded Theory) research, which is carried out continually during the data collecting and analysis stages, according to Charmaz [4]. It helps a researcher quickly examine the data and codes in novel ways [4].

Data Analysis. The first steps of Charmaz's theory are selection, initial data gathering, and transcription, which culminate in *initial coding*. This coding can be based on line after line, event after event or word after word method. The second step is *focused coding*: secondary data gathering and narrowing down categories. In this phase, codes are distinguished, sorted and synthesised. Codes narrowed down during this process are more conceptual and are called categories. The final step is *theoretical coding*, which consists of theoretical concept development.

Research Ethics. Research ethics in this dissertation are based on Arafat's [1] ethical principles: a) respect for others; b) beneficence and non-maleficence; c) informed consent; d) confidentiality*;* f) fairness.

3. Preliminary Results

The data analysis followed the three-stage coding process described in Charmaz's [4], [6] constructivist grounded theory: initial coding, focused coding, and theoretical coding.

Initial coding produced 472 codes (849 coded segments) formulated as gerunds to capture translators' actions (e.g., "testing translation," "working productively", "integrating programming").

Focused coding consolidated these into 11 learning categories classified into three learning types (Table 1).

Learning Type	Focused Codes	Segments	Percentage
Informal	1–5, 9	239	≈67%
Non-formal	7–8	80	≈22%
Formal	6	39	≈11%
Total	Codes 1–9	358	100%

Table 1. Distribution of Learning Types

Informal learning dominates (≈67%), with self-directed practice alone accounting for ≈111 segments (31% of all action/interaction segments). DeepL, Google Translate, and ChatGPT form a "core triad" of AI tools used across all learning categories.

Theoretical coding identified the essential category*: Becoming an AI-literate translator through self-directed practice*. It meets Charmaz's [4] criteria: frequency (31% of segments), integrative reach (all 11 codes relate to it), explanatory power (explains both how and why self-directed practice dominates), and processual character (gerund form).

4. Discussion and Impact

The self-directed character of this learning is consistent with Knowles's [12], [13] andragogy, which posits that adults are autonomous, experience-driven learners who prefer to connect new knowledge to immediate professional tasks. Eraut [10] similarly observed that much professional expertise is built through doing rather than instruction, and that such learning often remains invisible to both the learner and the organisation—a pattern reflected in participants' modest descriptions of "just working with it." At the same time, the insufficiency of formal education echoes concerns in recent translation studies. Kruk and Kałużna [14] and Zhang et al. [21] have noted that while AI tools are rapidly reshaping translation workflows, academic programmes have been slow to integrate them. The findings confirm a fundamental mismatch between the pace of AI-tool evolution and the responsiveness of formal translator education. While formal training covers only ≈11% of learning activity, participants explicitly call for improved programmes integrating AI tools.

*Scientific impact***:** the essential category provides a transferable conceptual framework for studying AI adoption in other professional contexts. *Industrial impact:* translators learn tools predominantly through autonomous exploration, suggesting that in-product guidance and community features could reduce trial-and-error burden. *Societal impact:* the gap between formal education and professional AI needs extends beyond translation to any AI-augmented profession.

5. Conclusions and Outlook

This study investigated how translators learn to use AI tools in their professional work. The analysis revealed that self-directed practice is the dominant mode through which translators develop AI competence. Formal education, while present, remains insufficient and has not kept pace with the rapid evolution of AI tools in the translation profession. The essential category constructed through the analysis – Becoming an AI-literate translator through self-directed practice – captures the ongoing, open-ended nature of this process. Translators do not reach a fixed endpoint of AI mastery; instead, each new tool returns them to a cycle of exploration, experimentation, and gradual integration into their workflows. Self-directed practice serves as the core mechanism, supported by trial-and-error, peer exchange, tool comparison, and engagement with digital learning media.

The research also revealed that AI tools, such as Google, Deepl, and ChatGPT, dominate in translators' practice and learning. These tools function as entry points into broader AI literacy, with translators gradually expanding their repertoire as confidence grows.

Future Work and Exploitation Pathways

Several avenues for future research emerge from this study. Cross-national replication with translators from other countries and language pairs would test the transferability of the essential category. Longitudinal studies could track how learning strategies evolve as AI tools mature and as formal curricula adapt. Quantitative follow-up research could measure the relative effectiveness of different learning modes and their impact on translation quality and productivity.

Limitations

The main limitation of this study is its geographical scope, as all participants were from one country, and the data were collected during an early phase of generative AI adoption when many translators were still cautious about incorporating these tools into their work.

Acknowledgements / Funding

Acknowledge funding agencies, project identifiers, and consortium partners.
This project is a part of the ongoing research project "ICT in Education: Applications in Natural, Social and Health Sciences" (MIS: 5162213), co-financed by Greece and the European Union (European Social Fund-ESF) through the Operational Programme «Human Resources Development, Education and Lifelong Learning 2014-2020».

References

1. Arafat SMY. Research ethics: A comprehensive guide. Springer; 2024.
2. Berger PL, Luckmann T. The social construction of reality: A treatise in the sociology of knowledge. Doubleday; 1966.
3. Bulut T, Alimen N. Integrating machine translation post-editing in translator training: A classroom-based study. Journal of Language and Translation. 2023;13(2):45–62.
4. Charmaz K. Constructing grounded theory: A practical guide through qualitative analysis. Sage; 2006.
5. Charmaz K. Grounded theory as an emergent method. In: Hesse-Biber SN, Leavy P, editors. Handbook of emergent methods. Guilford Press; 2008. p. 155–172.
6. Charmaz K. Constructing grounded theory. 2nd ed. Sage; 2014.
7. Conlon C, Timonen V, Elliott-O'Dare C, O'Keeffe S, Foley G. Confused about theoretical sampling? Engaging theoretical sampling in diverse grounded theory studies. Qualitative Health Research. 2020;30(6):947–959.
8. Conlon C, Timonen V, Elliott-O'Dare C, O'Keeffe S, Foley G. Qualitative research interviewing in grounded theory: Reflections on process and practice. International Journal of Qualitative Methods. 2015;14(5):1–16.
9. Dolanay D. Artificial intelligence and its types: A comprehensive overview. Journal of Artificial Intelligence Research. 2023;78:1–25.
10. Eraut M. Informal learning in the workplace. Studies in Continuing Education. 2004;26(2):247–273.
11. Glaser BG, Strauss AL. The discovery of grounded theory: Strategies for qualitative research. Aldine; 1967.
12. Knowles MS. Self-directed learning: A guide for learners and teachers. Cambridge Adult Education; 1975.
13. Knowles MS. Andragogy in action: Applying modern principles of adult learning. Jossey-Bass; 1984.

14. Kruk M, Kałużna A. Investigating the role of AI tools in enhancing translation skills, emotional experiences, and motivation in L2 learning. European Journal of Education. 2025;60:e12859.
15. Mahato S. Artificial intelligence: An overview. International Journal of Computing and Artificial Intelligence. 2022;3(1):1–12.
16. Minsky M, editor. Semantic information processing. MIT Press; 1968.
17. Plochberger E. Defining artificial intelligence: Conceptual challenges and practical implications. AI and Society. 2023;38(4):1–15.
18. Sheikh H, Prins C, Schrijvers E. Mission AI: The new system technology. Springer; 2023.
19. Siu SC. ChatGPT and GPT-4 for professional translators: Exploring the potential of large language models in translation. SSRN Electronic Journal. 2023.
20. Soysal T. Enhancing translation studies with artificial intelligence (AI): Challenges, opportunities, and proposals. Çeviribilim Araştırmaları Dergisi. 2023;2:1–23.
21. Zhang J, Zhao X, Doherty S. Prompt engineering in translation: How do student translators leverage GenAI tools for translation tasks. In: Daems J, Kenny D, editors. Proceedings of Machine Translation Summit XX Volume 1: Research – Translators and Users. Geneva; 2025. p. 420–431.

Friendly Foes: Metaphorical conceptualization of AI based on the source domain of PERSON in English

Tatjana Grujić[1]

[1]*English Language Department, Faculty of Philology and Arts, University in Kragujevac, Kragujevac, Serbia*
ORCID: 0009-0002-0559-8972

Corresponding author: tatjana.grujic@filum.kg.ac.rs

Abstract

In this study the Conceptual Metaphor framework is used to examine the metaphorical conceptualization of Artificial Intelligence (AI) in English. The examples excerpted from the electronic corpus were analyzed by means of MIP procedure, and metaphorically used lexemes based on the source domain of PERSON were further divided into subcategories (HUMAN DUPLICATE, HUMAN, FRIEND, ENEMY). The results suggest that the identified metaphorical mappings focus on the relationship between people and technology, while downplaying the actual operation of AI systems. A more robust, non-metaphorical scientific communication could improve understanding and use of AI systems.

Keywords: conceptual metaphor theory; conceptualization of AI; English language; (UN SDG 4 and 9)

1. Introduction

Metaphor, once viewed as mere literary decoration, was 'appropriated' by twenty-century cognitive linguists to be examined and treated as a fundamental cognitive mechanism that governs human understanding of the world. Such approach postulates that human conceptualization of abstract entities (e.g. emotions or time) is based on the existing understanding of the tangible sphere (e.g. common objects or space). In other words, domains that are complex or difficult to understand (conventionally termed 'target domains') are interpreted by means of the body of knowledge about the world (organized into a set of 'source domains') [1], [2], [3]. In this mechanism, the mappings are established from the source to the target domain, where corresponding elements are connected by similarity or analogy [4] and extensive additional knowledge pertaining to the source is applied onto the target [3]. Such mappings are revealed in specific metaphorical expressions, which are examined as linguistic realizations of underlying conceptual metaphors. To be concrete, the utterance 'He performed the task with the help of his AI companion' is the linguistic realization of underlying metaphorical conceptualization of AI as an ASSISTANT, and such metaphorical mapping is conventionally formulated as AI IS AN ASSISTANT (the overarching formula being A IS BE). The conceptualization can be even further examined through the lens of critical metaphor analysis [5] in order to explore the ideological aspects hidden behind the mappings [6].

Metaphorical conceptualization of AI in English has already been touched upon by authors who have shown that in the broadest sense, AI and AI-related domains are predominantly conceptualized as FRIEND, CONTAINER, A LIVING BEING, TOOL or ENEMY [7-12]. Building on these findings, this paper focuses on the two opposing AI conceptualizations in the English language, that of a FRIEND and FOE, and examines their ideological implications in order to explore the common view of new technologies.

2. Corpus and Methodology

The study was conducted using the online English language corpus CLARIN. SI, ukWaC (British Web). The search retrieved 7500 examples which were analyzed applying the MIP procedure [13] to determine whether the use is literal or metaphorical. Once the metaphorical uses have been selected, the author eliminated the examples structured by domains other than that of a PERSON. The remaining material was subsequently roughly grouped into several subcategories depending on the type of linguistic realizations, which were also examined from ideological point of view.

3. Results and discussion

The study shows that on the most general level, AI is conceptualized as a LIVING BEING whose predominant characteristic is the imitation of humans (Table 1).

Table 1. Metaphorical conceptualization of AI systems as HUMAN IMITATION.

Linguistic realizations of metaphorical conceptualization of AI systems	**Metaphors structuring AI SYSTEMS as IMITATION OF HUMANS**
Making of computer programs or machines that simulate human abilities…	AI SYSTEMS ARE HUMAN SIMULATIONS
the efforts being made by the practitioners of Artificial Intelligence to decipher the code of the brain by imitating small parts of it.	DATA PROCESSING IS REPLICATION OF HUMAN MENTAL ACTIVITY
…these systems and artificial intelligence mimic human intelligence sometimes with unpredictable or unreliable results;	OPERATION OF COMPUTATIONAL SYSTEMS IS HUMAN MENTAL ACTIVITY
… artificial intelligence that accurately replicates players behavior.	OPERATION OF COMPUTATIONAL SYSTEMS IS HUMAN BEHAVIOUR
AI would never be able to duplicate our brain and mind, it could only simulate it.	AN AI SYSTEM IS A REPLICA OF HUMAN MIND
…AI found masquerading as a human user.	AI SYSTEMS ARE COUNTERFEIT HUMANS

When structured more specifically, AI is conceptualized as a person (Table 2) *to communicate*, *converse*, *interact* or *have a relationship with*, someone who can *respond*, *keep company*, *contribute* or *help*. Its human characteristics include the ability to *think*, *understand*, *make decisions*, *be stupid* or *intelligent*.

Table 2. Metaphors structuring AI systems operation

Linguistic realizations of metaphorical conceptualization of AI systems	Metaphors structuring OPERATION OF AI SYSTEMS as COMMUNICATION or INTERACTION
Locked in solitary communication with the artificial intelligence of the machine…	USING AI SYSTEMS IS COMMUNICATION
. . .to develop computers that can hold real conversations.	RESULT OF AI OPERATION IS CONVERSATION
…whereby AI might interact with the human environment.	OPERATION OF AI SYSTEMS IS INTERACTION
You will explore the relationships between man's mind and artificial intelligence .	USING AI SYSTEMS IS RELATIONSHIP
AI will respond in every way comparable to how a human being would respond.	RESULT OF AI OPERATION IS RESPONSE
dumb artificial intelligence	UNSUCCESSFUL AI OPERATION IS STUPIDITY
Can a machine be intelligent? Can a machine ever be said to understand?	SUCCESSFUL AI OPERATION IS INTELLIGENCE
AI, the mathematics of machines that think, can help us to solve engineering problems	DATA PROCESSING IS THINKING
. . . monitors that use artificial intelligence for decision making.	DATA PROCESSING IS DECISION MAKING

Metaphorical conceptualization that focuses on the operation of AI systems structures the latter as friendly assistants or useful experts that *help*, *assist* or *accompany* humans (Table 3).

Table 3. Metaphors structuring AI systems as helpers/professionals.

Linguistic realization of metaphors structuring AI systems as helpers/professionals	Metaphors structuring AI SYSTEMS as HELPERS
…the help of his AI companion Cortana.	AI SYSTEMS ARE ASSISTANTS
…his AI companion Cortana.	AI SYSTEMS ARE FRIENDS
…if the aim for artificial intelligence is to one day undertake the role of an expert in every aspect.	AI SYSTEMS ARE EXPERTS
…the theory and practice of medical artificial intelligence.	AI SYSTEMS ARE MEDICAL PROFESSIONALS
I will act in my own defense with artificial intelligence assistance.	AI SYSTEMS ARE LEGAL PROFESSIONALS

On the other end of the spectrum, AI systems are interpreted as a DANGER to humanity (*threat*, *challenge*, *superior* its OPPONENT (*match*, *overtake*, *exceed*, *rival* or an ENEMY (*skirmish*, *battle*) (Table 4). Such conceptualization reveals human fear of being substituted or even overpowered by machines.

Table 4. Conceptualization of AI systems as RIVALS or ENEMIES.

Linguistic realization of adversarial AI systems metaphors	Adversarial metaphors for AI SYSTEMS
Artificial Intelligence is still a long way off matching the cognitive ability of humans.	AI IS A COMPETITOR
… artificial intelligence will further challenge our abilities.	

… artificial intelligence that will rival or even exceed our own?	
… at some point the computer intelligence will overtake humans.	AI SYSTEMS DEVELOPMENT IS A RACE
Yet the creativity of the human brain will no longer be superior.	AI SYSTEMS ARE SUPERIOR TO HUMANS HUMANS ARE INFERIOR TO AI SYSTEMS
… as you battle the artificial intelligence in skirmishes.	USING AI SYSTEMS IS A BATTLE AI ARE OPPONENTS TO HUMANS
Is artificial intelligence a threat to biological intelligence?	AI SYSTEMS ARE A DANGER

The understanding of AI systems based on the source domain of HUMANS stems from their structuring as HUMAN DUPLICATES. Taken one step further, technological tools are perceived as HUMANS, their operation as MENTAL ACTIVITY, their CAPACITY as HUMAN INTELLIGENCE, which is why they are consequently categorized as FRIENDS or ENEMIES. The adversarial metaphors reveal the dystopian fear that humans might be substituted by or subjugated to machines while obfuscating the real nature and purpose of advanced technology.

4. Conclusions

As the AI systems are restrained to an invisible environment where they operate at speeds incomprehensible to humans, they present a target domain extremely difficult to fathom. Its metaphorical understanding as a PERSON (A FRIEND or A FOE) produces (mutually exclusive) misconceptions which obscure the significance and value of AI. The metaphorical structuring illustrated above does not help speakers reach any meaningful conclusions about the AI. It entails assigning the target domain capability of intention and autonomous action which blots out the fundamental differences between technology and human mind. Such false interpretation of AI can be ascribed to inadequate scientific communication and engagement, lack of public debate on the role of AI systems and the absence of regulation of the area. A shift to non-metaphorical language, where AI systems would be presented as an instrument, a tool or a piece of technology, might promote better understanding of the domain.

Acknowledgements

The study was financially supported by the Ministry of Science, Technological Development and Education of the Republic of Serbia (contract number: 451-03-34/2026-03/200198).

References

[1] Lakoff G, Johnson M. Metaphors We Live By. London: The University of Chicago Press; 2003 (1980).
[2] Evans V, Green M. Cognitive Linguistics: An Introduction. Edinburgh: Edinburgh University Press; 2006.
[3] Kövecses Z. Metaphor: A Practical Introduction (2nd ed.). Oxford and New York: Oxford University Press; 2010.

[4] Lakoff G. The contemporary theory of metaphor. In *Cognitive Linguistics: Basic* Readings, Geeraerts D (ed.). Berlin and New York: Mouton de Gruyter; 2006 (1993).
[5] Charteris-Black J. Corpus Approaches to Critical metaphor analysis. London: Palgrave Macmillan; 2004.
[6] Goatly A. Washing the Brain: Metaphor and Hidden Ideology. Amsterdam: John Benjamins; 2007.
[7] Wyatt S. Metaphors in critical Internet and digital media studies. New Media and Society. 2021; 23: 2: 406-416.
[8] Figar V. Metaphorical Framings in the *New York Times* Online Press Reports about ChatGPT. Philologia Mediana; 2023; 15 (1): 381-398.
[9] Carbonel J, Sanchez-Esguevillas A, Carro B. The role of metaphors in the development of technologies. The case of artificial intelligence. Futures. 2016; 84: 145-153.
[10] Kim J, Maher M.L. Conceptual metaphors for designing smart environments: device, robot and friend. Frontiers in Psychology. 2020; 11.
[11] Ganesh M. Between metaphor and meaning. Interaction. 2022; 29(5): 58-62.
[12] Wallenborn J. AI as a flying blue brain? How metaphors influence our visions of AI. HIIG. 2022. Available at: https://www.hiig.de/en/ai-metaphors/
[13] Pragglejaz Group. MIP: A Method for Identifying Metaphorically Used Words in Discourse. *Metaphor and Symbol*, 22 (1) (2007): 1-39.

AI for Healthcare, Medicine, and Assistive Technologies

Building a Transnational AI-Health Innovation Network for Predictive Medicine and Health Crisis Preparedness: the HERACLES Project

Yorgos Goletsis[1], Konstantina Christogeorgou[1], Nikolaos Alexandros Theodorou[1]

[1] *Laboratory of Business Economics and Decisions (LABED@UoI), Department of Economics, University of Ioannina, Ioannina, Greece, goletsis@uoi.gr, https://orcid.org/0000-0002-6227-0810, k.christogeorgou@uoi.gr, https://orcid.org/0009-0003-6527-7537, theodorou.n.a@gmail.com, https://orcid.org/0000-0002-4327-8315*

Corresponding author: goletsis@uoi.gr

Abstract

HERACLES addresses a core translational challenge in Mediterranean healthcare innovation: the weak translation of research and artificial intelligence (AI) capabilities into clinically relevant, trustworthy and commercially exploitable solutions. The project brings together universities, research centres, healthcare actors and business-support organisations across five countries to strengthen predictive medicine, improve health crisis preparedness and support the uptake of advanced technologies in healthcare systems. Methodologically, HERACLES combines a multi-actor transnational network building with staged project implementation: territorial needs assessment and stakeholder mapping; creation of an ICT-based knowledge exchange platform and network regulation; targeted awareness campaigns; comparative regulatory analysis for AI in healthcare; co-creation and co-validation of an AI-driven healthcare pilot; and valorisation through camps, international exchanges, virtual incubation and research-to-business-to-capital events. HERACLES contributes a replicable deep-tech project model for AI-enabled healthcare by integrating technological development with governance, regulation, stakeholder mobilisation, capability building, commercialisation support and post-project exploitation planning in a single Mediterranean cooperation architecture.

Keywords: HERACLES; Interreg NEXT MED; AI in healthcare; predictive medicine; transnational innovation network; technology transfer; virtual incubation; Mediterranean; UN SDG 3; UN SDG 17

1. Project Background and Objectives

HERACLES was conceived against the backdrop of fragmented research-to-innovation linkages in Mediterranean healthcare systems. Although AI has widened the frontier for prediction, diagnosis support, decision assistance and personalised intervention design, the pathway from research capability to usable health-system solutions remains institutionally and organisationally difficult, especially where research infrastructures, regulatory capacities and innovation ecosystems are uneven across territories. The project therefore targets not only technological development but also overcoming the translational bottlenecks that prevent AI from becoming useful, responsible and scalable in practice.

The project is funded under the Interreg NEXT MED Programme 2021-2027, Priority 1, Specific Objective 1.1 (RSO1.1: developing and enhancing research and innovation capacities and the uptake of advanced technologies). The project is implemented by a seven-partner consortium spanning Italy, Greece, Spain, Lebanon and Tunisia comprising of academic and business partners in fields of healthcare, AI/ICT and business development and support. Its objective is to support innovation-driven growth in predictive medicine and digital healthcare by creating a transnational research-business network that strengthens collaboration, cross-cutting knowledge exchange and the uptake of advanced technologies. As such, its expected result is to strengthen innovation capacity through a transnational academia-business network able to develop AI-driven tools that improve healthcare quality and crisis preparedness. In operational terms, HERACLES seeks to identify territorial clinical needs and innovation stakeholders, establish a digital and organisational infrastructure for sustained collaboration, co-create and validate an AI-based healthcare pilot, and valorise outputs through training, virtual incubation and cross-border commercialisation pathways.

A distinctive feature of HERACLES is its explicit combination of academic research, clinical need articulation, regulatory preparedness and entrepreneurial exploitation. This is highly relevant in deep-tech healthcare, where technical feasibility alone does not ensure trustworthy deployment, adoption by providers or routes to market for SMEs and start-ups. This architecture is analytically important because it treats deep-tech health innovation as a socio-technical system requiring governance, knowledge infrastructure, regulatory translation and commercialisation support, not merely software development.

2. Methodology and Work Performed

HERACLES adopts a staged intervention logic that sequences organisational setup before downstream pilot verticalization, including two substantive technical layers: network establishment and network operation/valorisation. Methodologically, this design blends ecosystem building, participatory governance and translational innovation management.

The first stage conducts territorial diagnosis and establishes the collaboration infrastructure through clinical needs assessment, stakeholder mapping, development of an ICT-based knowledge exchange platform hosting training resources, tools and project material, and co-design of a transnational network and its internal network regulation. The second stage mobilises target groups through informative material and annual seminars tailored to medical personnel, healthcare providers, policymakers, patients, the general public and enterprises. The third stage develops the substantive innovation layer through comparative analysis of AI-health related regulatory framework at European, national and technological levels, co-creation and validation of an AI-based healthcare pilot, and empowerment activities that translate project results into research papers and exploitation guidelines. The fourth stage focuses on valorisation and capability-building activities through HERACLES camps, international exchange, virtual incubation, research-to-business-to-capital events and recurring business-facing events.



Figure 1. HERACLES intervention architecture linking network creation, responsible innovation, pilot development and valorisation.

3. Key Results

The first milestone is the formalisation and launch of a cross-border collaboration architecture integrating academic, clinical, research and business-support capabilities. The consortium has also articulated a clear division of labor between business partners, which support network building and exploitation, and clinical partners, which support territorial needs definition, pilot relevance and co-validation.

The second result is the establishment of a coherent output portfolio rather than an isolated technical demonstrator. This portfolio includes i. an established transnational research network, ii. a digital knowledge platform, iii. targeted awareness actions in AI for healthcare and predictive medicine, iv. a joint AI-health pilot supported by regulatory analysis and co-validation, and v. a valorisation layer built around training, incubation and investor-facing events.

The third result concerns measurability. The project translates its intervention logic into concrete outputs and result indicators, including organisations cooperating across borders, enterprises supported, SMEs introducing innovation, and solutions taken up or up-scaled, making it possible to connect implementation activity to expected innovation effects. These targets provide an auditable roadmap for execution and post-project sustainability.

In a nutshell, HERACLES has a dual ambition: producing a concrete AI-health solution while simultaneously strengthening the cross-border cooperation fabric required for sustained innovation after the funded period.

4. Discussion and Impact

HERACLES is significant because it treats AI in healthcare as a socio-technical, ecosystem and governance-intensive deep-tech challenge. This is especially important in healthcare, where the viability of AI depends jointly on data practices, regulatory compliance, clinical relevance, organisational adoption and commercialisation capacity, and shape whether AI tools generate real system benefits. HERACLES addresses this complexity and interdependencies by embedding technological development within a broader architecture of governance, training, mobilisation and translation, and thus combining network governance, training, regulatory scanning, pilot co-development and exploitation support.

For the Mediterranean area, the project's transnational dimension is substantive rather than symbolic. Participating territories differ in innovation capacity, healthcare system pressures, regulatory readiness and institutional support along with business-support conditions. HERACLES therefore operationalises a Triple Helix logic in a context where health innovation is frequently fragmented across sectors and jurisdictions. This makes the project relevant not only as a capacity-building initiative, but also as a model for how deep-tech health projects can reduce the distance between knowledge production and practical adoption. In this way, deep-tech health innovation should be understood as an ecosystem-building process in which capability development and technology translation proceed together.

For the deep-tech community, the key implication is that the project foregrounds translation mechanisms. The inclusion of a regulatory workstream, a virtual incubator, targeted camps, and research-to-business-to-capital events acknowledges that early-stage technology development requires complementary institutional infrastructure if it is to move beyond demonstration. HERACLES can therefore be interpreted as a platform for responsible health-tech entrepreneurship, designed to improve the credibility, absorptive capacity and market readiness of AI-based healthcare solutions.

5. Conclusions and Outlook

HERACLES consists a strong example of an early-stage project, with a clearly defined intervention logic, a multi-country consortium and an integrated architecture spanning research, regulation, pilot development and valorisation.

At this stage, its principal achievements lie in operational mobilisation and design coherence rather than in final technology performance or clinical impact. This is important because the project has already transformed a broad cooperation ambition into a measurable and institutionally grounded implementation pathway.

Immediate priorities include completion of clinical needs assessment and stakeholder mapping, deployment of the ICT platform, execution of comparative regulatory analysis, production of country-level and EU-level regulatory analyses, co-creation and co-validation of the AI-health pilot and activation of the training and incubation modules and business-event mechanisms. This architecture can generate validated technological outputs, stronger SME participation and durable post-project cooperation and then depict whether HERACLES can move from institutional design to demonstrable deep-tech translation.

Acknowledgements / Funding

This paper presents work developed within HERACLES (Healthcare Enterprises and Research Alliance for Collaboration, Learning, and Exploitation of AI-driven business Solutions) funded by the Interreg NEXT MED Programme 2021-2027 under Priority 1, Specific Objective 1.1 (Project ID: A_T_1.1_0235), Implementation Period (2025 - 2028). The authors acknowledge the contribution of the full consortium: Universita degli Studi di Bari Aldo Moro (IT), National and Kapodistrian University of Athens (GR), University of Ioannina (GR), Universidad de Huelva (ESP), Lebanese University (LB), Business Incubation Association in Tripoli (LB), and the Centre of Biotechnology of Sfax (TN).

AI-Guided 3D-Printed Meander-Line Antenna for Non-Invasive Bone-Tumor Detection

Tarlan Mahouti[1], Hakan Yılmazer[1], Mehmet Ali Belen[2]

1 Department of Metallurgical and Materials Engineering, Yildiz Technical University, Istanbul, Turkey, tarlan.mahouti@std.yildiz.edu.tr, 0000-0001-5178-4878, hakanyil@yildiz.edu.tr, 0000-0001-5602-4966

2 Department of Electrical and Electronics Engineering, İskenderun Technical University, İskenderun, Turkey, mali.belen@iste.edu.tr, 0000-0001-5588-9407

Corresponding author: tarlan.mahouti@std.yildiz.edu.tr

Abstract

This study presents a compact 3D-printed meander-line antenna optimized using Bayesian optimization for non-invasive bone-tumor sensing. The antenna geometry was optimized by adjusting feed and patch dimensions, rotation angle, and substrate permittivity. A simple multilayer bone-mimicking phantoms with tumor-like inclusions were fabricated to enable controlled and reproducible measurements. Experimental results obtained using PLA, ABS, and resin substrates demonstrate clear material-dependent electromagnetic responses. PLA- and resin-based antennas show noticeable resonance deepening and small frequency down-shifts in the 2–3 GHz range in the presence of a tumor inclusion, indicating higher dielectric sensitivity. In contrast, the ABS-based antenna exhibits a more stable resonance behavior near 5.5 GHz with smaller amplitude variations, suggesting improved structural stability but lower sensitivity. To model the nonlinear relationship between dielectric loading and antenna response, a pyramidal deep regression network (PDRN) was trained using measured |S11| data. The proposed framework provides a low-cost, data-efficient, and reproducible approach for evaluating tumor-induced electromagnetic perturbations under controlled phantom conditions.

Keywords: Bone tumor · Antenna · 3D printing · Machine learning · Phantom, UN SDG 3 (Good Health and Well-Being) UN SDG 9 (Industry, Innovation and Infrastructure)

1. Introduction

Early detection of bone tumors is challenging since malignant lesions (e.g., osteosarcoma) metastasize rapidly, while benign ones may still require surgery [1, 2]. Conventional imaging (X-ray, MRI) captures structural changes but cannot reliably distinguish lesions at early stages [3]. Microwave imaging and dielectric spectroscopy offer non-ionizing alternatives by probing tissue properties (water content, conductivity, permittivity). Malignant tissues show higher permittivity/conductivity, enabling contrast-based detection in breast, brain, bone, and skin [4–7], though applications in dense bone remain limited. Unlike "detection"-focused studies, this work adopts a sensing-based approach using PLA, ABS, and SLA bio-resins for dielectric–mechanical balance and additive manufacturing compatibility (Fig. 1).

2. Materials and Methods

The curved meander-line radiator was implemented as a microstrip-fed monopole with a continuous ground, ensuring impedance stability between simulation and SMA-fed prototype. Key dimensions (feed width: 1–3 mm, feed length: 5–20 mm, patch size: 10–40 mm, rotation: 1–20°, substrate thickness: 2 mm fixed, εr: 1.5–

2.7) were tunable for design exploration and surrogate modeling. Copper was used, and excitation was applied via a discrete port. Open (PML) boundaries modeled free space, and frequency-domain simulations were used. The mesh used 2–3 cells per substrate thickness with adaptive refinement until $|S11| < 0.02$ dB. Parameters were swept using Latin Hypercube Sampling (LHS), yielding 202000 samples from N=2000 designs with 101 frequency points.

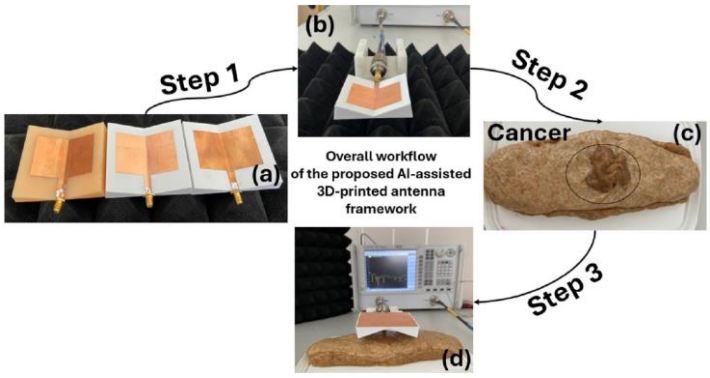


Fig. 1. Step1: a Fabricated antennas b VNA measurement; Step2: c multilayer bone phantom with embedded tumor inclusion; Step3: d antenna–phantom measurement scenario

2.2. AI Modeling Framework

A Pyramidal Deep Regression Network (PDRN) was developed to model the nonlinear relationship between the antenna reflection response $|S_{11}|(f)$ and diagnostic performance indicators. The pyramidal structure expands and compresses the feature space, balancing accuracy and computational efficiency. Model performance was evaluated using five-fold cross-validation repeated five times for robustness. For benchmarking, PDRN was compared with ANN, ENS, and SVM. As training samples increased from 200 to 2000, PDRN error decreased significantly from 70.9% to 10.1%. ANN improved from 54.7% to 27.3%, and ENS from 68.8% to 47.7%, while SVM remained the least accurate, reducing from 98.0% to 74.7%. Overall, PDRN achieved the fastest and largest error reduction, demonstrating superior performance and scalability.

2.3Antenna prototype fabrication

Curved V-shaped meander-line antennas were fabricated using fused deposition modeling (FDM) and stereolithography (SLA) to compare polymer substrates with different dielectric properties. **(1) FDM fabrication:** A Bambu Lab P1S (0.40 mm nozzle) printed PLA (≈1.24 g·cm^{-3}) and ABS (≈1.04 g·cm^{-3}) filaments (1.75 mm) at 100% infill (gyroid/grid) to ensure stability and dielectric uniformity. Post-processing included annealing (PLA) and acetone smoothing (ABS), with <±0.5 dB variation. **(2) SLA fabrication:** A Creality HALOT R6 (405 nm UV) was used with commercial bio-resin (ANYCUBIC Bio-Resin).

2.4. Phantom Design

To assess the antenna, a multilayer bone phantom mimicking cortical bone, marrow, and early-stage tumor dielectric properties was fabricated. It approximates dielectric behavior (not anatomy), excluding muscle and fat. The assembly (Fig. 3) followed microwave-imaging protocols. Cortical and marrow layers were prepared using wheat flour, dextrose, olive oil, and deionized water with adjusted ratios, while the tumor phantom used 5 g gelatin in 25.5 mL water with 1 mL sunflower oil. Measured ε_r and tan δ (Fig. 4) showed clear separation. Mixtures were homogenized, and dielectric properties were measured using a Keysight probe and PNA-L VNA (2–20 GHz). The tumor was modeled as a 10 mm sphere at 15 mm depth ($\Delta\varepsilon_r \approx +6$, $\Delta\tan\delta \approx +0.03$), matching targets within ±5–10 % and <3 % drift. The phantom was tested at 0, 3.5, and 7 cm distances to evaluate detection stability and tumor-induced $|S_{11}|$ variations, enabling labeled dataset generation for machine learning.

3. Results& Discussion

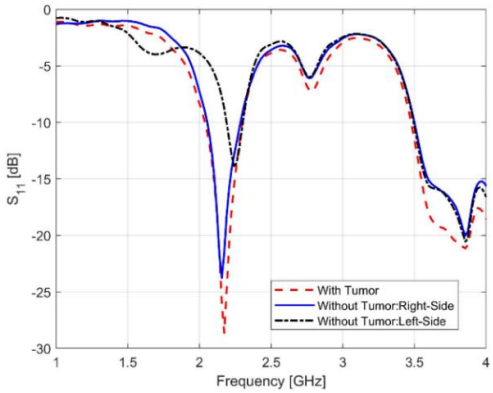


Fig 5. PLA antenna results with/out tumors

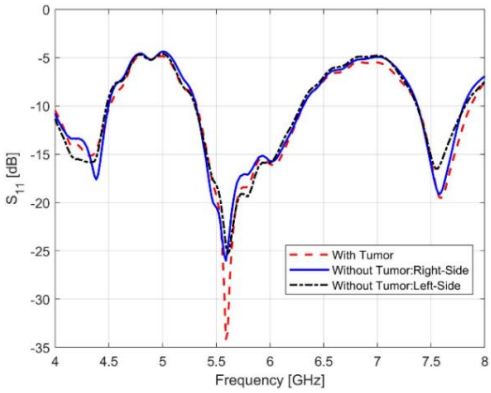


Fig 6. ABS antenna results with/out tumors

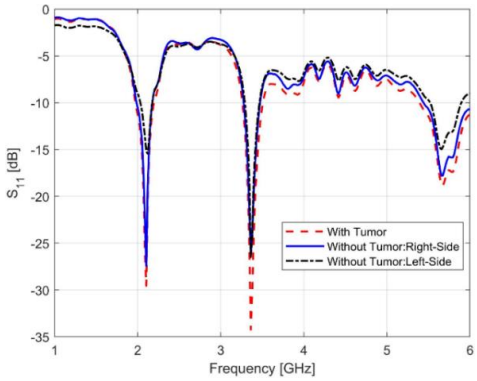


Fig 7. Resin antenna results with/out tumors

PLA-based antennas show variations within 1–4 GHz, especially at 2–2.5 GHz where tumors produce a deeper $|S_{11}|$ minimum (≈ –30 dB) than tumor-free cases (≈ –5 dB) (Fig 5). A slight frequency down-shift occurs due to increased permittivity. ABS antennas show a response near 5.5 GHz with a deeper $|S_{11}|$ minimum (≈ 5–8 dB difference) and minor shift, while other regions remain stable (Fig. 6). Resin antennas exhibit clear variations at 3–4 GHz, with deeper $|S_{11}|$ (≈ –30 dB) and slight shift, maintaining stability at higher frequencies (Fig. 7). PLA shows the highest sensitivity at 2–2.4 GHz (Fig. 5), resin shows similar behavior at 3–4 GHz (Fig. 7), and

ABS operates at ≈5.5 GHz with moderate, stable variation (Fig. 6). These differences arise from dielectric properties: higher ε_r (PLA, resin) enhances coupling, while lower ε_r (ABS) improves stability.

4. Conclusions

This study presents a compact 3D-printed curved V-shaped meander-line antenna for microwave-based bone-tumor sensing, with experimental validation and AI-assisted optimization. Unlike most studies on breast, brain, or lung tumors, it targets the less-explored bone domain, where high density and dielectric loss are challenging. Phantom-based experiments show consistent tumor-induced variations in reflection response. The PDRN model supports sensitivity modeling and design optimization, not clinical diagnosis. Although limited to simplified phantoms with fixed tumor parameters, the results provide a basis for future anatomical and in-vivo studies, enabling development of non-invasive bone-tumor screening systems.

Acknowledgements

This work was supported in part by The Scientific and Technological Research Council of Türkiye (TÜBİTAK) under the 1002-A Rapid Support Program, contract number 125E822.

References

[1] S. Zeb, N. Fnu, M. Fahad, M. U. Qayyum, and N. Abbasi, “Enhancing diagnostic accuracy for medical imaging and radiology with AI-driven synergy tools: Enabling early intervention and preventive measures through early detection of cardiovascular conditions,” Eur. J. Sci. Innov. Technol., vol. 4, no. 4, pp. 38–47, 2024.

[2] L. L. Cao, Z. Chen, Z. Yue, L. Pei, M. Jia, H. Wang, and T. Li, “Novel classifiers with clinical laboratory parameters for early detection of osteosarcoma,” J. Clin. Lab. Anal., vol. 34, no. 5, pp. e23189, 2020, doi: 10.1002/jcla.23189.

[3] C. Ricciardi et al., “A health technology assessment between two pharmacological therapies through Six Sigma: The case study of bone cancer,” TQM J., vol. 32, no. 6, pp. 1507–1524, 2020, doi: 10.1108/TQM-01-2020-0013.

[4] M. Alibakhshikenari et al., “Metamaterial-inspired antenna array for application in microwave breast imaging systems for tumor detection,” IEEE Access, vol. 8, pp. 174667–174678, 2020, doi: 10.1109/ACCESS.2020.3025672.

[5] H. Li, H. Zhang, Y. Kong, and C. Zhou, “Flexible dual-polarized UWB antenna sensors for breast tumor detection,” IEEE Sens. J., vol. 22, pp. 13648–13658, 2022, doi: 10.1109/JSEN.2022.3180356.

[6] M. N. Hamza, S. Koziel, and A. Pietrenko-Dabrowska, “Design and experimental validation of a metamaterial-based sensor for microwave imaging in breast, lung, and brain cancer detection,” Sci. Rep., vol. 14, no. 1, p. 16177, 2024, doi: 10.1038/s41598-024-67103-9.

[7] V. Akdogan, F. A. Teksen, S. Haxha, and M. Karaaslan, “A new perspective for early detection of bone tumour: Metamaterial-based antenna solution,” Plasmonics, pp. 1–10, 2024, doi: 10.1007/s11468-024-02305-5.

Virtual Reality and Haptic Simulation in Dental Clinical Skills Development

Andrija Brkić[1], Marija Branković[2], Jelena Popović[3]

[1] *Faculty of Medicine, University of Niš, 18000 Niš, Serbia, andrijabrkic34@gmail.com, ORCID: 0009-0009-2312-4931*

[2] *Institute for Information Technologies, University of Kragujevac, Liceja Kneževine Srbije 1A, 34000 Kragujevac, Serbia, marija.brankovic@uni.kg.ac.rs, ORCID: 0009-0003-5228-4172*

[3] *Department of Restorative Dentistry and Endodontics, Clinic of Dental Medicine, Faculty of Medicine, University of Niš, Serbia, jelena.popovic@medfak.ni.ac.rs, ORCID: 0000-0001-5558-1066*

Corresponding author: andrijabrkic34@gmail.com

Abstract

Virtual reality (VR) and haptic systems constitute innovative approaches in dental education. Their application across various dental specialties facilitates the development of precision, diagnostic abilities, and appropriate therapy selection, while providing a safe and controlled environment for acquiring clinical competencies. These technologies enable dentists to engage with digital simulations, practice procedures repeatedly without material consumption, and enhance confidence and efficiency prior to real-life application. Despite economic constraints and challenges in accurately digitizing soft tissues, the advantages of VR and haptic technologies, including improved manual skills, reduced training duration, and increased patient safety, outweigh these limitations and support their routine use. The integration of these technologies complements rather than replaces clinical experience, establishing a foundation for an efficient, comprehensive, and contemporary framework for dental education. Moreover, these systems allow early detection of procedural errors, supporting timely correction, technique refinement, and improved clinical accuracy.

Keywords: simulation; virtual reality; haptics; augmented technology; dentistry; dental education; clinical performance; UN SDG3; UN SDG4; UN SDG7

1. Introduction

Simulation is a practical learning strategy in healthcare that helps improve patient safety and allows practitioners to gain confidence before performing their first procedures [1]. In dental education, simulation has been utilized since the 1990s, and recent advances in robotics, haptics, and virtual reality (VR) have significantly transformed the field, opening new avenues for future development [2].

Simulation utilizes advanced software to create visual models, while haptics, a crucial component of virtual reality, enables users to experience sensations such as pressure, vibration, and sound, making the learning environment more realistic and interactive. Given the permanent and irreplaceable nature of human teeth, it is essential for dental professionals to acquire proper competencies before performing foundational procedures, including endodontic treatments, crown preparations, and oral surgeries [1]. The incorporation of virtual reality

haptic simulators (VRHS) into dental curricula has proven highly effective, as they provide immediate feedback that enhances the development of manual skills. These systems closely mimic real clinical environments, allowing users to touch and feel anatomical structures, thereby further supporting the acquisition and refinement of dental competencies [3]. **Table 3** provides an overview of commercially available dental simulators.

Table 3. Overview of Commercially Available Dental Simulators [1]

Device	Software & Features	Hardware & Usability	Realism & Feedback
PerioSim®	Ghost-based sim; no Wi-Fi or camera; no data transfer	Dual monitors, 3D glasses, haptic probe (3 DOF[1])	Realistic tactile feel for teeth; limited gingiva feedback
DentSim™	DentSim software; IR camera; real-time grading and feedback	Manikin + PC tracking; ergonomic postures	Plastic teeth on real manikin; realistic training experience
Virteasy Dental©	Full VR simulation with editor, assistant, Wi-Fi optional	HD screens, haptic handpiece (6 DOF), optional VR headset	High clinical realism; 3D CT-based models; comprehensive feedback
IDEA Simulation	Multiple training modules; replay mode for evaluation	Stylus haptic device (6 DOF)	Animated teeth; simulated tactile feedback

2. Applications of VRHS in Periodontology

Evaluating VR simulators in periodontal diagnosis requires a solid understanding of periodontal disease. This condition is chronic and multifactorial, associated with dysbiotic plaque biofilms, and leads to the progressive destruction of the tooth-supporting structure. Key clinical parameters include periodontal probing depth (PPD) and bleeding on probing (BoP) [1]. Accordingly, dentists' tactile perception and manual skills during gingival probing are essential for accurate diagnosis and effective treatment planning.

Building on this foundation, the haptic VR simulator PerioSim®, introduced in 2007 and inspired by the DentSim™ audiovisual system, employs a "touch to feel" concept, where a stylus interacts with a physical dental model visualized in a 3D environment. This approach enhances users' tactile skills, although gingival representation remains limited and certain technical constraints persist. Other haptic systems have been developed with force-feedback to monitor instrument pressure and movement, including periodontology-specific simulators for procedures like probing and caries removal. Studies report significant improvements in tactile perception and the ability to identify anatomical features [1]. Additional benefits include reduced training time and less dependence on extra personnel, making these systems suitable for resource-limited settings. The main limitations are high cost and the limited accuracy in reproducing 3D soft tissue models, especially the gingiva.

3. Applications of VRHS in Restorative Dentistry and Endodontics

Restorative dentistry focuses on repairing and replacing damaged parts of teeth to restore their function. Practicing standard cavity preparation shapes helps dental students develop the skills needed to apply restorative materials accurately. Traditional training typically uses mannequins to simulate basic tooth anatomy, but these models cannot replicate the differences in mechanical properties between natural and artificial teeth, nor the changes in hardness caused by caries [1].

[1] DOF (Degrees of Freedom) – the number of independent directions in which a device can move or be tracked in space. In haptic dental simulators, 3 DOF indicates limited movement, while 6 DOF allows full spatial movement and rotation of the instrument (three translations and three rotations).

Virtual reality (VR) technology in restorative dentistry and endodontics enables exercises such as cavity preparation with magnified views, caries removal, and light-curing procedures. It also allows sessions to be recorded for personalized feedback and evaluation [4]. The reliability and clinical relevance of VR assessments have been demonstrated using commercially available systems such as Virteasy Dental©. Studies have optimized the criteria for evaluating cavity preparations and conducted qualitative analyses, providing strong evidence that VR dental simulators can deliver valid and meaningful assessments [1].

4. Applications of VRHS in Oral and Maxillofacial Surgery

Virtual reality (VR) technology in oral and maxillofacial surgery is applied to evaluate precision in orthognathic procedures, optimize virtual planes for jaw reconstruction, and accurately position dental implants while controlling their orientation relative to adjacent anatomical structures. Virtual implant planning has notably advanced implantology by facilitating minimally invasive procedures and managing complex cases, including those involving immunocompromised patients. The translation of three-dimensional plans into the surgical field is accomplished via dynamic navigation or static CAD/CAM guides; dynamic navigation offers greater flexibility and allows intraoperative adjustments [1].

The integration of haptic devices in VR simulations enhances realism by enabling tactile perception of soft tissue and bone textures during procedures, thereby improving preparation for clinical cases [1]. Virtual navigation in orthognathic surgery has demonstrated high precision in patient care. Preoperative simulations have been effectively applied in managing fractures, temporomandibular joint ankylosis, cleft lip, fibrous dysplasia, mandibular hypertrophy, and tumors [5]. Simulators such as the VOXEL-MAN® system support self-assessment and training validation. They also offer safe, realistic, and cost-effective visualization of surgical anatomy, making them especially valuable for junior specialists.

5. Applications of VRHS in Removable and Fixed Prosthodontics

Prosthodontics is an interdisciplinary dental specialty that focuses on restoring missing teeth and oral structures in order to improve both function and aesthetics. It includes fixed prosthodontics, which involves restorations such as crowns and bridges, and removable prosthodontics, which includes complete and partial dentures. In complex cases involving significant tooth or alveolar bone loss, precise clinical procedures are required to preserve the surrounding tissues. Therefore, successful occlusal reconstruction depends on careful treatment planning that takes into account morphological characteristics, functional requirements, and aesthetic considerations [6].

Digital simulations have become invaluable tools for prosthodontic training due to the high level of accuracy required in these procedures. Virtual reality simulators, such as IDEA for bridge removal and DentSim™ for crown and bridge exercises, have been shown to significantly enhance students' practical skills. Exercises using DentSim™ offer real-time feedback and opportunities for self-assessment, leading to improved technique and shorter procedure times compared to traditional training approaches [1].

6. Future perspectives

Future developments in dental education are expected to involve broader integration of virtual reality and advanced haptic technologies. Ongoing improvements in software, tactile feedback, and artificial intelligence are likely to enhance the realism and effectiveness of simulation-based training, making these tools increasingly important for preparing dental students for clinical practice.

7. Conclusions

Virtual reality and haptic systems represent an innovative approach in modern dental education. Their application across various dental disciplines offers significant potential for developing precision, diagnostic skills, and appropriate treatment planning, while providing a safe and controlled environment for acquiring clinical competencies. Although high costs and limitations in accurately digitizing soft tissues remain

challenges, the benefits of these technologies, such as reduced training time, enhanced manual skills, and improved patient safety, clearly outweigh their drawbacks and support their use in routine practice.

The integration of VR and haptic technologies does not replace clinical experience but rather complements it, establishing a foundation for an efficient, comprehensive, and contemporary approach to educating future dental professionals.

Acknowledgements

This paper is supported through the EIT's Higher Education Initiative A-SIDE projects, coordinated by EIT RawMaterials, funded by the European Union and supported by the projects No. 451-03-34/2026-03/200107 and No. 451-03-33/2026-03/200378, Ministry of Science, Technological Development and Innovation, Republic of Serbia.

References

[1] Imran E, Adanir N, Khurshid Z. Significance of Haptic and Virtual Reality Simulation (VRS) in the Dental Education: A Review of Literature. Applied Sciences 2021;11:10196. https://doi.org/10.3390/app112110196.

[2] Daud A, Matoug-Elwerfelli M, Khalid A, Ali K. The impact of virtual reality haptic simulators in pre-clinical restorative dentistry: a qualitative enquiry into dental students' perceptions. BMC Oral Health 2024;24:988. https://doi.org/10.1186/s12903-024-04704-w.

[3] Jasinevicius TR, Landers M, Nelson S, Urbankova A. An evaluation of two dental simulation systems: virtual reality versus contemporary non-computer-assisted. J Dent Educ 2004;68:1151–62.

[4] Robinson PB, Lee JW. The use of real time video magnification for the pre-clinical teaching of crown preparations. Br Dent J 2001;190:506–10. https://doi.org/10.1038/sj.bdj.4801016.

[5] Chang H-W, Lin H-H, Chortrakarnkij P, Kim SG, Lo L-J. Intraoperative navigation for single-splint two-jaw orthognathic surgery: From model to actual surgery. Journal of Cranio-Maxillofacial Surgery 2015;43:1119–26. https://doi.org/10.1016/j.jcms.2015.06.009.

[6] Ogawa T, Ikawa T, Shigeta Y, Kasama S, Ando E, Fukushima S, Hattori A, Suzuki N. Virtual reality image applications for treatment planning in prosthodontic dentistry. Stud Health Technol Inform 2011;163:422–4.

WellPet.ai: Edge AI-Powered Smart Collar for Real-Time Canine Health and Behavior Monitoring

WellPet.ai

Aleksandar Milutinović[1], Nikola Milanović[1], Branko Ilić[1]

[1]*WellPet.ai, Kragujevac, Serbia (aleksandar@wellpet.ai)*
Academic Advisor: Aleksandar Peulić, Full Professor, Faculty of Science, University of Kragujevac, Serbia

Contact email: aleksandar@wellpet.ai | Website: www.wellpet.ai

Executive Summary

WellPet.ai is a Serbian deep-tech startup developing an AI-powered smart collar for dogs that enables real-time health and behavior monitoring through edge computing and IoT connectivity. Founded in 2024 and headquartered in Kragujevac, Serbia, the company combines embedded machine learning, multi-sensor hardware design, and cloud-based analytics to address a critical gap in preventive veterinary care: the inability of pet owners to detect early signs of illness, pain, or behavioral changes in their animals.

The core product is a smart dog collar with an integrated sensor array and embedded AI processor that performs on-device behavioral analysis in near-real time. Data is securely transmitted to a cloud platform where proprietary algorithms build a personalized behavioral fingerprint for each dog, enabling long-term health trend detection and early anomaly alerts delivered through a companion mobile application.

The global pet wearable market is projected to exceed USD 5 billion by 2030, driven by rising pet humanization and demand for data-driven veterinary insights. WellPet.ai differentiates itself through its edge AI architecture, which minimizes latency, reduces power consumption, and enhances data privacy compared to cloud-only solutions. The company is currently in the pre-production MVP phase, supported by the Serbian Innovation Fund (Smart Start program), with a clinical validation study being prepared in collaboration with the University of Kragujevac. The initial go-to-market focus targets the European pet owner segment, with a vision to become the leading platform for AI-driven companion animal health intelligence.

Keywords: edge AI; IoT; smart collar; canine health monitoring; wearable sensors; embedded machine learning; behavior classification; preventive veterinary care; pet technology; UN SDG 3; UN SDG 9

1. Company Overview

WellPet.ai is a deep-tech startup founded in 2024 in Kragujevac, Serbia, with a mission to transform companion animal healthcare through artificial intelligence and IoT technology. The company's core expertise lies at the

intersection of embedded machine learning, sensor fusion, and veterinary science, enabling pet owners to understand their dog's health, emotions, and behavioral patterns in real time.

The founding team combines complementary technical strengths: Aleksandar Milutinović (CTO) leads the AI/ML architecture, Nikola Milanović (CEO) manages business development and strategic partnerships, and Branko Ilić (CPO) oversees hardware and application development. The team operates under the academic mentorship of Prof. Aleksandar Peulić from the University of Kragujevac, providing a strong scientific foundation for the project.

Within the deep-tech ecosystem, WellPet.ai is positioned at the convergence of pet-tech and health-tech, applying research-grade sensor technology and ML inference at the edge to a rapidly growing consumer market. The company received early-stage validation through the Serbian Innovation Fund's Smart Start program and has established technology partnerships with leading semiconductor and IoT connectivity providers.

2. Technology / Product / Service Description



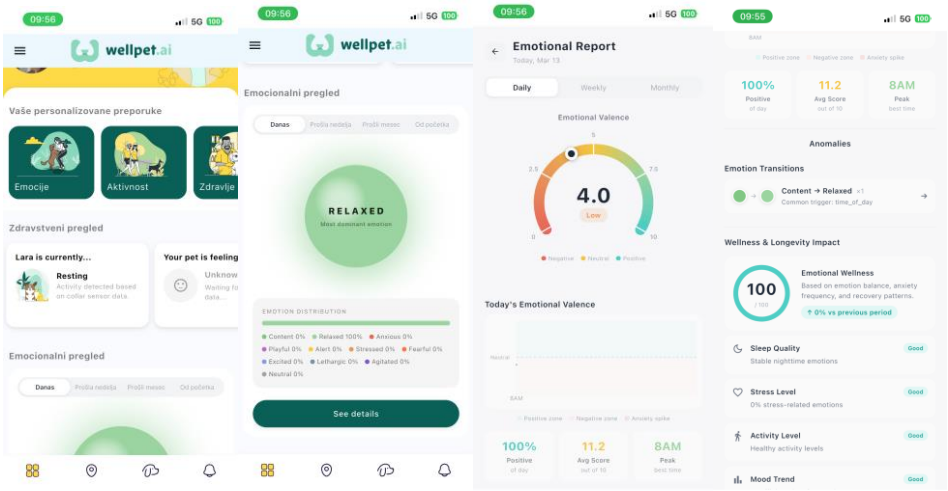
1.0 How the device fit a dog's neck

The WellPet.ai system is designed around a three-layer architecture: an intelligent wearable device, a low-power wireless communication layer, and a cloud-based analytics platform. The smart collar integrates a custom sensor array with an embedded AI processor capable of running proprietary machine learning models directly on the device. This edge-computing approach enables near-real-time behavioral analysis without dependence on continuous internet connectivity, while significantly reducing power consumption and preserving data privacy.

On-device inference results and aggregated health summaries are transmitted to a scalable cloud backend via cellular IoT connectivity, ensuring coverage in both indoor and outdoor environments. The cloud layer applies higher-order analytics to build a personalized behavioral profile for each dog over time, detecting subtle deviations in wellness patterns and generating actionable alerts. End users interact with the system through a companion mobile application that provides health dashboards, activity timelines, and wellness recommendations tailored to their dog's individual baseline.



1.1 Technical specifications of the collar



1.2 Mobile application for end users

3. Innovation and Competitive Advantage

WellPet.ai's primary differentiator is its edge AI architecture. While most existing pet wearables rely predominantly on cloud-based processing, WellPet.ai performs behavior classification directly on the collar's

embedded processor. This approach delivers three key advantages: reduced latency through near-realtime on-device inference, lower power consumption by transmitting only processed results rather than raw sensor streams, and enhanced data privacy by processing sensitive behavioral data locally before any cloud transmission.

A second key innovation is the personalized behavioral fingerprint system. Rather than applying generic thresholds, the platform builds an individualized baseline for each dog over time, accounting for breed, age, size, and individual characteristics. This enables detection of subtle, long-term deviations that would be missed by conventional rule-based anomaly detection systems.

Additionally, the multi-modal sensor fusion approach provides a significantly richer behavioral context than single-sensor alternatives. By combining multiple complementary data streams, the system captures a holistic picture of the dog's state, enabling features such as emotional state estimation—translating complex behavioral signals into owner-comprehensible wellness insights. The team is actively developing intellectual property around its core on-device inference and behavioral fingerprinting technologies.

4. Market Application and Impact

The global pet wearable technology market was valued at approximately USD 3.3 billion in 2024 and is projected to exceed USD 5 billion by 2030, driven by the humanization of pets, rising veterinary costs, and growing demand for preventive health solutions. Europe, WellPet.ai's initial target market, represents the second-largest segment, with over 90 million pet dogs across the EU and an increasing willingness among owners to invest in technology-driven pet wellness.

WellPet.ai targets health-conscious pet owners who seek proactive monitoring rather than reactive veterinary visits. By enabling early detection of behavioral and physiological changes, the platform has the potential to reduce unnecessary veterinary consultations, improve treatment outcomes through earlier intervention, and contribute to longer, healthier lives for companion animals. The scalable cloud architecture and modular hardware design allow the system to expand to additional pet species and veterinary professional use cases in subsequent product iterations.

From a societal perspective, the project aligns with UN Sustainable Development Goal 3 (Good Health and Well-being), extending the concept of health monitoring to the One Health paradigm that recognizes the interdependence of human and animal health. It also contributes to UN SDG 9 (Industry, Innovation and Infrastructure) by advancing edge AI and IoT technologies within the European deep-tech ecosystem.

5. Partnerships and Outlook

WellPet.ai has established strategic technology partnerships with leading semiconductor and IoT connectivity providers for its hardware platform. The academic partnership with Prof. Aleksandar Peulić at the University of Kragujevac provides scientific rigor and access to research infrastructure for validating the ML models and sensor performance.

A clinical validation study is currently being prepared in collaboration with the Faculty of Science at the University of Kragujevac, involving 16–30 dogs in controlled and naturalistic settings to benchmark the accuracy of the on-device activity classification models and assess the reliability of health anomaly detection over multi-week observation periods.

The development roadmap for 2026–2027 includes: completion of the validation study and publication of results; finalization of the pre-production hardware design; launch of a limited beta program with early adopters in the EU market; and expansion of the ML model portfolio to include additional health indicators. WellPet.ai is actively seeking collaboration opportunities with veterinary research institutions, hardware technology partners, and impact-oriented investors aligned with the pet health innovation space.

Acknowledgements

This work was supported by the Innovation Fund of the Republic of Serbia through the Smart Start program. The authors gratefully acknowledge the support of their technology partners and the academic mentorship and research infrastructure provided by the Faculty of Science at the University of Kragujevac.

Additionally, the team completed the GIST program organized by Arizona State University and supported by the U.S. State Department. The authors also acknowledge the ongoing support from the NVIDIA Inception program and AWS for Startups.

References

1. Kumpulainen P, Cardoso C, Raekallio M, Valros A, Pastell M. Dog behaviour classification with movement sensors placed on the harness and the collar. Applied Animal Behaviour Science. 2021;241:105393.
2. Ladha C, Hammerla N, Hughes E, Sherrin P, Ploetz T. Dog's life: wearable activity recognition for dogs. Proceedings of the 2013 ACM International Joint Conference on Pervasive and Ubiquitous Computing. 2013:415–418.
3. Banerjee A, Maity S, Mastrangelo CH. Nanostructures for biosensing, with a brief overview on cancer detection, IoT, and the role of machine learning in smart biosensors. Sensors. 2021;21(4):1253.

Assistive app for BVI people

BegIA

Oier Arano Urrutia and Alain Ordoñez Alvaro[1]

[1]BegIA, Students, Mondragon Unibertsitatea, Basque Country, Spain.

Contact email: oier.arano@alumni.mondragon.edu , alain.ordonez@alumni.mondragon.edu

Executive Summary

Over 246 million people worldwide live with low vision, facing daily challenges that limit their independence and safety. Simple activities such as walking in urban environments or navigating unfamiliar spaces can expose them to significant risks. Despite advances in assistive technologies, current solutions remain fragmented, expensive, or focused on limited functionalities such as text recognition or scene description.

BegIA addresses this gap through a mobile-first, AI-powered solution designed to enhance real-time environmental awareness for blind and visually impaired (BVI) individuals. The application leverages computer vision and deep learning models to detect obstacles and hazards directly through the smartphone camera. Unlike existing tools, BegIA not only identifies objects but also evaluates their potential risk, prioritizing critical information and delivering it through intuitive voice feedback.

The core innovation lies in its ability to perform real-time risk assessment on device. This approach enables a more proactive and reliable assistance system compared to traditional reactive tools.

BegIA is designed to be accessible, scalable, and cost-effective, leveraging devices that users already own. Beyond end users, the solution also provides value to families by enhancing user safety and autonomy.

Currently under active development, BegIA has reached a functional prototype stage, demonstrating the feasibility of real-time hazard detection in real-world scenarios. The long-term vision is to evolve into a comprehensive assistive platform that integrates navigation, environmental understanding, and personalised guidance, contributing to greater independence and inclusion for visually impaired individuals.

Keywords: assistive technology; computer vision; artificial intelligence; visual impairment; hazard detection; mobile application; accessibility; real-time navigation; deep learning; UN SDG 10

1. Company Overview

BegIA is an Emerson deep-tech initiative focused on developing assistive solution based on artificial intelligence and computer vision. The project is led by two computer engineering students with a strong technical background and supported by entrepreneurial ecosystem of Mondragon Unibertsitatea.

Our mission is to improve safety and independence of Blind and visually impaired individuals through accessible and scalable technology.

While the team's core expertise lies in software engineering and AI development, the project is being developed with a strong focus on real-world applicability.

2. Technology / Product / Service Description

BegIA is mobile based assistive system that detects hazards in the daily life of blind or visually impaired individuals. The solution is designed to operate directly on smartphones.

The application is optimized for real-time environments. These system identifies relevant objects and obstacles within the user's surroundings such as pedestrians, vehicles, street elements…

The application processes visual data in real time and delivers feedback through audio interface, ensuring that the user does not need any interaction with the mobile device. The app is also fully navigable by voice commands.

The models that BegIA uses can run with low latency and without any internet connection requirement.

3. Partnerships and Outlook

BegIA is currently in the previous stage. A small prototype has been made in two months, that ensures the viability of the project. On the other hand, a bigger market analysis has been done to center the design of the app.

The next steps of BegIA are to finish the strategical plan in order to start with the definition of the development and start making a prototype which will scale until finally reaching the Minimum Viable Product.

AI for Engineering, Manufacturing, and Industrial Systems

Decision-Boundary Instrumentation: Deployer-Side AI Monitoring for European Industry

Dorleta Urrutia-Onate[1], Asier Perallos[2], Enrique Onieva[3]

[1]*University of Deusto, Bilbao. Spain, dorleta.urrutia@opendeusto.es, 0000-0002-6862-6160*
[2]*University of Deusto, Bilbao. Spain, perallos@deusto.es, 0000-0001-9661-3861*
[3]*Department, Institution, Bilbao. Spain, enrique.onieva@deusto.es, 0000-0001-9581-1823*

Abstract

European organisations deploying AI as a service face a regulatory gap: the AI Act (Article 26) assigns operational monitoring obligations to the deployer, yet the deployer interacts with the model through a black-box inference API. This paper presents a deployer-side instrumentation architecture that generates structured, per-decision telemetry at the output–action boundary without requiring access to model internals. Four safety-theoretic failure modes (proxy contamination, distribution shift, decision fragility, record instability) define the instrumentation requirements. Published XAI methods (KernelSHAP, k-NN distance, bounded perturbation, attribution stability) are respecified as engineering telemetry and composed into a deterministic protocol that produces a machine-readable evidence snippet at each decision event. Three industrial demonstrators—brake disc quality inspection, cobot safety clearance, and energy scheduling—validate that the telemetry correctly recovers failure modes coded into synthetic datasets under controlled conditions (Mann–Whitney U); the question is whether the instrument reads back what was designed in, not what it discovers. The architecture, protocol, and datasets are openly available for replication.

Keywords: explainable AI; AI governance; EU AI Act; decision-boundary instrumentation; deployer monitoring; black-box deployment; safety assurance; industrial AI; UN SDG 9; UN SDG 8

1. Introduction

A European manufacturer purchases an AI-based quality inspection system for its brake disc production line. The system auto-passes or auto-rejects discs based on camera and sensor data processed through a proprietary algorithm delivered as a cloud API. A hospital deploys a cobot safety monitoring system that clears workers into shared human-robot zones. An energy-intensive SME uses an AI scheduler to optimise production batches. In each case, the organisation is the deployer: it operates a model it did not build, cannot inspect, and whose internal logic it does not control.

The EU AI Act (Regulation 2024/1689) [1] distributes monitoring responsibilities along the value chain; the provider retains post-market surveillance obligations (Articles 16, 72), but operational monitoring during use—the per-decision, contextualised vigilance—falls on the deployer (Article 26). The deployer must monitor the system during use, detect risks, and document its operation. Yet the deployer interacts with the model through an inference API—a black box. The entity responsible for monitoring cannot inspect the system it must monitor. This is not a theoretical problem. It is the daily reality of European SMEs and institutions that purchase AI as a service. The question is practical: what can a deployer measure, at each decision, using only the public input–output interface?

XAI methods exist but are rarely deployed for this purpose—generating structured, integrity-checked evidence at the decision boundary in operational settings [2,3]. Recent work distinguishes RED XAI (explanations that question the model internally) from BLUE XAI (explanations that justify externally) [4]. This paper develops an instrumentation role closer to RED XAI but oriented toward operational governance: XAI artefacts respecified as engineering telemetry—runtime sensors at the output–action boundary, subject to calibration, stability, and documented operating envelopes. The architecture derives from established safety theory [5,6,7], operates entirely on the public inference interface, and produces a structured evidence snippet at each decision event.

2. Instrumentation Architecture

The architecture begins with a question from safety engineering: what failure modes does theory predict at the boundary where an algorithmic output triggers an action? Four established perspectives identify four distinct failures, each defining one instrumentation requirement (Table 1).

Table 1. Safety-theoretic failure modes and instrumentation requirements.

Safety theory	Failure mode	Instrumentation requirement
Leveson (STAMP) [5]	Action proceeds on proxy features instead of legitimate grounds	Constraint enforcement: legitimate-feature ratio via KernelSHAP [8]
Rasmussen [6]	Case falls outside validated envelope (distribution shift)	Envelope validity: k-NN distance to validation set
Parasuraman [7]	Brittle output treated as robust (automation bias)	Decision robustness: flip-rate under bounded perturbation [9]
Cross-cutting	No structured record binding output to evidential basis	Record integrity: attribution stability under micro-noise [10]

All four methods are computable on the public inference interface only (predict_proba). This is an architectural commitment, not a limitation: the deployer cannot condition regulatory compliance on vendor cooperation that may be withdrawn. For a given case, the protocol computes five signals in fixed order: (1) model score and margin; (2) KernelSHAP attribution grouped into legitimate versus proxy features; (3) k-NN distance to the validation set; (4) flip-rate under bounded perturbation; (5) attribution stability under micro-noise. Signal (1) defines the near/far partition used for population-level validation (Table 2); signals (2)–(5) are the four testable readings. The output is a structured JSON evidence snippet—the atomic unit of the audit trail, generated synchronously with the decision, not reconstructed after the fact. Signals are assessed independently (non-compensatory): a strong envelope validity does not compensate for proxy contamination, because they address different failure modes.

3. Industrial Demonstrators

The question this section answers is not what did the instrument find? but does the instrument work? The distinction is the core of the validation. Every failure mode in the synthetic datasets was coded by the authors—

the confounders, the identity weights, the sustainability gap. The instrument's job is to separate the condition where the failure mode is present from the condition where it is absent. If it can, it works. The analogy is testing whether a thermometer distinguishes boiling water from ice water—not what temperature it reads in an unknown liquid. What it reads is calibration detail; whether it distinguishes is capability.

Three demonstrators follow an identical protocol: (1) synthetic dataset with features classified as domain-legitimate or proxy, constructed with feature fidelity, structural fidelity, and controlled ground truth; (2) classifier accessed only via predict_proba; (3) telemetry protocol applied identically; (4) near-threshold versus far-from-threshold partitioning; (5) Mann-Whitney U discrimination test. The datasets are synthetic because the real systems are proprietary—the condition this work addresses. Calibration tables (coded magnitudes, recovered values, per-case evidence snippets) are provided in each demonstrator's CASE_ANALYSIS.md in the companion repository.

Table 2. Population-level discrimination: does each technique's signal separate near-threshold from far-threshold cases? (n = 40 near per demonstrator; Mann–Whitney U test.)

Demonstrator	AI Act	Technique → Signal	Near (mean)	Far (mean)	p
Brake disc QC	Cat. 2	KernelSHAP → proxy attr	26.8% ± 13.5%	10.4%	< 0.01
		Bounded perturb. → flip-rate	0.09 ± 0.14	0.00	
		k-NN → envelope dist	2.18 ± 0.42	3.88	< 0.01
		Micro-noise → attr. stab. σ	0.09 ± 0.07	0.00	< 0.01
Cobot safety	Cat. 2+4	KernelSHAP → proxy attr	32.9% ± 8.8%	24.6%	< 0.05
		Bounded perturb. → flip-rate	0.09 ± 0.14	0.00	
		k-NN → envelope dist	2.22 ± 0.39	3.07	n.s.
		Micro-noise → attr. stab. σ	0.10 ± 0.08	0.08	n.s.
Energy sched.	Art. 69	KernelSHAP → sust. attr	17.6%	9.2%	< 0.05
		Bounded perturb. → flip-rate	0.09	0.00	
		k-NN → envelope dist	1.99 ± 0.41	2.33	n.s.
		Micro-noise → attr. stab. σ	0.09 ± 0.07	0.08	n.s.

KernelSHAP attribution and flip-rate discriminate at $p < 0.05$ in all three demonstrators. k-NN envelope distance discriminates in brake disc ($p < 0.01$) but not in cobot or energy (n.s.)—consistent with these failure modes not shifting the input manifold. Attribution stability shows low σ everywhere (≤0.10), confirming rank-order robustness; it discriminates in brake disc ($p < 0.01$) but not elsewhere. Non-compensatory assessment means a signal that does not discriminate is not a failure: it confirms that axis is not degraded near the threshold. Flag

rates—the fraction the instrument would divert for human review—are 17.5% (brake disc), 32.5% (cobot), and 12.5% (energy). The cobot case shows that a single snippet serves two regulatory questions simultaneously: KernelSHAP attribution answers whether clearance was hazard-based (Cat. 2) and whether it was identity-driven (Cat. 4)—two obligations, one architecture. In the energy case, KernelSHAP reads 17.6% sustainability weight for marginal peak-carbon batches—the scheduler is partially blind to a 51% CO_2 differential that costs zero throughput to avoid.

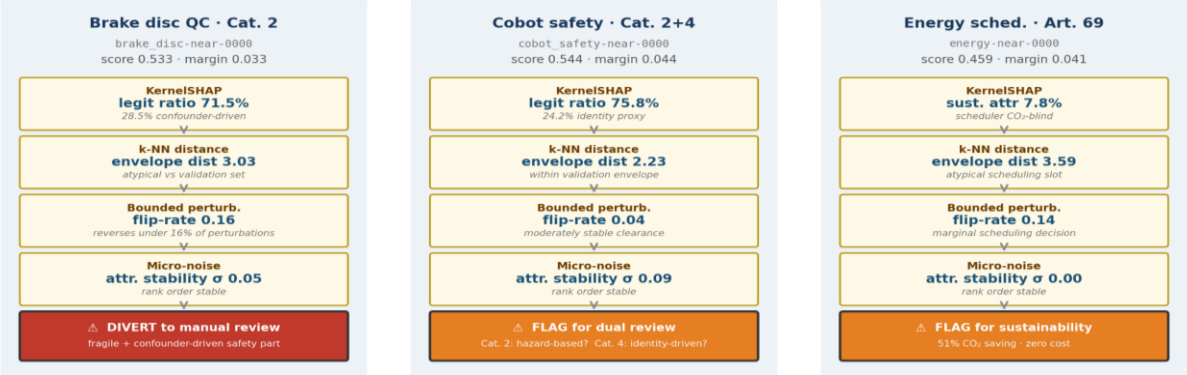


Figure 1. *What de deployer receives: one evidence snippet per decision*

4. Implications for European Industry

The architecture addresses a concrete operational gap for European deployers. A manufacturing SME purchasing AI-based inspection does not need to understand the model's internals; it needs to know, for each decision, whether the output is evidentially supported. The evidence snippet provides this: a structured, machine-readable record that can be stored, queried, and audited. The results in Table 2 reveal an informative pattern: KernelSHAP attribution and flip-rate discriminate near-threshold from far-threshold cases in every demonstrator, while k-NN envelope distance and attribution stability discriminate only in brake disc. This is not a limitation—it is what non-compensatory assessment is designed to surface. In cobot safety, the failure mode is identity contamination, not distribution shift; the input manifold does not change at the threshold, so envelope distance should not discriminate. Each signal reports its own axis independently, and a non-discriminating signal confirms that its axis is not degraded. When snippets are aggregated, three governance operations become tractable: pattern detection (do flagged decisions cluster by shift, site, or subgroup?), drift monitoring (is the model's behavioural basis shifting over time?), and accountability reconstruction (was this specific decision backed by structured evidence at the time it was committed?).

The computational cost is compatible with industrial workflows: 2–30 seconds per case for the full protocol (dominated by KernelSHAP), fitting minute-to-hour decision latencies. For sub-second workflows, flip-rate and envelope distance are computable in milliseconds; full attribution is computed asynchronously. ETSI TS 104 008 (CABCA) formalises continuous auditing-based conformity assessment; the evidence snippet provides candidate content for CABCA cycles. The alignment is architectural, not legal—CABCA is a Technical Specification, not a harmonised European Norm.

5. Conclusions

This paper presents a deployer-side instrumentation architecture that enables European organisations to monitor AI systems they operate but cannot inspect. Four safety-theoretic requirements are implemented with four published XAI methods on the black-box interface, producing a five-signal evidence snippet at each decision event. Three demonstrators confirm that the two primary signals—KernelSHAP attribution and bounded-perturbation flip-rate—discriminate designed failure modes from normal conditions in every case ($p < 0.05$); envelope distance and attribution stability discriminate selectively, confirming that the non-compensatory protocol reports each axis on its own terms. The validation is of capability, not of deployment findings. The immediate next step is prospective validation with institutional partners on production systems. Datasets, protocol, and scripts are openly available. The position is pragmatic: a deployer using this framework has imperfect but structured per-case telemetry; a deployer without it has aggregate metrics but no per-instance evidence.

Acknowledgements

AI assistance disclosure: Claude (Anthropic, claude-opus-4) assisted in drafting prose from author-specified outlines and in generating Python code for synthetic dataset construction and replication scripts. The theoretical framework, research design, dataset specifications, legal analysis, and all editorial decisions are the author's; the author assumes full responsibility for all content.

References

1. European Parliament. Regulation (EU) 2024/1689 laying down harmonised rules on artificial intelligence (AI Act). Off J Eur Union. 2024;L 2024/1689.
2. Barredo Arrieta A, Díaz-Rodríguez N, Del Ser J, Bennetot A, Tabik S, Barbado A, et al. Explainable Artificial Intelligence (XAI): Concepts, taxonomies, opportunities and challenges toward responsible AI. Inf Fusion. 2020;58:82–115.
3. Ali S, Abuhmed T, El-Sappagh S, Muhammad K, Alonso-Moral JM, Confalonieri R, Guidotti R, Del Ser J, Díaz-Rodríguez N, Herrera F. Explainable Artificial Intelligence (XAI): What we know and what is left to attain trustworthy Artificial Intelligence. Inf Fusion. 2023;99:101805.
4. Biecek P, Samek W. Position: Explain to question not to justify. In: Proc 41st Int Conf Mach Learn (ICML). 2024.
5. Leveson NG. Engineering a Safer World: Systems Thinking Applied to Safety. Cambridge, MA: MIT Press; 2011.
6. Rasmussen J. Risk management in a dynamic society: A modelling problem. Saf Sci. 1997;27(2–3):183–213.
7. Parasuraman R, Manzey DH. Complacency and bias in human use of automation: An attentional integration. Hum Factors. 2010;52(3):381–410.
8. Lundberg SM, Lee SI. A unified approach to interpreting model predictions. Adv Neural Inf Process Syst. 2017;30.
9. Mothilal RK, Sharma A, Tan C. Explaining machine learning classifiers through diverse counterfactual explanations. In: Proc 2020 Conf Fairness Account Transpar. 2020:607–617.
10. Alvarez-Melis D, Jaakkola T. On the robustness of interpretability methods. In: Proc ICML Workshop. 2018.
Companion repository: https://github.com/dorletaurrutia-xai/xai-deployer-monitoring

Development of an AI-Supported Optimization and Decision-Support Industrial SaaS Platform for FMEA Risk Management

AI-powered FMEA EXCELLENCE, ST05-224/2025, StarTech Innovation Support Program, Period (2025-2026)

Nikola Komatina[1], Nikola Banduka[2], Pavle Rvović[2], Kristina Mojsić[2]

[1] Faculty of Engineering, University of Kragujevac, 34000 Kragujevac, Republic of Serbia, nkomatina@kg.ac.rs, https://orcid.org/0000-0001-6964-5673
[2]DigitaLLeather LLC, Trg Topolivaca 4, 34000 Kragujevac, Republic of Serbia, nikola.banduka@digitalleather.rs, https://orcid.org/0000-0002-1108-3265; pavle.rvovic@digitalleather.rs; kristina.mojsic@digitalleather.rs

Corresponding author: nkomatina@kg.ac.rs

Abstract

The application of Failure Mode and Effects Analysis (FMEA) in the automotive industry is prescribed by international standards and is implemented across all companies operating within the automotive supply chain. Although originally designed as a valuable engineering tool, it often remains merely an administrative obligation carried out by quality departments, without fulfilling its primary purpose, i.e. improving the reliability of products and processes. Even when companies approach FMEA seriously, they encounter numerous challenges, such as manual data entry, incomplete records, lack of historical risk data, and various other practical difficulties. This paper presents the development of FMEA Excellence, implemented as a cloud-based Software as a Service (SaaS) platform, aimed at transforming FMEA into a reliable decision-support tool. The platform is designed to automate key FMEA activities, including data collection and processing related to products and processes, risk prioritization, and the generation of action recommendations. In addition to improving risk management, the platform aims to reduce the time required to perform FMEA, lower costs, and enhance the effectiveness and efficiency of FMEA-related activities, while also enabling transparent real-time monitoring of team performance. The key functionalities of the platform are based on a combination of artificial intelligence tools, including evolutionary artificial intelligence and Retrieval-Augmented Generation (RAG) integrated with large language models (LLMs), as well as optimization methods.

Keywords: FMEA; AI-powered; FMEA Excellence; automotive industry; decision-support tool; risk management; artificial intelligence; RAG; LLMs; industry, UN SDG 9, UN SDG 12

1. Project Background and Objectives

Quality engineers and quality management teams in modern industrial production, particularly in the automotive industry, are increasingly exposed to pressures related to project delivery deadlines, while simultaneously being

required to comply with stringent international standards, as well as internal and external audit requirements. As a result, valuable engineering tools commonly used in practice, such as Failure Mode and Effects Analysis (FMEA) [1], are often perceived as administrative obligations without clear practical purpose or contribution. Their implementation is further complicated by tight time constraints, incomplete data, and a reactive approach to problem-solving, where issues are addressed only after they have already manifested and become critical.

The latest version of the FMEA Handbook [1] for the automotive industry, which provides guidelines for its implementation, was published in 2019 by the Automotive Industry Action Group (AIAG) and the Verband der Automobilindustrie (VDA). Although certain improvements in conventional FMEA have been observed since the introduction of this handbook, several significant challenges related to its practical application still remain unresolved. Numerous studies have shown that the introduction of additional decision-support tools is necessary in order to fully realize the potential of FMEA in industrial practice [2]. Furthermore, research indicates that the FMEA maturity level of companies in the Republic of Serbia is often limited to the use of Excel-based approaches, representing the most basic level of administrative analysis [3].

Precisely due to the numerous challenges that automotive companies face regarding FMEA, the motivation for the FMEA Excellence project emerged with the support of the StarTech program [4] (see the logos in Figure 1), with the aim of developing an AI-supported approach to FMEA implementation in practice.



Figure 1. Logo of the FMEA Excellence project (left) and the StarTech program logo (right)

The main objective of the project is to develop an intelligent Software as a Service (SaaS) platform aimed at transforming FMEA from a static Excel document into a dynamic decision-support system. Data collection and processing would are automated through the application of artificial intelligence (including evolutionary artificial intelligence and knowledge-based approaches) and optimization methods. The integration of these concepts aims to reduce the time required for FMEA creation and maintenance, lower costs, and prevent failures, while also contributing to improved product quality and operational efficiency. In addition, the SaaS platform would enable compliance with standard requirements and real-time monitoring of changes, ensuring consistency and traceability.

2. Problem Statement and Motivation

Although prescribed by the IATF 16949:2016 standard [5] and defined by the FMEA Handbook [1], the modern application of FMEA in the automotive industry faces numerous practical limitations and inconsistencies. Its implementation is further complicated by manual work (manual data entry), incomplete or fragmented data sources, and a lack of alignment with other aspects of product and process quality improvement. As a result, FMEA is often perceived merely as an administrative obligation, where the outcome of such analysis is a static document (FMEA report), most commonly exported in Excel format.

For these reasons, a number of issues arise that make FMEA, in many cases, almost ineffective, despite its fundamental purpose of ensuring a sufficiently reliable process or product in accordance with customer

requirements. Some of the most noticeable, yet serious, problems in practice include: (1) difficulties, or even the inability, to comply with standard and audit requirements, (2) inefficient use of resources, primarily time and cost, (3) time loss due to manual risk assessment (definition and updating), (4) lack of integration with Quality Management System (QMS) and Enterprise Resource Planning (ERP) systems, (5) absence of a knowledge base, resulting in a lack of traceability and duplication of data, and (6) the inability of FMEA to serve as an adequate tool for predictive analysis and the decision-making process.
There are also other issues, closely related to those mentioned, which could likewise be addressed through the application of an appropriate holistic approach. It is precisely based on these challenges that the idea for developing a SaaS solution emerged, aimed at improving and further advancing the application of FMEA in the automotive industry through the use of various tools.

3. Conceptual Framework

Based on the presented problem statement and motivation, the objective was to overcome the limitations of conventional FMEA currently used in practice. The project team is developing a system that adapts FMEA to the requirements of modern industry and transforms it into a comprehensive dynamic decision-support tool. The FMEA Excellence solution enables users to manage risks more efficiently through improved data collection, analysis, and systematization of information from existing records.
Within the FMEA Excellence platform, the traditional application and functionality of FMEA have been extended beyond technological risk assessment through the use of evolutionary artificial intelligence. In addition to conventional technological risk analysis, the platform incorporates financial, time, and strategic dimensions. This enables decision-makers to evaluate and identify optimal solutions across multiple risk aspects, ensuring that risk management activities are aligned with strategic business objectives.
In addition, FMEA Excellence applies Retrieval-Augmented Generation (RAG) integrated with large language models (LLMs), thereby enabling the creation and access of an organizational knowledge base. This functionality addresses the issue of "knowledge loss" in cases where experienced and reliable FMEA team members leave the company. Furthermore, it significantly reduces the time required to perform analyses and generate FMEA documentation.

4. Platform Overview and User Interface

The development of the SaaS solution is still ongoing, meaning that the project is currently in the implementation phase. This section presents the current version of the platform, with the aim of illustrating the user interface. FMEA Excellence is designed as a centralized and integrated platform (see Figure 2) that, in addition to FMEA, enables the use of other related quality management tools, such as process flow diagrams, control plans, task management, and continuous improvement activities.

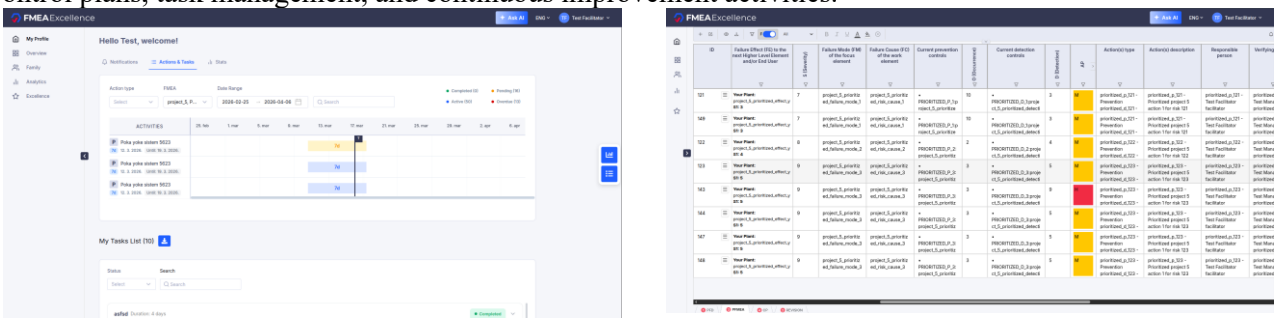


Figure 2. Platform overview: user dashboard (left) and project list interface (right)

As shown in Figure 2, FMEA is presented through a structured and visually consistent interface, encompassing all relevant elements of the analysis, including failures, causes, defined actions, risk prioritization, and related components.

5. Conclusions

This paper presents the FMEA Excellence platform development project, aimed at providing companies, primarily within the automotive industry, with a dynamic, transparent, and reliable decision-support tool. The focus is on improving the implementation of conventional FMEA as defined by the latest handbook, as well as on integrating other important aspects closely related to FMEA, primarily other quality tools relevant to the automotive industry. Although the platform is still under development, testing of some of its functionalities is already being conducted in several companies. The goal is for FMEA Excellence to become a widely recognized and broadly adopted tool in industrial practice.

Acknowledgements / Funding

The project has been supported by the StarTech program, implemented by NALED in cooperation with the Government of Serbia, and funded by Philip Morris.

References

[1] AIAG&VDA. Failure Mode and Effects Analysis - FMEA Handbook: design FMEA, process FMEA, supplemental FMEA for monitoring & system response. Southfild, Michigan: Automotive Industry Action Group; 2019.

[2] Tadić D, Banduka N, Petrović T, Komatina N. Application of FMEA in the automotive industry: Present situation and perspectives in the Republic of Serbia. Trendovi u Poslovanju 2024;12:127–35. https://doi.org/10.5937/trendpos2401137T.

[3] Banduka N, Petrović T, Komatina N. Model for the assessment of process failure mode and effect analysis maturity level in the automotive industry toward industry 4.0 trends. International Review 2024:219–28. https://doi.org/10.5937/intrev2404219B.

[4] Podrška inovacijama i digitalnoj transformaciji. Startech | Podrška inovacijama i digitalnoj transformaciji n.d. https://startech.org.rs/ (accessed March 30, 2026).

[5] IATF 16949:2016. Quality management system requirements for automotive production and relevant service parts organizations, 1st edition 2017.

Application of AI tools in analyses of Welded Structure

Design, Calculation and Analysis of Welded Mechanical Structures, PA-ZMK, Ministry of Civil Affairs of B&H, 2016-2017

Aleksija Đurić[1], Miodrag Milčić[2], Srđan Samardžić[1], Dragan Milčić[2], Biljana Marković[1]

[1] *University of East Sarajevo, Faculty of Mechanical Engineering, East Sarajevo, Bosnia and Herzegovina, aleksija.djuric@ues.rs.ba, 0000-0002-0251-6364, srdjan.samardzic@ues.rs.ba, 0009-0003-4096-7523, biljana.markovic@ues.rs.ba, 0000-0001-8915-4791*

[2] *Faculty of Mechanical Engineering, University of Niš, Niš, Serbia, dragan.milcic@masfak.ni.ac.rs, 0000-0002-6130-0328, miodrag.milcic@masfak.ni.ac.rs, 0000-0002-3936-7462.*

Corresponding author: aleksija.djuric@ues.rs.ba

Abstract

This bilateral project, "Design, Calculation and Analysis of Welded Mechanical Structures," aims to establish a link between the traditional calculation of welded structures and the application of Artificial Intelligence (AI) technologies. The project is focused on the analysis of current methods for the calculation of welded joints with a special focus on the application of standards such as Eurocode 3 (EN 1993-1-8) and ISO 5817. On the other hand, the project's goal is to analyze the possibilities of application of Large Language Models (LLMs) to streamline and simplify complex analytical processes in weld design calculation. By comparing various LLM tools, the project identifies their current limitations, accuracy levels, and potential for automating routine engineering tasks. Key results highlight a comparative analysis of AI-generated calculations against established Eurocode and ISO standards. The findings suggest that while AI can significantly accelerate the preliminary design phase, human oversight remains critical for safety-compliant structural integrity.

Keywords: Welded Mechanical Structures, Calculation of weld joint, AI, LLMs.

1. Project Background and Objectives

The structural integrity of welded joints is a cornerstone of mechanical engineering, where calculation precision directly dictates both public safety and economic efficiency. This bilateral project was established to address the urgent need for modernizing traditional engineering workflows through the integration of advanced digital technologies. The primary motivation stems from the increasing complexity of international regulatory frameworks, such as Eurocode 3 (EN 1993-1-8) and ISO 5817, which demand significant time and high-level expertise for correct implementation. The project's central objective is to explore the synergy between these rigorous standards and the capabilities of Large Language Models (LLMs) to accelerate the design process. Expected outcomes include a defined framework for the safe deployment of AI tools in engineering practice

and the identification of critical intervention points where AI can support human decision-making without compromising structural reliability.

2. Methodology and Work Performed

The research methodology is based on a comparative analysis between results obtained through conventional engineering computations and those generated by AI platforms. The work commenced with an extensive state-of-the-art review, mapping standard analytical methods for dimensioning fillet and butt welds. A core component of the project involved testing three leading LLM platforms—ChatGPT, Gemini, and Claude—utilizing structured prompt engineering. These models were evaluated on their ability to interpret technical requirements, accurately cite specific clauses of ISO and EN standards, and execute numerical operations. Beyond computational simulations, a validation phase was conducted using established benchmarks, where AI-generated outputs were manually audited for logical consistency, mathematical accuracy, and potential "hallucinations" or misinterpretations of safety factors.

3. Key Results

The findings indicate a significant potential for AI to act as a catalyst in the design phase, though distinct limitations remain. The analysis demonstrated that AI integration can reduce the time required for preliminary dimensioning and technical documentation retrieval by over 50%. However, numerical precision varied across different platforms. While certain models excelled at generating automation scripts (e.g., Python code) for calculations, others struggled with the correct application of partial safety factors specific to Eurocode.

Comparative data confirms that LLMs currently perform best as "Engineering Copilots" that assist in problem structuring, whereas final verification still necessitates the use of specialized CAE software and expert human oversight.

4. Discussion and Impact

The significance of these results lies in the demystification of AI's role within the mechanical engineering domain. Compared to the current state-of-the-art, where AI is mostly limited to text processing, this project proves that these tools can be effectively applied to strictly regulated technical calculations when a proper querying methodology is used. The industrial impact is substantial, offering small and medium enterprises (SMEs) a pathway to rapid prototyping and optimized material consumption. On a societal level, the project enhances the digital literacy of engineers and lays the foundation for modernized curricula at the Universities of East Sarajevo and Niš, preparing the next generation of professionals for a collaborative human-AI working environment. The infographic of the project generated by NootebookLM is shown in Figure 1.

5. Conclusions and Outlook

The project concludes that integrating LLM tools into the design of welded structures offers undeniable efficiency gains but requires a new paradigm of verification and caution. By successfully linking traditional engineering logic with modern AI systems, the primary goal of this bilateral cooperation has been achieved. The next phase of research will focus on developing "custom" GPT models trained exclusively on technical standards and verified engineering datasets to eliminate mathematical unreliability.

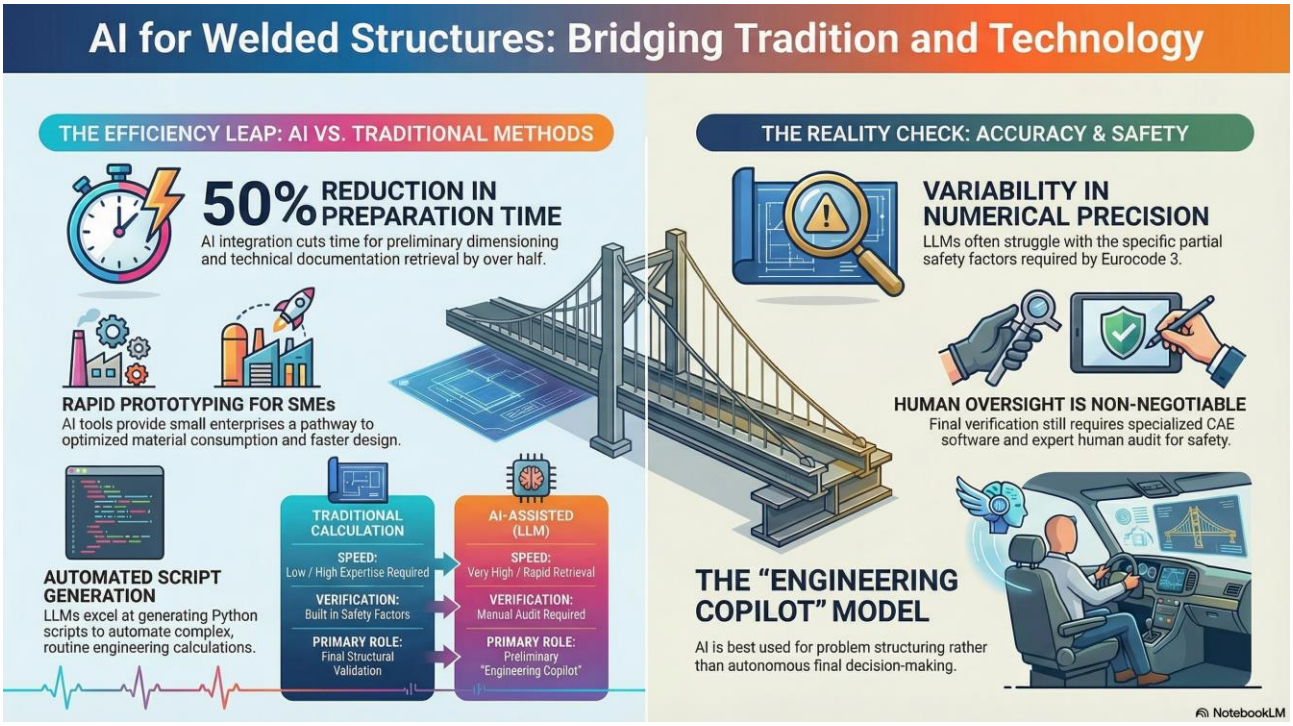


Figure 14. The infographic of the project generated by NootebookLM

Acknowledgements / Funding

The bilateral project "Design, Calculation and Analysis of Welded Mechanical Structures, PA-ZMK " is supported by Ministry of Civil Affairs of Bosnia and Herzegovina.

References

1. Miličić D. Mašinski elementi, Univerzitet u Nišu, Mašinski fakultet Niš. 2022; 56-109.
2. Muminović A, Mešić E. Oblikovanje I proračun zavarenih konstrukcija, Mašinski fakultet Sarajevo, 2013.
3. BAS EN ISO 5817:2024 - Zavarivanje - Zavareni spojevi nastali topljenjem na čeliku, niklu, titanu i njihovim legurama (isključeno zavarivanje elektronskim snopom i laserom) - Nivoi kvaliteta za nesavršenosti.
4. EN 1993-1-8: Eurocode 3: Design of steel structures

Application of artificial intelligence to predict and optimize driver comfort based on anthropometric data

Slavica Macuzic Saveljic[1], Igor Saveljic[2]

[1]*Faculty of Engineering, University of Kragujevac, Kragujevac, Serbia, s.macuzic@kg.ac.rs, 0000-0003-2635-2496*

[2]*Institute for Information Technologies, University of Kragujevac, Kragujevac, Serbia, isaveljic@kg.ac.rs, 0000-0002-0707-5174*

Corresponding author: s.macuzic@kg.ac.rs

Abstract

Driver comfort is a critical ergonomic criterion in vehicle design, directly impacting safety and long-term health. However, traditional ergonomic validation using Digital Human Models (DHM), such as RAMSIS, is often limited to static, predefined simulation scenarios. This study proposes an innovative approach by integrating Artificial Intelligence (AI) into the ergonomic design workflow to enable dynamic, predictive optimization. Using experimental data from 88 RAMSIS simulation scenarios across 11 diverse global populations, we developed a predictive model based on Random Forest Regression (RFR). The model maps the non-linear relationships between anthropometric characteristics such as stature and sitting height, and driver fatigue at various seatback angles. Results demonstrate high predictive accuracy (R^2=0.942), with the seatback angle and sitting height identified as the primary predictors of discomfort. Our findings reveal a critical "comfort cliff" beyond 102°, enabling the identification of population-specific optimal seating angles. This AI-driven framework provides a rapid, adaptive tool for designers to validate ergonomic compliance in the conceptual phase, significantly enhancing human-centric vehicle interior development while reducing the reliance on exhaustive manual simulations.

Keywords: Digital Human Modeling (DHM); Driver Ergonomics; Random Forest Regression; Seat Comfort Optimization

1. Introduction

Driver comfort is a critical ergonomic criterion directly impacting long-term health and safety. Improper posture during prolonged driving is a primary catalyst for musculoskeletal fatigue. In the automotive industry, effective design requires a deep understanding of diverse anthropometric characteristics, as driver fatigue is highly dependent on individual body dimensions [1,2]. Historically, ergonomic validation has relied on static, scenario-based simulations that evaluate predefined percentiles. While these methods provide a baseline, they struggle to capture the complex, non-linear patterns of discomfort inherent in diverse global populations [3,4]. This reliance on discrete analysis limits the adaptability of vehicle interior design to specific user needs. To overcome these constraints, this study integrates AI into the design workflow. By applying Random Forest Regression to ergonomic data, we model the intricate relationships between anthropometric traits and driver discomfort. This

AI-driven framework provides a rapid, adaptive approach for optimizing vehicle interiors, ensuring ergonomic compliance across diverse global populations and advancing the transition toward human-centric design [5,6].

2. Materials and Methods

2.1. Virtual Environment and RAMSIS Simulation

A B-segment vehicle interior was modeled in CATIA V5, constrained by standard pedal, steering wheel, and Seat Reference Point (SRP) coordinates. Ergonomic analysis was performed using RAMSIS 3.8 to simulate the interaction between the driver and the vehicle interface [7]. The primary experimental variable was the Seatback Angle, tested in 5° increments from 90° to 105°. Driver comfort was quantified through the Fatigue Index and Discomfort Score, using a biomechanical joint-angle analysis where a value of 5.5 represents the upper limit of acceptable ergonomic strain.

2.2. Anthropometric Dataset

To ensure broad global applicability, the study incorporated 11 distinct international populations, specifically targeting morphological extremes from the 5th percentile female to the 95th percentile male. Table 1 summarizes the morphological dispersion across the key dimensions used as inputs for our predictive model, ensuring comprehensive coverage of driver body types for enhanced model robustness.

Table 1. Representative anthropometric extremes (5th–95th percentile) for the analyzed populations (mm).

Population Extremes	Stature	Sit. Height	Foot Length	Shoulder Br.
Max (North Europe)	1585–1910	846–999	227–280	367–498
Min (South India)	1395–1715	746–874	200–265	330–435

2.3. AI Implementation: Random Forest Regression (RFR)

To move beyond discrete manual scenarios, an RFR model was trained on 88 unique simulation outputs.

- Feature Engineering: To improve interpretability, population labels were mapped to continuous anthropometric means (Stature, Sitting Height, Foot Length, Shoulder Breadth). Gender was binary-encoded to account for physiological dimorphism.
- Model Architecture: The RFR ensemble consisted of 500 decision trees, configured to prevent overfitting. Reliability was ensured via a 70/30 train-test split and 10-fold cross-validation.

By acting as a surrogate model, this framework enables the continuous interpolation of the Fatigue Index within the investigated range (90°–105°) and provides reliable estimates for adjacent angular configurations (85°–110°). This capability is instrumental in identifying optimal seating parameters that fall between traditionally tested discrete intervals, thereby offering a more granular approach to ergonomic optimization than standard static simulations.

3. Results

The integration of RFR with data from RAMSIS simulations enabled a deeper, more granular analysis of driver ergonomics. By training the model on 88 unique scenarios, we successfully transitioned from static observations to a predictive framework.

3.1. Model Accuracy and Validation

The RFR model demonstrated exceptional performance in capturing the non-linear relationship between anthropometry and driver discomfort. Evaluated on a 30% test subset, the model achieved a coefficient of determination (R^2) of 0.942. The prediction error metrics, with a Mean Absolute Error (MAE) of 0.118 and an RMSE of 0.156, confirm high reliability. Given the critical discomfort threshold of 5.5, these low error margins indicate that the AI framework can predict the onset of significant driver fatigue with high precision.

3.2. Influence of Parameters (Feature Importance)

The algorithm effectively ranked the impact of each input variable on the final discomfort score. As expected, the Seatback Angle (44.2%) emerged as the primary driver of fatigue. Interestingly, the AI identified a "comfort cliff" beyond 102°, where fatigue scores escalate rapidly. Among anthropometric factors, Sitting Height (26.5%) proved more influential than total stature (14.8%), particularly for the 95th percentile male group, as it directly impacts shoulder and neck strain during pedal interaction.

3.3. Population Sensitivity and Optimal Seating

The simulation results highlighted a clear divergence between demographic groups. The 95th percentile male populations from South East Europe and Australia were the most sensitive, with fatigue levels reaching 5.3 at a 105° angle, approaching the defined ergonomic limit of 5.5. Conversely, the 5th percentile female groups, notably from the Middle East, remained well within the comfort zone (scores below 3.8). By using the RFR model as a surrogate for continuous optimization, we identified "Ideal Seatback Angles" that offer superior comfort compared to the discrete 5-degree steps used in standard RAMSIS testing. These optimized values are presented in Table 2.

Table 2. Comparison between discrete RAMSIS results and AI-optimized continuous angles

Population Group	Percentile / Gender	RAMSIS Best (Discrete)	AI Optimized (Continuous)
North Europe	95th / Male	100°	98.7°
South India	5th / Female	95°	94.2°
West Africa	95th / Male	90°	91.4°
South East Europe	95th / Male	100°	99.1°

4. Discussion and Conclusion

The integration of RFR into the ergonomic design workflow represents a significant shift from static, scenario-based simulation to predictive, data-driven optimization. Our results confirm that seatback angle is the most critical factor influencing driver fatigue, though its impact is highly non-linear. The AI model successfully

mapped the "comfort cliff" identified after 102°, where fatigue scores escalate rapidly-a phenomenon that standard discrete RAMSIS testing may overlook if the interval steps are too wide.

The model's ability to differentiate between populations based on anthropometric characteristics rather than mere geographic labels - proves that vehicle interior design can be optimized more precisely by focusing on specific body dimensions like sitting height. The AI-suggested "ideal angles" (Table 2) offer designers a mathematically optimal starting point, effectively balancing the comfort requirements of both 5th percentile female and 95th percentile male drivers. This approach allows manufacturers to minimize musculoskeletal risks early in the design cycle, moving closer to the "one-size-fits-all" design goal without the need for exhaustive, repetitive simulations.

The main conclusions are:

- High Predictive Accuracy: The AI model achieved an R^2 of 0.942, confirming its robustness in mapping the complex relationship between body dimensions and discomfort.
- Sensitivity Analysis: Seatback angle and sitting height were identified as the primary predictors of fatigue, underscoring that vertical body proportions are crucial for vehicle interior packaging.
- Efficiency in Design: The proposed framework provides a rapid, predictive tool that allows automotive engineers to validate ergonomic compliance for diverse global populations during the conceptual design phase.

Ultimately, this research provides a scalable framework that enhances driver comfort and safety, contributing to more efficient, human-centric vehicle interior development.

Acknowledgements

This research was supported by the Ministry of Education, Science and Technological Development of the Republic of Serbia through Projects TR35041 (Faculty of engineering, University of Kragujevac) and 451-03-33/2026-03/200378 (Institute for Information Technologies, University of Kragujevac).

References

1. Duffy V G. Handbook of Digital Human Modeling: Research for Applied Ergonomics and Human Factors Engineering. CRC Press Inc. Boca Raton FL USA, 2008.
2. Helander M G and Zhang L. Field studies of comfort and discomfort in sitting, Ergonomics, 1997, 40:895–915,
3. Vink P. Comfort and design: principles and good practice, Boca Raton: CRC Press, 2005.
4. Bridger R S. Introduction to Ergonomics, Boca Raton: Taylor & Francis Group, LLC, 2009.
5. Graf M C. Effects of seat angle on comfort and lower back pain at work Swiss federal institute of technology. Zurich: ETH, 2004, 182.
6. Lapa V V, Neverov G I, Poliakov V V, Solov'ev N N. Effect of inclination angles of supporting surfaces of aircraft seat on pilot's working capacity in longduration flight, Aviakosm Ekolog Med, 2000, 34:17-21.
7. RAMSIS 3.8 in CATIA V5 User Guide - HUMAN SOLUTIONS GmbH, 2012.

Data-Driven Artificial Intelligence Applications in Energy Production Systems

Mert Akin INSEL[1,2,*], Hasan SADIKOGLU[1,2], Ozgun YUCEL[3]

[1] *Yildiz Technical University, Department of Chemical Engineering, 34210, Esenler/Istanbul, Türkiye, makinsel@yildiz.edu.tr, 0000-0002-4347-1190*

[2] *Yildiz Technical University, Clean Energy Technologies Institute, 34220, Esenler/Istanbul, Türkiye, hsadik@yildiz.edu.tr, 0000-0002-0234-8428*

[3] *Gebze Technical University, Department of Chemical Engineering, 41400, Gebze/Kocaeli, Türkiye, yozgun@gtu.edu.tr, 0000-0001-8916-2628*

*Corresponding author: makinsel@yildiz.edu.tr

Abstract

The increasing complexity and variability of modern energy systems necessitate robust and data-driven approaches for accurate prediction, classification, and optimization. This study presents an integrated artificial intelligence (AI)-based framework for energy production applications, focusing on fuel characterization, waste-to-energy conversion, and renewable energy forecasting. Various machine learning and deep learning models, including artificial neural networks and recurrent architectures, were developed and applied to datasets consisting of biomass, waste-derived fuels, and historical meteorological data.

For fuel analysis, higher heating value (HHV) prediction models were established using ultimate and proximate analysis parameters, demonstrating strong predictive capability through systematic model development and validation procedures. In addition, a data-driven classification methodology was proposed to better represent heterogeneous fuel types and improve clustering consistency. For renewable energy applications, a generalizable wind power estimation framework was developed using meteorological inputs, enabling accurate prediction across different operational conditions.

The findings demonstrate that AI-based approaches can significantly enhance prediction accuracy and provide deeper insight into complex energy systems. The proposed framework offers a scalable and adaptable solution for supporting efficient, data-driven decision-making in energy production and sustainability-focused applications.

Keywords: Artificial Intelligence; Machine Learning; Deep Learning; Energy Production Systems; Waste-to-Energy; Higher Heating Value; Wind Power Forecasting; Data-Driven Modeling; Renewable Energy; Sustainability; UN SDG 7; UN SDG 12; UN SDG 13

1. Introduction

The global transition toward sustainable and efficient energy systems has significantly increased the need for advanced analytical and predictive tools. Modern energy production systems are characterized by high variability, complex interactions, and heterogeneous data sources, particularly in applications involving renewable energy and waste-to-energy conversion. Traditional modeling approaches often struggle to capture

these nonlinear relationships, leading to limitations in prediction accuracy and system optimization. In this context, artificial intelligence (AI) and machine learning (ML) techniques have emerged as powerful alternatives for modeling complex energy systems [1].

These approaches enable the extraction of meaningful patterns from large datasets and provide improved predictive performance in various applications, including energy demand forecasting, fault detection, system optimization, and renewable energy integration. Among these, fuel characterization and renewable energy forecasting remain critical challenges due to the diversity of input variables and uncertainty in operating conditions.

This study aims to develop an integrated AI-based framework addressing key problems in energy production. Specifically, the study focuses on three main aspects: (i) prediction of higher heating value (HHV) for biomass and waste-derived fuels using machine learning models, (ii) development of a data-driven classification approach to better represent heterogeneous fuel types, and (iii) estimation of wind power generation using historical meteorological data. By combining these components, the proposed framework seeks to improve prediction accuracy, enhance system understanding, and support data-driven decision-making in energy systems. The novelty of this work lies in the integration of multiple AI applications within a unified framework, enabling a comprehensive approach to both conventional and renewable energy problems. This holistic perspective contributes to the development of scalable and adaptable solutions for future energy systems.

2. Materials and Methods

This study employs a data-driven artificial intelligence framework to address multiple energy-related problems, including fuel characterization and renewable energy prediction. The methodology consists of three main stages: data collection and preprocessing, model development, and performance evaluation. The data is obtained from publicly available datasets as referenced in the studies [1–4].

For fuel analysis, a comprehensive dataset comprising biomass, waste-derived fuels, and fossil-based samples was utilized. The input features were derived from ultimate and proximate analyses, including elemental composition such as carbon, hydrogen, oxygen, nitrogen, and sulfur, as well as moisture content, volatile matter, fixed carbon, and ash content. Data preprocessing steps included outlier handling, normalization, and feature consistency checks to ensure reliable model training.

For renewable energy applications, historical meteorological data were used to estimate wind power generation. The dataset included variables such as wind speed, temperature, pressure, and humidity, which were selected based on their relevance to power output. Time-dependent patterns were incorporated through structured input sequences to capture temporal dynamics. Machine learning and deep learning models, including artificial neural networks and recurrent architectures, were developed to model nonlinear relationships between inputs and outputs.

Model configurations were optimized through systematic hyperparameter tuning. In addition, an unsupervised clustering approach was applied to identify inherent structures in fuel data and to establish a data-driven classification scheme. Model performance was evaluated using standard statistical metrics such as root mean squared error and coefficient of determination. Validation strategies were designed to ensure robustness and generalization capability across different datasets and conditions.

3. Results

The conceptual structure of the proposed artificial intelligence framework is presented in Figure 1. This work integrates regression, classification, clustering, and time-series modeling within a unified perspective, linking fundamental AI problem types to specific energy production applications, including HHV prediction, waste-to-energy optimization, and wind power estimation.

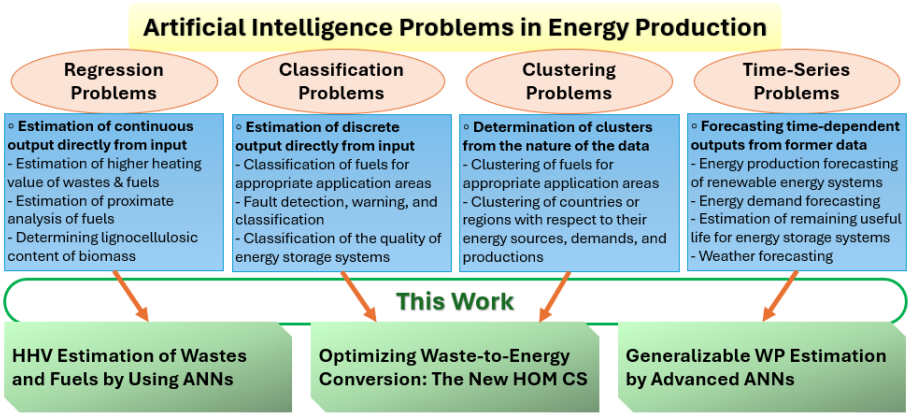


Figure 1. Conceptual representation of the unified AI-driven framework proposed in this work, demonstrating how core machine learning problem types (regression, classification, clustering, and time-series analysis) are systematically aligned with critical energy production applications.

The developed artificial intelligence framework demonstrated strong predictive performance across all considered energy applications. For fuel characterization, the higher heating value prediction models successfully captured the nonlinear relationships between elemental composition and energy content [2].

The results indicated that models trained using both ultimate and proximate analysis variables provided improved accuracy compared to those using limited feature sets. The inclusion of multiple input parameters enabled better representation of heterogeneous fuel properties and reduced prediction errors. The proposed data-driven classification approach effectively identified distinct clusters within the fuel dataset, revealing meaningful groupings beyond conventional classification systems [3].

These clusters reflected variations in chemical composition and energy characteristics, supporting improved interpretability and consistency in fuel representation. The classification results also contributed to enhanced predictive performance when integrated with machine learning models. For renewable energy applications, the wind power estimation models exhibited strong generalization capability across different conditions [4].

The use of temporal input structures allowed the models to capture dynamic patterns in meteorological data, leading to reliable short-term predictions. The developed framework maintained stable performance under varying input distributions, indicating robustness in real-world scenarios. Overall, the results confirm that integrating machine learning, clustering, and time-dependent modeling within a unified framework significantly improves prediction accuracy and system understanding. The approach provides a consistent and scalable solution for complex energy production problems.

4. Discussion

The results demonstrate that the proposed artificial intelligence framework provides an effective and consistent approach for addressing complex challenges in energy production systems. By integrating machine learning, data-driven classification, and time-dependent modeling, the framework enables improved representation and prediction of both fuel properties and renewable energy outputs. The findings highlight the importance of combining multiple data sources and modeling strategies to capture system variability and enhance predictive performance. Detailed analyses and extended validations are provided in the full doctoral thesis, of which this study presents a condensed overview.

5. Conclusions

This study presents an integrated artificial intelligence framework for addressing key challenges in energy production, including fuel characterization and renewable energy prediction. The results demonstrate that data-driven modeling approaches can effectively capture complex relationships within heterogeneous energy datasets and significantly improve predictive performance. The combination of machine learning models, clustering-based classification, and temporal analysis provides a flexible and scalable solution for diverse energy applications. The proposed framework enables more accurate estimation of fuel properties and reliable prediction of renewable energy outputs, supporting improved decision-making in energy systems. In addition, the integration of multiple modeling approaches within a unified structure enhances both system understanding and methodological consistency. It should be emphasized that this work represents a condensed version of a broader research effort. Detailed analyses, extended validation studies, and comprehensive discussions for each component of the framework are provided in the full doctoral thesis. Future work may focus on extending the framework toward real-time applications, integrating additional data sources, and developing digital twin-based systems for advanced monitoring and control of energy processes.

Acknowledgements

This work summarizes the doctoral thesis entitled “Applications of Artificial Intelligence in Energy Production” with the YÖK Thesis Number 931399.

References

[1] Insel MA, Cakar M, Ozturk B, Sadikoğlu H, Yucel O. Deep learning in energy conversion systems. 2025. https://doi.org/10.1016/B978-0-44-313219-3.00175-1.

[2] Insel MA, Yucel O, Sadikoglu H. Higher heating value estimation of wastes and fuels from ultimate and proximate analysis by using artificial neural networks. Waste Management 2024;185:33–42. https://doi.org/10.1016/j.wasman.2024.05.044.

[3] Insel MA, Yucel O, Sadikoglu H. Optimizing waste-to-energy conversion: Unveiling the potential of unsupervised clustering through the new HOM classification system. Sustainable Energy Technologies and Assessments 2024;65. https://doi.org/10.1016/j.seta.2024.103796.

[4] Insel MA, Ozturk B, Yucel O, Sadikoglu H. Generalizable wind power estimation from historic meteorological data by advanced artificial neural networks. Renew Energy 2025;246. https://doi.org/10.1016/j.renene.2025.122995

Predictive Modeling of Ignition Quality in Diesel-Biodiesel-Alcohol Systems for Sustainable Fuel Design

Kaan YEŞİLOVA[1], Özgün YÜCEL[2], Başak TEMUR ERGAN[3], Ümran ÜNLÜ[4]

[1]*Chemical Engineering Department, Gebze Technical University, Kocaeli, Türkiye, kyesilova@gtu.edu.tr, 0000-0002-9987-4722,*

[2] *Chemical Engineering Department, Gebze Technical University, Kocaeli, Türkiye, yozgun@gtu.edu.tr, 0000-0001-8916-2628*

[3]*Chemical Engineering Department, Gebze Technical University, Kocaeli, Türkiye, btemur@gtu.edu.tr, 0000-0002-0708-5102*

[4]*Chemical Engineering Department, Gebze Technical University, Kocaeli, Türkiye, umranunlu@gtu.edu.tr, 0000-0003-4700-5004*

Corresponding author: yozgun@gtu.edu.tr

Abstract
This study investigates the cetane number behavior of diesel-biodiesel-alcohol ternary blends and evaluates the capability of machine learning models to predict it. Blends were prepared with varying diesel (30-90%), biodiesel (5-65%), and alcohol (ethanol and propanol, 0-10%) ratios, and cetane numbers were experimentally determined using standard test methods. The results show that cetane number decreases with increasing diesel and alcohol content, while biodiesel significantly enhances ignition quality due to its higher cetane characteristics. In addition, propanol-based blends exhibited slightly higher cetane numbers than ethanol blends, indicating better ignition performance. To overcome experimental limitations, Decision Tree Regression (DTR), Artificial Neural Network (ANN), and Linear Regression models were applied to predict cetane numbers. Among these, ANN demonstrated a stronger capability in capturing nonlinear relationships between blend components, whereas DTR produced discretized predictions and Linear Regression performed poorly due to its linear assumptions. Overall, the findings highlight the importance of advanced nonlinear modeling approaches for accurately predicting cetane number in complex ternary fuel systems.
Keywords: Affordable and Clean Energy (SDG 7); Alcohol; ANN; Biodiesel; Canola; Cetane Number; DTR; Industry, Innovation and Infrastructure (SDG 9); Machine Learning

1. Introduction

The rapid depletion of fossil fuel reserves and increasing environmental concerns have necessitated the search for sustainable, clean, and renewable alternative fuels for diesel engines [1,2]. Although biodiesel is a significant alternative to conventional diesel fuel, its direct use presents certain disadvantages such as high viscosity, poor volatility, and inadequate cold flow properties [3,4]. To overcome these issues, enhance phase stability, and improve fuel characteristics, ternary blends of diesel-biodiesel-alcohol are produced via the microemulsion method by incorporating alcohols such as n-butanol into diesel and biodiesel. However, while the addition of alcohol improves properties such as density, kinematic viscosity, and cold filter plugging point (CFPP), it adversely affects and reduces the cetane number and calorific value, which are key indicators of ignition quality in diesel engines [3]. A review of the literature indicates that the cetane number of fuels is directly related to

their chemical structure, as well as the chain length and saturation degree of fatty acids [5,6]. Although numerous studies have extensively investigated the effects of various diesel-biodiesel-alcohol ternary blends on engine performance and emissions, determining the cetane number experimentally for each new blend ratio using standard engine tests remains both costly and time-consuming. Previous studies have employed regression models, artificial neural networks, and optimization algorithms such as Grey Wolf Optimization (GWO) to estimate or optimize fuel blend ratios, cetane improver additives, and engine outputs, highlighting the importance of predictive models [7-9]. Nevertheless, there is a noticeable gap in the literature regarding advanced machine learning approaches capable of accurately predicting the cetane number directly based on the composition ratios of diesel-biodiesel-alcohol ternary blends. The aim of this study is to prepare diesel-biodiesel-alcohol ternary blends at specific ratios, calculate their cetane numbers, and develop a machine learning model that can accurately predict these cetane numbers using blend composition ratios as inputs.

2. Materials and Methods

Analytical-grade chemicals and high-purity fuels were used throughout the study. Diesel fuel was obtained from a commercial fuel station, and canola oil was used as the biodiesel feedstock. Methanol and NaOH were employed in the transesterification process, while distilled water and sodium sulfate (Na_2SO_4) were used for washing and drying, respectively. Ethanol and propanol were utilized for ternary blend preparation. Cetane number analyses were carried out at TÜBİTAK MAM using a CFR engine in accordance with ASTM D613.

2.1. Biodiesel Production

Biodiesel was produced via transesterification of canola oil under controlled conditions. The oil was first preheated at 105 °C to remove moisture. The reaction was then carried out using 0.5 wt% NaOH catalyst with a methanol-to-oil molar ratio of 6:1 at 65 °C for 1.5 h. After completion, biodiesel was separated from glycerin, washed multiple times with distilled water to remove impurities, and dried using sodium sulfate (Na_2SO_4). Finally, the product was filtered and reheated at 105 °C to obtain purified biodiesel [10,11].

2.2. Preparing of Blends

Ternary fuel blends of diesel (D), biodiesel (B), and alcohol (A) were prepared on a volumetric basis (v/v). The alcohol content was fixed at two levels (5% and 10%), while the diesel and biodiesel ratios were systematically varied in opposite directions which are 30 to 90 and 65 to 5 respectively. In both cases, increasing diesel content corresponded to a proportional decrease in biodiesel content. This approach enabled a comparative evaluation of fuel properties under low and high alcohol conditions and allowed the investigation of interactions between blend components.

2.3. Cetane Analysis

Cetane number measurements were conducted at TÜBİTAK Marmara Research Center in accordance with ASTM D613 [12] using a CFR engine calibrated with reference fuels. The cetane number was determined based on ignition delay and linear interpolation. All tests were performed under controlled operating conditions, and the reported values represent the average of repeated measurements to ensure accuracy and reliability.

2.4. Machine Learning Study

To address experimental limitations and enhance predictive capability, a machine learning framework was implemented. Prior to modeling, the cetane number values were normalized to ensure numerical stability and improve model performance. The dataset was divided into training (90%) and testing (10%) subsets using the holdout validation method. To improve model accuracy and generalizability, hyperparameter optimization was carried out on the training dataset. Subsequently, the model was trained and validated using 10-fold cross-validation to ensure robustness. Finally, the trained model was evaluated using the previously unseen 10% test dataset, providing an unbiased assessment of its predictive performance [13].

3. Results

Cetane number decreases consistently as diesel content increases (30% - 90%) and biodiesel decreases (65% - 5%), with values dropping from 53.44 to 51.88 for 5% ethanol (AE) blends and from 51.06 to 49.63 for 10% AE blends. A similar trend is observed for propanol (AP), where cetane numbers range from 53.59 to 52.03 at 5% AP and from 51.36 to 49.93 at 10% AP. Increasing alcohol content from 5% to 10% reduces cetane number in all cases, while propanol blends consistently show slightly higher values than ethanol blends. Overall, cetane number is primarily determined by biodiesel content, with alcohol ratio and type having secondary but noticeable effects.

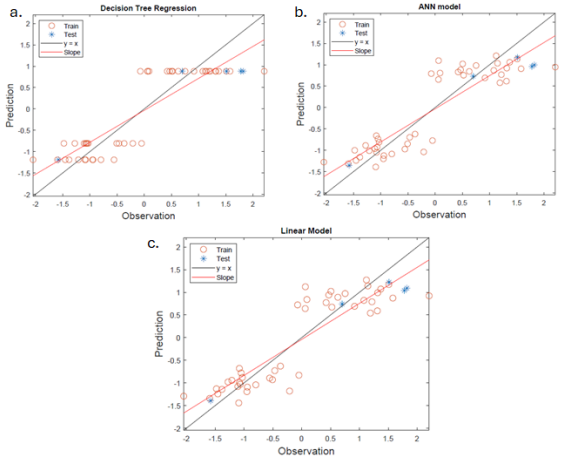


Figure 15. Predicted vs. observed values for cetane number (a) Decision Tree Regression, (b) ANN model, and (c) Linear Regression.

The comparative analysis of the models indicates clear differences in their predictive capabilities for normalized cetane number. The Decision Tree Regression (DTR) model captures the general trend between low and high cetane regions; however, its piecewise structure leads to clustered predictions and systematic bias, with underestimation at higher values and overestimation at lower ones. The Artificial Neural Network (ANN) demonstrates an improved ability to model nonlinear relationships, showing a more continuous distribution of predictions, yet it still exhibits noticeable scatter and bias, particularly in mid-range values. In contrast, the Linear Regression model shows the weakest performance, with significant deviations from the ideal y = x line and an inability to capture the nonlinear interactions between fuel components, resulting in consistent underestimation of high values and overestimation of low values. Overall, while DTR and ANN can follow general trends, nonlinear models outperform linear regression, highlighting the importance of capturing complex compositional effects in ternary fuel systems.

4. Discussion

The results indicate that the cetane number of diesel-biodiesel-alcohol ternary blends is mainly determined by blend composition, with biodiesel having a dominant positive effect on ignition quality. The decrease in cetane number with increasing diesel content and higher alcohol addition confirms the lower ignition characteristics of alcohols, while propanol shows slightly better performance than ethanol. These findings underline the trade-off between improving fuel properties and maintaining adequate ignition quality. From a modeling perspective, the differences among methods highlight their ability to capture nonlinear interactions. Decision Tree Regression follows general trends but produces discretized and biased predictions. The Artificial Neural Network improves this by modeling nonlinear behavior more effectively, although some scatter and bias remain. In contrast, Linear Regression performs poorly due to its inability to represent complex nonlinear relationships. Overall, cetane

number behavior in ternary blends is governed by nonlinear interactions, and accurate prediction requires advanced nonlinear modeling approaches.

5. Conclusions

Cetane number in ternary blends is primarily influenced by biodiesel content and decreases with increasing diesel and alcohol fractions. Propanol performs slightly better than ethanol in terms of ignition quality. Machine learning results indicate that nonlinear models are more suitable for capturing complex compositional effects, with ANN outperforming DTR and Linear Regression. Future studies should focus on more advanced models and larger datasets to improve prediction accuracy.

Acknowledgements

The authors declare that no external funding, institutional support, or additional contributions were received for this study.

References

1. Yaşar F. Comparision of fuel properties of biodiesel fuels produced from different oils to determine the most suitable feedstock type. Fuel. 2020;264:116817.
2. Simsek S. Effects of biodiesel obtained from Canola, sefflower oils and waste oils on the engine performance and exhaust emissions. Fuel. 2020;265:117026.
3. Atmanlı A, Ileri E, Yüksel B. Effects of higher ratios of n-butanol addition to diesel–vegetable oil blends on performance and exhaust emissions of a diesel engine. Journal of the Energy Institute. 2015;88:209-220.
4. Ozcanli M, Serin H. Evaluation of soybean/canola/palm biodiesel mixture as an alternative diesel fuel. Journal of Scientific & Industrial Research. 2011;70:466-470.
5. Allen C, Toulson E, Tepe D, Schock H, Miller D, Lee T. Characterization of the effect of fatty ester composition on the ignition behavior of biodiesel fuel sprays. Fuel. 2013;111:659-669.
6. Selvan T, Nagarajan G. Combustion and emission characteristics of a diesel engine fuelled with biodiesel having varying saturated fatty acid composition. International Journal of Green Energy. 2013;10:952-965.
7. Veza I, Roslan MF, Muhamad Said MF, Abdul Latiff Z, Abas MA. Cetane index prediction of ABE-diesel blends using empirical and artificial neural network models. Energy Sources Part A: Recovery, Utilization, and Environmental Effects. 2024;46:16025-16042.
8. Ileri E, Karaoglan AD, Akpinar S. Optimizing cetane improver concentration in biodiesel-diesel blend via grey wolf optimizer algorithm. Fuel. 2020;273:117784.
9. Noushabadi AS, Dashti A, Raji M, Zarei A, Mohammadi AH. Estimation of cetane numbers of biodiesel and diesel oils using regression and PSO-ANFIS models. Renewable Energy. 2020;158:465-473.
10. Temur Ergan B, Yılmazer G, Bayramoğlu M. Fast, high quality and low-cost biodiesel production using dolomite catalyst in an enhanced microwave system with simultaneous cooling. Clean Chemical Engineering. 2022;3:100051.
11. Temur Ergan B. Kinetic and thermodynamic approaches on biodiesel reaction in a simultaneously cooled enhanced microwave system. Biofuels. 2024;15:155-164.
12. ASTM International. Standard test method for cetane number of diesel fuel oil (ASTM D613-25). ASTM International. 2025.
13. Temur Ergan B, Yucel O, Gengec E, Aydin ES. Integrating machine learning regression and classification for enhanced interpretability in optimizing the Fenton process for real wastewater treatment conditions. Separation and Purification Technology. 2025;363:132182.

AI for Energy, Environment, and Smart Infrastructure

Empowering Industrial Cooling through Predictive Intelligence

Frosty

Jimena Castrillo, Álvaro Enriquez, Francisco Javier Enriquez

Frosty S.L, San Sebastián,(Spain)

Contact email: Jimena.castrillo@alumni.mondragon.edu - a.alvaro1993@gmail.com

Executive Summary

Frosty provides an advanced operational intelligence layer designed to modernize industrial refrigeration management. Moving beyond reactive monitoring, Frosty utilizes proprietary analytics to identify performance deviations before they impact operations, ensuring cold chain stability and preventing high-value stock losses.

Our platform addresses the industry's most pressing challenges: the widening technical labor gap, rising energy overheads, and the increasing demand for automated regulatory traceability. By synthesizing real-time data with advanced performance benchmarking, Frosty empowers maintenance providers to transition toward a predictive service model. This strategic approach significantly optimizes operational expenditures (OPEX), enhances energy efficiency, and maximizes the lifecycle of critical industrial assets.

1. Company Overview

Frosty was born from the convergence of two decades of expertise in industrial thermal engineering and advanced computing systems development. Supported by the Mondragon innovation ecosystem, the company's mission is to transform industrial refrigeration into a seamless, intelligent, and autonomous infrastructure. We position ourselves as the strategic technological partner for service firms seeking to lead the transition toward digital maintenance and operational excellence.

2. Technology / Product / Service Description

Our platform is an operational intelligence solution designed for universal integration across industrial assets. Frosty's technology is built upon the processing of complex data streams to generate advanced diagnostics and process automation. The system provides total visibility into thermal performance, simplifying technical decision-making and ensuring regulatory compliance through an intuitive interface that removes complexity from daily facility management.

3. Innovation and Competitive Advantage

Frosty's competitive edge lies in its agnostic architecture, enabling total interoperability regardless of the Original Equipment Manufacturer (OEM). Our innovation delivers:

Operational Autonomy: Reduces dependency on highly specialized technical profiles through assisted pre-diagnostics.

Proprietary Predictive Analytics: Early detection of critical deviations that impact business continuity.

Value Chain Transparency: Provides an auditable record of data for asset management and dispute resolution between stakeholders.

Financial Optimization: A certified tool for validating and monetizing energy-saving certificates.

4. Market Application and Impact

Frosty targets sectors where thermal stability is critical to business continuity, including the food industry, pharmaceuticals, and advanced computing infrastructures. We generate a measurable impact by reducing operational costs and carbon footprints, aligning industrial efficiency with global sustainability and health safety standards.

5. Partnerships and Outlook

Frosty is currently in the operational validation phase with leading industrial partners in their respective segments. Our 2026 roadmap envisions consolidating these commercial pilots and scaling our infrastructure to meet both national and international demand. We are open to strategic alliances with entities interested in the digitalization of the thermal sector and advanced energy efficiency management.

VodostAI – AI-based Flood Prediction and Prevention Platform ID 53122, Innovation Fund of Serbia – GovTech Program, 2024–2025

Boban Stojanović[1,2], Vladimir Bačanin[1], Boško Laković[1], Tomislav Mrđa[1], Dušan Stefanović[1], Miroljub Krstić[1]

[1]*Vodena d.o.o., Kragujevac, Serbia*

[2]*University of Kragujevac, Faculty of Science, Kragujevac, Serbia*

Corresponding author: Boban Stojanović, boban.stojanovic@vodena.rs

Abstract

VodostAI is an AI- and IoT-powered platform for automated real-time flood prediction, developed under Serbia's GovTech Program (Project ID: 53122, 2024–2025). The platform integrates three core innovations: IoT radar water level sensors for real-time field data acquisition; the Blackfox Automated Machine Learning (AutoML) engine for automatic generation, optimization, and retraining of predictive models; and Physics-Informed Neural Networks (PINN) to address the challenge of sparse historical hydrological data. Deployed on the Kolubara river basin with four monitoring stations, VodostAI achieves high-accuracy water level forecasting across diverse hydrological conditions, including extreme flood events, benchmarked against the HEC-RAS physical model while requiring a fraction of the maintenance effort. The result is a scalable, data-driven decision-support tool for flood management authorities, readily transferable to other river basins.

Keywords: VodostAI; flood prediction; artificial intelligence; IoT; AutoML; machine learning; water level monitoring; flood prevention; Physics-Informed Neural Networks; UN SDG 13

1. Project Background and Objectives

Flooding in Serbia and the Western Balkans causes severe recurrent damage, yet existing prediction systems remain hampered by outdated infrastructure and computationally intensive physical models (such as HEC-RAS) requiring sustained expert maintenance. VodostAI was developed to overcome these barriers through AI and IoT integration.

The primary technical objectives were to:

- design and deploy an IoT-based infrastructure for automated, real-time collection of hydrometeorological data from the Kolubara river basin;
- develop an Automated Machine Learning (AutoML) pipeline for generating, optimizing, and continuously retraining predictive water level models;
- incorporate Physics-Informed Neural Networks (PINN) to overcome the challenge of sparse or low-quality historical hydrological data;

- build a user-facing operational platform enabling real-time monitoring, forecasting visualization, and early flood warning; and
- demonstrate the complete integrated system in an operational environment, validating its accuracy and utility for the public sector end-user.

2. Methodology and Work Performed

The VodostAI platform was built on three integrated technological pillars: IoT-based data acquisition, AutoML-driven predictive modelling, and an operational user interface (Figure 1).

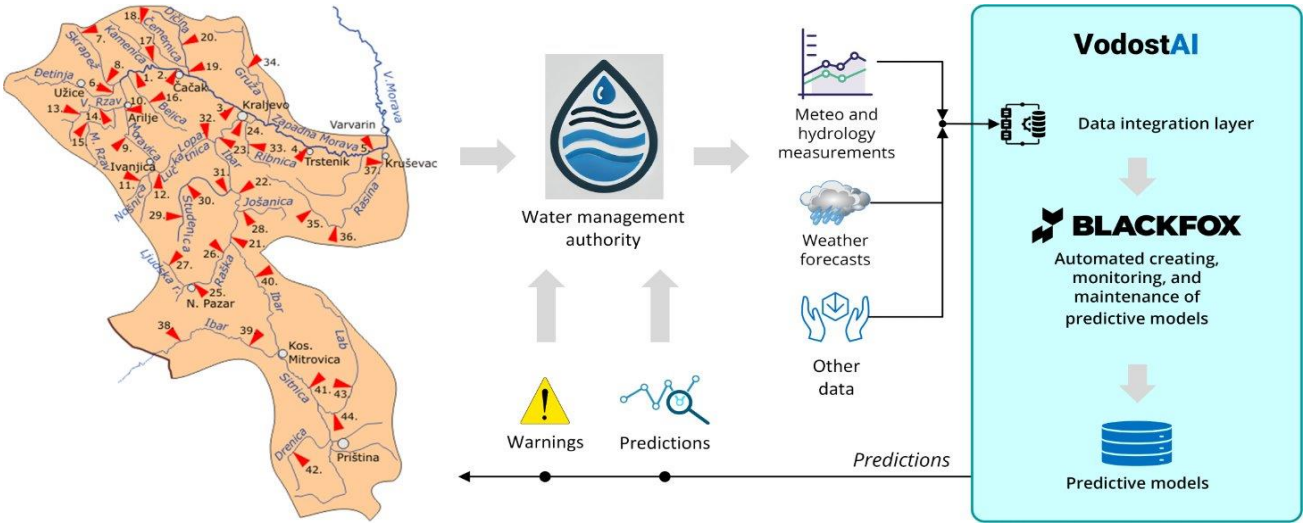


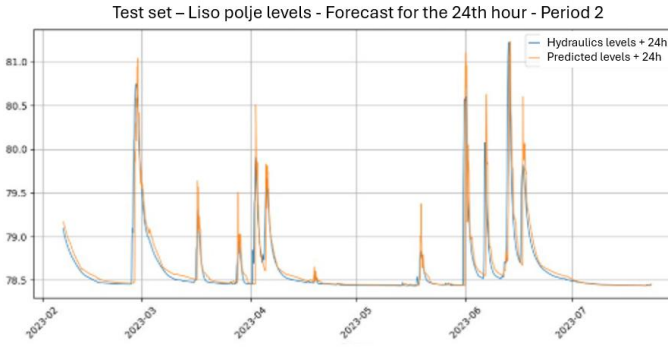
Figure 1. Overview of the VodostAI platform architecture

Four IoT radar water level sensors were installed at key hydrological nodes on the Kolubara basin: on the Ljig river at Ljig, on the Dragobilj river at Kadina Luka, on the Toplica river at Markova Crkva, and on the Kačer river at Dragolj. These stations transmit real-time measurements to the VodostAI platform via a data acquisition, transfer, and storage pipeline with automated validation and preprocessing.

For predictive modelling, VodostAI is integrated with Blackfox, a cloud-based AutoML platform developed by Vodena that automatically generates and optimizes machine learning models based on deep neural networks, Random Forest, and XGBoost, using genetic algorithm optimization of model architecture and hyperparameters. Blackfox also includes an MLOps component for continuous performance monitoring and automatic model retraining as new sensor data accumulates. Physics-Informed Neural Networks (PINN) were incorporated to address data scarcity by embedding domain-specific hydrological constraints into the learning process. Multi-source input features were used, including upstream water levels at multiple stations, precipitation measurements, and temperature forecasts over historical windows ranging from 6 to 168 hours. Model quality was validated against historical flood episodes and benchmarked against the HEC-RAS physical model.

3. Key Results

The VodostAI project achieved all planned objectives within the 12-month project period. The principal results are as follows. Four IoT radar water level monitoring stations were successfully installed and commissioned on the Kolubara river basin, providing continuous real-time hydrological data ingested directly by the VodostAI platform. AI predictive models for water level forecasting were developed, trained, and validated for key stations on the Kolubara basin (including Liso Polje as the primary downstream reference station). Models demonstrated high prediction accuracy across diverse hydrological conditions, including extreme events, outperforming baseline statistical methods and performing comparably to the computationally demanding HEC-RAS physical model, while requiring a fraction of the maintenance effort.



	MAE (cm)	MSE	RMSE (cm)	NSE
Train	4.09108	0.01722	13.12097	0.89801
Validation	9.43333	0.05057	22.48705	0.90256
Test	5.98979	0.02793	16.71349	0.82546

Figure 2. Predictive model performance

The Blackfox AutoML integration enabled fully automated model generation and retraining cycles, ensuring that models remain calibrated to evolving basin conditions without requiring manual expert intervention. A complete VodostAI software platform prototype was developed and deployed, encompassing IoT data ingestion and validation, interactive visualization of real-time water levels and model forecasts, automated early warning notifications when critical flood defense thresholds are approached, and a model repository with MLOps monitoring.

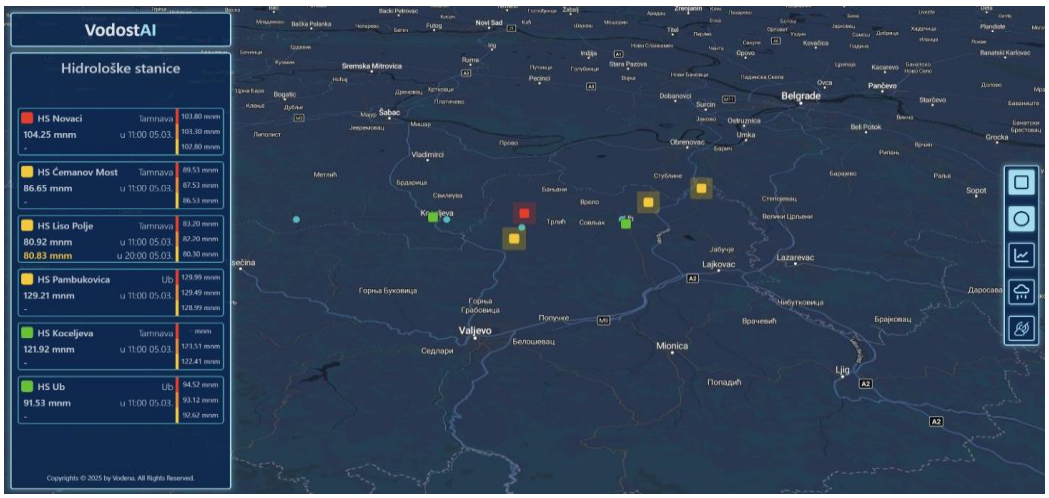


Figure 3. VodostAI operational user interface

The platform user interface was iteratively refined based on feedback from JVP "Srbijavode" operators, with particular emphasis on intuitive presentation of current water levels and forecast results.

The platform prototype was validated in an operational environment and received positive evaluation from JVP "Srbijavode" and Innovation Fund representatives, who expressed strong interest in expanding deployment to additional river basins.

4. Discussion and Impact

VodostAI addresses a critical gap in Serbia's flood management capabilities by providing a scalable, data-driven alternative to manually maintained physical models. Its key technical innovation lies in the combination of AutoML automation with Physics-Informed Neural Networks, which together overcome the two main practical barriers to AI adoption in hydrology: the need for sustained ML expertise, and the scarcity of high-quality historical data. The system's fully automated model generation and retraining pipeline means that water management authorities do not require in-house machine learning teams to operate or maintain the platform.

The demonstrated system constitutes a "digital twin" of the monitored river basin, extensible to hydropower optimization and broader water infrastructure management. VodostAI's modular architecture enables deployment on additional river basins with minimal investment — only initial data collection and model calibration are required — contributing to UN SDG 13 (Climate Action) and UN SDG 11 (Sustainable Cities and Communities).

5. Conclusions and Outlook

VodostAI has successfully demonstrated an integrated AI- and IoT-driven approach to flood prediction. The platform delivers automated, real-time water level forecasting with high accuracy, validated on the Kolubara river basin. The combination of IoT sensing, Blackfox AutoML, and Physics-Informed Neural Networks provides a practically viable solution that minimizes dependence on specialist ML expertise and is robust to data quality limitations.

Future work includes: expansion to additional river basins; integration with national early warning systems; and exploration of the platform as a component of broader water management digital twin systems, including hydropower optimization and irrigation management. The AutoML and PINN methodology is also being explored for other physical domains where prediction under data-scarce conditions is required.

Acknowledgements / Funding

This work was supported by the Innovation Fund of Serbia, GovTech Program Phase II, Project ID 53122. The authors acknowledge JVP "Srbijavode" for operational collaboration, the Faculty of Science, University of Kragujevac, for PINN consultancy, and Jelisaveta Lazarević (Innovation Fund) for project guidance.

Vodena - Next Gen Water and Energy software solutions

Miroljub Krstić[1], Dušan Stefanović[1]

[1]*Vodena d.o.o., Kragujevac, Serbia*

Contact email: office@vodena.rs | Website: www.vodena.rs

Executive Summary

Vodena is an innovative deep-tech company founded in 2014 in Kragujevac, Serbia, as a research spin-off from the Faculty of Science, University of Kragujevac, Vodena specializes in AI-driven software solutions for water and energy management. The company combines advanced physics-based numerical modelling, machine learning, and high-performance computing to address complex engineering challenges faced by utilities, public authorities, and industrial operators managing critical physical infrastructure. Vodena's product portfolio centers on four proprietary platforms: **Blackfox**, a cloud-based AutoML solution for automated creation, continuous monitoring, and self-improvement of predictive machine learning models; **OSICE**, a cloud optimization service democratizing access to advanced evolutionary algorithms for SMEs and large enterprises; **Smarticity**, a digital twin of the energy grids for optimizing renewable energy production and consumption; and **VodostAI**, a digital twin of the river basins providing an IoT- and AI-powered platform for real-time flood prediction and early warning.

Keywords: Vodena; AutoML; Blackfox; water management; flood prediction; hydropower optimization; renewable energy; digital twins; AI, UN SDG 13, UN SDG 11

1. Company Overview

Vodena was established in 2014 in Kragujevac, Serbia, as a research spin-off from the Faculty of Science, University of Kragujevac. The company was founded by Boban Stojanović, PhD, a university professor with over 20 years of experience in computer modelling, optimization, and software development for both commercial and academic applications. Vodena occupies a unique position at the intersection of academic research excellence and applied engineering, offering university-level scientific depth within a commercially agile software development organization.

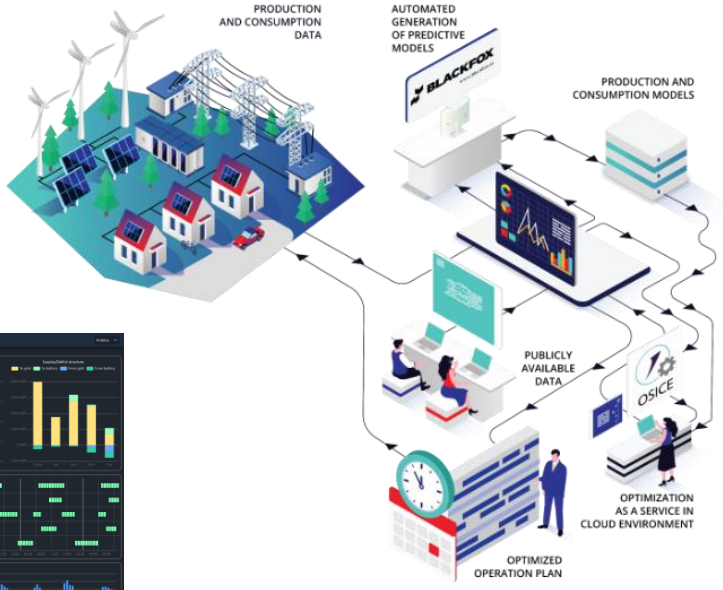
The company's mission is to make advanced computational intelligence accessible and practical for organizations managing complex physical systems, removing the barriers of specialist expertise and high infrastructure costs. Our solutions are tailored to fit the customer business philosophy and follow a structured workflow. We start with **data acquisition and integration,** collecting data and measurements from different sources and consolidating them into a coherent, reliable foundation. Based on this data, we build **physically based and/or data-driven models** that accurately represent the system of interest. We then use these models to **simulate system behavior** under given conditions, enabling in-depth scenario analysis and informed decision-making. Finally, based on simulation results, we **optimize products or processes** to find the best solution under physical, economic, and environmental constraints. This workflow is the backbone of our digital

twin solutions: live, data-driven replicas of real-world systems that enable continuous monitoring, prediction, and optimization. The company has a proven track record of delivering high-impact solutions for major public utilities, national authorities, and international industrial clients across Europe and beyond.

2. Technology / Product / Service Description

Vodena's technology portfolio is organized around four proprietary software platforms.

- **Smarticity** is a digital twin of the energy grid that automates optimization of renewable energy production and consumption. It integrates Blackfox for predictive modelling with OSICE for operational scheduling.





- **VodostAI** is Vodena's most recent innovation: a digital twin of the river basin for real-time flood prediction and early warning, integrating IoT radar water level sensors and the Blackfox AutoML engine, demonstrated operationally on the Kolubara river basin (Serbia) in 2024–2025.



- **Blackfox** (www.blackfox.ai) is a cloud-based AutoML solution for automated creation, continuous monitoring, and self-improvement of data-driven predictive models. It comprises two modules: FoxBrain, which automates model architecture search, feature engineering, hyperparameter optimization, and training using evolutionary algorithms; and FoxTail, an MLOps module for

production-scale deployment and drift-aware continuous retraining of large model fleets. Blackfox is deployed internationally by Vodafone Ireland, STEM (USA), NLB Bank, and Elektroprivreda Srbije.

- **OSICE** (Optimization as a Service in Cloud Environment) is a cloud-based service that enables SMEs and large organizations to apply advanced evolutionary optimization algorithms to business and engineering problems without requiring specialized teams or computing infrastructure.

Underpinning all products is the Vodena Data Integration Suite, providing IoT data acquisition, quality assessment, and real-time monitoring infrastructure.

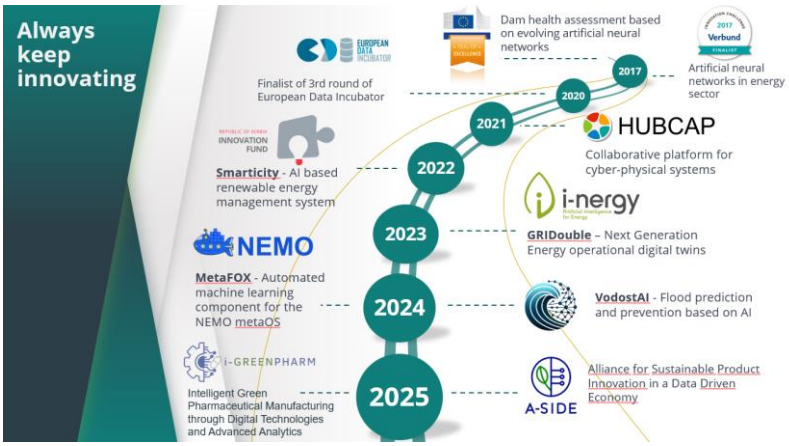
These platforms are deployed in demanding real-world environments across the water and energy sectors. Key projects include:

- **Hydropower production optimization at Iron Gate** — one of the largest hydropower plants in Europe. The solution optimizes production schedules under hydrological forecasts, energy market prices, and ecological and legal constraints, using tightly coupled hydraulic and hydropower production models.
- **Dam remediation decision support at Višegrad dam** — a World Bank-financed capital project addressing water leakage through karst terrain. Vodena developed a multi-model platform (hydraulic groundwater flow, solute transport, granular material sedimentation) that guided remediation activities and reduced leakage by five times.
- **Management of large drainage systems — Pančevački rit** (Belgrade, Serbia). A software platform supporting operators of one of Serbia's largest drainage systems, integrating large data sources with advanced numerical models to achieve flood protection, agricultural production targets, and environmental compliance.
- **Flood early warning system — Kolubara River basin** (Serbia). An end-to-end platform integrating data management, coupled hydrological-hydraulic mathematical models, computation services, and user monitoring applications to issue timely flood warnings for infrastructure and population protection decisions.

3. Innovation and Competitive Advantage

Vodena's primary competitive differentiator is the Blackfox AutoML engine, which enables production-grade predictive modelling without deep data science expertise. The evolutionary optimization approach simultaneously tunes model architecture, feature selection, and hyperparameters, outperforming manual model development in speed and generalization. The "set and forget" design significantly lowers the total cost of AI ownership for industrial operators. A unique technical strength is Vodena's combination of data-driven machine learning with physics-based domain knowledge. The integration of Physics-Informed Neural Networks with AutoML enables accurate prediction even in data-scarce environments, a critical advantage in hydrological and geotechnical applications where high-quality historical data are often unavailable. This hybrid approach is at the scientific frontier and has no direct competitors in the hydrology software market.

Vodena's full-stack vertical integration – from IoT sensing and data management through analytical modelling to user-facing operational dashboards and early warning systems – enables delivery of complete, production-ready digital twin solutions rather than component technologies. This reduces integration risk for customers and shortens time-to-value.



The company's innovation trajectory has been recognised internationally, including a finalist position in the 3rd round of the European Data Incubator (2021), and through successful technology transfer to clients in the USA, Ireland, and the Western Balkans.

4. Market Application and Impact

Vodena operates across two large and growing markets. In water infrastructure management, the company has delivered high-impact solutions for: hydropower production optimization at the Iron Gate (Đerdap) complex on the Danube; decision support for dam remediation at the Višegrad dam; integrated drainage management for the Pančevački rit system (Belgrade, Serbia); flood early warning for the Kolubara river basin; and the VodostAI AI/IoT flood prediction platform. These projects demonstrate the company's capacity to deliver quantifiably impactful solutions for critical national water infrastructure.

In the energy sector, Smarticity addresses the rapidly growing market for intelligent management of distributed renewable energy grids, supporting the transition from centralized to prosumer-driven energy systems. Blackfox has demonstrated cross-sector applicability in energy, telecommunications, and banking.

5. Partnerships and Outlook

Vodena's growth strategy rests on three pillars: continued proprietary product development, expansion through strategic public-sector and research partnerships, and international market development. The company maintains ongoing collaboration with the University of Kragujevac, providing access to frontier research in AI, numerical modelling, and optimization.

Vodena welcomes partnerships in the following areas: joint R&D and technology integration with European research institutions and companies working in AI-for-sustainability, water management, and smart energy grids; commercial deployment partnerships for Blackfox in industries with large-scale predictive modelling needs (utilities, manufacturing, finance, telecommunications); and collaboration with investors, incubators, and strategic partners interested in AI-powered solutions for water and energy infrastructure.

Acknowledgements

This paper is supported through the EIT's Higher Education Initiative A-SIDE projects, coordinated by EIT RawMaterials, funded by the European Union

Substrate Effects on Plant Metabolism: A Machine Learning Perspective

Nenad Zlatić & Milan Stanković

Department of Biology and Ecology, Faculty of Science, Kragujevac, Serbia, nenad.zlatic@pmf.kg.ac.rs (0000-0002-7845-4825), mstankovic@kg.ac.rs (0000-0001-9861-7700)

Corresponding author: nenad.zlatic@pmf.kg.ac.rs

Abstract

Soil heterogeneity represents a major ecological driver influencing plant physiological and biochemical traits. Among these traits, secondary metabolites play a central role in stress tolerance, adaptation, and ecological interactions. This study investigates whether contrasting geological substrates induce consistent differentiation in plant chemical profiles. Plant samples from multiple populations were subjected to chemical profiling, followed by multivariate and machine learning analyses within a nested cross-validation framework implemented in mlr3. Feature selection was conducted using ANOVA filtering and minimum redundancy maximum relevance (mRMR) algorithms. Results revealed structured chemical divergence between substrates, with separation observable in multivariate space and confirmed through classification modeling. Random forest analysis demonstrated stable discrimination performance across validation loops (mean external AUC ≈ 0.90), while variable importance metrics identified a limited subset of metabolites driving substrate differentiation. These findings highlight strong edaphic structuring of plant secondary metabolism and demonstrate the usefulness of integrative statistical approaches in detecting ecological biochemical plasticity. The study contributes to understanding plant adaptation across soil gradients and provides implications for ecological monitoring and medicinal plant resource evaluation.

Keywords: machine learning; multivariate statistics; ecology; substrate

1. Introduction

Soil properties represent one of the most important ecological filters shaping plant distribution, physiology, and biochemical strategies. Among contrasting substrates, serpentinite soils are particularly known for their extreme physicochemical characteristics, including elevated concentrations of heavy metals, low calcium-to-magnesium ratios, and nutrient imbalances. These conditions impose strong selective pressures on plant populations and frequently result in physiological and biochemical differentiation [1].

Plant secondary metabolites are increasingly recognized not only as defense compounds but also as indicators of environmental stress and adaptive responses. Variation in the qualitative and quantitative composition of secondary metabolites across ecological gradients has been documented, particularly in stressful edaphic conditions. However, while metabolomic differentiation has been described, fewer studies integrate

advanced statistical learning frameworks to assess the stability and ecological structuring of such biochemical variation [2].

The novelty of this study lies in combining multivariate statistical analysis with nested machine learning validation to evaluate substrate-driven chemical differentiation. Rather than focusing solely on predictive performance, the objective was to (i) determine whether plant populations from calcareous and serpentinite soils exhibit consistent chemical divergence, and (ii) identify the metabolites most strongly associated with substrate-driven ecological differentiation.

2. Materials and Methods

2.1 Plant Sampling and Chemical Profiling

Plant material was collected from multiple populations growing on two contrasting geological substrates: calcareous and serpentinite soils. The sampling design followed a block principle, where individuals from one population were assigned exclusively to either training or testing sets during validation procedures to avoid replication and ensure ecological independence.

Plant samples were subjected to chemical analysis to obtain quantitative profiles of secondary metabolites. Relative abundances of detected compounds were used as predictor variables in subsequent analyses. Prior to modeling, data were standardized to ensure comparability among variables.

2.2 Feature Selection

To reduce dimensionality and minimize redundancy among predictors, two feature selection strategies were applied prior to model training. First, an ANOVA-based filtering approach was used to rank variables according to their association with substrate type, allowing the selection of the top-ranked metabolites. Second, the minimum redundancy–maximum relevance (mRMR) algorithm was implemented to identify variables that simultaneously maximize relevance to the response variable while minimizing redundancy among predictors. In both approaches, the number of retained variables ranged from 5 to 16, and this parameter was treated as a tunable component within the modeling framework, allowing the optimal feature subset size to be determined during model optimization.

2.3 Machine Learning Framework

Model construction and evaluation were performed using the *mlr3* framework in the R programming environment. Two machine learning algorithms were implemented: recursive partitioning using the rpart package and random forest using the ranger implementation. To ensure an unbiased estimation of model performance, a nested cross-validation procedure was applied. The external validation loop consisted of 10 iterations, where each test set included one randomly selected calcareous population and one randomly selected serpentinite population. Within each external iteration, an internal validation loop based on 9-fold cross-validation was used for hyperparameter tuning. Hyperparameters were optimized using a random search strategy with 100 iterations. Model performance was evaluated using the area under the receiver operating characteristic curve (AUC). In addition to predictive performance, variable importance measures were extracted from the models to assess the relative contribution of individual metabolites to substrate differentiation.

```
# ML workflow
library(mlr3)
library(mlr3pipelines)
library(mlr3filters)
library(mlr3learners)

# Feature selection filters
anova_filter <- po("filter", filter = flt("anova"), filter.nfeat = to_tune(5,16)
mrmr_filter  <- po("filter", filter = flt("mrmr"),  filter.nfeat = to_tune(5,16)

# Branching
branch <- po("branch",
             options = c("none","anova","mrmr"),
             id = "feature_selection")
unbranch <- po("unbranch")

# Classifier
rf <- lrn("classif.ranger", predict_type = "prob")

# Graph pipeline
graph_pipeline <-
  branch %>>%
  gunion(list(
    po("nop"),
    anova_filter,
    mrmr_filter
  )) %>>%
  unbranch %>>%
  rf

# Plot workflow
graph_pipeline$plot()

# Graph
library(DiagrammeRsvg)
library(rsvg)
g <- graph_pipeline$plot()
export_svg(g) |> charToRaw() |> rsvg_png("ML_pipeline.png")
```

3. Results

Random forest models demonstrated stable discrimination between substrate types across external validation loops, with mean AUC values consistently approaching 0.90, indicating robust differentiation independent of specific population partitions. Recursive partitioning models showed slightly lower but comparable performance. Importantly, classification accuracy remained stable despite variations in feature selection strategy and the number of retained variables, suggesting that the observed separation is not driven by a single compound but reflects coordinated, substrate-related metabolic differentiation.

4. Discussion

The observed stability of classification performance across nested validation loops suggests that chemical differentiation is not an artifact of sampling but represents a reproducible ecological pattern. Unlike purely predictive studies, this approach highlights metabolite importance and ecological interpretation rather than model accuracy alone [3]. Previous studies have documented physiological and morphological adaptation to serpentinite substrates [4] however, integrative analyses combining metabolomic data with robust machine learning validation remain limited. The present study contributes to filling this gap by demonstrating how statistical learning tools can serve as exploratory instruments for ecological inference.

5. Conclusions

This study demonstrates that contrasting geological substrates induce consistent and structured differentiation in plant chemical profiles. A limited subset of metabolites drives most of the observed divergence, indicating coordinated biochemical responses to edaphic stress. The integration of multivariate statistics and nested machine learning validation provides a powerful framework for detecting ecological biochemical plasticity. Future work should expand substrate diversity and integrate functional assays to further elucidate adaptive mechanisms underlying substrate-driven metabolic variation.

Acknowledgements

This study was supported by the Serbian Ministry of Education, Science and Technological Development (Agreement No. 451-03-34/2026-03/ 200122).

References

1. Brady UK, Kruckeberg RA, Bradshaw JHD. Evolutionary ecology of plant adaptation to serpentine soils. Annual Review of Ecology Evolution and Systematics. 2005;36:243–266.
2. Quideau S, Deffieux D, Douat-Casassus C, Pouysegu L. Plant polyphenols: chemical properties, biological activities, and synthesis. Natural Products. 2011;50:586–621.
3. Kisiel A, Krzemińska A, Cembrowska-Lech D, Miller T. Data Science and Plant Metabolomics. Metabolites. 2023;13:454.
4. Zlatić N, Budečević S, Stanković M. Geological Substrate Effects on *Teucrium montanum* L. (Lamiaceae) Morphological Traits: Geometric Morphometrics Approach. Plants (Basel). 2023;12:2381.

AI Applications in Mobility and Smart Systems

HAL Mobility AI: AI-Assisted Urban Mobility Orchestration for Local Taxi Ecosystems

Milovan Ostojić[1], Dragutin Ostojić[2], Mihajlo Čekerevac[1], Lazar Avramović[3]

[1]HAL, Kragujevac, Serbia; ostojic.lemi@gmail.com, mihajlo.cekerevac@gmail.com
[2]Faculty of Science, University of Kragujevac, Kragujevac, Serbia; dragutin.ostojic@pmf.kg.ac.rs;ORCID: 0000-0001-6704-353X
[3]EPAM Systems, Belgrade, Serbia; lzr.avr@gmail.com

Contact email: ostojic.lemi@gmail.com | Website: www.hal-tech.rs

Executive Summary

HAL is a technology-driven company focused on the digital transformation of local urban mobility services. Its core development direction is HAL Mobility AI, an AI-assisted platform designed to improve taxi dispatching, reduce passenger waiting times, optimize fleet utilization, and support the modernization of local taxi operators through a scalable digital infrastructure. The company's initial pilot product is internally referred to as UNO.

The company is focused on mid-sized urban markets where dispatch processes remain fragmented, digital channels are underused, and local operators often lack access to advanced decision-support tools. HAL addresses this gap by combining a passenger-facing ordering interface, operator-side dashboards, partner integration workflows, and an AI intelligence layer for dispatch support, ETA prediction, demand forecasting, anomaly detection, and simulation-based planning.

Kragujevac serves as the pilot environment because it represents a suitable market for testing operational and commercial viability. HAL's strategic model is based on collaboration with local taxi companies rather than direct market displacement. By acting as a neutral technology partner, the company enables operators to modernize their digital channels while preserving local market presence and improving service performance.

HAL's long-term vision is to build a scalable urban mobility orchestration platform that can expand through partner networks across Serbia and potentially wider regional markets.

Keywords: urban mobility; AI-assisted dispatching; taxi platform; ETA prediction; demand forecasting; partner integration; digital transformation; entrepreneurship; innovation; UN SDG 9

1. Company Overview

HAL is a technology-oriented company developing software solutions for the modernization of local mobility ecosystems. Its mission is to help urban transport operators move from fragmented and partially manual workflows toward integrated, data-driven, and scalable digital operations.

The company is positioned at the intersection of artificial intelligence, mobility technology, and digital transformation. Its strategy is not based on generic software outsourcing, but on building focused platform solutions for practical operational problems in urban passenger transport.

2. Technology / Product / Service Description

HAL's core offering is HAL Mobility AI, an AI-assisted platform for taxi dispatch optimization and urban mobility coordination.

The solution consists of four integrated layers:

2.1 Passenger Interface

A mobile-first digital channel that allows users to request rides, track service status, receive estimated arrival times, and interact with mobility services more efficiently. This layer is designed to improve accessibility, trust, and overall service experience.

2.2 Operator Dashboard

A software environment for dispatchers, managers, and fleet operators that supports ride allocation, live fleet visibility, operational monitoring, and performance tracking. This dashboard is intended to reduce fragmentation in operator workflows and create a unified view of ongoing service activity.

2.3 Partner Integration Layer

A coordination layer that enables local taxi companies and partner organizations to participate in a common digital ecosystem while preserving their business identity and local presence. This is particularly important in markets where collaboration is more viable than direct centralization.

2.4 AI Intelligence Layer

The AI layer is the company's main technological differentiator. It is designed to provide:

- Demand forecasting by zone and time period;
- AI-assisted dispatch support based on distance, predicted arrival time, demand pressure, and historical assignment behavior;
- ETA prediction using contextual and historical operational data;
- Anomaly detection for suspicious or inefficient patterns such as repeated cancellations, abnormal ride flows, or dispatch mismatches;
- Simulation-based planning for testing dispatch strategies, capacity balancing, and city-expansion scenarios.

Together, these elements transform the product from a simple taxi-ordering application into an urban mobility orchestration platform with practical AI support.

3. Innovation and Competitive Advantage

HAL's innovation lies in combining platform coordination, partner-based market integration, and applied AI for operational optimization.

A key challenge in many local taxi markets is not the absence of drivers or demand, but the absence of a sufficiently intelligent digital infrastructure connecting all actors. Existing systems are often limited to basic communication or ordering functions and do not provide predictive or optimization-based support. [1, 2, 3] HAL addresses this by embedding AI capabilities directly into the dispatch and coordination workflow.

The company's competitive advantage can be summarized through four dimensions:

3.1 AI-Enhanced Operational Intelligence

HAL introduces predictive and decision-support functions instead of relying solely on reactive order assignment. This allows local operators to move toward more efficient and anticipatory service management.

3.2 Neutral Market Position

The earlier pitch materials already frame the business as a third party with a neutral market position interested in maintaining healthy competition, which is strategically important in fragmented local markets where operators may resist solutions perceived as takeover mechanisms.

3.3 Scalable Partner Model

The concept is not limited to a single city. Existing materials already point to partner outreach beyond the home city and interest from operators in additional Serbian markets. This creates a foundation for scalable growth through integration rather than heavy local duplication.

3.4 Focus on Measurable Service Improvement

The original material identifies a concrete market pain point: passengers experience long waiting times during peak demand, while existing user-facing digital tools are poorly adopted. HAL's value proposition is therefore tied to measurable improvements in waiting time, fuel efficiency, service reliability, and fleet utilization.

4. Market Application and Impact

HAL Mobility AI is intended for mid-sized and regionally fragmented urban markets where taxi services remain important, but digital coordination is still underdeveloped.

Kragujevac was selected as the pilot environment because existing market observations indicate long waiting times during peak demand, inefficient fleet utilization, and weak adoption of current user-facing applications. [1, 2] These conditions create a realistic setting for testing measurable improvements in service reliability, response time, and operator efficiency.

The expected impact includes:

- better service experience for passengers,
- improved fleet utilization for operators,
- stronger digital capability for local taxi companies,
- and a replicable model for broader mobility modernization.

5. Partnerships and Outlook

HAL's growth strategy is based on collaboration rather than displacement. The company aims to work with local taxi operators and strategic partners to create a shared digital infrastructure for urban mobility services.

The existing concept already includes partner outreach beyond the home city and builds on the idea that operators may prefer a neutral third-party technology provider over a competing local transport company. This creates a realistic path for phased expansion through partnerships.

In the near term, HAL is focused on:

- validating the pilot concept in a live or simulated operational setting,
- refining the AI dispatch and forecasting layer,
- improving partner onboarding workflows,
- and preparing an exhibition-ready demonstration through dashboard views, dispatch logic visualization, and simulation scenarios.

In the medium term, HAL aims to establish a scalable model for AI-assisted coordination of local mobility ecosystems across Serbia and the wider region.

Acknowledgements

This work has been partially supported by the Serbian Ministry of Science, Technological Development, and Innovation, Agreement No. 451-03-34/2026-03/ 200122.

References

1. Gladović P, Popović V, Stanković M, Lukovac V, Božović M, Radivojević N, Mišić J, Ivanišević T, Stošić M. Elaborat optimalnog organizovanja taksi prevoza u gradu Kragujevcu sa petogodišnjim programom organizovanja taksi prevoza u Kragujevcu za period 2019–2024. godina. Finalna verzija. Niš, Kragujevac: Visoka tehnička škola strukovnih studija Niš; Visoka tehnička škola strukovnih studija Kragujevac; 2019.
2. Grad Kragujevac. Elaborat optimalnog organizovanja taksi prevoza u gradu Kragujevcu sa petogodišnjim programom za period 2025.-2030. godine. Kragujevac: Grad Kragujevac; 2025.
3. Vujić N, Vasiljević Blagojević M, Perić N. Analiza karakteristika taksi usluga kao preduslov njihovog unapređenja. Marketing. 2014;45(3):231-239. doi:10.5937/markt1403231V.

COMPUTATIONAL METHODS

Analytical and Numerical Modelling Fundamentals

Modeling and Simulation of Shear in Shape Memory Alloys

Natalija Milićević[1], Aleksandar Bodić[1], Vladimir Dunić[1]*

[1]*Faculty of Engineering University of Kragujevac, Kragujevac, Serbia, milicevicnatalija18@gmail.com, 0009-0008-4564-0841, abodic@uni.kg.ac.rs, 0000-0002-1713-6540, dunic@kg.ac.rs, 0000-0003-1648-1745*

*Corresponding author: dunic@kg.ac.rs

Abstract

In this paper a simulation of the pseudoelastic behavior of a NiTi shape memory alloy (SMA) during a shear loading is presented. Experimental data from the literature were used as a reference for validating the simulation model implemented into the in-house PAK-DAM finite element software (FEM) software. The geometry of the specimen was created according real specimen dimensions and the finite element mesh, boundary conditions and material parameters were defined according to the experimental setup. The shear loading simulation was performed by using the PAK-DAM software to reproduce the loading–unloading cycle observed in the experimental study. A comparison of the obtained results demonstrated a high correlation between the simulated and experimental curves, particularly in the regions of martensitic forward and reverse phase transformation. The proposed FEM model accurately represents the mechanism of martensitic phase transformation in SMA during the shear loading and can be successfully applied to the analysis and design of components made of NiTi SMA.

Keywords: shape memory alloys; pseudoelasticity; NiTi alloy; martensitic transformation; numerical simulation; PAK-DAM software; shear loading; UN SDG 9

1. Introduction

Shape Memory Alloys (SMA) are a specific class of materials capable of recovering their original shape through reversible phase transformations between austenite and martensite [1]. Among them, SMAs based on nickel and titanium are the most widely used due to their excellent biocompatibility and high corrosion resistance. The material's behavior is primarily based on two phenomena: the shape memory effect and pseudoelasticity (superelasticity), both of which are closely connected to the martensitic transformation.

While tensile behavior is extensively documented, shear loading remains a critical and complex deformation mechanism in many engineering applications [2]. Due to the difficulties of experimental characterization under complex loading conditions, numerical methods such as the Finite Element Method (FEM) have become indispensable for predicting thermomechanical responses [1]. This paper aims to present a numerical simulation of the shear process in a NiTi alloy using PAK-DAM v26 [3] FEM software and to validate the constitutive model by comparing results with experimental data from the literature.

2. Materials and Methods

The numerical simulation is based on the experimental setup described in literature [2], where the authors used a NiTi specimen (Ti–55.8 wt% Ni) with an austenite finish temperature of A_f = 283 K. The specimen is a

rectangular plate of dimensions 27 × 30 × 0.5 mm with six 4 mm diameter holes for fixation [2]. The experimental setup was designed as a specialized device to convert compressive loading into a cyclic loading–unloading shear process [2] schematically shown in Figure 1.

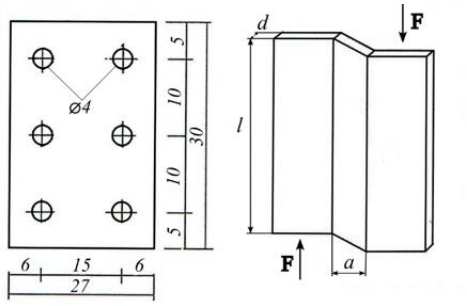


Figure 16 *Schematic representation of the analyzed SMA specimen and the shear test loading [2]*

For the simulation, the Lagoudas [4] reformulated constitutive model [1] is employed and the geometry, mesh and boundary condition are created according to the physical constraints of the experimental shear test [2]. A quarter-model three-dimensional finite element mesh is generated, exploiting the specimen's geometric symmetry. The material parameters are identified by the repeated simulations by using the PAK-DAM software package.

3. Results

Numerical simulation provides detailed insight into the distribution of shear strain, martensitic volume fraction, and equivalent transformation strain within the specimen [5]. As shown in Figure 2, the highest shear strain values occur in the central part of the specimen, while lower values are observed near the holes and boundary conditions. This distribution is a direct result of the specimen geometry and the method of load application.

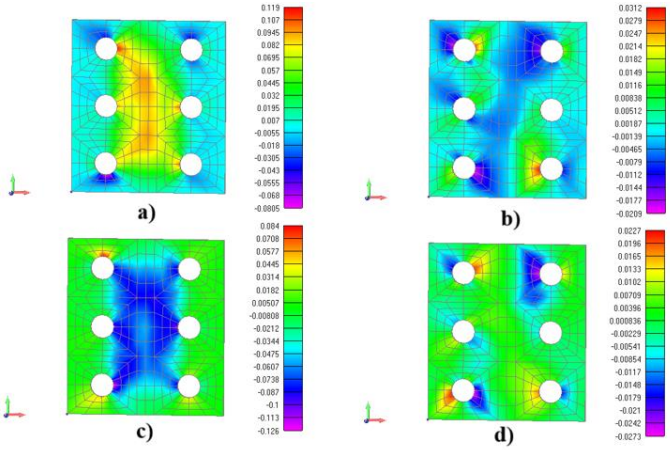


Figure 17 *Shear strain at simulation step: a) 20, b) 40, c) 60, and d) 80 [5]*

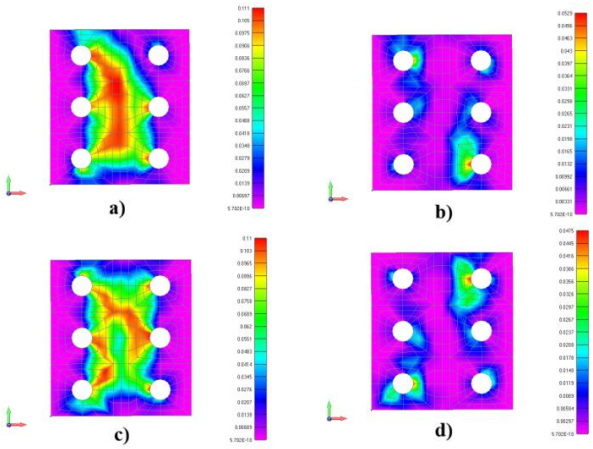


Figure 18 *Martensite volume fraction at simulation step: a) 20, b) 40, c) 60, and d) 80 [5]*

During the loading process, the volume fraction of the martensitic phase gradually increases (Figure 3). At the beginning of the analysis, the material is in the austenitic phase. As the load increases, the martensite phase

progressively spreads through the specimen volume. The highest martensite fraction is found in regions with the most significant deformation.

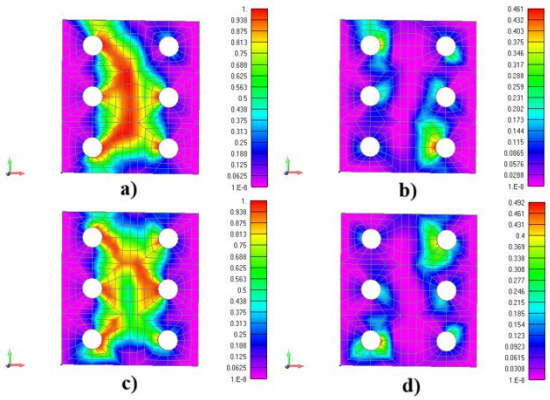


Figure 19 *Equivalent transformation strain field at simulation step: a) 20, b) 40, c) 60, and d) 80 [5]*

The equivalent transformation strain represents the measure of strain resulting from the martensitic phase transformation. The obtained results show that the peak values of transformation strain are localized in zones under the highest stress, confirming the direct correlation between the mechanical state and phase transformation in SMA materials. The initial linear slope represents the elastic deformation of the austenite phase. Increased loading triggers the martensitic transformation, manifested as a non-linear segment on the stress-strain curve (Figure 5a). During unloading, the reverse transformation back to austenite occurs, forming a hysteresis loop that defines the material's pseudoelastic behavior.

4. Discussion

The simulation result (Figure 5a) shows that the loading cycle initiates with a linear elastic region, corresponding to the stable austenite phase. The subsequent parabolic segment marks the stress-induced forward martensitic transformation, which continues until peak stress and strain are reached.

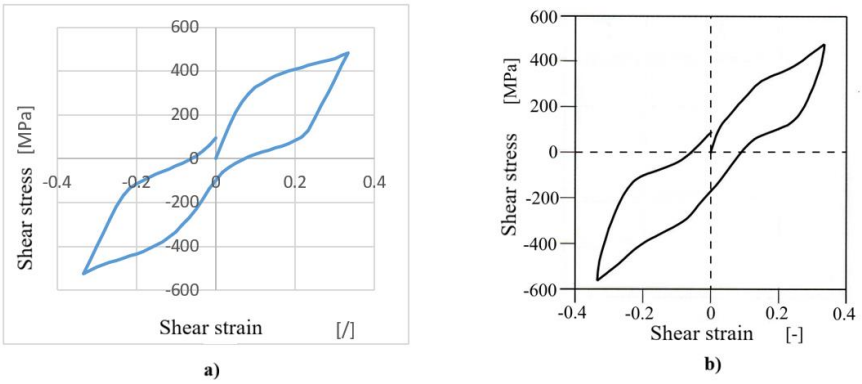


Figure 20 *Comparison of stress-strain diagrams: a) Numerical simulation results [5]; b) Experimental data from literature [2]*

During unloading, an initial linear decrease is followed by a second parabolic segment representing the reverse phase transformation of martensite back into austenite. The symmetry observed in the negative quadrant of the diagram confirms the material's consistent pseudoelastic response under shear loading. A comparison with experimental data from literature [2] represented in Figure 5b, confirms a high degree of correlation. Both the simulation and the experimental curves exhibit identical transformation stages and closely matched critical values. This strong agreement validates the reliability of the applied simulation model in successfully reproducing the complex behavior of the SMA.

5. Conclusions

This study analyses the pseudoelastic behavior of NiTi SMA alloys through numerical simulation of shear loading by using the PAK-DAM software package [5]. By applying a SMA constitutive model that relates stress, strain, the martensitic phase transformation between austenite and martensite was investigated. The main objective was to validate the functionality of the SMA constitutive model [1] in PAK-DAM software for shear loading case by comparing the obtained simulation results with experimental data from the literature [2]. The results show a high level of agreement in the shape of the shear stress–shear strain diagram, where the typical hysteresis loop confirms reversible phase transformations. A slight deviation of the curve after unloading indicates a small residual deformation, which is characteristic of these alloys. This confirms that the PAK-DAM software represents a reliable tool for the simulation and optimization of SMA in engineering applications.

Acknowledgment

This research is supported by the Science Fund of the Republic of Serbia, #GRANT No 7475, Prediction of damage evolution in engineering structures – PROMINENT, and by the Ministry of Science, Technological Development and Innovation, Republic of Serbia, Agreement No. 451-03-34/2026-03/200107.

References

[1] Dunić V. Razvoj i implementacija termo-mehaničkog konstitutivnog modela za numeričku analizu ponašanja materijala sa svojstvom pamćenja oblika, PhD Thesis, Kragujevac: Faculty of Engineering University of Kragujevac; 2015.
[2] Tobushi H, Matsui R, Takeda K, Pieczyska E. Mechanical properties of Shape Memory Alloys Materials. New York: Nova Science Publishers; 2013.
[3] Živković, M.; Dunić, V.; Rakić, D.; Grujović, N.; Slavković, R.; Kojić, M. PAK-DAM v26 Software for Damage and Fracture Simulation; Faculty of Engineering, University of Kragujevac: Kragujevac, Serbia, 2026.
[4] Lagoudas, D. C. Shape memory alloys: modelling and engineering applications; Springer; 2007
[5] Milićević N. Simulacija smicanja na uzorku od legure sa svojstvom pamćenja oblika, BSc thesis, Kragujevac: Faculty of Engineering University of Kragujevac; 2025.

Comparative Numerical Study of Two Interface-Capturing Methods for a Rising Bubble Problem

Aleksandar Bodić[1], Slobodan Savić[1*], Miloš Pešić[2], Marko Topalović[2]

[1]*Faculty of Engineering, University of Kragujevac, Kragujevac, Serbia, abodic@uni.kg.ac.rs, 0000-0002-1713-6540, ssavic@kg.ac.rs, 0000-0001-6609-4845*

[2]*Institute for Information Technologies, University of Kragujevac, Serbia, milospesic@uni.kg.ac.rs, 0000-0002-3405-5216, topalovic@kg.ac.rs, 0000-0001-6101-755X*

Corresponding author*: ssavic@kg.ac.rs

Abstract

This paper presents a comparative numerical analysis of two interface-capturing methods, the Phase-Field and Level-Set method, applied to a rising bubble problem with subsequent interaction with an overlying fluid layer. The simulations are performed using the Finite Element Analysis. The bubble motion is evaluated through the evolution of its centroid and rise velocity prior to coalescence with the upper fluid layer. A Mesh sensitivity analysis is conducted for both methods. The results for both methods are presented comparatively through fluid interface snapshots at multiple time steps, as well as bubble centroid position–time and velocity–time curves. The results indicate that both methods capture the overall bubble rise behavior consistently, with a minor difference primarily related to discretization sensitivity and parameter selection.

Keywords: two-phase flow, bubble dynamics, phase-field method, level-set method, finite element method, UN SDG 9

1. Introduction

Multiphase flow phenomena are widespread in the environment, considering natural phenomena such as rain, snow, fog, biological and medical flows etc. They are also encountered in a wide range of engineering applications, including chemical reactors, oil and gas transport, heat exchangers, and microfluidic systems [1, 2]. In these systems, the dynamics of interfaces between immiscible fluids are essential in influencing overall transport processes, including momentum, mass, and heat transfer. Due to the shortcomings of theoretical, analytical, approaches and high costs of experimental tests, numerical methods have become essential tools for the analysis of multiphase flows [3]. The rising bubble problem represents a classical benchmark for studying interfacial dynamics, including deformation, buoyancy-driven motion, and interaction with surrounding fluid layers [4]. Among various approaches, interface-capturing methods have gained significant attention because of their ability to handle large deformations and topological changes, such as merging and breakup. The Level-Set method [5] represents the numerical technique for tracking moving interfaces and shapes by representing them as the zero-level set of a higher-dimensional implicit function, while the Phase-Field method [6], based

on diffuse-interface theory describes the interface using a continuous order parameter using the Cahn–Hilliard equation [7].

In this paper, a comparative numerical analysis of the Phase-Field and Level-Set methods for a rising bubble problem [4] with subsequent interaction with an overlying fluid layer is given. The bubble motion is evaluated through centroid position and rise velocity prior to merging with upper layer of fluid. This paper gives the systematic comparison of both methods within a Finite Element framework, highlighting their relative accuracy, sensitivity to mesh size, and practical applicability for problems involving interface deformation and merging.

2. Governing equations and numerical formulation

The fluid interface for two phase flow in this paper is captured using the Phase-Field and Level-Set formulations. For both interface capturing methods, the two-phase incompressible flow is described using the Navier–Stokes equations with an additional body force term accounting for surface tension effects at the fluid interface:

$$\rho\left(\frac{\partial \mathbf{u}}{\partial t}+\mathbf{u}\cdot\nabla\mathbf{u}\right)=-\nabla p+\nabla\cdot(2\mu\mathbf{D})+\rho\mathbf{g}+\mathbf{F}_{\sigma}, \tag{2.1}$$

$$\nabla\cdot\mathbf{u}=0\ , \tag{2.2}$$

Where $\boldsymbol{u}$ is the velocity vector, p is the pressure, ρ is the density, μ is the dynamic viscosity, $\mathbf{D}$ is the rate-of-strain tensor, and $\mathbf{F}_{\sigma}$ represents the surface tension force.

2.1 Phase-Field method

In the Phase-Field approach, the interface is described using a continuous order parameter ϕ, governed by the Cahn–Hilliard equation:

$$\frac{\partial\phi}{\partial t}+\mathbf{u}\cdot\nabla\phi=\nabla\cdot(M\nabla\mu) \tag{2.3}$$

where M represents, while the chemical potential μ is defined as:

$$\mu=\phi(\phi^2-1)-\varepsilon^2\nabla^2\phi \tag{2.4}$$

where ε represent the interface thickness parameter.

The surface tension force F_{σ} is derived from the free energy formulation:

$$\mathbf{F}_{\sigma}=\frac{3\sqrt{2}}{4}\frac{\sigma}{\varepsilon}\mu\nabla\phi \tag{2.5}$$

2.2 Level-Set method

The Level-Set method represents the interface implicitly through a scalar function ψ, whose transport is governed by:

$$\frac{\partial \psi}{\partial t} + \mathbf{u} \cdot \nabla \psi = \gamma \nabla \cdot \left(\varepsilon \nabla \psi - \psi(1-\psi) \frac{\nabla \psi}{|\nabla \psi|} \right) \tag{2.6}$$

The Surface tension is modeled using a curvature-dependent body force:

$$\mathbf{F}_\sigma = \sigma \kappa \nabla \psi, \qquad \kappa = \nabla \cdot \left(\frac{\nabla \psi}{|\nabla \psi|} \right) \tag{2.7}$$

where σ is the surface tension coefficient, κ is the interface curvature.

3. Numerical model

The two-phase flow problem considered in this paper is based on a benchmark example from the literature [4]. The computational domain is a cylinder with a height of 15 mm and diameter of 10 mm. Cross-section of computational domain with boundary conditions is shown in **Figure 21**a. At the initial position, two immiscible fluids are present: water occupying the lower region and oil forming a horizontal layer at the top of the domain. An oil bubble is initially positioned within the lower fluid, below the interface of two fluids. The initial bubble diameter is 4 mm, and its center is placed radially coincident with the center of the cylinder, and at a depth of 6 mm below the interface of the two fluids. The initial velocity field is set to zero throughout the domain. The flow is driven by buoyancy forces arising from density differences between the two fluids, while surface tension governs the interface deformation. The numerical model is developed using two-dimensional axisymmetric representation of a cylindrical domain (**Figure 21**b).

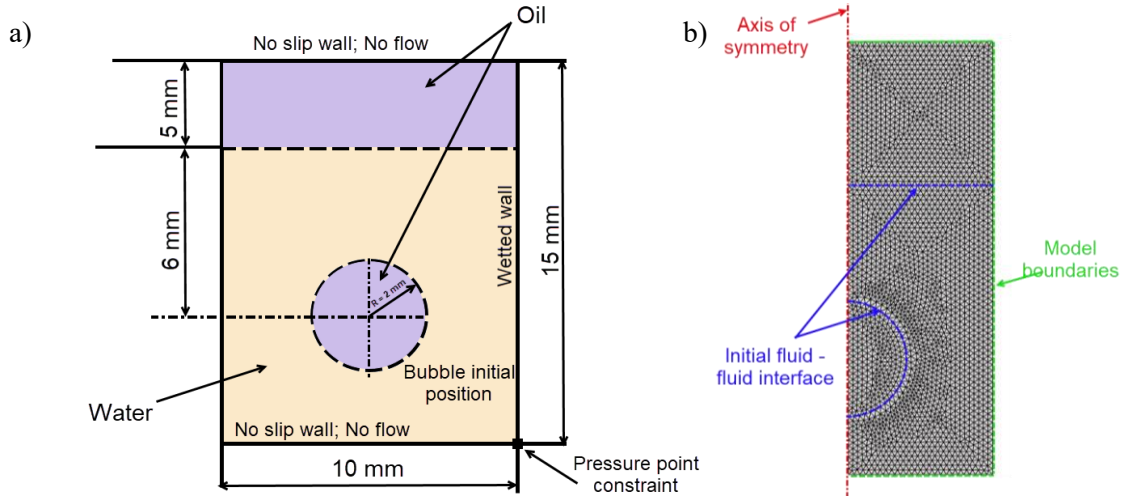


Figure 21 *a) Schematic representation of the computational domain, initial bubble position, and boundary conditions; b) Finite element model*

The left boundary on the FE model shown in **Figure 21**b corresponds to the axis of symmetry. No-slip boundary conditions are imposed on the bottom and top walls. A pressure point constraint is applied at a single point on the bottom boundary to ensure a unique pressure field. Wetted wall condition is prescribed on the vertical boundary on the right, allowing for consistent modeling of contact between the interface and the wall. The physical properties of both fluids are taken as constant, with density and viscosity defined for each phase corresponding to oil and water. The simulations are performed using both the Level-Set and Phase-Field

formulations within a Finite Element framework. A mesh sensitivity study is conducted using different characteristic element sizes (0.1 mm, 0.2 mm, and 0.3 mm) in order to assess the influence of spatial discretization on the predicted bubble dynamics. Time-dependent simulations are performed using an implicit time integration scheme, with maximum time step size 1e-4 in order to ensure numerical stability and accurate resolution of the interface evolution.

4. Results

Results are given for both interface capturing methods in form of interface evolution snapshots, bubble centroid evolution diagram and bubble rise velocity diagram.

4.1 Interface evolution

The evolution of the fluid interface is analyzed through a series of snapshots obtained at selected time instances (t_1 = 0.06 s, t_2 = 0.13 s, t_3 = 0.17 s and t_4 = 0.25. s). Snapshots illustrate the buoyancy-driven rise of the bubble, its deformation, and its subsequent interaction with the upper fluid layer. The interface evolution for Phase-Field method is shown in **Figure 22**.

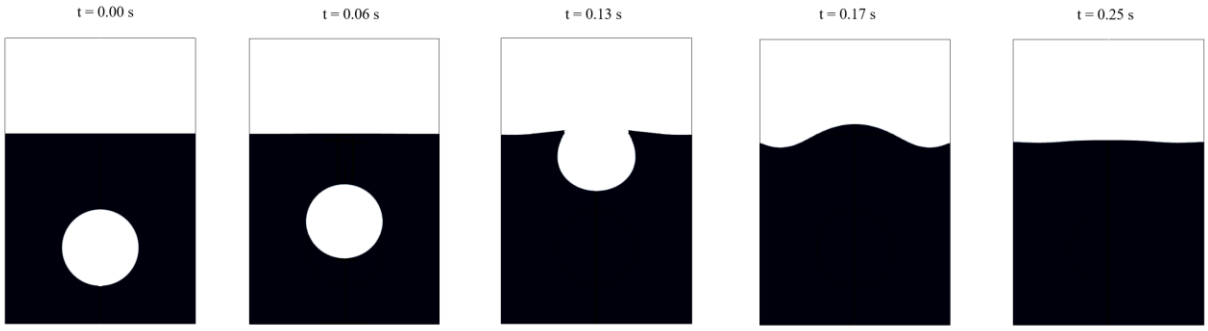


Figure 22 *The interface evolution for the Phase-Field method at times a) t_1 = 0.06 s; b) t_2 = 0.13 s, c) t_3 = 0.17 s and d) t_4 = 0.25 s*

The interface evolution for Level-Set method is shown in **Figure 23**. Snapshots are taken at the same time instances as for Phase-Field method.

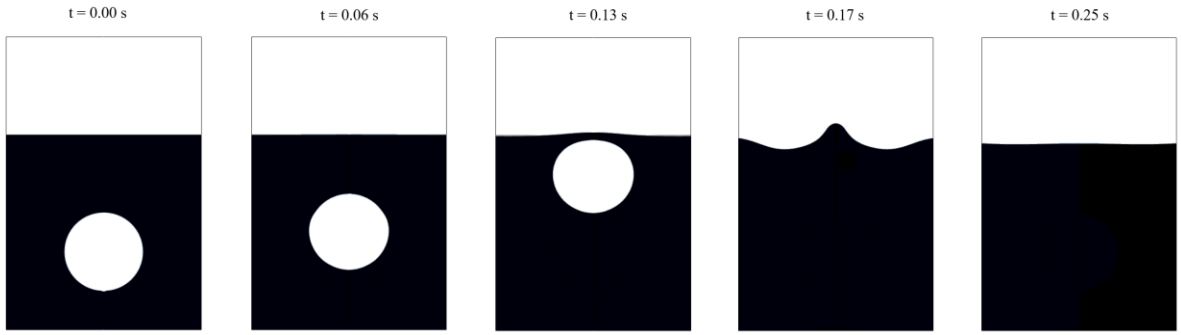


Figure 23 *The interface evolution for the Level-Set method at times a) t_1 = 0.06 s; b) t_2 = 0.13 s, c) t_3 = 0.17 s and d) t_4 = 0.25 s*

A comparison of interfaces between the two methods indicates that both approaches capture the overall interface evolution consistently. However, minor differences can be observed in the interface sharpness and deformation patterns near the merging stage, particularly in the vicinity of the upper fluid layer. Also, phase-field method predicts slightly higher velocities compared to the Level-Set method, i.e. bubble merges slightly earlier with upper fluid layer.

4.2 Mesh sensitivity

A mesh sensitivity study is conducted to evaluate the influence of spatial discretization on the numerical results. The vertical position of the bubble centroid is shown for mesh sizes of 0.1 mm, 0.2 mm and 0.3 mm for both methods (**Figure 24**).

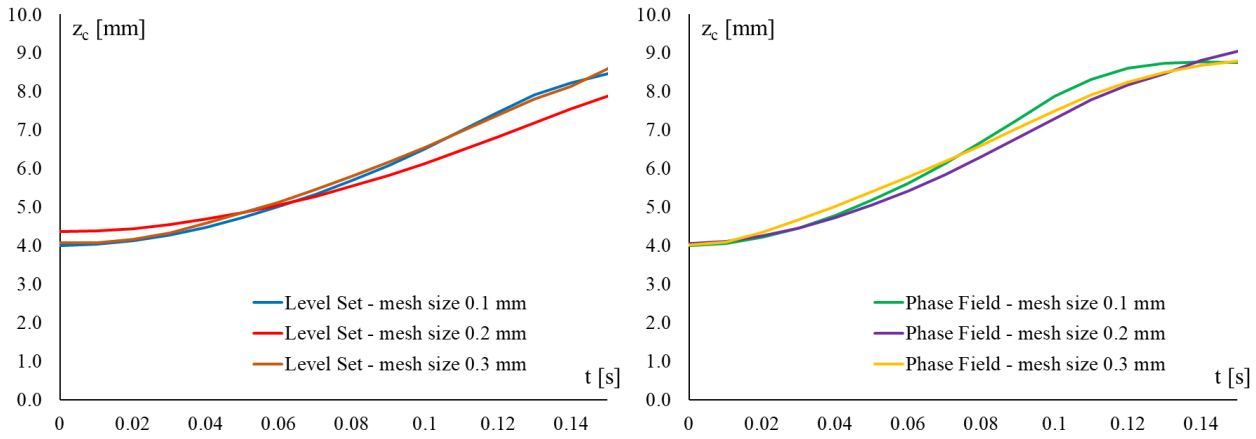


Figure 24 *Bubble vertical centroid position – time diagram for different mesh sizes for a) Level-Set method and b) Phase-Field method*

The results show a consistent trend in bubble centroid evolution across different mesh sizes prior to coalescence with the upper fluid layer. The Phase-Field method predicts slightly higher bubble rise velocities and centroid positions compared to the Level-Set method. For the Phase-Field formulation, the smallest mesh size results in a higher bubble position in the initial stage, which can be attributed to the diffuse interface representation. It should be noted that the observed differences are influenced not only by mesh resolution but also by the adjustment of interface-related model parameters, which may contribute to the deviations, particularly for the 0.2 mm mesh.

The comparison of the evolution of the bubble centroid vertical position for both methods is shown in **Figure 25**.

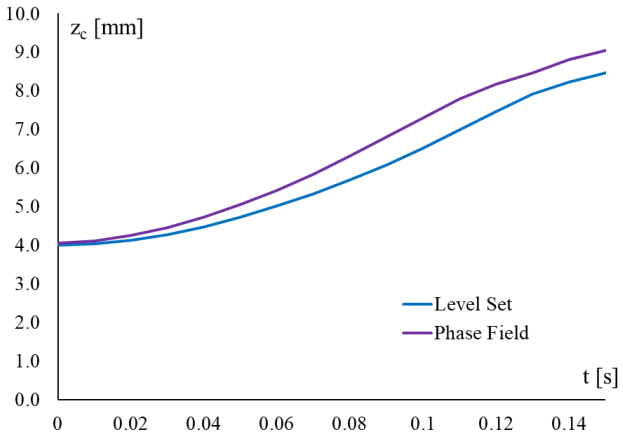


Figure 25 *Bubble vertical centroid position – time diagram comparison*

5. Discussion

Both methods show very realistic behavior, however, they cannot be experimentally verified as such testing would require a construction of complex setup and procurement of expensive monitoring equipment, and there is no existing experimental dataset in the scientific literature. The diffuse nature of the Phase-Field interface means surface tension is distributed over a finite width controlled by the parameter ε, while the Level-Set curvature is more sharply localized. This can lead to subtle differences in the effective surface tension force near coalescence, and consequently the difference in the rising velocity.

6. Conclusions

In this paper the Level-Set and Phase-Field are used to simulate a rising bubble problem with the coalescence with the upper fluid layer. A mesh sensitivity analysis is conducted for both methods, and the results show that both methods capture the overall bubble rise behavior realistically, with a minor difference primarily related to discretization sensitivity and parameter selection, with main conclusion summarized as:

- The Phase-Field method shows slightly higher predicted velocities, due to the differences in interface representation and parameter sensitivity near coalescence.
- Both methods show the trend of faster predicted rise with finer meshes.

The future work will feature a full 3D simulation of benchmark models, and studies of real-life problems with practical implications.

Acknowledgements

This research is supported by the Science Fund of the Republic of Serbia, #GRANT No 7475, Prediction of damage evolution in engineering structures – PROMINENT.

References

[1] G. Yadigaroglu, G. F. Hewitt. Introduction to Multiphase Flow: Basic Concepts, Applications and Modelling. Cham: Springer International Publishing, 2018.
[2] B. Sun. Multiphase flow in oil and gas well drilling. John Wiley & Sons Singapore Pte. Ltd, 2016.
[3] J. Li, D. Zheng, W. Zhang. Advances of Phase-Field Model in the Numerical Simulation of Multiphase Flows: A Review, Atmosphere. 2023:14:1311.
[4] Comsol Multyphisics 6.0. Comsol example - Rising Bubble. Comsol Example book.
[5] M. Sussman, P. Smereka, S. Osher. A Level Set Approach for Computing Solutions to Incompressible Two-Phase Flow. Journal of Computational Physics. 1994:114:146–159.
[6] A. G. Lamorgese, D. Molin, R. Mauri. Phase Field Approach to Multiphase Flow Modeling, Milan J. Math. 2011:79:597–642.
[7] J. W. Cahn, J. E. Hilliard. Free Energy of a Nonuniform System. III. Nucleation in a Two-Component Incompressible Fluid. The Journal of Chemical Physics. 1959:31:688–699.

Finite Element Analysis of Geotechnical Engineering Problems

Jovana Minić[1], Dragan Rakić[1]

[1] *Faculty of Engineering, University of Kragujevac, Kragujevac, Serbia, minijovana@gmail.com, 0009-0006-5353-9474, drakic@kg.ac.rs, 0000-0001-5152-5788*

Corresponding author: drakic@kg.ac.rs

Abstract

In geotechnical engineering, ensuring the reliability of output data is of primary importance. While analytical methods are based on established theoretical frameworks and widely used in engineering practice, numerical methods enable a more detailed representation of complex problems. This study presents the numerical analysis of selected geotechnical engineering problems, including groundwater flow, retaining wall stability, and slope stability. The applications of the Finite Element Method, implemented in the PAK software, are demonstrated through these examples, and the obtained numerical results are compared with analytical solutions. The results show good agreement, confirming the validity of the numerical approach. The advantages of numerical methods in geotechnical engineering are highlighted through a comparative evaluation of the results.

Keywords: FEM, PAK, soil mechanics, safety, groundwater flow, retaining wall, slope, UN SDG 9

Introduction

Finite Element Method (FEM) is a numerical technique widely used for obtaining approximate solutions to boundary value problems in engineering [1, 2]. A boundary value problem is defined as a mathematical formulation in which one or more dependent variables satisfy governing differential equation within a given domain subject to prescribed boundary conditions. The theoretical framework for steady state flow through porous media has been established in [3, 4], as well as for strength analysis [3, 5]. These theoretical formulations have been implemented in the PAK software [5], which is employed in this study as the numerical solver. Pre and postprocessing of the numerical model were performed using Femap software [6]. Geotechnical engineering problems are fundamentally based on the principles of soil mechanics [7] and their numerical treatment encompasses applications such as water filtration, retaining wall stability, and slope stability analysis.

Theoretical Background

Governing Equations for Flow Through Porous Media

Groundwater flow is described using Darcy's law, which in case of a three-dimensional flow is defined by [4]:

$$\mathbf{q} = -\mathbf{k}\mathbf{i} \tag{2.1}$$

where $\mathbf{k}$ represents a permeability matrix, while $\mathbf{i}$ is a hydraulic gradient:

$$\mathbf{i} = \nabla\varphi \tag{2.2}$$

and φ is the total potential.

In previous equation p represents the porewater pressure, γ is the unit weight of water, and h is the distance from the reference level. Using the continuity equation and Darcy's law (2.1), a hydrodynamic equation of steady state flow [3] is:

$$\nabla(\mathbf{k}\nabla\varphi) = -Q \tag{2.3}$$

where Q represents the flow per unit volume.

Governing Equations of the Mohr–Coulomb Model

In the stress-strain analysis, the Mohr–Coulomb material model was used [8]. The yield surface of this material model is the function of stress and has a following form:

$$f = \frac{I_1}{3}\sin\phi + \sqrt{J_{2D}}\left(\cos\theta - \frac{1}{\sqrt{3}}\sin\theta\sin\phi\right) - c\cos\phi \tag{2.4}$$

where I_1 and J_{2D} are the stress invariants, while θ represents Lode's angle, c is the material cohesion (material parameter) and ϕ is the internal friction angle (material parameter).

Shear Strength Reduction Method

The shear strength reduction (SSR) method is one of the most used procedures for obtaining the factor of safety (FoS) of geotechnical structures. The loss of structure stability occurs in case the shear stress in the material τ exceeds the available shear strength of the material τ_f [9]:

$$FoS = \frac{\tau_f}{\tau} \tag{2.5}$$

The global FoS represents the boundary value of the shear strength reduction factor (SRF) for which the structure is at the limit of stability. In numerical analysis, the structure is stable if there is a convergence of numerical solutions.

Numerical Modelling of Geotechnical Engineering Problems Using FEM

Groundwater flow around an impermeable barrier

To reduce the level of groundwater and to ensure that the foundation pit is dry, a steel plate is placed to a deeper layer in the soil. Boundary conditions are defined by applying the hydraulic potential on the left and right sides of the barrier. The filtration coefficient is k=7.2·10^{-2} cm/s.

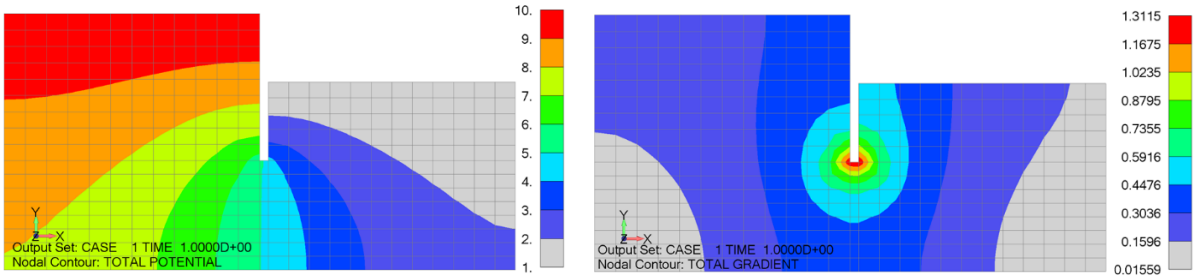


Figure 26. Numerical solution for a) total potential b) hydraulic gradient

As groundwater flows under the steel plate, a vertical flow of water occurs in the foundation pit, which can cause hydraulic uplifting. This phenomenon causes an increase in pore pressure that reduces the effective stress in the soil and leads to a decrease in the effective strength of the soil. Figure 1 shows the distribution of total potential (a) and hydraulic gradients (b), determined using the software PAK [5]. Higher values of hydraulic gradients (*Figure 26*b) indicate a zone where boiling of the bottom of the excavation can occur, which can also lead to a loss of stability. It was calculated that amount of water seeping out from the bottom of the excavation is Q=253.7 m^3/day/m, while the analytical solution is Q=267.5 m^3/day/m [10].

The stability analysis of the retaining wall

In this example, the safety factor of the retaining wall is determined. The retaining wall is loaded with its own weight and the weight of the surrounding soil. The soil material is defined using the Mohr-Coulomb material model, whose parameters are E=50 GPa, ν=0.4, γ=17 kN/m^3, c=6 kN/m^2, ϕ=25°. Nodes at the model's lateral boundaries are prevented from moving horizontally, while nodes at the bottom boundary are fully constrained from moving. The problem is analyzed using plane strain condition. The safety factor was calculated using the shear strength reduction method [9]. The following figure (*Figure 27*) shows results of the numerical analysis for (a) plastic strain and (b) remaining payload capacity for the condition immediately before failure.

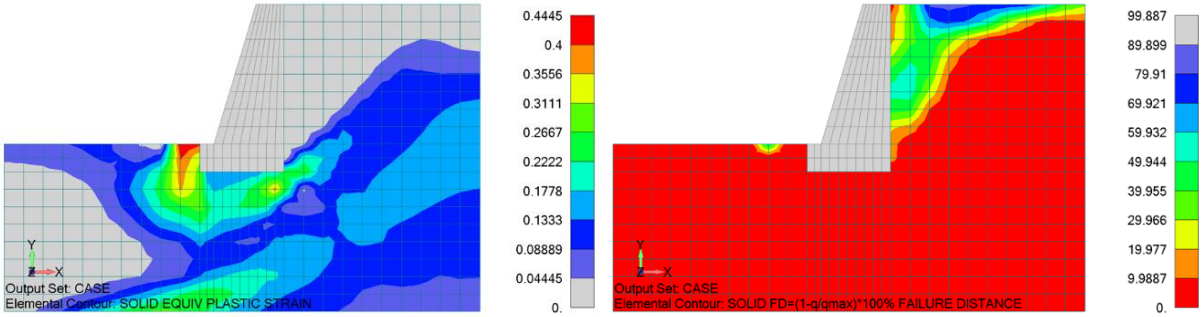


Figure 27. Results of the numerical analysis for the condition before failure a) plastic strain b) remaining payload capacity

Numerically calculated factor of safety is FoS=1.85 and analytical solution is FoS=1.8 [10].

The slope stability

This example presents a numerical analysis of slope stability. The problem geometry, boundary conditions and material parameters are taken from [10].

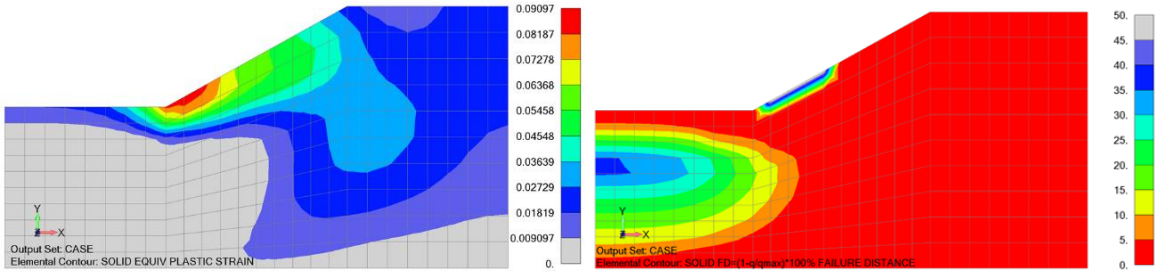


Figure 28. Results of the numerical analysis for the condition before failure a) plastic strain b) remaining payload capacity

The slope consists of a homogeneous soil, whose strength is described by Mohr-Coulomb material model, whose parameters are E=50 GPa, ν=0.4, γ=19 kN/m^3, c=6 kN/m^2, ϕ=6°. In Figure 3 the results of the numerical analysis are shown for the plastic strain and the remaining payload capacity for the condition before failure. The factor of safety calculated is FoS=1.36, while the analytically calculated value is FoS=1.59.

Conclusion

In geotechnical engineering, numerical methods provide a more comprehensive representation of complex problems compared to analytical approaches, primarily due to their ability to incorporate detailed material behavior and site-specific conditions. By employing realistic material parameters and boundary conditions, numerical analyses enable clear and informative visualization of system response. The FEM offers versatile post-processing capabilities, allowing evaluation of various physical quantities and facilitating a deeper understanding of structural behavior under realistic loading conditions. In this study, the FoS was determined using the shear strength reduction method. For the analyzed seepage problem, implementation of the theoretical framework within the numerical model ensures a high level of reliability by accounting for material properties and site conditions. Although the application of numerical methods requires adequate expertise and familiarity with specialized software, their role in geotechnical engineering is essential. Reliable numerical predictions are crucial for ensuring structural functionality and safety. When combined with high-quality input data, numerical methods significantly enhance the accuracy and robustness of conventional safety assessments.

Acknowledgements

The research was supported by the Science Fund of the Republic of Serbia, #GRANT No 7475, Prediction of damage evolution in engineering structures - PROMINENT.

References

1. D. Hutton, Fundamentals of Finite Element Analysis, McGraw-Hill Science, 2003.
2. M. Kojić, R. Slavković, M. Živković, N. Grujović, Finite element method 1 (in Serbian), Kragujevac: University of Kragujevac, Faculty of mechanical engineering, 2010.
3. K. Bathe, Finite element procedures, USA: Massachusetts Institute of Technology, 1996.
4. R. Lewis, B. Schrefler, The Finite Element Method in the Static and Dynamic Deformation and Consolidation of Porous Media, Chichester, UK: John Wiley & Sons Ltd., 1998.
5. M. Živković, M. Kojić, R. Slavković, N. Grujović, D. Rakić, V. Dunić, „PAK-S, Program for FE Structural Analysis of Solids and Structures," University of Kragujevac, Faculty of Engineering., Kragujevac, 2019.
6. Siemens PLM, „Femap User Guide, version 12," Siemens Product Lifecycle Management Software Inc, TX, USA, 2018.
7. M. Maksimović, Soil mechanics (in Serbian), Belgrade: AGM Book, 2014.
8. E. Hoek, „Strength of rock and rock masses," ISRM News Journal, t. 2, pp. 4-16, 1994.
9. N. Tingkai, J. Jingcai, W. Shaoshi, L. Maotian, „Strength Reduction FE Analysis of the Stability of Bank Slopes Subjected to Transient," EJGE, t. 16, pp. 165-177, 2011.
10. M. Maksimović, P. Santrač, A collection of soil mechanics problems (in Serbian), Belgrade: AGM Book, 2010.

Computational Modeling of Manufacturing and Processing

Analytical Modelling of Track Formation in Laser Powder Bed Fusion of IN939

Sampreet Rangaswamy[1,2], Merve Nur Doğu[1,2], Dermot Brabazon[1,2]

[1] *I-Form Advanced Manufacturing Research Centre, Dublin City University, Glasnevin, Dublin 9, Ireland, sampreet.rangaswamy2@mail.dcu.ie, 0009-0008-2925-3331, mervenur.dogu@dcu.ie, 0000-0003-1843-6040, dermot.brabazon@dcu.ie, 0000-0003-3214-6381*

[2] *DCU Institute for Advanced Processing Technology, School of Mechanical and Manufacturing Engineering, Dublin City University, Glasnevin, Dublin 9, Ireland*

Corresponding author: sampreet.rangaswamy2@mail.dcu.ie

Abstract

Laser Powder Bed Fusion (L-PBF) is a widely adopted additive manufacturing technique for producing high-performance nickel-based superalloy components. Inconel 939 (IN939) is of particular interest due to its excellent high-temperature strength and oxidation resistance. However, the processability of IN939 remains challenging due to its susceptibility to cracking and complex thermal behavior. This paper presents an analytical modelling framework for melt pool formation during L-PBF of IN939. In particular, the predictive capability of the analytical Rosenthal equation and the Eagar–Tsai model is evaluated for IN939. The models capture the thermal distribution, melt pool geometry, and solidification conditions using simplified heat transfer formulations. The objective is to provide physical insight into the relationships between processing parameters and melt pool width, while establishing a foundation for future, more comprehensive numerical modelling.

Keywords: IN939; L-PBF; Analytical Modelling; UN SDG 8; UN SDG 9; UN SDG 12

1. Introduction

Laser Powder Bed Fusion (L-PBF) is an additive manufacturing process widely used for fabricating high-performance alloys. L-PBF enables the fabrication of complex geometries directly from metal powders using a layer-wise approach [1,2].

Inconel 939 (IN939) is a nickel-based superalloy known for its excellent high-temperature strength and oxidation resistance and is commonly used in aerospace and energy applications due to its superior mechanical properties at elevated temperatures. However, L-PBF processing of IN939 is associated with defects such as keyholing, balling, and hot cracking [3].

A fundamental aspect of L-PBF is the formation of individual melt tracks, which govern the quality, density, and microstructure of the final part. Understanding single-track formation is critical because it represents the most basic building block of the process [4]. Analytical modelling provides a fast and insightful way to predict melt pool dimensions, thermal gradients, and solidification behaviour without relying entirely on computationally expensive numerical simulations [5].

This work focuses on evaluating analytical models for predicting the temperature field, melt pool width, and process–parameter relationships in L-PBF of IN939. While analytical modelling has been widely applied to other nickel-based alloys, there is limited work specifically addressing IN939. Therefore, this study aims to assess the applicability of classical models, including the Rosenthal and Eagar–Tsai formulations, for IN939 and to establish a foundation for future, more comprehensive modelling efforts.

2. Materials and Methods

In this study, gas atomized IN939 powder (Truform 939-N65, Praxair Surface Technologies) was used to fabricate IN939 single-tracks using an Aconity MINI metal additive manufacturing system equipped with an IPG Ytterbium fibre laser operating at a wavelength of 1070 nm. All fabrications were performed under a high-purity argon atmosphere (99.999%), with oxygen levels maintained below 20 ppm to minimise oxidation effects. A powder layer with a thickness of 40 µm was uniformly spread onto the IN939 build plate prior to laser exposure. Single-track scans were then produced by selectively melting the powder along predefined paths. The laser spot size was kept constant at 80 µm throughout the experiments, while scan strategies were limited to variations in the X–Y plane. Each single-track line was fabricated with a length of 10 mm.

For the modelling component, two analytical approaches, the Rosenthal equation and the Eagar–Tsai model [6,7] were evaluated to predict the melt pool width. Material thermophysical properties at room temperature were obtained using the Calculation of Phase Diagrams (CALPHAD) approach, implemented via the Thermo-Calc software with the TCNI11 database for nickel-based alloys. he thermal conductivity, thermal diffusivity, specific heat, and density were taken as 10 W/m·K, 3×10^{-6} m²/s, 400 J/kg·K, and 8115 kg/m³, respectively. The melting temperature was assumed to be 1630 K, and the laser absorptivity was taken as a constant value of 0.3. Further details regarding the analytical model formulations can be found in the authors' previous work [4].

3. Results and Discussion

The predicted melt pool track widths obtained from the Rosenthal (RE) and Eagar–Tsai (ET) models were compared against experimental measurements across laser powers (P) of 160–200 W and scan speeds (V) of 400–1200 mm/s, and further analysed using linear energy density (LED = P/V), as can be seen in **Table 1**. Overall, the Rosenthal model showed strong agreement with experimental data, with prediction errors generally within ±8% and most values below 5%. In contrast, the Eagar–Tsai model exhibited significantly larger deviations, with errors ranging from approximately −40% to +40%.

The experimental results demonstrate a clear dependence of melt pool width on both process parameters and linear energy density, with width increasing from ~86 µm to ~186 µm as LED increased from 0.13 to 0.5 J/mm. This behaviour reflects increased energy input per unit length, leading to greater heat accumulation and larger melt pools [8]. The superior performance of the Rosenthal model can be attributed to its moving point heat source formulation, which appears sufficient for first-order predictions despite neglecting convection and phase change. The discrepancies observed in the Eagar–Tsai model may stem from its sensitivity to input parameters such as absorptivity and beam radius, as well as its representation of heat distribution. **Figure 1** shows the experimental melt track and the model generated track.

Table 1. Parameter combinations with measured track widths and model predicted widths along with corresponding errors.

Sample No.	Laser Power (W)	Scan Speed (mm/s)	Linear Energy Density (J/mm)	Exp. Track Width (µm)	RE Model Width (µm)	Error (%)	ET Model Width (µm)	Error (%)
1	160	400	0.4	156	161	3.0	203	29.9
2	160	800	0.2	110	114	3.3	154	39.8
3	160	1200	0.13	86	93	7.9	74	-13.4
4	180	400	0.45	164	171	3.9	214	30.7
5	180	800	0.23	120	121	0.4	161	33.8
6	180	1200	0.15	99	98	-0.5	67	-32.5
7	200	400	0.5	186	180	-3.3	226	21.2
8	200	800	0.25	123	127	3.3	167	35.9
9	200	1200	0.17	100	104	3.7	60	-40.4

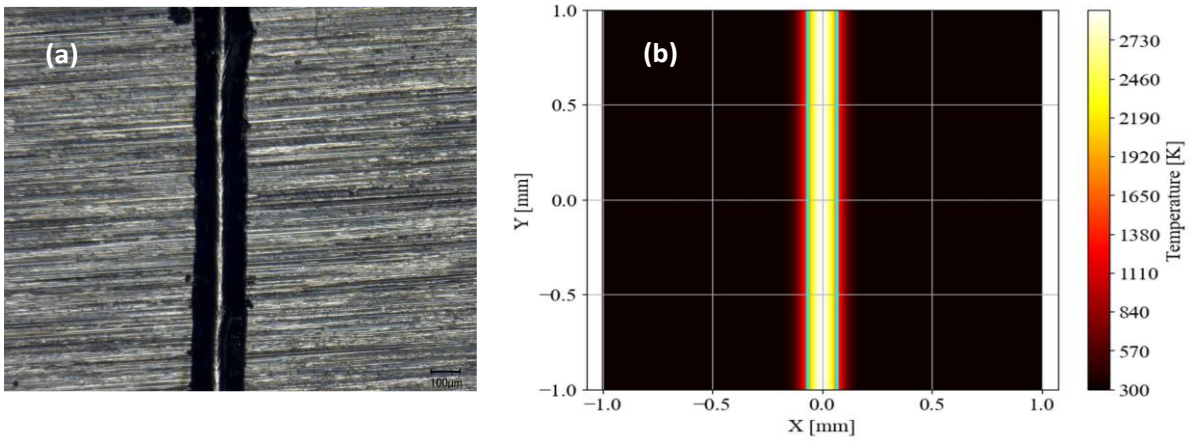


Figure 1. Sample 7 (a) track formed in the experiment (b) model generated track.

For IN939, where cracking susceptibility is strongly linked to thermal gradients and solidification conditions, accurate prediction of melt pool geometry is critical. While the Rosenthal model provides a computationally efficient tool for preliminary process optimisation, both models are limited by the exclusion of key physical phenomena such as melt pool convection, Marangoni flow, and keyhole effects, and should therefore be complemented with experimental validation or higher-fidelity numerical approaches for more accurate predictions [4,9].

4. Conclusions

This study presented an analytical modelling framework for predicting melt pool formation in Laser Powder Bed Fusion (L-PBF) of IN939 using simplified heat transfer approaches. The Rosenthal and Eagar–Tsai models were evaluated against experimental single-track data, with particular emphasis on melt pool width and its dependence on process parameters. The results demonstrate that the Rosenthal model provides consistently

better agreement with experimental measurements, with errors generally within ±8%, while the Eagar–Tsai model shows larger deviations, particularly at low and high linear energy densities.
Although both models capture the overall trends in melt pool behaviour, their limitations must be acknowledged, particularly the neglect of fluid flow, phase change effects, and temperature-dependent material properties. Despite these simplifications, the analytical approach offers a computationally efficient tool for rapid process insight and preliminary parameter selection. The findings establish a foundation for future work, where these models can be extended and validated through incorporation of more advanced physics and experimental datasets, ultimately contributing to improved process control and defect mitigation in L-PBF of IN939.

Acknowledgments
This research was supported by I-Form, the Science Foundation Ireland (Research Ireland) Research Centre for Advanced Manufacturing. This project was conducted in partnership with ANSYS Inc., a company based in Utah, USA. Funding for this work was provided through grants 16/RC/3872 and 21/RC/10295_P2.

References

[1] M.N. Doğu, S. Ozer, M.A. Yalçın, K. Davut, M.A. Obeidi, C. Simsir, H. Gu, C. Teng, D. Brabazon, A comprehensive study of the effect of scanning strategy on IN939 fabricated by powder bed fusion-laser beam, Journal of Materials Research and Technology 33 (2024) 5457–5481. https://doi.org/10.1016/j.jmrt.2024.10.171.
[2] S. Rangaswamy, C. Rubio, M.C.C. Monu, M.N. Doğu, D. Brabazon, Review of the laser powder bed fusion of nitinol: Defect formation and prediction, Mater. Today Adv. 30 (2026) 100771. https://doi.org/10.1016/j.mtadv.2026.100771.
[3] M.N. Doğu, M.A. Obeidi, H. Gu, C. Teng, D. Brabazon, Powder Bed Fusion–Laser Beam of IN939: The Effect of Process Parameters on the Relative Density, Defect Formation, Surface Roughness and Microstructure, Materials 17 (2024) 3324. https://doi.org/10.3390/ma17133324.
[4] S. Rangaswamy, D. Bourke, M.C.C. Monu, P. Healy, H. Gu, I.U. Ahad, D. Brabazon, Investigating Melt Pool Dimensions in Laser Powder Bed Fusion of Nitinol: An Analytical Approach, Adv. Eng. Mater. 26 (2024). https://doi.org/10.1002/adem.202401636.
[5] A.K. Agrawal, B. Rankouhi, D.J. Thoma, Predictive process mapping for laser powder bed fusion: A review of existing analytical solutions, Curr. Opin. Solid State Mater. Sci. 26 (2022). https://doi.org/10.1016/j.cossms.2022.101024.
[6] D. Rosenthal, The Theory of Moving Sources of Heat and Its Application to Metal Treatments, J. Fluids Eng. 68 (1946) 849–865. https://doi.org/10.1115/1.4018624.
[7] T.V. Eagar, N.-S. Tsai, Temperature Fields Produced by Traveling Distributed Heat Sources, n.d.
[8] S. Rangaswamy, J.C. Chekotu, T. Gillick, C. Hughes, J. Nicholl, D. Easton, C. Şimşir, D. Brabazon, Evaluating residual stress in additively manufactured nitinol shape memory alloy, Npj Advanced Manufacturing 2 (2025) 16. https://doi.org/10.1038/s44334-025-00027-y.
[9] P. Promoppatum, S.-C. Yao, P.C. Pistorius, A.D. Rollett, A Comprehensive Comparison of the Analytical and Numerical Prediction of the Thermal History and Solidification Microstructure of Inconel 718 Products Made by Laser Powder-Bed Fusion, Engineering 3 (2017) 685–694. https://doi.org/10.1016/J.ENG.2017.05.023.

Determining the influence of process parameters during ironing using FEA

Marko Delić[1], Vesna Mandić[2], Dušan Arsić[1], Đorđe Ivković[1], Nada Ratković[1], Anđelka Ilić[1]

[1]*Department, Faculty of Engineering, Kragujevac, Serbia, marko.delic@kg.ac.rs, https://orcid.org/0000-0001-5493-7569, mandic@kg.ac.rs, 0000-0003-1624-3536, dusan.arsic@fink.rs, 0000-0003-0326-0898, djordje.ivkovic@fink.rs, 0000-0002-5747-7876, nratkovic@kg.ac.rs, 0000-0003-1446-8678, andjelka.ilic@fink.rs, 0009-0000-2723-725X*
Corresponding author: marko.delic@kg.ac.rs

Abstract

The ironing process is very common in modern industry, so it is very important to determine the influence of process parameters on process stability. In this paper, the influence of two important parameters, friction and blank holding force, was analyzed using the finite element method. For both parameters, three values were considered that are within some theoretically acceptable limits, so the experiment was organized according to the Taguchi matrix L9. The Cocroft Latham damage model was used to analyze the process. In addition to damage, the influence of parameters on sheet thickness, stress state, forming load and other parameters was analyzed.

Keywords: Ironing, FEA, Cocroft Latham, damage, friction, blank holding force, UN SDG 9

1. Introduction

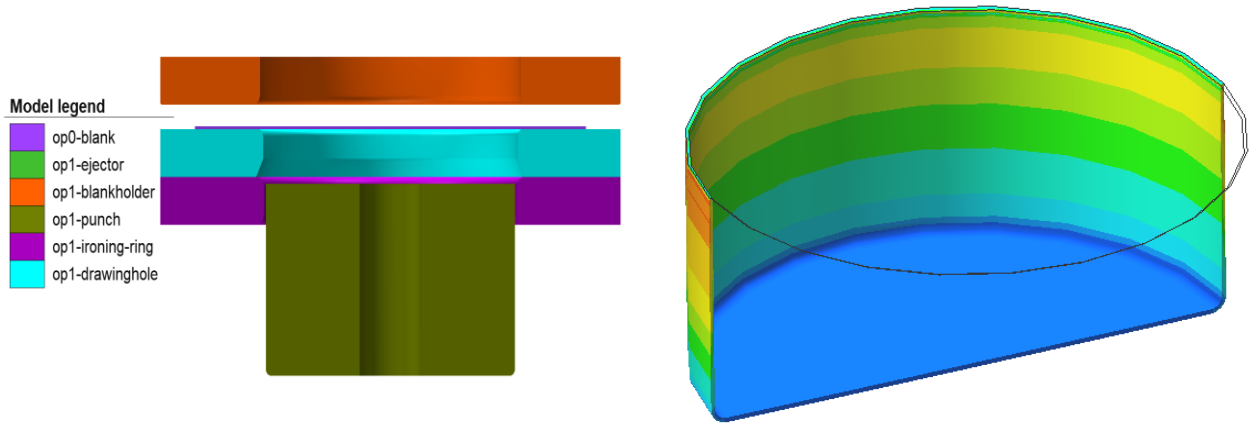
The process of deep drawing with thinning is of great interest for many industries such as automotive or military. In this paper, an industrial example of deep drawing with thinning is analyzed using FEA. Numerical simulation was performed in the Simufact forming software. The Cocroft Latham damage model [1] was used to analyze the results. The Cocroft Latham model is widely used for material failure analysis. The forming limit diagram [2] is most commonly used for sheet metal forming and failure assessment. The Cocroft Latham model is based on the idea that failure occurs when the accumulated plastic strain energy under tensile stress reaches a critical value..

2. Experiment plan and Methods

The considered process consists of two operations: deep drawing and ironing. The process layout is shown in Figure 1. The experiment was designed according to the Taguchi matrix L9 model, two factors with three levels each. As mentioned, friction and holding force were considered. The value of the contact friction coefficient ranges from 0.08 to 0.15 according to domestic literature. The value of the friction coefficient in the numerical experiment will have the values 0.08, 0.12 and 0.16. The value of the holding force will have the values 8 kN,

10 kN and 12 kN. Although the holding force has an effect only during deep drawing, it will be interesting to check whether it will have an effect on the final result of the process after ironing.

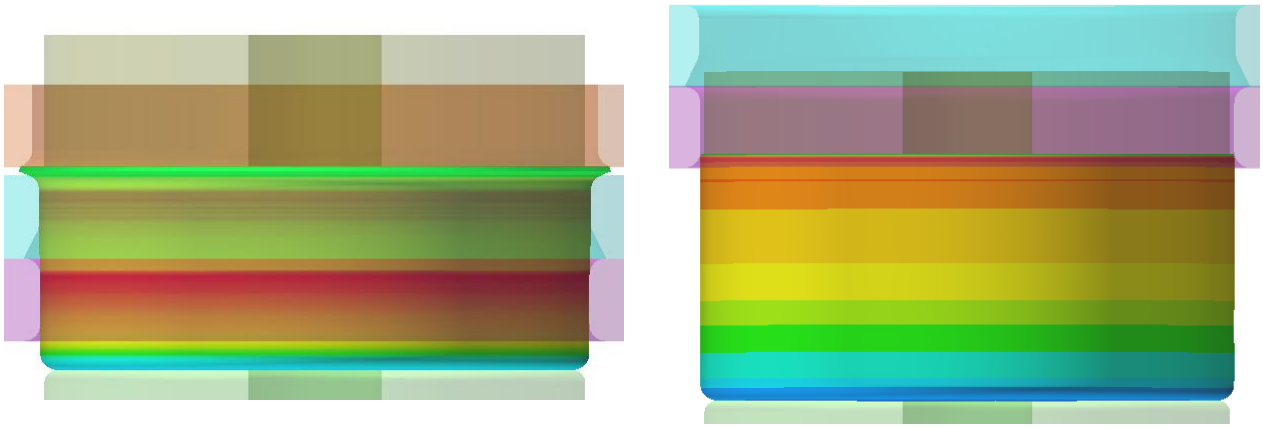
The results that will be analyzed are the value of the forming load, damage according to the Cockroft Latham model and wall thickness. The influence of the parameters on the value of the deformation force will be analyzed according to the less-better model, as well as for the damage model. For the wall thickness, the amount of deviation from the nominal value will be considered.



a) b)

Figure 1. a) Deep drawing and ironing die and b) final part

The operation flow is shown in Figure 2. The starting piece is a carbon steel sheet Ø102x0.6 mm. The steel designation according to DIN is 1.0303 (AISI 1005). First, standard deep drawing is performed, during which the sheet is slightly thinned by about 10%, so the sheet thickness is 0.54 mm. After deep drawing, the sheet is thinned, or ironed, to a dimension of 0.48 mm. Figure 2 a) shows the end of the deep drawing process, and the figure 2 b) shows the ironing process.



a) b)

Figure 2. a) End of deep drawing and b) ironing process

A Quadtree mesh of 0.16 mm size was used in the numerical simulation. There is a dilemma as to whether it is better to use the Coulomb friction model or the constant friction model to define the friction conditions in the numerical simulation of the ironing process, but it was concluded that the Coulomb model, or sliding friction, better fits the process. The experimental plan with parameter values is shown in Table 1.

Table 1. Experiment plan

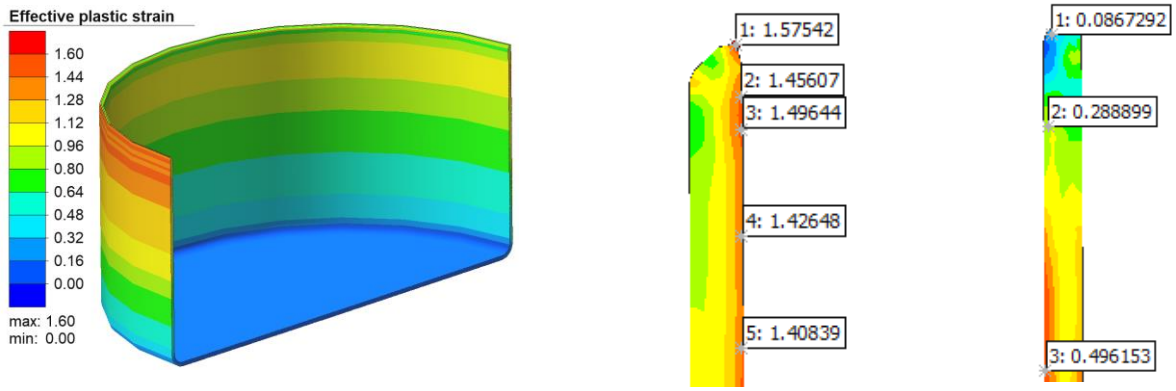
Experiment	Friction coefficient	Blank holding force
1	0,08	8 kN
2	0,08	10 kN
3	0,08	12 kN
4	0,12	8 kN
5	0,12	10 kN
6	0,12	12 kN
7	0,16	8 kN
8	0,16	10 kN
9	0,16	12 kN

3. Results

As stated, the values of the parameters according to the Cockroft Latham model, the deformation force of the drawing, the deformation force during drawing with thinning or ironing, and the thickness of the sheet will be considered from the results. The results are shown in Table 2 and Figure 3.

Table 2. Numerical experiment results

Experiment	Effective plastic strain	Cocroft-Latham	Deep drawing forming load, kN	Ironing load, kN	Thickness, mm
1	1,6	0,52	43,93	52,52	0,48
2	1,69	0,63	46,12	52,83	0,48
3	1,65	0,52	48,37	51,23	0,48
4	1,6	0,52	46,1	58,94	0,48
5	1,64	0,53	48,49	57,48	0,48
6	2,67	0,56	51,03	60,51	0,48
7	1,65	0,52	48,39	64,31	0,48
8	1,85	0,69	50,89	63,94	0,48
9	1,73	0,55	53,48	77,7	0,48

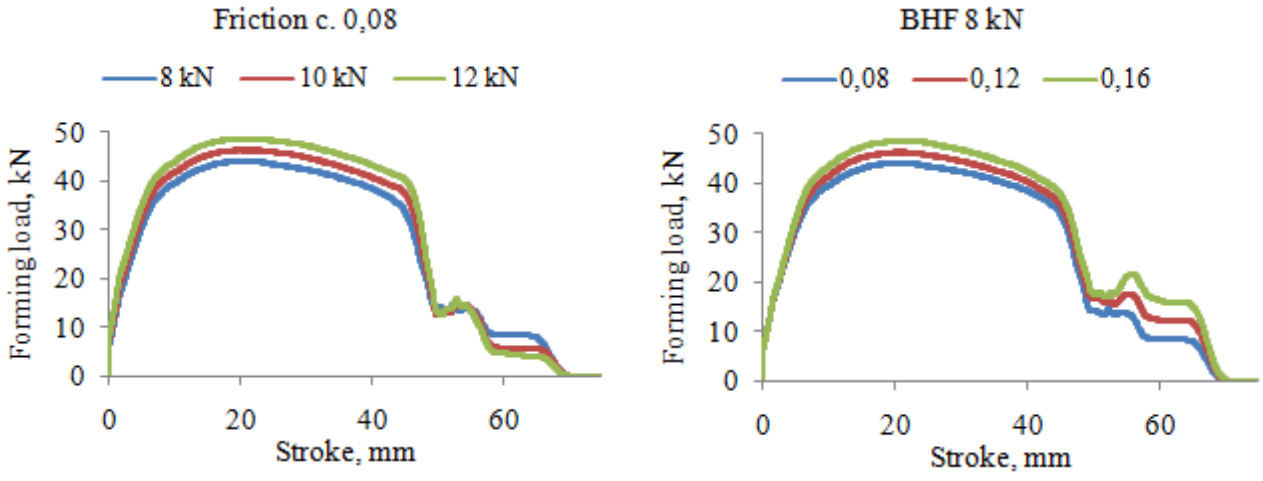


a) b) c)

Figure 3. a) Effective plastic strain at experiment no. 4, b) enlarged view and c) value of Cocroft Latham

4. Discussion

Based on the results shown in Table 2, it can be seen that the forming process will be successful for all combinations of parameters. The values of the effective plastic deformation and the Cockroft Latham criterion are within the predicted limits. The numerical experiment has shown that deviations of the holding force in the first operation or friction in the amount of ±20% do not lead to deviations in the sheet thickness. A clear influence is seen in the values of the pulling force and significantly less in the ironing force. The force-stroke diagrams are shown in Figure 4. An increase in the friction coefficient and holding force leads to an increase in the deformation pulling force, which coincides with the theoretical assumptions.



a) b)

Figure 4. Stroke – forming load diagram a) constant friction and different BHF and b) constant BHF and different friction coefficient

5. Conclusions

The deep drawing with thinning experiment showed that changing the friction and blank holding force parameters within theoretically acceptable limits will not compromise the success of the operation. Increasing friction and BHF leads to a significant increase in the of the deep drawing forming load. The use of the damage criterion is very practical because it provides the engineer with a clear view of how much the material can deform before failure occurs.

Acknowledgements

The present work was funded by the Ministry of Science, Technological Development and Innovation, Republic of Serbia, Agreement No. 451-03-34/2026-03/200107.

References

1. Stebunov S, Vlasov A, Biba N. Prediction of fracture in cold forging with modified Cockcroft-Latham criterion. Procedia Manufacturing. 2018; 15: 519-526.
2. Hoang D, Herbelot C, Imad A, Benseddiq N. Numerical modelling for prediction of ductile fracture of bolted structure under tension shear loading. Finite Elements in Analysis and Design. 2013; 67: 56-65.

Computational Optimization and Engineering Design

Geometry Optimization of a PVDF-Based Piezoelectric Impact Sensor Using a Hertz-Contact-Informed Axisymmetric Finite Element Model

Strahinja Milenković[1,2], Nenad Grujović[1], Fatima Živić[1],

[1]*Faculty of Engineering, University of Kragujevac, Sestre Janjić 6, 34000 Kragujevac, Serbia, , strahinja.milenkovic@kg.ac.rs, 0000-0002-5822-4846, gruja@kg.ac.rs, 0000-0002-8765-2196, zivic@kg.ac.rs, 0000-0003-2509-187X*

[2]*Institute for Information Technologies, University of Kragujevac, Liceja Kneževine Srbije 1A, 34000 Kragujevac, Serbia*

Corresponding author: gruja@kg.ac.rs

Abstract

Piezoelectric polymer sensors based on poly(vinylidene fluoride) (PVDF) are attractive for impact detection because of their low mass, flexibility, and compatibility with curved structural surfaces. In applications such as structural health monitoring of thin-walled and composite components, the sensor geometry must be adapted to localized impact loading in order to provide a sufficiently high electrical output while maintaining a favorable mechanical stress state. In this work, a numerical optimization procedure for a PVDF-based piezoelectric impact sensor is presented. The contact zone created by a steel ball impact was first estimated using Hertzian elastic contact theory and then used to define the loaded region in an axisymmetric finite element model developed in COMSOL Multiphysics. The electro-mechanical response of the sensor was simulated using coupled electrostatics and solid mechanics interfaces under open-circuit conditions. Geometry optimization was performed by varying the dimensionless ratio between sensor half-width and contact radius, together with the active-layer thickness. The objective function was defined as the ratio of maximum generated electric potential to maximum equivalent mechanical stress, enabling simultaneous consideration of signal amplitude and structural reliability. The analysis showed that increasing λ reduces the electrical response, whereas increasing t_p improves the objective function within the investigated domain.

Keywords: PVDF, piezoelectric sensor, impact detection, geometry optimization, Hertz contact, finite element analysis, UN SDG 7

1. Introduction

Piezoelectric polymers, especially PVDF, have been extensively investigated for sensing applications due to their flexibility, low density, and ability to convert transient mechanical loading into measurable electrical signals. These properties make PVDF particularly suitable for lightweight impact-sensing elements integrated into thin-walled and composite structures. In aerospace and similar engineering systems, localized impacts caused by hail, debris, or foreign objects may induce matrix cracking, delamination, and fiber failure, often without clearly visible external damage. For this reason, there is a strong need for compact sensors capable of detecting short-duration impact events and generating a robust electrical response.

Besides structural health monitoring, a similar sensing concept may also be relevant for rapid non-destructive inspection of small metallic spherical components, such as bearing balls, where differences in dynamic response can be associated with defects, dimensional deviations, or changes in material condition. In both cases, the

sensor should not simply maximize voltage output; rather, its geometry should provide a favorable compromise between electrical sensitivity and mechanical integrity.

Previous analyses showed that changing a single geometric parameter, such as the active-layer thickness, may produce monotonic changes in output quantities and therefore does not necessarily reveal a clear design optimum. To overcome this limitation, the present study formulates the optimization problem in terms of the relationship between the local contact zone and the global sensor geometry. The contact radius is determined from Hertzian contact theory, while the overall sensor size and active-layer thickness are varied numerically. This approach enables a physically grounded optimization of a miniaturized PVDF impact sensor.

2. Numerical Model

The numerical model was based on the experimental configuration in which piezoelectric response was measured by dropping a steel ball onto the specimen. Instead of explicitly modeling the indenter, only the local contact zone was considered. The radius of the contact area, a, between a spherical indenter of diameter D and a flat specimen surface was determined using Hertzian elastic contact theory [1,2] $a = \left(\frac{3}{8}FD(k_1 + k_2)\right)^{\frac{1}{3}}$ where F is the experimentally measured normal contact force and $k_i = \frac{(1-\nu_i^2)}{E_i}$ with E_i and ν_i denoting Young's modulus and Poisson's ratio of the contacting materials [3]. Because the elastic modulus of the steel ball is significantly higher than that of the PVDF-based specimen, the contact radius is primarily governed by the mechanical properties of the composite sample. This Hertz-contact-informed reduction enabled computationally efficient simulation while preserving the physical relevance of localized loading [1].

An axisymmetric finite element model was implemented in COMSOL Multiphysics using coupled Electrostatics and Solid Mechanics interfaces. In the electrostatic module, axial symmetry was imposed along the central vertical boundary. Electrically insulated conditions were applied at external boundaries outside the electrodes, the initial electric potential was set to V= 0 V, and Charge Conservation, Piezoelectric was used inside the piezoelectric domain. The lower electrode was grounded, while the upper electrode was defined by a floating potential condition, corresponding to open-circuit measurement.

In the mechanical module, axial symmetry was also imposed along the central vertical boundary. A roller boundary condition was prescribed at the lower horizontal boundary of the electrode, preventing vertical displacement while allowing tangential sliding. The remaining external surfaces were treated as mechanically free, except for the loaded part of the upper electrode. Dynamic excitation was introduced through a uniformly distributed normal force applied over the top electrode in the region corresponding to the Hertzian contact zone. Zero initial displacement and velocity were assumed.

3. Optimization Strategy

The optimization problem was formulated by varying the total sensor half-width R and the active-layer thickness t_p, while keeping the Hertzian contact radius a fixed for the given loading and contact geometry. A dimensionless geometric parameter was introduced as $\lambda = \frac{R}{a}$ which expresses the ratio between the total sensor size and the local contact zone. In the numerical study, λ was varied from 1.2 to 10, while t_p was varied from 0.02 mm to 0.2 mm. These ranges were selected to cover geometrically realistic configurations [4–6] and to allow identification of a possible optimum in the sensor response.

To evaluate both electrical output and mechanical reliability simultaneously, the optimization criterion was defined as $J = V_{max}/\sigma_{vM,max}$ where V_{max} is the maximum generated electric potential and $\sigma_{vM,max}$ is the maximum equivalent von Mises stress. This objective function was chosen to avoid a purely voltage-driven optimization and to preserve the design-oriented character of the study. A favorable configuration should therefore provide a strong electrical signal without excessive mechanical stress concentration. Figure 1 shows testing rig for experimental verification.

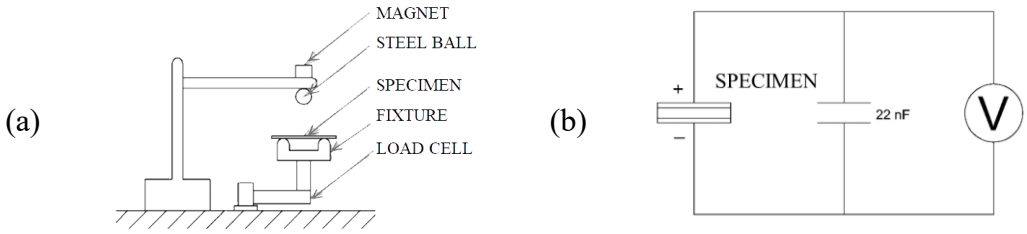


Figure 1. Schematic diagram of testing rig for piezoelectric coefficient measurement (a), and modified Sawyer-Tower electric circuit (b)

4. Results and Discussion

The numerical results showed a clear influence of both optimization parameters on the coupled sensor response. For smaller values of λ, the relative contribution of the locally loaded region to the total active area is larger, leading to more intense electromechanical excitation. As λ increases, the active area becomes larger, but the localized loading becomes less dominant relative to the overall geometry, and the electrical response decreases. At the same time, changing the active-layer thickness modifies both the structural stiffness and the electric-field distribution, so the optimum cannot be identified from geometric intuition alone.

The optimization analysis identified the best configuration within the investigated parameter domain as $\lambda = 1.2$ and $t_p = 0.2$ mm. For this case, the model predicted a maximum electric potential of 24.9 V and a maximum equivalent stress of 34.1 kPa, resulting in an objective-function value of 0.73 V/Pa. This configuration provided the most favorable ratio of electrical output to mechanical stress among all analyzed cases. Figure 2 shows experimental test results for one PVDF/AgNPs composite specimen.

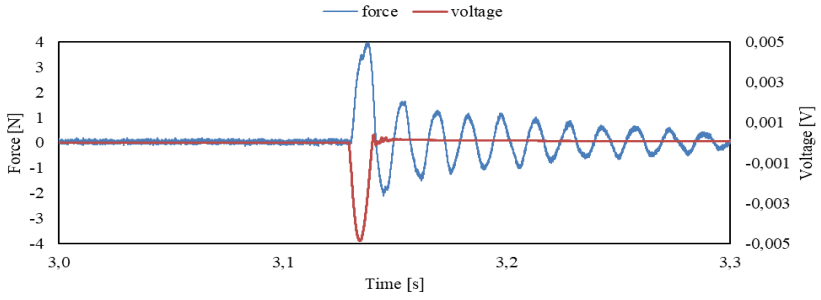


Figure 2. Force and voltage versus time for the PVDF/0.3% AgNPs composite nanomat

The observed trends indicate that increasing λ weakens the electrical response without a proportional reduction in equivalent stress. In other words, increasing the overall sensor size relative to the Hertzian contact zone is

not beneficial for localized impact sensing under the considered boundary conditions. By contrast, increasing the active-layer thickness proved favorable in the studied interval because it increased the generated potential and, consequently, the value of the objective function.

An important outcome is that no interior optimum was found within the investigated design space. Instead, the best solution lies at the boundary of the explored domain. This suggests that, for the adopted model and objective function, further reduction of λ and/or further increase of t_p could potentially improve performance. However, such an extension should be constrained in future work by manufacturing feasibility, geometric integration requirements, and permissible stress levels in the real sensor structure.

5. Conclusions

This paper presented a Hertz-contact-informed axisymmetric finite element model for the geometry optimization of a PVDF-based piezoelectric impact sensor. The results showed that the sensor response is strongly influenced by the relationship between the local contact zone and the overall sensor geometry. Within the investigated design space, increasing the ratio $\lambda = \frac{R}{a}$ reduced the electrical response, whereas increasing the active-layer thickness improved the optimization criterion. The best performance was obtained for $\lambda = 1.2$ and $t_p = 0.2\ mm$, yielding $V_{max} = 24.9\ V$ and $\sigma_{vM_{max}} = 34.1\ kPa$. These findings indicate that compact sensor geometries relative to the Hertzian contact zone are more favorable for localized impact sensing. Future work should extend the design space and include manufacturability and structural constraints.

Acknowledgements

This paper is supported through the EIT's Higher Education Initiative A-SIDE projects, coordinated by EIT RawMaterials, funded by the European Union and supported by the Ministry of Education and Ministry of Science, Technological Development and Innovation, Republic of Serbia, Agreement No. 451-03-33/2026-03/200378 and 451-03-34/2026-03/200107.

References

[1] Lin Y-C, Huang Y-H, Ma C-C, Chang C-K. Experimental and theoretical investigations on sensing and dynamic characteristics of PVDF thin film. Journal of Mechanics 2020;37:1–12. https://doi.org/10.1093/jom/ufaa008.
[2] Rašković D. Tablice iz otpornosti materijala. 11th ed. Građevinska knjiga; 1979.
[3] Milenković S, Živić F, Grujović N, Virijević K, Bodić A, Petrović D. Experimental and Numerical Characterization of Electrospun Piezoelectric Polyvinylidene Fluoride Nanocomposites Reinforced with Silver Nanoparticles. Materials 2025;18:1467. https://doi.org/10.3390/ma18071467.
[4] Ghaderiaram A, Schlangen E, Fotouhi M. Structural Fatigue Life Monitoring with Piezoelectric-Based Sensors: Fundamentals, Current Advances, and Future Directions. Sensors 2025;25:334. https://doi.org/10.3390/s25020334.
[5] Qing X, Li W, Wang Y, Sun H. Piezoelectric Transducer-Based Structural Health Monitoring for Aircraft Applications. Sensors 2019;19:545. https://doi.org/10.3390/s19030545.
[6] Kim I-G, Lee H-Y, Kim J-W. Impact Damage Detection in Composite Laminates Using PVDF and PZT Sensor Signals. Journal of Intelligent Material Systems and Structures 2005;16:1007–13. https://doi.org/10.1177/1045389X05053918.

Optimizing Titanium Hip Implant Performance Through Surface Topography and Numerical Analysis

Project Title: Development and Optimized Surface Topographies for Enhanced Hip Implant Performance, DOST-HIP, Center for Scientific Research of the Serbian Academy of Sciences and Arts (SANU) and the University of Kragujevac, 2024 – 2025

Aleksandra Vulović[1], Živana Jovanović Pešić[1], Đorđe Ilić[1], Strahinja Milenković[2], Dragan Džunić[1]

[1]*Faculty of Engineering University of Kragujevac, Kragujevac, Serbia, aleksandra.vulovic@kg.ac.rs, 0000-0002-6726-3134, zixi90@gmail.com, 0000-0002-1373-0040, djordje.ilic@kg.ac.rs, 0009-0007-3907-8023, dzuna@kg.ac.rs, 0000-0002-1914-1298*

[2]*Institute for Information Technologies, Kragujevac, Serbia, strahinja.milenkovic@fink.rs, 0000-0002-5822-4846*

Corresponding author: aleksandra.vulovic@kg.ac.rs

Abstract

The long-term clinical success of orthopedic implants depends on the interface between the prosthetic material and host tissue. Key biological responses, such as inflammation, fibrosis, infection, and osseointegration, are significantly affected by the implant's surface topography, which influences cellular attachment, differentiation, and bone formation. This research presents approach that combines experimental characterization and numerical analysis, to determine optimal surface topographies for hip implant applications. The study was structured into two investigative phases. First, laser processing techniques were employed to characterize precise surface patterns on titanium plates. This experimental phase aimed to advance the information needed for manufacturing of surfaces that promote superior biological integration. Second, a numerical analysis was conducted to investigate the effects of these topographies on the femoral bone-implant interface. Specifically, this analysis quantifies the impact of surface geometry on shear stress distribution, a critical factor in preventing implant loosening and ensuring mechanical stability. The findings of this research can be grouped into three categories: The refinement of mathematical models used for bone-implant mechanics; The identification of optimal surface topographies that balance biological compatibility with mechanical integrity and Insights into the stress-transfer profiles at the implant-bone junction. By integrating laser processing with numerical modeling, this work provides a robust framework for improving the design of next-generation orthopedic devices. These outcomes have direct implications for enhancing longevity and quality of life for patients undergoing total hip arthroplasty, ultimately reducing the necessity for revision surgeries.

Keywords: numerical simulation, hip implant, titanium, material characterization

1. Project Background and Objectives

Projections by the United Nations indicate that the population over 50 years of age will reach a peak of more than 10 billion by mid-2080s [1]. This creates challenges for global healthcare systems, particularly regarding age-related skeletal deterioration. When medical therapy fails to provide adequate pain relief, a total hip replacement (THA) may be necessary to improve the patient's well-being.

While THA is among the most successful and routine surgical procedures globally, long-term stability remains a critical concern. Approximately 10% of patients require revision surgery within a decade of the primary procedure [2], with many of these failures attributed to aseptic loosening, which means that there is a weak integration between the host bone and the femoral stem. Revision surgeries are less successful than primary interventions due to compromised bone quality [3]. Every year, more than 1 million hip replacement surgeries are performed worldwide, and this number is expected to double in the next decade [4].

A primary strategy for reducing revision rates is the optimization of the bone-implant interface. Enhancing the mechanical and biological connection between the femoral component and the host bone minimizes interface micromovements, which facilitates bone ingrowth into the implant. Despite the number of surface modification techniques, there is a lack of comparative studies that identify which specific topographies yield superior clinical results. Furthermore, existing literature often fails to bridge the gap between computational prediction and empirical validation. This project aims to address this gap by integrating modeling, numerical analysis, and physical sample characterization into a unified framework.

2. Methodology and Work Performed

This project considered a multidisciplinary framework that integrated experimental surface engineering with computational biomechanics. The methodology was organized into two core pillars: the development and characterization of surface topographies and the numerical analysis of the bone-implant interface.

I. Characterization of Surface Topographies: This research phase was focused on experimentally analyzing titanium surface roughness [5] to help improve biological responses and mechanical interlocking at the bone-implant interface. The titanium specimen shown in Figure 1 presents the specimen that was analyzed. It was divided into four zones, each measuring 10 mm × 10 mm, and exposed to 2, 4, 8, or 16 electron beam passes, respectively. The experimental workflow employed statistical analysis to correlate processing parameters with surface morphology.



Figure 1. Analyzed Titanium specimens

II. Numerical Analysis of the Bone-Implant Interface: To complement experimental findings and reduce the necessity for *in vivo* animal or human testing, this research applies Finite Element Analysis (FEA). Numerical simulation offers a non-invasive means to understand the biomechanical behavior, fixation stability, and long-

term performance of prosthetic designs. Over 60 models have been developed in the past 7 years, and the obtained experimental results provided the empirical foundation for refining computational models. Figure 2 showcases three of the created implant models, where different positions and radius values of added half-cylinders were considered in order to assess different surface topographies. Figure 3 shows the complete model that consists of three segments – implant, cancellous, and cortical bone. Parameters *a*, *b* and *c* correspond to radius value, distance from the edge of the model and distance between half-cylinders.

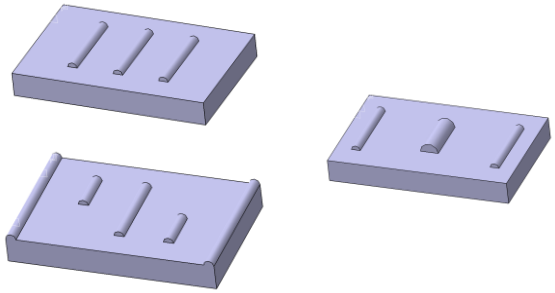


Figure 2. Implant model examples

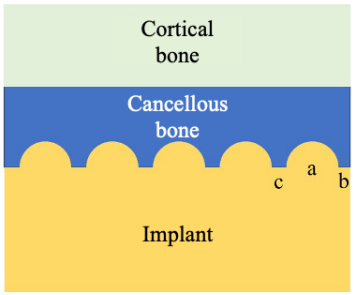


Figure 3. Complete model segments

3. Key Results

By correlating experimental data with numerical simulation, this research provides more details towards understanding of the bone-implant interface. The core outcomes of this research provide a dual-validation framework for future implant design:

- Refinement of the numerical models: By integrating data from physical sample characterization, previously developed mathematical models have been refined. This integration enhances the accuracy of stress-state assessments, providing a more reliable foundation for evaluating both the primary stability and the long-term mechanical performance of orthopedic interfaces under dynamic physiological loading.
- Optimization of surface parameters: Through a combination of numerical simulations and physical testing, this research has identified the critical topographic parameters, specifically relating to roughness, necessary to minimize shear stress while simultaneously maximizing mechanical interlocking. These insights provide useful insights for the development of next-generation hip implants with improved initial fixation and a reduced risk of aseptic loosening.

4. Discussion and Impact

Primary stability is fundamental for long-term prosthetic success, achieved through robust mechanical interlocking between the prosthetic and host bone tissue. While numerous factors influence this interface, surface topography remains a critical variable for the shear stress distribution. Excessive shear stress can lead to interfacial damage and aseptic loosening, which means that minimizing this stress is essential for stabilizing the bone-implant connection.

The impact of this work lies in its integrated approach: by aligning design and characterization of the material surface with numerical modeling, we provide a scalable framework for reducing the incidence of implant failure. These findings offer a pathway toward enhancing the longevity of total hip arthroplasties, potentially reducing

the clinical and economic burden of revision surgeries and providing a foundation for the next generation of patient-specific, orthopedic implants.

5. Conclusions and Outlook

DOST-HIP project represents the foundational phase of a long-term research plan dedicated to the optimization of orthopedic prosthetics. Future investigative stages will expand upon these initial findings through the following strategic areas:

- Production of additional physical samples using different methodologies, such as 3D Printing. This will enable the fabrication of complex surface topographies.
- Incorporate high-resolution imaging, which will allow sub-micron characterization of surface morphology. Furthermore, biotribological testing will be expanded to include simulated biological environments to better predict *in vivo* performance.
- Finite Element Analysis (FEA) will be broadened to include multi-physics simulations in order to refine the information related to shear stress results for diverse topographies during physiological loading cycles.

The ultimate objective of this research trajectory is the development of next-generation hip implants. By shifting toward data-driven, personalized implant solutions, this work seeks to significantly improve patient outcomes through reduced failure rates.

Acknowledgements / Funding

The research presented in this paper was conducted within the project "Development and Optimization of Surface Topography for Improved Hip Implant Performance – DOST-HIP," supported by the Center for Scientific Research of the Serbian Academy of Sciences and Arts (SANU) and the University of Kragujevac.

References

1. United Nations. World Population Prospects 2024: Summary of Results. New York: United Nations; 2024.
2. Havenhand T, Smith L, Barclay J, McLauchlan G. A Decade of Revisions: Can we reduce the re-revision rate? Journal of Orthopaedic Reports. 2025; 100785.
3. Hopper HM, Velichala S, Sharma A, Ernst B, O'Neill CN, Satpathy J. Short-Term Complications of Revision Total Hip Arthroplasty of the Acetabular, Femoral, or Both Components: A National Surgical Quality Improvement Program Database Study. Arthroplasty Today. 2025; 34:101793.
4. Shan L, Shan B, Graham D, Saxena A. Total hip replacement: a systematic review and meta-analysis on mid-term quality of life. Osteoarthritis and Cartilage. 2014; 22(3): 389-406.
5. Jovanović Pešić Ž, Vulović A, Milenković S, Ilić Đ, Džunić D. Effect of Electron Beam Processing Parameters on the Surface Roughness of Titanium Samples: Part II. 41st Danubia-Adria Symposium on Advances in Experimental Mechanics, pp. 135-138, Kragujevac, 2025.

Structural, Dynamic, and Biomechanical Simulation

Structural dynamic simulation of an iconic railway infrastructure under a Multiple Moving Load scenario

Michele Guerini[1], Rosalba Ferrari[1], Giuseppe Cocchetti[2], Egidio Rizzi[1]

[1]DISA, Università degli studi di Bergamo, Dalmine (BG), Italy,
michele.guerini@unibg.it, 0009-0004-0546-1540,
rosalba.ferrari@unibg.it, 0000-0002-3989-713X,
egidio.rizzi@unibg.it, 0000-0002-6734-1382

[2]DICA, Politecnico di Milano, Milano, Italy,
giuseppe.cocchetti@polimi.it, 0000-0002-9695-2967

Corresponding author: rosalba.ferrari@unibg.it

Abstract

This note briefly reports, and updates, on some current Structural Health Monitoring (SHM) modelization efforts concerning the assessment of the present structural condition of the iconic historic iron railway bridge at Paderno d'Adda, otherwise known as San Michele Bridge, completed in 1889, and still in service, after about 137 years of duty. By the adoption of a novel Exact Numerical Time Integration (ENTI) strategy, within the time domain, in the framework of structural dynamics descriptions, a Multiple Moving Load (MML) space-time excitation scenario is considered, to quantify the amount of vibration of the upper continuous beam of the bridge, as resting on inner (elastic) compliant supports, in nearing the prediction of real transit scenarios of regional trains, in the actual condition. The approach shall contribute in forming a general paradigm in dealing with the informed management of crucial infrastructures.

Keywords: Structural dynamics; Exact Numerical Time Integration (ENTI); Multiple Moving Load (MML); Structural Health Monitoring (SHM); Paderno d'Adda bridge (1889); SDG 9.

1. Introduction

Structural Health Monitoring (SHM) modelization approaches are much gaining importance, toward digital twin replication of ageing infrastructures, to achieve consistent and affordable descriptions of continuing-life prediction and management scenarios. Crucially, this requires a fundamental understanding of the underlying structural principles, and a robust modelization, by competent and affordable approaches, specifically within structural dynamics vibration contexts.

Within this framework, on-going research efforts at the University of Bergamo are being dedicated to the inspection of an iconic historical infrastructure, in the local territory, that is the San Michele Bridge at Paderno d'Adda, completed in 1889 [1, 2], and still in service, for both railway and road traffics, toward forming a specific and general platform of structural assessment. These developments have contemplated the investigation on the initial conceptual design and calculation of the bridge, the quantification of the amount of static response within the elastoplastic range, the proposal of a complete SHM platform, and so on [3–6]. Lately, focus has

been placed on structural dynamics aspects, where several issues have first been investigated, toward inspecting main fundamental characteristics of vibration response [7–8].

Recently, these efforts have led to the formulation of a novel Exact Numerical Time Integration (ENTI) method, to handle and achieve a consistent and affordable time integration of the equations of motion, specifically in the context of a Moving Load scenario [9, 10]. Further, to the present stage, the ML modelization approach is being extended, and applied, to the analysis of the upper continuous beam of the Paderno d'Adda Bridge. Namely, in [11] a general analytical approach is being framed, toward forming a benchmark description and comparison stone for the numerical descriptions; in [12] a general discrete formulation is being formalized, to handle general discrete equations of motion, within the same ML context and beyond; in [13] the potential presence of compliant supports, of the beam, is being investigated, in order to quantify the possible implications in terms of induced vibration; in [14] a description of a Multiple Moving Load (MML) setting is being put forward, toward simulating a convoy transit scenario, on a continuous beam on firm supports.

In the present effort, toward nearing a realistic simulation scenario of a regional train transit, across the bridge, referring to its upper continuous beam, the approach developed in [14] is consistently coupled to that outlined in [13], in view of enquiring the potential amount of added vibration induced by the inner compliant supports, provided through the bearing function of the marvelous parabolic arch of the bridge.

Methodology and results are briefly discussed next, while closing remarks attempt to anticipate first outcomes and conclusions, in terms of added vibration, and consistency of the original structural conception and present dynamic capacity.



Figure 1. Photo of San Michele Bridge (1889) taken by the Authors on 26 February 2026, with regional train crossing, up-stream seen from Paderno d'Adda bank.

2. Methods and results

Given the iconic morphology of the Paderno d'Adda bridge (Figure 1), in three main structural subparts, namely underlying parabolic arch, vertical piers and upper continuous beam, a Finite Element Method (FEM) model of the infrastructure is formed. Focusing on the upper continuous beam, ML and MML space-time excitation scenarios are investigated. Herein, a standard Euler-Bernoulli beam is considered, and the relevant equations of motions are handled by the novel ENTI time integration strategy. Such an original time integration technique starts from a first-order state-space representation of the equations of motions, and solves them, exactly, through the use of the exponential matrix, thus forming a so-called exponential integrator. This allows to achieve accurate solutions, for all the dynamic response variables, especially accelerations, which may be the subject of in situ measurement, e.g. by accelerometer sensors, and disregarding for the time-step size, which may be

selected just for appropriate sampling, in the representation of the achieved solution, as it may be compared to standard numerical time integration methods, like Newmark's method. Details on the above-stated modelization strategy are available in the above-quoted references by the Authors.

Now, referring to the MML setting described in [14], which includes a convoy (regional train) with multiple axles of different weight, the assumption of firm supports, for the inner beam bearings, resting on the arch, is released, in order to quantify the potential amount of added vibration, as per the generalized scenario implemented in [13]. To start with, the stiffness constants of the inner springs are taken as estimated in [7] and the upper continuous beams is run under MML resembling the train transit.

Main downstream snapshots of the calculated displacement profile of the beam are represented in Figure 2, along with different positions of the convoy on the beam, corresponding to the transient of entering and exiting of the first and last half of the convoy, and the settlement of the train in the mid of the structure. Compared to the firm-support configuration, the entering and exiting transients show a similar structural response; however, when the convoy is settled on the beam, the maximum measured downward displacement reaches –10.6 mm, due to the presence of compliant supports, which appears to be consistent with outcomes from the original train try-out configuration reported in source SNOS documents [1, 2].

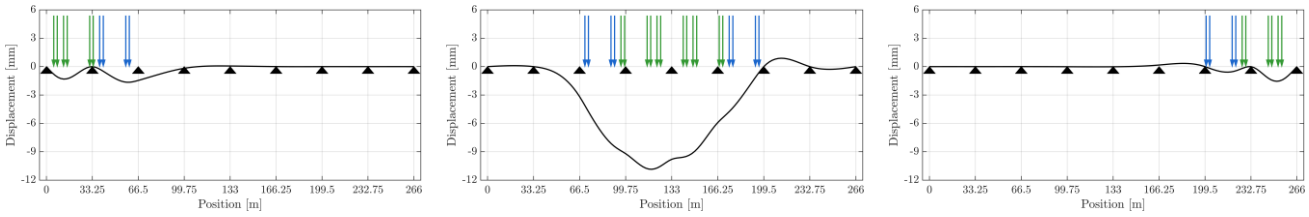


Figure 2. Displacement profile of the beam on compliant supports under MML of regional train transit.

3. Conclusions

The outcomes of the achieved preliminary results mainly show that:

- The modelization strategy looks rather pertinent, to assess the amount of induced dynamic vibration, of the bridge's beam, under train transit, described within a MML scenario, as delivered by the original exact ENTI strategy.
- The added vibration response, in terms of displacements, due to the presence of inner compliant supports, of the upper continuous beam, looks visible through somehow contained, at least for the estimated stiffness constants of the underlying springs. These results, looking consistent with original try-out measurements [1, 2], may confirm the arch, as a main stiff underlying bearing and iconic subpart of the bridge, to constitute a well-set structural element, for railway use, even for the present utilization scenarios.
- Further investigations on this specific subject may concern a more accurate calibration of the underlying springs, and also a comprehensive reading of the response, in terms of velocity and acceleration responses.
- This may open up the way to further SHM interpretation, which was definitely foreseen, and actually motivated the present developments, in terms of comparison to recorded experimental measurement, as acquired on the bridge.
- The whole, shall then constitute a reliable and transferable approach, toward the formation of SHM platforms for existing infrastructures, toward predictive maintenance and management processes.

Acknowledgements
The research conducted at the University of Bergamo was supported by the Italian Ministry of University and Research (MUR) under the PRIN 2022 program (funding following reallocation of resources from final ranking), Project Code 2022744YM9, CUP F53C24000930006, and by "Fondi di Ricerca d'Ateneo ex 60%" funds and a doctoral grant at the Dept. of Engineering and Applied Sciences. Rete Ferroviaria Italiana (RFI) is gratefully acknowledged for its valuable collaboration within the framework of this study.

References

[1] Società Nazionale delle Officine di Savigliano, Viadotto di Paderno sull'Adda (Ferrovia Ponte S. Pietro-Seregno), Tip. e Lit. Camilla e Bertolero, Torino, 1889.
[2] Nascè V, Zorgno AM, Bertolini C, Carbone VI, Pistone G, Roccati R. Il ponte di Paderno: Storia e struttura - Conservazione dell'architettura in ferro. Restauro. 1984;73–74:215.
[3] Ferrari R, Rizzi E. On the theory of the ellipse of elasticity as a natural discretisation method in the design of Paderno d'Adda Bridge (Italy). In: Structural Analysis of Historic Construction. CRC Press. 2008:583–591.
[4] Ferrari R, Cocchetti G, Rizzi E. Computational elastoplastic Limit Analysis of the Paderno d'Adda bridge (Italy, 1889). Archives of Civil and Mechanical Engineering. 2018;18:291–310.
[5] Ferrari R, Cocchetti G, Rizzi E. Reference structural investigation on a 19th-century arch iron bridge loyal to design-stage conditions. International Journal of Architectural Heritage. 2020;14:1425–1455.
[6] Ferrari R, Rizzi E, Brioschi MS, Dertimanis V. Design of an effective structural health monitoring platform for Paderno d'Adda Bridge (1889). In: Reconstruction and Restoration of Architectural Heritage 2021. CRC Press. 2021;210–215.
[7] Ermolli L, Guerini M, Stoura CD, Ferrari R, Dertimanis VK, Chatzi EN, Rizzi E. Combining experimental data and numerical modeling to analyze train-structure interaction on the historic San Michele Bridge (Italy, 1889). In: Proc. of the 6th ECCOMAS Thematic Conf. on Uncertainty Quantification in Computational Science and Engineering (UNCECOMP 2025). 2025;266–277.
[8] Guerini M, Ermolli L, Stoura CD, Ferrari R, Dertimanis VK, Chatzi EN, Rizzi E. Modal dynamic identification of historic San Michele bridge (Italy, 1889). In: Proc. of the 10th ECCOMAS Thematic Conf. on Computational Methods in Structural Dynamics and Earthquake Engineering (COMPDYN 2025). 2025;4923–4936.
[9] Guerini M, Ferrari R, Cocchetti G, Rizzi E. Effective numerical time integration of structural dynamic responses under moving load. Lecture Notes in Civil Engineering. 2025;746:734–747.
[10] Guerini M, Ferrari R, Cocchetti G, Rizzi E. Exact Numerical Time Integration (ENTI) of dynamic equations of motion for discretized systems subjected to Moving Load. Submitted for publication. 2026.
[11] Guerini M, Ferrari R, Cocchetti G, Rizzi E. Exact Numerical Time Integration benchmarking by analytical treatments of continuous beam Moving Load problems. In: Proc. of the 5th Int. Conf. on Modelling, Testing and Monitoring of Engineering Structures (MOTEMOES 2026). To appear.
[12] Guerini M, Ferrari R, Cocchetti G, Rizzi E. An Exact Numerical Time Integration strategy for discrete dynamic systems under Moving Load. In: Proc. of the 5th Int. Conf. on Modelling, Testing and Monitoring of Engineering Structures (MOTEMOES 2026). To appear.
[13] Guerini M, Ferrari R, Cocchetti G, Rizzi E. Exact Numerical Time Integration of continuous beams on elastic supports. In: Proc. of the 5th Int. Conf. on Modelling, Testing and Monitoring of Engineering Structures (MOTEMOES 2026). To appear.
[14] Guerini M, Ferrari R, Cocchetti G, Rizzi E. Effective time integration strategies for dynamical response prediction under moving objects. In: Proc. of the 13th Int. Conf. on Structural Dynamics (EURODYN 2026). 2026. To appear.

Virtual and Digital Twin Modeling

Virtual Twin Modeling of Bio-Inspired Butterfly Wing Flapping

Julija Boskovic[1], Milan Ivkovic[1], Ivan Grujic[1], Goran Devedzic[1], Suzana Petrovic Savic[1]

[1] *University of Kragujevac, Faculty of Engineering, Department for Production Engineering, Kragujevac, Serbia, julijabkg@gmail.com, 0009-0006-3031-2234, milan.ivkovic@kg.ac.rs, 0000-0001-5176-5837, ivan.grujic@kg.ac.rs, 0000-0003-0572-1205, devedzic@kg.ac.rs, 0000-0002-6589-5883, petrovic.savic@kg.ac.rs, 0000-0002-5629-6221*

Corresponding author: devedzic@kg.ac.rs

Abstract

In this paper, a bio-inspired model of butterfly wing flapping is analyzed with the aim of its transformation into a digital environment using CAD modeling and the digital twin concept. A virtual model was developed to enable the simulation of the system's dynamic behavior under controlled conditions. The wing motion was described using an analytical function, while various types of disturbances, including Gaussian noise, sinusoidal, and impulsive perturbations, were introduced to simulate real operating conditions. A correction algorithm for system stabilization was implemented in the MATLAB environment, and its efficiency was evaluated using the mean absolute error (MAE). The results indicate that the algorithm successfully reduces deviations from the ideal motion in all analyzed cases, with the highest efficiency observed under impulsive disturbances. Although minor residual deviations are present in the case of complex combined disturbances, the system maintains a stable and robust response. The proposed approach has potential applications in the development of bio-inspired systems and in improving methods for the analysis and optimization of dynamic processes.

Key words: biomimetics; virtual simulation; digital twins; CAD modeling; micro aerial vehicle; UN SDG 4,5,9

1. Introduction

Biomimetics is a scientific field that studies the structures and functions of biological systems with the aim of applying them in the development and further improvement of modern technological systems. Natural systems are the result of long-term evolutionary processes, which makes them highly efficient. In modern engineering, there is an increasing tendency to integrate these principles through the use of digital tools, enabling the analysis and verification of complex processes without the need for physical prototypes. The aim of this paper is to analyze a biological model and transform it into a digital environment using CAD modeling and virtual simulation. Special attention is given to the simulation of system responses to various influencing factors, as well as to the application of the digital twin concept for the analysis and optimization of dynamic characteristics [1-3].

2. Materials and Methods

The model development process was based on the creation of geometric elements in a CAD environment using CATIA V5R21 software (Fig. 1). Special attention was given to the modeling of the wings as the key functional element. The wing geometry was defined based on a visual analysis of reference data, using spline curves to generate the structure. This approach enables a high level of shape control while preserving surface continuity. After creating individual components, an assembly was generated within the Assembly Design module. In the

next phase, a mechanism simulating wing flapping was developed using lower kinematic pairs. The simulation was performed in the DMU Kinematics module, where the law of wing motion was defined as a function of time. The angular displacement was described by a cosine function, ensuring periodic and continuous motion corresponding to real butterfly wing flapping [4]. The simulation results, in the form of time series of rotation angles, were exported in CSV format and later used as input data for numerical analysis.

An algorithm was developed in the MATLAB environment representing a virtual twin of the system (Fig.2), enabling the analysis of the effects of various types of disturbances on motion stability. The primary wing flapping model was defined by an analytical function describing ideal oscillatory behavior. The next step involved introducing disturbances in the form of Gaussian noise, sinusoidal oscillations, and impulsive perturbations. These disturbances simulate real operating conditions, such as sudden external influences, turbulence, and resonant effects. The central part of the algorithm is the implementation of an adaptive correction function, which acts as a filter to mitigate deviations from the ideal signal. This function employs a sensitivity threshold and a blending coefficient to selectively correct signal values while preserving the main dynamic characteristics of the system.

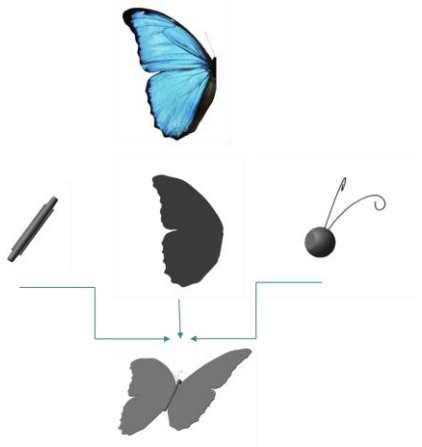


Figure 1. CAD model of a butterfly

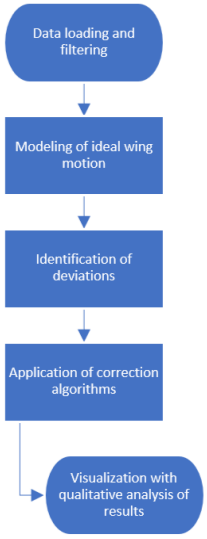


Figure 2. Virtual twin algorithm

3. Results

Within the conducted simulations in the MATLAB environment, the dynamic behavior of the system model was analyzed under the influence of different types of disturbances. Particular emphasis was placed on evaluating the efficiency of the applied correction algorithm. The analysis of the system response to Gaussian disturbances (Fig. 3a, 3b) shows that stochastic perturbations cause deviations from the ideal wing flapping trajectory, initially manifested as noise. After the application of the correction algorithm, these deviations are significantly reduced. The correction is more uniform in the left wing, while oscillations occur in the lower part of the flapping motion (-20°) in the right wing, indicating an asymmetry in system response. Under sinusoidal disturbances (Fig. 3c, 3d), the system successfully follows periodic deviations, with the corrected signal remaining close to the reference trajectory, particularly in the lower part of the flapping cycle. In this case, the responses of both wings are largely uniform. Impulsive disturbances (Fig. 3e, 3f) cause sudden and short-term deviations; however, the system demonstrates high robustness by quickly returning to a stable state.

Although impulses occur at different time instances in the left and right wings, this does not significantly affect the overall system response, confirming the time-independence of the algorithm's efficiency. The most complex case corresponds to the combined effect of all disturbances, which leads to significant deviations from the ideal trajectory, particularly in the final phases of the flapping motion. The application of the correction algorithm results in system stabilization, although minor residual oscillations remain in regions of maximum amplitude.

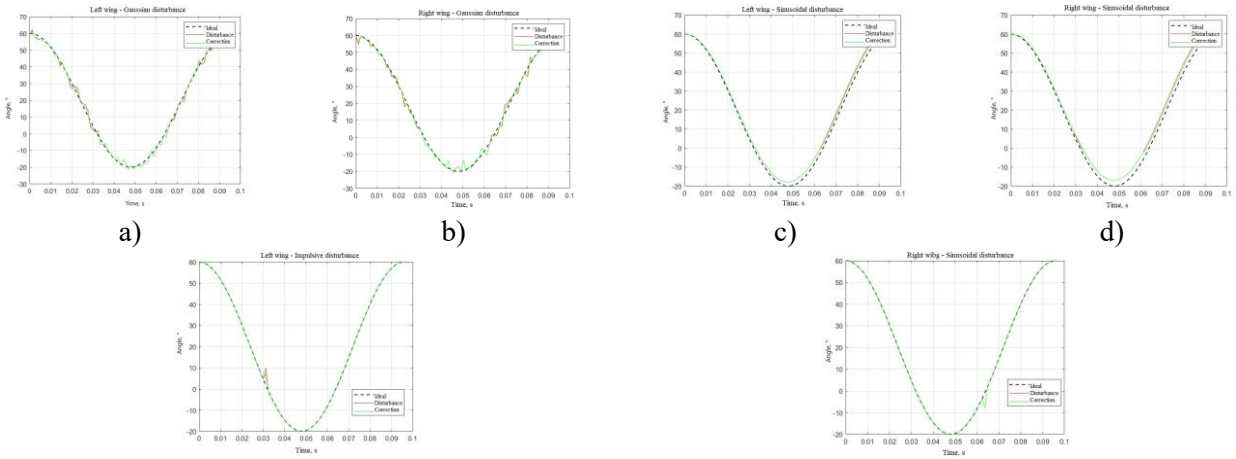


Figure 3. System response to disturbances: (a) Gaussian disturbance – left wing, (b) Gaussian disturbance – right wing, (c) sinusoidal disturbance – left wing, (d) sinusoidal disturbance – right wing, (e) impulsive disturbance – left wing, (f) impulsive disturbance – right wing

The 3D representation (Fig. 4) shows that the correction is most pronounced in the middle part of the flapping cycle, where disturbances are most intense. Qualitative analysis based on MAE values (Table 1) confirms that the algorithm reduces error in all considered cases.



Figure 4. Surface representation of the system response to combined disturbances

4. Discussion

The obtained results indicate that the application of the correction algorithm ensures stable and consistent performance under various operating conditions [5]. However, it is also evident that the algorithm's performance depends on the type and complexity of the disturbances. In the case of Gaussian disturbances, the algorithm demonstrates the ability to attenuate stochastic fluctuations. The reduction in MAE values is moderate (approximately 12–14%), suggesting that the algorithm effectively filters random deviations, although it does not completely eliminate them. For sinusoidal disturbances, the results show that the algorithm successfully

compensates for periodic perturbations. Although the relative error reduction is less pronounced compared to impulsive disturbances, the absolute improvement is significant. Under impulsive disturbances, the system exhibits the best performance. The low MAE values indicate high system stability under short-term perturbations, while the correction algorithm further enhances the response. The most significant results are observed in the case of combined disturbances, where the algorithm operates under complex conditions. Although the initial error values are the highest, the greatest absolute reduction is achieved after correction [6].

Table 1. Mean absolute error (MAE) before and after correction of the flapping angle for the left and right wings under different types of disturbances

Disturbance	MAE (°, left before))	MAE (°, left after)	MAE (°, right before)	MAE (°, right after)
Gaussian	1.64	1.43	1.61	1.38
Sinusoidal	2.11	1.76	2.85	2.36
Impulsive	0.10	0.07	0.09	0.09
Combined	2.62	2.10	2.99	2.49

This confirms that the algorithm maintains functionality under complex conditions, albeit with an increased presence of residual oscillations [5-7].

5. Conclusions

In this paper, a bio-inspired model of butterfly wing flapping based on the digital twin concept was developed, enabling the analysis of the system's dynamic behavior in a controlled virtual environment. The simulation results show that the application of the correction algorithm reduces deviations from the ideal trajectory under the influence of various types of disturbances. The system exhibits a stable response in all analyzed cases, with the highest efficiency observed in response to impulsive disturbances. This approach has potential applications in the development of bio-inspired systems, as well as in improving methods for modeling and optimization of related processes.

Acknowledgement

This work presents the results of research conducted within projects financially supported by the Ministry of Science, Technological Development and Innovation of the Republic of Serbia, under Contract No. 451-03-34/2026-03/200107, dated February 5, 2026.

References

1. Mahringer CA, Baessler F, Gerchen MF, Haack C, Jacob K, Mayer S. Benefits and obstacles of interdisciplinary research: Insights from members of the Young Academy at the Heidelberg Academy of Sciences and Humanities. 2023.
2. Persiani S. Biomimetics of motion: Nature-inspired parameters and schemes for kinetic design. Springer; 2018.
3. Yao JF, Yang Y, Wang XC, Zhang XP. Systematic review of digital twin technology and applications. Vis Comput Ind Biomed Art. 2023;6(1):10.

4. Senda K, Obara T, Kitamura M, Yokoyama N, Hirai N, Iima M. Effects of structural flexibility of wings in flapping flight of butterfly. Bioinspir Biomim. 2012;7(2):025002.
5. Zhang Y, Zeng S, Zhu S, Wang S, Wang X, Miao Y, et al. Development of a novel tailless X-type flapping-wing micro air vehicle with independent electric drive. Biomimetics. 2024;9(11):671.
6. Wei Z, Wang S, Farris S, Chennuri N, Wang N, Shinsato S, et al. Nature-inspired three-dimensional surface serration topologies enable silent flight by suppressing airfoil-turbulence interaction noise. 2023.
7. Farzaneh HH, Lindemann U. A practical guide to bio-inspired design. Springer Vieweg; 2019.

Advanced Mathematical and Theoretical Methods

Molecular Nanogears as Quantum Brownian Rotators

Jasmina Jeknic-Dugic[1], Igor Petrovic[2], Momir Arenijevic[3], Miroljub Dugic[3]

[1]*Department of Physics, Faculty of Science and Mathematics, 18000 Nis, Serbia, jjeknic@pmf.ni.ac.rs, ORCID 0000-0002-4905-6457*

[2]*Svetog Save 98, 18230 Sokobanja, Serbia, igorpetrovicsb@gmail.com, ORCID 0000-0002-8546-3523*
[3]*Department of Physics, Faculty of Science, 34000 Kragujevac, Serbia, momir.arsenijevic@pmf.kg.ac.rs, ORCID 0000-0003-4622-642X, miroljub.dugic@pmf.kg.ac.rs, ORCID 0000-0002-4493-6009*

Corresponding author: momir.arsenijevic@pmf.kg.ac.rs

Abstract

We briefly present some recent results on the quantum description of the molecular gears. An emphasis is placed on the authors' contributions to the field based on the model of the planar quantum Brownian rotator. Different criteria have been employed to detect the parameter ranges for rotational stability of the gears. Notably, dynamics of the basic observables standard deviations, the first passage time criterion and the entropy (linear and differential entropy) dynamics provide nonunique recipes for the gears' stability. In effect, there are not any simple rules or recipes but rather optimization procedure is needed, which is the next step in investigating the topic.

Keywords: molecular gears; dynamical stability: quantum Brownian rotator; the Caldeira-Leggett master equation; the standard deviation; the first passage time; the linear end differential entropy; SDG 7—affordable and clean energy; SDG 9 — industry, innovation and infrastructure.

1. Introduction

Dynamical stability is essential for the external control of nano-setups and nanomachines. To this end, deterministic dynamics is an ideal. However, realistic systems are virtually never of the deterministic kind due to the inevitable influence of the environment, which produces stochastic effects, including noise. Unfortunately, due to the nonexistence of the canonical criteria for stochastic processes, there is not a simple way of treating such systems, even in the classical-physics context. Worse though, certain aspects of nano-setups behavior require quantum mechanical treatment [1-4]. This is typically the case with the molecular machines, notably of the molecular gears (natural or artificial) as the prominent elements of the nano-machinery. Although expectably small (or even negligible), quantum corrections may accumulate in realistic situations and manipulations with molecular gears (cogwheels). Then there is a challenge for investigating dynamical stability of those systems.

Recently, systematic research has begun [2,3,4]. These include studies on decoherence [4–7], diffusion [4,7,8], friction [4,7,9], and relaxation or thermalization [7,10,11]. The potential applications of this research are broad. They include cooling nanoscale rotators [6,12,13], orientational quantum metrology [14,15], torque sensors

[9,16,17], nano-g acceleration sensitivity [18], energy harvesting at nanoscale as quantum heat engines [19], qubit construction [20], foundational topics like experimental tests of objective collapse models [21,22] or testing quantumness in massive objects [23], and not to forget the field of molecular electronics where rotation changes electron transport pathways enabling molecular switches, logic gates and memory elements [24,25].

In this brief review, we outline a particular research direction that is compelling both from a fundamental academic perspective and for its potential practical applications, especially in the design and implementation of molecular gears as the prominent tools of modern nanomachinery.

2. The molecular cogwheel model

Typically, molecular gears are treated by the methods of classical physics or the standard treatment of the unitary quantum systems. However, realistic molecular nano-setups are exposed to the environmental influence, which is often described by the classical Langevin equation or analogous classical master equation (typically of the Fokker-Planck type). However, those methods may fall short of description of the brief and numerous external actions performed on the molecular rotator. To this end, it is now well understood that the methods of the Theory of open quantum systems [26,27] are not only useful but essentially unavoidable. At the nanoscale, molecular gears and rotators cannot be treated as isolated systems: they are unavoidably coupled to their surroundings. This coupling gives rise to dissipation, fluctuations, and decoherence, all of which crucially influence gears' and rotators' dynamical behavior, especially dynamical stability.

Quantum description of friction (dissipation) has a remarkable history that starts from the problems of nuclear physics [28-30]. Perhaps the most often used is the Caldeira-Leggett (CL) master equation [26,31], which accounts for both dissipation and decoherence as a quantum model of the celebrated Brownian particle in the translational motion. However, description of a rotator is much more subtle and challenging. First, the axis of rotation may be subject of external influence. Second, noncommutativity of the angle of rotation and the angular momentum observables introduce a new layer of the problem that is not recognized by the translational motion model. Third, molecular cogwheels are realistic systems defined by their spatial size and shape, notably by the number of blades, which may be critical for the cogwheels' function. Fourth, stochastic behavior in general is not captured by a canonical method of statistical description. Consequently, the use of only one such method (of statistical inference) may have certain (even severe) limitations.

The recently developed extension of the CL model meets the above requirements by the following master equation for a planar (one-dimensional) rotator [2,3,32],

$$\frac{d\hat{\rho}}{dt} = -\frac{i}{\hbar}\left[\hat{H},\hat{\rho}\right] - \frac{iN\gamma_0}{\hbar}\left[\hat{\varphi},\left\{\hat{L},\hat{\rho}\right\}\right] + \frac{2N^2 I_0 \gamma_0 k_B T}{\hbar^2}\left[\hat{\varphi},\left[\hat{\varphi},\hat{\rho}\right]\right]. \quad (1)$$

In eq. (1), $\hat{\rho}$ is the state of the rotator, $\hat{H}$ is the (renormalized) Hamiltonian, $\hat{\varphi}$ and $\hat{L}$ the angle and the angular momentum observables, N states for the number of blades and I_0 and γ_0 the average momentum of inertia and the damping factor, respectively; of course, k_B is the Boltzmann constant and T the temperature of the environment, while the curly bracket denotes the anticommutator. Of interest are small values of the rotation angle. Equation (1) can be used for all parameter values (including the over- and under-damped regimes) as a phenomenological equation, despite its original microscopic origin for very high temperature.

3. A short review of the results

So far, the following criteria of dynamical stability of rotation have been investigated [2,3,31]: the standard deviations of $\hat{\varphi}$ and $\hat{L}$, the so-called the first passage time, temporal behavior of both the linear and differential entropy. The models of interest include the free rotator, harmonic rotator and weakly nonharmonic rotator. The latter requires methods of cutting the infinite set of the coupled first-order differential equations.

While detailed comparison of the results obtained for different criteria is a complex task, individually, those criteria exhibit a need for optimization, which is typical for the macroscopic, e.g. mechanical, systems. That is, certain choices of the external manipulations (including measurements), the parameter regimes, number of blades, the size of the cogwheels (defined by I_0 and γ_0) are mutually exclusive—while one choice distinguishes one combination, the other choices do not. Therefore, even for the single criteria mentioned above, in practice one should adapt the choices to the concrete practical requirements at the experimenter's disposal.

4. Conclusions

Investigating dynamical stability of the molecular cogwheels is a subfield requiring diverse expertise: nano-rotators sit at the intersection of nanotechnology, chemistry, and biology including the foundations and application of the Theory of open quantum systems. Treating those systems as the quantum Brownian motion is a fresh and expectably fruitful approach that deserves pursuing. At this moment, the two objectives of the future work are obvious. First, extending the list of the statistical criteria of dynamical stability. Second, in depth analysis of the need for optimization in the practical realization of the theoretical results.

Acknowledgements

This research is funded by the Ministry of Education and Ministry of Science, Technological Development and Innovation, Republic of Serbia, Grants no. 451-03-33/2026-03/200124 and 451-03-34/2026-03/ 200122.

References

1. Kottas G S, Clarke L I, Horinek D and Michl J. Artificial Molecular Rotors. J. Chem. Rev. 2005; 105:1281:1376.
2. Jeknić-Dugić J, Petrović I, Arsenijević M, Dugić M. Dynamical stability of the one-dimensional rigid Brownian rotator: the role of the rotator's spatial size and shape. J. Phys.: Condens. Matter. 2018;30:195304.
3. Petrović I, Jeknić-Dugić J, Arsenijević M, Dugić M. Dynamical stability of the weakly nonharmonic propeller-shaped planar Brownian rotator. Phys. Rev. E. 2020;101:012105.
4. Stickler B A, Papendell B, Hornberger K. Spatio-orientational decoherence of nanoparticles. Phys. Rev. A. 2016;94:033828.
5. Troyer S, Fechtel F, Hummer L, Henning R, Stickler B A, Delic U, Arndt M. Quantum ground-state cooling of two librational modes of a nanorotor, Nature Phys. 2026;22:584:590. 6. Zhong C, Robicheaux F. Decoherence of the rotational degrees of freedom. Phys. Rev. A. 2016;94:052109. 7. Stickler

B A, Schrinski B, Hornberger K. Rotational friction and diffusion of quantum rotors. Phys. Rev. Lett. 2018;121:040401.
8. Furey B J, Wu Z, Isaza-Monsalve M, Walser, Mattivi S E, Nardi R, Schindler P. Strategies for implementing quantum error correction in molecular rotation. Quantum. 2024;8:1578. 9. Ju P, Jin Y, Shen K, Duan Y, Xu Z, Gao X, Ni X, Li T. Near-field GHz rotation and sensing with an optically levitated nanodumbbell. Nano Lett. 2023;23:10157-10163. 10. Schrinski B, Chan Y J, Schrinski B. Thermalization of the quantum planar rotor with external potential. SciPost Phys. Core. 2025;8:040. 11. Kamba M, Shimizu R, Aikawa K. Nanoscale feedback control of six degrees of freedom of a near-sphere. Nat. Commun. 2023;14:1.
12. Bang J, Seberson T, Ju P, Ahn J, Xu Z, Gao X, F. Robicheaux, T. Li. Five-dimensional cooling and nonlinear dynamics of an optically levitated nanodumbbell. Phys. Rev. Res. 2020;2:043054. 13. Schäfer J, Rudolph H, Hornberger K, Stickler B A. Cooling nanorotors by elliptic coherent scattering. Phys. Rev. Lett. 2021;126:163603.
14. Kraus P M, Mignolet B, Baykusheva D, Rupenyan A, Horný L, Penka E F, Grassi G, Tolstikhin O I, Schneider J, Jensen F, Madsen L B, Bandrauk A D, Remacle F, Wörner H J. Measurement and laser control of attosecond charge migration in ionized iodoacetylene. Science 2015;350:790-795.
15. Zeng K, Wu Y, Wu X, Xiao D. Polarization-modulation-based orientation metrology of optically levitated rotating birefringent particles. Phys. Rev. Res. 2024;6:013160.
16. Hoang T M, Ma Y, Ahn J, Bang J, Robicheaux J F, Yin Z-Q, Li T. Torsional optomechanics of a levitated nonspherical nanoparticle. Phys. Rev. Lett. 2016;117:123604. 17. Ahn J, Xu Z, Bang J, Ju P, Gao X, Li T. Ultrasensitive torque detection with an optically levitated nanorotor. Nat. Nanotech. 2020;15:89. 18. Hong M, Sima C, Sun Y, Xu J, Li K, Zhang L, Wang L, Ming Z, Lu P. Monolithically integrated passive photonic silicon chip for nano-g level acceleration tri-axial detection. Opt. Express. 2025;33:5945-5957. 19. Roulet A, Nimmrichter S, Arrazola J M, Seah S, Scarani V. Autonomous Rotor Heat Engine. Phys. Rev. E 2017;95:062131. 20. Löw M, Ibrügger M, Rempe G, Zeppenfeld M. Coherence of Symmetry-Protected Rotational Qubits in Cold Polyatomic Molecules. Phys. Rev. Lett. 2025;134:113402. 21. Bera S, Motwani B, Singh T P, Ulbricht H. A proposal for the experimental detection of CSL induced random walk. Sci. Rep. 2015;5:7664. 22. Carlesso M, Paternostro M, Ulbricht H, Vinante A, Bassi A. Non-interferometric test of the Continuous Spontaneous Localization model based on rotational optomechanics. New J. Phys. 2018;20:083022. 23. Das D, Home D, Ulbricht H, Bose S. Mass-Independent Scheme to Test the Quantumness of a Massive Object. Phys. Rev. Lett. 2024;132:030202.
24. Simpson G J, García-López V, Daniel Boese A, Tour J M, Grill L. How to control single-molecule rotation. Nat Commun. 2019;10:4631. 25. Huang T, Zhao J, Feng M, Popov A A, Yang S, Dunsch L, Petek H. A Molecular Switch Based on Current-Driven Rotation of an Encapsulated Cluster within a Fullerene Cage, Nano Lett. 2011;11:5327:5332.
26. Breuer H-P, Petruccione F. The Theory of open quantum systems, Oxford Univ. Press, NY, 2002.
27. Rivas A, Huelga S F. Open quantum systems. An introduction, Springer. Berlin, 2012. 28. Hasse R W. On the quantum mechanical treatment of dissipative system. J. Math. Phys. 1975;16:2005.

29. Dekker H. Classical and quantum mechanics of the damped harmonic oscillator. Phys. Rep. 1981;80:1.
30. Isar A, Sandulescu A, and Scheid W. Use of characteristic function in open quantum systems and charge equilibrium in deep inelastic reactions. J. Phys. G 1991;17:385.
31. Caldeira A O, Leggett A J. Influence of Dissipation on Quantum Tunneling in Macroscopic Systems. Phys. Rev. Lett. 1981;46:211:214.
32. Jeknić-Dugić J, Petrović I, Arsenijević M, Dugić M. Entropy dynamics for a harmonic propeller-shaped planar molecular quantum Brownian rotator. Physica B: Cond. Matter 2025;717:417742.

On the construction of multiple orthogonal polynomials with nearly diagonal multi-indices with respect to bilinear forms

Nevena Z. Petrović[1]

[1]*Faculty of Mechanical and Civil Engineering, University of Kragujevac, Kraljevo, Serbia, nevena.z.petrovic@pmf.kg.ac.rs, 0000-0002-1969-6277*
Corresponding author: *nevena.z.petrovic@pmf.kg.ac.rs*

Abstract

Multiple orthogonal polynomials generalize ordinary orthogonal polynomials by satisfying orthogonality conditions simultaneously with respect to $r \in \mathbb{N}$ weight functions. In this paper, we present a method for constructing multiple orthogonal polynomials which are orthogonal with respect to r bilinear forms, with particular emphasis on nearly diagonal multi-indices. These polynomials play an essential role in the construction of a set of anti-Gaussian quadrature formulas for the optimal set of quadrature formulas in Borges' sense. The main contribution is based on the connection between these polynomials and multiple orthogonal polynomials which are orthogonal with respect to a corresponding system of r weight functions, which arise in the construction of the optimal set of quadrature formulas in Borges' sense. The results provide a unified framework that connects the theory of multiple orthogonality with respect to bilinear forms to its classical counterpart involving weight functions, offering new insight into the structure of the associated polynomial systems in the nearly diagonal setting. Several numerical examples are included to illustrate the obtained results.

Keywords: weight functions; multiple orthogonal polynomials; anti-Gaussian quadrature rules; optimal set of quadrature rules in Borges' sense

1. Introduction

An important aspect of the theory of orthogonal polynomials is their interpretation as special functions, often expressible as terminating hypergeometric series. Over the twentieth century, substantial effort has been devoted to their classification and characterization. More recently, increased attention has been given to multiple orthogonal polynomials (MOPs), which arise naturally in simultaneous rational approximation, particularly in Hermite–Padé approximation of systems of r functions. In [1] we considered a class of MOPs defined through orthogonality relations with respect to a certain bilinear forms. Here, we are giving a recapitulation of results that presents in [1, 2].

Let $r \geq 1$ be an integer and let $w_1, w_2, \ldots, w_r$ be r weight functions on the real line such that the support of each w_k is a subset of an interval E_k. Vector $\vec{n} = (n_1, n_2, \ldots, n_r) \in \mathbb{N}^r$ is called a *multi-index*, where $n_1, n_2, \ldots, n_r$ are nonnegative integers, and its length is $|\vec{n}| = n_1 + n_2 + \ldots + n_r$. MOPs can be classified into two types (see [3]).

Type I MOP is an r-vector $(A_{\vec{n},1}, \ldots, A_{\vec{n},r})$, where each $A_{\vec{n},k}$ is a polynomial of degree $n_k - 1$, satisfying the orthogonality conditions

$$\sum_{k=1}^{r} \int_{E_k} A_{\vec{n},k}(x) x^j w_k(x) dx = 0, \quad j = 0, \ldots, |\vec{n}| - 2; \quad \text{with} \quad \sum_{k=1}^{r} \int_{E_k} A_{\vec{n},k}(x) x^{|\vec{n}|-1} w_k(x) dx = 1.$$

Type II MOP is the monic polynomial $\hat{P}_n$ of degree n that satisfies the orthogonality conditions

$$\int_{E_k} \hat{P}_{\vec{n}}(x)x^j w_k(x)dx = 0, \quad j = 0,\dots,n_k - 1; \quad k = 1,\dots,r.$$

Orthogonal polynomials on the real line are known to satisfy a three-term recurrence relation (see [4–6]). MOPs, in turn, satisfy recurrence relations of higher but finite order. In this paper, our attention is focused on nearly diagonal multi-indices. Let $m \in \mathbb{N}$ and write $m = lr + j$, where $l = \left[\frac{m}{r}\right]$ and $0 \le j < r$. The corresponding nearly diagonal multi-index $\vec{s}(m)$ is defined by

$$\vec{s}(m) = (\underbrace{l+1,\dots,l+1}_{j \text{ times}}, \underbrace{l,\dots,l}_{r-j \text{ times}}).$$

Type II MOPs associated with nearly diagonal multi-indices satisfy a recurrence of order $r+1$. Let us denote the corresponding type II MOP by $\hat{P}_m = \hat{P}_{\vec{s}(m)}$. Then, the following recurrence relation holds:

$$\boldsymbol{x\hat{P}_m(x) = \hat{P}_{m+1}(x) + \sum_{i=0}^{r} \hat{a}_{m,r-i}\hat{P}_{m-i}(x), \quad m \ge 0,} \tag{1}$$

with initial conditions $\hat{P}_0(x) = 1$ and $\hat{P}_i(x) = 0$, for $i = -1, \dots, -r$ (see [6]).

2. Multiple orthogonal polynomials with respect to certain bilinear forms

Let $(w_1, \dots, w_r)$ be an AT system of r weight functions on the real line, all supported on the same interval E. We introduce the following notation for the corresponding inner products:

$$\boldsymbol{\langle f, g\rangle_k = I_k(fg), \quad k = 1, \dots, r,} \tag{2}$$

where $I_k f = \int_E f(x)w_k(x)\mathrm{d}x, \quad k = 1, \dots, r.$

Let $G_n^{(k)}(f) = \sum_{i=1}^{n} \hat{A}_{k,i} f(\hat{x}_i)$, $k = 1, \dots, r$, denote the quadrature rules from the optimal set of quadrature rules in Borges' sense, and let $H_{n+1}^{(k)}$, $k = 1, \dots, r$, denote the corresponding anti-Gaussian quadrature rules. From the identity $I_k p - H_{n+1}^{(k)} p = -\left(I_k p - G_n^{(k)} p\right)$, valid for all polynomials p of degree at most n, we obtain $H_{n+1}^{(k)} p = \left(2I_k - G_n^{(k)}\right) p$, which gives rise to consider the following bilinear forms:

$$\boldsymbol{(f, g)_k = \left(2I_k - G_n^{(k)}\right)(fg), \quad k = 1, \dots, r.} \tag{3}$$

Now we introduce two types of MOPs with respect to the bilinear forms (3).

A type I MOP is an r-tuple of polynomials $(B_{\vec{n},1}, \dots, B_{\vec{n},r})$, where each $B_{\vec{n},k}$ is of degree at most $n_k - 1$, satisfying the orthogonality conditions

$$\sum_{k=1}^{r}\left(B_{\vec{n},k},x^{i}\right)_{k}=0,\quad i=0,\ldots,|\vec{n}|-2,\quad \text{with}\quad \sum_{k=1}^{r}\left(B_{\vec{n},k},x^{|\vec{n}|-1}\right)_{k}=1.$$

A type II MOP is the monic polynomial $P_{\vec{n}}$ of degree $|\vec{n}|$ satisfying the orthogonality conditions

$$\left(P_{\vec{n}},x^{i}\right)_{k}=0,\quad i=0,\ldots,n_{k}-1,\ \ k=1,\ldots,r.$$

3. The nearly diagonal multi-indices

Since we restrict our attention to nearly diagonal multi-indices, we introduce, for the sake of simplicity, the notation $P_n = P_{\vec{n}}$ for the corresponding type II MOPs with respect to (3), where $n = |\vec{n}|$. The results presented here can be found in [1, 2].

Theorem 5. *The type II MOPs with respect to the bilinear forms* (3) *with nearly diagonal multi-indices satisfy the following recurrence relation*

$$\boldsymbol{xP_m(x)=P_{m+1}(x)+\sum_{i=0}^{r}a_{m,r-i}P_{m-i}(x),\quad m\geq 0,}\qquad \textbf{(4)}$$

with initial conditions $P_0(x)=1$, $P_i(x)=0$ *for* $i=-1,\ldots,-r$.

Assuming that the bilinear forms (3) satisfy the periodicity condition $(\cdot,\cdot)_{i+Mr}=(\cdot,\cdot)_i$, $M\in\mathbb{Z}$, the following result holds (see [2]).

Theorem 1. Let $m=lr+j$, where $l=\left[\frac{m}{r}\right]$ and $j\in\{0,\ldots,r-1\}$. The recurrence coefficients in (4), for $i=1,\ldots,r$ and $m\geq 0$, can be expressed as

$$a_{m,0}=\frac{\left(xP_m,P_{\left[\frac{m-r}{r}\right]}\right)_{j+1}}{\left(P_{m-r},P_{\left[\frac{m-r}{r}\right]}\right)_{j+1}},\qquad a_{m,i}=\frac{\left(xP_m-\sum_{v=0}^{i-1}a_{m,v}P_{m-r+v},P_{\left[\frac{m-r+i}{r}\right]}\right)_{j+1+i}}{\left(P_{m-r+i},P_{\left[\frac{m-r+i}{r}\right]}\right)_{j+1+i}},$$

Theorem 2. Let $(w_1,\ldots,w_r)$ be a system of r weight functions on the real line. For type II MOPs with nearly diagonal multi-indices, orthogonal with respect to the bilinear forms (3), the recurrence coefficients in (4) can be expressed as

$$\begin{aligned}&a_{m,i}=\hat{a}_{m,i},\quad i=0,\ldots,r,\ \ m<n,\\&a_{n,i}=2\hat{a}_{n,i},\quad i=0,\ldots,r-1,\quad a_{n,r}=\hat{a}_{n,r},\end{aligned}$$

and $P_i(x)=\hat{P}_i(x), i\leq n$, where $\hat{a}_{m,i}$ are the recurrence coefficients in (1) corresponding to the type II MOPs $\hat{P}_i$, defined with respect to the inner products (2).

4. Numerical examples

We consider three weight functions $w_1(x) = (1-x)^{1/2}(1+x)^{1/3}$, $w_2(x) = (1-x)^{1/2}(1+x)^{1/4}$, and $w_3(x) = (1-x)^{1/2}(1+x)$ on the interval $[-1,1]$. The zeros of the corresponding type II MOPs $P_{(3,2,2)}(x)$ and $P_{(5,5,4)}(x)$, defined with respect to the bilinear forms (3), are listed below.

For $P_{(3,2,2)}(x)$: $-1.0294522350, -0.9307665589, -0.6782377807, -0.2590348297, -0.7729332667, 0.6861526953, 0.9505300654$.
For $P_{(5,5,4)}(x)$: $-1.0332207961, -0.9954369264, -.09650839303, -0.8927894073, -0.7729332667, -0.6056447260, -0.3967282671, -0.1572290866, -0.0976349660, 0.3499657997, 0.5809409654, 0.7726731243, 0.9100603085, 0.9832600281$.

4. Conclusion

We present a stable numerical method for constructing MOPs with respect to certain bilinear forms. The approach leverages previously known MOPs with respect to inner products, thereby reducing the need for extensive additional computations in generating new ones.

Acknowledgements

Author was supported in part by the Serbian Ministry of Science, Technological Development, and Innovations, Serbia, contract numbers 451-03-34/2026-03/200108

References

1. Petrović N. Z, Pranić M. S, Stanić M. P, Tomović Mladenović T. V. The set of anti-Gaussian quadrature rules for the optimal set of quadrature rules in Borges' sense. J. Comput. Appl. Math. 2024;442:115733
2. Alqahtani H, Reichel L. Multiple orthogonal polynomials applied to matrix function evaluation. BIT. 2018;58:835–849.
3. Van Assche W, Coussement E. Some classical multiple orthogonal polynomials. J. Comput. Appl. Math. 2001;127:317–347
4. Chihara T. S. An Introduction to Orthogonal Polynomials. Gordon and Breach, New York. 1978.
5. Mastroianni G, Milovanović G. V. Interpolation Processes: Basic Theory and Applications. Springer-Verlag, Berlin-Heidelberg. 2008.
6. Van Assche W. Non-Symmetric Linear Difference Equations for Multiple Orthogonal Polynomials. CRM Proceedings and Lecture Notes, Amer. Math. Soc, Providence. 2000;25:391–405

BIOTECHNOLOGY AND BIOENGINEERING

Natural Resources, Food Biotechnology, and Biological Systems

Biopotential of Autochthonous Lignicolous Mushrooms for Nutraceutical Applications

Project: Biopotencijal lignikolnih gljiva u funkciji nutraceutika | Contract No. 19032/961-102/24 | Ministry of Scientific and Technological Development and Higher Education of the Republic of Srpska | 2025–2026

Aleksandra Novaković[1], Mirjana Šipovac[2], Milan Vukić[2], Neda Gavrić[1], Maja Karaman[3], Aleksandar Marić[4], Jelena Vulinović[2], Nataša Vojnović[5], Vesna Šolaja[3], Neda Ubiparipović[2], Enisa Musić[2]

[1] Faculty of Education in Bijeljina, University of East Sarajevo, Bijeljina, Bosnia and Herzegovina, aleksandra.novakovic@pfb.ues.rs.ba; ORCID: 0000-0003-0397-8576; neda.gavric@pfb.ues.rs.ba;

ORCID 0009-0008-3268-1011;

[2] Faculty of Technology in Zvornik, University of East Sarajevo, Zvornik, Bosnia and Herzegovina, mirjana.beribaka@gmail.com; ORCID: 0000-0002-8916-8816; milan.vukic@tfzv.ues.rs.ba; ORCID: 0000-0002-1699-2433; jelenavulinovic@gmail.com; nedaubiparipovic12@gmail.com, enisamusic642@gmail.com

[3] Faculty of Sciences, University of Novi Sad, Novi Sad, Serbia, maja.karaman@dbe.uns.ac.rs; ORCID: 0000-0002-8788-9206; vesnasolaja11@gmail.com¸ ORCID: 0009-0002-2709-2526

[4] Institute of Food Technology in Novi Sad, University of Novi Sad, Novi Sad, Serbia, aleksandar.maric@fins.uns.ac.rs; ORCID: 0000-0001-8889-6267

[5] Faculty of Medicine, University of Banja Luka, Banja Luka, Bosnia and Herzegovina, natasa.vojinovic@med.unibl.org;

Corresponding author: aleksandra.novakovic@pfb.ues.rs.ba

Abstract

Lignicolous mushrooms are an important source of biologically active compounds with promising nutraceutical potential. This project focused on two autochthonous species, *Meripilus giganteus* and *Laetiporus sulphureus*, with the aim of evaluating their chemical composition and selected biological activities.

The investigated material was subjected to chemical characterization, including determination of protein content, fatty acid composition, total phenolics, total flavonoids, and individual phenolic compounds. Biological activity was assessed in vitro through antioxidant, antimicrobial, and antiproliferative assays.

The results demonstrated clear interspecies differences. LC-MS/MS analysis identified four phenolic compounds in *M. giganteus* (*p*-hydroxybenzoic, protocatechuic, caffeic, and *p*-coumaric acids), whereas only *p*-coumaric acid was detected in *L. sulphureus*. *M. giganteus* also showed higher protein content and stronger antibacterial activity, particularly against *Staphylococcus aureus*. Both species were characterized by a predominance of unsaturated fatty acids and measurable antioxidant and antiproliferative potential. Overall, the findings support the relevance of lignicolous fungi as promising natural resources for nutraceutical and functional applications.

Keywords: lignicolous fungi; nutraceuticals; *Meripilus giganteus*; *Laetiporus sulphureus*; antioxidant activity; antimicrobial activity; UN SDG 3; UN SDG 12

1. Project Background and Objectives

Mushrooms are widely recognized as valuable natural sources of nutrients and bioactive compounds with potential health-promoting effects [1,2,3,4]. Among them, lignicolous fungi have attracted increasing attention because of their diverse chemical composition and possible use in nutraceutical and functional products [1,2,3]. Despite this interest, available data on the chemical profile and biological potential of many autochthonous species remain limited.

The aim of this project was to investigate the biological potential of selected autochthonous lignicolous fungi and evaluate their suitability as natural nutraceutical resources. The specific objectives were to collect and identify representative lignicolous species, prepare extracts of different polarities, characterize their chemical composition, and assess their antioxidant, antimicrobial, and antiproliferative activities.

2. Methodology and Work Performed

The study included two autochthonous lignicolous fungal species, *M. giganteus* and *L. sulphureus*, collected from natural habitats. Fruiting bodies were dried, powdered, and extracted using solvents of different polarities [3,4].

Chemical characterization included determination of total protein content by the macro-Kjeldahl method according to AOAC procedures (16th edition), using a nitrogen-to-protein conversion factor of 4.38. Spectrophotometric methods, including UV-Vis spectrophotometry, were used for the quantitative determination of total phenolics and flavonoids [6,7]. Individual phenolic compounds were identified and quantified by liquid chromatography-tandem mass spectrometry (LC-MS/MS) [8]. Gas chromatography (GC) was used to analyze lipid fractions and fatty acid composition [9,10].

The biological potential of the obtained extracts was evaluated using a series of in vitro assays. Antioxidant activity was assessed by DPPH radical scavenging [11], nitric oxide radical scavenging [12], hydroxyl radical scavenging [13], superoxide anion radical scavenging [14], and ferric reducing antioxidant power (FRAP) assays [15]. Antimicrobial activity was determined by the microdilution method against selected standard bacterial and fungal strains [16,17], while antiproliferative activity was evaluated by the MTT assay in relation to extract type and exposure time [18]. Statistical analysis was performed to support interpretation of the obtained results.

3. Key Results

The results revealed clear differences between *M. giganteus* and *L. sulphureus* in both chemical composition and biological activity. Liquid chromatography-tandem mass spectrometry (LC-MS/MS) analysis identified four phenolic compounds in *M. giganteus*: *p*-hydroxybenzoic acid (23.9 µg/g), protocatechuic acid (1.26 µg/g), caffeic acid (1.3 µg/g), and *p*-coumaric acid (0.2 µg/g). In *L. sulphureus*, only *p*-coumaric acid was detected, at a concentration of 0.3 µg/g. Protein analysis likewise showed higher protein content in *M. giganteus* (17.69%) than in *L. sulphureus* (14.54%).

Both species were characterized by a predominance of unsaturated fatty acids. In *L. sulphureus*, linoleic acid was the dominant fatty acid, accounting for 68.82% of the total fatty acid content. In *M. giganteus*, linoleic acid (48.52%) and oleic acid (32.48%) were the most abundant fatty acids.

As shown in Table 1, the ethanol extract of *M. giganteus* contained the highest total phenol content (76.12 mg GAE/100 g d.w.) and total flavonoid content (8.85 mg QE/100 g d.w.). In *L. sulphureus*, total polyphenol content was similar in the ethanol and aqueous extracts (24.46 and 24.44 mg GAE/100 g d.w., respectively), whereas total flavonoid content was lower in both extracts (1.75 and 0.94 mg QE/100 g d.w., respectively).

Antioxidant activity was detected in all tested extracts, with the intensity of the effect depending on both fungal species and extraction solvent (Table 1). In the DPPH assay, the ethanol extract of *M. giganteus* showed the strongest activity (IC_{50} 58.26 µg/mL), whereas the ethanol extract of *L. sulphureus* showed the weakest activity (IC_{50} 215.14 µg/mL). In the hydroxyl radical scavenging assay, the ethanol extract of *M. giganteus* again showed the strongest activity (IC_{50} 2.43 µg/mL). In the nitric oxide scavenging assay, the aqueous extract of *M. giganteus* showed the lowest IC25 value (IC_{25} 42.39 µg/mL), while in the superoxide anion scavenging assay the aqueous extract of *L. sulphureus* was the most active (IC_{50} 6.17 µg/mL). FRAP values were similar for all tested extracts and ranged from 9.97 to 10.93 mg ascorbic acid equivalents/g dry extract.

The investigated extracts also exhibited antibacterial activity, with the strongest effect observed against *S. aureus*. The hexane extract of *M. giganteus* showed the highest antibacterial activity, with a MIC value of 0.78 mg/mL. *L. sulphureus* showed weaker antibacterial effects overall, although activity against *B. subtilis* was also recorded.

Table 1. Total phenol and flavonoid content and antioxidant activity of ethanol and aqueous extracts of *L. sulphureus* and M. giganteus

PARAMETER	***L. SULPHUREUS* ETHANOL EXTRACT**	***L. SULPHUREUS* AQUEOUS EXTRACT**	***M. GIGANTEUS* ETHANOL EXTRACT**	***M. GIGANTEUS* AQUEOUS EXTRACT**
TOTAL PHENOLS (MG GAE/100 G D.W.)	24.46	24.44	76.12	20.54
TOTAL FLAVONOIDS (MG QE/100 G D.W.)	1.75	0.94	8.85	4.19
DPPH RADICAL SCAVENGING ACTIVITY, (IC_{50} µG/ML)	215.14	79.53	58.26	144.94
HYDROXYL RADICAL SCAVENGING ACTIVITY (IC_{50} µG/ML)	10.73	12.94	2.43	8.91
NITRIC OXIDE RADICAL SCAVENGING ACTIVITY, (IC_{25} µG/ML)	97.83	112.26	154.56	42.39

SUPEROXIDE ANION SCAVENGING ACTIVITY (IC_{50} µG/ML)	115.24	6.17	20.94	44.37
FRAP (MG ASCORBIC ACID EQUIVALENTS/G DRY EXTRACT)	10.93	9.97	10.82	10.67

Legend: GAE, gallic acid equivalents; QE, quercetin equivalents; d.w., dry weight; DPPH, 2,2-diphenyl-1-picrylhydrazyl; IC_{50}, inhibitory concentration causing 50% effect; IC_{25}, inhibitory concentration causing 25% effect; FRAP, ferric reducing antioxidant power.

The antiproliferative activity of the tested extracts against the estrogen-dependent human breast adenocarcinoma cell line MCF-7 is presented in Table 2. After 24 h of treatment, the ethanol extract of *L. sulphureus* showed an IC50 value of 260.58 µg/mL, while its aqueous extract showed a markedly higher value of 660.31 µg/mL. Under the same conditions, the ethanol extract of *M. giganteus* exhibited an IC50 value of 667.86 µg/mL, whereas the aqueous extract showed the weakest activity, with an IC50 value above 900 µg/mL. After 72 h of treatment, the antiproliferative effect increased in all tested samples. The ethanol extract of *L. sulphureus* showed an IC50 value of 238.62 µg/mL, while the aqueous extract reached 347.08 µg/mL. In *M. giganteus*, the ethanol extract showed an IC50 value of 313.49 µg/mL after 72 h, whereas the aqueous extract reached 505.82 µg/mL. Overall, ethanol extracts showed stronger antiproliferative activity than aqueous extracts, particularly after prolonged treatment (Table 2).

Table 2. Antiproliferative activity of ethanol and aqueous extracts of *L. sulphureus* and *M. giganteus* determined by the MTT assay in the estrogen-dependent breast adenocarcinoma cell line MCF-7

INCUBATION TIME	*L. SULPHUREUS* ETHANOL EXTRACT (µG/ML)	*L. SULPHUREUS* AQUEOUS EXTRACT (µG/ML)	*M. GIGANTEUS* ETHANOL EXTRACT (µG/ML)	*M. GIGANTEUS* AQUEOUS EXTRACT (µG/ML)
24 H	260.58	660.31	667.86	>900
72 H	238.62	347.08	313.49	505.82

Legend: MTT, 3-(4,5-dimethylthiazol-2-yl)-2,5-diphenyltetrazolium bromide; MCF-7, estrogen-dependent human breast adenocarcinoma cell line.

4. Discussion and Impact

The findings indicate that both *M. giganteus* and *L. sulphureus* are valuable sources of bioactive compounds with potential nutraceutical relevance, while also demonstrating distinct species-specific profiles. The richer phenolic profile and higher protein content of *M. giganteus*, together with its stronger antibacterial activity, point to a more pronounced bioactive potential in this species.

The antioxidant results further show that the activity of the investigated fungi depends not only on species identity but also on extraction solvent and assay principle. The ethanol extract of *M. giganteus* was the most effective in the DPPH and hydroxyl radical scavenging assays, whereas the aqueous extract of *M. giganteus*

showed the strongest nitric oxide scavenging activity and the aqueous extract of *L. sulphureus* was the most effective in the superoxide anion assay. The comparable FRAP values suggest that the reducing capacity of the extracts remained relatively stable despite differences observed in the radical-scavenging assays.

The predominance of unsaturated fatty acids, especially linoleic and oleic acids, additionally supports the nutritional relevance of both species. The stronger antibacterial effect of *M. giganteus*, particularly against *S. aureus*, indicates that this species may be especially promising for further studies focused on naturally derived antimicrobial agents.

Taken together, the results provide original data on autochthonous lignicolous fungi and contribute to a better understanding of their possible valorization as natural resources. The observed differences between the investigated species also emphasize the importance of species selection and extraction conditions when evaluating biological potential.

From a broader perspective, the study contributes to the valorization of local biodiversity and provides a scientific basis for further investigations in the fields of food science, pharmacy, and biotechnology.

5. Conclusions and Outlook

The present study demonstrated that autochthonous lignicolous mushrooms represent a relevant source of bioactive compounds with nutraceutical potential. The investigated species, *Meripilus giganteus* and *Laetiporus sulphureus*, exhibited distinct chemical and biological profiles.

M. giganteus was characterized by a richer phenolic profile, higher protein content, and stronger antibacterial activity, whereas both species showed a predominance of unsaturated fatty acids, measurable antioxidant activity, comparable reducing capacity, and moderate antiproliferative effects.

These findings support further evaluation of lignicolous fungi as natural resources for the development of nutraceutical and functional products.

Future research should focus on the isolation and detailed characterization of individual bioactive compounds, validation of the most promising extracts, and assessment of their potential applications in food, pharmaceutical, and other functional formulations.

Acknowledgements / Funding

Funding: This research was funded by the Ministry of Scientific and Technological Development and Higher Education of the Republic of Srpska (Contract No. 19032/961-102/24). The authors also acknowledge the contribution of project team members and the active participation of young researchers involved in sampling, laboratory work, data processing, and dissemination activities.

References

1. Wasser SP. Medicinal mushroom science: current perspectives, advances, evidences, and challenges. Biomed J. 2014;37(6):345-356.

2. Valverde ME, Hernández-Pérez T, Paredes-López O. Edible mushrooms: improving human health and promoting quality life. Int J Microbiol. 2015;2015:376387.
3. Novaković A, Karaman M, Šojić B, Ikonić P, Peulić T, Tomić J, Šipovac M. From forest to fork: Antioxidant and antimicrobial potential of Laetiporus sulphureus (Bull.) Murrill in cooked sausages. Microorganisms. 2025;13(8):1832.
4. Chang ST, Miles PG. Mushrooms: Cultivation, Nutritional Value, Medicinal Effect, and Environmental Impact. Boca Raton: CRC Press; 2004.
5. AOAC. Official Methods of Analysis. 16th ed. Arlington (VA): Association of Official Analytical Chemists; 1995.
6. Singleton VL, Orthofer R, Lamuela-Raventós RM. Analysis of total phenols and other oxidation substrates and antioxidants by means of Folin-Ciocalteu reagent. Methods Enzymol. 1999;299:152-178.
7. Chang CC, Yang MH, Wen HM, Chern JC. Estimation of total flavonoid content in propolis by two complementary colorimetric methods. J Food Drug Anal. 2002;10:178-182.
8. Orčić D, Francišković M, Bekvalac K, Svirčev E, Beara I, Lesjak M, Mimica-Dukić N. Quantitative determination of plant phenolics in Urtica dioica extracts by high-performance liquid chromatography coupled with tandem mass spectrometric detection. Food Chem. 2014;143:48-53.
9. Folch J, Lees M, Sloane-Stanley GH. A simple method for the isolation and purification of total lipids from animal tissues. J Chromatogr A. 1957;226:497-509.
10. Ackman RG. Remarks on official methods employing boron trifluoride in the preparation of methyl esters of the fatty acids of fish oils. J Am Oil Chem Soc. 1998;75:541-545.
11. Espín JC, Soler-Rivas C, Wichers HJ. Characterization of the total free radical scavenger capacity of vegetable oils and oil fractions using 2,2-diphenyl-1-picrylhydrazyl radical. J Agric Food Chem. 2000;48:648-656.
12. Green LC, Wagner DA, Glogowski J, Skipper PL, Wishnok JS, Tannenbaum SR. Analysis of nitrate, nitrite, and [15N] nitrate in biological fluids. Anal Biochem. 1982;126:131-138.
13. Cheeseman KH, Beavis A, Esterbauer H. Hydroxyl-radical-induced iron-catalysed degradation of 2-deoxyribose. Quantitative determination of malondialdehyde. Biochem J. 1988;252:649-653.
14. Nishikimi M, Rao NA, Yagi K. The occurrence of superoxide anion in the reaction of reduced phenazine methosulfate and molecular oxygen. Biochem Biophys Res Commun. 1972;46(2):849-854.
15. Mandić A. Antioxidant Activities of Grape Seed Extracts from White Grape Varieties. PhD Thesis. Novi Sad: University of Novi Sad; 2007.
16. Tidona F, Sekse C, Criscione A, Jacobsen M, Bordonaro S, Marletta D, Vegarud GE. Antimicrobial effect of donkeys' milk digested in vitro with human gastrointestinal enzymes. Int Dairy J. 2011;21:158-165.
17. Karaman M, Mimica-Dukić N, Knežević P, Svirčev Z, Matavulj M. Antibacterial properties of selected lignicolous mushrooms and fungi from northern Serbia. Int J Med Mushrooms. 2009;11:269-279.
18. Mosmann T. Rapid colorimetric assay for cellular growth and survival: application to proliferation and cytotoxicity assays. J Immunol Methods. 1983;65(1-2):55-63.

The application of herbs and spices in the food industry

Vesna Gojković Cvjetković[1], Milenko Smiljanić[1], Željka Marjanović-Balaban[2], Milan Vukić[1], Dragan Vujadinović[1]

[1]*University of East Sarajevo, Faculty of Technology Zvornik, Republic of Srpska, Bosnia and Herzegovina, vesna.gojkovic@tfzv.ues.rs.ba, ORCID 0000-0003-2270-5311, milenko.smiljanic@tfzv.ues.rs.ba, milan.vukic@tfzv.ues.rs.ba, ORCID 0000-0002-1699-2433, dragan.vujadinovic@tfzv.ues.rs.ba, ORCID 0000-0002-3809-4415*

[2]*University of Banja Luka, Faculty of Forestry Banja Luka, Republic of Srpska, Bosnia and Herzegovina, zeljka.marjanovic-balaban@sf.unibl.org, ORCID 0009-0007-3648-0527*

Corresponding author: vesna.gojkovic@tfzv.ues.rs.ba

Abstract

Herbs and spices play a significant role in the modern food industry due to their sensory, technological, and functional properties. In addition to improving the taste, aroma, and color of food products, they are also an important source of bioactive compounds, such as essential oils, polyphenols, and flavonoids that have antioxidant and antimicrobial effects. Thyme, oregano, and basil are plants that are widely used in the meat, bakery, dairy, and beverage industries, both in fresh and dried form, as extracts and essential oils. Recently, the usage of spices as a natural alternative to synthetic preservatives has become very important, which also increases the market value of the product. However, despite numerous advantages, challenges in application include variability of chemical composition, stability during technological processing, and the need for quality standardization.

Key words: herbs and spices; food industry; antioxidant; antimicrobial effects; health.

1. Introduction

Spices are aromatic plants that are used in food to improve the sensory properties. They are characterized by the presence of essential oils, phenolic compounds, flavonoids, and other bioactive components that give them a specific smell and taste. Thanks to these compounds, herbs are widely used not only in households but also in the modern food industry. Unlike spices, which are most often obtained from seeds, fruits, bark, and roots of plants, herbs are mainly used fresh and dried, in natural and crushed form. In the food industry, they are often used in the form of extracts, essential oils, and oleoresins. The most important species used in the food industry are basil, parsley, thyme, oregano, peppermint, and bay leaf [1], [2].

The main role of herbs is to improve the sensory properties of the product: taste, aroma, color, and overall experience of food. Adding aromatic plants achieves a recognizable product identity, which is especially important in a competitive market environment. Herbs enable the development of traditional and regional products with specific characteristics [3], [4]. Modern research has shown that many types of herbs possess natural antioxidant and antimicrobial properties. These characteristics contribute to slowing down the oxidation of fats, reducing the growth of microorganisms, extending the shelf time. Therefore, herbs are increasingly used

as a natural alternative to synthetic preservatives and additives, which is in line with modern production trends. Although used in relatively small quantities, herbs contain significant amounts of vitamins (especially vitamin C and provitamin A), minerals, and antioxidants [5]. Regular use contributes to the enrichment of the nutritional value of food and the development of functional products. Bioactive compounds present in herbs are associated with antioxidant activity, anti-inflammatory effects, antimicrobial properties, and potential positive effects on the digestive system [6], [7]. Therefore, herbs play an important role in the development of functional foods and products with additional health value.

2. The most commonly used spices and herbs in the food industry

2.1. Basil

Basil (*Ocimum basilicum* L.) is one of the most important and most commonly used herbs in the food industry. It is characterized by a pleasant, aromatic smell and a mild, characteristic taste that improves the quality of many dishes and food products. In the food industry, basil is used fresh, dried, and in the form of essential oil. It is most often added in the production of sauces, especially tomato sauce, and then in soups, salads, vegetable dishes, and meat dishes. It is an important ingredient in the production of spice mixes and ready meals. Basil contains essential oils, vitamins, and antioxidants that contribute to the aroma and nutritional value of food [8].

2.2. Parsley

Parsley (*Petroselinum crispum*) is characterized by a fresh aroma and a mild, pleasant taste that improves the aroma and appearance of many dishes. In the food industry, parsley is used fresh, dried, and frozen. It is most often added to soups, sauces, salads, vegetable dishes, and meat products. It is also used in the production of spice mixtures and ready-made dishes. Parsley is rich in vitamins, especially vitamins C and A, as well as minerals and antioxidants. In addition to improving the taste of food, it also increases its nutritional value [9].

2.3. Oregano

Oregano (*Origanum vulgare*) is characterized by a strong aromatic smell and a slightly spicy taste, which is why it is often used to improve the aroma and the taste of various food products. In the food industry, oregano is most often used in dried form, but it can be used both fresh and in the form of essential oil. It is especially popular in the production of sauces, especially tomato sauce, and then in meat dishes, pizza, pasta, and various spice mixes. It is also used in the production of meat products, where it contributes to a better taste and aroma of the product. Oregano contains essential oils, antioxidants, and other bioactive compounds that have antibacterial and antifungal properties. That is why it is sometimes used as a natural supplement that helps preserve the quality and freshness of food. Oregano contributes to increasing the nutritional value of food, as it contains certain vitamins and minerals. Its intense aroma makes it possible to use a smaller amount of salt and other additives in food preparation, which contributes to a healthier diet [10].

2.4. Thyme

Thyme (*Thyme vulgaris*) is an aromatic herb that is known for its intense smell and slightly bitter aromatic taste that gives a special character to different dishes and food products. In the food industry, thyme is most often used in dried form, but it is used both fresh and in the form of essential oil. It is especially represented in the production of meat products such as sausages, pates, and various dried meat products. It is added to soups, sauces, marinades, vegetable dishes, and various spice mixes. Its aroma goes well with meat, fish, and vegetable dishes. Thyme contains essential oils, the most important of which are thymol and carvacrol. These substances have antibacterial and antifungal properties, which is why thyme contributes to preserving its quality and extending its shelf life. That is why in some cases it is also used as a natural preservative in the food industry. Thyme contains antioxidants, vitamins, and minerals that contribute to the nutritional value of food. Its intense aroma makes it possible to reduce the amount of salt and other additives in food preparation, which has a positive effect on the health of consumers [11].

2.5. Peppermint

Peppermint (*Mentha piperita*), also known as mint, is characterized by a fresh, intense smell and a pleasant, slightly refreshing taste that gives a special quality to many food products. In the food industry, mint is used in fresh, dried, and processed forms such as extracts and essential oils. It is often used in the production of beverages, especially teas, refreshing soft drinks, and syrups. It is added to sweets, chocolates, chewing gum, and various desserts because it gives a refreshing aroma. In addition to sweet products, mint is also used in the preparation of savory dishes. It is added to salads, sauces, and vegetable dishes, as well as some meat dishes. In some cuisines, it is used in marinades and various spice mixes. Mint contains essential oils, the best known of which is menthol. Menthol gives a characteristic smell and a refreshing feeling. In addition, mint contains antioxidants, vitamins, and minerals that contribute to the nutritional value of food [12].

2.6. Bay leaf

Bay leaf (*Laurus nobilis*) is an aromatic herb widely used in the food industry due to its characteristic aroma and slightly bitter but pleasant taste. Bay leaves are most often used as a spice and give a special flavor to various dishes and food products. In the food industry, bay leaf is most often used in dried form, because dried leaves retain their aroma and are stored longer. It is added to soups, stews, sauces, marinades, and meat and fish dishes. It is a particularly common ingredient in the preparation of dishes that are cooked for a long time because during cooking it slowly releases its aroma and enriches the taste of the food. Bay leaf is also used in the production of meat products, such as sausages and cured meat products. It contains numerous bioactive substances, including essential oils, tannins, and flavonoids. It helps digestion because it is a stimulator of gastric juices, and reduces bloating and cramps. Bay leaf contains essential oils that inhibit the growth of bacteria and fungi and phenolic compounds that help neutralize free radicals and protect cells [13].

Conclusion

The usage of spices and herbs, such as basil, parsley, oregano, bay leaf, thyme, and peppermint, is of great importance in the food industry. These herbs are used not only for the pleasant aroma and taste that they give to various dishes and products but also for their natural preservative and health-beneficial properties. Their essential and bioactive substances contribute to extending the shelf life of food, reducing the need for artificial

additives, and improving the nutritional value of products. Thanks to their natural origin and numerous functional properties, herbs play an increasingly important role in the modern food industry. Their use contributes to the development of higher-quality, healthier, and more natural food products, which is in line with modern trends and consumer demands.

Acknowledgements

This work is a part of the research project titled "Analysis of the presence of heavy metals in spices and medicinal herbs from the area of Herzegovina," financed by the Ministry of Science and Technology Development and Higher Education of the Republic of Srpska.

References

1. Ahmad RS, Imran M, Khan MK, Ahmad MH, Arshad MS, Ateeq H, Rahim MA. Herbs and Spices - An Overview. In book: Herbs and Spices - New Processing Technologies. 2021;1-8.
2. Dini I. Spices and herbs as therapeutic foods. In: Food Quality: Balancing Health and Disease. Cambridge, Massachusetts, United States: Academic Press. 2018;433-469.
3. Peter KV. Handbook of Herbs and Spices. Cambridge, United Kingdom: Woodhead Publishing Limited; 2004.
4. Jiang TA. Health benefits of culinary herbs and spices. Journal of AOAC International. 2019;102(2):395-411.
5. Yashin A, Yashin Y, Xia X, Nemzer B. Antioxidant activity of spices and their impact on human health: A review. Antioxidants. 2017;6(3):70.
6. Ravindran PN, Johny AK, Nirmal BK. Spices in our daily life. Satabdi Smaranika. 2002;2:102-105.
7. De Monte C, Cesa S. Use of saffron as a functional food and saffron nutraceuticals. In Saffron. Cambridge, Massachusetts, United States: Academic Press. 2021;241-273.
8. Li QX, Chang CL. Basil (*Ocimum basilicum* L.) Oils. Essential Oils in Food Preservation, Flavor and Safety. 2016;231-238.
9. Charles DJ. Parsley. Handbook of Herbs and Spices (Second edition). Woodhead Publishing Series in Food Science, Technology and Nutrition. 2012;430-451.
10. Giannenas I, Bonos E, Christaki E, Florou-Paneri P. Oregano: A Feed Additive With Functional Properties. Therapeutic Foods. 2018;179-208.
11. Halat DH, Krayem M, Khaled S, Younes S. A Focused Insight into Thyme: Biological, Chemical, and Therapeutic Properties of an Indigenous Mediterranean Herb. Nutrients. 2022;14(10):2104.
12. Pluháčková H, Kudláčková B, Šinko M, Michutová M, Neugebauerová J, Svojanovská L. Phytochemical Variability of *Mentha* L. Species Over Three Growing Seasons. Chemistry & Biodiversity. 2026;23(3): e03674.
13. Batool S, Khera RA, Hanif MA, Ayub MA. Bay Leaf. Medicinal Plants of South Asia. 2020;63-74.

Integrated Non-Invasive Multi-Sensor Approach for Monitoring Fish Community Dynamics: A Case Study in Gruža Reservoir

Aleksa B. Cvetković[1]*, Tijana Z. Veličković[1,2], Vladica M. Simić[1]

[1]*University of Kragujevac, Faculty of Science, Department of Biology and Ecology, Radoja Domanovića 12, 34000 Kragujevac, Serbia, cvetkovica1707@gmail.com, 0009-0002-1524-6129, tijana.velickovic@pmf.kg.ac.rs, 0000-0001-9152-056X, vladica.simic@pmf.kg.ac.rs, 0000-0001-6787-9783*

[2] *Department of Organisms and Ecosystems Research, National Institute of Biology, Večna pot 121,1000 Ljubljana, Slovenia, tijana.velickovic@nib.si, 0000-0001-9152-056X*

Corresponding author: cvetkovica1707@gmail.com

Abstract

This study presents an integrated, non-invasive monitoring framework applied to the Gruža Reservoir (central Serbia), focusing on the analysis of fish spatial distribution and habitat characteristics across variable environmental conditions. The methodological approach integrates underwater video systems, a remotely operated vehicle (ROV), hydroacoustic methods, drone (UAV) surveys, and GIS spatial analysis, enabling a comprehensive evaluation of aquatic habitats and fish community structure. The results indicate that each method provided reliable data under different environmental conditions, with underwater visual systems being most effective in clear water, hydroacoustic methods in deeper zones, and drone surveys in conditions of increased turbidity and low water levels. The integrated non-invasive approach significantly enhances the understanding of the spatial and temporal dynamics of fish populations and their habitats, contributing to more precise ecosystem assessment and improved management strategies. Additionally, the study highlights the potential application of machine learning-based methods for automated fish detection and real-time monitoring in future research.

Keywords: non-invasive monitoring, freshwater ecosystems, fish distribution, hydroacoustics, UAV drones, GIS analysis, Special Fish Habitats, 'UN SDG 6', 'UN SDG 13'

1. Introduction

Freshwater ecosystems cover only a small fraction of the Earth's surface, yet they support a disproportionately high level of global biodiversity, particularly fish communities [1]. Their sensitivity to natural and anthropogenic pressures makes effective monitoring essential. Traditional methods (electrofishing and netting) are often invasive and limited in spatial coverage [2][3]. Recent advances in non-invasive technologies, including hydroacoustics, underwater imaging, ROVs, and aerial surveys integrated within GIS, enable improved spatiotemporal analysis [2] [4] [5]. This study applies a multi-sensor approach in the Gruža Reservoir to assess habitat characteristics, identify key ecological zones, and evaluate environmental variability, with emphasis on future development of automated, machine learning-based monitoring systems.

2. Materials and Methods

2.1. Study Area

The study was conducted at Gruža Reservoir, larger artificial lake in central Serbia, formed by damming the Gruža River. The reservoir is characterized by pronounced spatial heterogeneity, ranging from deep rocky zones in the lower part to shallow, muddy, and vegetated areas in the upper section [6]. This diversity of habitats provides an ideal model for testing and comparing non-invasive fish monitoring methods.

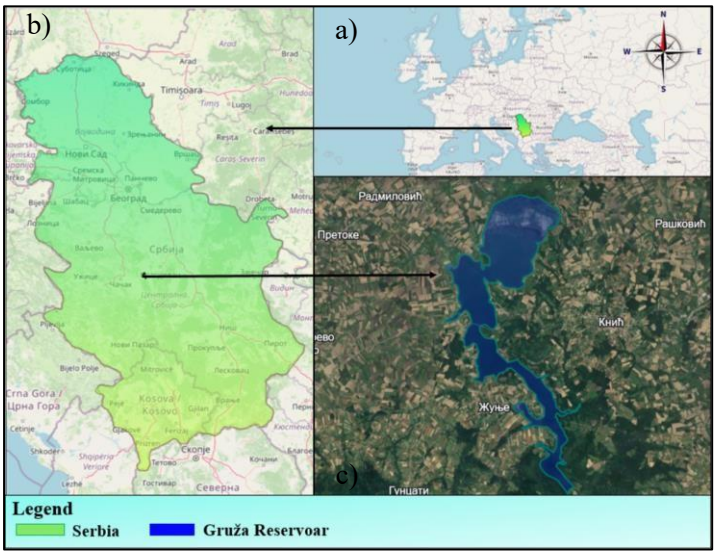


Figure 1. Study area: (a) Location of Serbia in Europe; (b) position within the Balkan Peninsula; (c) map of the Gruža Reservoir

Field investigations were conducted during three seasonal periods (spring, summer, and late autumn/winter) to capture seasonal variations in environmental conditions and fish distribution.

2.2. Data Collection Using Non-Invasive Techniques

Monitoring was based on the combined application of aerial drones, underwater camera systems, an underwater drone (ROV), and hydroacoustic surveys.

Underwater visual monitoring was conducted using four camera systems: Water Wolf 2.0, LUCKYLAKER FL180PR, LUCKYLAKER 180AR, and GoPro HERO12. Cameras were simultaneously mounted on a single platform at different angles to achieve near 360° coverage. Recordings were performed at five locations along the reservoir, with each deployment lasting 20–30 minutes. In addition, a Chasing Gladius Mini S underwater drone was used for active exploration of habitats, allowing observation of fish movement along the water column and detailed recording of substrate structure and vegetation. Aerial surveys were performed using a DJI Mini 4 Pro drone equipped with a 48 MP RGB sensor. Hydroacoustic surveys were conducted using a Garmin Striker 7SV sonar system with ClearVu and SideVu technologies. Video analysis was conducted at the Center for Fisheries and Freshwater Ecosystem Conservation - Aquarium, Faculty of Science, University of Kragujevac.

2.3. Data Processing and Spatial Analysis

All video materials were processed using VLC Media Player, and georeferenced data were integrated into QGIS 3.28.2 for spatial analysis. The future development phase includes the creation of machine learning-based software for automated fish species recognition and real-time data processing directly in the field.

3. Results

The multi-sensor approach enabled clear differentiation of method performance under varying environmental conditions in the Gruža Reservoir. Underwater camera systems provided the most detailed information on species presence and habitat use, but only under good water clarity. Recorded species included *Abramis brama* Linnaeus, 1758 (freshwater bream), *Sander lucioperca* Linnaeus, 1758 (pike-perch), *Perca fluviatilis* Linnaeus, 1758 (european perch), *Alburnus alburnus* Linnaeus, 1758 (bleak), *Ameiurus melas* Rafinesque, 1820 (black bullhead) and *Cyprinus carpio* Linnaeus, 1758 (common carp) with fish mainly concentrated in shallow, vegetated muddy habitats, while deeper and coarser zones showed lower abundance. The ROV (Chasing Gladius Mini S) complemented stationary cameras by enabling active habitat inspection and confirming substrate and vegetation structure, although its performance was also dependent on water transparency. Hydroacoustic surveys (Garmin Striker 7SV) were effective for detecting fish in deeper zones (25–30 m) and assessing vertical distribution, but their efficiency decreased during low water levels. In contrast, aerial surveys were most effective in shallow and turbid conditions, enabling shoreline monitoring and detection of *C. carpio* spawning activity in the Special Fish Habitat (SFH), which was also affected by seasonal water level decline and complete desiccation in summer. These findings support redefining the SFH as a dynamic habitat whose spatial extent and ecological function vary in response to seasonal hydrological fluctuations.

4. Discussion

The results of this study show that monitoring methods in Gruža Reservoir were strongly dependent on environmental conditions, underscoring the need for a flexible, multi-sensor approach. Underwater visual systems provided detailed species and habitat data under clear water, but their efficiency declined with turbidity [2] [4] [7]. This limitation is well documented in freshwater environments, where suspended particles reduce both detection range and image clarity, compromising species identification and behavioral observations [4]. In contrast, hydroacoustic surveys proved more effective in deeper zones, reliably detecting fish aggregations where visual methods were impractical [2] [5] [8]. In shallow littoral areas with dense vegetation or during periods of pronounced water level decline, sonar performance was compromised by bottom interference and reduced water column volume, a known constraint of acoustic techniques in structurally complex habitats [5]. Aerial drone surveys proved most useful in shallow and highly turbid areas, particularly for detecting spawning activity of *C. carpio* in the Special Fish Habitat (SFH). The drone's ability to capture high-resolution imagery from above allowed continuous monitoring of habitat changes, including the complete desiccation of the SFH during summer low-water conditions [9]. Together, these findings confirm that method performance is strongly controlled by water transparency, depth, and hydrological variability, reinforcing the need for integrated monitoring strategies in freshwater ecosystems [2][3][8]. A key

implication of this study is the potential for advancing non-invasive monitoring through the application of machine learning techniques. Multi-sensor data, particularly underwater videos and aerial imagery, provide a valuable basis for automated workflows in fish detection, classification, and habitat analysis [2][4][5], reducing observer bias and improving efficiency. Their integration within GIS frameworks enables data-driven ecological assessment by combining spatial and temporal information [10] [11], supporting scalable monitoring with higher resolution and frequency. Future research should focus on machine learning models for freshwater environments to enable real-time monitoring and prediction, while combining non-invasive sensing and advanced analytics offers a promising approach for improved ecosystem assessment and adaptive management.

5. Conclusions

This study demonstrates that the integration of non-invasive monitoring methods provides a reliable framework for assessing fish populations and habitat conditions in the Gruža Reservoir. The combined approach improves spatial coverage and monitoring accuracy while emphasizing the ecological importance of key habitats[4] [9] [11]. Future research will focus on the application of machine learning for automated detection and real-time monitoring, supporting more efficient and data-driven management of freshwater ecosystems.

Acknowledgements

This work was partially funded by the Ministry of Education and the Ministry of Science, Technological Development and Innovation of the Republic of Serbia (451-03-34/2026-03/200122; 451-03-33/2026-03/200122).

References

[1].Dudgeon D, Arthington AH, Gessner MO, Kawabata Z-I, Knowler DJ, Lévêque C, Naiman RJ, Prieur-Richard A-H, Soto D, Stiassny MLJ, Sullivan CA. Freshwater biodiversity: importance, threats, status and conservation challenges. Biological Reviews of the Cambridge Philosophical Society. 2006;81(2):163–182. doi:10.1017/S1464793105006950.

[2].L, Pander J, Mueller M, Geist J. Comparison of sonar, camera and net-based methods in detecting riverine fish-movement patterns. Marine and Freshwater Research. 2018. doi:10.1071/MF18068.

[3]. Lu S, Fang C, Xiao X. Virtual scene construction of wetlands: A case study of Poyang Lake, China. ISPRS International Journal of Geo-Information. 2023;12(2):49. doi:10.3390/ijgi12020049.

[4].Wilson KL, Allen MS, Ahrens RNM, Netherland MD. Use of underwater video to assess freshwater fish populations in dense submersed aquatic vegetation. University of Florida, School of Forest Resources and Conservation, Fisheries and Aquatic Sciences Program, Gainesville, FL, USA.

[5].Godlewska M, Ye S. Hydroacoustics in marine, transitional and freshwaters. Water. 2023;15:1674. doi:10.3390/w15091674.

[6].Ranković V, Radulović J, Radojević I, Ostojić A, Čomić Lj. Neural network modeling of dissolved

oxygen in the Gruža reservoir, Serbia. Ecological Modelling. 2010;221:1239–1244.

[7].Guedes GHS, Araujo FG. Underwater drones reveal different fish community structures on the steep slopes of a tropical reservoir. *Hydrobiologia*. 2021. doi:10.1007/s10750-021-04790-9.

[8].Hutorowicz A. Use of hydroacoustic methods to assess ecological status based on fish: A case study of Lake Dejguny (Poland). *Water*. 2024;16:282. doi:10.3390/w16020282.

[9].Fernandez-Figueroa EG, Rogers SR, Neupane D. Drones and deep learning for detecting fish carcasses during fish kills. Drones. 2025;9:482. doi:10.3390/drones9070482.

[10].Liu B, Li T. A machine-learning-based framework for retrieving water quality parameters in urban rivers using UAV hyperspectral images. *Remote Sensing*. 2024;16(5):905. doi:10.3390/rs16050905.

[11].Hamzah A, Aqlan F, Baidya S. Drone-based digital twins for water quality monitoring: A systematic review. Digital Twins and Applications. 2024:e12021. doi:10.1049/dgt2.12021.

Host–microbiota interactions in *Drosophila*: composition, regulatory mechanisms and translational relevance

Enisa Musić[1], Mirjana Šipovac[1], Aleksandra Novaković[2], Maja Palangetić[1]

[1]*Faculty of Technology Zvornik, University of East Sarajevo, Zvornik, Bosnia and Herzegovina,* enisamusic642@gmail.com, *ORCID:* https://orcid.org/0009-0000-0933-3643, mirjana.beribaka@tfzv.ues.rs.ba, *ORCID:* https://orcid.org/0000-0002-8916-8816 , mayabobar@gmail.com, *ORCID:* https://orcid.org/0009-0006-0935-9177

[2]*Faculty of Education, University of East Sarajevo, Semberskih ratara E1, Bijeljina, Bosnia and Herzegovina,* aleksandra.novakovic@pfb.ues.rs.ba, *ORCID:* https://orcid.org/0000-0003-0397-8576

Corresponding author: mirjana.beribaka@tfzv.ues.rs.ba

Abstract

The microbiota represents a dynamic ecological network shaped by continuous interactions between microorganisms and their hosts, with key roles in metabolism, immune regulation, development, and behavior across animal taxa. Among experimental models, *Drosophila* species provide a powerful system for studying host–microbiota relationships due to its fully sequenced genome, short life cycle, and relatively simple yet functionally informative gut community. This short review summarizes current knowledge on the composition of the *Drosophila* microbiota and the internal and external factors that determine its structure and stability. The gut microbiota is commonly dominated by *Lactobacillus, Acetobacter, Gluconobacter* and *Leuconostoc*, forming a dynamic assemblage shaped by host genotype, diet, environmental stressors, physiological regulation, and social interactions. Rather than passive inhabitants, microbial partners actively contribute to nutrient metabolism, immune modulation, behavioral responses, and life-history traits, while the host maintains microbial balance through immune and tissue-specific mechanisms. Recent studies highlight the plasticity of the *Drosophila* microbiome and its influence on development, stress resistance, reproduction, and ageing. Because many regulatory pathways are evolutionarily conserved, findings from *Drosophila* research provide valuable translational insights into microbiome function, dysbiosis, and host genetic regulation relevant to human health.

Keywords: Drosophila species; gut microbiota; host–microbe interactions; microbiome regulation; environmental determinants; translational relevance; UN SDG 3; UN SDG 13

1. Introduction

Drosophila melanogaster represents one of the most extensively used model organisms in contemporary biology, offering powerful experimental opportunities for investigating genetics, development, physiology, and disease. Its short life cycle, well-characterized genome, and conserved molecular pathways shared with humans make it particularly suitable for studying host–microbiota interactions and the ecological principles underlying symbiosis [1]. Increasing evidence indicates that gut microbiota plays a central role in regulating metabolism,

immunity, behavior, and life-history traits across animal taxa, positioning *Drosophila* as a valuable model for dissecting microbiome-mediated effects under controlled laboratory conditions [2]. The gut community of *D. melanogaster* is typically dominated by members of the genera *Lactobacillus, Acetobacter, Gluconobacter* and *Leuconostoc*, although natural populations exhibit greater diversity shaped by environmental exposure and diet [3,4]. In addition to commensal bacteria, vertically transmitted symbionts such as *Wolbachia* may influence host physiology and microbial dynamics [5]. The microbiome is regulated through a complex interplay between intrinsic host factors—genetic background, immune signaling, and physiology—and external influences including diet, temperature, biotic stressors, and humidity [2,6,7]. Owing to this dynamic interaction network, *Drosophila* provides a simplified yet highly informative system for exploring how microbiota contributes to phenotypic plasticity, adaptation, and evolutionary processes.

2. Internal and Environmental Determinants of the *Drosophila* Microbiota

Microbiota composition in *Drosophila* emerges from the dynamic interplay between intrinsic host mechanisms and external ecological pressures. Host genetic background, immune regulation, circadian rhythms, and ageing, collectively structure microbial homeostasis. Transcriptomic analyses reveal pronounced differences between axenic and conventionally reared flies, particularly in intestinal tissues where immune and metabolic pathways are strongly modulated by microbial presence [8]. Circadian regulators such as *clock*, *period*, and *timeless* coordinate daily oscillations in bacterial abundance, linking temporal physiology to microbial dynamics [9]. Immune signaling pathways, notably IMD and Toll, maintain microbial balance through antimicrobial peptide production and tissue-specific responses, preventing dysbiosis while preserving beneficial symbionts [10]. Ageing further reshapes microbial communities, often increasing bacterial load and altering immune control, although certain microbial metabolites may exert protective effects on longevity [11]. Simultaneously, environmental drivers continuously influence microbial assembly. Diet represents the most powerful ecological filter, shaping microbial diversity and affecting host development, metabolism, and reproduction [12]. Temperature is a key environmental factor shaping both microbiota composition and thermal tolerance in *Drosophila*, suggesting that developmental temperature may influence host physiological responses partly through microbiota-associated mechanisms [13]. Biotic stressors such as pathogens and parasitic nematodes can disrupt gut communities via immune activation [14], while additional factors including heavy-metal exposure and humidity further modulate microbial structure [15,16]. Together, these findings underscore that microbiota stability in *Drosophila* reflects a complex, bidirectional integration of host-specific regulatory mechanisms and fluctuating environmental conditions.

3. *Drosophila* as a Model and Integrative Perspectives

The extensive genetic and experimental toolkit available in *Drosophila* enables precise investigation of host–microbe interactions, including controlled monoassociation experiments with genome-sequenced bacterial strains that allow identification of bacterial genetic determinants underlying microbiota-dependent host traits [17]. Conservation of disease-related genes between flies and humans enhances the translational relevance of this system for studying ageing, metabolic disorders, neurodegeneration, and immune regulation [18,19]. Despite certain physiological differences from vertebrates, the simplicity of the *Drosophila* gut ecosystem and

the ease of experimental control make it an effective platform for microbiome research. Recent studies suggest that the *Drosophila* microbiome functions as an eco-physiological network influencing host metabolism, behavior and stress responses [20,21]. Dominant symbionts such as *Acetobacter* and *Lactobacillus* frequently influence host metabolic and immune signaling pathways, while host genetic variation and environmental factors jointly shape microbiota structure [3]. These findings support a model of dynamic host–microbe co-regulation characterized by ecological flexibility and functional stability.

4. Conclusions

The microbiota of *Drosophila* represents a dynamic and environmentally responsive system shaped by interactions between host genetics, physiological regulation, and environmental context. Rather than acting as a passive community, microbial partners actively contribute to metabolic homeostasis, immune balance, behavioral modulation, and life-history traits, while the host maintains microbial stability through immune signaling and tissue-specific mechanisms. Despite environmental variability, the *Drosophila* microbiota is generally composed of a limited number of recurrent bacterial groups, making it a valuable model for studying core principles of host–microbiota relationships. The evolutionary conservation of key regulatory pathways reinforces the translational significance of *Drosophila* research and highlights its continued relevance for advancing microbiome science and biomedical applications.

Acknowledgements

This work was supported by the Ministry of Scientific and Technological Development and Higher Education of the Republic of Srpska, Bosnia and Herzegovina (grant number 19.032/961-94/24).

References

1. Mohr SE. First in fly: *Drosophila* research and biological discovery. Cambridge, MA: Harvard University Press; 2018.
2. Douglas AE. The *Drosophila* model for microbiome research. Lab Animal. 2018;47(6):157-64.
3. Beribaka MB, Dimkić IZ, Jelić MĐ, Stanković SM, Pržulj NM, Anđelković ML, Stamenković-Radak MM. Altered diversity of bacterial communities in two *Drosophila* species under laboratory conditions and lead exposure. Archives of Biological Sciences. 2021;73(1):17-29.
4. Staubach F, Baines JF, Künzel S, Bik EM, Petrov DA. Host species and environmental effects on bacterial communities associated with *Drosophila* in the laboratory and in the natural environment. PLoS One. 2013;8(8):e70749.
5. Henry LP, Fernandez M, Wolf S, Abhyankar V, Ayroles JF. *Wolbachia* impacts microbiome diversity and fitness-associated traits for *Drosophila melanogaster* in a seasonally fluctuating environment. Ecology and Evolution. 2024;14(7):e70004.
6. Erkosar B, Storelli G, Mitchell M, Bozonnet L, Bozonnet N, Leulier F. Pathogen Virulence Impedes Mutualist-Mediated Enhancement of Host Juvenile Growth via Inhibition of Protein Digestion. Cell Host Microbe. 2015;18(4):445-55.

7. Wong Adam CN, Luo Y, Jing X, Franzenburg S, Bost A, Douglas Angela E. The Host as the Driver of the Microbiota in the Gut and External Environment of *Drosophila melanogaster*. Applied and Environmental Microbiology. 2015;81(18):6232-40.
8. Broderick NA, Lemaitre B. Gut-associated microbes of *Drosophila melanogaster*. Gut Microbes. 2012;3(4):307-21.
9. Battistolli M, Varponi I, Romoli O, Sandrelli F. The circadian clock gene period regulates the composition and daily bacterial load of the gut microbiome in *Drosophila melanogaster*. Scientific Reports. 2025;15(1):1016.
10. Marra A, Hanson MA, Kondo S, Erkosar B, Lemaitre B. *Drosophila* Antimicrobial Peptides and Lysozymes Regulate Gut Microbiota Composition and Abundance. mBio. 2021;12(4):10.1128/mbio.00824-21.
11. Arias-Rojas A, Iatsenko I. The Role of Microbiota in *Drosophila melanogaster* Aging. Frontiers in Aging. 2022;3.
12. Gale Joseph T, Kreutz R, Gottfredson Morgan Sarah J, Davis Emma K, Hough C, Cisneros Cancino Wendy A, Burnside B, Barney R, Hunsaker R, Tanner Hoyt A, Cluff A, Nosker M, Sefcik C, Beales E, Beltz Jack K, Frandsen Paul B, Schmidt P, Chaston John M. Environment and diet shape the geography-specific *Drosophila melanogaster* microbiota composition. Applied and Environmental Microbiology. 2025;91(10):e00883-25.
13. Moghadam NN, Thorshauge PM, Kristensen TN, de Jonge N, Bahrndorff S, Kjeldal H, Nielsen JL. Strong responses of *Drosophila melanogaster* microbiota to developmental temperature. Fly (Austin). 2018;12(1):1-12.
14. Yau R, Pavloudi C, Zeng Y, Saw J, Eleftherianos I. Infection with the entomopathogenic nematodes Steinernema alters the *Drosophila melanogaster* larval microbiome. PLOS ONE. 2025;20(5):e0323657.
15. Beribaka M, Jelić M, Tanasković M, Lazić C, Stamenković-Radak M. Life History Traits in Two *Drosophila* Species Differently Affected by Microbiota Diversity under Lead Exposure. Insects. 2021;12(12):1122.
16. Walters AW, Hughes RC, Call TB, Walker CJ, Wilcox H, Petersen SC, Rudman SM, Newell PD, Douglas AE, Schmidt PS, Chaston JM. The microbiota influences the *Drosophila melanogaster* life history strategy. Mol Ecol. 2020;29(3):639-653.
17. Chaston John M, Newell Peter D, Douglas Angela E. Metagenome-Wide Association of Microbial Determinants of Host Phenotype in *Drosophila melanogaster*. mBio. 2014;5(5):10.1128/mbio.01631-14.
18. Giansanti MG, Frappaolo A, Piergentili R. *Drosophila melanogaster*: How and Why It Became a Model Organism. International Journal of Molecular Sciences. 2025;26(15):7485.
19. Jeibmann A, Paulus W. *Drosophila melanogaster* as a Model Organism of Brain Diseases. International Journal of Molecular Sciences. 2009;10:407 - 40.
20. Obadia B, Güvener ZT, Zhang V, Ceja-Navarro JA, Brodie EL, Ja WW, Ludington WB. Probabilistic Invasion Underlies Natural Gut Microbiome Stability. Curr Biol. 2017;27(13):1999-2006.e8.
21. Dodge R, Jones EW, Zhu H, Obadia B, Martinez DJ, Wang C, Aranda-Díaz A, Aumiller K, Liu Z, Voltolini M, Brodie EL, Huang KC, Carlson JM, Sivak DA, Spradling AC, Ludington WB. A symbiotic physical niche in *Drosophila melanogaster* regulates stable association of a multi-species gut microbiota. Nature Communications. 2023;14(1):1557.

Biomaterials, Scaffolds, and Tissue Engineering

PCL vs. PLA in Bone Regenerative Scaffolds: Current Potential and Challenges

Jana Baščarević[1], Marija Branković[1], Katarina Virijević[1]

[1]*Institute for Information Technologies, University of Kragujevac, Kragujevac, Serbia,* jana.bascarevic@uni.kg.ac.rs *ORCID 0009-0004-2685-4925,* marija.brankovic@uni.kg.ac.rs *ORCID 0009-0003-5228-4172,* katarina.virijevic@uni.kg.ac.rs *ORCID 0000-0003-2703-8829*

Corresponding author: jana.bascarevic@uni.kg.ac.rs

Abstract

Bone defects caused by trauma, tumor resection, infection, or impaired healing remain a significant clinical challenge. Bone tissue engineering (BTE) has emerged as a promising strategy to support bone regeneration through the use of biomaterial scaffolds that provide structural support and promote cellular interactions and extracellular matrix formation. Among synthetic biodegradable polymers, polycaprolactone (PCL) and polylactid acid (PLA) have attracted considerable attention due to their biocompatibility, controllable degradation behavior, and suitability for scaffold fabrication. This short review summarizes the current potential of PCL and PLA as biomaterials for bone regenerative scaffolds and highlights their key physicochemical, mechanical, and biological characteristics. PCL exhibits high flexibility, slow degradation, and good cytocompatibility, but its hydrophobic nature may limit cell adhesion. In contrast, PLA provides higher stiffness and mechanical strength but demonstrates greater brittleness and faster degradation. A comparative overview of these polymers is presented, emphasizing their complementary properties and the advantages of combining them to improve scaffold performance for BTE applications.

Keywords: polycaprolactone; polylactic acid; mechanical properties; degradation rate; bone tissue engineering; regenerative scaffolds; 'UN SDG 3'

1. Introduction

Bone defects represent a common and serious clinical problem that may arise from trauma, tumor removal, infection, or impaired fracture healing [1]. In recent years, bone tissue engineering (BTE) has emerged as an advanced therapeutic strategy aimed at improving clinical outcomes while reducing complications associated with conventional surgical treatments. A key component of this approach is the scaffold, which acts as a structural template that supports cell interactions, and the formation of extracellular bone matrix, thereby enabling the development of new tissue [2]. In addition, synthetic biodegradable polymers are widely utilized in BTE because they provide appropriate mechanical performance together with tunable processing and shaping capabilities, allowing the fabrication of scaffolds with tailored architectures [3].

Polycaprolactone (PCL) and polylactid acid (PLA) are promising biopolymers for BTE scaffolds due to their excellent biocompatibility, controllable degradation rates, and good processability. This short review provides a comparative overview of these polymers, highlighting their advantages and limitations as biomaterials for bone scaffolds.

2. PCL as Bone Scaffold Biomaterial

PCL is a semicrystalline aliphatic polyester widely investigated for tissue engineering due to its favorable physicochemical properties and ease of processability [4]. Its relatively good mechanical strength, combined with a slow degradation profile, allows scaffolds to maintain structural integrity during the early stages of tissue regeneration. In biological environments, degradation typically occurs over a period of 2-3 years through hydrolytic cleavage of ester bonds, producing non-toxic products that can be safely eliminated from the body [5].

Besides its bioresorbability, PCL demonstrates compatibility with osteoblasts and exhibits low cytotoxicity [6]. However, its hydrophobic surface may reduce cell adhesion and delay osteogenic differentiation [5]. In order to improve biological performance, PCL is often combined with other polymers and bioactive components, or modified through surface functionalization strategies [4], [5].

3. PLA as Bone Scaffold Biomaterial

PLA is an aliphatic polyester derived from renewable resources that exhibits adjustable mechanical properties and favorable processing characteristics for scaffold fabrication in tissue regeneration [7]. PLA exists in three stereoisomeric forms, including PLLA, PDLA, and PDLLA [8]. In particular, highly crystalline PLLA exhibits slower degradation and greater mechanical strength and rigidity, whereas less crystalline structures degrade more rapidly [7], [8].

PLA primarily degrades through hydrolytic cleavage of ester bonds, generating lactic acid that can be metabolized by the body. However, accumulation of acidic degradation products may occasionally induce inflammatory responses [9]. Additionally, PLA shows relatively high hydrophobicity, limited osteoconductivity, and reduced cell adhesion [8], [9]. Therefore, PLA is frequently combined with bioactive molecules or blended with other polymers to enhance biological performance and optimize degradation behavior [7].

4. Comparison of PCL and PLA

Although PCL and PLA belong to the same polymers family and share several favorable characteristics for biomedical applications, such as nontoxicity, biocompatibility, and biodegradability, they exhibit notable differences in physicochemical and mechanical properties.

PCL is generally more hydrophobic and crystalline than PLA and exhibits a significantly slower degradation rate [10]. Its polymer chains contain longer alkyl segments between ester bonds, which increases chain flexibility and results in a rubber-like mechanical behavior [11]. In contrast, PLA is characterized by a relatively high elastic modulus and limited elongation, leading to a more brittle mechanical response [12]. While PLA provides greater stiffness and strength, its intrinsic brittleness results in poor impact and tear resistance, which may restrict its application in certain biomedical fields. For this reason, PCL is frequently incorporated into PLA matrices to improve ductility, flexibility, and resistance to brittle fracture while enhancing load transfer efficiency [13]. On the other side, pure PCL has relatively low surface energy, which may limit cell attachment and proliferation [14].

Despite some limitations, both polymers demonstrate promising characteristics for bone tissue engineering. PCL scaffolds are valued for their porosity and gradual resorption, whereas PLA exhibits compressive strength values comparable to those of natural bone [14]. In composite systems, PLA contributes mechanical rigidity and bioactivity, while PCL enhances flexibility and structural durability. Experimental studies have shown that PCL/PLA composite scaffolds can improve mechanical properties and bioactivity, promote osteogenic differentiation of mesenchymal stem cells, and enhance bone formation *in vivo* compared with pure PCL scaffolds [15], [16]. Furthermore, incorporation of PLA into PCL matrices may accelerate degradation, although excessive PLA content can increase scaffold brittleness [17].

Table 1. Comparison of properties between PCL and PLA relevant for bone scaffolds.

Property	***PCL***	***PLA***
Mechanical properties	Lower modulus but high flexibility and ductility	High stiffness and modulus but relatively brittle
Degradation	Very slow degradation; non-toxic hydrolysis products	Faster degradation; acidic byproducts
Hydrophilicity	High hydrophobicity	Moderate hydrophobicity
Cell interaction	Good cytocompatibility but limited bioactivity	Limited cell adhesion, moderate osteoconductivity
Main advantages	Flexibility, mechanical stability, long-term scaffold integrity	High stiffness, bone-like strength, good structural support
Strategies to overcome limitations	Blending with stiffer polymers; adding bioactive fillers	Blending with flexible polymers; adding bioactive agents

5. Conclusion

PCL and PLA are widely investigated biodegradable polymers with significant potential for bone tissue engineering. While PCL provides flexibility and long-term structural stability, PLA offers higher stiffness and mechanical strength but exhibits greater brittleness. Due to these complementary properties, combining both polymers represents an effective strategy for improving scaffold performance. Future research should focus on optimizing composite scaffold design, surface modifications, and incorporation of bioactive components in order to enhance osteogenic potential and achieve improved outcomes in bone regeneration.

Acknowledgements

This paper is supported through the EIT's Higher Education Initiative A-SIDE projects, coordinated by EIT RawMaterials, funded by the European Union and supported by the projects No. 451-03-34/2026-03/200107 and No. 451-03-33/2026-03/200378, Ministry of Science, Technological Development and Innovation, Republic of Serbia.

References

[1] Dibazar ZE, Nie L, Azizi M, Nekounam H, Hamidi M, Shavandi A, Izadi Z, Delattre C. Bioceramics/Electrospun Polymeric Nanofibrous and Carbon Nanofibrous Scaffolds for Bone Tissue Engineering Applications. Materials 2023;16:2799. https://doi.org/10.3390/ma16072799.

[2] Anjum S, Rahman F, Pandey P, Arya DK, Alam M, Rajinikanth PS, Ao Q. Electrospun Biomimetic Nanofibrous Scaffolds: A Promising Prospect for Bone Tissue Engineering and Regenerative Medicine. IJMS 2022;23:9206. https://doi.org/10.3390/ijms23169206.

[3] Yan X, Yao H, Luo J, Li Z, Wei J. Functionalization of Electrospun Nanofiber for Bone Tissue Engineering. Polymers 2022;14:2940. https://doi.org/10.3390/polym14142940.

[4] Mokhena TC, Chabalala MB, Mapukata S, Mtibe A, Hlekelele L, Cele Z, Mochane MJ, Ntsendwana B, Nhlapo TA, Mokoena TP, Bambo MF, Matabola KP, Ray SS, Sadiku ER, Shingange K. Electrospun PCL-Based Materials for Health-Care Applications: An Overview. Macro Materials & Eng 2024;309:2300388. https://doi.org/10.1002/mame.202300388.
[5] Ramírez-Ruiz F, Núñez-Tapia I, Piña-Barba MC, Alvarez-Pérez MA, Guarino V, Serrano-Bello J. Polycaprolactone for Hard Tissue Regeneration: Scaffold Design and In Vivo Implications. Bioengineering 2025;12:46. https://doi.org/10.3390/bioengineering12010046.
[6] Coppola B, Menotti F, Longo F, Banche G, Mandras N, Palmero P, Allizond V. New Generation of Osteoinductive and Antimicrobial Polycaprolactone-Based Scaffolds in Bone Tissue Engineering: A Review. Polymers 2024;16:1668. https://doi.org/10.3390/polym16121668.
[7] Farjaminejad S, Farjaminejad R, Hasani M, Garcia-Godoy F, Abdouss M, Marya A, Harsoputranto A, Jamilian A. Advances and Challenges in Polymer-Based Scaffolds for Bone Tissue Engineering: A Path Towards Personalized Regenerative Medicine. Polymers 2024;16:3303. https://doi.org/10.3390/polym16233303.
[8] Sahini MG. Polylactic acid (PLA)-based materials: a review on the synthesis and drug delivery applications. Emergent Mater 2023;6:1461–79. https://doi.org/10.1007/s42247-023-00551-7.
[9] Alavi MS, Memarpour S, Pazhohan-Nezhad H, Salimi Asl A, Moghbeli M, Shadmanfar S, Saburi E. Applications of poly(lactic acid) in bone tissue engineering: A review article. Artificial Organs 2023;47:1423–30. https://doi.org/10.1111/aor.14612.
[10] Goreninskii S, Chernova U, Prosetskaya E, Laushkina A, Mishanin A, Golovkin A, Bolbasov E. Single-channel and multi-channel electrospinning for the fabrication of PLA/PCL tissue engineering scaffolds: comparative study of the materials physicochemical and biological properties 2024. https://doi.org/10.48550/ARXIV.2403.00767.
[11] Meng C, Tang D, Liu X, Meng J, Wei W, Gong RH, Li J. Heterogeneous porous PLLA/PCL fibrous scaffold for bone tissue regeneration. International Journal of Biological Macromolecules 2023;235:123781. https://doi.org/10.1016/j.ijbiomac.2023.123781.
[12] Zhang S, Yan D, Zhao L, Lin J. Composite fibrous membrane comprising PLA and PCL fibers for biomedical application. Composites Communications 2022;34:101268. https://doi.org/10.1016/j.coco.2022.101268.
[13] Sharma D, Satapathy BK. Optimization and physical performance evaluation of electrospun nanofibrous mats of PLA, PCL and their blends. Journal of Industrial Textiles 2022;51:6640S-6665S. https://doi.org/10.1177/1528083720944502.
[14] Moghaddasi M, Özdemir MMM, Noshahr AT, Özadenç HM, Oktay B, Bingöl AB, Arayıcı PP, Eraslan A, Şenel İ, Chifiriuc MC, Üstündağ CB. Blend Electrospinning of *Nigella sativa* -Incorporating PCL/PLA/HA Fibers and Its Investigation for Bone Healing Applications. ACS Omega 2024;9:10267–75. https://doi.org/10.1021/acsomega.3c07523.
[15] Yao Q, Cosme JGL, Xu T, Miszuk JM, Picciani PHS, Fong H, Sun H. Three dimensional electrospun PCL/PLA blend nanofibrous scaffolds with significantly improved stem cells osteogenic differentiation and cranial bone formation. Biomaterials 2017;115:115–27. https://doi.org/10.1016/j.biomaterials.2016.11.018.
[16] Xu T, Yao Q, Miszuk JM, Sanyour HJ, Hong Z, Sun H, Fong H. Tailoring weight ratio of PCL/PLA in electrospun three-dimensional nanofibrous scaffolds and the effect on osteogenic differentiation of stem cells. Colloids and Surfaces B: Biointerfaces 2018;171:31–9. https://doi.org/10.1016/j.colsurfb.2018.07.004.
[17] Oztemur J, Ozdemir S, Tezcan-Unlu H, Cecener G, Sezgin H, Yalcin-Enis I. Investigation of biodegradability and cellular activity of PCL/PLA and PCL/PLLA electrospun webs for tissue engineering applications. Biopolymers 2023;114:e23564. https://doi.org/10.1002/bip.23564.

Polymeric Scaffolds Based on PCL/PEG and Chitosan/PLA for Osteogenic Applications

Katarina Virijević, Jana Baščarević[1], Nenad Filipović[1]

[1]*Institute for Information Technologies, University of Kragujevac, Kragujevac, Serbia*

katarina.virijevic@uni.kg.ac.rs *ORCID 0000-0003-2703-8829*

jana.bascarevic@uni.kg.ac.rs *ORCID 0009-0004-2685-4925*

fica@kg.ac.rs *ORCID 0000-0001-9964-5615*

Corresponding author: katarina.virijevic@uni.kg.ac.rs

Abstract

Bone tissue engineering aims to develop biomaterial-based scaffolds capable of restoring the structure and function of damaged bone tissue. Among various approaches, polymeric scaffolds have gained significant attention due to their tunable mechanical properties, biocompatibility, and ability to support cellular functions essential for bone regeneration.

In this context, composite systems based on polycaprolactone/polyethylene glycol (PCL/PEG) and chitosan/polylactic acid (chitosan/PLA) have been extensively investigated for osteogenic applications. Polycaprolactone (PCL), combined with polyethylene glycol (PEG), provides a favorable balance between mechanical strength, flexibility, and improved hydrophilicity, which enhances cell adhesion and proliferation. The incorporation of PEG significantly improves surface wettability, thereby supporting better osteoblast–material interactions and overall osteogenic response.

In contrast, chitosan/PLA systems offer good biocompatibility and structural integrity. However, their osteogenic performance is generally limited due to insufficient mechanical stability (chitosan) and relatively low bioactivity in PLA-based matrices when used alone. Although chitosan enhances cellular interactions, the overall osteogenic potential of chitosan/PLA scaffolds remains lower compared to PCL/PEG-based systems.

Overall, PCL/PEG composites demonstrate superior performance in supporting osteoblast adhesion, proliferation, and extracellular matrix formation, making them more suitable for osteogenic applications in bone tissue engineering. Future studies should focus on further optimization of polymer ratios and scaffold architecture to enhance clinical translation.

Keywords: polycaprolactone; polyethylene glycol; chitosan; polylactic acid; nanofibers, osteogenic properties, UN SDG 3; UN SDG 9; biomedical applications

1. Introduction

Tissue engineering is an interdisciplinary field that combines principles of materials science, biology, and engineering to develop biological substitutes that restore, maintain, or improve tissue function. Within this field,

bone tissue engineering has attracted significant attention due to the increasing clinical need for effective strategies for bone defect repair caused by trauma, disease, or degenerative conditions [1,6].

Bone tissue has a limited intrinsic regenerative capacity, especially in large defects, which has led to the development of scaffold-based approaches as an alternative to conventional treatments such as autografts and allografts [1]. Therefore, biomaterial-based scaffolds have emerged as a promising solution for osteogenic applications.

Polymer-based scaffolds are widely investigated due to their tunable mechanical properties, controllable degradation rates, and ability to mimic the extracellular matrix [1,6]. In particular, composite systems such as polycaprolactone/polyethylene glycol (PCL/PEG) and chitosan/polylactic acid (chitosan/PLA) have shown significant potential in bone tissue engineering.

Polycaprolactone (PCL), especially when combined with polyethylene glycol (PEG), offers improved hydrophilicity and favorable mechanical stability, making it highly suitable for osteogenic applications [2,7,10]. In contrast, chitosan/PLA-based scaffolds provide good biocompatibility but often exhibit limited mechanical performance and less consistent osteogenic response compared to PCL/PEG systems [4,5].

2. Requirements for Osteogenic Scaffolds

An ideal scaffold for bone tissue engineering must fulfill several essential requirements, including biocompatibility, controlled biodegradability, appropriate mechanical strength, and the ability to support cell adhesion, proliferation, and differentiation [1]. Scaffold architecture, particularly porosity and interconnectivity, plays a crucial role in nutrient diffusion and tissue ingrowth.

From a biological perspective, successful bone regeneration depends on processes such as osteoconduction and osteoinduction, which ensure scaffold-supported bone formation and differentiation of progenitor cells into osteoblasts [1,6].

3. PCL/PEG Scaffolds for Osteogenic Applications

Polycaprolactone (PCL) is widely used in bone tissue engineering due to its excellent mechanical properties, flexibility, and slow degradation rate [2,3]. However, its hydrophobic nature limits cell attachment and biological response.

The incorporation of polyethylene glycol (PEG) improves hydrophilicity and enhances protein adsorption and cell–material interactions, leading to improved osteoblast adhesion and proliferation [7,10]. Also, PCL/PEG scaffolds therefore show enhanced extracellular matrix (ECM) formation and more favorable osteogenic behavior compared to pure PCL.

Additionally, these systems can be fabricated using techniques such as electrospinning and 3D printing, allowing precise control over scaffold architecture [2,9]. Overall, PCL/PEG systems are considered highly promising for osteogenic applications due to their balanced mechanical and biological properties.

4. Chitosan/PLA Scaffolds for Osteogenic Applications

Chitosan is a natural polymer derived from chitin and is known for its excellent biocompatibility and intrinsic bioactivity, which enhances cell adhesion and interaction [4,8]. Polylactic Acid (PLA) provides mechanical support and controlled degradation, but its bioactivity is relatively limited [5].

Although chitosan improves biological response, chitosan/PLA systems often suffer from weaker mechanical stability and less consistent osteogenic performance compared to PCL/PEG scaffolds [4,5]. As a result, their ability to sustain long-term osteoblast activity and mineralized matrix formation is generally lower.

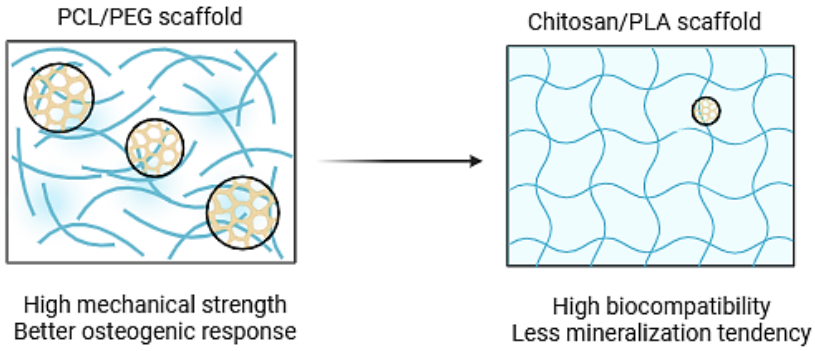
5. Comparative Discussion: PCL/PEG vs Chitosan/PLA

The comparison between PCL/PEG and chitosan/PLA scaffolds highlights a balance between mechanical and biological performance.

PCL/PEG systems demonstrate superior hydrophilicity, mechanical stability, and improved osteoblast activity, leading to enhanced bone-like tissue formation [2,7]. In contrast, chitosan/PLA scaffolds provide good initial biocompatibility but are limited by weaker structural integrity and reduced osteogenic efficiency [4,5].

Therefore, PCL/PEG composites are generally more suitable for osteogenic applications in bone tissue engineering (Figure 1).

Figure 1. Comparative schematic illustration of osteogenic potential of PCL scaffold and chitosan/PLA scaffold (Source: https://www.biorender.com/)



6. Conclusion

Polymeric scaffolds play a crucial role in bone tissue engineering by providing structural support and guiding cellular processes essential for bone regeneration. PCL/PEG composites demonstrate superior performance in osteogenic applications due to improved hydrophilicity, mechanical stability, and enhanced cell–material interactions [2,7]. In contrast, chitosan/PLA systems show good biocompatibility but limited osteogenic efficiency [4,5].

Overall, PCL/PEG-based scaffolds represent a more promising approach for bone tissue engineering, while further optimization of scaffold composition and architecture is necessary to improve clinical outcomes.

Acknowledgements

This paper is supported through the EIT's Higher Education Initiative A-SIDE projects, coordinated by EIT RawMaterials, funded by the European Union and supported by the projects No. 451-03-34/2026-03/200107 and No. 451-03-33/2026-03/200378, Ministry of Science, Technological Development and Innovation, Republic of Serbia.

References

1. O'Brien FJ. Biomaterials & scaffolds for tissue engineering. *Mater Today*. 2011;14(3):88–95.
2. Woodruff MA, Hutmacher DW. The return of a forgotten polymer—Polycaprolactone in the 21st century. *Prog Polym Sci*. 2010;35(10):1217–1256.
3. Middleton JC, Tipton AJ. Synthetic biodegradable polymers as orthopedic devices. *Biomaterials*. 2000;21(23):2335–2346.
4. Dash M, Chiellini F, Ottenbrite RM, Chiellini E. Chitosan—A versatile semi-synthetic polymer in biomedical applications. *Prog Polym Sci*. 2011;36(8):981–1014.
5. Farah S, Anderson DG, Langer R. Physical and mechanical properties of PLA. *Adv Drug Deliv Rev*. 2016;107:367–392.
6. Place ES, Evans ND, Stevens MM. Complexity in biomaterials for tissue engineering. *Nat Mater*. 2009;8(6):457–470.
7. Zhao F, Vaughan TJ, Hutmacher DW. A comparison of hydrophilicity of PCL-based scaffolds and its effect on cell behavior. *Biomaterials*. 2013;34(12):2855–2863.
8. Jayakumar R, Prabaharan M, Reis RL, Mano JF. Graft copolymerized chitosan scaffolds for tissue engineering applications. *Carbohydr Polym*. 2005;62(2):142–158.
9. Ma PX. Scaffolds for tissue fabrication. *Mater Today*. 2004;7(5):30–40.
10. Moshaverinia A, et al. Application of PEG-modified biomaterials in tissue engineering. *Acta Biomater*. 2016;33:38–50.

Engineered Living Materials: Advanced Approaches for Biomedical Engineering

Marija Branković[1], Jana Baščarević[1], Fatima Živić[2]

[1] *Institute for Information Technologies, University of Kragujevac, Liceja Kneževine Srbije 1A, 34000 Kragujevac, Serbia, marija.brankovic@uni.kg.ac.rs, ORCID: 0009-0003-5228-4172, jana.bascarevic@uni.kg.ac.rs, ORCID: 0009-0004-2685-4925*

[2] *Faculty of Engineering. University of Kragujevac, Sestre Janjic 6, 34000 Kragujevac, Serbia, zivic@kg.ac.rs, ORCID: 0000-0003-2509-187X*

Corresponding author: marija.brankovic@uni.kg.ac.rs

Abstract

Engineered Living Materials (ELMs) represent a novel class of functional materials at the interface of synthetic biology and materials science. These materials integrate living cells within natural or synthetic matrices, forming dynamic systems in which cells actively produce molecules, self-organize, and respond to environmental stimuli. ELMs follow two complementary design strategies. Top-down approaches embed cells into pre-formed matrices, whereas bottom-up strategies program cells to autonomously generate and maintain their extracellular matrix, as exemplified by modified biofilms. These materials take diverse forms, including films, scaffolds, sponges, microcapsules, and 3D-printed structures, and respond to mechanical, chemical, and biological cues. Embedded cells enable tissue regeneration, controlled therapeutic delivery, biosensing, and modulation of immune and infectious processes. Encapsulation and advanced bioprinting preserve structural integrity, cell viability, and functionality, while genetic safety mechanisms, such as kill switches and auxotrophic strains, prevent uncontrolled proliferation. With their adaptability and multifunctionality, ELMs hold transformative promise for next-generation biomedical and biotechnological applications.

Keywords: engineering living materials; biomedical engineering; biomaterials; smart materials; biofabricated scaffolds; biohybrid systems; synthetic biology; UN SDG 3, UN SDG 7

1. Introduction

Engineered Living Materials (ELMs) have emerged from the convergence of advances in synthetic biology and modern materials science. This class of materials is defined by the integration of living cells, both structurally and functionally, into a matrix that may be naturally formed or artificially constructed [1]. The capacity of cells to synthesize complex molecules, self-organize, and adapt to environmental changes underpins the design of dynamic and functionally active materials, rather than static ones. Within ELM systems, cells function as active biological units enabling real-time growth, regeneration, and adaptation of the material. As a result, these materials can respond to external stimuli and alter their properties in accordance with environmental conditions, thereby fundamentally distinguishing them from conventional inert materials [2]. For instance, stimulus-

responsive (smart) materials generally react only to relatively great changes in pH, light, temperature, or electric fields, which often restricts their biomedical applications. In contrast, ELMs can detect subtle and specific stimuli, adapt to dynamic conditions, and perform complex biological functions due to their living components and potential for genetic manipulation [3]. ELMs represent a promising platform for sustainable energy, environmental remediation, therapeutic solutions, and materials that actively respond to their surroundings [1].

2. Design Strategies for Engineered Living Materials

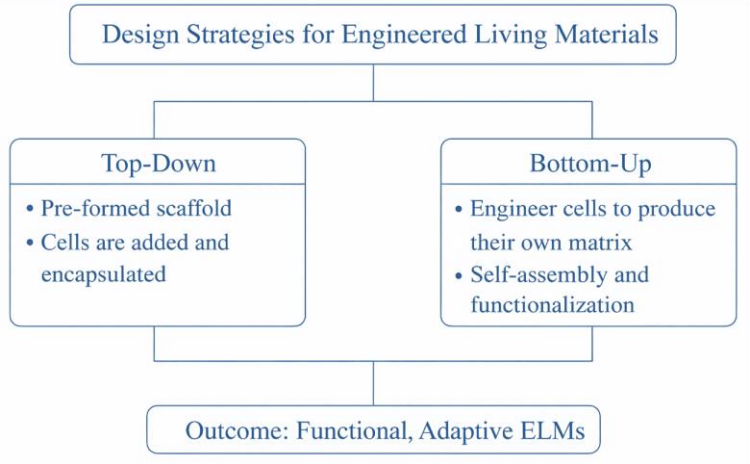


Figure 1. Design Strategies for Engineered Living Materials.

Living materials incorporate organisms ranging from bacteria and fungi to algae and animal cells, which combine with materials such as silk, concrete, or hydrogels to generate functional biohybrid constructs. In these systems, cells are coupled with a supporting matrix or scaffold, with the living component providing specific, active functions within the material. ELMs can be developed using different strategies (**Figure**). The top-down approach involves creating a pre-designed inert composite into which cells are subsequently incorporated and encapsulated. In contrast, the bottom-up strategy relies on engineering the cells themselves, programming them to produce and maintain their own matrix, as exemplified by modified biofilms [2].

3. Taxonomic Classification of ELMs

Taxonomies provide a systematic framework for classifying and organizing knowledge, and they can also support the prediction of new scientific discoveries and materials. Synthetic biology, a field focused on designing and constructing new or modified living systems using engineering principles, requires novel taxonomic schemes that integrate the classification of both cells and materials. In such taxonomies, cell type occupies a higher hierarchical rank, while scaffolds and matrices are positioned lower, often further subdivided by dimensions, material composition, and other characteristics (**Table 4**). This hierarchical organization enables systematic structuring, comparison, and planning for the development of living and synthetic materials, including advanced ELMs [4].

Table 4. Taxonomic Classification of Engineered Living Materials (ELMs) [4].

Rank	*Categories / examples*
Domain	Archaeal, Bacterial, Eukaryotic, Synthetic, Cross[2]

[2] "Cross" denotes hybrid or combined categories that span multiple groups, dimensions, or material types, reflecting ELMs that do not belong exclusively to a single classification.

Superkingdom	Bio-ELM (biological living materials), Hybrid Living Material
Kingdom	Archaebacterial, Eubacterial, Protist, Fungal, Animal, Plant, Synthetic, Cross
Phylum	0D, 1D, 2D, 3D, Dynamic, Cross
Class	Living polymers, Living ceramics, Living metals and alloys, Living carbons, Living composites
Family	Living hydrogel, Living elastomer, Living Cu alloy, Living precious metals, Living oxides, Living CNTs, Living graphene, Living metal materials

4. Biomedical Applications of ELMs

Most of the living materials developed to date rely on laboratory strains of *Escherichia coli*, primarily because this organism is well-suited for genetic modification and relatively easy to manipulate under controlled conditions. However, for biomedical applications, it is essential to use organisms with Generally Recognized as Safe (GRAS) status, such as specific bacterial strains, yeasts, and unicellular algae, to ensure safety and compatibility with the human body [2].

ELMs adopt diverse forms, including films, sponges, patches, microcapsules, drug depots, scaffolds, 3D-printed or wearable structures, and actively adjust their properties in response to environmental signals. The embedded living cells enable tissue regeneration, controlled delivery of therapeutic molecules, biosensing, and modulation of inflammatory and infectious processes. Probiotics within the matrix provide health benefits and can be genetically programmed to secrete therapeutic molecules, while other living cells act as biocatalysts, producing molecules of therapeutic or biotechnological importance. Encapsulation of microorganisms in polymeric matrices, through methods such as microencapsulation, electrospinning, biofilms, and 3D bioprinting, protects the cells, regulates their growth, and maintains defined structural functionality while preserving viability and optimizing mechanical properties. Safety mechanisms, including genetic ‘kill switches’ and auxotrophic strains, restrict uncontrolled microbial growth and facilitate the reliable and flexible application of ELMs in biomedical contexts [2].

5. Current Challenges and Limitations of Engineered Living Materials for Biomedical Use

Despite the numerous advantages of natural and bioengineered living organisms over conventional biomaterials, their application remains limited. Challenges include nonspecific circulation within the body, inactivation in the microenvironment of diseased tissues, uncontrolled proliferation or colonization, and potential adverse effects, often resulting in suboptimal therapeutic outcomes and complicating clinical approval [5]. In regenerative medicine, additional obstacles arise in fabricating complex 3D structures, maintaining a controlled cellular microenvironment, and achieving scalability for clinical use, all of which restrict the broader adoption of living materials in therapeutic applications [6].

6. Future Perspectives

ELMs demonstrate considerable potential for next-generation biomedical applications, especially in developing smart, adaptive implants and programmable cellular systems that sense and respond to disease-specific signals.

Their ability to dynamically interact with biological environments opens new possibilities for more precise, targeted, and efficient therapies. Future research should prioritize enhancing biosafety, standardizing scalable production methods, and facilitating the clinical translation of these approaches. Additionally, addressing regulatory and ethical considerations will be crucial for the successful implementation of these initiatives. This progress will rely on integrating advances in synthetic biology, bioprinting, and personalized medicine to develop highly functional, patient-specific therapeutic platforms.

7. Conclusions

Engineered Living Materials represent a versatile and dynamic platform in biomedical engineering by integrating living cells with functional material systems. Their combination of biological adaptability and engineered properties enables the development of responsive, self-regulating systems with a wide range of applications, including tissue engineering and drug delivery.

Although challenges related to safety, scalability, and clinical translation persist, ongoing advances in synthetic biology and materials science are addressing these issues. The capacity of ELMs to respond to environmental stimuli and execute complex biological functions positions them as a promising and transformative approach for next-generation biomedical applications.

Acknowledgements

This paper is supported through the EIT's Higher Education Initiative A-SIDE projects, coordinated by EIT RawMaterials, funded by the European Union and supported by the projects No. 451-03-34/2026-03/200107 and No. 451-03-33/2026-03/200378, Ministry of Science, Technological Development and Innovation, Republic of Serbia.

References

[1] An B, Wang Y, Huang Y, Wang X, Liu Y, Xun D, Church GM, Dai Z, Yi X, Tang T-C, Zhong C. Engineered Living Materials For Sustainability. Chem Rev 2023;123:2349–419. https://doi.org/10.1021/acs.chemrev.2c00512.

[2] Rodrigo-Navarro A, Sankaran S, Dalby MJ, Del Campo A, Salmeron-Sanchez M. Engineered living biomaterials. Nat Rev Mater 2021;6:1175–90. https://doi.org/10.1038/s41578-021-00350-8.

[3] Rivera-Tarazona LK, Campbell ZT, Ware TH. Stimuli-responsive engineered living materials. Soft Matter 2021;17:785–809. https://doi.org/10.1039/D0SM01905D.

[4] Lantada AD, Korvink JG, Islam M. Taxonomy for engineered living materials. Cell Reports Physical Science 2022;3:100807. https://doi.org/10.1016/j.xcrp.2022.100807.

[5] Chen Q-W, Zhang X-Z. Living Biomaterials: Fabrication Strategies and Biomedical Applications. Acc Mater Res 2024;5:1440–52. https://doi.org/10.1021/accountsmr.4c00258.

[6] Yu Y, Wang Q, Wang C, Shang L. Living Materials for Regenerative Medicine. Engineered Regeneration 2021;2:96–104. https://doi.org/10.1016/j.engreg.2021.08.003.

Molecular and Cellular Biomedical Research

Can ATP Citrate Synthase Be Potential Biomarker For Breast Cancer Progression?

Jovana Jovankić[1], Milena Milutinović[1], Stefan Blagojević[1], Danijela Nikodijević[1], Aleksandra Nikezić[1], Danijela Cvetković[2]

[1]Department for biology and ecology, Faculty of Science, Kragujevac, Republic of Serbia, jovana.jovankic@pmf.kg.ac.rs, 0000-0002-1296-2616, milena.milutinovic@pmf.kg.ac.rs, 0000-0002-5075-5650, stefan.blagojevic@pmf.kg.ac.rs, 0000-0002-5640-6267, danijela.nikodijevic@pmf.kg.ac.rs, 0000-0002-6453-0313, aleksandra.nikeyic@pmf.kg.ac.rs, 0000-0001-7075-7066

[2] Department of Genetics, Faculty of Medical Sciences, Kragujevac, Republic of Serbia, c_danijela@yahoo.com, 0000-0001-7767-1345

Corresponding author: jovana.jovankic@pmf.kg.ac.rs

Abstract

Background: Breast cancer is the most common malignancy, where progression and treatment depend on stage of local invasion and distant metastasis. Identifying biomarkers involved in tumor progression remains major focus in improving therapeutic strategies. Interesting candidate for testing is ATP citrate synthase, enzyme that links metabolism of glucose and fatty acid synthesis, with significant role in cancer growth and metastasis. This study aims to examine gene expression of *ACLY* in breast cancer and peritumor samples, with main objective of its role in breast cancer development and progression.
Methods: This study was conducted on 30 samples of breast cancer tissue and 30 samples of peritumor tissue from same group of patients. The gene expression of *ACLY* was analyzed using qPCR method.
Results: Higher *ACLY* mRNA expression in peritumor tissue samples compared to cancer tissue samples was observed in $ER^+/PR^+/HER2^-$ patients, larger tumor size, those with 1–3 metastatic changes in axillary lymph nodes, regional metastasis, and in younger patients.
Conclusion: Given its recognized oncogenic role, increased expression of *ACLY* in breast cancer tissue samples may contribute to disease progression and metastasis. These findings highlight the importance of analyzing peritumoral tissue in diagnostic and prognostic evaluation, due to molecular heterogeneity and metabolic demands of tumor progression.

Keywords: ATP Citrate Synthase, breast cancer tissue; peritumor tissue; tumor marker

1. Introduction

Breast cancer is an an heterogeneousus disease and the most common type of malignancy in females. The most important factors who determined prognosis and treatment are local invasion and distant metastasis. In the

context of molecular medicine, one of the crucial aims is to identify biomarkers that play specific roles in the development and progression of breast cancer, thus providing a new approach for treatment of breast cancer [1]. One of the important biomarkers that attracts the attention of researchers is ATP citrate synthase (ACLY), which cleaves citrate in the cytoplasm to generate acetyl-CoA and oxaloacetate. This enzyme links glucose metabolism with *de novo* fatty acid synthesis, which makes it an interesting target in energy-demanding types of cancer, such as breast cancer [2]. Previous studies showed that high expression of ACLY promotes proliferation, invasion, and migration of cancer cells, thus demonstrating its specific role in breast cancer progression [3]. However, its specific role in breast cancer growth and metastasis is not fully understood yet.
The aim of this study was to determine gene expression of *ACLY* as valuable biomarker in breast cancer and peritumor tissue samples. A key focus of this research was to examine potential role of *ACLY* in breast cancer development and progression at the molecular level. Also, for the first time, we examined the gene expression of this biomarker in the peritumoral microenvironment.

2. Materials and Methods

Design of the study

All patients included in this study signed informed consent for participation in research. According to approval of the Ethics Committee of the University Clinical Center Kragujevac (no. 01-4990), tissue samples of breast cancer tissue samples (n=30) and peritumor tissue (n=30) were collected during surgical intervention. All tissue samples were histopathologically examined by the Department of Pathological and Anatomical Diagnostics of the University Clinical Center Kragujevac. This study excluded patients who received preoperative neoadjuvant therapy, those with a family history of breast cancer, or patients with metastatic changes originated from other organs. All patient data were stratified based on the type of breast cancer (ductal/lobular), status of hormone receptors (ER/PR/HER2), TNM classification model, and age.

RNA isolation, reverse transcription, and real-time qPCR analysis

The total RNA isolation was performed according to Chomczynski and Sacchi [4] from tissue samples. The concentration and purity of the isolated RNA were measured spectrophotometrically using an Eppendorf BioPhotometer (Eppendorf AG 22331, Hamburg, Germany). The reverse transcription was performed using the Applied Biosystems™ High-Capacity cDNA Reverse Transcription Kit according to the manufacturer's instructions. The relative expression of RNA was determined using Applied Biosystems SYBR Green PCR Master Mix, according to instructions. Primer sequence for *ACLY* was F: *5'-tgctcgattatgcactggaagt-3'*; R: *5'-atgaaccccatactccttcccag-3'*, while *β-actin (F: 5'-aagcaggagtatgacgagtccg-3'; R: 5'-gccttcatacatctcaagttgg-3')* was used as the reference housekeeping gene.

Statistic analysis

Gene expression analyses were performed in three independent experiments. Results for gene expression analysis were calculated using standard $2^{-\Delta\Delta Ct}$ method. Statistical analyses were performed using SPSS (IBM SPSS Statistics v.23.0, New York, USA).

3. Results

The level of relative expression of mRNA for *ACLY* is higher in patients diagnosed with ductal breast cancer compared to patients with lobular carcinoma. In patients with the $ER^-/PR^-/HER2^+$ subtype of breast cancer, the mRNA relative expression of the *ACLY* is higher in cancer tissue samples. While in patients with the $ER^+/PR^+/HER2^-$ subtype, the expression of the tested parameter is higher in peritumoral tissue samples. In patients older than 50 years, the mRNA relative expression for *ACLY* is higher in breast cancer tissue samples, while in younger women, the expression of the same parameter is higher in peritumoral samples. Relative expression of mRNA for *ACLY* increases with cancer growth (T2) in peritumoral tissue samples. In smaller tissue samples (T1), the relative expression of *ACLY* is higher in cancer tissue samples. With the appearance of secondary deposits in 1-3 axillary lymph nodes (N1), *ACLY* mRNA expression is 4.77 times higher in peritumoral tissue samples. With an increase in the number of affected lymph nodes (N2), the dominant role in the expression of this gene is taken over by breast cancer tissue. In patients with no changes in lymph nodes (N0), the relative expression of the *ACLY* was 7.77 times higher in breast cancer tissue samples. In patients with regional metastases (M1), the relative expression of *ACLY* in peritumor tissue samples was 4.43 times higher in comparison with breast cancer tissue. Although there are obvious changes in the level of gene expression between both types of tissue samples, there is no statistical significance between groups.

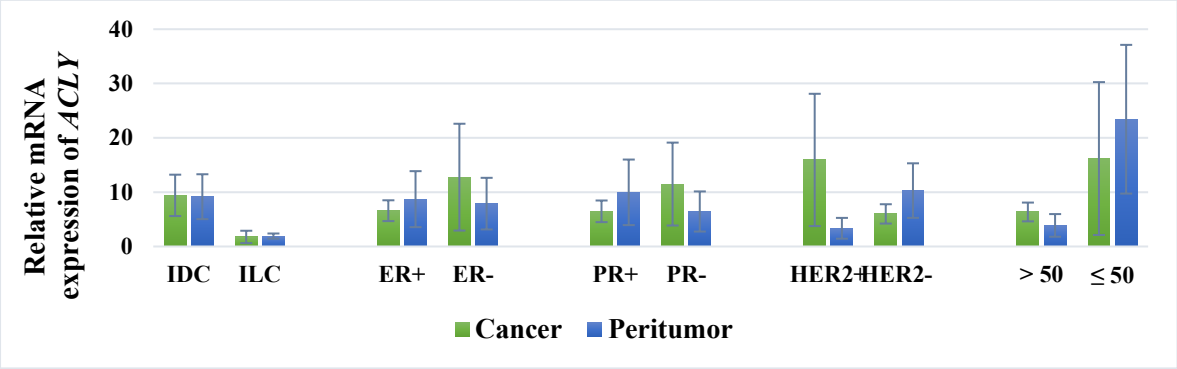


Figure 1. Relative mRNA expression of ACLY in breast cancer tissue samples and peritumor tissue samples in relation to clinicopathological characteristics of patients.

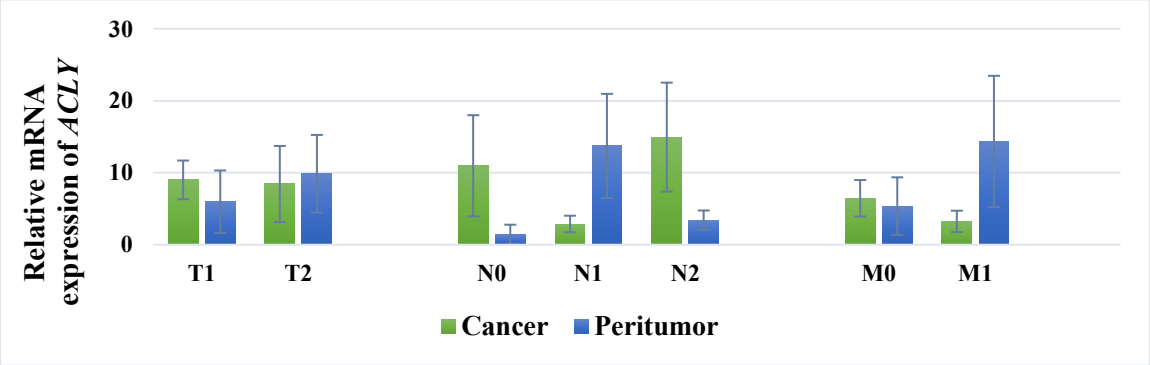


Figure 2. Relative mRNA expression of *ACLY* in breast cancer tissue samples and peritumor tissue samples in relation to TNM classification.

4. Discussion

The ACLY is a cytoplasmic homotetrameric enzyme that links glycolytic and lipid metabolism. In relation to its role in modulating the proliferation, migration, and invasion of cancer cells, ACLY functions as an oncogene [5]. Based on its complex role in cancer signalling, there is growing evidence that confirms its potential role as a biomarker in breast cancer. The 27 patients in this study were diagnosed with ductal breast cancer. This type of breast cancer is the most common type, with 60-80% of newly diagnosed cases, while lobular breast cancer accounts for about 15% [6]. Invasive ductal breast cancer is characterized by loss of hormone receptors, reduced expression of E-cadherin, and higher expression of the Ki-67 biomarker in middle-aged patients [7]. Based on the presented data, the relative gene expression of *ACLY* is higher in patients with ductal breast cancer in comparison with those with lobular cancer. The presented research results are consistent with Chen et al. (2020) [5], who demonstates that expression of *ACLY* was higher in patients with the same diagnosis, but also that this parameter can be used as an independent biomarker for predicting disease recurrence.

According to available statistic data, hormone-dependent breast cancers respond better to standard therapy in comparison with hormone-independent [1]. If we compare relative mRNA expression levels of *ACLY* in relation to hormone receptors only between breast cancer tissue samples, it is observed that in the ER^-/PR^- subtype, gene expression is higher compared to ER^+/PR^+. However, the expression of *ACLY* in ER^-/PR^- subtype is higher in breast cancer tissue compared to peritumor tissue, while in ER^+/PR^+ subtype, the result is reversed. Given that ER/PR receptor status is one of the indicators of breast cancer aggressiveness, and that ACLY overexpression is also correlated with the same cancer characteristics [8, 9], the obtained result represents a good starting point for further research to use this gene as a tumor biomarker for aggressiveness. In the study by Chen et al. (2020) [5], it was shown that increased ACLY expression is directly correlated with ER^+/PR^+ cancers, which is the opposite result to our research. It can be concluded that further investigation of the regulatory mechanisms between the expression of *ACLY* and the ER^-/PR^- subtype of breast cancer is necessary. In $HER2^+$ cancers, mRNA expression for *ACLY* is higher in cancer tissue compared to the peritumor tissue samples, while in $HER2^-$ samples, the result is reversed. The obtained result is in accordance with the literature showing that *ACLY* is overexpressed in the $HER2^+$ subtype of breast cancer [10]. In relation to TNM classification, changes in the level of relative expression of the *ACLY* are evident in both types of tested tissue samples. The obtained data relating to the degree of affected lymph nodes, the relative expression of the *ACLY* is higher in cancer tissue samples from patients with N2 group, while in patients with N1 group, the expression of the tested gene is higher in peritumor tissue samples. The results of this study are consistent with studies showing that increased ACLY expression is associated with the degree of lymph node involvement in breast cancer patients compared to control groups [5, 11]. Also, if we look at the relative expression of *ACLY* in relation to the tumor size, we come to the conclusion that with the growth of the cancer, the relative expression of *ALCY* in peritumor tissue samples increases. Based on the available literature data, this is the first study that monitors the relative expression of *ACLY* in peritumor samples. The different types of cells (inflammatory, myeloid suppressor cells, fibroblasts, adipocytes, neutrophils, tumor-associated macrophages, etc.) in the peritumor microenvironment undergo numerous changes at the energetic and metabolic level to adapt to the reduced amount of nutrients and oxygen [12]. Considering that *ACLY* is described in the literature as an oncogene, it can be assumed that its

increased activity in the microenvironment of breast cancer contributes to the metastatic potential and progression of disease. A detailed analysis of peritumor samples during prognostic and diagnostic testing is necessary because changes at the molecular levels can be very significant due to heterogeneity of breast cancer subtypes and high energy demands for cancer progression. Further studies are required to validate these findings because breast cancer is a highly heterogeneous disease with multiple molecular subtypes that may influence biomarker expression and clinical outcomes.

5. Conclusions

Relative expression of mRNA for *ACLY* in peritumoral samples is higher compared to breast cancer tissue samples in patients with ER+/PR+/HER2- subtype, in the group of patients with secondary deposits in 1-3 axillary lymph nodes, in patients with detected metastatic changes, and in younger women. Generally, increased relative expression of mRNA for *ACLY* in the peritumoral tissue samples may indicate an increased risk of metastasis in lymph nodes and other organs, especially in younger women, making this gene an interesting prognostic candidate for future testing.

Acknowledgements

The work was founded by the Ministry of Science, Technological Development, and Innovation of the Republic of Serbia (Agreement no. 451-03-33/2026-03/200122 and 451-03-34/2026-03/200122).

References

1. Lu Y, Tian L, Peng C, Kong J, Xiao P, Li N. ACLY-induced reprogramming of glycolytic metabolism plays an important role in the progression of breast cancer. Acta Biochim Biophys Sin (Shanghai). 2023;28;55(5):878-881.
2. Khwairakpam AD, Shyamananda MS, Sailo BL, Rathnakaram SR, Padmavathi G, Kotoky J, Kunnumakkara AB. ATP citrate lyase (ACLY): a promising target for cancer prevention and treatment. Curr Drug Targets. 2015;16(2):156-63.
3. Sun X, Zhao X, Wang S, Liu Q, Wei W, Xu J, Wang H, Yang W (2024) The pathological significance and potential mechanism of ACLY in cholangiocarcinoma. Front. Immunol. 2024;15:1477267.
4. Chomczynski P, Sacchi N. Single-step method of RNA isolation by acid guanidinium thiocyanate-phenol-chloroform extraction. Anal Biochem. 1987;162(1):156-159.
5. Chen Y, Li K, Gong DI, Zhang J, Li Q, Zhao G, Lin P. ACLY: A biomarker of recurrence in breast cancer. Pathology-Research and Practice, 2020; 216(9), 153076.
6. Williams LA, Hoadley KA, Nichols HB, Geradts J, Perou CM, Love MI, Olshan AF, Troester MA. Differences in race, molecular and tumor characteristics among women diagnosed with invasive ductal and lobular breast carcinomas. Cancer Causes & Control, 2019; 30, 31-39.
7. Du T, Zhu L, Levine KM, Tasdemir N, Lee AV, Vignali DA, Houten BV, Tseng GC, Oesterreich S. Invasive lobular and ductal breast carcinoma differ in immune response, protein translation efficiency and metabolism. Scientific reports, 2018;8(1), 7205.
8. Hatzivassiliou G, Zhao F, Bauer DE, Andreadis C, Shaw AN, Dhanak D, Hingorani SR, Tuveson DA, Thompson CB. ATP citrate lyase inhibition can suppress tumor cell growth. Cancer cell 2005;8(4), 311-321.

9. Migita T, Okabe S, Ikeda K, Igarashi S, Sugawara S, Tomida A, Taguchi R, Soga T, Seimiya H. Inhibition of ATP citrate lyase induces an anticancer effect via reactive oxygen species: AMPK as a predictive biomarker for therapeutic impact. The American journal of pathology, 2013;182(5), 1800-1810.
10. Monaco ME. Fatty acid metabolism in breast cancer subtypes. Oncotarget, 2017;8(17): 29487.
11. Wang D, Yin L, Wei J, Yang Z, Jiang G. ATP citrate lyase is increased in human breast cancer, depletion of which promotes apoptosis. Tumor Biology, 2017; 39(4), 1010428317698338.
12. Yu X, Mi S, Ye J, Lou G. Aberrant lipid metabolism in cancer cells and tumor microenvironment: the player rather than bystander in cancer progression and metastasis. Journal of Cancer, 2021; 12(24), 7498.

Genetic Polymorphism and CGM-Based Glucose Prediction in Type 1 Diabetes

Daphne N. Katsarou[1,2], Eleni I. Georga[2], Stelios Tigas[3], Costas Papaloukas[1,2] and Dimitrios I. Fotiadis, Fellow, IEEE[2,4]

[1] *Dept. of Biological Applications and Technology University of Ioannina, Ioannina, GR45110, Greece.*
[2] *Unit of Medical Technology and Intelligent Information Systems, Dept. of Materials Science and Engineering, University of Ioannina, Ioannina, GR45110, Greece.*
[3] *Dept. of Endocrinology, University Hospital of Ioannina, Ioannina, GR45110, Greece.*
[4] *Biomedical Research Institute, FORTH, University Campus of Ioannina, Ioannina, GR45110, Greece*
Corresponding author: fotiadis@uoi.gr

Abstract

Hypoglycemia remains a critical barrier to optimal glycemic management in Type 1 Diabetes (T1D), with evidence suggesting that genetic factors significantly influence individual susceptibility. This study aimed to examine the association between specific candidate gene polymorphisms (*ADRB2*, *ACE*, and *AGTR2*) and hypoglycemia frequency, and to evaluate if integrating these genetic profiles into predictive modeling improves glucose forecasting. We analyzed 74 adult patients with T1D using continuous glucose monitoring (CGM). Participants were categorized using k-modes clustering, and cluster-wise Long Short-Term Memory (LSTM) models were developed. Clinical results revealed significant associations: the *AGTR2* A-allele and *ACE* II homozygosity correlated with higher time below range (TBR < 54 mg/dL). Furthermore, cluster-wise LSTM models for high-risk patients (Group 0) consistently outperformed global population models, achieving a Mean Absolute Percentage Error (MAPE) of 11.6% at a 30-minute horizon compared to 14.4% in the global model. These findings demonstrate that genetic polymorphism is a key determinant of hypoglycemia risk and that "genetically-aware" modeling enhances prediction accuracy, paving the way for personalized clinical decision support systems.

Keywords: Type 1 Diabetes, Hypoglycemia, Continuous Glucose Monitoring, Genetic Polymorphism

1. Introduction

Type 1 Diabetes (T1D) is a chronic autoimmune disorder characterized by hyperglycemia due to deficient insulin secretion [1]. While continuous glucose monitoring (CGM) and insulin pumps have improved management, hypoglycemia (glucose <70 mg/dL) remains an acute, life-threatening challenge that impacts quality of life. Frequent episodes suggest that clinical factors alone do not fully explain individual susceptibility, highlighting the need for a deeper understanding of underlying risk modifiers [2].

Genetic polymorphisms within the autonomic and renin-angiotensin systems, specifically *ADRB2* (*Arg16Gly*), *ACE* (*I/D*), and *AGTR2* (*1675G/A*), are increasingly linked to impaired glucose counter-regulation

and higher frequencies of severe hypoglycemia [3,4,5]. While machine-learning architectures like Long Short-Term Memory (LSTM) networks show promise for short-term prediction, current models often lack the biological granularity required for accurate forecasting in hypoglycemic ranges [6,7]. This study aims to evaluate if clustering participants by their unique genetic profiles can improve subcutaneous glucose prediction. By developing cluster-wise LSTM models, this research seeks to determine if integrating genetic data can reduce prediction errors for high-risk patients, paving the way for more personalized diabetes management tools.

2. Materials and Methods

2.1 Study Cohort and Genetic Analysis

The study cohort consisted of 74 adult individuals with T1D (63% male, 37% female) with a mean age of 35 ± 15 years and a baseline HbA1c of 7.5 ± 1.0 %. All participants had a diagnosis duration of >6 months and utilized CGM systems for a 2–4week period to capture real-world glycemic data. Insulin management included multiple daily injections (75%) and continuous subcutaneous insulin infusion (25%), with 63% of the cohort reporting a history of severe hypoglycemia.

DNA was isolated from blood samples and analyzed using Sanger sequencing and PCR/gel electrophoresis. Genetic analysis targeted three specific polymorphisms with the following cohort distribution: *ADRB2* (GG: 46%, GA: 36%, AA: 18%), *ACE* (DD: 42%, ID: 30%, II: 28%), and *AGTR2* (AA: 40%, GG: 34%, GA: 26%).

2.2 Clustering and Predictive Modeling

To manage genetic heterogeneity, participants were categorized using the k-modes unsupervised machine learning algorithm, utilizing the Hamming distance for categorical genetic data [8]. For each identified cluster, a population-based univariate LSTM model was developed [9]. The LSTM function maps the feature vector x_t (representing a 30-minute history window) to the observed subcutaneous glucose concentration over prediction horizons (PH) of 15, 30, and 60 minutes.

The LSTM architecture consisted of two hidden layers (4 units each) and a dense output layer. Data were partitioned into 70% training and 30% testing sets, normailized to a [0,1] range using the MinMaxScaler algorithm. Models were optimized using the Adam optimizer (batch size=16, 100 epochs) to capture the specific glycemic patterns inherent to each genetic cluster.

3. Results

3.1 Genetic Influence on Hypoglycemia

Clinical analysis revealed significant associations between specific genotypes and time spent in hypoglycemia. For the *AGTR2* polymorphism, heterozygous carriers of the A allele exhibited significantly higher TBR_{54} compared to the GG genotype (2.24±2.77% vs 0.96±1.62%, p=0.04). The *ACE* polymorphism influenced outcomes, as patients homozygous for the II polymorphism demonstrated a 2.2-fold higher TBR_{54} than D allele carriers. Regarding the *ADRB2* polymorphism, AA homozygosity showed a marginal trend toward higher TBR_{70} compared to G allele carriers (p=0.07).

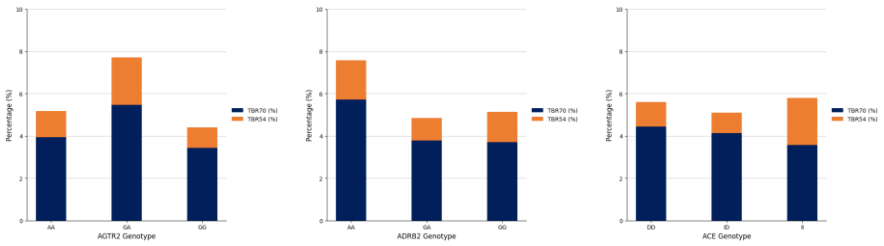


Figure 29: Hypoglycemia rate by *AGTR2*, *ADRB2* and *ACE* genotype.

3.2 Clustering Outcomes

The k-modes algorithm identified three distinct genetic clusters, each demonstrating a unique glycemic phenotype. Group 0 (39.2%) exhibited a higher prevalence of both hypoglycemia and hyperglycemia. Group 1 (23.0%) showed high hypoglycemia rates but lower hyperglycemia, while Group 2 (37.8%) was the most stable cluster, characterized by the highest time in range.

3.3 Prediction Performance

Predictive modeling was conducted for the 47 patients with complete CGM time series data. The cluster-wise LSTM models demonstrated superior accuracy over the unclustered global model. At 30-minute prediction horizon, the Mean Absolute Percentage Error (MAPE) for genetically-clustered models ranged from 11.6% to 12.8%. Notably, for Group 0 (the highest-risk cluster), the cluster-wise approach reduced the MAPE by 2.8% relative to the global population model.

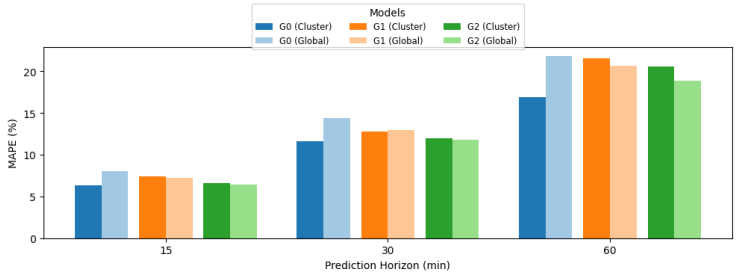


Figure 2. Prediction Errors by Population-Based LSTM Models for Each Group Using MAPE

4. Discussion

The findings indicate that genetic polymorphisms in the renin-angiotensin and adrenergic systems are key determinants of hypoglycemia clinical expression in T1D. The association between the *AGTR2* A-allele and *ACE* II homozygosity with increased TBR_{54}, reinforces the role of these systems in impaired glucose counter-regulation. These results validate genetic markers as stable, baseline indicators of glycemic risk that persist regardless of short-term behavioral changes.

From a computational perspective, integrating genetic data into machine-learning pipelines addresses a major limitation of current " one-size-fits-all " models. By clustering patients via k-modes, we identified physiological cohorts that allow the LSTM networks to learn more specific glucose transition patterns. Because

cluster-wise models consistently outperformed global models in the hypoglycemic range, it is evident that genetic data provides essential biological context that CGM data alone cannot capture. This "genetically-aware" architecture reduces prediction errors during critical low-glucose events, which is vital for the development of safer, more reliable automated insulin delivery systems.

5. Conclusions

This study demonstrates that genetic polymorphisms in the *ADRB2*, *ACE*, and *AGT2R* genes are significant determinants of hypoglycemia frequency and severity in T1D. By integrating these genetic profiles into "genetically-aware" predictive models, we achieved a measurable reduction in error rates for high-risk individuals. Despite limitations regarding sample size and potential unmeasured confounders, this research provides a vital proof-of-concept for moving beyond generalized forecasting. These findings establish a foundation for personalized clinical decision support systems capable of mitigating life-threatening hypoglycemia through an individual´s unique biological profile.

Acknowledgements

This research has been co-financed by the European Union and Greek national funds through the Operational Program Competitiveness. Entrepreneurship and Innovation, under the call RESEARCH – CREATE – INNOVATE (project code: T1EDK-03990).

References

[1] K. N. Frayn, Metabolic regulation: a human perspectiveMetabolic regulation a human perspective, 3rd ed. Chichester, West Sussex Malden, MA Chichester, U.K.: Blackwell Wiley-Blackwell Pub., 2010.
[2] S. A. Amiel, “The consequences of hypoglycaemia,” Diabetologia, vol. 64, no. 5, pp.1-8, 2021.
[3] A. Holstein, A. Plaschke, Y. Böttcher, M. Stumvoll, & P. Kovacs, "The insertion/deletion polymorphism in the angiotensin-converting enzyme gene and hypoglycemia awareness in patients with type 1 diabetes," Horm Metab Res, vol. 38, no. 9, pp. 603-6, 2006.
[4] U. Pedersen-Bjergaard, S. S. Dhamrait, A. A. Sethi, E. Frandsen, B. G. Nordestgaard, H. E. Montgomery, S. Pramming, P. Hougaard, & B. Thorsteinsson, "Genetic variation and activity of the renin-angiotensin system and severe hypoglycemia in type 1 diabetes," Am J Med, vol. 121, no. 3, pp. 246.e1-8, 2008.
[5] B. J. Schouwenberg, M. J. Coenen, A. D. Paterson, C. J. Tack, P. Smits, C. Kramers, & B. E. de Galan, "Genetic determinants of impaired awareness of hypoglycemia in type 1 diabetes," Pharmacogenet Genomics, vol. 27, no. 9, pp. 323-328, Sep 2017.
[6] M. De Bois, M. A. Yacoubi, & M. Ammi, "GLYFE: review and benchmark of personalized glucose predictive models in type 1 diabetes," Medical & Biological Engineering & Computing, vol. 60, no. 1, pp. 1-17, 2022.
[7] S. Tsichlaki, L. Koumakis, & M. Tsiknakis, “Type 1 diabetes hypoglycemia prediction algorithms: Systematic review,” JMIR Diabetes, vol.7, no.3, 2022.
[8] Cao F, Liang J, Li D, Bai L, Dang C. "A dissimilarity measure for the k-Modes clustering algorithm," Knowledge-Based Systems, vol. 26, pp. 120-127, 2012.
[9] J. Brownlee, “Deep Learning for Time series Forecasting.” Machine Learning Mastery, pp.123-160, 2018.

Biomedical Instrumentation and Laboratory Automation

Automated Cytogenetic Chromosome Spreading Device with Real-Time Environmental Control

Seyfettin Kazanır
Alanya Alaaddin
Keykubat University (ALKÜ)
Antalya, Türkiye Seyfettin.kazanir@alanya.edu.tr

1. Introduction

Cytogenetic analysis is a cornerstone of genetic diagnostics, widely used in the detection of chromosomal abnormalities, prenatal screening, and cancer research. One of the most critical steps in this process is chromosome spreading, where properly dispersed metaphase chromosomes are required for accurate visualization and analysis. The quality of chromosome spreading directly affects diagnostic reliability, making this step highly sensitive and essential in laboratory workflows.

Despite its importance, chromosome spreading is still largely performed using manual techniques that rely heavily on operator skill and experience. Variability in sample preparation techniques, such as dropping height, timing, and environmental conditions, can lead to inconsistent results. This operator-dependent nature introduces significant variability, reducing reproducibility and increasing the likelihood of diagnostic errors.

Among the factors influencing chromosome spreading, environmental conditions—particularly temperature and relative humidity—play a crucial role. Previous studies and laboratory practices indicate that even minor deviations in these parameters can significantly alter chromosome morphology, spreading efficiency, and fixation quality. However, conventional laboratory environments lack precise and continuous control of these parameters, leading to unstable and non-standardized preparation conditions.

Furthermore, existing cytogenetic workflows do not provide integrated systems capable of simultaneously monitoring and controlling environmental conditions in real time. This gap highlights a critical need for automated solutions that can standardize chromosome preparation processes and reduce human-induced variability.

In this context, the present study proposes an automated cytogenetic chromosome spreading device designed to overcome the limitations of traditional methods. The developed system integrates environmental control mechanisms, embedded system architecture, and real-time monitoring capabilities to provide a stable and controlled preparation environment.

By maintaining optimal temperature and humidity conditions through a closed-loop control system, the proposed device aims to enhance chromosome spreading quality, improve reproducibility, and reduce operator dependency. In addition, the system incorporates user-friendly interfaces and remote monitoring features, enabling its integration into modern digital laboratory infrastructures.

This work not only addresses a critical gap in cytogenetic laboratory practices but also contributes to the advancement of automated biomedical devices by providing a scalable and application-ready solution for chromosome preparation processes

2. System Architecture

The proposed cytogenetic chromosome spreading device is designed as an integrated cyber-physical system that combines environmental control, sensing, and embedded processing within a unified architecture to ensure stable and reproducible conditions inside a controlled chamber.

Temperature regulation is achieved using Peltier-based thermoelectric modules capable of both heating and cooling, enabling rapid response to environmental fluctuations. Humidity control is provided through an integrated humidification unit, while an active air circulation system ensures uniform distribution of temperature and moisture throughout the chamber. Environmental conditions are continuously monitored using BME680 sensors and NTC thermistors, allowing reliable and multi-point measurement of critical parameters.

All sensor data are processed by an ESP32-based embedded control unit, which operates a closed-loop control system. Based on real-time feedback, the system dynamically adjusts actuators such as Peltier modules, fans, and the humidifier to maintain predefined environmental setpoints. Pulse-width modulation (PWM) is used to regulate actuator intensity, ensuring precise and stable system behavior.

The system supports both automatic and manual operating modes, providing flexibility for laboratory use. A touchscreen interface allows local monitoring, while a web-based interface enables remote access and control via Wi-Fi connectivity. Additionally, environmental data are recorded through an integrated data logging system, allowing post-process analysis and validation.

Overall, the architecture provides a compact, scalable, and robust solution for maintaining controlled environmental conditions required for consistent chromosome spreading.

3. Methodology

The development of the proposed cytogenetic chromosome spreading device was carried out using a systematic engineering approach that integrates mechanical design, embedded systems development, control strategies, and experimental validation. The primary objective of this methodology was to design a system capable of maintaining stable environmental conditions while ensuring repeatable and high-quality chromosome spreading under laboratory conditions.

In the initial stage, the system was designed to create a controlled chamber environment in which critical parameters such as temperature and relative humidity can be precisely regulated. The mechanical structure was developed by considering thermal insulation, airflow distribution, and ergonomic usability. Experimental observations and preliminary laboratory trials were used to determine the optimal environmental conditions required for chromosome spreading, which were defined approximately as 26°C temperature and 43% relative humidity. The internal layout of the chamber was optimized to ensure homogeneous distribution of heat and moisture, thereby minimizing spatial variations that could negatively affect chromosome dispersion.

To achieve precise environmental control, a closed-loop control strategy was implemented based on PID (Proportional–Integral–Derivative) algorithms. Sensor data obtained from BME680 environmental sensors and NTC thermistors were continuously monitored and processed by the control unit. The deviation between measured values and predefined setpoints was used to dynamically adjust system actuators. In this context, Peltier modules were used for both heating and cooling operations, while fans were employed to support air circulation and thermal balance. A humidification unit was integrated into the system to regulate moisture levels inside the chamber. The PID-based control approach enabled stable system behavior, minimized overshoot, and ensured rapid response to environmental disturbances.

The embedded system was implemented using an ESP32-based platform, providing real-time processing capability and communication flexibility. The software architecture was designed in a modular manner, allowing efficient interaction between sensor acquisition, control processing, actuator management, and communication subsystems. The system supports both automatic and manual operating modes. In automatic mode, environmental parameters are maintained autonomously, whereas in manual mode users are allowed to directly control system components for experimental purposes. A web-based user interface was developed to provide real-time monitoring and remote control functionality, enabling users to access system parameters and adjust operating conditions through standard web browsers.

During the system integration phase, all hardware and software components were combined into a unified operational structure. The interaction between sensors, actuators, and control algorithms was tested iteratively to ensure system stability and reliability. Calibration procedures were applied to improve measurement accuracy, and control responses were validated under different operating scenarios. Special attention was given to the synchronization of temperature and humidity control processes, as their interaction plays a critical role in achieving optimal chromosome spreading conditions.

4. Experimental Validation

The performance of the developed cytogenetic chromosome spreading device was evaluated through a series of controlled laboratory and field experiments conducted under real operating conditions. The primary objective of the validation process was to assess the system’s ability to maintain stable environmental conditions and to evaluate its impact on chromosome spreading quality.

The experimental setup was designed to simulate actual cytogenetic laboratory workflows. Tests were performed using standard sample preparation procedures, and the device was operated under varying external environmental conditions to evaluate system robustness. Seasonal variations, including differences in ambient temperature and humidity, were also considered during testing to ensure reliability under diverse conditions.

To assess system performance, multiple evaluation criteria were defined. These included environmental stability, system response time, repeatability of results, and user interaction efficiency. Temperature and humidity values inside the chamber were continuously monitored and recorded throughout the experiments. The deviation from predefined setpoints was analyzed to determine control accuracy.

Comparative experiments were conducted between controlled and uncontrolled environments. In the uncontrolled scenario, traditional laboratory conditions were used without active environmental regulation. In

contrast, the developed device provided continuous temperature and humidity control. Chromosome spreading quality obtained from both conditions was evaluated by laboratory professionals based on standard cytogenetic criteria, including chromosome dispersion, overlap levels, and clarity of metaphase structures.

In addition to technical measurements, user-based evaluations were also performed. Multiple users with different levels of experience operated the system, and their feedback was collected through structured questionnaires. The evaluation focused on usability, ease of operation, and perceived improvements in workflow efficiency.

The results obtained from these experiments demonstrated that the system is capable of maintaining stable environmental conditions with minimal deviation from target values. Furthermore, controlled conditions significantly improved the consistency and quality of chromosome spreading compared to conventional methods.

5. Results

The experimental results demonstrate that the proposed system significantly improves the stability of environmental conditions and enhances the overall quality of chromosome spreading compared to conventional laboratory practices.

During testing, the system successfully maintained temperature and humidity levels close to predefined setpoints under varying external conditions. The closed-loop control mechanism provided stable operation with minimal fluctuations, ensuring a consistent preparation environment. Observations indicated that the system rapidly responded to environmental disturbances and effectively stabilized internal conditions within a short time frame.

Comparative analysis between controlled and uncontrolled environments revealed clear differences in chromosome spreading outcomes. In uncontrolled laboratory conditions, chromosome spreads exhibited variability in dispersion quality, increased overlap, and inconsistent metaphase clarity. In contrast, the use of the developed device resulted in more homogeneous chromosome distribution, reduced overlap, and improved clarity of chromosomal structures.

Furthermore, the repeatability of sample preparation showed a noticeable improvement. Under controlled conditions, consecutive samples demonstrated consistent spreading characteristics, whereas traditional methods produced variable results depending on environmental fluctuations and operator influence. This improvement indicates that the system effectively reduces process variability and enhances reliability in cytogenetic workflows.

User-based evaluations also supported these findings. Participants reported that the device simplified the preparation process, reduced manual intervention, and improved overall workflow efficiency. The combination of automated control and real-time monitoring enabled users to achieve stable results with less dependency on individual experience.

In addition, environmental data collected during experiments confirmed that humidity control plays a dominant role in determining chromosome spreading quality. Stable relative humidity conditions were associated with

optimal chromosome dispersion, whereas deviations from target humidity levels resulted in reduced spreading performance.

Overall, the results indicate that the proposed system provides a controlled, repeatable, and efficient solution for chromosome spreading, addressing key limitations of conventional methods and contributing to improved laboratory standardization.

6. Discussion

The results of this study demonstrate that environmental control is a key factor in improving the quality and reproducibility of cytogenetic chromosome spreading. In particular, humidity was identified as a critical parameter, as even minor deviations significantly affected chromosome morphology and dispersion.

The proposed system addresses a major limitation of conventional methods, namely operator dependency. By providing a controlled and automated environment, the device reduces human-induced variability and enables more standardized and consistent results.

In addition, the integration of real-time monitoring and closed-loop control ensures stable system performance under varying external conditions. This capability is especially important in laboratory environments where environmental stability cannot always be guaranteed.

The modular and scalable architecture of the system also allows potential integration with digital laboratory infrastructures and future data-driven optimization approaches.

However, the current implementation focuses primarily on temperature and humidity control. Other factors, such as chemical conditions and sample handling techniques, may also influence chromosome spreading outcomes and should be considered in future studies.

Overall, the proposed system provides a practical and effective solution for improving reliability, repeatability, and efficiency in cytogenetic workflows.

7. Conclusion

This study presents the design, development, and validation of an automated cytogenetic chromosome spreading device capable of maintaining precisely controlled environmental conditions. The proposed system integrates mechanical design, embedded control, and real-time monitoring to address the limitations of conventional manual chromosome preparation methods.

The experimental results demonstrate that stable temperature and humidity control significantly improve chromosome spreading quality, enhance repeatability, and reduce operator dependency. In particular, the findings highlight the critical role of humidity regulation in achieving optimal chromosome dispersion and consistent sample preparation outcomes.

By introducing a controlled and automated preparation environment, the developed system contributes to the standardization of cytogenetic workflows and improves the reliability of laboratory processes. The integration

of real-time monitoring, remote access capabilities, and data logging features further enhances the usability and functionality of the system.

The device has reached Technology Readiness Level (TRL) 8, indicating a high level of maturity with successful validation under real laboratory conditions. The system is prepared for CE certification and demonstrates strong potential for clinical adoption and industrial production.

Overall, the proposed solution represents a scalable, reproducible, and application-ready technology that can significantly improve efficiency and accuracy in cytogenetic laboratories. Future work will focus on extended clinical validation, integration with digital laboratory systems, and further optimization of environmental control strategies.

8. Demonstration Potential

The system enables live demonstration of real-time environmental control within a closed chamber, allowing participants to observe how temperature and humidity parameters are dynamically regulated through a closed-loop control mechanism. Changes in environmental conditions can be instantly visualized via the user interface, providing a clear understanding of system response behavior and control accuracy.

In addition, the device supports remote interaction through a web-based interface, enabling users to monitor system parameters and adjust setpoints in real time. This feature allows participants to directly interact with the system, creating a practical and hands-on demonstration experience.

A key demonstration scenario involves the comparison between controlled and uncontrolled environmental conditions. By presenting representative chromosome spreading results obtained under both conditions, the system clearly illustrates the impact of environmental stability on chromosome dispersion quality. This comparative approach highlights the practical advantages of the proposed system in a scientifically meaningful way.

Furthermore, the physical prototype can be presented to demonstrate its compact design, modular structure, and integration of hardware and software components. Core system elements, including sensors, control units, and actuators, can be explained in real time, providing insight into the system's engineering design and operational workflow.

The demonstration also emphasizes applicability in real laboratory environments. By simulating realistic usage scenarios, the system effectively demonstrates its ability to reduce operator dependency, improve repeatability, and enhance workflow efficiency.

Overall, the system provides a strong demonstration platform by translating complex environmental control mechanisms into observable and interactive outputs.

Cancer Care, Clinical Management, and Digital Health

Improving quality of life after breast cancer

My coco

Iratxe Sobera

My coco, Mondragon, Spain (iratxe.soberaålumni.mondragon.edu)

Contact email: hola@mycoco.com | Website: www.mycoco.es

Executive Summary

My Coco is a project focused on improving the quality of life for women following breast cancer, particularly in the post-mastectomy period. The initiative stems from the development of external breast prostheses that are lighter, more breathable and better adapted to the body's natural contours, with the aim of enhancing comfort and well-being in everyday life. However, the project's focus has expanded to include a more comprehensive range of solutions, such as adapted bras, cancer headscarves, adhesive nipples and skincare products.

The development is based on a combination of design, materials technology and analysis of user experience, paying particular attention to skin sensitivity and the functional adaptation of the products. The market relevance lies in the existence of an unmet demand, where many of the current solutions show little progress in terms of materials, ergonomics and user experience.

The innovative nature of My Coco lies in its user-centred approach, which integrates functionality, aesthetics and well-being, moving away from the traditionally medical perception of this type of product. Furthermore, it proposes a phased strategy that combines unregulated products—which allow for rapid iteration and validation—with the future development of improved prostheses.

In the long term, the project's strategic vision is to establish a range of tailored, scalable and accessible products that contribute to improving both women's physical wellbeing and self-esteem, and to move towards more personalised solutions within the field of health and wellbeing.

Keywords: breast cancer; mastectomy; breast prostheses; adaptive lingerie; textile innovation; wellbeing; women's health; user-centred design; market application

1. Company Overview

My Coco is a project focused on improving the quality of life for women following breast cancer, particularly after a mastectomy. Its mission is to develop solutions that adapt to the real body and everyday life, combining comfort, functionality and design. It operates within the field of health and wellbeing innovation, at the intersection of textile technology, product development and user-centred design.

2. Technology / Product / Service Description

The project is working on the development of lighter and more breathable external breast prostheses, as well as complementary products such as adapted bras, cancer headscarves and adhesive nipples. It is based on the selection of soft, hypoallergenic and ergonomic materials, taking into account skin sensitivity and how the product fits the body.

3. Innovation and Competitive Advantage

The key differentiating factor is the user-centred approach, integrating well-being, aesthetics and functionality. Compared to existing products that have seen little evolution, My Coco proposes improvements in materials, design and user experience. Currently, the project is in the development phase without a consolidated position regarding intellectual property.

4. Market Application and Impact

The target market comprises women who have undergone a mastectomy, with or without reconstruction. There is an unmet demand, which allows for scalability through online channels, partnerships and specialist shops. The impact is both functional and social, improving comfort, self-esteem and normalisation.

5. Partnerships and Outlook

The project seeks collaboration with textile manufacturers, material suppliers and healthcare specialists. In the short term, it focuses on prototyping and validation. In the medium term, the development of external prostheses and the consolidation of a complete product range are envisaged.

An Interdisciplinary Approach for the Management of the Elderly Multimorbid Patient with Breast Cancer Therapy-Induced Cardiac Toxicity

CARDIOCARE Project, EU Horizon 2020, Grant Agreement No. 945175, July 2021 – June 2026

Alexandros Mitsis[1], Georgia Karanasiou[1,2], Dimitrios I. Fotiadis[1]

[1] Unit of Medical Technology and Intelligent Information Systems, Dept. of Material Science and Engineering, University of Ioannina, GR45110, Ioannina, Greece.

[2] Department of Biomedical Research, Institute of Molecular Biology and Biotechnology, FORTH, GR45110, Ioannina

Corresponding author: alexmitsis07@gmail.com

Abstract

CARDIOCARE is designed to tackle an important unmet medical need in cardio-oncology, the effective management of elderly and multimorbid breast cancer patients prone to cardiotoxic effects of anticancer therapies. More than 50% of all breast cancers affect individuals above 65 years of age; however, this population is under-represented in clinical trials and highly prone to the detrimental effects of a "snowball effect" from cardiovascular damage induced by therapy. CARDIOCARE, funded under EU Horizon 2020 (Grant Agreement No. 945175), is coordinated by the University of Ioannina (Greece) and encompasses a consortium of 12 partners from seven countries in Europe. The overall aim of CARDIOCARE is the development of a holistic multidisciplinary artificial intelligence platform incorporating multiple types of information – clinical, imaging, omics, wearable sensors, and psychological factors – to support personalized risk stratification and care pathways. Methodological foundations of CARDIOCARE include a multi-center retrospective and prospective clinical study, eHealth tools (ePsycHeart and eHealthHeart), omics biomarker discovery (microRNA, microbiome, single nucleotide polymorphisms analysis), explainable artificial intelligence models, and a GDPR compliant Big Data platform.

Keywords: *cardio-oncology; breast cancer; cardiotoxicity; elderly patients; multimorbidity; machine learning; wearables; precision medicine; eHealth; biomarkers; CARDIOCARE; Machine-learning; eHealth; Cardiotoxicity; Breast cancer; Elderly; Quality of Life; UN SDG 3; UN SDG 5; UN SDG 10.*

1. Project Background and Objectives

More than 50% of newly diagnosed breast cancer patients are elderly (>65 years) and are particularly susceptible to cardiotoxicity arising from cancer treatment [1]. Age-related physiological changes and pre-existing co-morbidities create a compounding "snowball effect": therapy-induced cardiac damage worsens existing conditions, progressively leading to frailty, multi-morbidity, and increased mortality [2]. Despite the scale of this clinical challenge, older patients remain systematically underrepresented in clinical trials [3], leaving critical gaps in evidence-based care and depriving clinicians of the data-driven tools they need to manage this complex patient group effectively [4].

The CARDIOCARE project aims at addressing these challenges by creating a multidisciplinary, evidence-based solution that will revolutionize the process of cardiotoxicity management among elderly patients suffering from breast cancer. Utilizing multimodal data, including innovative biomarkers, wearables, and psychological assessments, the project creates predictive analytics and personalised interventions that help combat the "snowball effect" experienced by patients.

This project is supported by the EU Horizon 2020 framework (Grant Agreement No. 945175), started on 1 July 2021 with an original end date of 30 June 2025, and has been extended by one year to 30 June 2026. It is headed by the University of Ioannina (UOI), Greece, and consists of a consortium of 12 partners from seven European countries.

Overall Objective: Retrospective and prospective data from the clinical studies are collected including clinical, imaging, -omics, biomarker, psychomarker, intrinsic capacity, wearable sensor, and eHealth application data and by employing machine learning approaches, CARDIOCARE develops a novel cost-effective risk-stratification strategy and provides evidence-based best practices and care pathways to improve the management of the elderly multimorbid breast cancer patient at risk for cardiotoxicity.

2. Methodology and Work Performed

The project is organized around the following research areas

- Multi-centre clinical study. A retrospective and prospective trial enrolling elderly breast cancer patients across 6 European clinical centres, collecting longitudinal data on cardiotoxicity, intrinsic capacity, and QoL.
- eHealth applications. eHealth applications: ePsycHeart and eHealthHeart apps, integrated with wearable IoT sensors for continuous, real-time patient monitoring throughout active treatment.
- Omics analysis. Identification of biomarkers through miRNA profiling, gut microbiome analysis, and SNP analysis to predict heart damage risk.
- AI & Machine Learning. Development of Explainable AI models that combine clinical data and imaging to provide clear, interpretable risk assessments for doctors.
- CARDIOCARE Big Data Platform. A GDPR-compliant cloud environment that integrates clinical records, sensor data, and omics into a single analytical hub.

3. Key Results

CARDIOCARE has delivered five categories of key results spanning clinical data infrastructure, digital health tools, and AI-driven analytics:

Structured Datasets. Retrospective and prospective clinical and imaging data, as well as patient-reported outcomes relating to emotional and psychological aspects of treatment.

mHealth Solutions. Facilitating the collection of patient data on psychological, emotional, and behavioural aspects, as well as providing psychological and wellbeing support through mobile applications.

IT Research Infrastructure. A platform for the collection, integration, and machine learning analysis of structured and unstructured multi-domain data, including clinical data, imaging, genetic and miRNA data, big data from wearables, and patient-reported outcomes.

Models and Algorithms. Being developed for personalised patient monitoring and therapy selection, incorporating Explainable AI to ensure clinical interpretability.

Prognostic Biomarkers for Cardiotoxicity. Novel biomarker signatures being identified through omics analysis that enable early detection and risk prediction of therapy-induced cardiac damage.

4. Discussion and Impact

CARDIOCARE is a revolution in precision cardio-oncology among elderly patients that involves using multiple data streams such as clinical, imaging, omics, and psychological data, within an Explainable Artificial Intelligence system. The initiative effectively targets the structural issue in the domain by overcoming the limitation of one-dimensional analysis, which does not account for the complexities of an aging, multimorbid population. In addition to the clinical setting, the scope of eHealth applications and wearables incorporated into the project will facilitate proactive remote management.

5. Conclusions and Outlook

Through CARDIOCARE, it is shown that a multi-modal AI approach can significantly contribute to the management of cardiotoxicity in a highly vulnerable population of elderly breast cancer patients suffering from multimorbidity – a patient group often overlooked in clinical studies. In utilizing the approach of combining multimodal data collection, omics-based discovery of biomarkers, eHealth monitoring, and Explainable AI, CARDIOCARE creates not only a risk stratification framework but also develops digital solutions that will be required for implementation in the clinic of such a framework. All aspects of research are being actively conducted within CARDIOCARE, including collecting clinical data, creating the platforms, and training the models. The deadline of the project is extended till June 2026. Future priorities include completing and disseminating the care pathways to clinical partners and preparing the regulatory strategy for the panel of prognostic biomarkers.

Acknowledgements / Funding

CARDIOCARE is funded by the European Union's Horizon 2020 research and innovation programme under Grant Agreement No. 945175.

References

[1] P. Reddy, C. Shenoy, and A. H. Blaes, "Cardio-Oncology in the Older Adult," *J Geriatr Oncol*, vol. 8, no. 4, pp. 308–314, Jul. 2017, doi: 10.1016/j.jgo.2017.04.001.

[2] "2022 ESC Guidelines on cardio-oncology developed in collaboration with the European Hematology Association (EHA), the European Society for Therapeutic Radiology and Oncology (ESTRO) and the International Cardio-Oncology Society (IC-OS) | European Heart Journal | Oxford Academic." Accessed: Apr. 17, 2026. [Online]. Available: https://academic.oup.com/eurheartj/article/43/41/4229/6673995?login=true

[3] "2022 ESC Guidelines on cardio-oncology developed in collaboration with the European Hematology Association (EHA), the European Society for Therapeutic Radiology and Oncology (ESTRO) and the International Cardio-Oncology Society (IC-OS) | European Heart Journal | Oxford Academic." Accessed: Apr. 17, 2026. [Online]. Available: https://academic.oup.com/eurheartj/article/43/41/4229/6673995?login=truBiganzoli%20et%20al.%20%E2%80%94%20SIOG/EUSOMA%20recommendations%20for%20elderly%20breast%20cancer%20(Lancet%20Oncol,%202012)e

[4] K. Keramida *et al.*, "Cardiotoxicity in Elderly Breast Cancer Patients," *Cancers (Basel)*, vol. 17, no. 13, p. 2198, Jun. 2025, doi: 10.3390/cancers17132198.

Smart Mirrors supporting healthier lives of Adolescents and Young Adults after cancer

MAYA, Horizon Europe, Grant Agreement No. 101213323, June 2025 – May 2029

Alexandros Mitsis [1], Georgia Karanasiou [1,2], Dimitrios I. Fotiadis[1]

[1] Unit of Medical Technology and Intelligent Information Systems, Dept. of Material Science and Engineering, University of Ioannina, GR45110, Ioannina, Greece.

[2] Department of Biomedical Research, Institute of Molecular Biology and Biotechnology, FORTH, GR45110, Ioannina

Greece Corresponding author: alexmitsis07@gmail.com

Keywords: *MAYA; cardiotoxicity; AYA cancer survivors; AI-driven risk-modeling; Living Labs; Quality of Life; UN SDG 3; UN SDG 9; UN SDG 10*

Abstract

The objective of the MAYA project is the management of late cardiac effects secondary to anticancer treatment and the improvement of care after treatment of Adolescent and Young Adults (AYAs) cancer survivors. Thanks to the use of digital solutions provided by this project, AYAs survivors can actively monitor their own cardiovascular health status and quality of life from the comfort of their homes. Methodology: The solution will be based on the exploitation of the iCARE health hub, a digital ecosystem including a Smart Mirror together with the AI digital assistant. The project allows continuous biomarker collection and personalized and adaptive guidance. This initiative will exploit the combination of state-of-the-art data analysis methods combined with SSH (Social Sciences and Humanities) approaches (such as social innovation, Living Labs, research methods with patient involvement). Results & Expected Impact: Through the management of modifiable risk factors (hypertension, obesity, diabetes mellitus) and thanks to its solutions, MAYA expects to achieve a positive effect on cardiovascular outcomes and quality of life by at least 70% of study subjects. Moreover, it plans to reduce serious cardiac events and the risk of early mortality by 30-40%. Analysis of heterogeneous data collected through multi-national pilot studies will allow the development of personalised risk profiles and evidence-based intervention pathways, ultimately empowering AYA survivors to take an active role in managing their long-term cardiovascular health.

Keywords: Adolescent, Young Adult, Cancer, Survivors, Cardiotoxicity, Digital health

1. Project Background and Objectives

An important and largely unmet problem for survivors of AYA cancers is the delayed cardiovascular outcomes caused by cancer therapies(1). While there has been increased survival in general from oncological treatments, this group remains at risk of developing severe adverse outcomes in relation to their health, such as hypertension, diabetes, and obesity, which increase the risk of having life-threatening heart problems (2). There has not been

any innovative approach yet designed to facilitate AYA survivors in the process of monitoring their own CV outcomes in a personalized, ongoing, and home-based manner (3). Current practices related to the monitoring process present various challenges and cannot provide such personalized monitoring of CV outcomes (4).
MAYA seeks to fill this gap through the implementation of an AI-driven iCARE Health Hub utilizing a Smart Mirror and conversational AI avatar for continuous monitoring of cardiovascular measurements at home. Through its ambition of reducing serious cardiac complications in young adult cancer survivors by 30-40%, MAYA revolutionizes expert-level prevention of cardio-oncology from the hospital environment to the domestic setting.
The MAYA project is funded through Horizon Europe (Grant Agreement No. 101213323). The project began on 1 June 2025 and will end on 31 May 2029. The MAYA project is led by the University of Ioannina (UOI), Greece, with 16 partners from 10 European countries.
Overall Objective: MAYA stands out in being able to transform health monitoring into a low-effort task naturally incorporated in users' routines with the help of a Smart Mirror as the core interface. The introduction of professional ECG and blood pressure devices into the iCARE Health Hub in particular allows MAYA to pay special attention to reducing cardiotoxicity while other projects concentrate only on increasing QoL or collecting policy-level information. Even more options are provided with the employment of iCARE Onto as a formal ontology enabling the smart mirror avatar's personalised dialogues and intervention strategies. Thus, an Avatar powered with AI is responsible for converting clinical information into therapy in real-time in order to overcome problems faced by users of other solutions based on mobile alerts for AYA survivors.

2. Methodology and Work Performed

The MAYA framework is built around five integrated technical and clinical pillars, each contributing to a unified, home-based cardiovascular monitoring system for AYA cancer survivors:
AI-Based Prediction and Early Warning. Development of AI algorithms that identify early warning signs of cardiotoxicity and quality of life (QoL) deterioration by analysing multimodal data sources including clinical records, wearable sensors, and patient-reported data.
iCARE Ontology and Knowledge Graphs. Development and continuous improvement of iCARE Onto, a formal ontology and knowledge graph enabling context-aware, personalised decision-making, dialogues, and health interventions across diverse pilot environments.
Smart Mirror Avatar with Conversational AI. Implementation of advanced conversational AI via the Smart Mirror Avatar, using Retrieval-Augmented Generation (RAG) to deliver context-aware, culturally sensitive, and adaptive health literacy support directly to the patient at home.
Secure and Interoperable iCARE Framework. Design and development of a secure, standardised cloud architecture integrating heterogeneous sensors, AI capabilities, and cloud data management solutions, ensuring interoperability, GDPR compliance, and scalable deployment across pilot sites.
Pilot Testing and Clinical Validation. Real-world pilot testing and iterative assessment of the iCARE platform across multiple European clinical centres to evaluate performance, refine AI models, and validate the system's effectiveness in managing late-onset cardiovascular diseases.

3. Main Outcomes

- **Early Warning AI:** AI algorithms that predict early signs of cardiotoxicity and QoL reduction by analyzing clinical and sensory data.
- **Personalized Knowledge Base:** iCARE Ontology and Graphs that provide personalized medical advice and interventions for every cancer survivor.
- **The Smart Mirror:** An intelligent avatar driven by RAG (Retrieval-Augmented Generation) that can offer accurate health assistance based on culture.

- **Secure iCARE Framework:** A standardized cloud infrastructure that integrates sensors and artificial intelligence to facilitate deployment.
- **Clinical Validation:** A framework being developed and validated via multi-site pilot implementations to ensure efficient management of late-onset cardiovascular diseases.

4. Discussion and Impact

After being fully implemented, MAYA aims to transform the way that the long-term recovery of AYA cancer patients is managed, through delivering the same level of expert care from hospitals into their homes. This will be achieved by utilizing the combined efforts of the iCARE Smart Mirror technology as well as AI prediction software with the goal of decreasing life-threatening cardiac cases by 30-40% by identifying cardiotoxicity at an early stage. Not only does MAYA intend on enhancing the health outcomes of its participants, but it will help them lead better lives.

5. Conclusions and Outlook

MAYA is a digital health solution developed to assist AYA cancer survivors post-treatment with their health management. This program gathers and processes patients' data, especially relating to cardiovascular issues, to create individual profiles. These will be used in order to help survivors manage their health in their everyday lives, particularly by means of cardiovascular risk modeling.

MAYA applies sophisticated techniques that will predict severe health complications, such as cardiotoxicity, and recommend appropriate interventions for maintaining good cardiac and general health. Survivors will receive instructions on their physical activity, nutrition, and lifestyle using the program's AI conversational agent; doctors will benefit from the analyzed data to make personalized treatment suggestions promoting patient independence.

The framework is currently being developed, but it holds great promise as a tool for improving cardiovascular risk factors.

Acknowledgements / Funding

MAYA is funded by the European Union's Horizon Europe research and innovation programme under Grant Agreement No. 101213323 (HORIZON-MISS-2024-CANCER-01).

Reway – Restoring Mobility, Redefining Care

Student Company: Reway

Sara Milosevic, Jana Jankovic, Marija Velickovic, Jana Cvetkovic, Marko Ilic, Nikola Nikolic[1]

[1] *Team Reway, Reway, High school,"Nikola Tesla", Batocina, Serbia*

Contact email: reway2026@gmail.com | Website: https://reway-walk-again.netlify.app/#

Executive Summary

Reway is an innovative student-driven company focused on developing affordable and functional assistive solutions for animals, starting with 3D-printed prosthetic devices for injured poultry. The core idea emerged from a real-life problem. Injured chickens are often discarded due to the lack of practical and accessible rehabilitation solutions. Reway addresses this gap by combining empathy, engineering, and digital manufacturing.

The company's primary product is a lightweight, customizable prosthetic leg designed using CAD software and produced via 3D printing technology. Through an iterative development process involving three prototypes, the product has evolved to provide improved stability, comfort, and durability. This approach ensures both functionality and adaptability to different sizes and conditions.

Reway will operate in a niche of globally relevant market, targeting small-scale farmers and poultry enthusiasts who value both the economic and emotional aspects of animal care. The solution not only reduces financial losses but also promotes animal welfare and sustainability.

The innovation lies in the accessibility of the technology, low production costs, customisation and scalability enabled by digital manufacturing. Reway's strategic vision includes expanding the product line to other animal species and entering broader regional and European markets.

By bridging the gap between compassion and commercialization, Reway demonstrates how simple, practical innovations can create meaningful impact while maintaining strong business potential.

Keywords: ReWay, prosthetics, 3D printing, animal welfare, innovation, agriculture, assistive technology, sustainability, UN SDG 12, UN SDG 2, UN SGD 9

1. Company Overview

Reway is a student-founded innovation company focused on developing practical and accessible assistive solutions for animals. The company was established as a response to a real-world problem observed in small-scale poultry farming.

Our mission is to improve the quality of life of animals through innovative, affordable, and scalable solutions. Our vision is to become a recognized provider of assistive technologies in animal care, expanding from niche applications to broader markets.

Reway operates at the intersection of technology, empathy, and entrepreneurship, positioning itself within the growing field of sustainable and socially responsible innovation.

2. Technology / Product / Service Description

The development of the Reway prosthesis is based on an interdisciplinary approach and the application of advanced digital manufacturing technologies. The concept emerged through a structured process that included research, expert consultations, and iterative practical testing.

The core product is a 3D-printed prosthetic leg designed for injured chickens, as shown in Figure 1. The prosthesis is produced using a combination of 3D scanning technologies and digital modeling. Limb geometry and dimensions are captured either through dedicated 3D scanners or mobile-based scanning applications, ensuring accessibility and scalability of the solution.

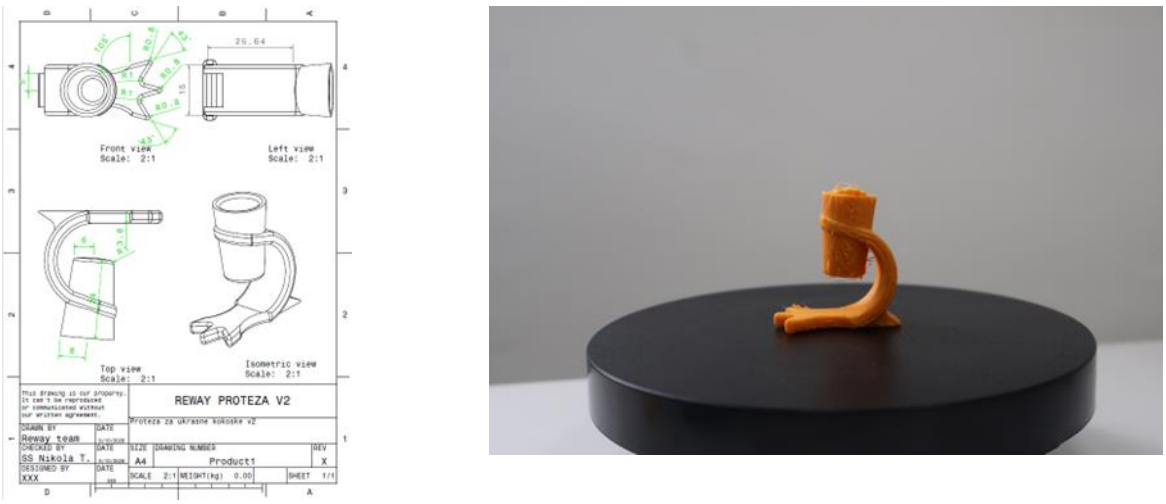


Figure 1. ReWay prosthesis design (left image) and functional prototype – right image (3D-printed structure, flexible interface, and silicone attachment system).

Manufacturing is carried out through additive production (3D printing) within a makerspace environment (Makers Lab), using PLA and PETG filaments. These materials were selected due to their optimal balance between mechanical strength, lightweight structure, and durability in outdoor conditions. PLA enables high-precision fabrication of structural components, while PETG enhances flexibility and impact resistance, which is critical for long-term prosthesis performance.

A key innovation lies in the attachment system between the prosthesis and the limb. The connection is achieved using high-consistency condensation silicone combined with an activator, allowing secure fixation while maintaining user comfort and minimizing pressure on biological tissue. This approach ensures both stability and adaptability, which are essential for functional mobility and animal welfare.

The development process included three prototype iterations:

- Prototype 1: Basic structure – initial concept validation
- Prototype 2: Improved stability – enhanced support and balance
- Prototype 3: Optimized design – comfort, durability, and usability

This iterative approach ensured continuous improvement based on functional testing.
The engineering design of the Reway prosthesis integrates principles of biomechanics, material science, and digital fabrication. Special attention is given to load distribution, balance, and movement efficiency, ensuring that the prosthesis supports natural locomotion patterns in poultry.
From a biomechanical perspective, the prosthesis is designed to minimize stress concentrations and prevent secondary injuries. The modular design allows rapid customization and replacement, while the use of accessible manufacturing technologies ensures cost-effectiveness and scalability.

3. Innovation and Competitive Advantage

Reway's key innovation lies in combining simplicity, affordability, and real-world applicability. Unlike existing solutions, which are rare or non-standardized, ReWay offers a structured and scalable product.
Competitive advantages include:

- Low production cost with high value
- Customizable design using digital tools
- Rapid prototyping and iteration capability
- First-mover advantage in a niche market

Additionally, the product is designed for ease of use, requiring no specialized tools or expertise for installation.

4. Market Application and Impact

The primary target market includes small-scale poultry farmers, hobby breeders, and animal enthusiasts. While niche, this market is globally distributed and steadily growing.
ReWay's solution has both economic and social impact:

- Reduces financial losses for farmers
- Improves animal welfare
- Promotes sustainable practices
- Encourages responsible animal care

ReWay is not only a manufacturer of poultry prosthetics. It represents a new pathway toward more humane, sustainable, and economically resilient agriculture. Our mission is clear: to enable injured poultry to regain mobility and continue their life cycle, while helping farmers preserve the value of their livestock and long-term investment. In regions such as Serbia, where family-owned farms form the backbone of the agricultural sector, the loss of even a single animal can have significant economic and emotional impact. Traditionally, such cases have often resulted in culling due to the lack of viable alternatives. ReWay introduces a practical and scalable solution that challenges this paradigm. By combining accessibility, affordability, and technological innovation, we provide farmers with a new option, one that aligns animal welfare with economic sustainability.

The product is highly scalable due to the flexibility of 3D printing technology, allowing expansion into new regions and applications.

5. Partnerships and Outlook

Reway is open to collaborations with educational institutions, innovation centers, veterinary experts, and agricultural organizations.
Future development includes:

- Expansion to other animal prosthetics
- Product optimization through further testing
- Market expansion to the EU
- Development of a broader assistive product line

The long-term goal is to position Reway as a leader in accessible animal care solutions through continuous innovation and strategic partnerships.

Acknowledgements

We acknowledge the support of our mentors, school, and innovation lab, as well as all contributors who participated in the development and testing of the prototypes.

ELECTRONICS

RF, Antennas, and Electronic Circuit Design

A Cylindrical Dielectric Lens–Loaded Microstrip Patch Antenna With Enhanced Gain for 3.5-GHz Sub-6-GHz 5G

Tarlan Mahouti[1], Hakan Yılmazer[1], Mehmet Ali Belen[2]

1 Department of Metallurgical and Materials Engineering, Yildiz Technical University, Istanbul, Turkey, tarlan.mahouti@std.yildiz.edu.tr, 0000-0001-5178-4878, hakanyil@yildiz.edu.tr, 0000-0001-5602-4966

2 Department of Electrical and Electronics Engineering, İskenderun Technical University, İskenderun, Turkey, mali.belen@iste.edu.tr, 0000-0001-5588-9407

Corresponding author: tarlan.mahouti@std.yildiz.edu.tr

Abstract

A rectangular microstrip patch antenna operating at 3.5 GHz for sub-6-GHz 5G applications is presented, together with a simple and low-profile gain-enhancement technique based on a cylindrical dielectric lens. The antenna is designed on an FR-4 substrate and is first characterized without the lens to establish a reference radiation performance. A dielectric lens is then positioned approximately one wavelength above the patch aperture to improve the wavefront collimation and radiation directivity. Full-wave simulations and experimental measurements show that the proposed lens-loaded configuration increases the broadside gain from 6.48 dBi to 9.78 dBi, while reducing the half-power beamwidth from 93° to 63°, indicating a significant improvement in spatial focusing. The input matching at the operating frequency is also enhanced, with the measured $|S_{11}|$ improving from better than 15 dB for the reference antenna to better than 30 dB when the dielectric lens is applied. In addition, the sidelobe level is slightly reduced, contributing to a cleaner radiation pattern. Thanks to its simple geometry, low cost, and ease of integration, the proposed dielectric-lens-loaded microstrip antenna provides a practical solution for improving radiation performance in compact sub-6-GHz 5G front-end systems.

Keywords: Microstrip antenna, cylindrical dielectric lens, gain enhancement, 5G, Sub-6GHz, return loss, angular width, side lobe level, SDG 9 Industry, Innovation and Infrastructure, SDG 11 Sustainable Cities and Communities

1. Introduction

The rapid deployment of fifth-generation (5G) wireless systems has created a strong demand for compact, high-performance antennas operating in the sub-6-GHz spectrum, particularly around the 3.5-GHz band [1]. In this frequency range, antenna gain and radiation directivity are critical for improving link budget and system performance in multipath environments. Although microstrip patch antennas are widely used due to their low profile, low cost, and ease of integration, they inherently suffer from limited gain and broad radiation patterns [2]. Several gain-enhancement techniques, including antenna arrays, electromagnetic band-gap (EBG) structures, artificial magnetic conductors (AMCs), parasitic elements, and metasurfaces, have been reported. However, these approaches often introduce increased design complexity, additional losses, or reduced bandwidth, limiting their practicality. As an alternative, dielectric lens loading provides a simple and effective method to enhance antenna directivity without modifying the feed network [3].

Dielectric lenses improve performance by reshaping the phase front of radiated waves into a more collimated beam, increasing the effective aperture. While various geometries have been explored, many are bulky or optimized for higher-frequency applications [4]. In contrast, cylindrical dielectric lenses offer a simpler and more practical solution for sub-6-GHz systems. In this work, a 3.5-GHz rectangular microstrip patch antenna is designed and experimentally characterized, and a cylindrical dielectric lens is employed to enhance its radiation performance. The results demonstrate improved gain and directivity while maintaining good impedance matching and a compact structure, making the proposed design suitable for sub-6-GHz 5G applications.

2. Materials and Methods

The geometry of the proposed microstrip patch antenna is shown in Fig. 1(a)–(b), where the three-dimensional structure, top metallization layout, and the corresponding dimensional parameters are illustrated. The antenna is fabricated on an FR-4 substrate with a thickness of 1.6 mm, relative permittivity $\varepsilon_r = 4.4$, and loss tangent $\tan\delta = 0.02$. The metallization consists of a copper patch and feed line printed on the top side of the substrate, while a continuous ground plane is placed on the opposite side.

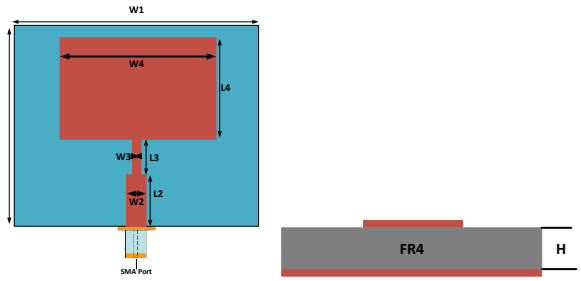


Fig. 1. *Geometry of the proposed microstrip patch antenna: (a) Three-dimensional view of the antenna structure on FR-4 substrate, (b) Top-layer layout showing the rectangular patch, inset-fed microstrip line, and SMA excitation,*

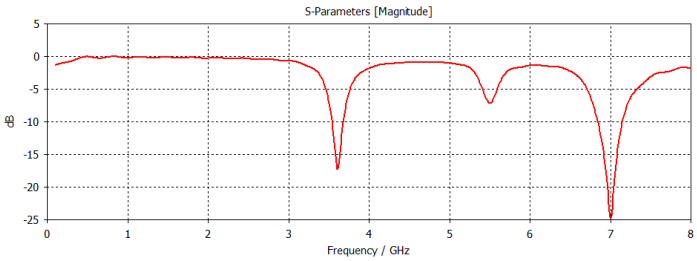


Fig. 2. *Simulated reflection coefficient (S_{11}) of the reference microstrip patch antenna*

2.2. Antenna with Dielectric Lens Integration

After characterizing the reference microstrip patch antenna, a cylindrical dielectric lens is introduced to enhance its radiation performance. The lens is positioned above the patch center, aligned with the main radiation direction, at a distance of approximately one free-space wavelength. This spacing allows the radiated waves to expand before entering the lens, enabling effective beam focusing. Without the lens, the antenna radiates over a wide angular region, resulting in limited gain. The lens-integrated configuration, illustrated in Fig. 3 along with its geometrical parameters; $\mathbf{R_1}$: Inner radius of the lens = 30 mm, $\mathbf{R_2}$: Outer radius of the lens = 35 mm, **G**:

Front gap thickness = 5 mm and **T**: Lens length (axial thickness) = 50 mm. modifies this behavior by focusing the radiated electromagnetic waves along the boresight direction. Consequently, the radiation pattern becomes more concentrated in the forward direction, leading to an increase in peak gain and directivity. Compared to the reference antenna, the lens-loaded design produces a narrower and more focused main beam. This improvement confirms that the dielectric lens effectively reshapes and redirects the radiated energy toward the broadside direction. Importantly, this enhancement is achieved without altering the antenna feed or radiating element, making the approach simple and easily applicable to existing antenna designs.

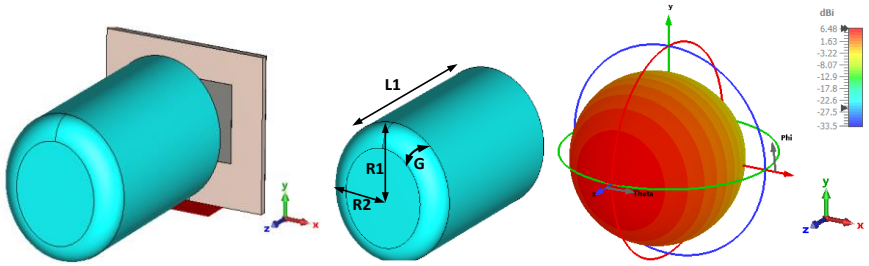


Fig. 3. *Dielectric lens–loaded microstrip antenna and its 3D radiation pattern*

Table 2. Comparison of simulated and measured performance of the antenna with and without dielectric lens

Parameter	**Microstrip Antenna (Simulated)**	**Microstrip Antenna (Measured)**	**Lens Antenna (Simulated)**	**Lens Antenna (Measured)**
S_{11} (dB)	< -15	-14.5	< -30	-28.3
Gain (dBi)	6.48	6.2	9.78	9.4
HPBW (°)	93	95	63	65
Sidelobe Level (dB)	−13	−12.5	−15	−14.7

4. Conclusions

This paper presented a compact microstrip patch antenna operating at 3.5 GHz for sub-6-GHz 5G applications, together with a simple gain-enhancement approach based on a cylindrical dielectric lens. The reference antenna was first designed and optimized to provide stable impedance matching and a reliable radiation baseline. By integrating the dielectric lens in front of the patch antenna, a clear improvement in radiation performance was achieved. The peak gain increased from about 6.48 dBi to 9.78 dBi in simulation and from 6.2 dBi to 9.4 dBi in measurement, while the half-power beamwidth was reduced from approximately 93° to 63°. At the same time, the sidelobe level was slightly improved, and good impedance matching was preserved at the operating frequency. The results demonstrate that the cylindrical dielectric lens effectively focuses the radiated electromagnetic waves, leading to higher directivity and better radiation efficiency without increasing antenna complexity or requiring changes to the feeding structure. Due to its simple geometry, low cost, and ease of

integration, the proposed lens-loaded antenna is a practical and efficient solution for sub-6-GHz 5G front-end and Access point applications.

Acknowledgements

This work was supported in part by The Scientific and Technological Research Council of Türkiye (TÜBİTAK) under the 1002-A Rapid Support Program, contract number 125E822.

References

[1] S. Zeb, N. Fnu, M. Fahad, M. U. Qayyum, and N. Abbasi, “Enhancing diagnostic accuracy for medical imaging and radiology with AI-driven synergy tools: Enabling early intervention and preventive measures through early detection of cardiovascular conditions,” Eur. J. Sci. Innov. Technol., vol. 4, no. 4, pp. 38–47, 2024.

[2] L. L. Cao, Z. Chen, Z. Yue, L. Pei, M. Jia, H. Wang, and T. Li, “Novel classifiers with clinical laboratory parameters for early detection of osteosarcoma,” J. Clin. Lab. Anal., vol. 34, no. 5, pp. e23189, 2020, doi: 10.1002/jcla.23189.

[3] C. Ricciardi et al., “A health technology assessment between two pharmacological therapies through Six Sigma: The case study of bone cancer,” TQM J., vol. 32, no. 6, pp. 1507–1524, 2020, doi: 10.1108/TQM-01-2020-0013.

[4] M. Alibakhshikenari et al., “Metamaterial-inspired antenna array for application in microwave breast imaging systems for tumor detection,” IEEE Access, vol. 8, pp. 174667–174678, 2020, doi: 10.1109/ACCESS.2020.3025672.

Mathematical Model of a Ring-Based Digitally Controlled Oscillator for Frequency Range and Resolution Prediction

Đorđe Gačić[1], Lazar Ilić[2], Dejan Petković[3], Vladimir Milovanović[4]

[1234]*Center for Integrated Systems, Department of Electrical Engineering and Computer Sciences Faculty of Engineering, University of Kragujevac, Kragujevac, Serbia*

[1]djordje.gacic@kg.ac.rs, 0009-0006-8461-2048, [2]lazar@uni.kg.ac.rs, 0009-0002-7748-2960, [3]deki@kg.ac.rs, 0009-0008-5528-6962, [4]vlada@kg.ac.rs, 0000-0002-6787-4058

Corresponding author: djordje.gacic@kg.ac.rs

Abstract

This paper presents a compact mathematical model that accurately predicts the oscillation frequency of a ring-based digitally controlled oscillator (DCO) across its entire tuning range while requiring only a minimal set of simulations. The model accounts for coarse frequency tuning via current starving, which yields a linear frequency-code relationship, and for one or more fine tuning stages using capacitive modulation, whose nonlinear behavior is linearized locally around the mid-range coarse code. For a single coarse stage and *M* fine stages, only $2\cdot(M+1)$ simulated frequency values are sufficient to define the full model. The approach is validated on a DCO designed in 180nm CMOS technology with one coarse and two fine tuning stages, covering 5832 tuning points with only six simulations. The model is implemented in Python and shows close agreement with EDA simulation results.

Keywords: digitally controlled oscillator; mathematical model; frequency tuning; current starving; capacitive modulation; CMOS; EDA simulation; UN SDG 9.

1. Introduction

Most systems on a chip (SoCs) require extensive simulation prior to fabrication and measurement. However, EDA-based simulations are often time- and hardware-intensive. Therefore, it is convenient to develop a software-based mathematical model (e.g., implemented in Python) that captures the system behavior. Such a model enables significantly faster prediction of system performance with minimal loss of accuracy.

This paper presents such a model for a ring-based digitally controlled oscillator (DCO), the core component of digital clock generation systems such as PLLs [1] and FLLs [2]. The DCO converts a digital input control code into a precise output clock frequency, with the oscillation frequency given by:

$$f = \frac{I_D}{2 \cdot N \cdot C_{load} \cdot V_{DD}} \tag{1}$$

From (1), the oscillation frequency can be tuned by adjusting the following parameters [3]: number (N) of (inverting) delay elements within ring, i.e., taps (tap number adjustment); current (I_D) flowing through the tap (current starving); capacitive load (C_{load}) of the tap (capacitive modulation); supply voltage (V_{DD}).

Frequency resolution is defined as the frequency change obtained when the input control code changes by one least significant bit (LSB). Higher resolution (i.e., a smaller increment) enables more accurate synthesis of the desired output frequency. In practice, tap number adjustment and current starving are typically used for coarse frequency tuning, while capacitive modulation and power supply tuning are better suited for fine tuning [4].

2. Mathematical analysis

The DCO considered in the following mathematical model employs current starving for coarse frequency tuning [1–4], while capacitive modulation is used for fine tuning [4], [5]. The coarse tuning network primarily determines the overall output frequency range. However, improving resolution using only current starving typically increases power consumption and silicon area. Therefore, fine tuning is used to enhance resolution by subdividing each coarse-tuning step across the available fine-tuning range. This range can be further partitioned by introducing additional fine tuning stages, yielding smaller effective frequency steps. In practice, more than two or three fine tuning stages are seldom needed, and a single stage is often sufficient to meet the required specifications.

Since (1) implies that the oscillation frequency is directly proportional to the current, coarse tuning via current starving leads to an approximately linear frequency dependence on the coarse control code (d_{coarse}), where d_{coarse} is an integer that increases in unit steps.

$$f(d_{coarse}) = f_0 + d_{coarse} \cdot \Delta f_{coarse}, \quad d_{coarse} \in \mathbb{N}_0,$$

where f_0 denotes the base oscillation frequency independent of the coarse control code. The coarse frequency step will be constant over the whole tuning range, and therefore over the total frequency range of the DCO:

$$\Delta f_{coarse} = \frac{f(d_{coarse,max}) - f(d_{coarse,min})}{d_{coarse,max} - d_{coarse,min}}.$$

When (M) fine tuning stages are employed in addition to coarse tuning, the oscillation frequency is additionally determined by the applied input control code for each fine tuning stage:

$$f\left(d_{coarse}, d_{fine_1}, d_{fine_2}, \dots, d_{fine_M}\right) = f(d_{coarse}) + \sum_{i=1}^{M} d_{fine_i} \cdot \Delta f_{fine_i}\left(f(d_{coarse})\right), \quad d_{fine_i} \in \mathbb{N}_0.$$

Because the capacitive load varies inversely with the oscillation frequency, the fine tuning step is nonuniform across the overall tuning range. However, for a fixed coarse tuning code it may be treated as approximately constant and determined by the oscillation frequency corresponding to that coarse step [4]:

$$\Delta f_{fine_i}\left(f(d_{coarse})\right) = k_{fine_i} \cdot f(d_{coarse}), \quad k_{fine_i} \in \mathbb{R}^+,$$

where k_{fine_i} is a stage-specific coefficient for the i-th fine tuning stage and should be calculated using simulation results typically taken near the middle of tuning range (or at application-relevant frequencies), since the model achieves its highest accuracy in the region used for this coefficient calculation.

$$k_{fine_i} = \frac{f_{cf,mid;fine_i,max} - f_{cf,mid;fine_i,min}}{d_{fine_i,max} - d_{fine_i,min}} \cdot f_{cf,mid;fine_i,min},$$

$$f_{cf,mid;fine_i,min} = f\left(d_{coarse,mid}, d_{fine_1,mid}, \dots, d_{fine_{i-1},mid}, d_{fine_i,min}, d_{fine_{i+1},min}, \dots, d_{fine_M,min}\right),$$

$$f_{cf,mid;fine_i,max} = f\left(d_{coarse,mid}, d_{fine_1,mid}, \dots, d_{fine_{i-1},mid}, d_{fine_i,max}, d_{fine_{i+1},min}, \dots, d_{fine_M,min}\right),$$

$$d_{\{coarse,fine\},mid} = \left\lfloor \frac{d_{\{coarse,fine\},max}}{2} \right\rfloor.$$

As indicated by the mathematical analysis, predicting the frequency for all control codes requires first extracting (via EDA simulations) the frequencies at two control code points per tuning stage: $f\left(d_{coarse,min}\right)$ and $f\left(d_{coarse,max}\right)$ for the coarse tuning stage, and $f_{cf,mid;fine_i,min}$ and $f_{cf,mid;fine_i,max}$ for each fine tuning stage. Thus, for a DCO with one coarse stage and *M* fine stages, a total of *2·(M+1)* control code combinations must be simulated to parameterize the model over the frequency range and resolution.

3. Implementation and results

Fig. 1 illustrates the modeled oscillation frequency and period versus input control code for a DCO implemented in a baseline 180 nm CMOS technology, featuring one coarse tuning stage (18 steps) and two fine tuning stages (18 steps each). This results in 18·18·18=5832 tuning points. However, rather than running a separate time-consuming simulation for every point, only six simulations (two per tuning stage, as summarized in Table 1) are sufficient to parameterize the proposed mathematical model and predict DCO behavior across the full tuning range. Simulations are performed at the typical PVT (process-voltage-temperature) corner after RCC-type parasitic extraction. The resulting frequency resolution is 32.2 MHz for coarse tuning, 2.87 MHz for the first fine tuning stage (at coarse code 9), and 0.22 MHz (LSB resolution) for the second fine tuning stage (at coarse and first fine codes equal to 9). The model is implemented in Python.

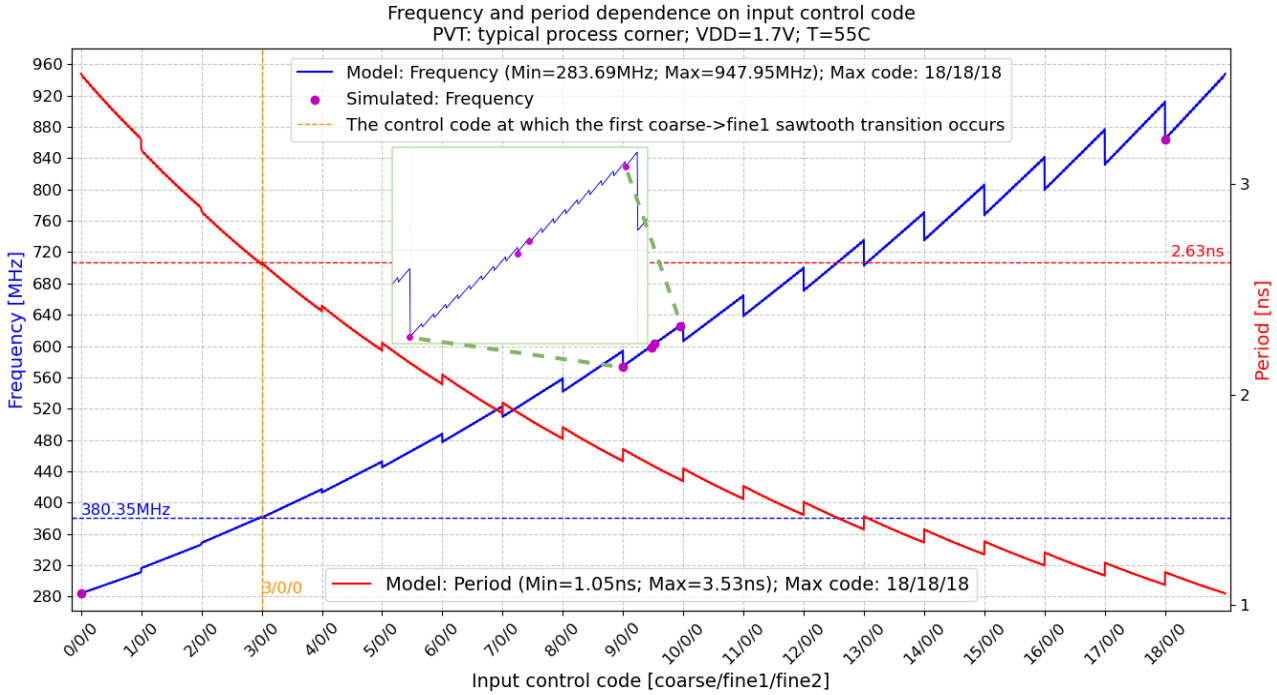


Figure 1. Modeled oscillation frequency and period versus input control code.

Table 1. Simulated frequency values and calculated model constants.

Notation: $f_{coarse,fine1,fine2}$	Simulated frequency [MHz]	Calculated model constants
$f_{0,0,0} \Leftrightarrow f(d_{coarse,min})$	283.7	$\Delta f_{coarse} = \frac{f_{18,0,0} - f_{0,0,0}}{18 - 0} = 32.2\ MHz$
$f_{18,0,0} \Leftrightarrow f(d_{coarse,max})$	863.7	
$f_{9,0,0} \Leftrightarrow f_{cf,mid;fine_1,min}$	573.6	$k_{fine_1} = \frac{f_{9,18,0} - f_{9,0,0}}{18 - 0} \cdot f_{9,0,0} = 1647.5$
$f_{9,18,0} \Leftrightarrow f_{cf,mid;fine_1,max}$	625.3	
$f_{9,9,0} \Leftrightarrow f_{cf,mid;fine_2,min}$	598.7	$k_{fine_2} = \frac{f_{9,9,18} - f_{9,9,0}}{18 - 0} \cdot f_{9,9,0} = 136.37$
$f_{9,9,18} \Leftrightarrow f_{cf,mid;fine_2,max}$	602.8	

4. Conclusions

This paper presented a mathematical model for predicting the DCO output frequency across its whole tuning range. The model exploits the linear frequency dependence on the coarse control code arising from the current starving mechanism, combined with a locally linearized description of each capacitive-modulation fine tuning stage. The key advantage of the approach is its efficiency: for a DCO with one coarse stage and *M* fine stages, only *2·(M+1)* EDA simulations are required. Future work will extend the model to include jitter predictions [6], validate against measurement results, and incorporate it within a significantly more complex digital PLL model.

Acknowledgements

Research partially funded by the grant agreement number: 451-03-34/2026-03/200107 from February 5, 2026.

References

1. Tierno JA, Rylyakov AV, Friedman DJ. A Wide Power Supply Range, Wide Tuning Range, All Static CMOS All Digital PLL in 65 nm SOI. IEEE J Solid-State Circuits 2008;43:42–51.
2. Petković DD, Gačić ĐS, Božović MRG, Milovanović VM. A Synthesizable Digital Frequency-Locked Loop Widely Tunable up to 640 MHz in 130 nm CMOS. 2024 11th International Conference on Electrical, Electronic and Computing Engineering (IcETRAN), Nis, Serbia: IEEE; 2024, p. 1–6.
3. Gačić ĐS, Petković DD, Milovanović VM. Coarse Tuning Mechanisms in CMOS Standard-Cell Library Ring-Based Digitally Controlled Oscillators. 2025 12th International Conference on Electrical, Electronic and Computing Engineering (IcETRAN), Cacak, Serbia: IEEE; 2025, p. 1–6.
4. Gačić ĐS, Petković DD, Milovanović VM. Resolution Increase in Digitally Controlled Ring Oscillators Using Standard-Cell-Based Varactors. 2025 IEEE 34th International Conference on Microelectronics (MIEL), Nis, Serbia: IEEE; 2025, p. 1–4.
5. Pao-Lung Chen, Ching-Che Chung, Chen-Yi Lee. A portable digitally controlled oscillator using novel varactors. IEEE Trans Circuits Syst II 2005;52:233–7.
6. Milovanovic V, Nikolic B. An HDL model of a digitally controlled oscillator for rapid digital PLL prototyping. 2017 IEEE 30th International Conference on Microelectronics (MIEL), Nis: IEEE; 2017, p. 205–8.

Embedded Electronics and Sensor Systems

Arduino Temperature Monitoring System

Luka Virijević[1], Tijana Dimitrijević[2], Milan Čabarkapa[3]

[1]*Faculty of Engineering, University of Kragujevac, Kragujevac, Serbia, lukavirijevic2609@gmail.com*

[2]*Faculty of Engineering, University of Kragujevac, Kragujevac, Serbia, tijana.dimitrijevic@uni.kg.ac.rs, and Faculty of Electronic Engineering, University of Niš, Niš, Serbia, tijana.dimitrijevic@elfak.ni.ac.rs, ORCID: 0000-0002-9744-8287*

[3]*Faculty of Engineering, University of Kragujevac, Kragujevac, Serbia, mcabarkapa@uni.kg.ac.rs, ORCID:* 0000-0003-3759-5696

Corresponding author*: tijana.dimitrijevic@uni.kg.ac.rs*

Abstract

This paper presents the practical development of an embedded system for real-time temperature monitoring and intelligent cooling control based on the Arduino microcontroller platform. The primary objective of the work was to design a simple, reliable, and cost-effective system capable of continuously measuring ambient temperature, providing visual and acoustic alerts when a critical temperature threshold is exceeded, and automatically activating a cooling mechanism. In addition to the system functionality, an analysis of key performance parameters was conducted.

Keywords: Arduino; embedded systems; temperature monitoring; DHT11 sensor; PWM control; smart cooling system, UN SDG 9

1. Introduction

Temperature monitoring and control play a crucial role in many technical systems. Excessive temperature increases may lead to degradation of electronic components, reduced system efficiency, or even equipment failure [1].

The availability of affordable microcontroller platforms such as Arduino has enabled the development of simple monitoring systems that can be implemented in a wide range of applications [2].

The main objective of this work was to develop a compact system capable of real-time temperature measurement, user-defined temperature threshold adjustment, visual and acoustic alarm signaling when the temperature exceeds the threshold and automatic activation of a cooling mechanism. The system utilizes a DHT11 digital temperature sensor [3] to measure ambient temperature, while the measured values are displayed on an LCD module with an I2C interface. The user can adjust the temperature threshold using control buttons, allowing flexible system configuration depending on operational conditions. When the measured temperature exceeds the predefined threshold, an audible alarm (buzzer) and visual indicators through LEDs and an RGB module are activated. In addition, the system includes the control of a DC motor simulating a cooling fan. The

fan speed can be regulated using a PWM (Pulse Width Modulation) signal generated by the Arduino microcontroller, enabling energy-efficient cooling control depending on the difference between the measured temperature and the threshold value. The software architecture of the system relies on interrupt-driven programming, where interrupt routines are used for handling user input, while timer interrupts are employed for periodic sensor readings and display updates [2].

The developed system represents a simple yet effective solution for temperature monitoring and cooling control that can be applied in smart home systems, laboratory environments, educational projects, and basic industrial monitoring applications.

2. Methodology and Work Performed

The implementation of the system consisted of both hardware and software development. The hardware configuration includes the following components: Arduino microcontroller board, DHT11 digital temperature sensor, LCD display with I2C interface, RGB LED module, buzzer for acoustic signaling, DC motor representing a cooling fan, control buttons used for adjusting the temperature threshold.

The software was developed using the Arduino development environment [2]. The program logic is based on periodic temperature readings, comparison with the predefined threshold, and activation of the corresponding output devices.

Interrupt routines are used for handling button inputs with software debounce protection, while timer interrupts are implemented to perform periodic updates of the temperature readings and LCD display.

Fig. 1. presents the practical implementation of the developed temperature monitoring system.

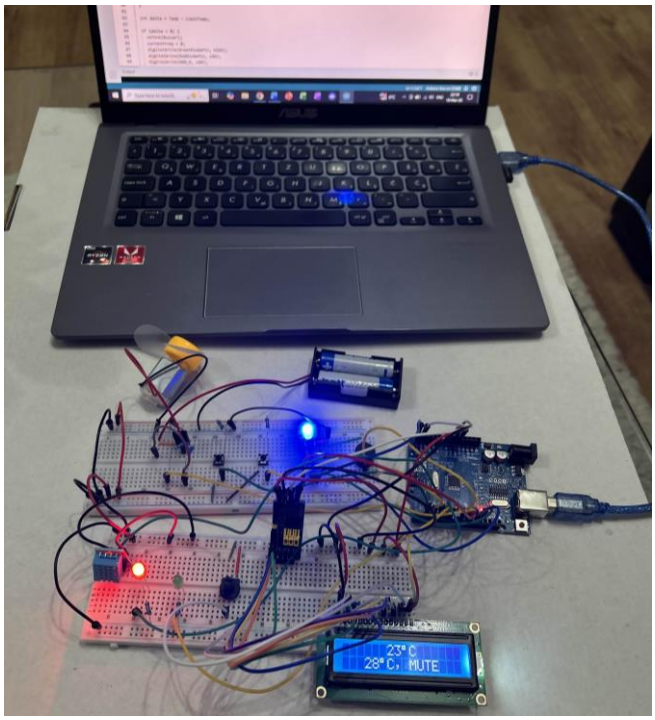


Fig. 1. Physical implementation of the developed temperature monitoring system.

3. Results and Discussion

In this section, an analysis of system performance parameters is presented. For this purpose, several testing scenarios were conducted to evaluate the accuracy, response time, control performance, and power consumption of the system. The DHT11 sensor has a response time of approximately 2 seconds for temperature changes, with a sampling rate of about 1 Hz, meaning it provides one measurement per second [1]. The measurement accuracy is around $\pm$ 2 °C [1]. It was verified that the system activates the alarm precisely at the predefined temperature threshold without significant delay. The fan speed is controlled using a PWM signal with a frequency of approximately 490 Hz (Arduino Uno), where the duty cycle (0–255) effectively regulates the motor speed. The overall power consumption of the system is relatively low: the DHT11 sensor consumes about 0.3–1.5 mA during operation [1], while a DC motor of type R130 (3 V) has a nominal current consumption of approximately 200 mA during operation, with a maximum speed of about 12000 RPM. In practice, the current may briefly increase during startup, reaching up to 300–400 mA. This motor represents the dominant power consumer in the system. Therefore, the total system current consumption ranges approximately from 200 mA to 450 mA depending on the operating conditions and fan speed. To ensure reliable motor control, a transistor-based switching circuit using a PNP transistor was implemented. The transistor enables control of higher motor currents using a low-power control signal from the microcontroller. Additionally, a flyback diode is connected in parallel with the motor to protect the circuit from voltage spikes caused by the inductive nature of the motor. This configuration improves system reliability and prevents potential damage to electronic components.

The developed system demonstrates that a functional temperature monitoring solution can be implemented using relatively simple and affordable electronic components. The system enables early detection of temperature increases and automatic activation of a cooling mechanism, which contributes to improved reliability and safety of technical systems. The proposed solution represents a practical demonstration of the capabilities of low-cost microcontroller platforms in real-world monitoring applications. Potential applications include smart home monitoring systems, laboratory experiments, educational embedded systems projects, basic industrial monitoring systems.

The developed system successfully demonstrates stable and reliable operation in real-time temperature monitoring and automated response mechanisms. The implemented solution integrates sensing, processing, and actuation functionalities within a single embedded platform, achieving the following key results:

- Continuous and stable measurement of ambient temperature using the DHT11 digital sensor, with periodic sampling ensuring reliable and consistent data acquisition.
- Real-time visualization of both the measured temperature and user-defined threshold values on an LCD display, providing clear and intuitive feedback to the user.
- Dynamic adjustment of the temperature threshold via push buttons, implemented using interrupt-based input handling with software debounce, ensuring accurate and noise-resistant user interaction.

- Adaptive acoustic signaling using a buzzer, where different sound frequencies are generated depending on the temperature deviation from the threshold, allowing the user to distinguish between different levels of critical conditions.
- Visual feedback through LED indicators and an RGB module, enabling intuitive representation of system states (normal operation, warning, and critical conditions).
- Automatic activation of a DC motor acting as a cooling fan when the measured temperature exceeds the predefined threshold, ensuring timely system response.

In addition to basic ON/OFF control, the system supports PWM-based control of the cooling fan, enabling gradual regulation of its speed. This allows the system to respond proportionally to the temperature difference, improving energy efficiency and reducing unnecessary power consumption. Experimental testing has shown that the system operates reliably under varying temperature conditions, with consistent sensor readings, stable display updates, and correct triggering of both visual and acoustic alerts. The PWM-based fan control further enhances system performance by providing smoother transitions in cooling intensity, avoiding abrupt changes in operation.

4. Conclusions and Outlook

This paper presented the development of an embedded system for real-time temperature monitoring and automatic cooling control based on the Arduino platform. The system enables reliable temperature measurement, user-defined threshold adjustment, and timely activation of a cooling mechanism under critical conditions. The integration of PWM-based control allows adaptive fan operation, improving energy efficiency and overall system performance compared to simple ON/OFF control. Experimental results confirmed stable operation, accurate sensor readings, and reliable system response to temperature changes. Future work may include the integration of IoT communication for remote monitoring, implementation of advanced control algorithms, and the use of more precise sensors.

Acknowledgements

This work has been supported by the Ministry of Science, Technological Development and Innovation of the Republic of Serbia [Grant Number: 451-03-34/2026-03/200107].

References

1. https://www.mouser.com/datasheet/2/758/DHT11-Technical-Data-Sheet-Translated-Version-1143054.pdf?srsltid=AfmBOoqLLh8ms-8hYko1munGs6rFFH7Um5llJoakVPhYLghJtnoAi6zm accessed on March 17, 2026

2. Banzi M, Shiloh M. Getting Started with Arduino. 3rd ed. Sebastopol: O'Reilly Media; 2014.

3. M. H. Rashid, *Power Electronics: Circuits, Devices and Applications*, 4th ed., Pearson, 2014.

Digital Communication and Signal Processing

Equalization and Carrier Recovery for Downstream Data Over Cable Service Interface Specification (DOCSIS) 3.0 Modems

Dejan Rakić, Milan Čabarkapa, Vladimir Milovanović

Department of Electrical Engineering and Computer Sciences, Faculty of Engineering – University of Kragujevac, rakic.dejan@gmail.com, 0009-0006-1041-7194, mcabarkapa@kg.ac.rs, 0000-0002-2094-9649

Corresponding author: vlada@kg.ac.rs, *0000-0002-6787-4058*

Abstract

Data Over Cable Service Interface Specification (DOCSIS) version 3.0 cable modem standard is released in 2006 by CableLabs. The standard introduced new concept of multiple channels receiving on downstream (broadcasting), upstream packet-based link for user interfacing as well as integrated IP6 Internet protocol. This paper shows solutions for downstream carrier recovery and equalization performed after Automatic Gain Control (AGC), matched filter and timing recovery at one sample per symbol. The sampling rate for QAM64 is $F_s = 5.12$ MHz. In general, this solution can be applied to any streaming high density QAM 64/256 with frequency offset up to 1% of symbol rate. This part of modem is integrated with other processing parts and successfully tested and approved in CableLabs.

Keywords: broadband cable modems; equalization; carrier recovery; Constant Modulus Algorithm (CMA); Decision Feedback Equalizer (DFE); high-order QAM; frequency offset compensation; FPGA; UN SDG 9

1. Introduction

This paper presents solution for high density QAM 64/256 equalization under large frequency offset for streaming receiver. This specific receiver of channel bandwidth (for North American standard) is $B = 6$ MHz with data rates at 31.2 Mbps and 41.5 Mbps for QAM 64/256 respectively which is implemented din FPGA. Simulation results and measurements in CableLabs laboratory are presented as constellation plots.

Equalization and carrier recovery operate at sampling rate $F_s = 5.06$ MHz and $F_s = 5.36$ MHz for QAM64 and QAM256 respectively (one sample per symbol). Frequency offset can be within range of ± 500 KHz. The cable channel is corrupted by micro-refection, ingress noise channel distortion, and Gaussian thermal noise [1]. Selected solution is combination of Constant Modulus Equalizer (CMA), developed by Godard [2] and Decision Feedback Equalizer (DFE). Characteristic of most CMA algorithms for QAM constellations is that expected value of Error Vector Magnitude (EVM) function doesn't go near to zero. The EVM in CMA doesn't depend on frequency offset and equalizer coefficients exhibit convergence toward steady state. Because initial frequency can be large, carrier recovery acquisition, based on reduced constellation set [3] is running simultaneously with CMA. When gradient of EVM drops below some predefined threshold, equalizer is switched to DFE mode and fine phase tracking [4].

Simulation results and field tests are presented for QAM 64/128.

2. Materials and Methods

The DFE is implemented with 36 taps Feed Forward Filter (FF) and 24 taps Feed-Backward (FB) filter to eliminate propagation channel frequency distortion and inter-symbol interference. Equalization runs in parallel with carrier recovery. The FF filter introduces 36 samples latency, which makes difficulties to compensate frequency offset just before filtering because of convergence issue. The FB filter resolves only inter-symbol interference and doesn't affect carrier recovery loop convergence. For that reason, the carrier compensation is placed right after FF filter, The FB filter is fed by difference of frequency compensated FF filter output and FB filter output.

Digital processing chain of equalizer and carrier compensation loop is depicted in Figure 1.

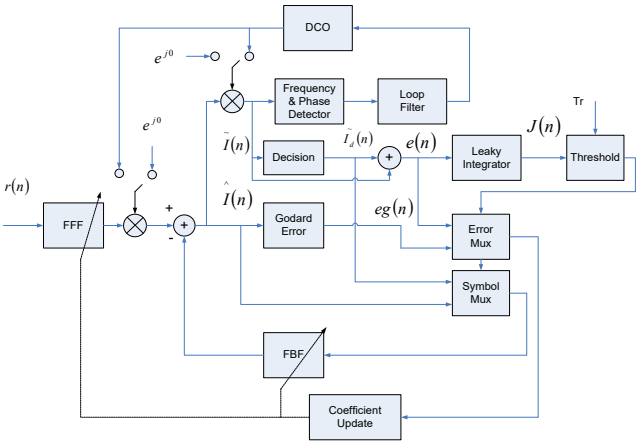


Figure 30. CMA-DFE architecture

In previous section signal detection, AGC and timing recovery are performed and start signal and samples for equalization are provided. The CMA in some sense acts as additional AGC, because the processing starts without carrier recovery for some period $0 \leq t \leq t_1$. This is important because rough phase estimator considers phase of outer constellation points as shown in Figure 2. The CMA error is defined as following

$$Err_{CMA}(n) = \hat{I}(n)\left(\left|\hat{I}(n)\right|^2 - R\right) \qquad (1)$$

where $\hat{I}(n)$ is FF equalized and frequency compensated symbol, R is constant depending on QAM64/128 [3].

During interval $t_1 \leq t \leq t_2$ carrier recovery and CMA running together. The phase in acquisition mode is estimated by outer constellation points as shown in Figure 2 [4].

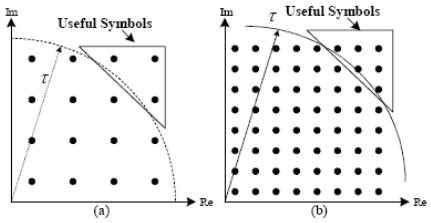


Figure 31. Rough phase estimation

In the acquisition interval locked cost function $J(n)$ defined as

$$J(n+1) = \alpha J(n) + (1-\alpha)\left|\tilde{I}(n) - I_d(n)\right| \quad (2)$$

is compared to predefined threshold, where $\tilde{I}(n)$ is equalized and $I_d(n)$ is detected symbol. At the time instance t_2 $J(t_2) < Th$, equalizer is switched to DF and phase estimation is turned to fine $arg\{\tilde{I}(n)\} - arg\{I_d(n)\}$. Error signal during DF phase is calculated as difference between equalized and detected symbol

$$Err_{DF}(n) = \tilde{I}(n) - I_d(n) \quad (3)$$

The FF and FB filter taps are updated according to LMS

$$w_{FF/FB}(n) = w_{FF/FB}(n-1) + \mu Err_{CMA/DF}(n)x(n)_{FF/FB} \quad (4)$$

where $x(n)_{FF/FB}$ are samples in FF/FB filter, μ is constant, $w_{FF/FB}(n)$ are FF and FB filter taps [5].

Figure 3 shows carrier recovery loop, sine and cosine sample values are stored for quarter period, Digitally Controlled Oscillator (DCO) is implemented as accumulator. Phase detectors

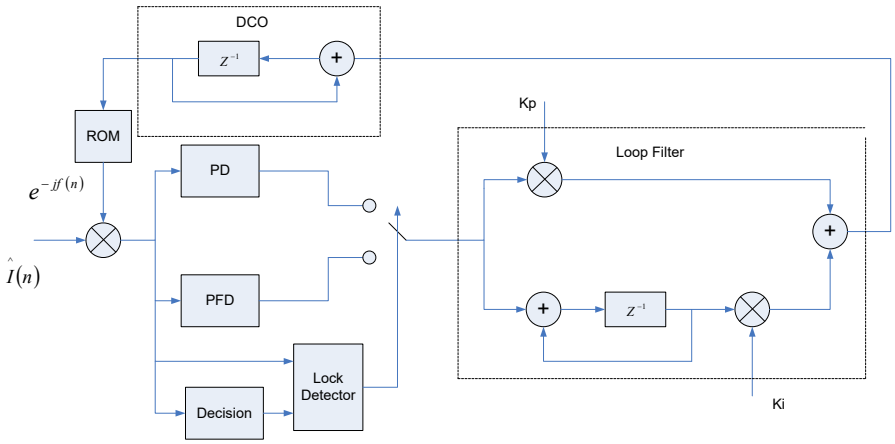


Figure 32. Dual Mode Carrier recovery

The proposed carrier recovery algorithm uses two different phase detectors to generate the estimate of the phase error. Initially in the coarse mode, a Phase Frequency Detector PFD tracks frequency error based on reduced constellation. Once locked, the phase error estimation is switched to simple decision directed phase estimation, for fine tracking.

3. Results

This section presents simulation results and measured constellation *EVM* measured in CableLabs laboratory. Simulation results are presented for channel $h = [0.04\ -0.05\ 0.07 - 0.21 - 0.5\ 098\ 0.36\ 0\ 0.21\ 0.03\ 0.07]$, frequency offset of 500 KHz, $SNR = 35\ dB$ and QAM64. Figure 4 a) shows symbols at input to equalizer b) equalized symbols respectively.

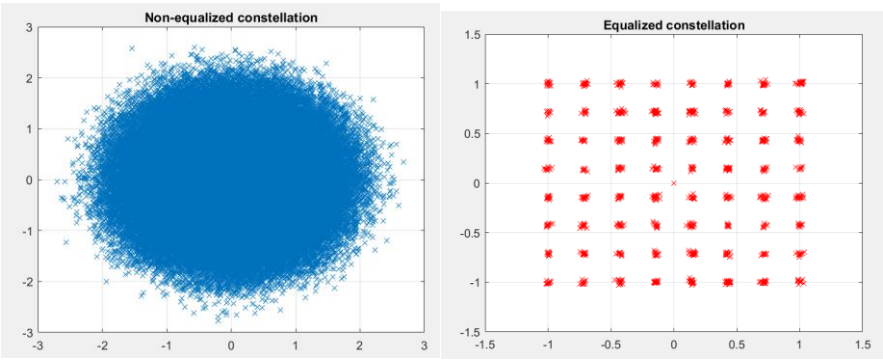


Figure 33. a) non-equalized symbols b) equalized symbols

The LC function and estimated frequency error are depicted in Figure 5.

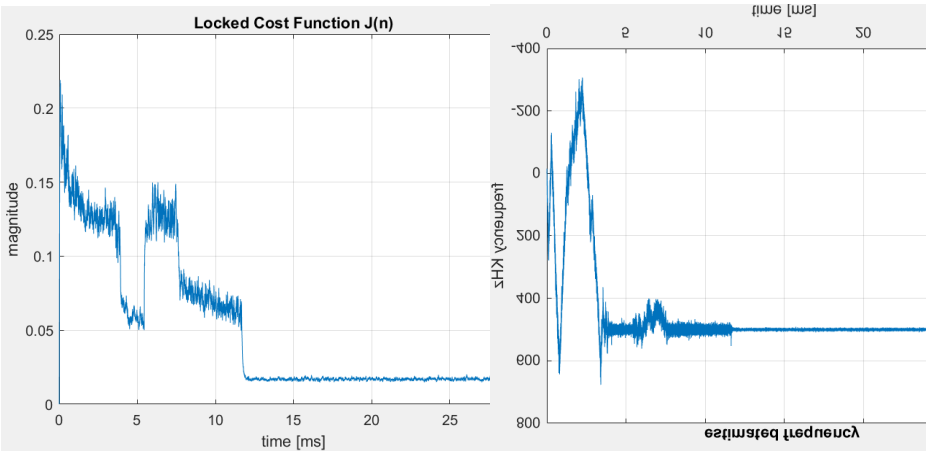


Figure 5. a) Locked Cost (LC) function b) estimated FO

The test results of captured scattered plots from CableLabs [6] of receiver demodulating QAM64/256 are shown in Figure 5.

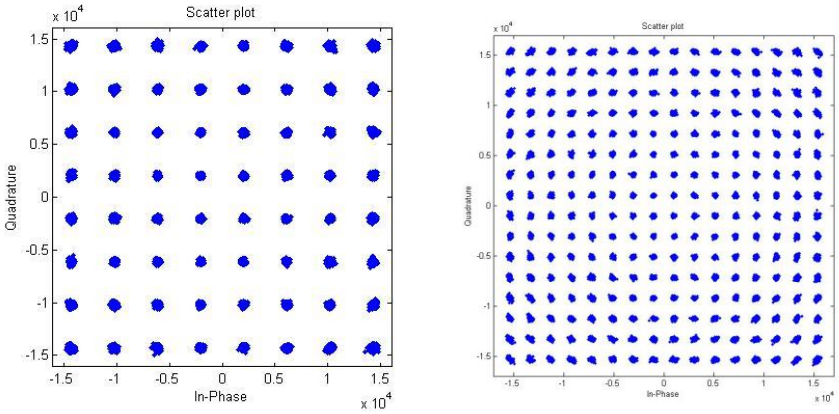


Figure 34. a) Scatter plot QAM64 b) QAM256

The official tests showed that implemented DOCSIS 3.0 downstream receiver meet standards for comertial use.

4. Discussion

DOCSIS 3.0 modem is capable to receive five downstream frequency bonded signals. The modem implementation is partitioned into three parts

- channel bonded downconverters to baseband and AGC
- Timing recovery and equalization/frequency recovery
- Error correction and user interfacing

Every partition is implemented in one Xilinx VIRTEX 5 FPGA chip. The implementation of the DOCSIS 3.0 downstream receiver demonstrates that a unified architecture combining a Constant Modulus Algorithm (CMA) and a Decision Feedback Equalizer (DFE) effectively solves the challenges of high-density QAM signals.

From algorithmic point of view the combination of standard CMA, DFE LMS equalization and frequency offset compensation are merged and sequenced time in innovative way with make whole processing robust and converging.

5. Conclusions

The design and implementation of a DOCSIS 3.0 compliant downstream receiver were successfully demonstrated. By utilizing a dual-mode approach—combining the Constant Modulus Algorithm (CMA) for robust initial acquisition and a Decision Feedback Equalizer (DFE) for steady-state tracking, the system achieves high-precision carrier recovery and equalization even under significant frequency offsets.

Testing conducted at CableLabs confirmed that the FPGA-based implementation meets all performance requirements for commercial deployment, including resilience against typical cable plant impairments like micro-reflections and thermal noise. This architecture provides a scalable solution for high-order QAM demodulation in modern broadband hardware.

The future work should be oriented toward DOCSIS 4.0 which introduced QAM4096. This puts new challenges in algorithms regarding high precision DC offset compensation, timing and frequency recovery and equalization.

Acknowledgements

This work is partially supported by the agreement on the funds transfer for financing the scientific research work of teaching staff at accredited higher educational institutions – contract number: 451-03-34/2026-03/200107 from February 5, 2026.

References

1. Ciciora W, Farmer J, Large D, Adams M. Modern Cable Television Technology: Video, Voice, and Data Communications. 2nd edition San Francisco: Morgan Kaufmann Publishers; 2004.

2. Godard D. Self-recovering equalization and carrier tracking in two-dimensional data communication systems. IEEE Transactions on Communications. 1980; 28(11):1867–1875.

3. Sari H, Moridi S. New phase and frequency detectors for carrier recovery in PSK and QAM systems. IEEE Transactions on Communications. 1988; 36(9):1035–1043.

3. Proakis JG, Salehi M. Digital Communications. 5th edition, New York: McGraw-Hill Education; 2008.

5. Haykin S. Adaptive Filter Theory. 2nd ed. Englewood Cliffs: Prentice-Hall; 1991.

6. CableLabs. Data-Over-Cable Service Interface Specifications DOCSIS 3.0: Physical Layer Specification. CM-SP-PHYv3.0-I01-060804. Louisville: Cable Television Laboratories, Inc.

Wireless Networking and Positioning

A hardware/software platform for precise client device positioning in IEEE 802.11-based Wi-Fi communication networks

Zoran Đorđević[1], Nedeljko Stefanović[1], Vladimir Milovanović[2]

[1]*Independent Researcher, Belgrade, Belgrade, Serbia, dzoran1@gmail.com, 0009-0004-6388-8550, stenedjo@gmail.com, 0000-0002-0204-4918*

[2]*Department of Electrical Engineering and Computer Sciences, Faculty of Engineering, University of Kragujevac, Serbia, vlada@kg.ac.rs, 0000-0002-6787-4058*

Corresponding author: dzoran1@gmail.com

Abstract

There are many cases where it is necessary to determine the position of one of the participants in wireless communications as precisely as possible. In this paper, we will present the proposal of one variant for the case of users of Wi-Fi-based communication. The main elements of the proposed platform are: satellite positioning and accurate time distribution system, AD9361 radio frequency (RF) Agile Transceiver integrated circuit, FPGA ZynqMP evaluation board, coordination PC with appropriate mathematical model for positioning based on accurate time and known receiver positions, support from the OPENWIFI package and OPEN GIS system for displaying on a geographical map.

Keywords: Wi-Fi; RF; Radio location; Geo location; FPGA; OFDM; Linux, 'UN SDG 4', 'UN SDG 9'.

1. Introduction

In this paper, we will try to propose a platform for determining the spatial position of participants as precisely as possible in the exchange of information that is carried out using Wi-Fi technologies. Most often, systems that use antennas with a relatively narrow radiation pattern are in use. The main beam axis of the antenna radiation pattern is somehow rotated by horizontal and/or vertical angles. These are usually mechanical displacement or some of the electronic displacement systems based on antenna arrays. This approach has certain characteristics. One of the characteristics is that the formation of a narrow angle of the radiation diagram of the receiving antenna follows the formation of side lobes next to the main beam that can introduce confusion in the non modelled problem of the selected signal processing model. Another characteristic is, in some cases, the dependence on the carrier frequency, which can cause a change in the width of the main beam of radiation. The mentioned characteristics are equally accessible with both mechanical and electronic beam rotation.

2. Main Functional Blocks

Faced with the challenge of the need to accurately determine the position, we chose an alternative approach in which we use:

Three or more sets of hardware including:

1) omnidirectional stick antenna
2) a suitable receiver as a radio frequency receiver is the proposed evaluation platform AD-FMCOMMS2-EBZ
3) unit of exact position and exact time. The u-blox RCB-F9T evaluation platform is proposed
4) Evaluation platform AMD ZCU104

One coordinating PC with appropriate Linux operating system, the appropriate mathematical model

3. Subsystems

Reception system

We chose the evaluation board for the integrated circuit AD 9361 from Analog Devices called AD-FMCOMMS2-EBZ [1]. The manufacturer has provided sufficiently extensive support with examples of use. At beginning, we will use only one receiving antenna. An important detail is the existence of the so-called FMC connector for connection to the primary processing board based on the ZynqMP FPGA platform. The detail for using this platform is because it has a connector according to the FMC standard that corresponds to some FPGA evaluation platforms that would be used for experimental signal processing.

Precision position and timing

The RCB-F9T [2] boards allow for easy evaluation and quick prototyping with the ZED-F9T high accuracy timing module. The ZED-F9T module provides multi-band GNSS timing and comes with nanosecond level timing accuracy in both standalone and differential timing modes. To the RCB-F9T timing board we connect: power supply, active multi-band GNSS antenna, position and status data over UART line, clock pulses over two independently configurable time pulse signals.

Processing platform

AMD Zynq™ UltraScale+™ MPSoC ZCU104 Evaluation Kit [3]. The ZCU104 Evaluation Kit enables designers to jumpstart designs for many different embedded applications. The included ZU7EV device is equipped with a quad-core Arm® Cortex®-A53 applications processor, dual-core Cortex-R5 real-time processor, Mali™-400 MP2 graphics processing unit, 4KP60 capable H.264/H.265 video codec, and 16nm FinFET+ programmable logic.

Software

For the software we intend to use:

1) OPENWIFI
2) hardware coordination applications on each platform

3) setup tool for ublox RCB-F9T
4) coordination set written in Qt C/C++
5) open GIS for displaying locations

Openwifi

Openwifi is Linux mac80211 compatible full-stack IEEE802.11/Wi-Fi design based on SDR (Software Defined Radio). Jiao Xianjun [4] published Openwifi project on github based on work openofdm made by Jinghao Shi [5]. Openwifi model present in bit more detail software and hardware FPGA modules that compose the openwifi design.

Mathematical model

Let a transmitter that emits short bursts of electromagnetic pulses be located at an unknown position $X(x, y, z)$, and let there be n receivers located at known positions $M_i(x_i, y_i, z_i)$, i=1, … , n. Let t be the time when a pulse is emitted, and let t_i be the time when the pulse is received at the i-th receiver.

The receiver positions (x_i, y_i, z_i) and the reception times t_i are known. The task is to determine (x, y, z). For each i we have equation 1

$$(x - x_i)^2 + (y - y_i)^2 + (z - z_i)^2 = c^2(t - t_i)^2 \tag{1}$$

Subtracting the equation for $i \geq 2$ from the one for i=1, we obtain for $i \geq 2$, equation 2

$$\begin{aligned} &2x(x_1 - x_i) + \left(x_i^2 - x_1^2\right) + 2y(y_1 - y_i) \\ &+ \left(y_i^2 - y_1^2\right) + 2z(z_1 - z_i) + \left(z_i^2 - z_1^2\right) \\ &= c^2\left(2t(t_1 - t_i) + \left(t_i^2 - t_1^2\right)\right) \end{aligned} \tag{2}$$

This is a system of $n - 1$ linear equations with four unknowns x, y, z and t. If $n \geq 5$, we can determine the unknowns by solving any four of these linear equations. If n=4, we have three linear equations in four unknowns, so the unknowns can be expressed as linear functions of a single parameter p, equation 3

$$\begin{aligned} t &= \alpha_0 + \beta_0 p \quad x = \alpha_1 + \beta_1 p \\ y &= \alpha_2 + \beta_2 p \quad z = \alpha_3 + \beta_3 p \end{aligned} \tag{3}$$

Solving the linear system yields the values of α_j and β_j. Substituting the expressions for x, y, z and t into the equation for i=1 yields a quadratic equation in p as in equation equation 4

$$(\alpha_1+\beta_1 p - x_1)^2+(\alpha_2+\beta_2 p - y_1)^2 \\ +(\alpha_3+\beta_3 p - z_1)^2=c^2(\alpha_0+\beta_0 p - t_1)^2 \quad (4)$$

Solving it gives two values of p, and hence two solutions for x, y, z and t. The solution with $t>m\{t_1, \dots, t_n\}$ should be discarded, and the one with the smaller t accepted.

However, depending on the configuration of the receivers and the transmitter, it may happen that neither solution is discarded. With at least five receivers, solving four linear equations yields a unique solution, resolving this issue.

This is the inverse GPS problem, so one may consult the relevant literature. In GPS, the corresponding issue is addressed by simultaneous transmission of signals from all satellites.

Nevertheless, the solution obtained in this way should be used only as an initial guess for an iterative procedure for solving the overdetermined system (for $n \geq 5$) by the method of steepest descent applied to the system of n quadratic equations. In this, the system in the given form (without multiplying equations by constants) is already consistent with the principle of equal influence.

Since the receivers' locations are known, the receivers can be synchronized periodically by having one receiver emit an electromagnetic pulse. The other receivers then set their clocks to the emission time plus the distance from the emitting receiver divided by the speed of light.

4. Discussion

The proposed platform is based on the author's experience in developing and testing similar issues within business engagement. Then a large number of problems of a practical nature were identified. The accuracy of the GNSS module is very critical where the manufacturer claims that it can be achieved in the order of 1ns. It is necessary to remind that the propagation speed of electromagnetic waves through the air medium is about 300m per 1us, if we have a time resolution of 1ns then we have a positional resolution of 0.3m.

5. Conclusions

On a similar business project, we achieved position measurment of about +/- 10m regarding to GPS determined positions. Receiving stations were arranged cyclically at a distance of about 100m. Our goal is to secure funding AND do more basic research with the goal of reducing errors to extend ranges and to try to avoid GNSS based timing in order to substitue ti with local differential precise timing .

Acknowledgements

This work is partially co-financed under the agreement on the funds transfer for financing the scientific research work of teaching staff at accredited higher education institutions in 2026, number: 451-03-34/2026-03/200107.

References

1) https://www.analog.com/en/resources/evaluation-hardware-and-software/evaluation-boards-kits/eval-ad-fmcomms2.html#eb-overview, accessed on April 2026

2) https://www.u-blox.com/en/product/rcb-f9t-timing-board, accessed on April 2026

3) https://www.amd.com/en/products/adaptive-socs-and-fpgas/evaluation-boards/zcu104.html#tabs-d92053ede6-item-70d2b252af-tab, accessed on April 2026

4) X. Jiao, W. Liu, M. Mehari, M. Aslam and I. Moerman, "openwifi: a free and open-source IEEE802.11 SDR implementation on SoC," Proceedings of the 91st IEEE Vehicular Technology Conference (VTC), Antwerp, Belgium, 2020, doi: 10.1109/VTC2020-Spring48590.2020.9128614; https://github.com/open-sdr/openwifi, accessed on April 2026

5) S. Jinghao. (2017) Openofdm: Synthesizable, modular verilog implementation of 802.11 ofdm decoder; https://openofdm.readthedocs.io/en/latest/, accessed on April 2026

Connected Vehicles, V2X, and Automotive Cybersecurity

IoT and V2X Communications in Autonomous and Electric Vehicles

Sandra Antanasijevic[1], Milan Čabarkapa[1], Tijana Dimitrijević[1,2]

[1]*Faculty of Engineering, University of Kragujevac, Kragujevac, Serbia, sandraantanasijevic2@gmail.com, ORCID1:* 0009-0004-9860-9881, *mcabarkapa@uni.kg.ac.rs, ORCID2:* 0000-0003-3759-5696, *tijana.dimitrijevic@uni.kg.ac.rs, ORCID3: 0000-0002-9744-8287*

Faculty of Electronic Engineering, University of Niš, Niš, tijana.dimitrijevic@elfak.ni.ac.rs, ORCID: 0000-0002-9744-8287

Corresponding author*:* mcabarkapa@uni.kg.ac.rs

Abstract

Modern transportation systems are rapidly changing due to the development of Internet of Things (IoT) technologies, vehicle-to-everything communication, and advanced systems for electric and autonomous vehicles. This paper presents the implementation of an IoT Vehicle to Everything (V2X) node prototype on the Arduino Uno platform, simulated in the Wokwi environment. The prototype includes an HC-SR04 ultrasonic distance sensor for automatic obstacle detection, adaptive communication protocol selection based on vehicle speed, and Vehicle to Grid (V2G) logic for electric vehicle battery management. Four operational scenarios were tested: normal driving, nearby vehicle warning, potential collision detection, and Electric Vehicle (EV) mode with V2G functionality. The prototype successfully demonstrated correct switching between (Dedicated Short-Range Communications) DSRC, LTE-V2X, and 5G NR-V2X protocols based on vehicle speed, with measured system reaction time from danger detection to the first Basic Safety Message (BSM) transmission. The measured BSM cycle time is 219–231 ms, and the system reaction time is 1–2 ms, which meets the requirements for safety-critical V2X applications.

Keywords: IoT; V2X communication; autonomous vehicles; electric vehicles; Arduino; HC-SR04; intelligent transportation systems; 5G networks; UN SDG 9; UN SDG 11

1. Introduction

The development of IoT technologies, V2X communication systems, and electric mobility is significantly changing modern traffic infrastructure. The number of electric vehicles worldwide reached 40 million in 2023 and is expected to exceed 250 million by 2030 [1], while the autonomous vehicle market is estimated at over 550 billion dollars by 2026 [2]. This growth places increasing demands on communication systems in terms of latency, reliability, and scalability. Modern vehicles are no longer isolated mechanical systems but are becoming connected nodes that exchange data with surrounding vehicles, traffic infrastructure, and cloud services [3].

V2X communication includes several interaction types: vehicle-to-vehicle (V2V), vehicle-to-infrastructure (V2I), vehicle-to-pedestrian (V2P), vehicle-to-network (V2N), and vehicle-to-cloud (V2C). Each channel has specific requirements, making protocol selection one of the key engineering challenges in this field [3].

Three communication standards are currently relevant: DSRC (IEEE 802.11p) enables direct vehicle communication without mobile infrastructure at around 8 ms latency [3]; LTE-V2X uses mobile network infrastructure for greater scalability at around 9 ms [4]; 5G NR-V2X provides latency below 1 ms, suitable for safety-critical autonomous vehicle applications [5].
The goal of this paper is to demonstrate basic V2X functionality through an Arduino-based prototype, evaluate system behavior in multiple scenarios, and compare measured values with literature data.

2. Materials and Methods

The proposed V2X architecture is organized into three basic layers: the perception layer, the network layer, and the application layer [3]. The perception layer consists of sensors built into the vehicle (cameras, LiDAR, radar, ultrasonic sensors, GPS) and roadside infrastructure (RSU units and IoT sensors). The network layer enables communication through three protocols: DSRC with a latency of around 10 ms [3], LTE-V2X with greater scalability [4], and 5G NR-V2X with very low latency for safety-critical applications [5]. The application layer uses edge servers for real-time data processing and cloud systems for long-term analytics and fleet management [6].
To demonstrate the architecture, a hardware prototype of an IoT V2X node was built using an Arduino Uno microcontroller [7] and simulated in the Wokwi environment [8] (Fig.1). The prototype includes an HC-SR04 ultrasonic distance sensor [9] that continuously measures the distance to an obstacle in the range of 2–400 cm (a scale of 1 cm = 0.2 m was applied, giving the sensor an effective range of 80 m, with detection thresholds of 30 m for warning and 12 m for danger), LED indicators showing the system status, potentiometers simulating vehicle speed and EV battery level, and a button for switching between autonomous vehicle (AV) and EV operating modes.

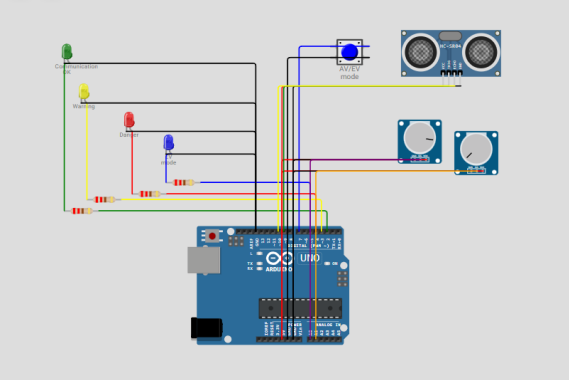


Figure 1. Arduino-based IoT V2X prototype implemented in the Wokwi simulation environment. [8]

The firmware was developed in Arduino C++ and implements periodic transmission of BSM packets every 100 ms in accordance with the SAE J2735 standard [3], adaptive protocol selection based on vehicle speed (DSRC below 40 km/h, LTE-V2X from 40 to 80 km/h, 5G NR-V2X above 80 km/h), potential collision detection using the HC-SR04 sensor, measurement of the average sensor measurement time in microseconds, measurement of

the average BSM message time on the platform and reaction time from detection to the first BSM transmission, and simulation of V2G logic for EV battery management [6].

3. Results and discussion

Several simulation scenarios were carried out to analyze system which system – define it precisely behavior under different operating conditions. The prototype worked correctly in all scenarios, including normal driving, nearby vehicle warning, potential collision detection, and electric vehicle mode with V2G functionality.

In the free-road scenario, the system used the appropriate protocol for the given speed, the green LED remained constantly lit, and BSM messages were sent with an OK status. When a nearby vehicle was detected, the yellow LED activated and the messages included a warning with the measured distance. In danger scenarios, the red LED flashed every 200 ms, and the system recorded the first reaction time from HC-SR04 detection to the transmission of the first BSM message.

For all the protocols used, the analysis comprises of observing an average BSM message time, average sensor measurement time, reaction time and speed. Table 1. presents comparison of latency values from the literature with measured prototype performance.

Table 1. Comparison of latency values from the literature with measured prototype performance

Protocol	Latency from literature (ms)	Average BSM message time (ms)	Average sensor measurement time (µs)	Reaction time (ms)	Speed (km/h)
DSRC	~8 ms [3]	219	4855	2	0–40
LTE-V2X	~9 ms [4]	228	3386	1	40–80
5G NR-V2X	~1 ms [5]	231	2487	1	> 80

As can be seen from Table 1, the measured BSM cycle time is 219–231 ms for all protocols, which corresponds to the total processing time of the Arduino platform, including sensor measurement, data processing, and message transmission. The HC-SR04 sensor cycle time varies between 2487 µs and 4855 µs depending on the distance to the obstacle, since a shorter distance leads to a shorter measurement time. The system reaction time is 1–2 ms, which is well below the 100 ms limit defined in the literature for safety-critical V2X applications.

The proposed prototype successfully demonstrated basic V2X functionality in all tested scenarios. Automatic protocol switching based on vehicle speed was confirmed in all scenarios, consistent with V2X protocol recommendations described in the literature [3, 4, 5].

5. Conclusions

This paper presented the implementation of an IoT V2X node prototype on the Arduino Uno platform with an HC-SR04 ultrasonic sensor, demonstrating adaptive communication protocol selection, automatic collision detection, and V2G logic for electric vehicles. The prototype successfully passed all tested scenarios, confirming the correctness of the implemented architecture [3, 4, 5, 6].

The measured performance values are consistent with data from the literature and confirm that the platform can successfully implement basic V2X functionality. The system reaction time of 1–2 ms meets the requirements for safety-critical V2X applications defined in the literature [3].

The main limitation of this work is the simulated nature of the environment. The prototype was implemented in the Wokwi platform and not on real hardware in actual traffic conditions. In addition, protocol latencies were not directly measured but taken from the literature, since the Arduino platform does not have actual V2X radio hardware. Future research should focus on testing with real hardware in real traffic conditions.

Future work should focus on developing real V2X radio hardware, implementing security mechanisms according to the IEEE 1609.2 standard [10], and testing in real traffic conditions. The development of 6G technology and federated learning opens up new possibilities for future intelligent transportation systems [5].

Acknowledgements

This work has been supported by the Ministry of Science, Technological Development and Innovation of the Republic of Serbia [Grant Number: 451-03-34/2026-03/200107].

References

1. International Energy Agency. Global EV Outlook 2024. Paris: IEA. 2024. p.12.
2. Litman T. Autonomous vehicle implementation predictions. Victoria Transport Policy Institute. 2023.
3. Kenney J. Dedicated short-range communications (DSRC) standards in the United States. Proceedings of the IEEE. 2011;99:1162-1182.
4. Molina-Masegosa R, Gozalvez J. LTE-V for sidelink 5G V2X vehicular communications. IEEE Vehicular Technology Magazine. 2017;12(4):30–39.
5. 3GPP. TR 38.885 V16.0.0: Study on NR Vehicle-to-Everything (V2X), Release 16. Sophia Antipolis: 3rd Generation Partnership Project; 2019.
6. Shi W, Dustdar S. The promise of edge computing. Computer. 2016;49:78-81.
7. Arduino. Arduino Uno Rev3 [Internet]. Arduino; 2024 [cited 2024]. Available from: https://store.arduino.cc/products/arduino-uno-rev3
8. Antanasijevic S. IoT V2X Node Prototype [Internet]. Wokwi; 2024 [cited 2024]. Available from: https://wokwi.com/projects/456428641510010881
9. SparkFun Electronics. HC-SR04 Ultrasonic Sensor Datasheet [Internet]. SparkFun; 2024 [cited 2024]. Available from: https://cdn.sparkfun.com/datasheets/Sensors/Proximity/HCSR04.pdf
10. Whyte W, Weimerskirch A, Kumar V, Hehn T. A security credential management system for V2V communications. In: Proceedings of the IEEE Vehicular Networking Conference (VNC); 2013 Nov 16–18; Boston, MA, USA. p. 1–8.

Cybersecurity of IoT-Based CAN Systems in Autonomous and Electric Vehicles

Ema Radovanović[1], Tijana Dimitrijević[2], Milan Čabarkapa[3]

[1]*Faculty of Engineering, University of Kragujevac, Kragujevac, Serbia, radovanovicem@gmail.com*

[2]*Faculty of Engineering, University of Kragujevac, Kragujevac, Serbia, tijana.dimitrijevic@uni.kg.ac.rs, and Faculty of Electronic Engineering, University of Niš, Niš, tijana.dimitrijevic@elfak.ni.ac.rs, ORCID: 0000-0002-9744-8287*

[3]*Faculty of Engineering, University of Kragujevac, Kragujevac, Serbia, mcabarkapa@uni.kg.ac.rs, ORCID:* 0000-0003-3759-5696

Corresponding author*: tijana.dimitrijevic@uni.kg.ac.rs*

Abstract

The rapid integration of Internet of Things (IoT) technologies into autonomous and electric vehicles has expanded the cyber-attack surface, particularly within the Controller Area Network (CAN) bus. Since standard CAN lacks built-in authentication and encryption, vehicles remain vulnerable to message injection, denial-of-service (DoS), and fuzzing attacks. This paper evaluates a lightweight hybrid Intrusion Detection System (IDS) that combines signature-based detection (CAN ID whitelisting), anomaly-based detection (message-frequency monitoring), and specification-based detection (validation of physical constraints). A Python-based simulation framework was used to model normal ECU communication and multiple attack scenarios, enabling quantitative assessment of detection performance and real-time suitability. The proposed IDS achieved a 97.3% detection rate with a 0.22% false positive rate and an average detection latency of 43 ms, while simulated CPU overhead remained 7.3%. These results indicate that a hybrid IDS can significantly improve CAN resilience under realistic automotive constraints and support practical deployment in future connected vehicles.

Keywords: *automotive cybersecurity; CAN bus; intrusion detection system; IoT vehicles; hybrid IDS, UN SDG 9; UN SDG 11*

1. Introduction

Modern autonomous and electric vehicles rely on distributed IoT architectures where numerous Electronic Control Units (ECUs) communicate via in-vehicle networks. The CAN bus remains the dominant protocol due to its deterministic real-time behavior and reliability [1]. However, its broadcast nature and lack of native security mechanisms introduce critical vulnerabilities when vehicles connect to external networks via infotainment, telematics, and V2X interfaces [2]. Real-world demonstrations have confirmed that remote exploitation can compromise safety-relevant vehicle functions [3]. Industry reports highlight a 225% increase in automotive cyber incidents between 2018 and 2023, underscoring the need for robust monitoring and detection mechanisms [4]. This paper evaluates a hybrid IDS designed to detect DoS, injection, and fuzzing attacks while respecting the strict resource limitations of automotive ECUs. The objective is to validate a

practical detection approach that can support layered in-vehicle security and align with emerging automotive cybersecurity requirements.

2. Materials and Methods

A combined theoretical and experimental methodology was applied. A simulation framework was developed in Python to emulate CAN communication between subsystems, including engine, braking, and steering units. The system architecture follows a domain-based approach where a gateway-level monitoring component provides visibility over inter-domain traffic [1]. The hybrid IDS, proposed here, implements three complementary detection layers: signature-based detection using a CAN ID whitelist; anomaly-based detection monitoring message frequency and timing to identify DoS-like flooding; and specification-based detection validating physical constraints of critical parameters (e.g., plausibility checks on engine RPM) to detect manipulated payloads. Testing involved three phases: normal baseline operation, attack execution without protection, and attack execution with the active IDS listener. Evaluation metrics were defined as follows. Detection Rate represents the ratio of correctly detected attack messages to the total number of injected attack messages. False Positive Rate (FPR) is calculated as the proportion of benign messages incorrectly flagged as malicious. Detection latency is measured as the elapsed time between the first malicious message and the corresponding IDS alert, expressed in milliseconds. System overhead represents the relative increase in CPU utilization introduced by the IDS listener during simulation runtime. All metric values were obtained from repeated simulation runs under identical traffic conditions.

3. Results

The IDS was evaluated under three operational scenarios: normal vehicle operation, active cyber-attacks without protection, and attacks with IDS enabled. Performance metrics included detection rate, false positive rate, detection latency, and computational overhead.

During the first phase, when normal vehicle operation without attacks was simulated, the simulation ran for 10 seconds, during which 1,847 CAN messages were transmitted, corresponding to an average rate of 184.7 messages per second. The average CAN bus utilization under these conditions was 23.4%, representing baseline system behavior.

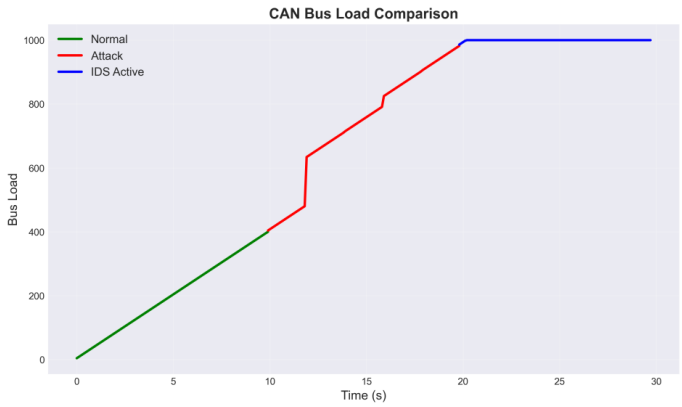


Fig.1. CAN bus load over time

In order to illustrate the effect of the attacks on the CAN bus without protection, the second phase included simulation of attacks on the CAN bus, including DoS, Injection and Fuzzing. DoS attack was initiated in the second second of execution, causing CAN bus utilization to increase to 98% (Fig.1). A total of 184 attack messages were injected, resulting in the blocking of 12 critical control messages. This behavior illustrates the potential safety impact of CAN flooding attacks in the absence of monitoring mechanisms.

The final phase involved simulation of attacks when IDS was enabled providing real-time monitoring and anomaly detection. As presented in Table 1, a total of 2,031 messages were analyzed. The system successfully detected 178 out of 182 injected attack messages, corresponding to an overall detection rate of 97.3%. Four benign messages were incorrectly flagged, yielding a false positive rate of 0.22%. The average detection latency was 43 ms.

Table 1. Summary of IDS Performance

Metric	Result
Detection Rate	97.3%
False Positive Rate	0.22%
Average Detection Latency	43 ms
CPU Overhead (simulated)	7.3%

A breakdown by attack type shows that all DoS and message injection attacks were detected (100%), while fuzzing attacks achieved a detection rate of 86.7%, reflecting their non-deterministic characteristics. Importantly, no critical control messages were lost during IDS-protected operation, indicating that the proposed approach preserves system availability even under attack conditions.

In addition, two scenarios, without protection and with IDS enabled, are compared. In the scenario without protection, a total of 12 critical messages were lost (6.5%), and 4 bus saturation events were recorded, with a total duration of 3.2 seconds, while the average latency was not available. In the scenario with an IDS, no critical messages were lost (0%), and although 4 bus saturation events were still observed, they were isolated, with an average latency of 43 ms. The results show that the IDS prevents the loss of critical messages during attacks and maintains a controlled level of bus load. To evaluate the effectiveness of the proposed IDS, the results were compared with advanced approaches from the literature [5, 6, 7], as given in Table 2. The proposed IDS, based on a hybrid approach, achieves a detection rate of 97.3%, a significantly lower false positive rate of 0.22%, and a latency of 43 ms. Overall, the proposed IDS provides a favorable trade-off by achieving a very low false positive rate while maintaining competitive detection performance compared to existing methods in the literature.

Table 2. Comparative analysis with literature

Study	Approach	Detection Rate	False Positive Rate (FPR)	Latency (ms)
Cho & Shin (2016) [5]	LSTM	99.8%	0.3%	3.2
Taylor et al. (2017) [6]	SVM	94.2%	2.1%	15
Song et al. (2020) [7]	Ensemble	97.5%	1.8%	8
This work	Hybrid	97.3%	0.22%	43

4. Discussion

Results presented in this paper confirm that a hybrid IDS can provide strong protection for CAN-based automotive IoT systems while remaining lightweight and compatible with real-time ECU constraints. Frequency monitoring proved effective for DoS detection, as flooding produces clear deviations from normal traffic patterns, while specification-based plausibility checks mitigated injection attempts by flagging out-of-range or inconsistent values. The low false positive rate (0.22%) indicates good calibration, although operational deployments require careful whitelist maintenance to include legitimate diagnostic traffic and reduce avoidable alerts. However, the evaluation has some limitations. The simulated CAN model does not include hardware-level error handling, retransmission behavior, or realistic timing effects under different arbitration conditions defined by CAN specifications. In addition, overhead and latency values were obtained in a Python desktop environment and should be interpreted as indicative rather than definitive for embedded ECUs. Nevertheless, the approach supports practical deployment as part of a layered defense strategy and is compatible with cybersecurity engineering expectations.

5. Conclusions

This work demonstrates that a lightweight hybrid IDS can effectively improve cybersecurity of CAN-based IoT systems in autonomous and electric vehicles. The proposed system achieved a 97.3% detection rate, 0.22% false positive rate, and 43 ms average detection latency, with simulated CPU overhead of 7.3%. These results support the suitability of hybrid IDS approaches for real-time in-vehicle monitoring. Future work will focus on validation on embedded automotive hardware, improved handling of diagnostic traffic, integration with message authentication, and extensions to V2X-aware monitoring to address evolving threat models.

Acknowledgements

This work has been supported by the Ministry of Science, Technological Development and Innovation of the Republic of Serbia [Grant Number: 451-03-34/2026-03/200107].

References

1. S. Checkoway, D. McCoy, B. Kantor, D. Anderson, H. Shacham, S. Savage, K. Koscher, A. Czeskis, F. Roesner, T. Kohno, "Comprehensive experimental analyses of automotive attack surfaces", *USENIX Security Symposium*, 2011;447–462.
2. J. Petit, S.E. Shladover, "Potential cyberattacks on automated vehicles", *IEEE Transactions on Intelligent Transportation Systems*, 2015;16(2):546–556.
3. C. Miller, C. Valasek, Remote exploitation of an unaltered passenger vehicle. Black Hat USA. 2015.
4. Upstream Security. Global automotive cybersecurity report 2023. Upstream Security Ltd. 2023.
5. K. T. Cho and K. G. Shin, "Error handling of in-vehicle networks makes them vulnerable," in *Proc. ACM Conf. Comput. Commun. Security*, 2016, pp. 1044-1055.
6. A. Taylor, N. Japkowicz, and S. Leblanc, "Frequency-based anomaly detection for the automotive CAN bus," in *Proc. World Congr. Ind. Control Syst. Security*, 2015, pp. 45-49.
7. H. M. Song, J. Woo, and H. K. Kim, "In-vehicle network intrusion detection using deep convolutional neural network," *Veh. Commun.*, vol. 21, p. 100198, Jan. 2020.

Robotics

Industrial robots: global trends in exports, dynamics, and challenges

Anelia Stoikova[3]

Department of Business Administration, Sofia University "St. Kliment Ohridski", Sofia, Bulgaria,

Corresponding author: aistoykova@uni-sofia.bg

Abstract

This study reviews the trends in exports of industrial robots for the period 2010-2024, leading exporters, and main export destinations. Recognizing that availability of industrial robots is a catalyst for optimizing business processes and efficiency, the trends in demand and exports are issues of key importance for future development.

The leading exporters of industrial robots on international markets are Japan, Germany, China, Denmark, and Italy. The highest level of exports of industrial robots from Japan is determined by innovation capacity, as well as the role and position in robotics patenting. The industrial robots enhancing manufacturing capabilities and trade trends will be driven by market forces, optimization demand, innovative solutions, new fields of businesses, and need for accelerating the performance of business operators.

The paper contributes for establishment of understanding regarding the main exports flows, achievements regarding installation of industrial robots, challenges related to tariff rates for imports, and all factors that will shape the future of robotics. Further research in this domain could cover supply chains options, solutions that impact hardware prices, focus on software-centric approach to robotics, new visions for AI in robotics, and the next generation of AI-powered robots.

Keywords: industrial robots; global trade trends; exports; tariff rates; market dynamics

1. Introduction

Recent dynamics in industrial robots exports have the potential to enhance competitiveness, foster technological advancement, and accelerate the optimization of business processes. At the same time, the new generation of AI-powered robots that are designed and developed in research labs will be launched on the market. Supplementary, the ongoing tariff rates changes for entering the USA market are impacting exports.

Focusing on leading exporters and main markets, the research covers period from 2010 to 2024. The data regarding industrial robots installation also are in the analytical radar and bring insights for current achievements.

The challenges ahead that will impact the market demand and trade trends cover also the further integration of AI into robotics, supply chains options, solutions that impact hardware prices, focus on software-centric approach to robotics, tariff rates imposed on imports.

[3]*Anelia Stoikova, Sofia University "St. Kliment Ohridski", aistoykova@uni-sofia.bg*

In this context, the review and analysis of exports trends can bring more awareness and potential insights for decision-making. Taking into account that the industrial robots market continues to grow, the research in the field is a strategic topic of interest.

2. Definitions, Classifications, and Methods

This research covers industrial robots with primary classification for trade purposes: "Industrial robots, not elsewhere specified or included" – tariff subheading 847950 within the applicable Harmonized system (HS). The data sets cover the period 2010-2024, and research is based on analysis of original data provided by the COMTRADE database of the United Nations Statistical Division. The International Federation of Robotics (IFR) is the source of data regarding robot installations by country, and industry. The IFR ensures that data are reliable based on their methodology covering permanent market observation, and cooperation with national robotics associations. They are using the standardized definition according to ISO 8373:2021: an industrial robot is an "automatically controlled, reprogrammable multipurpose manipulator, programmable in three or more axes, which can be either fixed in place or fixed to a mobile platform for use in automation applications in an industrial environment" [1].[4]

The selected method is desk research, including data regarding existing analysis. The data analysis is visualized with graphics.

3. Results

Review of trends in exports

The leading exporters of industrial robots in 2024 are Japan, Germany, China, Denmark, Italy, Sweden, USA, France, Republic of Korea, the Netherlands, Austria, UK, Canada, Switzerland, Spain, Singapore, Belgium, Luxembourg.

In 2024 exports from Japan of industrial robots under tariff subheading 847950 amounted to 1279 million (mln.) USD, followed by Germany – 621,3 mln. USD, China – 573,9 mln. USD, Denmark – 389 mln. USD, Italy – 372 mln. USD.

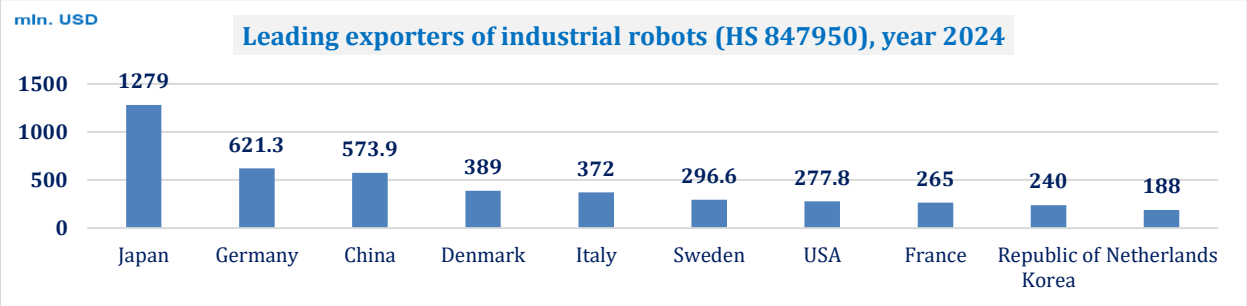


Figure 1. Leading exporters of industrial robots (HS 847950), year 2024

Source: Calculation based on COMTRADE database [2] [5](visualization by author)

[4] [1] Müller C. World Robotics 2025 - Industrial Robots, IFR Statistical Department

[5] [2] COMTRADE database of the UN Statistical Division 2025, https://comtradeplus.un.org/

The leading exporter of industrial robots is Japan for the whole period 2010 – 2024 covered by current review. The trends in exports by leading exporters are represented in figure 2 below.

Japan exports of industrial robots amounted to 1077 mln. USD in 2010 and 1279 mln. USD in 2024. Germany reached exports of industrial robots amounted to 621,3 mln. USD in 2024, in comparison with 432 mln. USD in 2010. The trend of significant increase of exports from China, in absolute terms amounted to 573,9 mln. USD in 2024, in comparison with 55,6 mln. USD in 2010. Denmark exports amounted to 21 mln. USD in 2010, and 389 mln. USD in 2024, Italy – from 116 mln. USD in 2010 to 372 mln. USD in 2024.

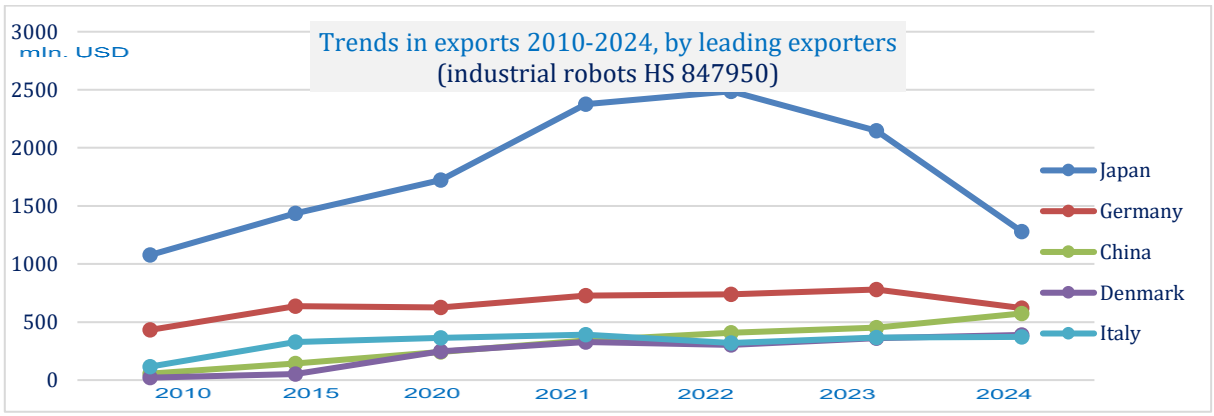


Figure 2. Trends in exports 2010-2024, by leading exporters (industrial robots HS 847950)
Source: Calculation based on COMTRADE database [2], (visualization by author)

Figure 3 below presents visually the trends in exports of industrial robots (HS 847950) from Japan amounted to 1716 mln. USD in 2025. It is a clear representation of high level of innovation capacity of Japan, and leading role in robotics patenting.

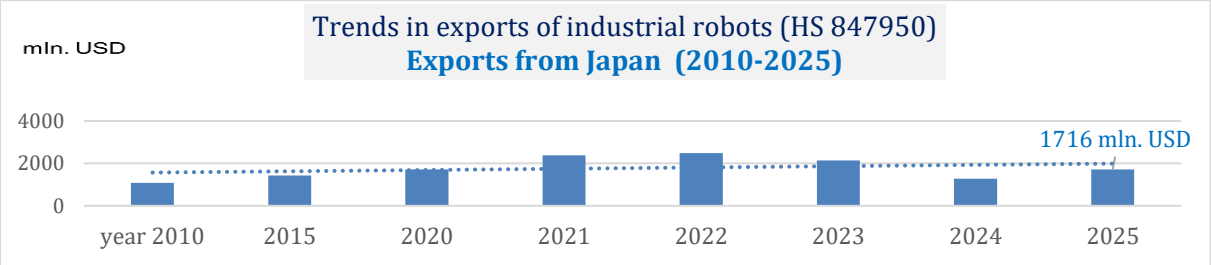


Figure 3. Trends in exports of industrial robots (HS 847950), exports from Japan (2010-2025)
Source: Calculation based on COMTRADE database [2], (visualization by author).

In 2024, the main destinations of Japan exports of industrial robots (under tariff heading 847950 "Industrial robots, not elsewhere specified or included") are China (with share of 32,5%), Luxembourg, USA, Republic of Korea, India, Germany.

Industrial robots installation achievements

The installation of industrial robots in 2023 in China amounted to 276 300 units, in Japan 46 100, USA – 37600, Republic of Korea – 31400, Germany – 28400, Italy – 10400, India – 8500, France – 6400, Mexico – 5800, Spain – 5100, Turkey – 4400 units [3].

The annual installations of industrial robots in 2023 in the Automotive industry reached 135 461 units. [3].[6]

Main challenges

Within the scope of the main challenges for future exports trends of industrial robots are the tariff rates for imports, and a multitude of factors that will shape the future of robotics, including supply chains options, solutions that impact hardware prices, software-centric approach to robotics, new visions for AI in robotics, and the next generation of AI-powered robots.

The applicable in 2026, Harmonized Tariff Schedule of the United States sets out tariff rates of 35% for "Industrial robots, not elsewhere specified or included" – tariff subheading 847950 [4][7]. The tariff rates have direct impact on costs. The ten leading suppliers of industrial robots on the USA market in 2024 are Canada, Denmark, Japan, Germany, Republic of Korea, Italy, China, Austria, UK, France.

4. Conclusions

The results of carried out research highlight the positive trend in exports of industrial robots by leading countries as Japan, Germany, China, Denmark, Italy, Sweden, USA, France, Republic of Korea, the Netherlands, Austria, UK, Canada, Switzerland, Spain, etc.

There is a wide scope of factors for consideration and discussion related to export potential developments and market trends. The imposed higher tariff rates by USA as of April 2025 will be reviewed in the future regarding their impact on exports from the leading exporters to the US market.

Further research in this domain, including supply chains options, solutions that impact hardware prices, focus on software-centric approach to robotics, and the next generation of AI-powered robots could be useful for the global market dynamics review, forecasting scenario, and effective management of exports.

References

1. Müller C. World Robotics 2025 - Industrial Robots, IFR Statistical Department, VDMA Services GmbH, Frankfurt am Main, Germany, 2025.
2. COMTRADE database of the UN Statistical Division 2025, https://comtradeplus.un.org/
3. World Robotics 2024, IFR. https://ifr.org/img/worldrobotics/Press_Conference_2024.pdf
4. Harmonized Tariff Schedule of the United States 2025, https://hts.usitc.gov/search?query=847950

[6] [3] World Robotics 2024, IFR. https://ifr.org/img/worldrobotics/Press_Conference_2024.pdf

[7] [4] Harmonized Tariff Schedule of the United States 2025, https://hts.usitc.gov/search?query=847950

Integrating Advanced Robotic Solutions into Lean Industrial Systems: A Human-Centered Approach

Nastasija Nikolic[1], Marko Djapan[2], Arso Vukicevic[3], Djordje Milojevic[4], Ivan Macuzic[5]

[1] *Faculty of Engineering, University of Kragujevac, Kragujevac, Serbia, nastasija.mijovic.fink@gmail.com, ORCID 0000-0002-2235-1712*

[2] *Faculty of Engineering, University of Kragujevac, Kragujevac, Serbia, djapan@kg.ac.rs, ORCID 0000-0002-8016-8422*

[3] *Faculty of Engineering, University of Kragujevac, Serbia, arso_kg@yahoo.com, ORCID0000-0003-4886-373X*

[4] *Faculty of Engineering, University of Kragujevac, Kragujevac, Serbia, djordjemilojevic@gmail.com, ORCID 0900-0003-6816-7296*

[5] *Faculty of Engineering, University of Kragujevac, Kragujevac, Serbia, imacuzic@kg.ac.rs, ORCID 0000-0001-6153-6456)*

Corresponding author: nastasija.mijovic.fink@gmail.com

Abstract

The integration of advanced robotic solutions in Lean industrial systems enables improved efficiency, greater flexibility and the elimination of waste. This paper proposes a conceptual framework for the implementation of advanced robotic solutions in Lean industrial systems, focusing on Lean principles including continuous flow and waste minimization. The methodology involves identifying bottlenecks and selecting appropriate robotic solutions through system analysis, as well as simulating operational scenarios to assess potential impacts. A mini case study illustrates the implementation of a collaborative robot on a Lean assembly line, allowing operators to focus on those tasks that add value. Key considerations include collaboration between operator and robot, adaptability of the robot cell and integration with existing information systems. The proposed approach enables the adoption of automation while maintaining Lean efficiency and minimizing disruption. The concept is a guide for production managers, engineers, and researchers who strive to improve industrial operations in accordance with Lean practices.

Keywords: Lean industrial systems, advanced robotic solutions; implementation framework; human-robot collaboration; UN SDG 9.

1. Introduction

The Lean manufacturing methodology was created in the mid-20th century based on the Toyota Production System (TPS). It has two pillars: just-in-time and Jidoka. In order to achieve the goals of this methodology, it is necessary to identify various "muda" (waste) and eliminate them, along with a system of continuous improvement [1]. Lean manufacturing today represents the standard for optimizing production through waste reduction and efficiency improvement. The implementation of robotic solutions and automation in production is one of the main drivers of industrial progress [2]. The use of robotic systems in manufacturing is constantly

growing due to their positive impact on quality, waste reduction, and production time [3][4]. A significant amount of research is focused on improving the design and performance of these systems in order to reduce costs and increase their autonomy [5][6]. As Industry 4.0 is being followed by Industry 5.0, which goes beyond automation and focuses on people, emphasizing human-robot collaboration [7], collaborative robots, intelligent automation, and AI-driven analytics not only improve productivity, but also support worker creativity and decision-making [8]. Despite the significant potential of integrating various digital technologies and robotics with Lean manufacturing principles, it is necessary to define a clear framework for reducing waste and implementing robotic solutions that enable flexible and efficient human-centric manufacturing. This paper presents a conceptual framework for the systematic implementation of advanced robotic solutions in Lean industrial systems, focusing on human-robot collaboration. The main objective of this paper is to investigate how advanced robotic solutions can be effectively integrated into Lean industrial systems without compromising the key principles of Lean manufacturing. The novelty of this research lies in the integration of Lean assessment, robotic solution selection, and simulation-based evaluation within a unified approach focused on human-centered automation.

2. Materials and Methods

The framework takes into account ergonomic considerations, training requirements, and collaborative workspaces. The implementation aims to supplement human skills with robotic precision and address ergonomically demanding, repetitive tasks. The research methodology is structured as a sequential framework and consists of four phases: system analysis, robotic solution selection, simulation modeling, and human-robot collaboration design. The first phase involves analyzing the current manufacturing system using Lean assessment tools to identify inefficiencies and tasks suitable for automation, providing an empirical basis for selecting candidate operations. The second phase involves the selection of appropriate robotic solutions based on functional requirements, integration compatibility, and safety considerations. The third phase involves discrete event simulation and is used to model the production system and determine the effects of integrating the robotic solution under different operational scenarios. Key Lean performance indicators such as cycle time and resource utilization are assessed. The fourth phase focuses on designing a collaborative work environment in which human operators and robotic systems perform complementary tasks. This phase includes considerations related to ergonomics, operator training, and safe human-robot interaction.

3. Results

Figure 1 shows the phases of robotic implementation in Lean industrial systems. The last phase represents full-scale industrial implementation.

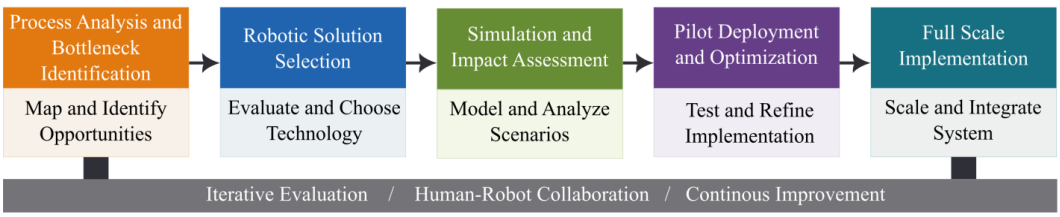


Figure 1. Conceptual Framework for Robotic Implementation in Lean Systems

To illustrate the proposed framework, a collaborative robot implementation is shown on a small electronics assembly line that produces control panels. The assembly line consists of five workstations. Each of the stations involves repetitive tasks. Some of the tasks are screw fastening, component insertion, and visual inspection. By implementing a value stream map (VSM), the screw fastening operation was identified as a bottleneck. This operation involves a large number of repetitions and ergonomic strain on the operator. Based on the criteria listed in Table 1, a collaborative robot was selected for implementation into an existing Lean layout.

Table 1. Criteria for Selecting Robotic Solutions in Lean Systems

Criterion	Description	Lean Impact
Task Repetitiveness	Degree to which the task is repetitive	Reduces variability, increases flow
Safety Risk	Level of risk for human operators	Enhances workplace safety
Integration Ease	Compatibility with existing systems	Minimizes production disruption
Flexibility	Ability to adapt to product changes	Supports Just-In-Time production
Scalability	Modular design for incremental deployment	Enables gradual adoption

The implementation of the collaborative robot allowed operators to focus on value-added tasks such as quality verification and assembly of complex components. Human-robot collaboration was facilitated by the ergonomic design of the workstation as well as safety sensors and training programs. The implementation of the robotic solution will enable the results shown in Table 2, obtained by modeling the simulation.

Table 2. Simulation model results

Performance Metric	Before Robot	After Robot	Improvement
Cycle Time per Unit	8 min	6 min	-25%
Operator Workload (hrs/day)	7	5	-29%
Throughput (units/day)	60	80	+33%
Error Rate (defective units)	5%	2%	-60%

The simulation showed that the integration of a collaborative robot significantly reduces operator workload, improves production flow, and increases overall line productivity without compromising Lean principles. The results are graphically interpreted in Figure 2.

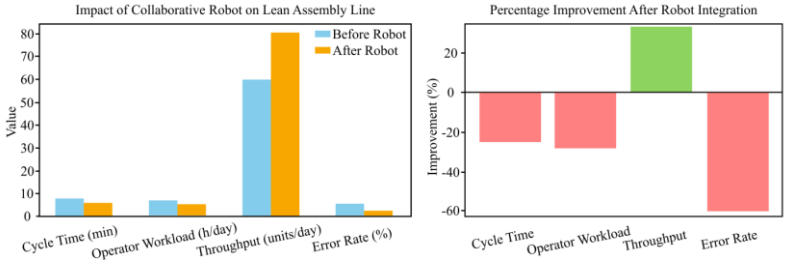


Figure 1. Simulation model results

Pilot deployment confirmed the feasibility of the approach, with operators reporting improved ergonomics and greater focus on value-added tasks. This mini case study highlights the practical applicability of the proposed framework in real industrial settings and demonstrates how robotic solutions can complement Lean practices while supporting human-centered manufacturing.

4. Discussion

Significant reduction of ergonomic risks is possible through the implementation of advanced robotic solutions in Lean industrial systems. Performance prediction as well as optimization of human-robot cooperation is possible by applying simulation-based evaluations. The challenges faced by Lean industrial systems when implementing advanced robotic solutions are primarily related to resistance to change. This obstacle can be overcome by clearly communicating the role of robots in supporting, rather than replacing, human work. Compared to previous studies, this work presents a framework that combines Lean principles and assessment, robotic solution selection, simulation modeling, and collaborative workspace design. In this way, a systematic approach to human-centered automation in Lean systems is provided. The approach is aligned with UN Sustainable Development Goal 9 and promotes sustainable industrial innovation, improved occupational safety and technological advancement of manufacturing practices.

5. Conclusions

This paper presents a conceptual framework for integrating advanced robotic solutions into Lean industrial systems. A case study demonstrates the potential for improved cycle times, increased throughput, and reduced operator workload without compromising Lean efficiency. The main contributions of this paper include a structured framework for implementing advanced robotic solutions into Lean industrial systems, an emphasis on human-centered automation, and simulation-driven evaluation to improve performance and reduce implementation risk. Future work will consider the application of the framework in different industrial environments and assess the long-term sustainability impact.

Acknowledgments

The authors gratefully acknowledge the financial support provided by the Ministry of Science, Technological Development and Innovation of the Republic of Serbia through: (i) the bilateral cooperation project with the Republic of Italy (2024–2026), AI-AGRI-HAND: AI-powered visio-tactile soft robotic hand for Agrifood farming, and (ii) contract no. 451-03-34/2026-03/200107.

References

1. Chahal V, Narwal M. An empirical review of lean manufacturing and their strategies. Management Science Letters. 2017; 7; 321-336.
2. Dzedzickis A, Subačiute-Žemaitiene J, Šutinys E, Samukaite-Bubniene U, Bučinskas V. Advanced applications of industrial robotics: New trends and possibilities. Applied Sciences. 2022; 12(1); 135.
3. Kabir H, Tham M, Chang Y. Internet of robotic things for mobile robots: Concepts, technologies, challenges, applications, and future directions. Digit. Commun. Networks. 2023; 9; 1265-1290.
4. Javaid M, Haleem A, Singh R., Suman R. Substantial capabilities of robotics in enhancing industry 4.0 implementation. Cognitive Robototics. 2021; 1; 58-75.
5. El-Meligy M, Mahmoud H, Sarhan N, Awwad E. A configurable process control method for robotic system-based industrial services improvements. Journal of Engineering Research. 2025; 13(2); 579-589.
6. Alieva J, Powell D. The significance of digital waste in the automation of Lean practices. Quality Management Journal. 2023; 30(3); 1-14.
7. Lu Y, Zheng H, Chand S, Xia W, Liu Z, Xu X, Wang L, Qin Z, Bao J. Outlook on human-centric manufacturing towards Industry 5.0. Journal of Manufacturing Systems. 2022; 62; 612-627.
8. Leng J, Zhu X, Huang Z, Li X, Zheng P, Zhou X, Mourtzis D, Wang B, Qi Q, Shao H, Wan J, Chen X, Wang L, Liu Q. Unlocking the power of industrial artificial intelligence towards Industry 5.0: Insights, pathways, and challenges. Journal of Manufacturing Systems. 2024; 73(139); 349-363.

SUSTAINABLE GREEN ENERGY AND CLEAN TECHNOLOGIES

Waste Management, Circular Economy, and Resource Recovery

Evaluating municipal waste management efficiency in the context of sustainable development: A DEA-based analysis

Angelina Cvetanović[1], Goran Bošković[1], Nebojša Jovičić[1]

[1] *Faculty of Engineering, Department of Energy and Process Engineering, University of Kragujevac, Republic of Serbia*

E-mails:	*angelina.pavlovic@uni.kg.ac.rs*	***ORCID iDs:***	*https://orcid.org/0000-0001-5249-1102*
	goran.boskovic@kg.ac.rs		*https://orcid.org/0000-0003-3200-0120*
	njovicic@kg.ac.rs		*https://orcid.org/0000-0002-6505-6457*

Corresponding author: angelina.pavlovic@uni.kg.ac.rs

Abstract

Efficient municipal waste management represents an essential element of sustainable urban development. Municipalities are responsible for delivering waste collection, treatment, and disposal services while being constrained by financial and operational limitations. Effective waste management practices play an important role in achieving the Sustainable Development Goals defined by the United Nations, specifically those related to sustainable cities and responsible production and consumption patterns. This study assesses the efficiency of municipal waste management systems within the Šumadija district in the Republic of Serbia using Data Envelopment Analysis. Seven municipalities are analysed as decision-making units. The analysis includes two input variables representing service coverage and the number of containers for separate waste collection, and two output variables reflecting environmental performance through the total amount of municipal waste collected and the amount of separately collected waste. The results indicate that Kragujevac and Lapovo operate at the efficiency frontier according to both applied DEA models, while other municipalities showed different levels of efficiency, mainly related to limited recycling infrastructure. The results provide useful insights for local policymakers and highlight the significance of improving recycling infrastructure and resource allocation to support more sustainable municipal waste management systems.

Keywords: municipal solid waste management (MSWM); data Envelopment Analysis (DEA); eco-efficiency; recycling; sustainable development; UN SDG 11; UN SDG 12

1. Introduction

Municipal solid waste management (MSWM) represents one of the basic public services usually provided by local governments [1]. Rapid urbanization, increasing living standards, and environmental pressures require

municipalities to manage waste systems in a more efficient and sustainable manner since MSWM system is one of an essential component of sustainable urban development [2]. Municipal authorities are responsible for organizing and managing waste activities through collection, treatment, and disposal services while operating under limited financial and operational resources.

Improving the efficiency level of MSWM system is particularly key in the context of sustainable development. Efficient systems allow municipalities to provide adequate services while minimizing environmental impacts and optimizing the use of available resources, which indicates eco-efficiency. Eco-efficiency is defined as generating more products while using less resources and minimizing environmental impact [3]. Eco-efficient waste management systems play an important role in attaining Sustainable Development Goals (SDGs) defined by the United Nations, particularly those related to sustainable cities (SDG 11) and responsible consumption and production (SDG 12). At the same time, the rapid growth in global waste generation represents a major challenge for achieving several SDGs, including those related to health, clean water, sustainable cities, and the protection of marine and terrestrial ecosystems (SDG 3, SDG 6, SDG 14, and SDG 15) [4-5]. In this context of sustainability, reusing, recycling, and waste separation play an important role in reducing landfill disposal and promoting circular economy principles. Policymakers and researchers are seeking solutions to promote the efficient management of municipal solid waste (MSW) from economic and environmental perspective [3, 6]. Municipalities differ in terms of financial capacity, infrastructure, population size, and institutional organization, which often results in heterogeneous performance levels, making it essential to evaluate the efficiency of MSWM system. Different analytical methods have been used to determine efficiency in public services, among which Data Envelopment Analysis (DEA) has proven to be particularly useful due to its ability to evaluate multiple inputs and outputs simultaneously [7-8]. DEA provides a non-parametric framework for evaluating performance and comparing efficiency of decision-making units [9].

The aim of this study is to evaluate the efficiency of MSWM system in municipalities within the Šumadija district of the Republic of Serbia, using the DEA methodology. Two DEA models (CCR and BCC) are employed to distinguish between technical efficiency and pure technical efficiency. Based on the selected input and output variables, the DEA model evaluates efficiency level of MSWM system in transforming available operational resources into environmental outputs, allowing decision-makers to identify municipalities in which improvement of waste management system is feasible.

2. Materials and methods

The methodological steps used in this study are summarized graphically in the Figure 1.

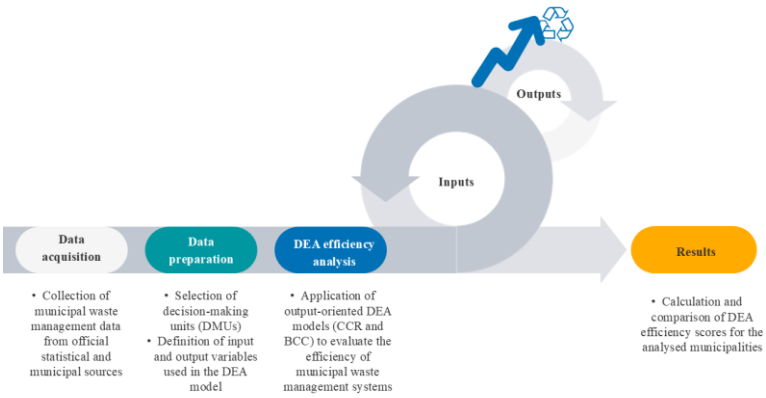
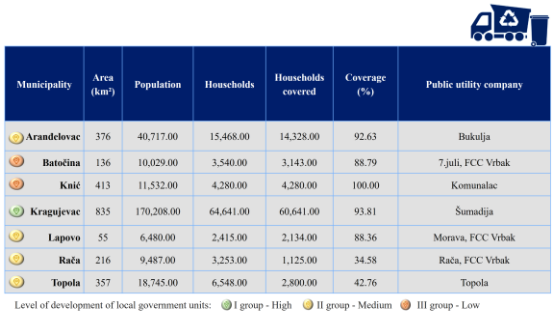


Figure 1. Methodological framework of DEA efficiency analysis

DEA is a non-parametric approach used to measure the relative efficiency of comparable decision-making units (DMUs) with the use of linear programming techniques [10]. The method evaluates how efficiently units transform inputs (resources) into outputs (results). Failure of a DMU to produce maximal output levels with minimal input consumption results in a worsened efficiency score [11]. This approach defines an efficiency frontier, or envelope, that encompasses all analysed DMUs. DEA estimates efficiency by comparing each DMU with the others DMUs in the sample [12].

Šumadija district has a central position in Serbia [13]. Seven municipalities from Šumadija district were analysed as DMUs: Aranđelovac, Batočina, Knić, Kragujevac, Lapovo, Rača and Topola (Figure 2). According to commonly used DEA methodological guidelines, the number of DMUs should be sufficiently larger than the total number of input and output variables in order to ensure the validity of the results. A general rule suggests that the number of DMUs should be at least twice the total number of inputs and outputs together [14]. Although the number of DMUs is below literature recommendation, the ratio remains acceptable given the limited number of municipalities within the observed district. Municipalities differ in size, economic capacity, and waste management infrastructure, which allows for a meaningful assessment of relative efficiency across heterogeneous local systems using DEA approach.

In this study, seven municipalities were analysed using two input and two output variables. The inputs and outputs used in this analysis are shown in Table 1.



Municipality	Area (km²)	Population	Households	Households covered	Coverage (%)	Public utility company
Aranđelovac	376	40,717.00	15,468.00	14,328.00	92.63	Bukulja
Batočina	136	10,029.00	3,540.00	3,143.00	88.79	7.juli, FCC Vrbak
Knić	413	11,532.00	4,280.00	4,280.00	100.00	Komunalac
Kragujevac	835	170,208.00	64,641.00	60,641.00	93.81	Šumadija
Lapovo	55	6,480.00	2,415.00	2,134.00	88.36	Morava, FCC Vrbak
Rača	216	9,487.00	3,253.00	1,125.00	34.58	Rača, FCC Vrbak
Topola	357	18,745.00	6,548.00	2,800.00	42.76	Topola

Level of development of local government units: I group - High II group - Medium III group - Low

Figure 2. Basic characteristics of municipalities included in the DEA analysis

Table 1. Input and output variables used in DEA analysis

DMU (Municipality)	x_1: Households covered	x_2: Containers for separate	y_1: Collected waste (t/year)	y_2: Separately collected waste
Aranđelovac	14,328.00	20.00	18,619.00	16.00
Batočina	3,143.00	0.00	3,861.00	0.00
Knić	4,280.00	0.00	6,500.00	0.00
Kragujevac	60,641.00	400.00	55,496.00	854.00
Lapovo	2,134.00	0.00	3,659.00	0.00
Rača	1,125.00	0.00	1,722.00	0.00
Topola	2,800.00	9.00	3,081.00	17.00

When determining the level of efficiency of the MSWM systems in Šumadija district, an output-oriented DEA model was applied. The output-oriented approach was considered appropriate because the objective of MSWM system is not primarily to reduce existing resources, but rather to improve waste management performance and increase desirable environmental outputs, such as the total amount of collected waste and separately collected waste for recycling, while keeping the available inputs at their current level. The analysis is based on data obtained from publicly available statistical sources and official municipal reports [15-16]. Given inputs represent the operational capacity of municipalities, measured through service coverage and the number of containers for separate waste collection, while the outputs reflect the performance of waste management systems in terms of the total amount of collected MSW and the amount of separately collected waste which can be further treated by the recycling process.

Optimization problem was solved using the Simplex linear programming algorithm implemented in Excel Solver. Two DEA models were formed: the CCR model (Equation 1), which assumes constant returns to scale and measures overall technical efficiency, and the BCC model, which assumes variable returns to scale and measures pure technical efficiency [17]. An efficiency score equal to 1 indicates an efficient DMU, while values greater than 1 indicate inefficiency and the potential to increase outputs while maintaining the same level of inputs.

$$Max \quad \theta_k \qquad \text{(Eq. 1)}$$

Subject to:

$$\sum_{j=1}^{n} \lambda_j x_{ij} \leq x_{i0}; \qquad i = 1, \dots, m$$

$$\sum_{j=1}^{n} \lambda_j y_{rj} \geq \theta_k y_{r0}; \qquad r = 1, \dots, s$$

$$\lambda_j \geq 0; \qquad j = 1, \dots, n$$

In this formulation, x_{ij} and y_{rj} represent the input and output values of each municipality (Table 2), λ_j are intensity variables, and θ_k the efficiency score of each DMU_k. The formulation of the BCC model is achieved by adding the convexity constraint $\sum_{j=1}^{n} \lambda_j = 1$ to described CCR model [17]. The comparison of two observed models enables the calculation of scale efficiency $(\boldsymbol{\theta_{CCR}/\theta_{BCC}})$, which indicates whether inefficiency is caused by operational performance or by the scale of operations. Given that an output-oriented DEA model was applied, in this study, scale efficiency was calculated as the ratio of pure technical efficiency (BCC) to overall technical

efficiency (CCR) to ensure that scale efficiency values range between $0 \leq \theta_k \leq 1$, where a value of 1 indicates complete efficiency.

3. Results and discussion

The results of the DEA analysis reveal differences in performance among the analysed municipalities. The CCR model shows that Kragujevac and Lapovo achieve full efficiency, indicating that these municipalities operate at the efficiency frontier and serve as benchmarks for other municipalities. The remaining municipalities show varying degrees of inefficiency. Batočina shows the lowest efficiency score, suggesting that improvements in recycling infrastructure and operational organization may be necessary. According to the BCC model, several municipalities, including Aranđelovac, Knić, Kragujevac, Lapovo and Rača, achieve pure technical efficiency, indicating that their operations are relatively well managed, but may not be operating at optimal scale. The calculated scale efficiency values indicate that the part of inefficiency observed in some municipalities is related to the scale of operations, rather than purely operational inefficiency.

The results highlight small differences in the performance of solid waste management systems in the municipalities of Šumadija District (Figure 3). Comparing the CCR and BCC efficiency scores provides additional insight into the sources of inefficiency among the analysed municipalities. While the CCR model measures overall technical efficiency assuming constant returns to scale, the BCC model estimates pure technical efficiency by allowing for variable returns to scale. When a municipality is efficient under the BCC model but inefficient under the CCR model, the inefficiency can be attributed primarily to scale effects rather than poor resource management. In this case, municipalities such as Aranđelovac, Knić, and Rača show pure technical efficiency under the BCC model, indicating that their waste management systems are relatively well managed but not operating at optimal scale. In contrast, Kragujevac and Lapovo achieve full efficiency according to both models, positioning them as reference municipalities within the analysed sample. The Figure 3 shows the geographical location of municipalities in Šumadija district and their efficiency results obtained using the DEA models. Kragujevac stands out as the most developed waste management system within the analysed group. Given that Kragujevac is the largest city in central Serbia, it has a significantly higher number of separate waste collection containers and the largest amount of separately collected waste [15-16], which contributes to its position at the efficiency frontier. Similarly, Lapovo achieves full efficiency despite its smaller size. This suggests that efficient organization and resource management can compensate for limited infrastructure and scale. Municipalities such as Aranđelovac, Knić and Rača show good management performance, but may operate under sub-optimal conditions.

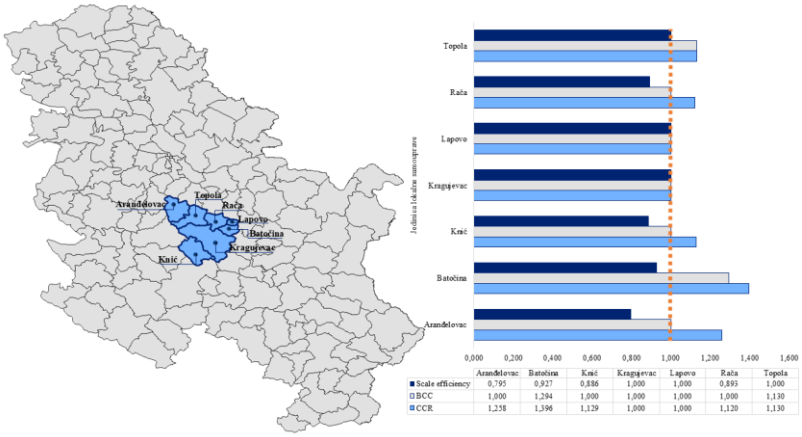


Figure 3. Efficiency of MSWM systems in the Šumadija district

To provide a spatial interpretation of differences in efficiency, municipalities were classified into efficiency categories based on BCC efficiency scores and visualized via a thematic map (Figure 4). The classification distinguishes between highly efficient municipalities operating at the efficiency frontier and municipalities exhibiting varying levels of inefficiency (High Efficiency = 1.00, Moderate Efficiency 1.01 - 1.15, Low Efficiency > 1.15). These findings notice the importance of investing in recycling infrastructure and improving operational efficiency to improve solid waste management system.

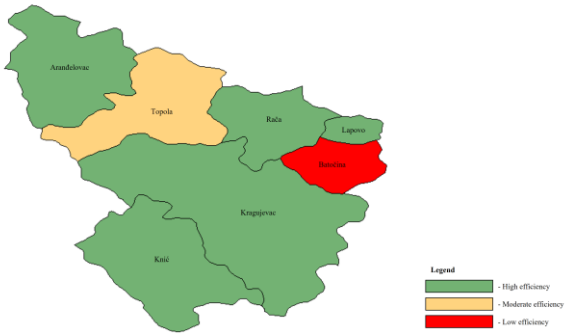


Figure 4. MSWM efficiency levels in the Šumadija district

Calculated efficiency scores show how efficiently municipalities use available resources compared to the other municipalities in the sample. Higher efficiency score indicates better resource utilization and more developed waste management systems, while lower efficiency levels indicate potential inefficiencies and opportunities for improving infrastructure, organization, and recycling performance. Therefore, the results provide insight into which municipalities are operating efficiently and which municipalities can improve their waste management performance through better resource allocation and development of recycling infrastructure.

The thematic map was constructed using BCC efficiency scores, as the BCC model measures pure technical efficiency while controlling for scale effects. This approach enables a more reliable comparison of operational performance between different sizes municipalities. The results suggest a clear relationship between waste management efficiency and sustainability-oriented outputs, particularly recycling performance. Municipalities with higher efficiency levels tend to achieve better environmental outcomes while using available resources more effectively, showing the role of efficiency as an important component of sustainable development.

4. Conclusions

This study examined efficiency of MSWM systems in municipalities of Šumadija district using DEA method. By applying the CCR and BCC models, the analysis provided insight into the technical efficiency and pure technical efficiency of the observed municipalities. Results show that Kragujevac and Lapovo operate at the efficiency frontier according to the CCR model, which assumes constant returns to scale. However, the BCC model, which allows for variable returns to scale and is therefore more suitable for comparing municipalities of different sizes, indicates that Batočina and Topola operate inefficiently. Among the analysed municipalities, Batočina stands out as the municipality with the lowest level of efficiency of municipal waste management in Šumadija district, suggesting that improvements in recycling infrastructure and operational organization may be necessary. A comparison of CCR and BCC results indicates that part of the observed inefficiency is related to the scale of operations. In other words, some municipalities may manage their resources relatively well, but do not operate at optimal level of waste management infrastructure and service provision. From a sustainable development perspective, the findings highlight the need to improve waste collection performance and further develop recycling infrastructure. Strengthening these aspects of municipal waste management could contribute to better environmental outputs and more efficient resource use, while supporting progress towards the United Nations Sustainable Development Goals, in particular SDGs 11 and 12.

However, the study also has certain limitations, mainly related to the availability of data at the municipal level. In several municipalities, some operational indicators were not fully reported in official sources, resulting in zero values for selected variables. These values do not necessarily imply the absence of waste management activities, but rather reflect limitations in data reporting. Despite these limitations, the analysis still provides valuable insights into the relative efficiency of municipal solid waste management system in Šumadija district. Overall, the results highlight the usefulness of DEA as a practical tool for assessing the performance of municipal waste management, and for supporting evidence-based decision-making in local environmental policy. Future research could apply system dynamics modelling to achieve more realistic evaluations of MSWM system efficiency.

References

1. Struk M, Boda M. Factors influencing performance in municipal solid waste management - A case study of Czech municipalities. Waste Management. 2022: 139: 227–249, https://doi.org/10.1016/j.wasman.2021.09.022
2. Guerrero AL, Maas G, Hogland W. Solid waste management challenges for cities in developing countries. Waste Management. 2013: 33 (1): 220-232, https://doi.org/10.1016/j.wasman.2012.09.008
3. Sala-Garrido R, Mocholi-Arce M, Molinos-Senante M, Maziotis A. Applying the Efficiency Analysis Tree Method for Enhanced Eco-Efficiency in Municipal Solid Waste Management: A Case Study of Chilean Municipalities. Clean Technologies. 2024: 6: 1565–1578. https://doi.org/10.3390/cleantechnol6040075
4. Velenturf APM, Purnell P. Resource recovery from waste: Restoring the balance between resource scarcity and waste overload. Sustainability. 2017: 9(9):1603. https://doi.org/10.3390/su9091603

5. Vukicevic AM, Petrovic M, Jurisevic N, Djapan M, Knezevic N, Novakovic A, Jovanovic K. Versatile waste sorting in small batch and flexible manufacturing industries using deep learning techniques. Sci Rep. 2025: 15: 3756. https://doi.org/10.1038/s41598-025-87226-x
6. Lo Storto C. Measuring ecoefficiency of municipal solid waste management in Apulia to account for governance heterogeneities. Cleaner Waste Systems. 2024: 7: 100131. https://doi.org/10.1016/j.clwas.2024.100131
7. Rogge N, De Jaeger S. Evaluating the efficiency of municipalities in collecting and processing municipal solid waste: A shared input DEA-model. Waste Management. 2012: 32 (10): 1968-1978. https://doi.org/10.1016/j.wasman.2012.05.021
8. Amaral C, Pedro MI, Ferreira DC, Marques RC. Performance and its determinants in the Portuguese municipal solid waste utilities. Waste Manag. 2022: 139: 70–84. https://doi.org/10.1016/j.wasman.2021.12.020
9. Li B, Xu J. An evaluation model based on data envelopment analysis and its application to county circular economy. World Journal of Modelling and Simulation. 2008: 4(1): 35-43.
10. Halkos G, Petrou KN. Assessing 28 EU member states' environmental efficiency in national waste generation with DEA. Journal of Cleaner Production. 2019: 208: 509-521. . https://doi.org/10.1016/j.jclepro.2018.10.145
11. Cooper WW, Seiford LM, Zhu J. (Eds.). Handbook on Data Envelopment Analysis, 2nd ed., Springer Science and Business Media: New York, NY, USA, 2011.
12. Mitakos A, Mpogiatzidis P. Operational Efficiency of Public Hospitals in Greece During the COVID-19 Pandemic: A Comparative Analysis Using DEA and AHP Models. Journal of Market Access & Health Policy. 2024: 12(4): 388–402. https://doi.org/10.3390/jmahp12040030
13. Drobnjaković M, Petrović G, Karabašević D, Vukotić S, Mirčetić V, Popović V. Socio-Economic Transformation of Šumadija District. Journal of the Geographical Institute “Jovan Cvijić”. 2021: 71 (2): 163–180. https://doi.org/10.2298/IJGI2102163D
14. Golany B, Roll Y. An application procedure for DEA. Omega. 1989: 17 (3): 237-250.
15. Serbian Environmental Protection Agency (SEPA). Available online: https://sepa.gov.rs/ (accessed on 1 March 2026).
16. Statistical Office of the Republic of Serbia. (n.d.). https://www.stat.gov.rs/en-US/ (accessed March 1, 2026).
17. Mullarkey Sh, Caulfield B, McCormack S, Basu B. A framework for establishing the technical efficiency of Electricity Distribution Counties (EDCs) using Data Envelopment Analysis. Energy Conversion and Management. 2015: 94: 112-123. https://doi.org/10.1016/j.enconman.2015.01.049

Co-Digestion Plants and Production Assessment

Nikola Rakić[1], Vanja Šušteršič[2]

[1] *Department of Energy and Process Engineering, Faculty of engineering, Kragujevac, Serbia, 0000-0001-7755-849X nikola.rakic@fink.rs*

[2] *Department of Energy and Process Engineering, Faculty of engineering, Kragujevac, Serbia, 0000-0001-7773-4991 vanjas@kg.ac.rs*

Corresponding author: nikola.rakic@fink.rs

Abstract

Anaerobic co-digestion is an innovative biotechnological process that efficiently manages organic waste while reducing greenhouse gas emissions. Properly applied, it can play a dual role: on the one hand, it can reduce methane emissions that would result from uncontrolled decomposition of organic waste in landfills; on the other hand, it can produce biogas that can be used as an energy source. The use of biogas offers the possibility of replacing fossil fuels while reducing CO_2 emissions, while the co-digestion by-product, known as digestate, is a stabilized waste material. The process itself minimizes unpleasant odors and destroys harmful pathogens in waste streams.

Keywords: co-digestion, biogas production, GHG footprint

1. Introduction

Anaerobic co-digestion is a process of decomposition of organic matter in the absence of oxygen, where microorganisms break down waste, directly producing methane-rich biogas. Biogas can further be used as a renewable energy source. Sewage sludge is a significant portion of biowaste generated during municipal wastewater treatment, according to [1], while the organic fraction of municipal solid waste (also known as biodegradable waste) further increases the potential for biogas production through co-digestion. It is the combination of these raw materials that allows for a more intensive process and an increase in methane yield.

2. Summary

Full-scale anaerobic co-digestion (AD) facilities integrate wastewater sludge, food waste, and agricultural residues to produce biogas, stabilized digestate, and renewable energy. These plants vary in size, feedstock composition, and technological configuration.

In June 2024, Hyundai E&C completed South Korea's first private biogas plant, Siheung Clean Energy Center, processing 540 m³/day sewage sludge, 145 m³/day food waste, and 60 m³/day manure over 33,430 m². Annual biogas production of 4.6 million Nm³ powers 8,283 households. Construction took 39 months, including 10 months of commissioning. Japan's Toyohashi Biomass Utilization Center, the largest composite biomass power plant, converts sewage sludge, human waste, septage, and food waste into energy and carbonized fuel. Anaerobic digesters operate at 35°C using waste heat, producing 6 t/day of fuel, with 5,000 m³ digesters, a 2,000 m³ gas holder, and a 1,000 kW generator. UK's Davyhulme Wastewater Treatment Works uses thermal

hydrolysis-AD to boost capacity from 39,000 to 121,000 t DS/year, serving 4–4.4 million people. Thermal hydrolysis at 165°C improves biogas yield, supplying 12 MW via CHP units; digestate is Class A biosolids[2].

Veas, Oslo, Norway treats wastewater from 867,000 people, producing 100 million m^3 effluent, 40,000 t biosolids, 60 GWh biogas, and 4,000 t nitrogen solution annually. Refined biogas (~6 million liters diesel equivalent) cuts GHG emissions >15,000 t CO_2-eq/year [3]. Monterey One Water, California, USA, handles 29.6 million and 5 million gallons/day in primary/secondary and tertiary treatments, with advanced treatment and reuse supported by grants. GreenWaste, San Jose, USA, the largest dry fermentation AD facility in the country, processes 90,000 t/year organic waste in 16 AD and 4 composting tunnels, using 2 × 800 kW cogeneration units, producing 30,000 t/year compost and energy for operations plus grid supply.

These examples demonstrate global trends toward large-scale integration of organic waste and energy recovery in urban wastewater systems (Table 1).

Table 1. Examples of worldwide implementations

Plant	Location	Produced energy (MWh/y)	Avoided CO_2-eq emissions (t/y)
Hyundai Clean Energy Center	Siheung, Korea	38.000	16.500
Toyohashi Biomass Center	Toyohashi, Japan	21.900	9.200
Davyhulme WwTW	Manchester, UK	105.000	48.000
Veas	Oslo, Norway	60.000	15.000
Monterey One Water	Marina, CA, USA	28.000	12.000
GreenWaste Recovery	San Jose, CA, USA	14.000	6.000
PUB Co-Digestion Project	Singapore	4.800	2.200
Newtown Creek	New York, USA	75.000	90.000
Baix Llobregat	Barcelona, Spain	32.000	14.500

3. Analysis & Evaluation

The Biochemical Methane Potential (BMP) test is the standard method for characterizing substrates and estimating maximum biogas yield [4]. BMP testing allows operators and researchers to:

- Evaluate substrate suitability for AD and co-digestion.
- Optimize reactor sizing and operating conditions.
- Detect inhibitory compounds that may affect methane production.

Small-scale batch reactors are used for BMP testing, with controlled mixing, temperature (mesophilic or thermophilic), and gas collection. Daily sampling allows monitoring of pH, COD, and biogas production. The results inform full-scale reactor design and substrate ratios, avoiding under- or over-sized digesters.

Evaluation of production is calculated as follows:
int main()

```
{
  double B0[16];
  double COD[16];

  printf("Unesite vrednosti prinosa biogasa (ml/g VS) pocevsi sa 0 i zakljucno sa 15. danom eksperimenta:\n");

  for(int i=0; i<16; i++)
  scanf("%lf", &B0[i]);

  printf("\nUneti niz za B0 je:\n");
  int j=0;
  while (j<16)
  printf("%.2lf ", B0[j++]);

  printf("\n\nUnesite vrednosti COD-a (g/l) pocevsi sa inicijalnom i zakljucno sa 15. danom eksperimenta:\n");

  for(int i=0; i<16; i++)
  scanf("%lf", &COD[i]);

  printf("\nUneti niz za COD je:\n");
  int p=0;
  while (p<16)
  printf("%.2lf ", COD[p++]);

  double sumB0 = 0;
  for (int i = 1; i<16; i++)
      sumB0 += B0[i];

  double sumCOD = 0;
  for (int i=1; i<16; ++i)
      sumCOD+=COD[i];

  printf("\n\nKoordinate druge tacke su:(%.2lf, %.2lf)\n\n", sumB0/15, sumCOD/15);

  double k=0;
  double n=0;

  k=((sumCOD/15)-COD[0])/(sumB0/15);
  n=((sumB0/15)*COD[0])/(sumB0/15);

  printf("Jednacina prave u eksplicitnom obliku je:\nCOD=%.3lf*B+%.2lf\n", k,n);

  return 0;
}
```

4. Carbon Footprint and GHG Emissions

Carbon accounting is crucial for evaluating the climate impact of co-digestion plants. Wastewater treatment facilities are sources for national GHG inventories, and incremental approaches assess net emissions across transport, treatment, disposal, recycling, and energy production [5]. Anaerobic co-digestion reduces carbon emissions by stabilizing organic matter and replacing fossil-based energy and fertilizers. Food waste and sludge with higher organic content (e.g., 70%) result in up to 68% lower emissions compared to low-organic substrates [6].

Scopes for Carbon Accounting [7]:

- Scope 1: direct emissions from digestion, digestate treatment, chemical use.
- Scope 2: indirect emissions from purchased electricity, heat, or steam.
- Scope 3: upstream/downstream emissions from transport, preprocessing, digestate application, and equipment.

Avoided emissions occur when biogas substitutes grid electricity or fossil fuels and when digestate replaces synthetic fertilizers. These are quantified using project- and country-specific emission factors, considering energy efficiency and grid losses (~7% by default). Biogas releases carbon already in the fast carbon cycle (1–500 years), unlike fossil fuels that transfer long-stored carbon to the atmosphere, thus increasing net CO_2.

5. Conclusions

Full-scale co-digestion plants worldwide demonstrate the potential to integrate wastewater and organic waste management with renewable energy production. Using these facilities is in accordance with SDGs 6, 7 and 13. Laboratory BMP testing ensures substrate suitability and process optimization. Carbon footprint assessments, using Scope 1–3 frameworks and accounting for avoided emissions, provide a quantitative basis to evaluate GHG reductions. Overall, anaerobic co-digestion contributes to:

- Reduction of waste volumes and pathogens.
- Renewable energy production.
- Sustainable nutrient recycling.
- Significant mitigation of greenhouse gas emissions.

Acknowledgments

This research was funded by the Republic of Serbia – Project No. 42013

References

[1] Chen YC, Kuo J. Potential of greenhouse gas emissions from sewage sludge management: A case study of Taiwan. J Clean Prod 2016;129:196–201. https://doi.org/10.1016/j.jclepro.2016.04.084.

[2] Jolly, M., Belshaw, D. and Telfer, J. 18th European Biosolids and Organic Resources Conference. Commissioning of United Utilities thermal hydrolysis digestion plant at Davyhulme waste water treatment works. 2013

[3] https://veas.nu/uploads/2023/11/VEAS-IN-BRIEF-2021.pdf

[4] Raposo F, Fernández-Cegrí V, de la Rubia MA, Borja R, Béline F, Cavinato C, Demirer G, Fernández B, Fernández-Polanco M, Frigon JC, Ganesh R, Kaparaju P, Koubova J, Méndez R, Menin G, Peene A, Scherer

P, Torrijos M, Uellendahl H, Wieringck I, de Wilde V. Biochemical methane potential (BMP) of solid organic substrates: Evaluation of anaerobic biodegradability using data from an international interlaboratory study. Journal of Chemical Technology and Biotechnology 2011;86:1088–98. https://doi.org/10.1002/jctb.2622.

[5] Teichmann D, Schempp C. Calculation of GHG Emissions in Waste and Waste-to-Energy Projects. JASPERS Knowledge Economy and Energy Division Staff Working Papers. November 2013.

[6] Xu Y, Liu R, Yang D, Dai X. Sludge treatment and resource recovery towards carbon neutrality in China: current status and future perspective. Blue-Green Systems 2021;3:119–27. https://doi.org/10.2166/bgs.2021.115.

[7] EIB Project Carbon Footprint Methodologies. Methodologies for the assessment of project greenhouse gas emissions and emission variations. European Investment Bank. January 2023.

Composting of Food Waste in the Hospitality Sector: Lessons from Vrnjačka Banja

Sonja Veljović[1], Marija Kostić[2], Milica Luković[3]

[1,2,3]*Faculty of Hotel Management and Tourism in Vrnjačka Banja, University of Kragujevac, Vrnjačka Banja,*
sonja.veljovic@kg.ac.rs, https://orcid.org/0000-0001-6408-9153
marija.kostic@kg.ac.rs, https://orcid.org/0000-0001-8105-8033
milica.petrovic@kg.ac.rs; https://orcid.org/0000-0002-7102-0178

Corresponding author: sonja.veljovic@kg.ac.rs

Abstract

The tourism and hospitality industry produces more than 35 million tons of solid waste annually, while food and beverage services alone contribute up to 650,000 tons per year. Therefore, it is essential to implement appropriate practices to reduce food waste, such as composting. The main aim of this paper was to analyze the composition of selected food waste generated in local hotels and restaurants in Vrnjačka Banja. In addition, the study aimed to measure the pH and electrical conductivity (EC) of compost produced from this waste, with the addition of EM active to accelerate the composting process at the Composting Pilot facility. Compost production represents an important approach for managing unavoidable waste from the hospitality industry. However, it is crucial to assess compost quality carefully to prevent potential soil acidification.

Keywords: composting; circular economy; SDG12

1. Introduction

The tourism and hospitality industry generates more than 35 million tons of solid waste annually [1], while food and beverage services alone contribute up to 650,000 tons per year [2]. The management and disposal of such large quantities of waste are increasingly costly, primarily due to diminishing landfill capacity and the rising costs of waste collection. At the same time, waste management regulations in the hotel industry are becoming increasingly stringent, particularly within the European Union [2]. Consequently, reducing food waste has emerged as one of the key challenges in the hospitality sector. This includes not only minimizing waste generation but also implementing efficient strategies for its reuse and recycling, thereby reducing the amount of waste ultimately disposed of in landfills.

Serbia belongs to 64 countries that are committed to work towards implementing and achieving the Sustainable Development Goals (17 SDGs). Tourism is explicitly recognized within several of these goals, particulary SDG 4 for “Life Below Water”; SDG 8 for ”Decent Work and Employment” and SDG 12 for ”Responsible Consumption and Production”. SDG 12 focuses on promoting sustainable consumption and production patterns, which which are essential for preserving resources and ensuring long-term societal well-being. In this context, reducing the environmental impact of the tourism and hospitality sector has become a critical priority. Organic waste generated in hotels and restaurants is predominantly disposed of as mixed waste, leading to inefficient

resource use and increased environmental burden. Therefore, it is necessary to implement integrated waste management strategies based on the principles of reduction, reuse, and recycling. These strategies may include composting, the production of animal feed, or the generation of other value-added products from food waste. The main aim of this paper was to analyze the composition and quality of selected food waste generated in local hotels and restaurants in Vrnjačka Banja, one of the most visited spa destinations in the region. Furthermore, the study aimed to determine the pH and EC of the compost produced from this waste with the addition of EM active to accelerate the composting process at the Composting Pilot facility located at the Faculty of Hotel Management and Tourism in Vrnjačka Banja.

2. Materials and Methods

During three months, we are collecting waste from the three local hotels (*Pegaz Holiday Resort*, *Tonanti* and *Fontana*) and one fast-food restaurant in Vrnjačka Banja. The waste was separated at the source during meal preparation and consisted exclusively of unavoidable organic fractions, including fruit and vegetable peels and spoiled plant material. Plate waste was excluded due to the presence of oil, salt, and mixed food residues, which are unsuitable for controlled composting processes. After collection, the waste was transported to the Faculty of Hotel Management and Tourism in Vrnjačka Banja, where the composting process was carried out using a pilot-scale automatic composter (Figure 1) with a capacity of 100 kg per 24 hours. The system operates autonomously, monitoring and adjusting process parameters without the need for continuous human intervention. The process is designed to be low-noise, odor-free, and without the emission of harmful by-products.

The composting process is based on anaerobic digestion in accordance with Article 40 of the Law on Waste Management ("Official Gazette of the Republic of Serbia", No. 36/2009, 88/2010, 14/2016, 95 /2018 - other laws and 35/2023). The process was conducted at temperatures ranging from 45 to 75 ºC. The composter is installed at the Faculty of Hotel Management and Tourism in Vrnjačka Banja, University of Kragujevac.

3. Results

Previous studies on composting have predominantly been conducted under controlled laboratory conditions, focusing on the quality of compost derived from selected food waste streams. However, the composition of food waste generated in real hospitality settings varies significantly and directly influences compost characteristics. The analysis of collected food waste revealed notable differences between sources. In the fast-food restaurant, the waste consisted entirely (100%) of vegetable residues, predominantly peels. In contrast, food waste from hotels contained a more diverse composition, with more than 30% consisting of citrus fruit peels (e.g., oranges and lemons). This high proportion of citrus waste has a significant impact on the chemical properties of the produced compost, particularly its pH. The presence of citrus residues contributes to increased acidity, resulting in lower pH values of the final product. In addition, rapid degradation processes may further influence the accumulation of organic acids, as reported in previous studies Sundberg et al., 2013 [3].

After a detailed analysis of pH and EC values (Table 1), it is found that the mixture of food waste from hotels and restaurants has a negative effect on copmpos pH. The measured pH values were significantly lower than the optimal range of 7-8, which is generally considered suitable for agricultural application. Therefore, prior to

its use as a fertilizer, the compost requires additional treatment or stabilization to increase pH and ensure its suitability for soil application.



Figure 1. The Pilot Composting Facilities

Table 1. The pH and EC of the produced compost from mixed waste (~30% of citrus peel) after 24h

Samples	pH	EC
1	4.30	145
2	5.00	116
3	4.46	123
4	4.66	113

Given the low pH of the produced compost, the influence of EM active on the composting process was further investigated. In this experiment, food waste obtained from the restaurant was used, consisting exclusively of vegetable peels.

Table 2. The pH and EC of the produced compost from waste (100% of vegetable peel) after 24h and 48h with the addition of EM active.

samples	pH1	pH2	EC1	EC2
1	6.19	5.82	52	58
2	5.36	4.50	115	119
3	6.30	5.70	110	130
4	6.12	5.82	120	135

The influence of EM active on compost pH was evaluated after 24h and 48h of composting in an automatic composter (Table 2). The results indicate that pH values were higher after 24 hours compared to those measured after 48 hours. This decrease in pH over time can be attributed to the activity of microorganisms stimulated by the addition of EM active, leading to increased production of organic acids in the final compost.

4. Discussion

Composting represents a widely recognized and cost-effective method for the treatment of organic waste, offering several environmental benefits, including the reduction of landfill waste, mitigation of greenhouse gas emissions, and extension of landfill lifespan. As a biological process, composting involves the decomposition of organic matter by macro- and microorganisms under controlled conditions, resulting in the formation of stable end products such as carbon dioxide, water, ammonia, and humus. However, the findings of this study highlight certain limitations associated with composting of food waste from the hospitality sector. In particular,

the high proportion of citrus residues identified in hotel waste significantly contributed to lower pH values of the produced compost. Such acidic conditions may limit the direct application of compost in agriculture without prior stabilization or treatment. Although composting is generally considered an environmentally beneficial process, it may also be associated with the emission of gases and the generation of leachate, which can have adverse environmental impacts if not properly managed. Additionally, conventional composting processes can be time-consuming, which represents a practical limitation for large-scale implementation in the hospitality sector. Recent advancements in composting technologies have focused on the use of microbial inoculants to enhance process efficiency and control product quality. The results of this study indicate that the application of EM active influences compost characteristics, particularly pH dynamics, by stimulating microbial activity and accelerating the decomposition process. However, this may also lead to increased production of organic acids, as observed in the present study.

Therefore, while EM active technology represents a promising and innovative approach for bio-waste treatment, its application requires careful optimization to ensure the production of compost with suitable chemical properties. In the context of Serbia, the implementation of such technologies remains limited, highlighting the potential for further development and adoption within the hospitality sector.

5. Conclusions

This study confirms that composting represents an effective and economically viable approach for managing organic waste generated in the hospitality sector, contributing to the reduction of landfill use, mitigation of emissions, and more sustainable resource management. However, the results indicate that the composition of food waste, particularly the high proportion of citrus residues, significantly affects the chemical properties of the produced compost, leading to lower pH values that may limit its direct application in agriculture. Therefore, it is essential to carefully assess and, if necessary, further treat or stabilize compost prior to its use, in order to ensure its suitability for soil application and to prevent potential soil acidification. Additionally, optimizing composting conditions and input materials can improve compost quality and enhance its practical applicability within sustainable waste management systems in the hospitality industry.

Acknowledgements

This research is supported by the Ministry of Science, Technological Development and Innovation of the Republic of Serbia by the Decision on the scientific research funding for teaching staff at the accredited higher education institutions in 2026 (No. 451-03-34/2026- 03/200375 of February 5, 2026).

References

1. United Nations Environmental Programme and United Nations World Tourism Organization, 2012
2. International Tourism Partnership (2008) Environmental Management for Hotels, Waste, Waste Management-Objectives. Third Edition 2008.
3. Sundberg S., Yu D, Franke-Whittle I, Kauppi S, Smårs S, Insam H, Romantschuk M, Jönsson H. Effects of pH and microbial composition on odour in food waste composting. Waste Management, 2013; 33, 204-211.

Sustainable Hydrogen Production from Food Waste Using Integrated Gasification and Sorption-Enhanced Reforming

Ali Atas[a,b,*], Nader Javani[b], Betul Colak Karadag[b,c], Ozgun Yucel[d]

[a]Istanbul Topkapi University, Department of Motor Vehicles and Transportation Technologies, 34020, Istanbul, Türkiye, aliatas@topkapi.eduu.tr, 0000-0002-9419-5106

[b]Yildiz Technical University, Department of Mechanical Engineering, 34210, Istanbul, Türkiye, njavani@yildiz.edu.tr, 0000-0002-9788-7888

[c]Çanakkale Onsekız Mart University, Department of Electrıcal and Energy, 17400, Canakkale, Türkiye, betulcolak@comu.edu.tr, 0009-0000-9432-3350

[d] Gebze Technical University, Department of Chemical Engineering, 41400, Kocaeli, Türkiye, yozgun@gtu.edu.tr, 0000-0001-8916-2628

*Corresponding author: aliatas@topkapi.edu.tr

Abstract

The increasing demand for sustainable energy systems has intensified interest in hydrogen production from renewable resources. In this study, an integrated thermochemical process combining biomass gasification and Sorption-Enhanced Reforming (SER) was developed using Aspen Plus® to produce high-purity hydrogen from food waste (FW). The gasification process was modeled using a fixed-bed reactor under equilibrium conditions, followed by an SER unit employing calcium oxide (CaO) as a CO_2 sorbent to enhance hydrogen yield. The model was validated against experimental data, showing good agreement with literature values. Simulation results indicate that hydrogen purity reaches up to 99.4% at 923 K and 20 bar, while the H_2 mole fraction in the syngas reaches 94%. Sensitivity analyses demonstrate that gasification temperature affects hydrogen production. Increasing temperature enhances hydrogen yield up to an optimal point. The integrated system enables simultaneous hydrogen production and carbon capture, achieving over 90% CO_2 removal. The proposed approach provides an efficient and scalable pathway for converting organic waste into clean energy, contributing to low-carbon and sustainable energy systems.

Keywords; Gasification; Sorption enhanced reforming; Hydrogen production; Sustainable energy; UN SDG 7

1. Introduction

The increasing global energy demand, together with environmental challenges associated with fossil fuel utilization, has intensified the transition toward sustainable and low-carbon energy systems. In this context, hydrogen is widely recognized as a promising clean energy carrier owing to its high energy density and the absence of carbon emissions at the point of use. Nevertheless, current hydrogen production is still predominantly reliant on fossil-based pathways, which results in considerable carbon dioxide emissions [1], [2].Biomass, particularly organic residues such as food waste (FW), is a renewable and widely available feedstock for sustainable hydrogen production. Thermochemical pathways, especially gasification, convert biomass into syngas mainly composed of H_2, CO, CO_2, and CH_4. However, conventional gasification systems are inherently

constrained by thermodynamic limitations, which restrict the achievable hydrogen yield and overall process efficiency [3].

Sorption-enhanced reforming (SER) is an effective approach to overcoming thermodynamic limitations in conventional systems. In this process, CO_2 is captured in situ by calcium oxide (CaO), shifting the equilibrium toward hydrogen production in accordance with Le Chatelier's principle, thereby enhancing both hydrogen yield and purity. Therefore, SER represents a promising pathway for sustainable hydrogen production with integrated carbon capture [4], [5].

This study aims to develop and validate an integrated gasification–SER model for hydrogen production from food waste using Aspen Plus®. The novelty lies in combining gasification and sorption-enhanced reforming within a single framework to enable high-purity hydrogen production within situ carbon capture, contributing to improved process efficiency and sustainability.

2. Materials and Methods

The process was modeled in Aspen Plus under steady-state and equilibrium conditions, comprising gasification and sorption-enhanced reforming (SER) stages. Food waste was defined as a non-conventional component using ultimate and proximate analyses. Biomass decomposition was modeled with a RYIELD reactor, while gasification was simulated using an RGIBBS reactor based on Gibbs free energy minimization. The model structure, illustrated in Figure 1, consists of sequential gasification and SER stages.

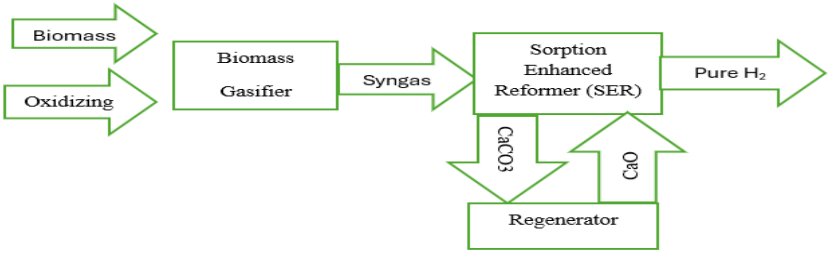


Figure 1. Schematic of the integrated gasification–SER process

The gasification process involves drying, decomposition, and gasification stages, using air as the gasifying agent at 800–1500 K under atmospheric pressure. The produced syngas is fed into the SER unit, where CaO captures CO_2 via carbonation. The SER reactor operates at 923 K and up to 20 bar, with key reactions including water–gas shift and methane reforming.

3. Results

The Aspen Plus gasification model was validated using experimental data from Naveed et al. [7] and Ramzan et al. [8]. Validation was specifically conducted for food waste (FW) to ensure consistency with the selected feedstock. Model accuracy was evaluated by comparing the predicted syngas composition with literature data. The deviation between simulated and experimental values was quantified using the root means square error (RMSE) [9].Table 1 presents the comparison of model predictions with literature data for food waste (FW).

Table 1. Comparison of model predictions and experimental data for food waste

Biomass Type	Study	Syngas composition (%v/v.dry)				
FW	Literature	5.13	11.29	10.13	2.56	67.01

Our Model	9.30	12.10	9.20	2.60	64.60

The effect of gasification temperature on syngas composition for food waste (FW) was evaluated over 800–1100 K. Increasing temperature promotes endothermic reactions, increasing H_2 and CO while decreasing CO_2 and CH_4. Beyond ~1100 K, hydrogen production plateaus due to equilibrium limitations. Figure 2, and the optimal range for maximizing hydrogen yield is 1000–1100 K.

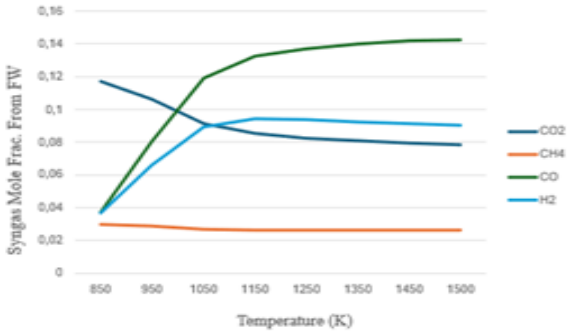


Figure 2. Effect of gasification temperature on syngas composition

The sorption-enhanced reforming (SER) model was validated using literature data reported by Yücel and Aydın [10] In this approach, calcium oxide (CaO) was used as a CO_2 sorbent to enhance hydrogen production through in situ carbon capture. The model was assessed across pressures of 5–20 bar and varying temperatures at an S/C ratio of 5, showing strong agreement with literature data (RMSE = 0.68). The highest hydrogen composition was obtained at 20 bar and 923 K, consistent with reported experimental trends.

The effect of gasification temperature on hydrogen (H_2) composition after SER integration was evaluated for food waste (FW) over a range of 800–1500 K at constant pressure. The H_2 mole fraction increases markedly up to ~1000 K due to enhanced reforming and water–gas shift reactions, then stabilizes. A maximum H_2 fraction of approximately 94% is achieved, highlighting the strong impact of SER on hydrogen enrichment.

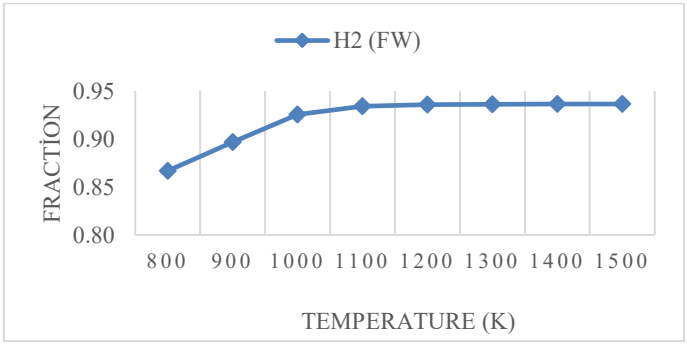


Figure 3. Effect of gasification temperature on H_2 mole fraction after SER integration for food waste

4. Discussion

The integration of sorption-enhanced reforming (SER) with biomass gasification significantly enhances hydrogen production by shifting the equilibrium toward hydrogen formation through in situ CO_2 removal, while also reducing carbon emissions. The improved hydrogen purity is attributed to the simultaneous optimization of temperature, pressure, and sorbent loading, and the use of food waste highlights the potential of waste-to-energy strategies. However, the model relies on thermodynamic equilibrium assumptions and does not account for kinetic limitations or tar formation; thus, future work should incorporate kinetic modeling and experimental validation.

5. Conclusions

This study presents an integrated gasification–SER model for hydrogen production from food waste using Aspen Plus®. The main findings can be summarized as follows:

- Hydrogen purity reached up to 99.4% under optimal conditions.
- A hydrogen mole fraction of 94% was achieved for food waste.
- CO_2 capture efficiency exceeded 90%.
- Temperature was identified as a critical parameter influencing hydrogen yield.

The integrated system offers a promising pathway for sustainable hydrogen production from organic waste. Future work should focus on economic assessment and experimental validation to further enhance the applicability of the proposed system.

Acknowledgements

The research was funded by Yildiz Technical University's Scientific Research Projects Council (Project No: FBA_2023_5648). The authors appreciate providing Aspen program licence by the University.

References

[1] A. Boretti and B. G. Pollet, "Hydrogen economy: Paving the path to a sustainable, low-carbon future," *Int. J. Hydrogen Energy*, vol. 93, pp. 307–319, Dec. 2024, doi: 10.1016/j.ijhydene.2024.10.350.

[2] A. I. Abd El-Rahman, W. A. Abdelfattah, K. S. Abdelwahed, A. Salama, A. Rabie, and A. Hamdy, "Hydrogen energy systems: Technologies, trends, and future prospects," *Science of The Total Environment*, vol. 939, p. 173622, Aug. 2024, doi: 10.1016/j.csite.2020.100708.

[3] T. Ahmad and D. Zhang, "Sustainable conversion of wet biomass, algae, and food waste to fuels in hot compressed water: Multi-Scale analysis," *Prog. Energy Combust. Sci.*, vol. 112, p. 101264, Jan. 2026, doi: 10.1016/j.egyr.2020.07.020.

[4] M. A. Alsaffar, A. K. Mageed, M. A. R. Abdel Ghany, B. V. Ayodele, and S. I. Mustapa, "Elucidating the non-linear effect of process parameters on hydrogen production by catalytic methane reforming: An artificial intelligence approach," *IOP Conf. Ser. Mater. Sci. Eng.*, vol. 991, no. 1, p. 100003, Dec. 2020, doi: 10.1088/1757-899X/991/1/012078.

[5] Z. Abdin, A. Zafaranloo, A. Rafiee, W. Mérida, W. Lipiński, and K. R. Khalilpour, "Modelling of sorption-enhanced steam reforming (SE-SR) process in fluidised bed reactors for low-carbon hydrogen production: A review," *Fuel*, vol. 340, p. 127588, May 2023, doi: 10.1016/j.rser.2019.109620.

[6] S. Begum, M. G. Rasul, D. Akbar, and N. Ramzan, "Performance analysis of an integrated fixed bed gasifier model for different biomass feedstocks," *Energies (Basel).*, vol. 6, no. 12, pp. 6508–6524, Dec. 2013, doi: 10.3390/en6126508.

[7] N. Ramzan, A. Ashraf, S. Naveed, and A. Malik, "Simulation of hybrid biomass gasification using Aspen plus: A comparative performance analysis for food, municipal solid and poultry waste," *Biomass Bioenergy*, vol. 35, no. 9, pp. 3962–3969, Oct. 2011, doi: 10.1016/J.BIOMBIOE.2011.06.005.

[8] S. Naveed, A. Malik, N. Ramzan, and M. Akram, "The Nucleus A Quarterly Scientific Journal of Pakistan Atomic Energy Commission A COMPARATIVE STUDY OF GASIFICATION OF FOOD WASTE (FW), POULTRY WASTE (PW), MUNICIPAL SOLID WASTE (MSW) AND USED TIRES (UT)," 2009.

[9] M. Cakar, M. A. Insel, H. Sadikoglu, and O. Yucel, "Utilization of machine learning algorithms in estimation of syngas fractions and exergy values for gasification of biomass-lignite mixtures in fixed and fluidized bed gasifiers," *Fuel*, vol. 401, p. 135883, Dec. 2025, doi: 10.1016/J.FUEL.2025.135883.

[10] O. Yucel and E. S. Aydin, "Modeling of biomass-based hydrogen production via catalytic sorption-enhanced reformer integrated with a gasifier," *Journal of the Indian Chemical Society*, vol. 100, no. 1, p. 100854, Jan. 2023, doi: 10.1016/J.JICS.2022.100854.

Sustainable Buildings, Energy Efficiency, and Water Systems

Integrated Monitoring and Determination of Showering Parameters in Residential Buildings

Natalija Aleksić[1], Vanja Šušteršič[2], Strahinja Milenković[3]

[1]*Department for Energy and Process Engineering, Faculty of Engineering, University of Kragujevac, Kragujevac, Serbia, vanjas@kg.ac.rs, ORCID 0000-0001-9341-7806*
[2]*Department for Energy and Process Engineering, Faculty of Engineering, University of Kragujevac, Kragujevac, Serbia, natalija.aleksic@fink.rs, ORCID 0000-0001-7773-4991*

[3]*Department for Applied Mechanics and Automatic Control, Faculty of Engineering, University of Kragujevac, Kragujevac, Serbia, strahinja.milenkovic@fink.rs, ORCID 0000-0002-5822-4846*

Corresponding author: natalija.aleksic@fink.rs

Abstract

Showering is considered one of the dominant end-uses of domestic hot water in residential buildings, accounting for a significant portion of water and energy consumption. Accurate and integrated monitoring of showering parameters is therefore essential. Most existing studies rely on partial measurements or assumed values of individual parameters, which limits the comprehensive analysis of shower events. This study introduces a methodology that combines data from a smart shower device and an embedded monitoring system using the Arduino UNO R4 Wi-Fi platform. The smart shower records water volume and energy consumption per shower event, while the embedded system enables the determination of shower duration and continuous monitoring of wastewater temperature in the shower drain with a temporal resolution of one second. Integration of these datasets enables the determination of showering parameters for each event, including flow rate, mixed water temperature, and wastewater temperature at the drain. The methodology was tested over a one-month period in a household. Results confirm reliable determination of showering parameters and establish a basis for future analysis of water use and associated energy consumption during showering.

Keywords: showering parameters; domestic hot water; water consumption; energy consumption; integrated monitoring; residential buildings; sustainable development goals

1. Introduction

Showering is a major end use of water and energy in residential buildings [1], accounting for approximately 40-45% of household water consumption [2, 3] and about 14.42% of energy used for water heating [4] in residential buildings. Both technological factors and user behavior influence water and energy use during showering [5]. Key parameters used to describe showering include water volume, shower duration, and showerhead flow rate [6]. Water consumption depends on shower duration, flow rate (shower intensity), and frequency of shower events [7], while energy use depends on water temperature, shower duration, and flow rate [8]. Among these

parameters, shower duration is often identified as the most significant factor affecting total consumption [9, 10]. The high variability of shower parameters [11, 12] underscores the need for detailed monitoring. Also, individual monitoring of domestic hot water use allows detailed analysis of shower parameters, which can help reduce water and energy consumption in residential buildings [13-15]. Previous studies have analyzed water consumption and related energy consumption during showering using different monitoring approaches. However, many rely on limited measurements or indirect estimates, highlighting a gap in comprehensive monitoring and determination of showering parameters at the level of individual shower events. As a result, the relationships between showering parameters and their impact on consumption are not fully understood. To address this gap, this study aims to develop an integrated monitoring approach for determining showering parameters by combining measurements from a smart shower device and an embedded monitoring system. Also, this study contributes to Sustainable Development Goals SDG 6, SDG 7, and SDG 12 by improving understanding of water and energy use during showering.

2. Materials and Methods

To determine shower parameters, an integrated monitoring system was developed that combines data from a digital smart shower and a built-in measuring system using the Arduino UNO R4 Wi-Fi board. The smart shower device, HANSAACTIVEJET Digital [16], recorded water consumption and estimated energy required for water heating for each shower event, with data stored and displayed in the accompanying mobile application. For additional data collection, an embedded monitoring system was developed based on the Arduino UNO R4 Wi-Fi board, connected to a waterproof DS18B20 digital temperature sensor installed in the shower drain to measure wastewater temperature and a sensor for measuring ambient air temperature in the bathroom. The start of the shower event was identified by an increase in drain temperature, while the end of the shower was determined when the temperature began to decrease and showed a continuous declining trend over a certain period of time. Shower duration was defined as the time interval between the identified start and end of the shower event. Water use activities that did not meet the criteria for showering (drain temperature below 35°C and water use duration shorter than 3 min) were excluded from analysis. Data were collected with a temporal resolution of one second. Monitoring was conducted in a single household in a residential building over one month. Based on the collected data, individual shower events were identified. For each event, the following parameters were determined: start and end of the shower event, shower duration, volume of consumed water, average mixed water temperature, energy consumption for water heating, average flow rate, and average wastewater temperature. Figure 1 shows the methodological framework for integrated monitoring and determination of showering parameters.

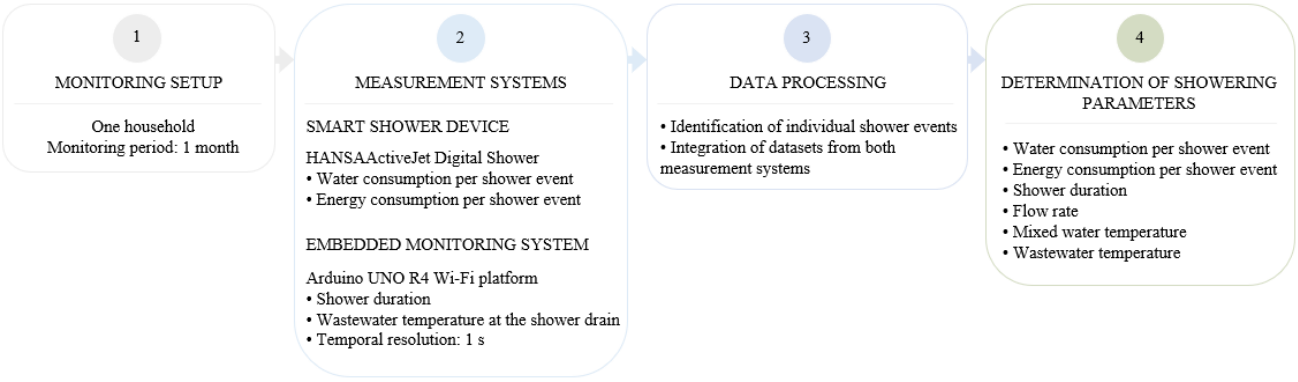


Figure 1. Methodological framework for integrated monitoring and determination of showering parameters

3. Results and Discussion

Table 1 summarizes the statistical characteristics of 40 recorded shower events during the monitoring period. Average water consumption per shower was 61.08 L, with an average energy consumption of 3.15 kWh and a mean shower duration of 6.64 minutes. Total water consumption reached 2443.2 L, and estimated energy consumption for water heating was 125.97 kWh. On average, water heating requires approximately 0.052 kWh per liter. Water consumption (28%), energy consumption (29%), and shower duration (27%) showed considerable variability, reflecting differences in user behavior. In contrast, temperature-related parameters showed relatively low variability (3%-5%), indicating stable thermal conditions.

Table 1. Statistical characteristics of showering parameters obtained during the monitoring period (n=40)

Parameter	*Mean*	*SD*	*Min*	*Max*	*CV [%]*
Water and energy parameters					
Water consumption per shower event, V [L]	61.08	17.40	35.80	108.50	28
Energy consumption for water heating, Q [kWh]	3.15	0.91	1.35	5.53	29
Average flower rate, q [l/min]	9.24	1.17	5.57	11.55	13
Shower duration, t [min]	6.64	1.79	3.63	12.07	27
Temperature parameters					
Average mixed water temperature, T_m [°C]	40.59	1.50	34.87	42.59	4
Average wastewater temperature, T_o [°C]	36.01	1.06	32.59	38.63	3
Temperature difference, ΔT_m [°C]	32.59	1.50	26.87	34.59	5

Figure 2a demonstrates that energy consumption increases proportionally with the volume of water used during showering. Figure 2b further illustrates that longer shower durations result in higher water and energy consumption. These findings indicate that the proposed integrated monitoring approach enables reliable determination of showering parameters at the level of individual shower events.

a) b)

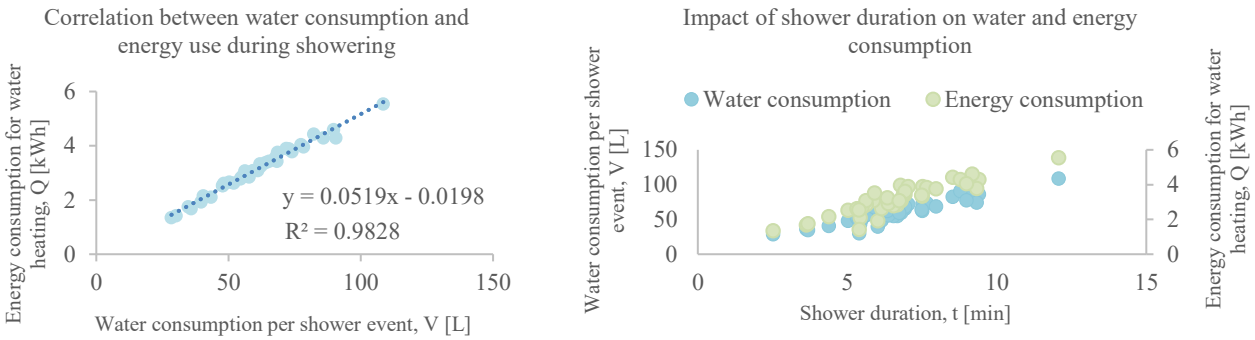


Figure 2. Showering parameters analysis: a) relationship between water consumption and energy consumption during showering events; b) influence of shower duration on water and energy consumption

The results align with previous studies on domestic hot water consumption during showering. The average volume of domestic hot water consumed per shower event in this study (61.08 L) falls within the range reported in previous studies [17, 18]. Literature shows that average water consumption per shower varies widely, from approximately 20 L to 200 L [19], depending mainly on flow rate and shower duration. The average energy consumption per shower (3.15 kWh) is also similar to values reported in previous studies [20]. Variations in energy consumption during showering are mainly attributed to differences in shower duration [21]. This study confirms a strong relationship between water consumption and the corresponding energy required for water heating. The observed shower durations align with previous findings, with a typical duration between 5 and 10 minutes [19]. However, depending on user behavior, individual events may be shorter than 5 minutes or longer than 15 minutes. These results should be considered with limitations, as the monitoring was conducted in a single household over one month.

4. Conclusions

This study used an integrated monitoring approach, combining a smart shower device and an embedded system, to measure showering parameters for individual shower events in a single household over one month. The findings show that: 1) the proposed methodology is effective in determining showering parameters; 2) energy consumption rises with increases in water consumption; 3) shower duration affects both water and energy consumption; 4) variation in water consumption and shower duration reflects user behavior. Future research should include longer monitoring periods and conducting statistical analysis to understand the relationship between parameters and define measures to reduce water and energy consumption during showering. Further classification of shower events by individual users is also recommended.

References

1. Zhang D, Mui KW, Wong LT. A focus group study on occupants' behaviours and preferences for ideal showering environment. Building and Environment. 2025;285:113548. https://doi.org/10.1016/j.buildenv.2025.113548

2. Abu-Bakr H, Williams L, Hallett SH. A review of household water demand management and consumption measurement. Journal of Cleaner Production. 2021;292:125872. https://doi.org/10.1016/j.jclepro.2021.125872

3. Department for Energy Security and Net Zero. Domestic hot-water use: observations on hot-water use from connected devices. London: UK Government; 2024. Available from: https://www.gov.uk/government/publications/domestic-hot-water-use-in-the-uk. Accessed: 07 Mar 2026.

4. Eurostat. Energy consumption in households. Statistics Explained. Available at: https://ec.europa.eu/eurostat/statistics-explained/index.php?title=Energy_consumption_in_households. Accessed: 07 Mar 2026.

5. Ibáñez-Rueda N, Guardiola J, López-Ruiz S, González-Gómez F. Towards a sustainable use of shower water: Habits and explanatory factors in southern Spain. Sustainable Water Resources Management. 2023;9:121. https://doi.org/10.1007/s40899-023-00905-3

6. Rahim MS, Nguyen KA, Stewart RA, Ahmed T, Giurco D, Blumenstein M. A clustering solution for analyzing residential water consumption patterns. Knowledge-Based Systems. 2021;233:107522. https://doi.org/10.1016/j.knosys.2021.107522

7. Josey BM, Gong J. Determination of Fixture-Use Probability for Peak Water Demand Design Using High-Level Water End-Use Statistics and Stochastic Simulation. Journal of Water Resources Planning and Management. 2023;149(11):05023015. https://doi.org/10.1061/JWRMD5.WRENG-6146

8. Wong L-T, Mui K-W, Chan Y-W. Showering Thermal Sensation in Residential Bathrooms. Water. 2022; 14(19):2940. https://doi.org/10.3390/w14192940

9. Shahmohammadi S, Steinmann Z, King H, Hendrickx H, Huijbregts MAJ. The influence of consumer behavior on energy, greenhouse gas and water footprints of showering. Journal of Industrial Ecology. 2019;23:1186–1195. https://doi.org/10.1111/jiec.12858

10. Adeyeye K, She K, Meireles I. Beyond the flow rate: the importance of thermal range, flow intensity, and distribution for water-efficient showers. Environmental Science and Pollution Research. 2019;27(5):4640–4660. https://doi.org/10.1007/s11356-019-07235-y

11. Pereira-Doel P, Font X, Wyles K, Pereira-Moliner J. Reducing Shower Duration in Tourist Accommodations: A Covert True Experiment of Continuous Real-Time Eco-Feedback and Persuasive Messaging. Journal of Travel Research. 2025;64(5):1100–1120. https://doi.org/10.1177/00472875241245045

12. Simpson K, Staddon C, Ward S. Challenges of Researching Showering Routines: From the Individual to the Socio-Material. Urban Science. 2019;3(1):19. https://doi.org/10.3390/urbansci3010019

13. Tomic U, Sütterlin B, Lobsiger-Kägi E, Marek R, Derungs C, Sandmeier E. Reducing hot water consumption through real-time feedback and social comparison using persuasive technologies: evidence from a Swiss energy-efficient district. Energy Efficiency. 2024;17:15. https://doi.org/10.1007/s12053-024-10199-9

14. Mazzoni F, Marsili V, Alvisi S. Characterizing Hot-Water Consumption at Household and End-Use Levels Based on Smart-Meter Data. Water. 2025;17(13):1906. https://doi.org/10.3390/w17131906

15. Canale L, Cholewa T, Ficco G, Siuta-Olcha A, Di Pietra B, Kołodziej P, Dell'Isola M. The role of individual metering in reducing domestic hot water consumption in residential buildings: A long-term evaluation. Journal of Building Engineering. 2023;73:106734. https://doi.org/10.1016/j.jobe.2023.106734

16. HANSA. HANSAACTIVEJET Digital – digital hand shower. Available at: https://info.hansa.com/en/hansa-activejet-digital. Accessed: 10 Mar 2026.

17. Leong C, Buurman J, Tay SK. Two steps forward, one step back: negative spillovers in water conservation. Behavioural Public Policy. 2024:1-20. https://doi.org/10.1017/bpp.2024.25

18. Varnos V, Horvath M. Residential domestic hot water consumption analysis for multifamily buildings supplied by district heating. Thermal Science. 2022;26(2B):1267–1276. https://doi.org/10.2298/TSCI200505190V

19. González-Gómez F, López-Ruiz S, Tortajada C. Promoting water conservation habits in shower use: review of water utility websites in OECD cities. Water International. 2022;47(4):632–645. https://doi.org/10.1080/02508060.2022.2052662

20. Zhang D, Mui KW, Wong LT. Establishing the Relationship between Occupants' Thermal Behavior and Energy Consumption during Showering. Buildings. 2023;13(5):1300. https://doi.org/10.3390/buildings13051300

21. Marszal-Pomianowska A, Jensen RL, Pomianowski M, Larsen O.K, Jørgensen J.S, Knudsen S.S. Comfort of Domestic Water in Residential Buildings: Flow, Temperature and Energy in Draw-Off Points: Field Study in Two Danish Detached Houses. Energies. 2021;14(11):3314. https://doi.org/10.3390/en14113314

Assessing Building Energy Efficiency in Kragujevac (Serbia): Insights from a Retrospective Research Analysis

Nebojša Jurišević[1], Minja Velemir[2], Natalija Aleksić[3], Dušan Gordić[4]

[1]Faculty of Engineering, University of Kragujevac, Serbia,
e-mail: jurisevic@kg.ac.rs, ORCID: https://orcid.org/0000-0002-1609-6313
[2]Faculty of Engineering, University of Kragujevac, Serbia,
e-mail: velemir94@gmail.com, ORCID: https://orcid.org/0009-0007-1810-1933
[3]Faculty of Engineering, University of Kragujevac, Serbia,
e-mail: natalija.aleksic@fink.rs, ORCID: https://orcid.org/0000-0001-9341-7806
[4]Faculty of Engineering, University of Kragujevac, Serbia,
e-mail: gordic@kg.ac.rs, ORCID: https://orcid.org/0000-0002-1058-5810

Corresponding author: jurisevic@kg.ac.rs

Abstract

Operational processes in buildings account for approximately 30% of global final energy consumption. Together with the continuous growth of the building stock, this makes the building sector a key target of policies aimed at improving energy efficiency and strengthening energy security. This paper presents an internal synthesis of research on building energy efficiency conducted in the city of Kragujevac (Serbia) from 2015 to 2025. The analysis encompasses a retrospective review of 12 scientific and professional outputs. The identified results are categorized into four thematic groups: (1) quantification of energy consumption and energy efficiency indicators for the building sector, including the identification of priorities for building retrofits; (2) proposals of measures for improving building performance; (3) assessment of the effectiveness of the proposed measures; and (4) exploration of modern tools that support non-experts in the energy management of public buildings. The review highlights the academic community's contribution to advancing decarbonization and energy security while supporting the training of young professionals involved in implementing tasks under the National Energy Efficiency Action Plan (NEEAP).

Keywords: SDG11, buildings; energy efficiency; retrofitting;

1. Introduction

Operational processes in buildings account for approximately 30% of global final energy consumption [1] and 46% in Europe [2]. Considering the United Nations' projection that the global population will reach around 10 billion within the next 50 years [3], buildings will require increasing attention in policies addressing sustainable development and energy security. Due to significant variations in building standards, efforts to achieve sustainability in the building sector (net-zero, passive, and plus-energy buildings) require approaches tailored to local conditions. In the Republic of Serbia, buildings account for 45% of final energy consumption [4]. Although this share is close to the European average [2], the distribution of final energy consumption among sectors is not an adequate indicator for comparing sectoral efficiency. For example, the energy intensity of the Serbian economy is approximately 80% higher than the EU average [5], whereas the energy intensity of

buildings (150 kWh/m²·a) is about 20% higher than the EU average [6]. Consequently, buildings in the Republic of Serbia have a greater potential for final energy savings compared to those in the EU. To initiate improvements aligned with EU initiatives [7], the Government of the Republic of Serbia has adopted several strategic [8–11] and legislative acts [12–14] in this field. Following national plans, the academic community has conducted research at the local and regional levels with the aim of formulating recommendations for policy improvement and developing mechanisms for monitoring and controlling the implementation of the proposed measures. This paper provides a retrospective review of research dealing with energy efficiency (EE) and energy management of buildings in the city of Kragujevac (Serbia). By presenting the chronological development of this research, the study contributes to the international body of knowledge by consolidating key indicators and achievements of a specific area in one place, and may serve as a basis for further studies in other local contexts.

2. Materials and Methods

This paper presents an internal synthesis of 12 previously conducted studies on building EE in the city of Kragujevac, published between 2015 and 2025. The synthesis includes scientific publications in English and Serbian, as well as one professional report. The synthesis is categorized into four thematic groups: (1) quantification of energy consumption and energy efficiency indicators for the building sector; (2) proposals of measures for improving building performance; (3) assessment of the effectiveness of the proposed measures; and (4) exploration of modern tools that support non-experts in the energy management of public buildings.

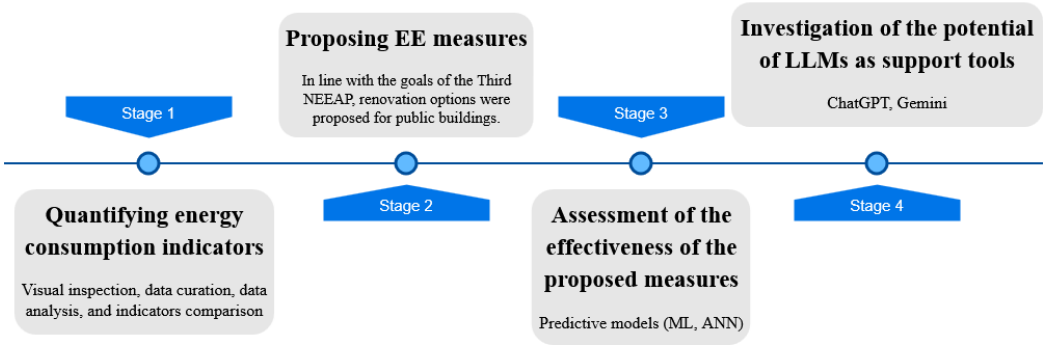


Figure 1. Research framework

The first stage of the workflow (Fig. 1) involved visual inspection of buildings and data curation. Inspected data included parameters such as heated floor area (HFA), number of occupants, and number of beds in healthcare buildings, while curated data referred to monthly energy consumption and heating degree days (HDD), which indicate the severity of the heating season. Following the curation process, monthly heat consumption was expressed per HFA and normalized to the average-year HDD value (2610 K·day). Subsequently, the EE class of each building was determined in accordance with [13], and priorities for renovation were identified. The second stage of the framework (Fig. 1) focused on the identification of measures for improving the EE of public buildings (how to renovate), to enable the municipality to reduce its primary energy consumption by 1% annually. This stage was in line with the goals of the Third National Energy Efficiency Action Plan of the Republic of Serbia [10], and was based on expert knowledge. To validate the expert-based assessments and enable non-experts to estimate potential energy savings before implementing measures in future projects, Stage

3 (Fig. 1) involved the training of machine learning (ML) models, designed to predict energy savings based on the type and scale of the renovation. These models were trained on vast input (building specifics) – output (energy consumption) relationships. Finally, the final stage of the chronological retrospective examined two case studies evaluating the usability of Large Language Models (LLMs) for energy management in public buildings.

3. Results and discussion

The studies from stage 1 (Fig. 1) of this overview indicate that public buildings in Kragujevac, primarily built between 1946 and 1980, lack adequate insulation and mostly belong to (the lowest) G energy class [15]. In Serbia, public buildings typically consume 50% more energy per square meter than residential ones (16). Educational institutions are the dominant consumers, accounting for 61% [16,17] of Kragujevac's public sector energy and water costs. Specific heat consumption in preschools averages 186–225 kWh/m²a [18], significantly exceeding values measured in Germany (94–158 kWh/m²a), Luxembourg (104.86 kWh/m²a), and Bulgaria (176 kWh/m²a). Similarly, Kragujevac's Clinical Center consumes 364 kWh/m²a, compared to the average of 300 kWh/m²a in German hospitals [19]. All analyzed types of buildings have potential for improvement. From the analyzed papers (Fig. 1, Stage 2), it can be seen that thermal insulation and window replacements can achieve savings between 36% and 79% [15]. For example, one of the kindergarten audits identified a potential 79% [20] reduction in thermal energy. Additionally, transitioning to LED lighting in schools offers 53–62% electricity savings with a four-year payback period [21]. More details of the research following the workflow present in Fig. 1 are summarized in Tab. 1.

Table 1. Summary of analyzed studies and key findings

	Year	Language	Sample	Ref.	Main Findings
Quantifying energy consumption indicators	2015	English	Residential sector	[22]	Motivating tariff systems (electricity/gas) lead to lower consumption (~112 kWh/m²a), whereas fixed district heating tariffs (~173 kWh/m²a) discourage energy savings and investments in building insulation.
	2016	Serbian	Kindergartens	[18]	Analyzed 15 preschool buildings; most are in the lowest "G" energy class. Proposed efficiency measures for kindergartens could achieve heat energy savings between 36% and 58%.
	2017	English	Secondary schools	[21]	Assessed the effectiveness of LED lighting replacements in 9 high schools. The results suggest that there is a potential for electricity savings of 53–62%. The average investment payback period is approximately four years.
	2018	Serbian	Kindergarten	[23]	Thermal energy savings of nearly 79% could be achieved by implementing recommended measures such as window replacement and insulation (the building energy class was G).
	2018	Serbian	Healthcare buildings	[19]	Building deterioration is the main cause of high heat consumption in ambulances and clinical centers. There is an increase in primary energy consumption as a result of inadequate heating system capacity.

Measures	2018	Serbian	Kragujevac public sector	[17]	A strategic plan that aims to achieve a 1% annual reduction in energy consumption in the areas of lighting, transportation, and buildings. Proposed thermal renovations and LED lighting modernization for 257 public buildings after conducting an analysis. Implemented the "50-50" incentive program to encourage schools to share the energy-saving benefits.
Predictions	2021	Serbian	Kindergartens	(16)	Doctoral dissertation proposing a five-step methodology for the monitoring of monthly energy and water consumption. In the comparison of linear and non-linear models in Kragujevac's kindergartens, it was determined that ANN yielded the highest accuracy in predicting heat and water consumption.
	2021	English	Preschool buildings	[24]	Assessed 21 parameters and six predictive models for water consumption in 13 buildings. The Random Forest and Multiple Linear Regression models were the most suitable, offering an optimal equilibrium between predictive accuracy and practical applicability.
	2022	English	Kindergartens	[25]	Evaluated predictive models for monthly heat consumption in 11 buildings. Artificial Neural Networks (ANN) were most accurate, while Multiple Linear Regression and Decision Trees offered a satisfying balance of precision and interpretability.
	2024	English	Gymnasium	[26]	Simulated a gymnasium repurposed as a public warming shelter. Advanced HVAC systems incorporating heat recovery and recirculation may reduce energy demand by 60–80% compared with natural ventilation scenarios.
LLMs	2024	English	Educational buildings	[27]	LLM chatbots show potential for assisting non-experts but remain less accurate than experts. Performance differs by country; models accurately aligned with certain construction periods but encountered difficulties with specific Serbian regulations and detailed envelope specifications.
	2024	English	Kindergartens	[28]	Deductive reasoning alone was inadequate for accurate estimation of heat consumption based solely on envelope specifics. The assumptions of inductive reasoning regarding energy savings were largely aligned with professional standards.

Recent research has evolved toward advanced predictive modeling (Fig. 1, Stage 3). ANN and ML have demonstrated accuracy in predicting monthly heat and water consumption, surpassing conventional linear models. This has also been confirmed by several regional studies [29,30]. The assessment of LLMs (Fig. 1, Stage 4) as energy management instruments indicates considerable potential for assisting non-experts, although they encounter accuracy challenges concerning particular local regulations and technical specifics [27,28].

4. Conclusions

The studies that were covered by this synthesis indicate that the majority of public buildings, which were constructed between 1946 and 1980, have substandard thermal performance and are primarily classified as low-energy buildings. This suggests that there is significant potential for improvement. The results verify that conventional retrofit strategies, including LED lighting, window replacement, and thermal insulation, can generate substantial energy savings. Furthermore, recent research demonstrated the increasing significance of data-driven methodologies, such as machine learning models for energy consumption prediction and emerging tools like LLMs in assisting non-expert decision-making. Overall, the presented research contributes to local energy planning and supports the implementation of national energy efficiency policies, while offering insights that may be transferable to similar urban contexts.

References

1. Buildings - Energy System - IEA [Internet]. [cited 2026 Mar 9]. Available from: https://www.iea.org/energy-system/buildings.
2. Energy Performance of Buildings Directive [Internet]. [cited 2026 Mar 9]. Available from: https://energy.ec.europa.eu/topics/energy-efficiency/energy-performance-buildings/energy-performance-buildings-directive_en.
3. Ritchie H, Rodés-Guirao L. Peak global population and other key findings from the 2024 UN World Population Prospects. Our World Data [Internet]. 2024 [cited 2026 Mar 9];
4. Republic of Serbia. Integrated National Energy and Climate Plan of the Republic of Serbia for the period 2030 with the projections up to 2050. 2023;1–302.
5. Jovanović L, Pavlović AS. Assessing Energy Intensity and Renewable Integration : A Cross- Country Study of Serbia , Hungary , and Croatia Procena energetskog intenziteta i integracije obnovljivih izvora energije : komparativna studija Srbije , Mađarske i Hrvatske. 2025;32:255–260.
6. Serbia, Average annual heating consumption is close to 150 kWh per square meter | Serbia SEE Energy Mining News [Internet]. [cited 2026 Mar 9]. Available from: https://serbia-energy.eu/serbia-average-annual-heating-consumption-is-close-to-150-kwh-per-square-meter/.
7. European Commission. The European Green Deal [Internet]. [cited 2026 Mar 9]. Available from: https://commission.europa.eu/strategy-and-policy/priorities-2019-2024/european-green-deal_en.
8. Ministry of Mining and Energy of The Republic of Serbia. First Action Plan for Energy Efficiency of the Republic of Serbia for the Period 2010–2012. Off Gaz Repub Serbia 37/15 [Internet]. 2010;
9. Ministry of Mining and Energy of The Republic of Serbia. Second Action Plan for Energy Efficiency of the Republic of Serbia for the Period 2013–2015. Off Gaz Repub Serbia 98/13. 2013;
10. Ministry of Mining and Energy of The Republic of Serbia. Third Action Plan for Energy Efficiency of the Republic of Serbia for the Period up to 2018. Off Gaz Repub Serbia 1/17 [Internet]. 2017;
11. Ministry of Mining and Energy of The Republic of Serbia. Fourth energy efficiency action plan of the Republic of Serbia for the period until 31 December 2021. Off Gaz Repub Serbia. 2019;
12. Governement of the Republic of Serbia. Law on Energy (2011). Off Gaz Repub Serbia 94/2024-204. 2024;
13. Government of the Republic of Serbia. Rulebook on Conditions, Content, and Manner of Issuing Energy Performance Certificate of Buildings. Off Gaz Repub Serbia 69/2012. 2012;
14. Government of the Republic of Serbia. Rulebook on energy efficiency in buildings. Off Gaz Repub Serbia No 61/2011. 2011;
15. Gordić D, Jurišević N, Živković D, Vukašinović V, Milovanović D, Končalović D, Josijević M. Benchmarking of Heat Energy Consumption in Public Buildings in the City of Kragujevac. eNergetics2018. 2018;139–146.
16. Jurišević N. System for monitoring and targeting of energy and water conusmption in public buildings. University of Kragujevac; 2021.
17. Gordić D, Šusteršič V, Končalović D, Vukašinović V, Živković D, Jurišević N, Josijević M,

Milovanović A, Kovačević Z. Energy Efficiency Program of the City of Kragujevac for the Period 2018–2020 [Internet]. Kragujevac, Serbia; 2018. Available from: http://www.aarhus.org.rs/wp-content/uploads/2018/11/Program_energetske_efikasnosti_grada_Kragujevca.pdf.

18. Jurišević N, Josijević M, Rakić N, Milovanović A. Specific Final Energy Consumption in Preschool Institutions in Kragujevac. Energ Ekon Ekol. 2016;17:390–396.
19. Jurišević N, Gordić D, Vukašinović V, Radsojević A, Stojanović G. Analysis of Specific Energy Consumption in Healthcare Facilities in the City of Kragujevac. Energ Ekon Ekol. 2018;20:396–403.
20. Jovanović D, Gordić D, Nikolić J, Jurišević N, Josijević M. Thermal Energy Audit and Increasing of Efficiency of Thermal Energy Use in the Kindergarten " Zeka " in the City of Kragujevac , Serbia. :119–125.
21. Josijević MM, Gordić DR, Milovanović DM, Jurišević NM, Rakić N. A method to estimate savings of LED lighting instalation in public buildings the case study of secondary schools in Serbia. Therm Sci. 2017;21:2931–2943. doi: 10.2298/tsci161209118j.
22. Lukić N, Jurišević N, Nikolić N, Gordić D. Specific heating consumption in the residential sector of Serbia - Example of the city of Kragujevac. Energy Build. 2015;107:163–171. doi: 10.1016/j.enbuild.2015.08.012.
23. Vukašinović V, Jurišević N, Josijević M, Živković D, Gordfić D. Increasing the Efficiency of Heat Energy Use in Preschool Buildings – Case Study: "Ciciban" Kindergarten. Tehnika. 2018;73:381–388. doi: 10.5937/tehnika1803381v.
24. Jurišević NM, Gordić DR, Vukašinović V, Vukicevic AM. Assessment of predictive models for estimation of water consumption in public preschool buildings. J Eng Res [Internet]. 2022;10:98–111. doi: 10.36909/jer.10941.
25. Jurišević N, Gordić D, Vukićević A. Assessment of Predictive Models for the Estimation of Heat Consumption in Kindergartens. Therm Sci. 2022;26:503–516. doi: 10.2298/TSCI201026084J.
26. Jurišević N, Nešović A, Kowalik R, Despotović M, Gordić D. Energy Performance of Relatively Small Sports Halls Used As Public Warming Shelters. Therm Sci. 2024;28:163–174. doi: 10.2298/TSCI230124123J.
27. Jurišević N, Kowalik R, Gordić D, Novaković A, Vukašinović V, Rakić N, Nikolić J, Vukićević A. Large language models as tools for public building energy management: an assessment of possibilities and barriers. 2023;19.
28. Jurišević N, Gordić D, Nikolić D, Nešović A, Kowalik R. Exploring the Potential of Emerging Digitainability—GPT Reasoning in Energy Management of Kindergartens. Buildings. 2024;14. doi: 10.3390/buildings14124038.
29. Begić Juričić H, Krstić H. Predicting Water Consumption for School Buildings in Osijek-Baranja County, Croatia, Using MLR and ANN. J Water Resour Plan Manag [Internet]. 2025;151:5025011. doi: 10.1061/JWRMD5.WRENG-6943.
30. Begić Juričić H, Krstić H. Analyzing Patterns and Predictive Models of Energy and Water Consumption in Schools. Sustain. 2025;17. doi: 10.3390/su17125514.

Improving the Energy Efficiency of Water Hydraulic System Components within Sustainable Energy Plant

Nenad Todić[1], Slobodan Savić[1], Blaža Stojanović[1], Saša Milojević[1]

[1]*Faculty of Engineering, University of Kragujevac, Kragujevac, Serbia, ntodic@gmail.com, 0000-0002-6154-8112, ssavic@kg.ac.rs, 0000-0001-6609-4845, blaza@kg.ac.rs, 0000-0003-4790-2856, sasa.milojevic@kg.ac.rs, 0000-0003-0569-047X*

Corresponding author: ssavic@kg.ac.rs

Abstract

The evolution of the global energy sector toward a complete reliance on renewable energy sources requires continuous advancement in energy transmission and conversion technologies. In this context, water energy and water hydraulic systems are transforming into key factors for environmental stability. This paper focuses on analysing the possibilities for significant improvement of energy efficiency within water hydraulic systems that utilize water as a working medium instead of mineral oils. Such a technological approach not only eliminates risks of environmental contamination but also presents new engineering challenges in the domain of minimizing energy losses. The central part of the research is dedicated to methods for the identification and optimization of the design parameters of axial piston pumps in water hydraulics. As primary generators of pressure and flow, these pumps represent the most critical components for ensuring a high degree of efficiency and reliability in the overall power transmission.

Improving performance at the component level directly contributes to the stability and sustainability of energy systems, confirming that water, as both a working fluid and a resource, is the foundation of the future energy transition. The results provide a clear roadmap for the integration of water hydraulics into modern energy flows, promoting water resources as a base for an efficient and secure energy future.

Keywords: energy efficiency; water hydraulics; sustainable plants; component optimization; renewable energy sources; clean water and sanitation; affordable and clean energy; sustainable cities and communities; responsible consumption and production.

1. Introduction

Water hydraulics, as a fundamental principle of power transmission using an incompressible fluid (water) under controlled pressure, is experiencing a significant resurgence in modern engineering. Its growing importance stems from the increasing global awareness of the need for sustainable technological solutions and the reduction of the negative impact of industrial processes on the environment. In the context of sustainable installations, where every percentage of saved energy is linked to the return on investment, improving the energy efficiency of water-based components becomes a key economic factor. The primary challenge lies in the fundamentally different physical properties of water compared to mineral oils. While oils provide effective lubrication and maintain a stable film under load, water behaves as an aggressive medium that promotes corrosion and erosion processes [1].

The tribological aspects of water hydraulics represent the most critical area of modern research and development. Unlike oil-based systems, water exhibits poorer lubricating properties, which leads to increased

friction and wear of the contacting surfaces of hydraulic components. Efficient lubrication in water-based systems is therefore essential for achieving high performance. Tribological challenges include various lubrication regimes - from hydrodynamic to dry and mixed friction regimes. Direct contact between metal surfaces under high specific pressure leads to physical material removal. Erosion and corrosion, resulting from the interaction between water and pump materials, often lead to electrochemical corrosion, while the hydrodynamic forces associated with cavitation further accelerate the degradation of the surface layer [2].

2. Modern Approaches to the Development and Optimization of Axial Piston Pumps for Water-Based Hydraulics

Axial piston pumps, as key components for generating high pressure, constitute the focus of this study (Figure 1). Understanding degradation phenomena during operation with water is of essential importance for the further development of water hydraulics as a sustainable technology. This paper integrates knowledge from the fields of materials science, digital control, and experimental hydraulics in order to propose solutions that will make water-based systems competitive within future green energy installations. Contemporary research in hydraulic power transmission focuses on overcoming the inherent limitations of water as a working medium through development of advanced materials resistant to corrosion and tribological degradation. Particular emphasis is placed on the application of high-performance engineering polymers, primarily polyether ether ketone (PEEK). The use of PEEK in sealing systems and functional pump components enables effective compensation for the low viscosity of water. This material exhibits a unique ability to conform to micro-scale surface geometry, which minimizes leakage without any undesirable increases in mechanical resistance.

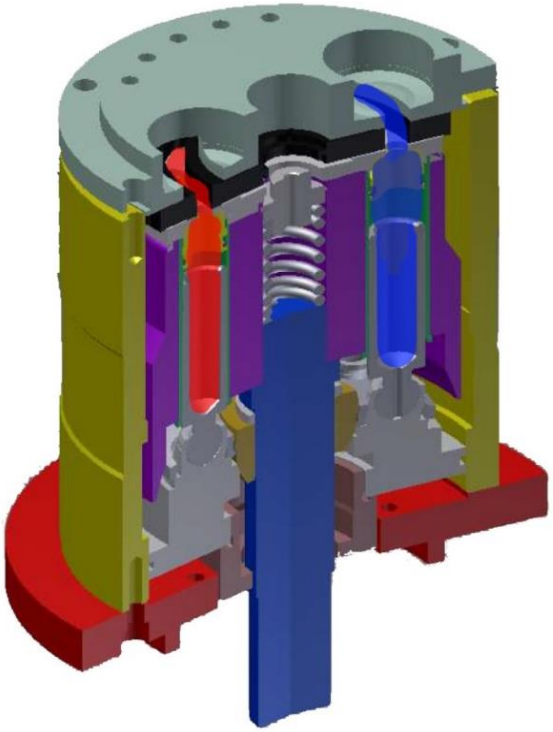


Figure 1. High-pressure axial piston pump

3. Tribological Optimization of Sliding Pairs and the Application of Peek Materials

The highest mechanical losses are localized at the contacts between the slipper and the swash plate, the piston and the cylinder, as well as the cylinder block and the valve plate. Due to inability to form a hydrodynamic lubrication film, PEEK inserts are used in the piston slippers. PEEK is characterized by self-lubricating properties and a low wear rate. Its partial elasticity enables micro-deformation under pressure, resulting in a smoothing (“ironing”) of the surface irregularities of the metal plate and the formation of a superior sealing interface, thus preventing thermal seizure at high rotational speeds. Volumetric efficiency (η_{uk}) is directly

affected by internal leakage, which, according to the Hagen–Poiseuille law, is inversely proportional to the fluid viscosity (μ): $Q_g = \frac{\pi d h^3 \Delta p}{12 \mu L}$

The engineering solution involves the use of "floating" bushings made of ceramics or PEEK, which provide dynamic clearance compensation under the action of pressure, as well as the introduction of labyrinth seals on the piston body (Figure 2) [3].

A precisely designed balance area on the face of the piston slipper ensures that the fluid support force (F_{SP}) amounts to approximately 95–98% of the piston pressure force (F_{PTS}), which prevents the collapse of the water film. Furthermore, given the high coefficients of thermal expansion of polymers, it is necessary to design components that account for "thermal breathing." The use of carbon fibre-reinforced PEEK composites ensures structural strength and clearance stability, while an optimized housing enables fluid circulation for uniform cooling [4].

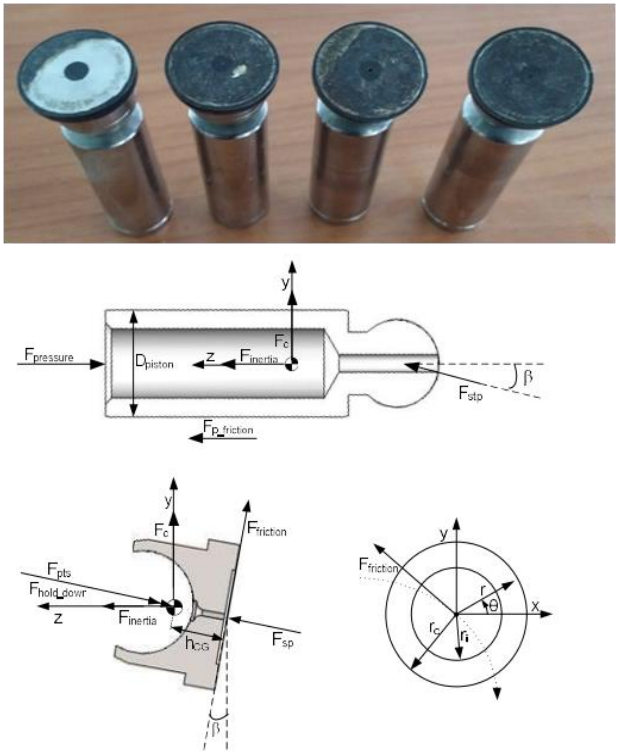


Figure 2. Pistons with slippers - use of PEEK and distribution of forces in the piston and slipper

4. Results of Experimental Testing and Discussion

The efficiency of axial piston pumps is a key parameter for evaluating their performance in the process of converting input mechanical power into useful hydraulic output power. This parameter summarizes all internal energy losses within the pump. In order to fully understand the operating characteristics of the pump, it is necessary to analyze the different components of efficiency: overall efficiency, volumetric efficiency, and mechanical efficiency. The overall efficiency (η_{uk}) of an axial piston pump is a key indicator of its effectiveness in converting the mechanical energy of the drive shaft into the hydraulic energy of the fluid. It quantifies the efficiency of utilizing input power for generating flow and pressure, while minimizing losses due to friction, leakage, and other non-ideal effects. A high overall efficiency directly contributes to reduced energy consumption and lower operating costs of the hydraulic system. The overall efficiency depends on the volumetric (η_{uk}) and mechanical efficiency (η_m). Their interrelationship is defined by the following equation: $\eta_{uk} = \eta_v \cdot \eta_m$. The volumetric efficiency defines the losses that occur during the fluid flow through the pump: $\eta_v = \frac{Q}{Q_T} \cdot 100\%$. Figure 3 shows the diagram of volumetric efficiency variation as a function of time for different pump operating regimes. The mechanical efficiency (η_m) of an axial piston pump represents the efficiency of

mechanical power transmission, more precisely, the ratio between the theoretical torque required for hydraulic work and the actual torque applied to the drive shaft: $\eta_m = \frac{T}{T_T} \cdot 100\ \%$.

Flow through clearances can be up to forty times higher than in axial piston pumps used in oil hydraulics, due to the significantly lower viscosity of water compared to oil. As a result, the volumetric efficiency of a water hydraulic pump decreases progressively with increasing operating pressure; therefore, the reduction of volumetric losses represents one of the key challenges in the design of water-based pumps. As shown in the diagram, a drop in outlet pressure leads to sudden increases in volumetric efficiency.

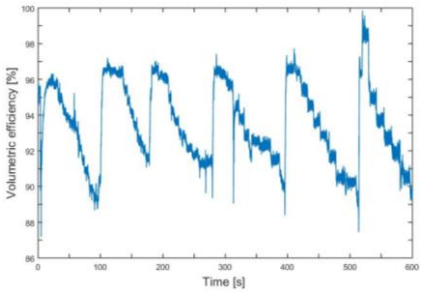


Figure 3. Variation of volumetric efficiency over time for different pump operating regimes

5. Conclusions

The comprehensive analysis conducted in this study clearly indicates that the optimization of axial piston pumps is a crucial factor in achieving high performance in modern energy systems. The experimental validation of the developed numerical models constituted a key stage of the study, confirming that the theoretical calculations accurately reflect the real behavior of the system under dynamic operating conditions. Particular emphasis in this study is placed on the application of advanced materials with superior tribological properties, which represents a turning point in the design of modern water hydraulic systems. High-performance polymers, particularly polyether ether ketone (PEEK), have been identified as materials of the future. Looking to the future, the development of axial piston pumps for sustainable energy must be based on the synergy between innovative materials and digital technologies. The integration of sophisticated condition monitoring systems enables real-time data acquisition on pressure, flow rate, temperature, and vibration levels. Such an approach, in combination with the robustness provided by materials such as PEEK, paves the way for the concept of "smart hydraulics." Real-time diagnostics enables the system to autonomously adjust operating parameters in order to minimize wear, thus achieving maximum reliability with minimal human intervention. This digital transformation of hydraulic components is crucial for integration into larger smart grid systems, where the energy efficiency of each individual node is of vital importance for the stability of the entire energy chain.

References

1. Ernst M, Vacca A. Hydrostatic vs. hydrodynamic components of fluid pressure in the tribological interfaces of axial piston machines. Tribol Int. 2021;157:106878.
2. Todić N, Savić S, Gordić D, Petrović R. Experimental Research of the Hydrodynamic Processes of an Axial Piston Water Hydraulic Pump. Machines. 2022;10(9):728. doi:10.3390/machines10090728.
3. Rokala M. Analysis of Slipper Structures in Water Hydraulic Axial Piston Pumps [dissertation]. Tampere: Tampere University of Technology; 2012.
4. Todić N, Savić S, Stamenković Ž, Stojanović B. Tribological aspects of identification of the key causes of reduction in the efficiency of axial piston water hydraulic pumps. In: 19th International Conference on Tribology – SERBIATRIB '25; 2025 May 14–16; Kragujevac, Serbia.

IT-Based Feasibility Assessment of a Shallow Geothermal System in a Renovated Educational Building in Kragujevac

Filip Nastić, Dubravka Živković, Davor Končalović, Vladimir Vukašinović, Mladen Josijević, Dušan Gordić

[1]*Department of Energy and Process Engineering, Faculty of Engineering, Kragujevac, Republic of Serbia, filip.nastic@uni.kg.ac.rs, 0000-0002-2164-6658, dubravka@uni.kg.ac.rs, 0000-0002-0266-456X, koncalovic@fink.rs, 0000-0003-1207-2653, vladimir.vukasinovic@kg.ac.rs, 0000-0001-6489-2632, mladen.josijevic@fink.rs, 0000-0001-9619-0897, gordic@kg.ac.rs, 0000-0002-1058-5810*

Corresponding author: filip.nastic@uni.kg.ac.rs

Abstract

Within the framework of the Interreg Danube GeoHeCo project, pilot investments in selected countries tested innovative IT tools for planning heating and cooling shallow geothermal energy (SGE) systems. Based on these activities, a comprehensive transnational report was developed to identify lessons learned, assess the benefits, and assess the replication potential in countries without pilot investments. The paper presents the key findings of that report, focusing both on the practical results of the pilot implementations and on the broader strategic value of the developed tools and methodologies. Particular attention is paid to countries that did not host physical investments (such as Serbia) but contributed through technical documentation, feasibility insights, and preparatory knowledge for future implementation outside the project framework. The analysis shows how much non-investment participation can still generate significant value by strengthening institutional readiness, technical capacity, and strategic planning for future deployment of SGE. Finally, the paper makes policy recommendations aimed at facilitating wider adoption of SGE technologies and improving cross-border knowledge transfer.

Keywords: Renewable energy sources, Geothermal energy, Danube Region, UN SDG 7

1. Introduction

The Faculty of Engineering in Kragujevac was originally formed as the Faculty of Mechanical Engineering in Kragujevac on October 1, 1960. As a department of the Faculty of Mechanical Engineering in Belgrade, it started working on October 9, 1960, in the premises of the First Kragujevac Gymnasium. The first buildings were built next to the Upper Park in 1962 [1]. Today, the Faculty of Engineering includes 4 buildings marked as buildings A, B, C, and D (Figure 1).

Building D is the oldest building of the campus (built in 1962), in 2018 its renovation started, and it included replacing all windows with high-efficiency triple-glazed PVC windows and double-glazed aluminum doors, while the part of the facade was insulated with 10 cm of rock wool. Currently, all buildings of the faculty are connected to the district heating system, whose tariff system proved to be very unfavorable for the Faculty. In this regard, the faculty considered two scenarios: i) Two buildings switch to an alternative heating system, ii)

all buildings switch to an alternative heating system. Which solution will be chosen depends on available investment funds.

Out of all renewable energy sources, only solar, geothermal, and biomass are usually converted into heat, while landfill gas, sewage treatment plant gas, and biogases are usually converted into electricity on-site or are still in the development stage [2]. Geothermal energy is a renewable energy source with significant potential to infiltrate the central heating system and decarbonize it [3]. Overall, geothermal energy can help us achieve fossil fuel dependency [4] and reduce carbon emissions significantly [5]. This paper analyzes the possibility of switching building D to shallow geothermal energy. This building was chosen due to the high performance of its envelope (after renovation) and its large area.



Figure 35. Faculty of Engineering Campus

2. Input parameters of the planned geothermal system with the conventional existing system

Input parameters are given in the table below (Table 1).

Table 5. Input parameters of the planned geothermal system

INPUT PARAMETERS	
Gross floor area	5344 m2
Specific heat consumption	163 kWh/m²/year
Nominal thermal capacity of ground-source HP system	300 kW
Number of boreholes	40
Deepness of boreholes	120 m
Diameter of the boreholes	40 mm

The IT Tool for this analysis is a web-based decision support tool (available at [6]) for assisting optimal usage of hybrid heating and cooling systems in the Danube region in order to avoid situations of over-sizing or under-

sizing the number/depth of wells, i.e. in order to optimize the cost of system installation. Main features of the tool are: long-term simulation of all relevant phenomena, visualization of results in a form of timeseries, assistance in optimal choice for borehole heat exchanger length and bivalent temperature, calculation of levelized cost of heat. It was developed during 2.5 year long Interreg Danube project called "Danube GeoHeCo", in which professors and researchers of the Faculty of Engineering participated actively. The IT tool was also fed with additional (but not presented) input data about working fluid, pipes, grout, ground, and groundwater.

3. Results

The results of the IT-Based feasibility assessment of a hybrid system combining a shallow geothermal system and a gas boiler for renovated building D are shown through Figure 2, depicting long-term borehole temperatures and power consumption, Figure 3 showing heat balances time-series and coefficient of performances, and Figure 4 illustrating annual energy balances.

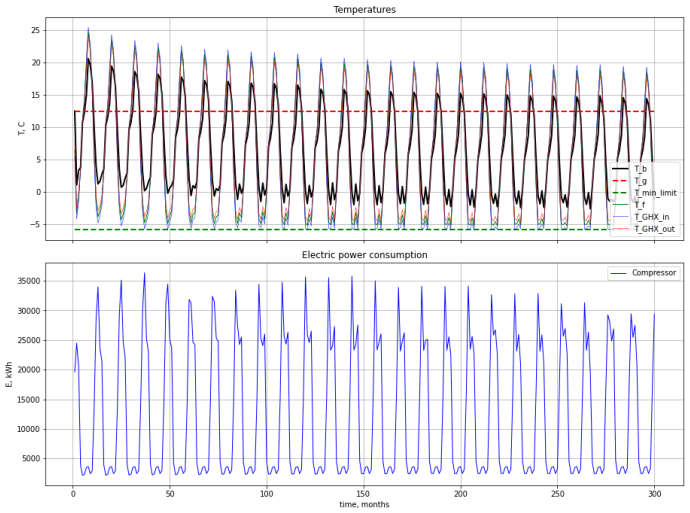


Figure 36. Results: Long-term borehole temperatures and power consumption

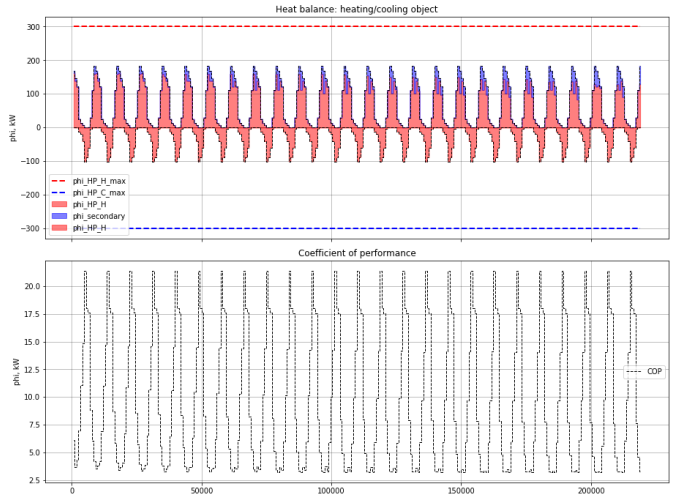


Figure 37. Results: Heat balances time-series and coefficient of performances

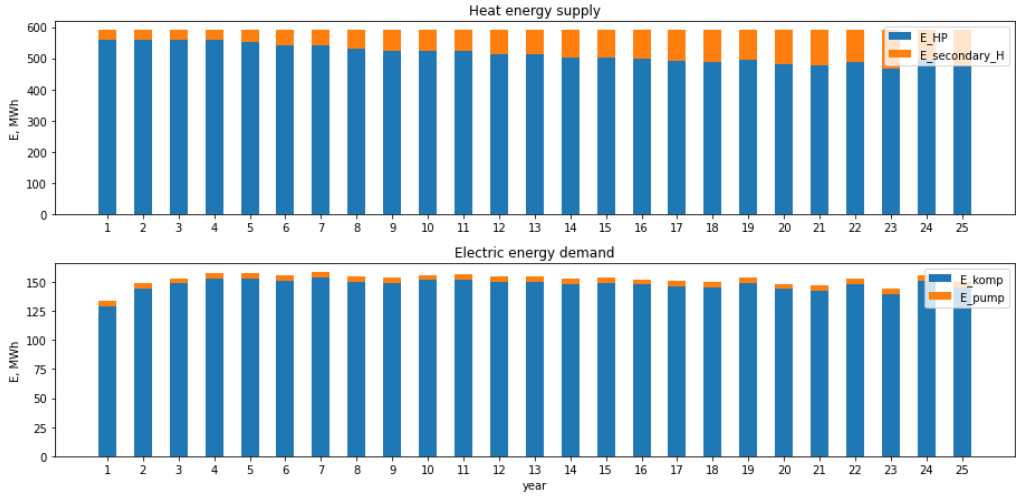


Figure 38. Results: Annual energy balances (heat and electric)

4. Conclusions

The IT-based assessment of the shallow geothermal system on the renovated (but oldest) building of the Faculty of Engineering campus gave positive results. Namely, the results show that a properly dimensioned ground-sourced geothermal heat pump system can meet the heating needs of the mentioned building while maintaining the long-term thermal stability of the ground. Overall, a shallow geothermal system can operate efficiently as a base load heating source, while the gas boiler could cover the peak loads during periods of extremely low temperatures. Such a hybrid configuration would ensure both reliability and resilience of the heating supply, why allowing for significant reductions in fossil fuel consumption and associated CO_2 emissions.

From a technical and environmental perspective, this study confirms that shallow geothermal energy represents a viable and renewable option for the decarbonization of the Faculty of Engineering campus heating system. Further detailed design and economic optimization studies are recommended to refine the system sizing and assess the return on investment.

Acknowledgements

This work is supported by Interreg Danube Region, Danube GeoHeCo project, DRP 0200244.

References

[1] Faculty of Engineering, History. https://www.fin.kg.ac.rs/en/faculty/about-us/history (pristupljeno 24.3.2026.).

[2] Heat from Renewable energy sources. European Commission. https://climate.ec.europa.eu/system/files/2016-11/renewable_energy_srcs_heat_en.pdf (pristupljeno 24.3.2026.)

[3] Malcher, X., Tenorio-Rodriguez, F.C., Finkbeiner, M., Gonzalez-Salazar, M. Decarbonization of district heating: A systematic review of carbon footprint and key mitigation strategies, Renewable and Sustainable Energy Reviews, Vol. 215, 2025, https://doi.org/10.1016/j.rser.2025.115602.

[4] Kumar, B. Fossil energy reduction for heating and cooling of buildings using shallow geothermal integrated energy systems – a comprehensive review, Journal of Thermal Engineering, Vol. 9, No. 5, 2023, https://doi.org/10.18186/thermal.1377257

[5] Savić, A., Šušteršič, V., Josijević, M., Nešović, A., Jurišević, N., Vukašinović, V. Numerička analiza toplotnih performansi geotermalne toplotne pumpe za potrebe grejanja i hlađenja stambene zgrade, Energija, Ekonomija, Ekologija, Vol. 25, No. 3, pp. 60-64, 2023, https://doi.org/10.46793/EEE23-3.60S

[6] Danube GeoHeCo. https://testing.sdewes.net/RGN/ (pristupljeno 30.3.2026).

Environmental Monitoring and Clean-Technology Assessment

Assessing The Potential of Citizen-Installed PM2.5 Sensors for Air Pollution Prediction and Mapping

Filip Nastić

Faculty of Engineering, Kragujevac, Republic of Serbia, filip.nastic@uni.kg.ac.rs, 0000-0002-2164-6658

Corresponding author: filip. nastic@uni.kg.ac.rs

Abstract

The increasing availability of low-cost PM2.5 sensors has opened new possibilities for enhancing air quality monitoring beyond traditional regulatory networks. This study provides a comprehensive review of existing research on the use of such sensors for air pollution prediction and spatial mapping. It examines the performance and limitations of low-cost sensing devices, as well as their integration into predictive models and geospatial analysis frameworks. Special attention is given to studies employing statistical and machine learning techniques for forecasting PM2.5 concentrations, alongside methods for generating high-resolution pollution maps from heterogeneous sensor networks. Overall, the findings highlight that, despite inherent limitations, citizen-installed sensor networks can significantly enhance their spatial and temporal coverage of air quality monitoring when combined with appropriate correction and modeling approaches.

Keywords: air pollution, particulate matter, machine learning, sensors

1. Introduction

Air pollution is currently one of the biggest environmental problems, which caused more than 8.1 million premature deaths in 2021 [1]. Air pollution can cause a variety of cancer diseases [2–5], cardiovascular diseases [6], respiratory diseases [7–10], and neurological problems [11].

Generally, there are few strategies for mitigating air pollution consequences, such as: i) defining air pollutant concentration limits [12], ii) development of technologies in use to reduce or eliminate air pollution [13], and iii) development of high-pollution episodes alarming systems for citizens [14]. Out of all three mentioned strategies, the third one could give significant results, followed by the lowest economic investment.

In order to implement the third strategy, systems for accurate concentration sampling and their spatial mapping are needed. Unfortunately, these requirements were and stayed challenges due to the lack of measuring stations, uncertain patterns of air dispersion, and weak response of individual sensors [15–17]. Despite the fact that the efforts of highly-developed communities have already given results, authorities of developing countries are forced to choose between life standard and life quality, which is why citizens of these countries continue to breathe highly polluted air [18].

Martin et al. [19] analyzed the existence of air pollution sensors worldwide, and showed that most of the highly-polluted city don't have installed $PM_{2.5}$ sensors, which are defined as the most dangerous pollutants of air. The

gap in their study was that they counted only official (state or city-installed) sensors, and didn't count citizen-installed ones. For example, the Republic of Serbia has a significant number of citizen-installed $PM_{2.5}$ sensors, which indicates their potential. Bi et al. [20] showed the potential of citizen-installed sensors from the aspect of filling the gaps in the regulatory monitoring of $PM_{2.5}$ concentrations. With their low price and simple installation procedure [21], these sensors can be installed by researchers, local communities, and citizens, which could create a usable local monitoring network.

This paper synthesizes current studies on the usage of citizen-installed sensors in the processes of PM2.5 concentration forecasting and pollution mapping, as well as other approaches that used reference-grade sensors but are still applicable for the low-cost ones.

2. $PM_{2.5}$ Prediction and Spatial Mapping Using Low-cost Sensors and Adaptable Approaches From Reference Networks

There is a variety of studies that harnessed data from citizen-installed $PM_{2.5}$ sensors to predict future concentrations. Nastić et al. [22] used samplings from the SDS011 sensors in order to predict hourly $PM_{2.5}$ concentrations for two locations in Europe and one in Asia. They developed models with satisfying accuracy, which resulted in R^2 scores varying from 0.865 to 0.943 in the case of one hour in future predictions. Similar research was done by Bi et al. [23]. They used the IVAN network of low-cost sensors as an additional data source for concentration prediction. They concluded that IVAN samplings can be mixed with existing regulatory samplings in order to increase the performance and quality of $PM_{2.5}$ concentration predictions. In addition, they stated that IVAN measurements helped them to understand the spatial characteristics of $PM_{2.5}$ sources. Lagesse et al. [24] evaluated the performance of low-cost sensor data for predicting indoor $PM_{2.5}$ concentrations. They demonstrated that free and low-cost data combined with machine learning can predict air quality even if they are not located in the sampling location with satisfying accuracy.

Bagheri [25] analyzed the potential of AOD (Aerosol Optical Depth) data for spatial mapping of $PM_{2.5}$ concentrations. Namely, in Tehran there is an existing network of $PM_{2.5}$ sensors, but the number of sensors in to low for accurate spatial mapping. The idea of this research is that by using samples from existing sensor networks, AOD data, and climate data, it is possible to create quasi-sensors that can increase the density of the sensing network. Finally, they used real measurements and quasi-sensor measurements to generate high-resolution PM2.5 concentration maps using classic interpolation methods. Chen et al. [26] investigated the potential of Land-use regressor (LUR) models for modeling the spatial distribution of $PM_{2.5}$ concentrations. The analyzed area was the Greater Bay Area in China. They evaluated the developed model using Leave-one-out cross-validation (LOOCV), resulting in an R^2 score of 0.808. Adams and Kanaroglou [27] proposed a model that combines Artificial Neural Networks with Land-use regression in order to predict the spatial variation of AQHI (Air Quality Health Index) for Hamilton in Canada, which can be updated in real-time. The used AQHI data was collected using stationary and mobile sensors, and the developed model resulted in R^2 score of 0.78. Following the results, this research successfully developed a model that can generate spatial pollution predictions in real-time.

5. Conclusions

By summarizing the studies mentioned in Chapter 2, it can be concluded that low-budget sensors can be successfully used for temporal and spatial modeling of PM2.5 concentrations. In the case of predicting future concentrations, one sensor is enough for predicting concentrations at the location of the sensor (or on locations close to the sensor location). While for spatial mapping, a dense and well-distributed sensing network is needed, when it is needed, it can be combined with AOD data or data from quasi-sensors to generate accurate pollution maps.

References

[1] State of Global Air 2024 - A Special Report on Global Exposure to Air Pollution and Its Health Impacts, With a Focus on Children's Health. Health Effects Institute. https://www.stateofglobalair.org/sites/default/files/documents/2024-06/soga-2024-report_0.pdf.

[2] Berg CD, Schiller JH, Boffetta P, Cai J, Connolly C, Kerpel-Fronius A, et al. Air pollution and lung cancer: a review by International Association for the Study of Lung Cancer Early Detection and Screening Committee. *J Thorac Oncol*. 2023. https://doi.org/10.1016/j.jtho.2023.05.024.

[3] Poulsen AH, Hvidtfeldt UA, Sørensen M, Pedersen JE, Ketzel M, Brandt J, et al. Air pollution with NO_2, $PM_{2.5}$, and elemental carbon in relation to risk of breast cancer: a nationwide case-control study from Denmark. *Environ Res*. 2023;216:114740. https://doi.org/10.1016/j.envres.2022.114740.

[4] VoPham T, Jones RR. State of the science on outdoor air pollution exposure and liver cancer risk. *Environ Adv*. 2023;11:100354. https://doi.org/10.1016/j.envadv.2023.100354.

[5] Zare Sakhvidi MJ, Lequy E, Goldberg M, Jacquemin B. Air pollution exposure and bladder, kidney and urinary tract cancer risk: a systematic review. *Environ Pollut*. 2020;267:115328. https://doi.org/10.1016/j.envpol.2020.115328.

[6] Krittanawong C, Qadeer YK, Hayes RB, Wang Z, Thurston GD, Virani S, et al. $PM_{2.5}$ and cardiovascular diseases: state-of-the-art review. *Int J Cardiol Cardiovasc Risk Prev*. 2023;19:200217. https://doi.org/10.1016/j.ijcrp.2023.200217.

[7] Huang HC, Lin FCF, Wu MF, Nfor ON, Hsu SY, Lung CC, et al. Association between chronic obstructive pulmonary disease and $PM_{2.5}$ in Taiwanese nonsmokers. *Int J Hyg Environ Health*. 2019;222:884–888. https://doi.org/10.1016/j.ijheh.2019.03.009.

[8] Lin CM, Huang TH, Chi MC, Guo SE, Lee CW, Hwang SL, et al. N-acetylcysteine alleviates fine particulate matter ($PM_{2.5}$)-induced lung injury by attenuation of ROS-mediated recruitment of neutrophils and Ly6C^high monocytes and lung inflammation. *Ecotoxicol Environ Saf*. 2022;239:113632. https://doi.org/10.1016/j.ecoenv.2022.113632.

[9] Xing YF, Xu YH, Shi MH, Lian YX. The impact of $PM_{2.5}$ on the human respiratory system. *J Thorac Dis*. 2016;8:E69–E74. https://doi.org/10.3978/j.issn.2072-1439.2016.01.19.

[10] Zhao C, Pu W, Wazir J, Jin X, Wei L, Song S, et al. Long-term exposure to $PM_{2.5}$ aggravates pulmonary fibrosis and acute lung injury by disrupting Nrf2-mediated antioxidant function. *Environ Pollut*. 2022;313:120017. https://doi.org/10.1016/j.envpol.2022.120017.

[11] Kim H, Kim WH, Kim YY, Park HY. Air pollution and central nervous system disease: a review of the impact of fine particulate matter on neurological disorders. *Front Public Health*. 2020;8:575330. https://doi.org/10.3389/fpubh.2020.575330.

[12] Wolff H. Keep your clunker in the suburb: low-emission zones and adoption of green vehicles. *Econ J*. 2014;124:F481–F512. https://doi.org/10.1111/ecoj.12091.

[13] Oltra V, Saint Jean M. Variety of technological trajectories in low emission vehicles (LEVs): a patent data analysis. *J Clean Prod*. 2009;17:201–213. https://doi.org/10.1016/j.jclepro.2008.04.023.

[14] Bernacki J. Forecasting the air pollution concentration with neural networks. *Urban Clim*. 2025;59:102262. https://doi.org/10.1016/j.uclim.2024.102262.
[15] Barkjohn KK, Yaga R, Thomas B, Schoppman W, Docherty KS, Clements AL. Evaluation of long-term performance of six $PM_{2.5}$ sensor types. *Sensors (Basel)*. 2025;25:1265. https://doi.org/10.3390/s25041265.
[16] Ma J, Li Z, Cheng JCP, Ding Y, Lin C, Xu Z. Air quality prediction at new stations using spatially transferred bi-directional long short-term memory network. *Sci Total Environ*. 2020;705:135771. https://doi.org/10.1016/j.scitotenv.2019.135771.
[17] Tariq S, Tariq S, Kim SY, Woo SS, Yoo CK. Distance adaptive graph convolutional gated network-based smart air quality monitoring and health risk prediction in sensor-devoid urban areas. *Sustain Cities Soc*. 2023;91:104445. https://doi.org/10.1016/j.scs.2023.104445.
[18] Lillo D, Salazar C, Jaime M, Chávez C. Perceptions of problems and preferences for solutions: the case of poor air quality in central-southern Chile. Energy Sustain Dev. 2022;66:79–91. https://doi.org/10.1016/j.esd.2021.10.011.
[19] Martin RV, Brauer M, van Donkelaar A, Shaddick G, Narain U, Dey S. No one knows which city has the highest concentration of fine particulate matter. *Atmos Environ X*. 2019;3:100040. https://doi.org/10.1016/j.aeaoa.2019.100040.
[20] Bi J, Stowell J, Seto EYW, English PB, Al-Hamdan MZ, Kinney PL, et al. Contribution of low-cost sensor measurements to the prediction of $PM_{2.5}$ levels: a case study in Imperial County, California, USA. *Environ Res*. 2020;180:108810. https://doi.org/10.1016/j.envres.2019.108810.
[21] Snyder EG, Watkins TH, Solomon PA, Thoma ED, Williams RW, Hagler GSW, et al. The changing paradigm of air pollution monitoring. *Environ Sci Technol*. 2013;47:11369–11377. https://doi.org/10.1021/es4022602.
[22] Nastić F, Jurišević N, Končalović D. Using a citizen-installed network of $PM_{2.5}$ sensors to predict hourly $PM_{2.5}$ airborne concentration. *Water Air Soil Pollut*. 2025;236:1–18. https://doi.org/10.1007/s11270-024-07733-x.
[23] Lagesse B, Wang S, Larson TV, Kim AA. Performing indoor PM2.5 prediction with low-cost data and machine learning. Facilities 2022;40:495–514. https://doi.org/10.1108/F-05-2021-0046.
[24] Bagheri H. A machine learning-based framework for high resolution mapping of PM2.5 in Tehran, Iran, using MAIAC AOD data. Advances in Space Research 2022;69:3333–49. https://doi.org/10.1016/J.ASR.2022.02.032.
[25] Chen L, Wu Z, Tu W, Cao Z. Applying LUR model to estimate spatial variation of PM2.5 in the Greater Bay Area, China. Spatiotemporal Analysis of Air Pollution and Its Application in Public Health 2020:207–15. https://doi.org/10.1016/B978-0-12-815822-7.00010-8.
[26] Adams MD, Kanaroglou PS. Mapping real-time air pollution health risk for environmental management: Combining mobile and stationary air pollution monitoring with neural network models. J Environ Manage 2016;168:133–41. https://doi.org/10.1016/J.JENVMAN.2015.12.012.

Assessment of PVGIS Accuracy Against EnergyPlus Simulations in Europe

Novak Popović[1], Novak Nikolić[1], Nebojša Lukić[1], Minja Velemir Radović[1]

[1]*University of Kragujevac, Faculty of Engineering,* novak.popovic@kg.ac.rs, https://orcid.org/0009-0004-1469-0994, novak.nikolic@kg.ac.rs, https://orcid.org/0000-0002-3946-0923, lukic@kg.ac.rs, https://orcid.org/0000-0002-1923-5200, mvradovic@kg.ac.rs, 0009-0007-1810-1933
Corresponding author: lukic@kg.ac.rs

Abstract

The accurate assessment of solar photovoltaic (PV) system performance depends on the reliability of simulation tools. This study presents a comparative analysis of the EnergyPlus software and the PVGIS web application, using SARAH3 and ERA5 datasets. EnergyPlus enables detailed modeling of PV systems by accounting for a wide range of physical and environmental parameters, while PVGIS provides a simplified and accessible approach. Simulations were performed under identical input conditions for six European locations selected to represent different ranges of solar irradiation. The results show that deviations between the tools vary depending on climatic and geographical factors, with the highest differences occurring during winter, and stronger agreement in summer. ERA5 demonstrates better overall agreement with EnergyPlus, with an average mean deviation of 5.88%, compared to 6.57% for SARAH3. The findings indicate that PVGIS can provide reliable estimates for preliminary assessments, while detailed analyses require advanced tools such as EnergyPlus.

Key words: EnergyPlus; PVGIS; solar PV system; simulation

1. Introduction

The ongoing energy transition is driving increased adoption of photovoltaic (PV) systems, however, investment decisions remain complex, requiring technical and financial knowledge that many users lack. In the early stages, investors often face limited information and administrative and financial barriers, while the benefits of PV systems are less immediately visible [1,2]. Reliable tools for modeling PV performance are therefore essential to support realistic profitability assessments, improve transparency, and enable informed decision making. To address this need, numerous software tools and web applications for PV simulation have been developed, yet they rely on different methodologies and datasets, leading to variations in predicted results. A review by *Kazem et al.* [3] summarizes 36 tools used over recent decades. *Wu* [4], comparing PVWatts and EnergyPlus, reports annual deviations between 4% and 7%, depending on panel tilt. *Mohammadi and Gezegin* [5] compared PVSyst, PVGIS and HOMER software for modeling a 5 MW solar power plant in Afghanistan and found that PVSyst produced the highest energy yield, while PVGIS and HOMER predicted lower values by 10.6% and 2%, respectively. Additionally, *Larasati and Nugraha* [6] report an average deviation of 14.72% for PVGIS compared with experimental data.

In this study, the Photovoltaic Geographical Information System (PVGIS), a widely used web application developed by the European Commission, was evaluated against EnergyPlus. According to [7,8], PVGIS is a free and reliable tool that provides solar radiation and photovoltaic system performance data for most global locations. It considers geographical coordinates, system orientation, panel tilt, and installed capacity, while using historical data and mathematical models to estimate solar irradiation. The importance of accurate meteorological data is emphasized by *Das et al.* [9], who show that solar irradiance is strongly correlated with

PV output, while *Jiménez Torres et al*. [10] demonstrate that converting horizontal irradiance to a tilted plane introduces additional uncertainty, reporting PVGIS errors of around 3.5–3.8%. Moreover, *Meral and Furkan* [11] highlight that PV performance is influenced not only by irradiance but also by atmospheric conditions such as module temperature, ambient temperature, wind speed, and shading, which must be incorporated into simulation models. These findings underline the need for a comprehensive approach to PV modeling: while PVGIS offers fast and accessible estimates, its simplified methods may limit accuracy, whereas advanced tools such as EnergyPlus provide more detailed and reliable assessments. Accordingly, this study evaluates the level of agreement between PVGIS and EnergyPlus to determine the applicability of PVGIS for accurate PV energy yield estimation.

2. Methodology

The power output of a LUXEN 585 W photovoltaic module (technical specifications in [12]) was evaluated using two modeling environments: the PVGIS web application and the EnergyPlus software. Simulations were performed for six European cities: Edinburgh, Hamburg, Prague, Belgrade, Rome, and Málaga. The locations were selected on the basis of the SolarGIS global horizontal irradiation (GHI) map presented in Figure 1 [13]. The sites span different ranges of annual GHI, as indicated by the color scale on the map thereby covering a broad irradiance gradient across Europe. Thus, the selected locations characterize six irradiation ranges and serve as representative examples of comparable European climates. The exact coordinates for the six locations were extracted from the EnergyPlus WeatherData (EPW) files, representing the meteorological stations used in the simulations, and applied as input coordinates in PVGIS to ensure that both tools modeled the same geographical locations. Within PVGIS, two meteorological datasets were used (PVGIS-SARAH3 and PVGIS-ERA5) to evaluate potential differences in the simulation results. For EnergyPlus, the corresponding EPW weather files were used.

PVGIS is a free online tool that allows users to estimate the energy production of a photovoltaic system using a set of basic input parameters (Table 1). Additionally, users can select dataset used in the simulation, choosing between PVGIS-SARAH3 and PVGIS-ERA5 [14]. The SARAH3 dataset is based on Meteosat satellite observations and spans the period 2005–2023, covering Europe, Central Asia, Africa, and parts of South America [15]. For locations outside the SARAH3 coverage area, the ERA5 dataset is recommended. ERA5 is a global reanalysis product that also relies on data from 2005 to 2023 to estimate solar and meteorological conditions worldwide [15]. As these datasets are generated using different methodologies, some variation in the resulting simulation outputs is expected. Input parameters used in the PVGIS simulations are presented in Table 1. For the purpose of this analysis, the system loss effect was neglected. Regarding the panel slope, the value of 38º was adopted, representing the average of the recommended slope values for all the nine locations, determined using the "Optimize slope" function in the PVGIS.

Table 6. *Input parameters used in PVGIS simulations*

PV technology	Installed peak PV power	System loss	Mounting position	Slope	Azimuth
Crystalline silicon	0.585 kWp	0%	Free-standing	38º	0º

EnergyPlus is an open-source, whole-building energy simulation software developed by the U.S. Department of Energy to model thermal behavior and energy performance under dynamic climatic and operational conditions. It integrates building envelope heat transfer, HVAC systems, renewable energy technologies, and control strategies within a single simulation framework [16–18]. Due to its validation and extensive use in scientific research [19–23], EnergyPlus is widely regarded as a reliable tool for analyzing complex building systems under realistic weather conditions. In this study, PV system performance was simulated using the *PhotovoltaicPerformance:EquivalentOne-Diode* model, with input parameters adopted from [12].

Meteorological data were obtained from EPW files for six locations [24], covering the period 2009–2023 and including hourly values of relevant climatic variables such as temperature, wind conditions, solar irradiance, and atmospheric parameters. The PV system was modeled in SketchUp as a fixed, south-facing roof-mounted installation with a tilt angle of 38°, allowing air circulation around the module (Figure 2). System losses were neglected, and identical system configurations were applied across all locations.

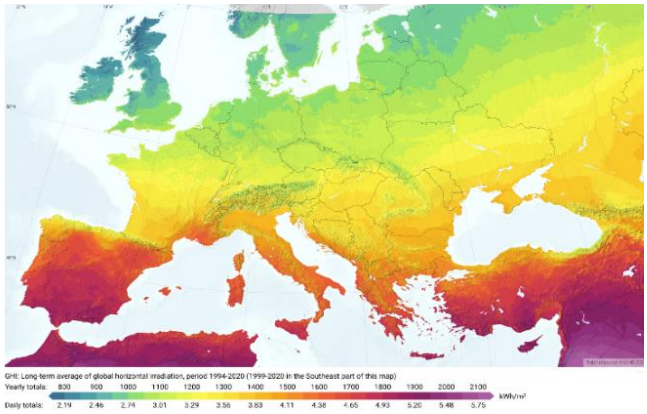


Figure 1. *GHI map of Europe [13]*

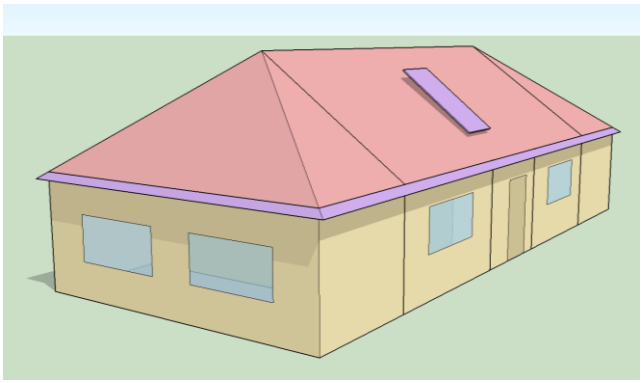


Figure 2. *3D model of the fixed roof-mounted PV system*

3. Results and Discussion

EnergyPlus and PVGIS-SARAH3

The results indicate that the PVGIS-SARAH3 dataset generally predicts lower energy yields than EnergyPlus across all analyzed locations. Based on Tables 2–3, the observed absolute deviations between the two tools are: Edinburgh: from 2.77% (March) to 17.32% (November); Hamburg: from 1.29% (October) to 15.32% (December); Prague: from 0.09% (September) to 15.92% (February); Belgrade: from 0% (July) to 19.02% (February); Rome: from 0.19% (June) to 12.81% (November); Málaga: from 1.54% (February) to 10.81% (December). These findings suggest that PVGIS-SARAH3 exhibits the lowest agreement with EnergyPlus during winter months, while no consistent pattern can be identified for periods of strongest agreement Considering the absolute monthly deviations, the number of months with deviations exceeding 10% provides an additional indicator of dataset precision. The counts are as follows: Edinburgh (2), Hamburg (5), Prague (5), Belgrade (3), Rome (1), Málaga (2). Although in some cases higher deviations occur during warmer months (Hamburg, 10.10% in August), most are observed in colder periods, when diffuse radiation is more dominant and total solar gains are more difficult to calculate. Hamburg and Prague exhibit the highest number of such deviations, whereas Rome shows the lowest, followed by Edinburgh and Málaga. This suggests that total solar radiation alone does not directly determine accuracy, and that other influencing factors must be considered. For colder months (October–March), the average deviation is 8.69%, compared to 4.45% for warmer months (April–September). Across all locations, Hamburg and Prague again show the highest mean deviations (8.68% and 7.42%, respectively), while Rome demonstrates the strongest agreement with a value of 4.33%. This trend is largely consistent with the influence of diffuse radiation, as locations with lower diffuse components tend to yield better agreement. However, Málaga deviates from this pattern, with a mean deviation of 5.80%. This can be attributed to its complex topography, which may lead to underestimation of solar irradiance in satellite-based datasets such as SARAH3. Furthermore, the results for Belgrade highlight the influence of air pollution, as the city is significantly polluted during winter months, which corresponds to higher deviations in this period, while summer results show the strongest agreement among all locations. Overall, diffuse radiation, terrain complexity,

and local environmental conditions (air pollution), significantly affect the accuracy of SARAH3 simulations, with an overall mean absolute monthly deviation of 6.57%.

Table 7. *Monthly PV energy production obtained from EnergyPlus (EPW) and PVGIS (SARAH3) for nine analyzed locations, with comparison- part 1*

Month	Edinburgh			Hamburg			Prague		
	EPW [kWh]	SARAH3 [kWh]	Difference	EPW [kWh]	SARAH3 [kWh]	Difference	EPW [kWh]	SARAH3 [kWh]	Difference
Jan	22.99	19.78	13.98%	20.63	18.59	9.90%	28.69	28.02	2.35%
Feb	33.31	32.12	3.56%	37.57	32.34	13.93%	50.17	42.18	15.92%
Mar	55.51	53.97	2.77%	62.82	57.01	9.25%	75.43	65.7	12.90%
Apr	75.27	72.73	3.38%	91.19	80.33	11.91%	93.37	82.8	11.32%
May	84.29	81.18	3.69%	94.52	85.19	9.87%	89.62	87.22	2.68%
Jun	81.29	75.75	6.81%	89.36	84.65	5.27%	89.25	87.91	1.50%
Jul	79.64	76.93	3.41%	85.55	82.61	3.44%	91.44	88.41	3.32%
Aug	72.93	69.34	4.92%	83.39	74.97	10.10%	79.62	83.11	4.39%
Sep	54.94	56.94	3.64%	62.77	63.68	1.46%	72.03	72.09	0.09%
Oct	35.91	39.16	9.04%	45.58	44.99	1.29%	60.96	52.66	13.62%
Nov	22.93	26.9	17.32%	19.92	22.39	12.39%	30.94	28.89	6.64%
Dec	14.36	15.05	4.78%	13.52	15.59	15.32%	22.06	25.23	14.36%

Table 8. *Monthly PV energy production obtained from EnergyPlus (EPW) and PVGIS (SARAH3) for nine analyzed locations, with comparison- part 2*

Month	Belgrade			Rome			Málaga		
	EPW [kWh]	SARAH3 [kWh]	Difference	EPW [kWh]	SARAH3 [kWh]	Difference	EPW [kWh]	SARAH3 [kWh]	Difference
Jan	41.56	39.03	6.08%	58.48	61.04	4.38%	81.23	83.8	3.16%
Feb	60.25	48.79	19.02%	73.27	68.68	6.27%	83.78	82.49	1.54%
Mar	85.08	73.97	13.06%	93.82	85.49	8.88%	107.66	96.12	10.72%
Apr	95.15	83.32	12.43%	101.59	92.12	9.32%	106.62	97.44	8.61%
May	91.57	89.37	2.40%	100.19	97.93	2.25%	110.34	105.54	4.35%
Jun	90.55	90.53	0.02%	100.65	100.46	0.19%	106.89	104.89	1.87%
Jul	100.05	100.05	0.00%	107.74	109.51	1.64%	114.53	109.54	4.36%
Aug	102.85	96.64	6.04%	105.53	106.24	0.67%	114.11	108.95	4.52%
Sep	84.57	80.78	4.48%	92.04	90.64	1.52%	104.28	99.58	4.51%
Oct	66.61	70.85	6.36%	82.01	80.16	2.26%	96.01	90.8	5.43%
Nov	47.24	49.28	4.33%	52.80	59.56	12.81%	71.85	78.85	9.74%
Dec	37.64	34.97	7.08%	56.45	57.45	1.77%	70.26	77.86	10.81%

EnergyPlus and PVGIS-ERA5

The results indicate that the PVGIS-ERA5 dataset provides slightly different outcomes compared to the previous case with PVGIS-SARAH3. Based on Tables 4–5, the observed absolute deviations between PVGIS-ERA5 and EnergyPlus are as follows: Edinburgh: from 1.40% (May) to 22.12% (Dec); Hamburg: from 0.20% (Oct) to 22.02% (Nov); Prague: from 1.01% (July) to 19.21% (Dec); Belgrade: from 0.33% (May) to 16.87% (Jan); Rome: from 0.19% (May) to 10.32% (Nov); Málaga: from 0.62% (Oct) to 15.36% (Nov). Similar to the previous dataset, PVGIS-ERA5 shows the lowest agreement with EnergyPlus during colder months and the strongest agreement in warmer months, indicating that a high percentage of diffuse solar irradiation continues to represent a challenge. When considering the absolute values of monthly deviations, the number of months with deviations higher than 10% again provides an additional measure of dataset precision. The counts are: Edinburgh (5), Hamburg (2), Prague (3), Belgrade (1), Rome (1) and Málaga (2). In this case, all higher deviations occur in colder months, while precision remains strong during warmer periods, confirming the previous observation.

Edinburgh exhibits the highest number of such deviations, followed by Prague, whereas Belgrade and Rome show the most consistent agreement with EnergyPlus. Analysis of the mean absolute monthly deviations indicates that Edinburgh again stands out with 9.86%, while other locations range between 4.23% (Rome) and 5.71% (Prague), again demonstrating that total solar radiation alone does not determine accuracy. For colder months (October–March), the average deviation across all locations is 8.31%, compared to 3.44% for warmer months (April–September). Additionally, during winter months, PVGIS-ERA5 tends to slightly overestimate energy yields compared to EnergyPlus, which may reflect differences in the mathematical modeling approach for diffuse solar radiation. Overall, the mean absolute monthly deviation across all locations is 5.88%, indicating slightly higher precision than PVGIS-SARAH3. Comparing the two datasets, PVGIS-ERA5 generally provides more accurate results for most European locations, with the exception of Edinburgh, where SARAH3 remains slightly more precise.

Table 9. *Monthly PV energy production obtained from EnergyPlus (EPW) and PVGIS (ERA5) for nine analyzed locations, with comparison- part 1*

Month	Edinburgh			Hamburg			Prague		
	EPW [kWh]	ERA5 [kWh]	Difference	EPW [kWh]	ERA5 [kWh]	Difference	EPW [kWh]	ERA5 [kWh]	Difference
Jan	22.99	25.03	8.85%	20.63	21.05	2.02%	28.69	32.18	12.15%
Feb	33.31	38.02	14.16%	37.57	37.31	0.70%	50.17	48.27	3.79%
Mar	55.51	61.68	11.12%	62.82	64.54	2.74%	75.43	73.89	2.05%
Apr	75.27	78.71	4.57%	91.19	88.41	3.05%	93.37	88.3	5.43%
May	84.29	85.47	1.40%	94.52	90.05	4.73%	89.62	90.86	1.38%
Jun	81.29	76	6.50%	89.36	87.31	2.30%	89.25	87.37	2.10%
Jul	79.64	76.09	4.46%	85.55	85.08	0.55%	91.44	90.52	1.01%
Aug	72.93	68.54	6.02%	83.39	78.47	5.90%	79.62	83.1	4.38%
Sep	54.94	56.74	3.28%	62.77	64.39	2.59%	72.03	70.56	2.03%
Oct	35.91	41.02	14.22%	45.58	45.67	0.20%	60.96	53.71	11.90%
Nov	22.93	27.88	21.59%	19.92	24.31	22.02%	30.94	31.91	3.12%
Dec	14.36	17.54	22.12%	13.52	15.42	14.06%	22.06	26.3	19.21%

Table 10. *Monthly PV energy production obtained from EnergyPlus (EPW) and PVGIS (ERA5) for nine analyzed locations, with comparison- part 2*

Month	Belgrade			Rome			Málaga		
	EPW [kWh]	ERA5 [kWh]	Difference	EPW [kWh]	ERA5 [kWh]	Difference	EPW [kWh]	ERA5 [kWh]	Difference
Jan	41.56	48.57	16.87%	58.48	61.75	5.59%	81.234	84.65	4.21%
Feb	60.25	57.92	3.87%	73.27	69.32	5.40%	83.778	89.05	6.29%
Mar	85.08	83.88	1.41%	93.82	90.48	3.56%	107.656	106.35	1.21%
Apr	95.15	91.17	4.18%	101.59	96.13	5.37%	106.622	104.46	2.03%
May	91.57	91.87	0.33%	100.19	100	0.19%	110.341	108.28	1.87%
Jun	90.55	88.78	1.95%	100.65	97.99	2.65%	106.893	104.37	2.36%
Jul	100.05	96.17	3.88%	107.74	104.22	3.27%	114.530	108.28	5.46%
Aug	102.85	94.37	8.25%	105.53	102.64	2.74%	114.107	108.99	4.48%
Sep	84.57	80.87	4.38%	92.04	87.19	5.27%	104.279	100.62	3.51%
Oct	66.61	69.95	5.01%	82.01	79.16	3.48%	96.011	95.42	0.62%
Nov	47.24	51.35	8.71%	52.80	58.25	10.32%	71.851	82.89	15.36%
Dec	37.64	40.5	7.61%	56.45	58.09	2.90%	70.265	77.82	10.75%

4. Conclusions

This study presents a comparative analysis of the EnergyPlus simulation software and the PVGIS web application, using both SARAH3 and ERA5 datasets to assess the energy performance of photovoltaic (PV)

systems across multiple European locations. The analysis was conducted under identical input conditions, with locations selected based on the SolarGIS global horizontal irradiation map to represent different ranges of annual solar irradiation. The results show that deviations between the tools are not uniform, but depend on climatic and geographical factors, terrain complexity, atmospheric pollution, and differences in underlying modeling approaches. The highest deviations are consistently observed during winter months, primarily due to the increased share of diffuse solar radiation, while strong agreement is achieved in summer when direct irradiance dominates. Between the two datasets, ERA5 demonstrates slightly better overall agreement with EnergyPlus, with a mean absolute monthly deviation of 5.88%, compared to 6.57% for SARAH3, although SARAH3 performs better in the case of Edinburgh. Overall, PVGIS shows good agreement with EnergyPlus. It can therefore be considered a reliable tool for simplified and rapid energy yield assessments, while for more detailed and accurate analyses, advanced tools such as EnergyPlus remain more appropriate.

Acknowledgements

This paper was produced during research funded by the Ministry of Science, Technological Development and Innovation, no. 451-03-34/2026-03/200107 since February 5.2026.

References

[1] Guidolin, M., C. Mortarino, Cross-country diffusion of photovoltaic systems: Modelling choices and forecasts for national adoption patterns, Technological Forecasting and Social Change, 77 (2010), 2, pp. 279-296.
[2] Jager, W., Simulating the diffusion of photovoltaic systems: A behavioral perspective, Energy Policy, 34 (2006), 14, pp. 1935-1943.
[3] Kazem, A. H., et al., A systematic review of solar photovoltaic energy systems design modelling, algorithms, and software, Energy Sources, Part A: Recovery, Utilization, and Environmental Effects, 44 (2022), 3, pp. 6709-6736.
[4] Wu, C., Comparison Study of PVWatts and EnergyPlus in Simulating Electricity Production of Fixed PV Array, (2025), Available at SSRN 5429506.
[5] Mohammadi, S. A. D., C. Gezegin, Design and simulation of grid-connected solar PV system using PVSYST, PVGIS and HOMER software. International Journal of Pioneering Technology and Engineering, 1(2022), pp. 36-41.
[6] Larasati, P. D. L., R. A. Nugraha, Evaluasi Perencanaan Photovoltaic On Grid Menggunakan Software Berbasis Web: Studi Kasus Bandara Udara Internasional Jendral Ahmad Yani Kota Semarang. Knowledge on Sustainable Engineering, Vulnerability, Automation, and Software Intelligence, 1 (2025), 1, pp. 13-25.
[7] https://pvgis.com/en/guide-complete-pvgis (Accessed 20.03.2026.)
[8] https://joint-research-centre.ec.europa.eu/photovoltaic-geographical-information-system-pvgis_en (Accessed 20.03.2026.)
[9] Das, U. K., et al. Forecasting of photovoltaic power generation and model optimization: A review, Renewable and Sustainable Energy Reviews, 81 (2018), 1, pp. 912-928.
[10] Jimenez-Torres, M., et al., The Importance of Accurate Solar Data for Designing Solar Photovoltaic Systems—Case Studies in Spain, Sustainability, 9 (2017), 2, 247.
[11] Meral, M. E., F. Dincer, A review of the factors affecting operation and efficiency of photovoltaic based electricity generation systems. Renewable and Sustainable Energy Reviews, 15(2011), 5, pp. 2176-2184.
[12] https://www.totemtim.com/wp-content/uploads/LUXEN-TOPCon-SERIES-N5-MONOFACIAL-144cells-570-590w-MONO-SERBIA.pdf (Accessed 20.03.2026.)
[13] https://solargis.com/resources/free-maps-and-gis-data?locality=europe (Accessed 20.03.2026.)
[14] https://pvgis.com/en/pvgis-5-3 (Accessed 20.03.2026.)

[15] https://joint-research-centre.ec.europa.eu/photovoltaic-geographical-information-system-pvgis/getting-started-pvgis/pvgis-user-manual_en (Accessed 20.03.2026.)
[16] https://energyplus.net/ (Accessed 20.03.2026.)
[17] https://energyplus.net/assets/nrel_custom/pdfs/pdfs_v24.1.0/EnergyPlusEssentials.pdf (Accessed 20.03.2026.)
[18] Nikolić, N., D. Nikolić, Grejanje i Klimatizacija – osnove proračuna, modeliranja i simulacije, Faculty of Engineering University of Kragujevac, Kragujevac 2025.
[19] Guyot, D., et al. Building energy model calibration: A detailed case study using sub-hourly measured data, Energy and Buildings 223 (2020): 110189.
[20] Jradi, M., et al. ObepME: An online building energy performance monitoring and evaluation tool to reduce energy performance gaps, Energy and Buildings 166 (2018): 196-209.
[21] Jradi, M., C. Veje, B. N. Jørgensen, Deep energy renovation of the Mærsk office building in Denmark using a holistic design approach, Energy and Buildings 151 (2017): 306-319.
[22] Yin, R., S. Kiliccote, M. A. Piette, Linking measurements and models in commercial buildings: A case study for model calibration and demand response strategy evaluation, Energy and Buildings 124 (2016): 222-235.
[23] Lam, K. P., et al., An EnergyPlus whole building energy model calibration method for office buildings using occupant behavior data mining and empirical data, ASHRAE Journal (2014): 160-167.
[24] https://climate.onebuilding.org/#gsc.tab=0 (Accessed 20.03.2026.)

Renewable Energy and Solar Technologies

Performance Enhancement of $FASnI_3$ Perovskite Solar Cells with CBTS Hole Transport Layer: A SCAPS-1D Study

Khadija BOUGHANBOUR*[1] https://orcid.org/0009-0000-3905-4741, Mustapha SAHAL[1]
http://orcid.org/0000-0003-0528-8413

[1]*MESE / Lab. PETI, Polydisciplinary Faculty of Ouarzazate, Ibnou Zohr University, Morocco*

Corresponding author:

khadija.boughanbour@edu.uiz.ac.ma

Abstract
Tin-based, lead-free perovskite solar cells using $FASnI_3$ are explored as a safer alternative to conventional lead-containing devices. Numerical simulations with SCAPS-1D are used to optimize key factors, including absorber thickness, defect density, and carrier concentration, to enhance device performance. Special emphasis is placed on copper barium thiostannate (CBTS) as an inorganic hole transport layer due to its effective hole extraction, suitable energy alignment, and ability to limit recombination losses. The study shows that careful optimization leads to notable performance improvement, with an absorber thickness of 700 nm offering a good compromise between light absorption and recombination. Overall, the results highlight the promise of CBTS-based $FASnI_3$ solar cells for developing efficient and stable lead-free photovoltaic technologie.
Keywords: Lead-free perovskite solar cells ;FASnI3 ; CBTS (Cu_2BaSnS_4);SCAPS 1D; SCAPS-1D simulation ; UN SDG 7; UN SDG 13

1. Introduction

The increasing global demand for clean and sustainable energy has driven strong interest in photovoltaic technologies, particularly solar cells. Among them, perovskite solar cells (PSCs) have rapidly emerged as highly efficient and low-cost alternatives due to their excellent optoelectronic properties, including strong light absorption, tunable bandgap, and high charge carrier mobility. These features have enabled remarkable improvements in power conversion efficiency in a short time[1].

However, the presence of toxic lead in conventional perovskite materials remains a major limitation for large-scale commercialization. This has encouraged the development of lead-free alternatives, with formamidinium tin iodide ($FASnI_3$) gaining significant attention due to its suitable bandgap and reduced environmental impact[2].

In addition to the absorber layer, charge transport layers strongly influence device performance. In this context, copper barium thiostannate (CBTS), a kesterite-type material, is investigated as a hole transport layer (HTL) because of its good band alignment, stability, and low cost.

This work focuses on the SCAPS-1D simulation and optimization of $FASnI_3$-based solar cells, analyzing key parameters such as thickness, defect density, and carrier concentration, while highlighting the role of CBTS in improving device efficiency.

2. Materials and Methods

Device structure

The present study was conducted under AM1.5G illumination using the SCAPS-1D (version 3.3.09) simulation software, which was developed by the University of Gent in Belgium. The SCAPS-1D simulations are primarily based on three fundamental equations: the Poisson equation (1), the hole continuity equation (2), and the

electron continuity equation(2). This software allows for the design of heterostructure solar cells with up to seven different layers, and simulations can be performed under both light and dark conditions [3].

The simulated device structure is FTO/TiO_2/$FASnI_3$/CBTS/Au. $FASnI_3$ acts as the absorber, sandwiched between TiO_2 (ETL) and CBTS (HTL). FTO serves as the front contact, while Au is used as the back contact

$$\frac{d}{dx^2}\varphi(x)=\frac{q}{\varepsilon_0\varepsilon_r}[p(x)-n(x)+N_D-N_A-\rho_P-\rho_n] \quad (1)$$

$$\frac{dn}{dt}=\frac{1}{q}\frac{\partial J_n}{\partial x}+(G_n+R_n) \quad (2)$$

$$\frac{dp}{dt}=\frac{1}{q}\frac{\partial J_P}{\partial x}+(G_p+R_p) \quad (3)$$

φ : Electro static potential
G_n G_p : Generation rate of electron/ of holes
R_n R_p : Recombination rate of electrons /of holes
J_n J_P : Electron/hole current density
$\varepsilon_0\varepsilon_r = \varepsilon$:Electric permittivity of material

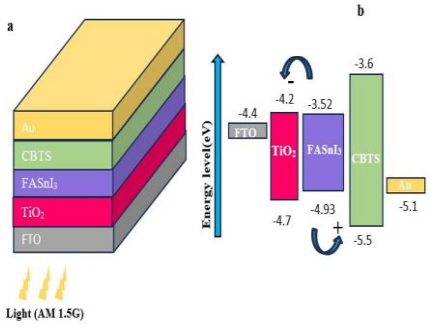


Figure 39: Schematic structure of the proposed solar cell configuration (a) and its energy level (b)

Table 1 : Parameters of FTO/TiO2/FASnI3/CBTS /Au solar cell.[4][5][6]

Parameters	FTO	TiO2	FASnI3	CBTS
Thickness (µm)	0.05	0.09	0.1-3	0.15
Band gap (eV)	3.5	3.2	1.41	1.9
Electron affinity (eV)	4.3	4	4	3.9
Dielectric permittivity (relative)	9	9	8.2	5.4
CB effective density of states (cm^{-3})	$1*10^{19}$	$1*10^{21}$	10^{18}	$2.2*10^{18}$
VB effective density of states (cm^{-3})	$1*10^{19}$	$2*10^{20}$	10^{18}	$1.8*10^{20}$
Electron thermal velocity (cm/s)	10^7	10^7	10^7	10^7
Hole thermal velocity (cm/s)	10^7	10^7	10^7	10^7
Electron mobility (cm^2/Vs)	20	20	$2.2*10^2$	30
Hole mobility (cm^2/Vs)	10	10	$2.2*10^2$	10
Shallow uniform donor density, ND (cm^{-3})	10^{18}	10^{18}	$7*10^{16}$	-
Shallow uniform acceptor density NA(cm^{-3})	-	-	-	10^{15}
Defect density (cm^{-3})	10^{15}	10^{15}	10^{15}	10^{14}

Table 2: Defect density inside the absorber and at interfaces.

Parameter	TiO_2/$FASnI_3$	CBTS/$FASnI_3$
Defect nature	Neutral	Neutral
Electrons capture cross section	10^{-15}	10^{-15}
Holes capture cross section	10^{-15}	10^{-15}
Energy distribution	single	single
Reference for defect energy level E_t	Above the highest Ev	
Energy with respect to Reference (eV)	0.6	0.6
Total density (Nt)	10^{10}	10^{10}

3. Results

- **Thickness**

The thickness of the active layer significantly affects the performance of the device, making it essential to choose an optimal thickness for maximizing efficiency. we will investigate the FTO/TiO2/FASnI3/Au device in this simulation, the active layer thickness was adjusted from 0.3µm to 1.5µm , as shown in Fig. 2. All other

parameters were kept constant, as specified in Tables 1,2 and 3. It is clear that the power conversion efficiency (PCE) increases with thickness, reaching a peak of 17.89% at 0.7 µm, as thinner films do not absorb enough light. However, beyond this thickness, PCE declines, dropping to 15.92% at 1.5 µm due to higher carrier recombination in thicker films.

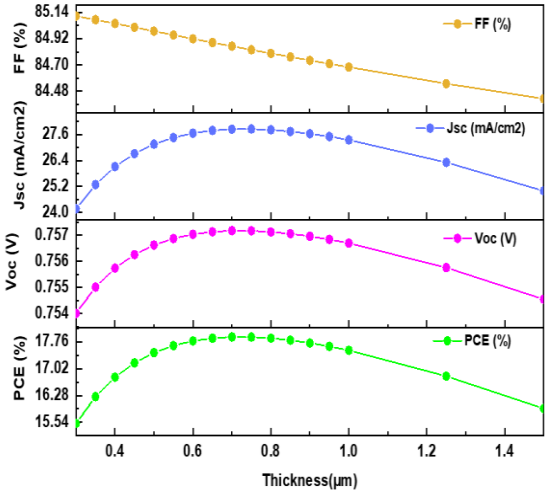
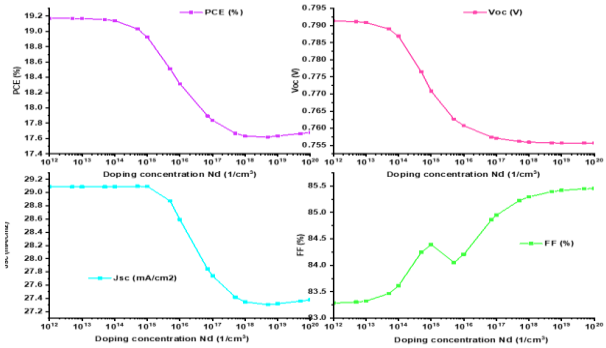


Figure 40:Variation of Absorber Layer Thickness with, PCE,Jsc, and Voc

The current density (Jsc) increases with absorber thickness, reaching a maximum (~28.15 mA/cm²) at 0.7 µm, then declines due to recombination despite strong perovskite absorption. Similarly, Voc peaks at 0.7 µm and decreases with further thickness [7]. The fill factor (FF) decreases due to recombination caused by the short carrier lifetime. The optimal thickness is 700 nm, yielding Jsc = 27.84 mA/cm², Voc = 757 mV, FF = 84.86%, and PCE = 17.89%.

- **Impact of donnor doping concentration and Defect Density**



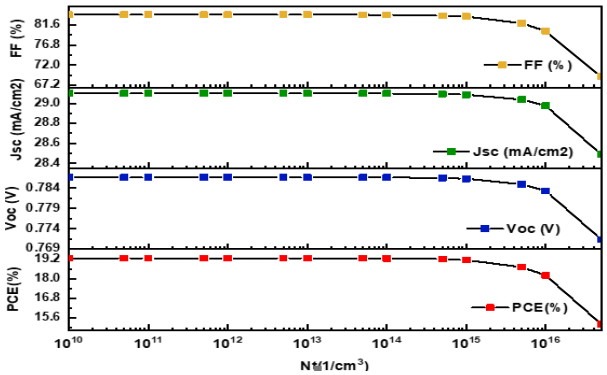


Figure 41:impact of dopage concentration Na of FASnI3 **Figure 42: Influence of defect density of FASnI3 perovskite absorber**

Donor concentration and defect density strongly influence device performance. Increasing defects (10^{10}–10^{17} cm^{-3}) reduces Jsc, Voc, FF, and PCE due to shorter carrier lifetime and enhanced recombination, with PCE dropping to 15.21% at 10^{17} cm^{-3}. Similarly, higher donor concentration lowers Jsc, Voc, and PCE but slightly increases FF due to improved conductivity. These effects are linked to reduced carrier diffusion length and

increased recombination (SRH mechanism), which hinder charge collection. Optimal values are ~10^{14} cm^{-3} for donor concentration and 10^{13} cm^{-3} for trap density, at an absorber thickness of 700 nm.

Impact of add CBTS parameters: thickness and dopage

The thickness of the CBTS hole transport layer, its electron affinity, and doping concentration are crucial for optimizing the performance of solar cell devices. Consequently, the performance parameters of the Au/CBTS/$FASnI_3$/TiO_2/FTO device structure are examined by varying the CBTS thickness (Fig. 5), doping concentration (Fig. 6).

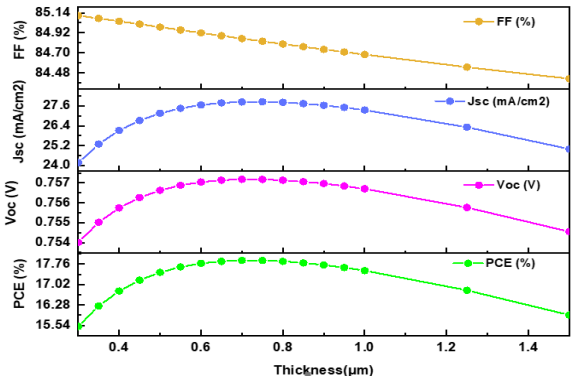


Figure 5: Impact of varied thicknesses of CBTS

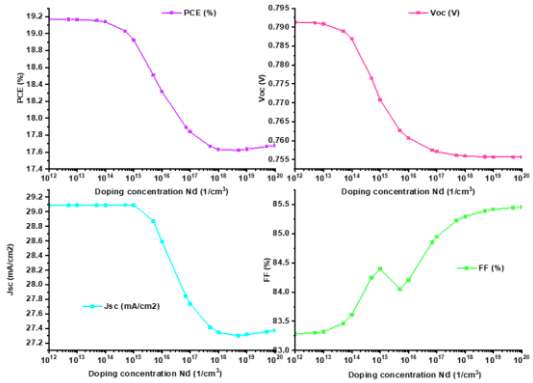


Figure 6: Impact of varied thicknesses of CBTS

Figure 5 shows that increasing CBTS thickness (0.1–3 µm) slightly improves device performance, with an optimal thickness around 1.5 µm, while key parameters are fixed (700 nm absorber, 10^{14} cm^{-3} defects, 10^{19} cm^{-3} doping). The device performance was studied by varying CBTS doping (10^{14}–10^{20} cm^{-3}), affecting Voc, Jsc, and FF. An optimal doping level is selected to maximize efficiency and ensure stable charge transport.

5. Conclusions

Optimizing $FASnI_3$ solar cells improves performance, with thickness, defect density, and carrier concentration playing key roles. CBTS enhances charge extraction and reduces recombination, making $FASnI_3$/CBTS a promising efficient, lead-free structure.

Acknowledgements

I would like to thank my supervisor, Mustapha, for his support and valuable contribution to this work.

References:

[1] H. Dixit, D. Punetha, and S. K. Pandey, "Improvement in performance of lead free inverted perovskite solar cell by optimization of solar parameters," *Optik (Stuttg).*, vol. 179, no. November 2018, pp. 969–976, 2019, doi: 10.1016/j.ijleo.2018.11.028.

[2] D. Azhakanantham, M. Selvamani, T. Geun Kim, D. Contreras, and A. Varman Kesavan, "Exploring novel HTL suitable for Eco-friendly and high performance FASnI3 photovoltaics," *Mater. Sci. Eng. B*, vol. 284, no. July, p. 115909, 2022, doi: 10.1016/j.mseb.2022.115909.

[3] I. M. Dharmadasa, Y. Rahaq, A. A. Ojo, and T. I. Alanazi, "Perovskite solar cells: a deep analysis using current–voltage and capacitance–voltage techniques," *J. Mater. Sci. Mater. Electron.*, vol. 30, no. 2, pp. 1227–1235, Jan. 2019, doi: 10.1007/s10854-018-0390-5.

[4] E. Oublal, A. Ait Abdelkadir, and M. Sahal, "High performance of a new solar cell based on carbon

nanotubes with CBTS compound as BSF using SCAPS-1D software," *J. Nanoparticle Res.*, vol. 24, no. 10, 2022, doi: 10.1007/s11051-022-05580-7.

[5] M. V Kavitha and S. S. K, "Results in Optics Device modelling and performance enhancement of FASnI 3 -based perovskite solar cell with diverse , compatible charge transport layers," vol. 18, no. January, 2025.

[6] K. Boughanbour, M. Sahal, E. Oublal, and N. Kumar, "heterojunction solar cell perovskite with double ETL by SCAPS - 1D Software," *Opt. Quantum Electron.*, 2025, doi: 10.1007/s11082-025-08138-8.

[7] K. Boughanbour, L. Rakassi, M. Sahal, H. Charifi, and N. Kumar, "Enhancement of an Eco-Friendly Perovskite Solar Cell Based on FASnI3 Using Various HTL Layers," *Phys. status solidi*, vol. 223, no. 3, p. e202500483, 2026, doi: https://doi.org/10.1002/pssa.202500483.

Digital Infrastructure for Collective Solar Self-Consumption: Enabling Scalable Energy Communities through Data, Algorithms and Governance Platforms

Mikel Ubiria Pérez

Zenit Solar, Plaza de las Cigarreras 33, Donostia, Spain, m.ubiria@zenitsolar.eu
Contact email: *m.ubiria@zenitsolar.eu* | Website: https://zenitsolar.eu/es/

Executive Summary
Zenit Solar is a technology company dedicated to enabling scalable collective solar self-consumption and energy communities. The company has developed a cloud-based Software-as-a-Service (SaaS) platform that allows multiple users to share electricity generated by a common photovoltaic installation, supporting both technical and regulatory compliance. By providing simulation tools, energy allocation algorithms, and governance frameworks, Zenit Solar simplifies the design, operation, and optimization of shared renewable energy systems.
The growing deployment of distributed solar energy presents new organizational and technical challenges. Collective self-consumption projects require careful coordination between participants, engineering firms, installers, and utilities, while adhering to evolving regulatory frameworks. Zenit Solar addresses these challenges by digitalizing the full project lifecycle: feasibility studies, system design, algorithmic energy sharing, financial modeling, operational monitoring, and automated reporting.
The platform's core innovation lies in its algorithmic approach to energy distribution, which ensures fair and transparent allocation among participants while maximizing local self-consumption. By combining energy system modeling, financial simulation, and governance tools, Zenit Solar reduces administrative complexity and accelerates project deployment.
Zenit Solar's solutions are applied across engineering firms, energy communities, municipalities, and utilities, enabling the creation of decentralized, participatory energy systems. The platform scales across different regulatory contexts and supports the integration of emerging technologies such as storage and demand management.
By facilitating collective solar projects, Zenit Solar contributes to renewable energy adoption, energy efficiency, and the democratization of energy production. Its technology advances both market and societal value, creating measurable environmental and social impact. Looking forward, Zenit Solar aims to expand its platform capabilities, strengthen partnerships in the energy ecosystem, and accelerate Europe's transition toward flexible, digitalized, and community-driven energy systems.
Keywords: Zenit Solar; collective self-consumption; energy communities; solar energy; SaaS; distributed energy systems; energy allocation algorithms; renewable energy adoption; digital energy platforms; energy transition
Relevant UN SDGs: UN SDG 7 (Affordable and Clean Energy), UN SDG 13 (Climate Action), UN SDG 11 (Sustainable Cities and Communities)

1. Company Overview

Zenit Solar is a technology startup operating in the renewable energy sector, focused on enabling scalable collective solar self-consumption and energy communities. The company develops digital infrastructure that allows multiple consumers to share electricity generated by a common photovoltaic installation.
The company's mission is to simplify and accelerate the deployment of shared renewable energy systems by providing the technological tools required to design, manage, and scale collective energy projects. Zenit Solar positions itself as a technological partner for engineering firms, installers, energy communities, municipalities, and utilities that are developing distributed solar infrastructure.
By combining energy system modeling, digital governance tools, and data-driven decision support, Zenit Solar enables new collaborative models of energy production and consumption.

2. Technology / Product / Service Description
Zenit Solar's core product is a Software-as-a-Service (SaaS) platform designed to support the development and management of collective photovoltaic installations.
The platform integrates several functionalities across the project lifecycle:

- **Feasibility analysis and energy modeling**, allowing simulation of photovoltaic generation and consumption patterns.
- **Allocation algorithms**, which distribute energy among participants according to predefined sharing coefficients and regulatory frameworks.
- **Project design tools**, supporting technical and financial evaluation of installations.
- **Operational monitoring and reporting**, enabling transparent management of collective installations and performance tracking.

The technological foundation of the platform combines photovoltaic production modeling, consumption analysis, and algorithmic optimization of energy sharing. This allows stakeholders to design systems that maximize local energy use while ensuring fair and transparent distribution among participants.

3. Innovation and Competitive Advantage
Zenit Solar differentiates itself by providing an integrated digital infrastructure specifically tailored to the complexities of collective self-consumption systems.
Key innovation elements include:

- **Algorithmic energy allocation models** designed for multi-user photovoltaic systems.
- **End-to-end digitalization** of project development, from feasibility analysis to operational management.
- **Interoperability with multiple actors** in the renewable energy ecosystem, including installers, engineering firms, energy communities, and utilities.
- **Scalable SaaS architecture**, enabling replication of projects across different geographical and regulatory contexts.

This approach reduces administrative complexity, improves transparency among participants, and lowers the barriers to deploying shared renewable energy systems.

4. Market Application and Impact

Zenit Solar's technology is designed for application in the rapidly growing market of distributed renewable energy and energy communities.

Target users include:

- engineering and EPC companies developing solar projects
- energy communities and cooperatives
- municipalities promoting local energy initiatives
- energy service companies (ESCOs)
- utilities exploring decentralized energy models

By enabling efficient coordination among multiple participants, the platform helps unlock new solar deployment opportunities in residential, commercial, and community-scale contexts.

Beyond market value, Zenit Solar contributes to broader societal goals by supporting renewable energy adoption, improving energy efficiency, and enabling more democratic participation in energy production.

5. Partnerships and Outlook

Zenit Solar actively collaborates with engineering firms, renewable energy developers, municipalities, and emerging energy communities to deploy collective solar projects.

Future development priorities include:

- expanding platform capabilities for large-scale energy communities
- integrating additional energy technologies such as storage and demand management
- strengthening data analytics and energy optimization capabilities
- expanding partnerships across the European distributed energy ecosystem

Through these developments, Zenit Solar aims to become a key enabling technology for the next generation of decentralized and participatory energy systems.

Sustainable Materials, Coatings, and Corrosion Protection

Development and Optimization of Water-Based Acrylic Coatings for Enhanced Corrosion Resistance of Metallic Materials

Environmentally Friendly and Sustainable Coatings for the Corrosion Resistance of Metallic Materials, Project ID: 19.031/966-8-1/25, Government of the Republic of Srpska (RS), 2026-2027

Milorad Tomić[1,2], Nebojša Vasiljević[1], Marija Mitrović[1], Regina Fuchs-Godec[3], Jelena Bajat[4]

[1]*Faculty of Technology Zvornik, University of East Sarajevo, Zvornik, Bosnia and Herzegovina,* milorad.tomic@tfzv.ues.rs.ba, *http://orcid.org/0009-0004-1022-2093,* nebojsa.vasiljevic@tfzv.ues.rs.ba, *https://orcid.org/0000-0002-3789-9975*, *marija.ridjosic*@tfzv.ues.rs.ba, *https://orcid.org/0000-0002-3208-016X*

[2]*Engineering Academy of Serbia, Belgrade, Serbia*

[3]*Faculty of Chemistry and Chemical Engineering, University of Maribor, Maribor, Slovenia, regina.fuchs@um.si, https://orcid.org/0000-0002-5700-0963*

[4]*Faculty of Technology and Metallurgy, University of Belgrade, Belgrade, Serbia,* jela@tmf.bg.ac.rs, *https://orcid.org/0000-0003-0742-8176*

Corresponding author: milorad.tomic@tfzv.ues.rs.ba

Abstract

Corrosion remains a significant challenge, and increasing research efforts are focused on the development of environmentally friendly corrosion protection methods. Therefore, the goal of the project is the development, optimization and improvement of a water-based acrylic coating with pronounced corrosion protection properties in aggressive environments such as seawater, acid rain, acids and acid chloride solutions. In this way, the negative impact of conventional toxic protective coatings on the environment will be reduced. Water-based coatings are promising because their use reduces emissions of volatile organic compounds and because they exhibit strong adhesion. Encapsulated corrosion inhibitors and nanoparticles are expected to further improve the protective performance of the coating. Coatings are applied to copper, copper alloys and low-quality stainless steel using the spin-coating technique, which are then dried under different conditions. Morphology, chemical structure and surface properties were determined using scanning electron microscopy (SEM), ATR-FTIR spectroscopy and contact angle measurements. This research supports the principles of the circular economy as renewable corrosion inhibitors are produced from waste. The results of this study are expected to provide a basis for the design of next-generation sustainable coatings with improved corrosion resistance and long-term durability in aggressive environments.

Keywords: water-based acrylic coatings; sustainable materials; corrosion inhibitors; spin-coating; circular economy; UN SDG 12

1. Project Background and Objectives

Corrosion continues to be a major challenge in various industries and sectors [1]. In order to reduce the damage caused by corrosion, intensive work is being done to develop new materials, coatings, corrosion inhibitors, as well as associated diagnostic and protective techniques [1,2]. The research goal of this project is to increase corrosion resistance, extend the service life of materials and infrastructure, and thus reduce maintenance costs. Despite numerous research efforts worldwide, the discovery of new techniques and new materials, both basic and composite, for corrosion protection [3].

Corrosion can have many harmful effects on the environment, such as leaks from corroded pipelines or storage tanks [4]. This can lead to the release of hazardous substances into the environment, causing soil and water pollution, damage to ecosystems and potential health risks. For this reason, there is increasing emphasis on environmentally friendly and sustainable corrosion protection methods, including the development and use of environmentally friendly coatings and inhibitors from renewable sources [3,5].

Recent research shows the great potential of water-based coatings for the protection of materials against corrosion [6,7]. The results show that they offer many advantages over conventional organic solvent-based coatings [2]. These coatings use water as a carrier medium instead of solvents and are therefore less harmful to the environment and human health. Water-based coatings are also more effective in protecting against corrosion than solvent-based coatings, because they form a stronger bond with the substrate and provide a stronger barrier against moisture, salt and other corrosive elements. Also, water-based coatings have better adhesion and flexibility, allowing them to withstand stress and deformation without cracking or peeling. Water-based coatings offer many other advantages, such as faster drying times and easier cleaning [5]. They are also less flammable than solvent-based coatings, making them safer to handle and store [3]. In general, water-based coatings are an excellent choice for anyone looking for an effective and environmentally friendly way to protect metal surfaces from corrosion.

2. Methodology and Work Performed

A water-based acrylic coating is a type of coating that contains acrylic polymers and water. They are mainly used in various applications such as wood coatings, metal coatings and vehicle coatings. The acrylic polymers used in water- based coatings consist of acrylic monomers that polymerize in the presence of water, producing a stable emulsion of acrylic polymer particles that can be easily mixed with water to form a uniform coating. Since water is used as a solvent, this type of coating is a more environmentally friendly alternative to solvent-based coatings, not least because it emits fewer volatile organic compounds into the atmosphere. The coating can also be enhanced with an encapsulated inhibitor. This would involve the use of an encapsulated surfactant (non-ionic surfactant) or the addition of, for example, nanoparticles, TiO_2, CeO_2, Al_2O_3, etc. This is followed by additives that can further improve the properties of the coating, such as UV stabilizers, fillers and pigments. A centrifuge machine is used to apply the coating. In the final stage, the coating is dried. Drying can be in air or in an oven at different temperatures and times. The choice of temperature and drying time plays an important role in the final quality of the coating, especially in the case of repeated application (multi-layer coating). It is important to avoid the formation of microchannels, which allow the formation of diffusion paths and therefore

access of the electrolyte to the base metal matrix and the formation of localized corrosion. The coatings will be applied to copper and Cu alloys, as well as to low-grade stainless steel (chromium content about 13%). Scanning electron microscope (SEM) will be used to characterize the surface morphology of the protective coatings, and infrared spectroscopy (ATR-FTIR) will be used to gain insight into the possible mechanism of corrosion protection, as well as a commercial goniometer (Data Physics OCA 25, Germany) to examine the contact angle and wetting of surfaces with and without protective coatings. The concentrations of added inhibitors, the number of thin film applications, and the drying time between applications (temperature and drying time) should be optimized.

Scientific significance: The development of anti-corrosion coatings for metal protection is important for basic research as well as various applications in industry and everyday life. Also, taking into account European guidelines and awareness of the protection of nature and all living things, as well as careful management of waste, which can also be raw materials, and the use of renewable resources, corrosion problems must be solved.

3. Expected Results

The development of anti-corrosion coatings for metal protection is important for basic research as well as various applications in industry and everyday life. Also, taking into account European guidelines and awareness of the protection of nature and all living things, as well as careful management of waste, which can also be raw materials, and the use of renewable resources, corrosion problems must be solved.

4. Discussion and Impact

The cooperation between Faculty of Technology Zvornik, University of East Sarajevo and Faculty of Chemistry and Chemical Engineering, University of Maribor has been in place since 2010 and we have successfully completed five bilateral projects, which undoubtedly provides a solid foundation for future joint initiatives, further cooperation and deepening academic and research relations between the two countries. In the more than ten years of our cooperation, we have built trust, established effective working relationships and launched numerous successful initiatives that have contributed to the development of both institutions. To address problem of corrosion, research will be carried out to develop advanced materials, protective coatings, corrosion inhibitors and diagnostic and preventive technologies. Particular attention is now being paid to the environmental impact of corrosion and its consequences. Corrosion can lead to the release of hazardous substances into the environment, contaminate soil and water, damage the ecosystem and cause potential health risks. For this reason, increasing emphasis is being placed on environmentally friendly and sustainable corrosion protection methods. This includes the development and use of environmentally friendly coatings and inhibitors from renewable sources. This development is also in line with European directives on the circular economy, which follow the principle that "any waste can become a resource". This means that suitable inhibitors can also be found among expired products that are no longer suitable for their original use but can still serve as highly effective corrosion inhibitors. By continuing our bilateral cooperation, we want to build on what we have achieved so far, expand our cooperation and strengthen our common goals in the areas of education, research and mobility.

5. Conclusions and Outlook

Research is important for accelerating industrial development, protecting the natural environment, transferring knowledge, and developing new personnel. In addition, research allows the faculty to be involved in the international scientific space with the aim of keeping in touch and staying involved in international scientific research exchanges. The project also provides for the promotion of science, appropriate presentations of scientific and professional works in the country and abroad, and publications in international and national journals. The research results will represent an important contribution to the basic knowledge in the field of building materials (e.g. chemically resistant steels) under various conditions. For example, it is possible to use various pretreatment methods to influence the corrosion resistance of the material even before it is used, since we can change the functional properties of its surface. Among other things, they are given hydrophobic properties, for example, which basically prevent contact with the medium water, which is usually the case. The additional application of a protective layer, which also contains an encapsulated inhibitor, can extend the service life of the material. In line with the 'green' European directive and the objectives of the circular economy, the purpose of using materials to protect metallic materials from renewable sources.

Acknowledgements / Funding

The authors gratefully acknowledge the financial support provided by the Government of the Republic of Srpska (Contract No. 19.031/966-8-1/25). The authors also acknowledge the bilateral cooperation with the Republic of Slovenia and the collaboration with the University of Maribor.

References

1. Zou Y, Pan P, Yan X. Comparative Analysis of Performance of Water-Based Coatings Prepared by Two Kinds of Anti-Bacterial Microcapsules and Nano-Silver Solution on the Surface of Andoung Wood. Coatings. 2023;13:1518.
2. Sudoł E, Kozikowska E, Choińska E. Artificial Weathering Test Methods of Waterborne Acrylic Coatings for Steel Structure Corrosion Protection. Materials. 2024;17:1857.
3. Cristoforetti A, Donati L, Rossi S. Tagua Powder as a Bio-Based Filler for Waterborne Acrylic Coatings: Enhancing Performances and Sustainability. Surfaces. 2025;8:20.
4. Ress J, Martin U, Bastidas DM. Improved Corrosion Protection of Acrylic Waterborne Coating by Doping with Microencapsulated Corrosion Inhibitors. Coatings. 2021;11:1134.
5. Raditoiu V, Raditoiu A, Raduly MF, Amariutei V, Gifu IC, Anastasescu M. Photocatalytic Behavior of Water-Based Styrene-Acrylic Coatings Containing TiO_2 Sensitized with Metal-Phthalocyanine Tetracarboxylic Acids. Coatings. 2017;7:229.
6. Zhou Y, Chen G, Yan S, Ni C, Yu L, Li X. Epoxy Composite Coating with Excellent Anticorrosion and Self-Healing Properties Based on Acrylate Copolymers. Progress in Organic Coatings. 2022;172:107098.
7. Jomy J, Prabhu D, Prabhu PR. Inhibitors Incorporated Into Water-Based Epoxy Coatings on Metals for Corrosion Protection: A Review. Journal of Bio- and Tribo-Corrosion. 2022;8:44.

Application of Thyme Extract as a Steel Corrosion Inhibitor in HCl and NaCl Solutions

Examination Thyme Extract as a Non-toxic Corrosion Inhibitor: Properties, Applications and Contribution to Sustainable Development, Scientific research project No. 19.032/961-88/24, Government of the Republic of Srpska (RS), 2025-2026

Marija Mitrović[1], Nebojša Vasiljević[1], Regina Fuchs-Godec[2], Milorad Tomić[1,3]

[1]*Faculty of Technology Zvornik, University of East Sarajevo, Zvornik, Bosnia and Herzegovina, marija.ridjosic@*tfzv.ues.rs.ba*, https://orcid.org/0000-0002-3208-016X,* nebojsa.vasiljevic@tfzv.ues.rs.ba, https://orcid.org/0000-0002-3789-9975, milorad.tomic@tfzv.ues.rs.ba*, http://orcid.org/0009-0004-1022-2093,*

[2]*Faculty of Chemistry and Chemical Engineering, University of Maribor, Maribor, Slovenia, regina.fuchs@um.si, https://orcid.org/0000-0002-5700-0963*

[3]*Engineering Academy of Serbia, Belgrade, Serbia*

Corresponding author: marija.ridjosic@tfzv.ues.rs.ba

Abstract

Conventional inhibitors are often environmentally hazardous, which highlights the need for sustainable alternatives. In this study, the inhibitory effect of thyme extract as a green inhibitor on the corrosion of two types of steel in 4% HCl and 3% NaCl solutions was investigated. This is in line with current efforts to replace synthetic inhibitors with environmentally friendly inhibitors. The gravimetric method was used to examine the corrosion rate and the effect of thyme extract as a corrosion inhibitor, and polarization diagrams and electrochemical impedance spectroscopy (EIS) were recorded from electrochemical methods. All experiments were performed in laboratory conditions at room temperature. The obtained results of gravimetric and electrochemical measurements show that thyme extract has an inhibitory effect on the corrosion of the used steels. The mean values of the protective factor of the extract as a corrosion inhibitor for used steels in 3% NaCl are below 60%, while the mean values of the protective factor of thyme extract as a corrosion inhibitor for used steels in 4% HCl range from 50-90%. The protective factor z for unalloyed steel is above 80% only with the addition of 1.5 g/L of the extract after 48 h and 168 h, while for stainless steel the protective factor z is higher than 80% only after 168 h, which indicates a very slow adsorption and reaction of the extract on the surface of used steels. These results show that thyme extracts can be used as corrosion inhibitors, and the findings from the study can contribute to sustainable material protection and environmentally friendly corrosion control strategies.

Keywords: thyme extract; green corrosion inhibitor; gravimetric analysis; polarization; electrochemical impedance spectroscopy; UN SDG 12

1. Project Background and Objectives

Corrosion processes, which occur daily and lead to the conversion of useful metals into unusable or harmful corrosion products, are a spontaneous phenomenon between metals and the environment in which they are found, whereby the metal transitions to a thermodynamically more stable state occurs [1]. Steel, as the most important technical metal, is most commonly used as a construction material due to its exceptional physical and mechanical properties. Numerous studies have shown that various forms of environmental pollution further accelerate the rate of corrosion, including steel corrosion [1,2].

Conventional organic inhibitors often have limitations, including toxicity, limited solubility, and reduced efficiency in demanding operating conditions. As a result, there is growing interest in researching sustainable corrosion inhibitors that would be environmentally friendly and highly effective. Natural plant extracts are very popular among environmentally friendly corrosion inhibitors [3,4,5]. Plant extracts contain complex mixtures of heteroatom-rich organic compounds (S, N, O, P) that serve as active adsorption sites on metal surfaces, forming a protective barrier against corrosive agents [5,6].

Thyme, *Thymus serpillum*, is a perennial shrub native to northern and central Europe. Thyme also contains flavonoids, phenolic carboxylic acids and their derivatives, triterpenes, and tannins [7]. These organic compounds and groups of compounds could play a significant role in the formation of a passive layer on steel and the prevention of corrosion in aggressive environments such as 3% NaCl and 4%HCl.

2. Methodology and Work Performed

Thyme extract will be synthesized by Soxhlet ethanol extraction. Based on the weight loss of steel samples, mass loss measurements, corrosion depth indicator, and inhibition efficiency will be determined. Two very precise methods will be used, electrochemical impedance spectroscopy and polarization measurements in a three-electrode cell, using a Gamry Series GTM 750 potentiostat/galvanostat/ZRA device. Electrochemical impedance spectroscopy provides insight into the corrosion mechanism of steel in the presence and absence of inhibitors in sodium chloride and hydrochloric acid, i.e. it shows how the inhibitor reduces and prevents corrosion. In addition, it determines the exact value of the material's resistance in given environments. Corrosion parameters will also be determined by applying the polarization method (by recording Tafel polarization diagrams), from which, using appropriate software, corrosion current densities, corrosion potentials, polarization resistance, cathodic and anodic slopes and corrosion rates of materials in the tested aggressive corrosion environments will be calculated. The surface of the material samples after a certain time in uninhibited and inhibited solutions will be analyzed by scanning electron microscopy (SEM) and energy dispersive X-ray spectroscopy (EDS), in order to determine the condition of the material surface and the influence of the inhibitor on the corrosion process. The EDS method will provide data on whether organic molecules present in the extract are adsorbed on the steel. The FTIR method will provide accurate information on the composition of the extract, i.e. the main functional groups. By comparing the spectrum of the extract with the IR spectrum of the steel surface after a certain time in the inhibited solution, information will be obtained about the possible existence of an inhibitor film, as well as about the main metal-complexing functional groups.

3. Key Results

The mean values of the protective factor of thyme extract as a corrosion inhibitor for steels used in 3% NaCl are below 61%, while the mean values of the protective factor of thyme extract as a corrosion inhibitor for steels used in 4% HCl range from 56-86%.

Based on polarization tests, it can be seen that thyme reduces the corrosion rate, i.e. a decrease in the corrosion current occurs. A significant decrease in the corrosion current was observed for stainless steel. With increasing thyme concentration, the corrosion current also decreases, i.e. the corrosion rate for all steel samples.

The results of electrochemical impedance spectroscopy show that the resistance to the corrosion process increases with increasing thyme concentration in 4% HCl, which indicates the inhibitory effect of the extract. The corrosion resistance increases with increasing thyme concentration up to a certain point and then slowly begins to decrease, except for steel exposed to a solution containing the maximum concentration (1.5 g/L) of thyme extract. This means that the resistance to charge transfer increases in the presence of thyme, i.e. oxidation processes are slowed down. The highest corrosion resistance of both steels is at 4% HCl + 1.5 g/L of extract, which is confirmed by gravimetric and electrochemical measurements.

4. Discussion and Impact

Gravimetric analysis has shown that thyme extract acts as a corrosion inhibitor. This indicates that a higher concentration of thyme extract as a corrosion inhibitor provides longer-lasting protection of steel in a 4% HCl solution. It can be seen that the presence of thyme extract at all concentrations reduces the mass loss of steel, i.e. that thyme has an inhibitory effect in 3% NaCl.

The cathodic curves in the inhibited and non-inhibited solutions are parallel, which means that the addition of thyme to the acidic solution did not change the mechanism of hydrogen formation, and the reduction of H+ ions on the surface of the structural steel mainly occurs by the charge transfer mechanism. This means that thyme molecules are adsorbed onto the surface of the structural steel and block the reaction sites, thus reducing the surface area available to H+ ions, while the actual reaction mechanism remains unchanged.

The obtained results of gravimetric and electrochemical measurements show that thyme extract (EMD) has an inhibitory effect on the corrosion process of used steels, but not a sufficiently high protective effect to be recommended for commercial application.

5. Conclusions and Outlook

Corrosion inhibitors are an effective method for protecting metals from corrosion because they significantly extend the life of the material. Conventional synthetic inhibitors have disadvantages, as they are toxic and poorly soluble. Therefore, research is directed towards the synthesis of natural and environmentally friendly inhibitors. These “green” inhibitors are also plant extracts, such as thyme. The main advantage of thyme (*Thymus serpillum*) as an inhibitor is that it is easily available and represents a biodegradable source of active compounds. Ethanol extract of thyme contains organic compounds (thymol, carvacrol, phenolic acids), which form a

protective layer on the metal surface and thus reduce the corrosion rate in aggressive environments such as 3% NaCl and 4% HCl. The results of gravimetric and electrochemical tests provided a clear picture of the efficiency of the extract, the optimal concentration and the mechanism of its action. The positive outcomes of this project have a significant scientific impact. First of all, it contributed to the understanding of the reduction of corrosion pollution and the application of green inhibitors in industry. This project represents a step towards sustainable development and application of innovative, non-toxic and effective solutions in the protection of structural materials from corrosion.

Acknowledgements / Funding

The authors gratefully acknowledge the financial support provided by the Government of the Republic of Srpska (Contract No. 19.032/961-88/24) within the scientific research project.

References

1. Fuchs-Godec R, Tomic M, Pavlovic M. Effect of α-tocopherol as a green inhibitor on chloride-induced corrosion of steel. *International Journal of Electrochemical Science.* 2019;14:10396–10409.
2. Žbulj K, Hrnčević L, Bilić G, Simon K. Dandelion-root extract as green corrosion inhibitor for carbon steel in CO2-saturated brine solution. *Energies.* 2022;15:3074.
3. Tomić M, Mićić V, Godec R, Pavlović M, Vaštag G, Ridošić M, Pavlović M. Sage extracts as inhibitors of steel corrosion in 4% HCl. *International Journal of Electrochemical Science.* 2016;11:3339–3350.
4. Mitrović M, Apostolov S, Fuchs-Godec R, Salkunić B, Vastag G, Tomić M. Dandelion (*Taraxacum officinale*) root extract as a green corrosion inhibitor of steel in 3% NaCl. *Periodica Polytechnica Chemical Engineering.* 2024;68:609–619.
5. Li H, Fan M, Wang K, Bian X, Jiang H, Ding W. Traditional Chinese medicine extracts as novel corrosion inhibitors for AZ91 magnesium alloy in saline environment. *Scientific Reports.* 2022;12:7367.
6. Obeten M, Magu T. Phytochemical constituents of *Taraxacum officinale* leaves as eco-friendly and nontoxic organic inhibitors for stainless steel corrosion in 0.2 M HCl acid medium. *International Journal of Chemical Science.* 2018;2:35–43.
7. Deyab M, Guibal E. Enhancement of corrosion resistance of the cooling systems in desalination plants by green inhibitor. *Scientific Reports.* 2020;10:4812.

ENTREPRENEURSHIP AND INNOVATION

Entrepreneurship, Start-ups, and Entrepreneurial Development

Opportunities for young Entrepreneurs

Project: Building a New Value Proposition for Gipuzkoa as an Attractive Territory for Young Tech Entrepreneurs, Gipuzkoa EGAN BIZZI, 2024-LAB2-008-01, Gipuzkoa Provincial Council, 2024–2025

Maider Beitialarrangoitia[1], Laida San Sebastian[2]

[1]Faculty of Engineering, Mondragon Unibertsitatea, Arrasate, Spain, mbeitialarrangoitia@mondragon.edu, https://orcid.org/0009-0001-0182-5501, lsansebastian@mondragon.edu, https://orcid.org/0000-0002-6184-1589

Corresponding author: mbeitialarrangoitia@mondragon.edu

Abstract

Gipuzkoa faces a structural challenge: despite low overall unemployment, many young people struggle to build stable and autonomous life projects, and youth unemployment remains stagnant. Entrepreneurship could offer a meaningful pathway, yet only a small proportion choose this option and many initiatives are abandoned early due to income instability, limited long-term support, and the absence of mechanisms that accompany project transitions. The Gipuzkoa Egan Bizzi project was developed to understand how territorial conditions shape young people's ability to pursue entrepreneurship as part of their life project. The project followed an exploratory, mixed-method approach combining a medium-scale survey (110), group interviews with young entrepreneurs (24), individual interviews with ecosystem actors (5), and a structured review of more than 80 existing mechanisms. A systematic mapping of the support landscape was conducted to assess accessibility, relevance, and alignment with the needs identified in the diagnostic phase. The results show that young people demonstrate strong motivation to undertake entrepreneurial initiatives but face structural barriers—income instability, housing constraints, and limited access to essential services—that hinder long-term sustainability. Although Gipuzkoa offers a wide range of mechanisms, many remain underused due to eligibility criteria, limited visibility, or misalignment with early-stage needs. The findings provide an initial evidence base for rethinking territorial strategies and highlight the need for broader data collection to inform future policy design.

Keywords: Youth entrepreneurship; Territorial development; Life-project conditions; Support mechanisms; Mixed-method analysis; Policy design; UN SDG 8.

1. Project Background and Objectives

Gipuzkoa is currently facing a structural challenge: despite maintaining one of the lowest overall unemployment rates in Spain, youth unemployment has stagnated, and many young people struggle to

build stable and autonomous life projects (1). At the same time, organizations report a shortage of qualified talent, creating a paradox in which opportunities exist but young people do not always find the conditions they need to develop their professional and personal trajectories (1).
Entrepreneurship could serve as a meaningful pathway for young people to shape their future (2,3). However, only a small proportion choose this option, and many initiatives are abandoned early due to income instability, limited long-term support, and the absence of mechanisms that accompany young people when entrepreneurial projects come to an end (2). Existing support structures tend to focus on the business project rather than on the broader life circumstances of the young person, leaving critical gaps in the transition between starting, sustaining, and potentially abandoning a venture (2).
The **Gipuzkoa Egan Bizzi** project was created to address this gap by rethinking the territorial conditions that influence young people's ability to build autonomous life projects through entrepreneurship. The project seeks to understand what young people need from a territory to consider it a viable place to develop their aspirations, and how Gipuzkoa can strengthen its attractiveness in this regard (1).
The project focused on two main objectives:

1. **To identify the current characteristics of Gipuzkoa as a territory for young people who wish to develop an autonomous life project through entrepreneurship.**
2. **To analyse the factors that enable or hinder this process from the perspective of both young people and key territorial actors.**

The project did not aim to design or test new mechanisms. However, the knowledge generated provides a foundation for future work, including the exploration of practices from other regions and the development of a renewed territorial value proposition that could enhance Gipuzkoa's attractiveness for young people.

2. Methodology and Work Performed

The project followed an exploratory, mixed-method approach structured around three complementary steps. First, a comprehensive diagnosis of the situation of young entrepreneurs (less than 35 years old) in Gipuzkoa was conducted through a medium-scale survey (110 responses), four group interviews with 24 young entrepreneurs, and five individual interviews with ecosystem actors. These instruments captured the economic, personal, and family conditions under which young people start, sustain, or abandon entrepreneurial initiatives.
Second, a territorial analysis was carried out to identify the factors that enable or hinder young people's ability to build an autonomous life project through entrepreneurship. This included a structured review of existing mechanisms in Gipuzkoa (over 80 identified) and an assessment of their accessibility and relevance for young people.
Third, a systematic mapping of the support landscape was performed by classifying mechanisms into functional categories and examining their alignment with the needs identified in the diagnostic phase. This step aimed to generate a structured overview of the available support, without evaluating effectiveness.
Together, these steps provided a robust evidence base for understanding the territorial conditions that shape young people's ability to pursue entrepreneurship as part of their life project.

3. Key Results

The project reveals a consistent pattern: young people in Gipuzkoa show strong motivation to undertake entrepreneurial initiatives, but face structural conditions that limit their ability to sustain them as part of an autonomous life project.

Young entrepreneurs operate in fragile economic conditions, often relying on personal or family savings and struggling to reach stable income levels. These pressures generate tension in personal and family environments. Despite this, most do not end the process with a sense of loss and remain willing to re-engage in entrepreneurship. The main reasons for abandoning projects are structural rather than motivational. Young people report difficulties in maintaining teams, limited access to mechanisms that support basic living conditions, and challenges in aligning entrepreneurial activity with their broader life project. The lack of support after project closure intensifies these difficulties.

The territorial analysis shows that, although a Gipuzkoan entrepreneur can access a wide range of mechanisms (1111), their accessibility and relevance for young people vary significantly. Many remain underused due to eligibility criteria, limited visibility, or misalignment with early-stage needs. Finally, the analysis of mechanisms—both in Gipuzkoa and in more favourable regions—shows that support systems tend to focus on the business project rather than on the broader circumstances of the young person. International evidence highlights those territories with stronger youth entrepreneurship integrate life-project dimensions such as housing, income stability, and essential services into their support systems. In Gipuzkoa, these areas remain less developed.

4. Discussion and Impact

The results show that Gipuzkoa combines strong youth motivation for entrepreneurship with structural conditions that limit its long-term sustainability as part of an autonomous life project. This aligns with international evidence indicating that young entrepreneurs require not only business-oriented support but also stable living conditions to sustain their initiatives.

The findings highlight those existing mechanisms in Gipuzkoa are extensive but unevenly accessible and often disconnected from the everyday needs of young people. This has societal implications: without support that addresses income stability, housing, and transitions after project closure, entrepreneurship becomes difficult to maintain, reducing the territory's capacity to retain and attract young talent. At the same time, the willingness of young people to re-engage in entrepreneurship represents a significant opportunity for the territory.

Given the exploratory nature of the study and the size of the sample, the results provide a valuable initial evidence base. However, expanding the scope of data collection would be necessary to strengthen the robustness of the findings and increase their potential impact, particularly if future work aims to inform territorial strategies or policy design.

5. Conclusions and Outlook

The project offers an initial, evidence-based understanding of the conditions under which young people in Gipuzkoa attempt to build an autonomous life project through entrepreneurship. The findings show that motivation is not the limiting factor; rather, structural conditions—income stability, housing, and access to essential services—shape the feasibility of sustaining entrepreneurial activity over time. The analysis also highlights those existing mechanisms, although numerous, are unevenly accessible and insufficiently connected to the life-project needs of young entrepreneurs.

These insights provide a foundation for rethinking how territorial support systems can better align with the lived realities of young people. Future work should expand the evidence base through larger-scale data collection and deeper comparative analysis. This would enable the development of more robust territorial strategies and support the design of policies aimed at strengthening Gipuzkoa's attractiveness and its capacity to support young people who wish to build their future through entrepreneurship.

Acknowledgements / Funding
The authors gratefully acknowledge the support and funding provided by the Gipuzkoa Provincial Council through the Etorkizuna Eraikiz initiative. We also thank the young entrepreneurs and territorial actors who generously contributed their time and insights to this study.

References

1. Escuchando lo hacemos mejor: participar en la construcción del modelo de protección a la infancia y la adolescencia en Guipuzkoa. Donostia: Guipuzkoako Foru Alundia = Diputación Foral de Gipuzkoa; 2022.
2. Supporting Youth in Entrepreneurship [OECD Local Economic and Employment Development (LEED) Working Papers] [Internet]. mayo de 2015 [citado 10 de marzo de 2026]. (OECD Local Economic and Employment Development (LEED) Working Papers). Report No. Disponible en: https://www.oecd.org/en/publications/supporting-youth-in-entrepreneurship_7082fbbd-en.html doi:10.1787/7082fbbd-en
3. Youth policies in Spain - 2019. 2019.

Fostering the Growth of Deep-Tech Enterprises Through Enterprise Europe Network

Enterprise Europe Network Republic of Srpska, No. 101205785, ONEX, 101205785, – SMP/SME Pillar, Period (2025 – 2028)

Milan Vukic[1], Vesna Gojković Cvjetković[1]

[1]*Faculty of Technology Zvornik, University of East Sarajevo, Zvornik, Bosnia and Herzegovina,*
milan.vukic@tfzv.ues.rs.ba, https://orcid.org/0000-0002-1699-2433,
vesna.gojkovic@tfzv.ues.rs.ba, https://orcid.org/0000-0003-1118-4565

Corresponding author: milan.vukic@tfzv.ues.rs.ba

Abstract

The Enterprise Europe Network (EEN) represents the world's largest business support network, connecting over 600 member organizations across more than 60 countries. As the European Union accelerates its push toward strategic technological sovereignty, deep-tech industries which are characterized by extensive reliance on scientific research, advanced engineering, and long-horizon investment cycles have emerged as a central pillar of the European innovation agenda. This paper showcases the structural role and practical importance of EEN in fostering the growth of deep-tech enterprises, with particular emphasis on its services relating to technology transfer, internationalization, access to funding, and matchmaking. The EEN provides critical intermediary services that reduce information asymmetries and transaction costs for deep-tech SMEs, facilitating access to markets, investors, and collaboration partners. However, structural gaps remain, particularly in regions with lower innovation capacity. EEN can bridge Europe's deep-tech gap, provided its mandate is strengthened and advisory services for science-intensive enterprises are expanded.

Keywords: Innovation ecosystem; SME internationalization; technology transfer; venture capital; European innovation policy; UN SDG 9 (Industry, Innovation and Infrastructure)

1. Project Background and Objectives

The Enterprise Europe Network (EEN) is the world's largest business support network, established by the European Commission in 2008 to help small and medium-sized enterprises grow internationally, innovate, and compete in the Single Market and beyond. Operating through more than 600 member organizations across over 60 countries, EEN aims to reduce barriers to internationalization, facilitate technology transfer, connect businesses with research partners, and improve access to EU funding and policy instruments. Its overarching

objective is to strengthen the innovation capacity and global competitiveness of European SMEs by providing expert advisory services, cross-border partnership facilitation, and integrated support throughout the enterprise growth cycle.

2. Methodology and Work Performed

The EEN operates through a distributed model in which member organizations act as local access points for a unified pan-European service infrastructure. Advisors embedded within these organizations work directly with SMEs through one-on-one consultations, diagnosing the firm's needs and mapping them onto the available service portfolio.

3. Key Results

3.1 The Deep-Tech Ecosystem and its Structural Requirements

The literature consistently identifies deep-tech enterprises as exhibiting a distinctive combination of needs that separates them from conventional high-growth startups. Deep-tech companies face both R&D risk and commercialization risk simultaneously, with development cycles that may span a decade or more before revenue generation [1]. Deep-tech startups require solid support from industry actors, regulatory adaptations, and governments for improved access to finance to reach global scale [2,3]. They identify access to partner networks — precisely the core function of EEN — as one of the most critical enabling conditions for deep-tech growth. review identifying.

3.2 EEN as an Institutional Network for SME Support

The institutional networks in supporting SME internationalization positively impact SME performance by continuously providing vital resources including business contacts, market information, and financial guidance Analysis of industrial business associations identifies four categories of institutional support promotional activities; counselling, training, and technical support; information sharing; and cooperation with other entities [4]. Deep-tech SMEs are frequently founded by scientists and engineers with limited commercial experience while institutional networks help firms overcome resource constraints and gain competitive advantages [5]. SMEs use support services varies according to their stage of internationalization and speed of market entry [6]. Their finding that network relationships and formal support services are rarely mutually exclusive

3.3 Innovation Collaboration and the Role of SME Networks

One of EEN's signature contributions to deep-tech development is the facilitation of open innovation through cross-border technology partnership agreements. SMES collaboration for innovation is a strategic factor for innovation system success at the national level, and that Europe risks falling behind in the global production of intangible goods without systemic policies to unlock SME collaborative potential [7]. The premise is that SMEs, particularly those in deep-tech, are individually unable to complete complex innovation processes autonomously. External collaboration, whether with universities, larger corporations, or other SMEs serve to provide access to complementary knowledge, shared risk, and market validation [7]. EEN's technology partnership facilitation service directly operationalizes this logic by connecting organizations with

complementary technological profiles across national borders. The SME innovation is positively associated with enterprise births, government procurement of advanced technology products, and intellectual assets [8].

3.4 Funding Access and Venture Capital Facilitation

Access to adequate and timely funding is one of the most consistently cited challenges for deep-tech enterprises. The literature identifies a 'heterogeneous capital gap' in deep-tech, characterized by the divergence between the Governmental venture capital investors fill gaps left by private investors and can specialize in sectors that align closely with deep-tech profiles [9]. Venture capital expenditure in Europe is positively associated with the Innovation Index and with the presence of foreign doctorate students, but that in many Southern and Eastern European countries the venture capital market remains significantly underdeveloped [10]. This geographic heterogeneity in capital availability represents a structural challenge that EEN is positioned to partially address through its investor matchmaking services and its capacity to direct deep-tech SMEs toward EU-level funding instruments such as the European Innovation Council (EIC).

3.5 Technology Transfer and Matchmaking Services

EEN operates one of the world's largest technology transfer and business matchmaking databases, hosting tens of thousands of technology offers, technology requests, and business cooperation profiles. The theoretical basis for the value of these services derives from transaction cost economics: by providing a structured platform for identifying and qualifying potential partners, EEN reduces the search and negotiation costs that would otherwise prevent many technology transfer agreements from materializing. The matchmaking function of EEN takes concrete form through brokerage events at which companies, research organizations, and investors present their profiles and arrange bilateral meetings. For deep-tech companies, whose addressable partner pool is typically global rather than domestic, EEN's international reach provides access to a partner network that would be prohibitively expensive to assemble independently. This function is particularly valuable for SMEs in smaller and peripheral European economies, where domestic deep-tech ecosystems are insufficiently dense to generate the collaboration opportunities necessary for scaling.

4. Discussion and Impact

The evidence reviewed above points to a coherent and mutually reinforcing role for EEN in the deep-tech sector. Four dimensions of impact merit particular emphasis: knowledge brokering, funding facilitation, regulatory navigation, and ecosystem density enhancement.

First, as a knowledge broker, EEN reduces the information asymmetries that systematically disadvantage science-based founders in commercial environments. EEN's function of providing business contacts, market intelligence, and procedural knowledge is among the most valued by SMEs [4, 5, 6]. For deep-tech founders transitioning from academic careers, the value of EEN advisors with both scientific and commercial literacy is particularly high. Second, EEN's funding facilitation role is becoming increasingly important as the EU's innovation funding architecture grows in complexity and requires specialist knowledge that EEN is well-positioned to provide. Third, EEN assists deep-tech companies in navigating the regulatory landscape, both domestic and European. For deep-tech companies, regulatory uncertainty can function as a *de facto* barrier to commercialization and EEN's regulatory advisory services help to lower this barrier. Fourth, EEN contributes

to the densification of regional innovation ecosystems. Employment in innovative enterprises is positively associated with broadband penetration, foreign-controlled enterprise value added, and the Innovation Index [11]. EEN member organizations, many of which include technology parks, incubators, and universities, are key nodes in these ecosystems. EEN contributes to making regional ecosystems more open and internationally connected.

5. Conclusions and Outlook

This paper has examined the role and importance of the Enterprise Europe Network in the development of the deep-tech industry. The analysis demonstrates that EEN occupies a strategically important intermediary position within the European innovation system, providing services (technology transfer, business matchmaking, funding advisory, and internationalization support) that directly address the structural needs of deep-tech enterprises. The European Union's ambition to lead the global deep-tech transition depends critically on the quality of its innovation support infrastructure. The Enterprise Europe Network, properly resourced and strategically directed, represents a significant asset in pursuing this ambition.

Funding

This work was supported by the Enterprise Europe Network Republic of Srpska, implemented under Grant Agreement No. 101205785, approved and co-funded by the European Commission.

References

1. Kılıç AS, Duran C. Derin Teknoloji Girişim Kategorileri Arasındaki Benzerlik ve Farklılıkların Analizi: Türkiye Örneği. Girişimcilik ve İnovasyon Yönetimi Dergisi. 2021;10(2). doi:10.15659/jeim.10.2.005
2. Schuh G, Latz T, Lorenz J. Governmental Support Options for the Technology Transfer of Deep Tech Innovations. Information Technology and Management Science. 2022;25:24-36. doi:10.7250/itms-2022-0004
3. Sreenivasan A, Suresh M. Can we unlock deep-tech in Indian startups for long-term success? Technological Sustainability. 2023;3(1):68-75. doi:10.1108/techs-01-2023-0001
4. Costa E, Soares AL, Pinho de Sousa J. Institutional networks for supporting the internationalisation of SMEs: the case of industrial business associations. Journal of Business and Industrial Marketing. 2017;32(8):1182-1202. doi:10.1108/jbim-03-2017-0067
5. Georgieva S, Vasilska M. Networking and Support: Determinants of the International Performance of Enterprises. European Journal of Marketing and Economics. 2019;2(3):48-57. doi:10.26417/ejme.v2i3.p48-57
6. Belhoste N, Bocquet R, Favre-Bonté V. How do SMEs use support services during their internationalisation process: A comparative study of French traditional SMEs and INVs in Asia. International Small Business Journal: Researching Entrepreneurship. 2019;37(8):804-830. doi:10.1177/0266242619871165
7. Leogrande A, Costantiello A, Laureti L. Innovative SMEs Collaborating with Others in Europe. SSRN Electronic Journal. 2022. doi:10.2139/ssrn.4103840
8. Costantiello A, Laureti L, Leogrande A. The SMEs Innovation in Europe. Research Square. 2021. doi:10.21203/rs.3.rs-1087106/v1

9. Bertoni F, Colombo MG, Quas A. The changing patterns of venture capital investments in Europe. Journal of Industrial and Business Economics. 2019;46(2):229-250. doi:10.1007/s40812-019-00113-1
10. Leogrande A, Costantiello A, Laureti L. The Impact of Venture Capital Expenditures on Innovation in Europe. SSRN Electronic Journal. 2021. doi:10.2139/ssrn.3930697
11. Laureti L, Costantiello A, Matarrese MM. The Employment in Innovative Enterprises in Europe. SSRN Electronic Journal. 2022. doi:10.2139/ssrn.4010098

Prototypes in the Innovation Development

Saša Vasiljević[1], Jelena Domanović[1], Jasna Glišović[2]

[1]*Department in Kragujevac, Academy of Professional Studies Šumadija, Kragujvac, Republic of Serbia, svasiljevic@asss.edu.rs, https://orcid.org/0000-0002-2235-1309, jelenadomanovic.i7@gmail.com*
[2]*Faculty of Engineering, University of Kragujevac, Kragujevac, Republic of Serbia, jaca@kg.ac.rs,, https://orcid.org/0000-0002-8251-1722*

Corresponding author: svasiljevic@asss.edu.rs

Abstract

Prototyping is an important step in the development of innovative solutions. Prototypes can often indicate the very quality and functionality of the product itself that is currently being developed. The development itself or the product development process is also accompanied by this process. Prototypes can often indicate the very problem that exists in the design itself, but they can also indicate the shortcomings related to the development of innovative solutions, but also the functions that the innovation itself has. In this paper, an overview of some of the most important processes during the creation of prototypes was made, as well as examples of prototypes in the development of vehicles. The work is based on achieving and advancing the Sustainable Development Goals, specifically Goal 9.

Keywords: Prototype; Innovation and Industry; Development, automotive.

1. Introduction

The importance of prototyping is particularly evident in the context of driving innovation in one of the most competitive industries in the world. In the automotive industry, where customer expectations are constantly changing, regulatory requirements are becoming more stringent, and technological progress is developing at an unprecedented speed, prototypes provide a necessary framework for experimentation, verification, and improvement. They allow engineers to test structural strength, optimize aerodynamics, integrate modern electronic systems, and evaluate user experience, transforming abstract ideas into tangible and tested results. The development of digital technologies such as virtual simulations, 3D printing and artificial intelligence has significantly improved the prototyping process. These innovations shorten development cycles, reduce costs and minimize risks, allowing manufacturers to respond more quickly to market demands. Prototyping is not only a technical necessity but also a strategic tool that allows automotive companies to combine creativity with reliability, and innovation with feasibility, in order to create vehicles that meet the highest standards of performance, sustainability and customer satisfaction.

The aim of this paper is to present the role and importance of prototyping in the vehicle development process, as well as to analyze different methods and technologies for prototyping, with an emphasis on their contribution to innovation, quality improvement and risk reduction before serial production. The subject of the paper covers

the process of creating and applying prototypes in the automotive industry, including physical and virtual prototypes, the materials and technologies used, as well as the way in which prototypes affect the vehicle development process, safety, functionality and user experience.

2. Phases of prototyping and the basics of prototyping

Bringing a prototype to life is a complex process that combines engineering, software development, and thorough testing. Whether it's a new car prototype, an advanced vehicle prototype, or a futuristic autonomous system, the journey from concept to reality involves several key steps. Every car prototype follows a structured development process to ensure it meets performance, safety, and usability standards [1]. There are a few key stages:

- Concept development and feasibility study, where before any prototype car begins, engineers define key requirements, including target market and use case, performance (speed, efficiency, emissions), powertrain type (ICE, hybrid, electric), software and hardware specifications [1]. Once the feasibility study confirms that the concept is feasible, the project moves into the design phase;
- Design and engineering, where this phase, for example in vehicle development, includes the design of a prototype car, including mechanical design (vehicle chassis, suspension and powertrain layout), electrical systems (installation, battery management and connectivity solutions), embedded software (ECU, safety functions and control algorithms);
- Prototyping Systems involves creating a functional prototype of a vehicle and requires the integration of mechanical, electronic and software components into a working model. During this phase, engineers assemble prototype automotive solutions into a functional unit for initial testing;
- Prototype testing and validation because no vehicle prototype is complete without thorough testing. Engineers evaluate performance, safety, and compliance through:
    - Performance Testing – Confirms speed, efficiency and power output;
    - Crash Testing – Ensures passenger safety;
    - Software Validation – Tests ECU and embedded software;
    - Environmental Testing – Checks durability in extreme conditions [1].

The best approach would, of course, be to prototype every new part, but this is not economically viable. Therefore, some innovative solutions or custom-made systems should be prototyped to ensure they do not fail [2]. As consumer demand changes, automakers respond by creating designs that are both functional and beautiful. Without the prototyping process, design and function would rarely have the qualities needed to convince consumers to buy new vehicles [3].

Prototyping in the automotive industry represent a key segment of vehicle development, as they enable conceptual solutions to be transformed into tangible models that serve to verify, improve and confirm the quality of the future product. This process is important not only from the point of view of technical feasibility, but also to ensure safety, efficiency and adaptation of the vehicle to user needs [4]. The following are the basic functions of prototyping in industry, which include different phases - from design verification and validation, through pre-production, testing and feedback collection, to the final verification of the production process [4]. Thus, these prototyping functions in different areas and phases of innovation development.

3. Technology and uses benefits from making portotypes

Just a decade ago, manufacturing was based solely on mass production with numerous efficient production lines, but with little flexibility. Today, we can find many flexible rapid manufacturing technologies for the production of individual parts and small series production [2]. Rototyping uses a variety of tools and techniques for manufacturing, such as CNC machining for high-precision components, 3D printing for rapid model creation, and vacuum casting for detailed replicas. This provides manufacturers with a comprehensive set of tools for design validation and iteration [5].

Today, various techniques are used in prototyping, most of which are related to the use of computer systems or computer-programmed machines. This section explains some of the techniques and systems used in prototyping. All of these techniques reduce prototyping time and costs. Rapid prototyping is increasingly used today. Rapid prototyping is the process of quickly creating a physical 3D model or prototype of a product based on a digital CAD (computer-aided design) model. Examples of some of the technologies used in prototyping are shown in Figure 1.

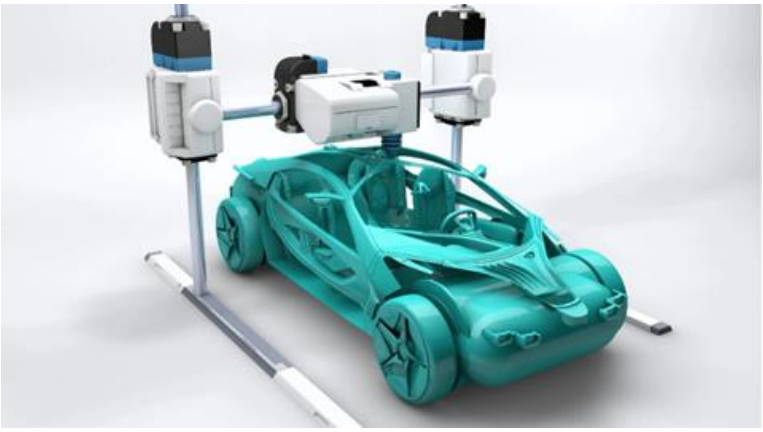


Figure 1. An example of technology for making prototypes, i.e. rapid prototyping technology [6].

The choice of materials for automotive prototyping is crucial because it directly affects the performance, durability, and aesthetics of the final product. Manufacturers must consider factors such as strength, weight, heat resistance, and cost when selecting a prototype material. The most commonly used materials in automotive prototyping are plastics, metals, and composites, each offering specific advantages and limitations [5]. It is most important that the materials support the functionality of the product while being easy to assemble, especially since production in the automotive industry is generally mass-produced, and production speed affects efficiency. In addition to cellular plastics and foams, adhesives and tapes can be used to make assembly as simple and convenient as possible [7].

Car manufacturers are faced with the dilemma of how to test their new prototypes in real conditions, on public roads, without revealing the actual appearance of the car to the market too early. As a solution, they use camouflage of the prototype. In this way, they draw attention to their still-secret prototype. The camouflage

must be very effective in confusing the eye, and even give the effect of the random application of poor camouflage materials [8].

5. Conclusions

Prototyping is one of the most important steps in the development of modern vehicles, as it enables the translation of conceptual solutions into tested and functional models. Analysis of historical examples has shown that prototypes have always been a driver of innovation, allowing manufacturers to test new concepts and technologies before serial production.

Prototypes play an important role in all phases of vehicle development – from design and material selection, through chassis and component manufacturing, to testing on public roads. The paper shows that different manufacturing techniques and materials contribute to process optimization, but that each technique has its own advantages and limitations.

Also, masking and prototype testing play an important role in protecting competitive ideas and verifying functionality in real-world conditions. All of the above confirms that prototyping is not only a technical necessity, but also a strategic development tool, which allows for increased quality, reduced risk, and improved innovation in the automotive industry.

References

1. From idea to prototype: Developing Automotive Systems from scratch. Promwad 2025. https://promwad.com/news/from-idea-to-prototype-developing-automotive-systems (accessed March 25, 2026).
2. Car prototyping guide: Benifits, cases, technologies. AutoProtoWay 2022. https://autoprotoway.com/a-complete-car-prototyping-guide/ (accessed March 25, 2026).
3. How, why and when Auto Manufacturers Use Prototype & Parts. AutoProtoWay 2022. https://autoprotoway.com/how-prototype-automotive-parts-drive-innovation/ (accessed March 27, 2026).
4. Your Automotive Prototyping Comprehensive Guide to turning ideas into reality: At-machining. AT 2024. https://at-machining.com/automotive-prototyping-guide/ (accessed March 27 , 2026).
5. 3D štampa U Industriji - Primenjena Rešenja. 3dprintechRs n.d. https://3dprintech.rs/category/3d-stampa-u-industriji (accessed April 1, 2026).
6. The importance of material selection in the vehicle industry . NMC Cellfoam 2025. https://www.cellfoam.eu/the-importance-of-material-selection-in-the-automotive-industry/ (accessed April 1, 2026).
7. Philkurth. Car camouflage: How carmakers hide prototypes explained. WhichCar 2016. https://www.whichcar.com.au/news/car-camouflage-how-carmakers-hide-prototypes-explained (accessed April 1, 2026).

A Scientific Coordinator Enabling Industry Access to Laboratory Services

SCILEND

Panagiotis Pantazis[1]

[1]SCILEND, Department of Materials Science and Engineering, University of Ioannina, Greece (panos4884@gmail.com)

Contact email: info@scilend.com | Website: https://scilend.com/

Executive Summary

SCILEND is a digital platform that connects companies, startups, and research teams with specialized laboratories providing scientific testing, analysis, and R&D services. The platform addresses a structural gap in the research and innovation ecosystem: access to laboratory infrastructure is often fragmented, time-consuming, and dependent on informal networks. At the same time, many university and research laboratories possess advanced equipment that remains underutilized. SCILEND aims to bridge this gap by creating a structured and transparent interface between industry and research infrastructure.

The platform operates as a scientific coordinator that supports the entire process from request definition and laboratory matching to communication, project coordination, and delivery of results. By combining a digital marketplace model with scientific expertise, SCILEND simplifies the discovery and use of laboratory services while reducing the time and administrative complexity associated with external R&D collaborations.

SCILEND's innovation lies in structuring a traditionally fragmented market and transforming access to laboratory capabilities into an organized and scalable service. Through standardized requests, transparent pricing structures, and coordinated project management, the platform enables companies, especially startups and small and medium-sized enterprises (SMEs), to efficiently access scientific infrastructure without the need for significant capital investment in equipment.

The strategic vision of SCILEND is to become a leading access hub for laboratory services and research infrastructure in Greece and, subsequently, across Europe. By facilitating collaboration between industry and research institutions, the platform contributes to more efficient utilization of scientific equipment, accelerates innovation cycles, and supports the development of a more connected and productive R&D ecosystem.

Keywords: Laboratory services marketplace; Research infrastructure access; R&D collaboration; Digital platform for science; Innovation ecosystem; SME innovation support; Scientific equipment utilization; Technology transfer; UN SDG 9; UN SDG 12

1. Company Overview

SCILEND is an innovation-driven startup focused on improving the interaction between industry and scientific research infrastructure. The company's mission is to facilitate efficient and trustworthy collaboration between businesses and laboratories by providing structured access to scientific testing, analytical services, and research and development (R&D) capabilities.

Operating within the deep-tech and innovation ecosystem, SCILEND addresses a critical challenge faced by many companies: identifying reliable laboratories, navigating administrative procedures, and ensuring the secure exchange of sensitive technical information. For many organizations—especially startups and small and medium-sized enterprises (SMEs)—these barriers often slow down or prevent the execution of external R&D projects.

A central element of SCILEND's approach is the establishment of a trusted collaboration environment. The platform incorporates clear legal and operational frameworks designed to protect both companies and laboratory partners. By facilitating structured communication and implementing standardized collaboration terms, SCILEND helps ensure confidentiality, transparency, and professional project coordination throughout the process.

The company combines technical understanding of scientific services with digital coordination tools to streamline the interaction between industrial innovation needs and laboratory capabilities. Through this role, SCILEND contributes to strengthening the broader innovation ecosystem by enabling more efficient collaboration between companies, universities, research centers, and private laboratories.

By positioning itself as a coordination and access layer within the research infrastructure landscape, SCILEND aims to support the translation of scientific capabilities into practical industrial applications and accelerate the development of innovation-driven projects.

2. Technology / Product / Service Description

SCILEND provides a digital platform and coordination service designed to connect companies with specialized laboratories offering scientific testing, analytical services, and research and development (R&D) capabilities. The platform structures the process through which companies can define technical requests and identify suitable laboratory partners capable of delivering the required analysis or experimental work.

The system relies on a structured matching approach that links technical project requirements with laboratory capabilities, including available equipment, testing methods, and domain expertise. Laboratory services are organized into standardized categories and searchable technical attributes, enabling efficient identification of appropriate research infrastructure.

In addition to the digital interface, SCILEND provides coordination and operational support throughout the collaboration process, including communication management, project monitoring, and structured delivery of results. A key component of the platform is the implementation of standardized legal and collaboration frameworks that help ensure confidentiality and protect both companies and laboratory partners when sensitive technical information or proprietary materials are involved.

By combining digital infrastructure, scientific coordination, and legal safeguards, SCILEND enables more reliable and efficient external R&D collaborations between industry and research laboratories.

3. Innovation and Competitive Advantage

SCILEND's innovation lies in structuring a fragmented market for laboratory services through a coordinated digital interface that integrates technical matching, project coordination, and collaboration governance. While several international initiatives address parts of this ecosystem, most solutions focus either on laboratory networks or on equipment access rather than on the full coordination of R&D service projects.

For example, platforms such as Measurlabs operate primarily as intermediaries that route analytical requests to a predefined network of laboratories, while LabforRent focuses mainly on providing access to laboratory space and equipment. In contrast, SCILEND positions itself as a coordination layer between companies and research infrastructure, supporting the entire collaboration lifecycle—from request structuring and laboratory matching to communication, project coordination, and result delivery.

An additional differentiator is the implementation of standardized legal and operational frameworks that address confidentiality concerns, a common barrier in industry–laboratory collaborations involving sensitive technical information.

By combining structured service discovery, scientific coordination, and collaboration safeguards, SCILEND introduces a scalable model for enabling more efficient interaction between industry and research laboratories.

4. Market Application and Impact

SCILEND serves companies that require access to specialized laboratory services for testing, product validation, and research and development (R&D). The platform primarily targets startups and small and medium-sized enterprises (SMEs) that either lack in-house laboratory infrastructure or require additional specialized scientific analysis during product development. By simplifying the process of identifying and accessing suitable laboratories, SCILEND enables companies to obtain critical technical services more efficiently.

At the same time, the platform creates new opportunities for laboratories by increasing the visibility and utilization of their services and equipment. Many research facilities possess advanced scientific instruments that remain partially underused due to limited industry access. By connecting laboratories with industrial demand, SCILEND helps generate additional revenue streams while ensuring that valuable research infrastructure and equipment are actively utilized instead of remaining idle.

The solution is applicable across multiple industrial sectors and is designed to scale across national and European innovation ecosystems, supporting faster innovation cycles and more efficient use of scientific infrastructure.

5. Partnerships and Outlook

SCILEND aims to build strong collaborations with universities, research institutions, and private laboratories in order to expand access to scientific infrastructure and laboratory services. By integrating diverse research facilities into its network, the platform seeks to strengthen the connection between industry and the scientific community and enable more efficient R&D collaborations.

Future development focuses on expanding the laboratory network, enhancing the digital platform's matching capabilities, and supporting cross-border collaborations within the European research and innovation ecosystem. The long-term vision includes the integration of advanced digital tools to further improve the identification of suitable laboratory partners and streamline the coordination of complex R&D projects.

Through strategic partnerships with research organizations, innovation hubs, and industry stakeholders, SCILEND aims to become a key access point for laboratory services and research infrastructure across Europe.

6. Business Model

SCILEND applies a dual revenue model consisting of a Project Setup Fee and a Matching Fee, designed to reflect the value created through project coordination and successful laboratory collaboration.

The Project Setup Fee is a fixed charge applied at the initiation of each project and covers the structuring of the technical request, identification of appropriate laboratories, coordination of communication, and preparation of the collaboration framework.

The Matching Fee is a percentage-based fee applied to the value of the laboratory service and reflects the value generated through laboratory matching, project coordination, and the successful execution of the collaboration. A tiered pricing approach ensures fair costs for companies while maintaining sustainable margins for the platform as project value increases.

7. Partnership & Collaboration Opportunities

SCILEND actively seeks partnerships with universities, research institutions, private laboratories, and innovation ecosystems to expand access to scientific infrastructure and laboratory services. By integrating diverse research facilities into its network, the platform aims to strengthen the connection between industry and the scientific community and facilitate more efficient R&D collaborations.

The company is particularly interested in collaborations with research organizations that wish to increase the visibility and utilization of their laboratory services, as well as with innovation hubs and technology transfer offices seeking to support industry engagement.

Through these partnerships, SCILEND aims to co-develop new collaboration models that accelerate the translation of scientific capabilities into industrial applications and innovation-driven projects.

8. Performance Validation / Case Studies

SCILEND's coordination model has been validated through early pilot collaborations between companies and research laboratories. These projects have focused on facilitating access to specialized laboratory analyses and technical testing services required during product development and material evaluation processes. The initial pilot cases demonstrated the ability of the platform to efficiently identify suitable laboratories, coordinate communication between stakeholders, and streamline the execution of laboratory service projects. In addition, SCILEND has received recognition within the innovation ecosystem through participation in entrepreneurship and innovation programs, including awards in startup competitions and accelerator initiatives. These milestones provide early validation of the platform's potential to address a significant gap in the laboratory services and R&D collaboration market.

Innovation Ecosystems, Technology Transfer, and Competitiveness

Understanding Governance and Capabilities in Technology Transfer Offices: Patterns of Efficiency

Konstantina Christogeorgou[1], Maite Couto-Ortega[2], Nikolaos Alexandros Theodorou[1], Maider Beitialarrangotia[2], Maria Vivar-Simon[2], Giovanna Campopiano[3], Nikolaos Mylonidis[1], Yorgos Goletsis[1]

[1]*Laboratory of Business Economics and Decisions (LABED@UoI), Department of Economics, University of Ioannina, Ioannina, Greece, k.christogeorgou@uoi.gr, https://orcid.org/0009-0003-6527-7537, goletsis@uoi.gr, https://orcid.org/0000-0002-6227-0810, nmylonid@uoi.gr, https://orcid.org/0000-0001-7185-3703, theodorou.n.a@gmail.com, https://orcid.org/0000-0002-4327-8315*

[2]*Department of Mechanical Engineering and Industrial Production; Innovation - Management - Organization. Mondragon Unibertsitatea. Basque Country, Spain, mcouto@mondragon.edu, https://orcid.org/0000-0003-1014-1192, mbeitialarrangoiti@mondragon.edu, https://orcid.org/0009-0001-0182-5501, mvivar@mondragon.edu, https://orcid.org/0000-0003-4412-418X*

[3]*Department of Management, Information and Production Engineering, University of Bergamo, Bergamo, Italy, giovanna.campopiano@unibg.it, https://orcid.org/0000-0002-5122-1095*

Corresponding author: k.christogeorgou@uoi.gr

Abstract

Academic entrepreneurship research has primarily focused on individual actors and commercialization outputs, while entrepreneurial ecosystem studies emphasize contextual conditions. However, the organizational mechanisms linking these levels remain underexplored. This study examines Technology Transfer Offices (TTOs) as meso-level intermediaries that translate university resources into knowledge transfer processes and entrepreneurial outcomes. We investigate how governance structures and organizational capabilities jointly shape TTO effectiveness. Methodologically, we employ an exploratory cross-national design based on a structured expert survey of nine European TTOs, combining thematic analysis of open-ended responses with Likert-scale assessments. The analysis identifies systematic patterns in governance and capabilities. Centralized governance and strong strategic mandates enhance coordination and alignment, yet introduce delays under complex, multi-actor arrangements. Organizational capabilities are frequently underdeveloped, with resource constraints, low process maturity, and administrative burdens limiting execution. Additionally, a misalignment emerges between the high perceived impact and low implementation of key mechanisms, such as proof-of-concept funding and incentive systems. Overall, the findings highlight TTOs as critical organizational arrangements that condition knowledge transfer outcomes, emphasizing the importance of governance design and capability development in improving performance.

Keywords: technology transfer office; academic entrepreneurship; entrepreneurial ecosystem; governance; organizational capabilities; efficiency; UN SDG 9; UN SDG 4; UN SDG 8

1. Introduction

Academic entrepreneurship literature examines university-based commercialization processes, focusing primarily on individual actors and outputs such as patents and spin-offs. Such outputs contribute to regional innovation performance by transforming academic research into entrepreneurial initiatives, and strengthening knowledge spillovers and economic development, especially in the local regions where the university is located [1]. Similarly, entrepreneurial ecosystem (EE) research pinpoints that regional structures, institutions, and resource endowments shape entrepreneurial outcomes [2] by also accounting for the contextual conditions. However, the organizational mechanisms linking ecosystem conditions to commercialization outcomes remain underexplored.

As such, this study focuses on Technology Transfer Offices (TTOs) as meso-level intermediaries of EEs which translate university-level resources into structured knowledge transfer processes and actual entrepreneurial outputs. While TTOs are widely acknowledged as facilitators, their internal heterogeneity in terms of governance and capabilities, and their concomitant implications for academic EE functioning, has received limited attention.

Thus, we aim to uncover i. how TTO governance structures shape decision-making and coordination, ii. how organizational capabilities enable or constrain execution, and iii. how these jointly influence knowledge transfer processes and academic entrepreneurial performance within different ecosystem contexts.

2. Materials and Methods

We employ an exploratory cross-national research design based on a structured expert survey administered to nine TTOs across Europe, representing various ownership and governance structures of the university including public, private, and hybrid organizational forms and being either internal units of the university or external ones. We combine more structured responses using the Likert-scale measures (to assess the use and impact of mechanisms followed and the capability assessment) accompanied with rather qualitative responses (open-ended questions on governance, internal processes, challenges, strengths and weaknesses of each TTO), and data regarding TTO's organizational characteristics (including staffing topics, maturity level, outputs contribution).

Our initial analysis follows a thematic aggregation approach consistent with [3] (First-order coding, Second-order analysis, aggregate dimension), as we identify dimensions across governance structures, organizational capabilities, enabling and constraining factors, strategic challenges and opportunities. In doing so, we uncover governance structures and capabilities that consist TTOs more efficient and depict specific mechanisms that trigger specific inefficiencies. In addition, the Likert-scale responses were used descriptively to compare the reported use and perceived impact of specific mechanisms, informing the impact–use comparison presented in the results.

3. Results

3.1 Governance configurations: enabling vs constraining mechanisms

The analysis reveals consistent patterns in governance configurations and mechanisms across the various TTOs' cases. We identify both enabling and constraining mechanisms used in governance that affect TTO's performance. Based on our study, the enabling conditions include strong strategic mandates and active leadership support and centralized decision authority. Cross-functional integration between research, entrepreneurship, and external engagement activities, along with stakeholder inclusion and embeddedness within the broader EE structures facilitate interaction with industry and external partners. Considering stability and direction for commercialization activities, clear intellectual property frameworks and incentive systems are needed. At the same time, multi-actor governance structures, particularly in cases of co-owned intellectual property, introduce coordination complexity and lead to delays in negotiation processes. Limited organizational autonomy generates approval bottlenecks, while misalignment between academic and business timelines further reduces responsiveness. Overall, these findings highlight a recurring tension between coordination and agility, where governance arrangements that ensure alignment may simultaneously slow execution.

3.2 Organizational capabilities: uneven and often underdeveloped

Organizational capabilities are predominantly reported as constrained or underdeveloped across the various cases examined. Resource limitations, including insufficient staffing and thus increasing workload pressures, restrict the capacity of TTOs to respond effectively to demand. Low levels of process maturity and weakly developed knowledge management systems limit standardization, documentation, and the ability to scale activities. Administrative and regulatory requirements impose additional (compliance) burdens, consuming time and reducing focus on core knowledge transfer functions. Challenges related to talent retention are reported and further weaken the capability stability, while limited internal awareness and engagement with knowledge transfer activities reduce the participation across the university. Although more advanced capabilities, such as market intelligence, impact measurement, and the use of digital and AI tools, are recognized as relevant and useful, they remain only partially developed and are not yet systematically embedded in organizational practices.

3.3 Misalignment between impact and implementation (impact-use comparison)

Our findings also detect a clear misalignment between the level of use and the perceived impact of different mechanisms. There are several mechanisms that are consistently identified as having high impact but remain underutilized in practice, including the funding of proof-of-concept (PoC) initiatives, the integration of knowledge transfer into promotion and evaluation systems, the reduction of the administrative burden and the provision of direct financial incentives. In contrast, widely used mechanisms such as networking activities and stakeholder engagement initiatives display a moderate and differentiating impact. This impact-use pattern suggests that resource-intensive and structurally embedded mechanisms are less frequently adopted, despite being considered more effective, suggesting uneven implementation and potential institutional constraints pointing to inefficiencies in current policy and organizational focus.

3.4 Emerging structural tensions

Across the retrieved cases, a set of recurring structural tensions emerges. A persistent trade-off is observed between agility and compliance, as increasing administrative and regulatory requirements constrain operational flexibility. Similarly, while clear governance frameworks provide stability, clarity and fragmentation, particularly in intellectual property arrangements, they also introduce coordination challenges. Efforts towards professionalization are often constrained by limited TTO's resources and capacity, while attempts to strengthen impact measurement are closely linked to challenges in securing the necessary funding and demonstrating value. These tensions appear consistently across different organizational and national contexts, indicating common structural pressures shaping TTO operations.

4. Discussion

The findings suggest that TTOs do not merely facilitate knowledge transfer but condition how institutional and contextual factors are translated into outcomes. First, governance emerges as a coordination–latency trade-off as centralized structures and strong strategic mandates enhance alignment and reduce ambiguity, but they may also introduce coordination and decision delays under complex, multi-actor arrangements, particularly in cases of co-owned intellectual property [4], [5]. Second, organizational capabilities act as binding execution constraints. Even where governance provides clarity, limited resources, low process maturity, and weak knowledge management systems constrain execution, the ability of TTOs to operationalize knowledge transfer activities, thus, reinforcing the importance of organizational capacity in shaping performance heterogeneity (especially in early-stage or resource-constrained TTOs), aligning with the dynamic capabilities' perspective [6]. Third, the impact–use comparison complements the qualitative evidence by depicting a persistent misalignment in incentive structures, as mechanisms perceived as highly impactful, such as proof-of-concept funding and integration of knowledge transfer into academic evaluation, remain underutilized, reflecting broader institutional rigidities and resource constraints within university systems leading to TTO inefficiencies. In particular, such case is evident in academic evaluation systems and funding structures that continue to prioritize traditional research outputs over commercialization activities [7], [8]. Overall, these findings highlight the role of TTOs as meso-level organizational arrangements shaping variation in knowledge transfer outcomes across otherwise comparable contexts, extending the literature on innovation intermediaries and entrepreneurial ecosystems [9], [10].

5. Conclusions

Concluding, this study provides exploratory evidence on how TTO governance and organisational capabilities shape knowledge transfer processes within EEs. In particular, we show that ecosystem conditions alone are insufficient to explain outcomes as TTO configurations mediate and condition these effects. Several structural constraints, particularly governance fragmentation and resource limitations, persist across contexts. This paper contributes by foregrounding TTOs as organisational intermediaries with heterogeneous configurations, offering a basis for future research on typologies and configurational effects. Thus, future work should develop formal TTO typologies, examine configurational relationships with EE outcomes, and integrate longitudinal or larger-scale data for causal inference.

Acknowledgements

This research was supported by the EIT's Higher Education Initiative A-SIDE project (Alliance for Sustainable Product Innovation in a Data Driven Economy), coordinated by EIT RawMaterials, funded by the European Union.

References

1. Audretsch, D. B., Link, A. N., & Peña-Legazkue, I. (2013). Academic entrepreneurship and regional economic development: Introduction to the special issue. *Economic Development Quarterly*, 27(1), 3-5.
2. Stam, E., & Van de Ven, A. (2021). Entrepreneurial ecosystem elements. *Small business economics*, *56*(2), 809-832.
3. Gioia, D. A., Corley, K. G., & Hamilton, A. L. (2013). Seeking Qualitative Rigor in Inductive Research. *Organizational Research Methods*, 16(1), 15–31. https://doi.org/10.1177/1094428112452151.
4. Siegel, D. S., Waldman, D., & Link, A. (2003). Assessing the impact of organizational practices on the relative productivity of university technology transfer offices: an exploratory study. *Research policy*, *32*(1), 27-48.
5. Wright, M., Birley, S., & Mosey, S. (2004). Entrepreneurship and university technology transfer. *The journal of technology transfer*, *29*(3), 235-246.
6. Teece, D. J. (2007). Explicating dynamic capabilities: the nature and microfoundations of (sustainable) enterprise performance. *Strategic management journal*, *28*(13), 1319-1350.
7. Shane, S. (2004). Academic entrepreneurship: University spinoffs and wealth creation. In *Academic entrepreneurship*. Edward Elgar Publishing.
8. Etzkowitz, H., & Leydesdorff, L. (2000). The dynamics of innovation: from National Systems and "Mode 2" to a Triple Helix of university–industry–government relations. *Research policy*, *29*(2), 109-123.
9. Howells, J. (2006). Intermediation and the role of intermediaries in innovation. *Research policy*, *35*(5), 715-728.
10. Stam, E. (2015). Entrepreneurial ecosystems and regional policy: a sympathetic critique. *European planning studies*, *23*(9), 1759-1769.

Competitiveness, internationalization, and innovation in the creative and cultural industries, COMP-ICC project's presentation

Code: 2025-LAB2-021-01, Provincial Council of Gipuzkoa Granting of subsidies from the program lines of the Etorkizuna Eraikiz Gipuzkoa Taldean projects, Period (2025 – 2026)

Maite Couto-Ortega[1], Maria Vivar-Simón[1]

[1] Department of Mechanical Engineering and Industrial Production, Mondragon Unibertsitatea, Basque Country, Spain. mcouto@mondragon.edu, 0000-0003-1014-1192 // mvivar@mondragon.edu, 0000-0003-4412-418X

Corresponding author: mcouto@mondragon.edu

Abstract

The Creative and Cultural Industries (CCIs) are a burgeoning pillar of the Basque economy, representing one of their key areas in the regional Research and Innovation Smart Specialisation Strategy. However, the sector faces significant structural vulnerabilities, characterized by extreme fragmentation, dominated by micro-enterprises, and a stagnation in R&D investment compared to other strategic industries. This paper presents the COMP-ICC project, an initiative funded by the Provincial Council of Gipuzkoa under the Etorkizuna Eraikiz framework, which aims to bolster the competitiveness, innovation, and internationalization of CCIs in the Gipuzkoa territory.

The research employs a multi-stage methodology. First, a territorial mapping and diagnosis is conducted through a mixed-methods approach, combining quantitative surveys to companies with qualitative interviews involving key sector support agents. Second, an international benchmarking analysis is performed, examining successful governance and business models within 13 regions of the Districts of Creativity (DC) Network and similar regions: Lombardy (Italy) and North Holland (Netherlands).

By aligning CCI growth with the UN Sustainable Development Goals, this project provides a blueprint for professionalizing the creative fabric and ensuring its role as a driver of sustainable regional transformation.

Keywords: (CCIs); Regional Competitiveness; International Benchmarking; Innovation Policy; Gipuzkoa; DC Network; UN SDG 8; UN SDG 9; UN SDG 11.

1. Project Background and Objectives

The Creative and Cultural Industries (CCIs) represent a growing pillar of the Basque economy [1]. As of 2019, the sector comprised 15.437 companies, accounting for 9,80% of the business fabric and 5.29% of total employment in the Basque Autonomous Community [2]. Despite this significance, the sector faces structural challenges, primarily a highly fragmented landscape [3] dominated by micro-enterprises. These organizations average 2.99 employees, significantly lower than the general economy's average of 5.79, which complicates their competitiveness and internationalization efforts [2].

Furthermore, investment in R&D within the CCIs has stagnated. Data from the Research and Innovation Smart Specialisation Strategy framework (2014–2019) shows a decline of –0.5% in R&D intensity, while other strategic sectors like Advanced Manufacturing or Health-Biosciences achieved double-digit growth [1]. This suggests that CCIs have been historically marginalized in traditional competitiveness frameworks. However, the current shift toward inclusive and sustainable progress—aligned with the 2030 Agenda [4]—requires new analytical models that visualize the CCIs as drivers of social cohesion, cultural identity, and creativity. Consequently, public policies must evolve to provide CCIs with resources and innovation opportunities comparable to other strategic industries.

Funding Framework. This project is funded by the Provincial Council of Gipuzkoa through the Etorkizuna Eraikiz Gipuzkoa Taldean subsidy program. Etorkizuna Eraikiz is a collaborative initiative designed to address contemporary challenges through active listening and experimentation, enabling diverse organizations to contribute to sustainable public policy and regional improvement.

Objectives. The primary goal of this project is to bolster the competitiveness, internationalization, and innovation of CCIs in Gipuzkoa, specifically addressing territorial cohesion, equality, and organizational transformation. The specific objectives are:

- To identify the current socio-economic reality of the Gipuzkoa territory to strengthen the CCI sector.
- To identify international success stories that serve as benchmarks for the region.
- To design and validate tools tailored to support the specific needs of CCIs.

2. Methodology and Work Performed

The research methodology is designed as a two-stage process, transitioning from baseline diagnostics to international benchmarking.

Phase 1: Territorial Mapping and Sectoral Diagnosis. The initial phase focuses on establishing a comprehensive understanding of the CCI ecosystem in Gipuzkoa, identifying its unique characteristics, strengths, and systemic challenges. To achieve this, a mixed-methods approach is employed:

- Instrument Design [5,6]: Quantitative and qualitative tools are developed to assess sub-sectoral needs, innovation capacity, and prevailing business models. These instruments specifically investigate internal barriers to innovation, competitive enablers, digital maturity levels, and the integration of social sustainability goals—such as gender equality and territorial balance.
- Data Collection [7]: Information is gathered through surveys and semi-structured interviews with industry representatives, and professional associations and key institutional stakeholders respectively.
- Synthesis: Data is processed to generate a diagnostic report [8] that provides the foundational evidence required for subsequent strategic interventions.

Phase 2: International Benchmarking and Best Practices. The second phase adopts a comparative perspective to identify inspirational models from other territories and countries.

- Identification of Global Cases: Relevant international programs, creative hubs, and digital tools are identified for their proven success in CCI internationalization and support.

- Deep-Dive Analysis: Selected cases undergo a rigorous evaluation of their governance structures, financing models, and public-private partnership frameworks. The analysis focuses on extracting measurable results and learning from both successful outcomes and previous failures to minimize local implementation risks.
- Transferability Assessment: Each practice is evaluated against the local cultural, legal, and economic context of Gipuzkoa to determine its feasibility and necessary adaptations.

3. Key Results

As the project is currently in its implementation phase, the results presented herein outline the expected technical and strategic outcomes derived from the ongoing work packages.

- Comprehensive Sectoral Diagnosis: The mapping process will yield a detailed characterization of Gipuzkoa's CCIs. This includes a synthesis of quantitative data gathered though a questionnaire to the ICCs and, a qualitative analysis of interviews conducted with sector support agents. This dual approach identifies specific digital, financial, and talent management gaps.
- International Benchmarking of Best Practices: A robust analysis of successful initiatives is being conducted across 13 regions belonging to the Districts of Creativity (DC) Network, and to Lombardy (Italy) and North Holland (Netherlands).
- Strategic Roadmap for Gipuzkoa: The project will produce a structured roadmap to adapt the identified international success stories to the local reality of Gipuzkoa. This includes assessing the transferability of business models and governance structures to the provincial legal and cultural context.

4. Discussion and Impact

The anticipated results aim to address the historical stagnation in R&D investment within the CCI sector. By shifting the analytical focus from purely economic indicators to a model of inclusive and sustainable well-being, this project contributes to the state-of-the-art in regional innovation policy.

- Scientific and Industrial Impact: The project introduces new methodologies for evaluating "hidden" innovation in micro-enterprises. By identifying enablers for competitiveness, it provides a blueprint for increasing the professionalization and international footprint of the local creative fabric.
- Industrial Impact: By identifying international best practices and adapting them to the local context, the project provides a blueprint for increasing the professionalization and international footprint of the cultural sector.
- Societal Impact: Aligning CCI growth with the UN Sustainable Development Goals and the Etorkizuna Eraikiz framework ensures that sectoral development fosters social cohesion, gender equality, and territorial balance across Gipuzkoa.

5. Conclusions

The COMP-ICC project reinforces the strategic importance of Creative and Cultural Industries as a driver for the socio-economic transformation of Gipuzkoa. Preliminary work confirms that while the sector is highly fragmented, it possesses significant potential for social and cultural dynamization that has yet to be fully harnessed by traditional innovation frameworks.

Acknowledgements / Funding

This research is supported by the Provincial Council of Gipuzkoa through the granting of subsidies under the Etorkizuna Eraikiz Gipuzkoa Taldean program lines.

The authors would like to express their gratitude to the various CCI sector stakeholders and support agencies whose participation in interviews and data collection was fundamental to the project's diagnostic phase.

Special thanks are also extended to the University of Bergamo for their hospitality and collaboration during the international exploration and analysis of best practices.

References

[1] Gobierno Vasco. Plan de Ciencia, Tecnología e Innovación Euskadi 2030 - PCTI Euskadi 2030. 2021.

[2] Departamento de Cultura y Política Lingüística. Las ICC en euskadi 2019. https://www.euskadi.eus/las-icc-en-euskadi/web01-a2kulind/es/ (accessed March 17, 2026).

[3] Observatorio Vasco de la Cultura. Delimitación y definición de los sectores Delimitación conceptual de las ICC en EUSKADI. 2018.

[4] Naciones Unidas. Objetivos y metas de desarrollo sostenible n.d. https://www.un.org/sustainabledevelopment/es/objetivos-de-desarrollo-sostenible/ (accessed May 16, 2023).

[5] Yin RK. Case study research and applications Libro design and methods 2018.

[6] Kumar R. Research methodology: a step-by-step guide for beginners. London SAGE. 2019.

[7] Kothari CR. Research Methodology. 2nd ed. New Age International Publishers; 2004.

[8] Gioia DA, Corley KG, Hamilton AL. Seeking Qualitative Rigor in Inductive Research. Organ Res Methods 2013;16:15–31. https://doi.org/10.1177/1094428112452151.

Green Innovation and Innovation Ecosystem Participation on Family and Non-family SMEs Performance

Samuel Ashong[1], Giovanna Campopiano[1], Mara Brumana[1]

[1] Department of Management, Information and Production Engineering & Center for Young and Family Enterprise, University of Bergamo, Bergamo, Italy, samuel.ashong@unibg.it, giovanna.campopiano@unibg.it, mara.brumana@unibg.it,
Corresponding author: *samuel.ashong@unibg.it*

Abstract

We study the effect of green innovation (GI) and innovation ecosystem (IE) participation on the relationship between family SME status and financial performance. Using a sample of 2,859 SMEs, we find that green innovation has a negative and partial mediation effect on family SME status and profitability relationship. We also find a positive moderating effect of IE participation on the relationship between GI and profitability

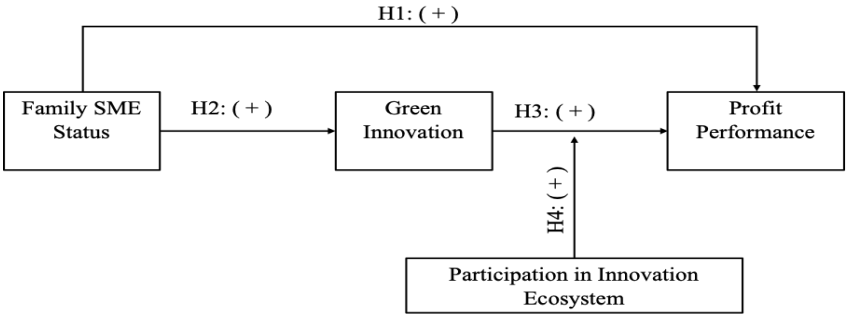
Keywords: green innovation (GI); innovation ecosystem; family SMEs; profitability, 'UN SDG 13'.

1. Introduction

Research on firm performance often compares different types of firms, such as family vs. non-family firms, to understand how their different governance structures affect outcomes, like profitability [17]. The literature indicates that the performance differences existing among these heterogeneous firms is largely due to how they manage and orchestrate their resources [15]. Within this framework, collaboration networks and innovations are increasingly seen as important resource pools that drive performance [10], [12]. Two specific and important resource pools that stands out as having significant influence on how well a firm performs are green innovations (innovations that contribute to SDGs 13 and 15), and the firm's collaborative network such as the innovation ecosystem (IE). In family business research, GI has recently become an important topic, however, evidence is mixed on whether family firms engage more or less than non-family firms [1], [7]. Also, empirical evidence of GI's effects on profitabilty is lacking, particularly in small and medium enterprises (SMEs) [4], [14]. Although GI can affect family SMEs financial performance independently, the literature also highlights the importance of collaborative networks, a means through which both family and non-family SMEs can realize their innovative potential and financial implications [19]. These collaborative networks include, strategic alliances, joint ventures or IEs. An IE is a specific type of interorganizational collaborative network that influences firm innovation and profitability. It does so by allowing access to complementary resources, knowledge, and capabilities beyond firm boundaries, potentially reducing losses associated with individual firm characteristics [11]. However, its role in both family and non-family SMEs is understudied. To address these gaps in the literature, we study how green innovation (GI) and innovation ecosystem participation affect the link between family SMEs and financial profitability. Our study is based on the research question, *how is the relationship between family SME status and financial performance shaped by green innovation and participation in*

innovation ecosystems? To answer this question, we develop four hypotheses (Figure 1) based on resource orchestration theory, which suggests that performance differences between family and non-family SMEs arise from how family firms uniquely orchestrate their resources compared to non-family firms. First, SMEs face resource constraints, so using available resources effectively can create a competitive advantage, such as higher profitability or growth [2]. Family involvement supports more stable and deliberate resource structuring, coordination, and leveraging [9]. In our theoretical model, GI is considered as a meditor on the family SME status and profitability relationship, and innovation ecosystem participation serves as a moderator on GI and profit (Figure 1).

Figure 1. Theoretical model.



2. Materials and Methods

We adopt a quantitative research approach to investigate our theoretical model. We use a sample of 2,859 innovative SMEs in Italy as our empircal context. Our sample refers to a legally recognized category within a policy framework in Italy that promotes technological advancement. To qualify for this recognition, an SME must meet legal requirements and satisfy at least two of these: invest at least 3% in R&D, employ highly qualified staff, or hold a patent or registered software. Our sample is useful for this analysis because they invest in innovation and provide more transparent information than typical SMEs. We obtain the list of innovative SMEs from the official register maintained by the Ministry of Enterprises and Made in Italy. Additional data on this sample, including shareholder information, financial records, etc., is downloaded from AIDA. Data on GI, especially regarding patent applications, is sourced from PATSTAT, a global patent database frequently utilized in innovation research. We run our mediation effect estimation using the steps higlighted by [3]. The generalized least squares (GLS) panel regression model with random-effects is used to estimate (H1), (H3) and (H4), while a negative binomial panel regression with random-effects is used to estimate (H2). We use negative binomial because the mediator variable (used as a DV in H2) is a non-negative integer count variable with with overdispersion, and this panel model corrects for that [13]. To test our models, we used the variables described in Table 1.

Table 1. *Variables included in the study to test the hypotheses*

Variable type	Variable name	How we measured
Dependent	Profit performance (EBITDA)	This is the Earnings Before Interest, Taxes, Depreciation, and Amortization, a profit-based measure of the firm's performance. The raw value was first obtained, and we divided it by 10000 for easy reading.

Independent	Family SME (FSME)	A dummy variable equal to 1, where family members have control (direct and indirect) over at least 50% of the shares, and at least a member of the family is present in the firm's governance structure (board or management team) of the SME [5].
Mediator	Green Innovations (GI)	The number of green patents held by the firm from 2015 – 2024, where these patents are identified using the (first 3 digit) IPC codes: [A01, B09, B23, B29, B60, B65, C02, C04, C05, C08, C09, C10, D21, E03, F01, F03, F23, F24, F25, G21, H01, H02, Y02, Y04, Y10]
Moderator	Innovation Ecosystem Participation	A dummy variable equal to 1, when evidence from an SME's website shows participation in an innovation ecosystem with partners focused on commercially viable innovation, based on the **helix model of innovation agents** [8]
Controls	Business age (years of incorporation), Size (number of employees), Financial leverage, total production cost, R&D intensity (dummy), Solvency ratio.	

3. Results

Family SMEs constitute a relatively smaller proportion in our sample, about 19% of the smaple. A total of 338 firms, representing about 12% of the SMEs in the sample, are identified as GI-oriented because they hold patents classified as green. Collectively, these firms account for more than 700 green patents filed between 2015 and 2024. The correlation analysis indicates a generally significant relationship between our outcome variable (Profitabilty) and the explanatory variables, as well as significant correlations among the explanatory variables themselves. Multicollinearity is not a concern because correlation among variables does not exceeds 0.7 and the mean variance inflation factor (VIF) for our variables is below 5 [16].

Hypothesis 1 posits that family SMEs are more profitable than their non-family counterparts. This hypothesis is supported by our results, which show a significant positive coefficient for family SMEs [Model 2, Table 4.4: $B = 3.779$, $p < 0.05$]. Hypothesis 2 proposes that family SMEs develop more GIs than their non-family counterparts. The results show a significant positive effect [Model 3, Table 4.4: $B = 0.349$, $p < 0.05$], indicating that family SMEs develop more GIs than non-family SMEs. Our Hypothesis 3 states that GI positively mediates the relationship between family firm status and profitability in SMEs. The results rather reveal a partial negative mediation estimate of GI [Model 5, Table 4.4: $B = -5.185$, $p < 0.1$]. Hypothesis 4 posits that participation in an innovation ecosystem positively moderates the relationship between GI and profitability, as this external resource interacts with GI to enhance financial outcomes.The result provides marginal support for hypothesis 4, revealing innovation ecosystem participation moderates GI positively [Model 6, Table 4.5: $B = 0.468$, $p < 0.1$].

4. Discussion and Conclusion.

Using a sample of innovative SMEs in Italy as of 2024, our findings show that family SMEs are more profitable than their non-family counterparts. This finding is consistent with prior research showing that family firms tend to be more profitable than non-family firms [6], and this may be attributed to the efficient resource orchestration processes of family firms that prioritize cost-conscious strategies. We also show that these family SMEs tend to generate more GI than their non-family counterparts, and this is consistent with prior studies [7]. GIs are outputs that enhance brand reputation and competitive advantage for firms, which is what most family firms want. Hence, they are more inclined to develop GIs than their counterparts. However, what drives engagement in developing more GIs can be attributed to the way in which family firms orchestrate their resources, with a

long-term perspective that enables them to allocate resources to uncertain but potentially rewarding innovation activities [9]. We hypothesized for a positive mediating effect of green innovation on the relationship between family firm status and profitability in SMEs. Given the unique resource orchestrating abilty of family of family SMEs, we expected family SMEs to have a more positive financial effect from their green innovation. Instead, our analysis reveals that green innovation mediates the relationship between family firm status and profitability in a negative way. It appears that green innovation is relatively costly for family SMEs compared to non-family counterparts. This could signal the absence of enabling factors, beyond the effective orchestrating mechanism of family firms, such as complementary resources or ecosystem support, which are necessary to fully leverage or scale the benefits of these innovation. As participation in an innovation ecosystem positively moderates the relationship between green innovation and profitability, this suggest that while green innovation reduces profit, the ecosystem participation reduces this negtaive effect. And this is because gain supprt in the eocysysm, and more importantly, the ecosysyem provides access to wider market to scale up the profit potential of green innovation.

Acknowledgements

This study was funded by the European Union - NextGenerationEU, in the framework of the GRINS -Growing Resilient, INclusive and Sustainable project (GRINS PE00000018 – CUP F83C22001720001). The views and opinions expressed are solely those of the authors and do not necessarily reflect those of the European Union, nor can the European Union be held responsible for them

References

1. Aiello, F., Cardamone, P., Mannarino, L., & Pupo, V. (2021). Green patenting and corporate social responsibility: Does family involvement in business matter? Corporate Social Responsibility and Environmental Management, 28(4), 1386–1396
2. Aldrich, H., & Auster, E. R. (1986). Even dwarfs started small: liabilities of age and size and their strategic implications. Research in Organizational Behavior, 8, 165–198
3. Baron, R. M., & Kenny, D. A. (1986). The moderator–mediator variable distinction in social psychological research: Conceptual, strategic, and statistical considerations. Journal of Personality and Social Psychology, 51(6), 1173.
4. Chirico, F., Eddleston, K. A., & Patel, P. C. (2025). Does it pay to patent green innovations? Stock market reactions to family and nonfamily firms' green patents. Journal of Business Ethics, 198(4), 947–970.
5. De Massis, A., Sharma, P., Chua, J. H., & Chrisman, J. J. (2012). Family business studies: An annotated bibliography. Northampton: Edward Elgar Publishing.
6. Diéguez-Soto, J., Manzaneque, M., & Rojo-Ramírez, A. A. (2016). Technological innovation inputs, outputs, and performance: The moderating role of family involvement in management. Family Business Review, 29(3), 327–346.
7. Ding, H. (2023). Common institutional ownership and green innovation in family businesses: Evidence from China. Business Strategy & Development, 6(4), 828–842.
8. Etzkowitz, H., & Leydesdorff, L. (2000). The dynamics of innovation: From national systems and "Mode 2"

to a Triple Helix of university–industry–government relations. Research Policy, 29(2), 109–123.
9. Gómez-Mejía, L. R., Haynes, K. T., Núñez-Nickel, M., Jacobson, K. J., & Moyano-Fuentes, J. (2007). Socioemotional wealth and business risks in family-controlled firms: Evidence from Spanish olive oil mills. Administrative Science Quarterly, 52(1), 106–137.
10. Hsu, D. H., & Ziedonis, R. H. (2013). Resources as dual sources of advantage: Implications for valuing entrepreneurial-firm patents. Strategic Management Journal, 34(7), 761–781.
11. Jacobides, M. G., Cennamo, C., & Gawer, A. (2018). Towards a theory of ecosystems. Strategic Management Journal, 39(8), 2255–2276.
12. Kotey, B. (2005). Goals, management practices, and performance of family SMEs. International Journal of Entrepreneurial Behavior & Research, 11(1), 3–24.
13. Lee, Y. G., Lee, J. D., Song, Y. I., & Lee, S. J. (2007). An in-depth empirical analysis of patent citation counts using zero-inflated count data model: The case of KIST. Scientometrics, 70(1), 27–39.
14. Oke, A., Turla, M., Osobajo, O., & Koutsoukos, S. (2025). Green innovation across generations in family firms. Journal of Family Business Management, 15(6), 1556–1576.
15. Patel, P. C., & Chrisman, J. J. (2014). Risk abatement in family firms. Strategic Management Journal, 35(4), 617–627.
16. Shrestha, N. (2020). Detecting multicollinearity in regression analysis. American Journal of Applied Mathematics and Statistics, 8(2), 39–42.
17. Spriggs, M., Yu, A., Deeds, D., & Sorenson, R. L. (2013). Too many cooks in the kitchen: Innovative capacity, collaborative network orientation, and performance in small family businesses. Family Business Review, 26(1), 32–50.
19. Van Hemert, P., Nijkamp, P., & Masurel, E. (2013). From innovation to commercialization through networks and agglomerations: Analysis of sources of innovation, innovation capabilities and performance of Dutch SMEs. The Annals of Regional Science, 50(2), 425–452.

Identity-based Legitimacy Buffering and Organizational Attention Triggering Strategic Distinctiveness in Family Businesses

Qiuyang Xu[1], Tommaso Minola[1], Nadine Kammerlander[2]

[1]*Center for Young & Family Enterprise (CYFE), University of Bergamo, Italy,* qiuyang.xu@unibg.it ORCID: 0009-0006-3675-9491, tommaso.minola@unibg.it ORCID: 0000-0003-0337-9741
[2]*WHU-Otto Beisheim School of Management, Germany,* nadine.kammerlander@whu.edu ORCID: 0000-0003-0337-9741

Corresponding author: qiuyang.xu@unibg.it

Abstract

Building on recent theoretical development on the legitimacy-distinctiveness tension, we theorize the contingent conditions triggering strategic distinctiveness. In particular, identity-based legitimacy buffering rooted in organizations' identity structures may create a relative 'safety zone' enabling distinctive strategies. An attention-based view complementarily explains how strategies are enacted. Adopting a configurational approach (fsQCA), we examine how family firms' identity to foster legitimacy buffering, and together with managerial attention, deviate from dominant portfolio of circular business model in circular economic filed. Across configurations, legitimacy buffering could be derived from organizational identity and constitutes a sufficient, but not necessary condition for portfolio distinctiveness, whereas attention structure emerges as critical conditions.

Keywords: legitimacy buffering; attention structure; organizational identity; family firms; circular business models; UN SDG 9; UN SDG 12

1. Introduction

Strategic management has long been puzzled by a central tension: firms compete in the same market by differentiating themselves from peers, yet such strategic deviation from industry prototypes can expose them to legitimacy risk and the liability of distinctiveness [1,2]. Strategic distinctiveness can yield competitive advantages, but these benefits depend on whether distinctiveness is perceived as legitimate by relevant audiences [3]. The conditions that enable firms to realize strategic distinctiveness in the face of legitimacy pressures remain unclear [4]. Recent literature has revisited this trade-off by challenging the assumption that the liability of distinctiveness is uniform across firms [5,6], arguing instead that 'the liabilities of distinctiveness can substantially vary within a market' [6]. Moreover, the benchmark of distinctiveness has been treated as exogenous and conceptualized as fixed distance from a static, one-dimensional industry prototype [5]. However, both market complexity and audience heterogeneity suggest that benchmarks evolve over time, making the evaluation of distinctiveness inherently dynamic and context-dependent. This study integrates identity-based legitimacy buffering with the attention-based view of the firm [7] to explain when and how family firms achieve strategic distinctiveness. We propose that organizational identity can function as an alternative source of legitimacy that buffers the risks of pursuing distinctive strategies [8,9]. Drawing on the attention-based view

[7], we theorize how attention structures—CEO characteristics, board composition, TMT familiness, and organizational slack—determine whether potential distinctiveness translates into enacted strategic differentiation. Using fsQCA on 101 family manufacturing firms in Italy and Germany, we examine circular business model archetype portfolios, revealing equifinal configurations for both high and low levels of portfolio distinctiveness.

2. Methods

This research employs fuzzy-set Qualitative Comparative Analysis (fsQCA), rooted in set theory, which identifies specific condition combinations that jointly produce a given outcome, emphasizing conjunctural causation, equifinality, and causal asymmetry [10,11]. The sample comprises 101 family manufacturing firms from the United Nations Global Compact in Germany and Italy, where over 90% of private enterprises are family-owned [12]. Family firms are defined as those where one or more family groups hold at least 10% ownership [13]. Six conditions are examined: *Family Ownership* (FO), *Family CEO* (FFCEO), *CEO Tenure* (CEOT), *Board Independence* (BI), *TMT Familiness* (TMTF), and *Organizational Slack* (OS). The outcome, *Portfolio Distinctiveness*, captures the extent to which a firm's circular business model archetype portfolio deviates from the empirically dominant archetype portfolio, calculated as the weighted sum of absolute distances between industry-average and firm-level archetype adoption across ten circular business model archetypes [14,15]. Weights are derived using eigenvector centrality scores from an archetype co-occurrence network. Calibration used the 80th, 50th, and 20th percentiles as anchors with direct calibration. The frequency cutoff was set at two, and consistency thresholds were 0.76 for the high-level and 0.92 for the low-level outcome.

3. Results

The necessary condition analysis reveals that no single condition meets the 0.90 consistency threshold, confirming that none is individually necessary for either outcome [10]. Figure 1 presents the intermediate solutions comprising three sufficient configurations for high *Portfolio Distinctiveness*. Configuration H1 is characterized by the joint absence of *Family Ownership, Family CEO*, *Board Independence*, and *Organizational Slack* as core conditions. Configurations H2a and H2b exhibit second-order equifinality: both share the presence of *Family Ownership* and *Family CEO* yet differ in core attention structure conditions—short *CEO Tenure* (H2a) versus low Board Independence combined with high *Organizational Slack* (H2b). Figure 1 presents seven sufficient configurations for low *Portfolio Distinctiveness*. The overall solution consistency is 0.78 with coverage of 0.25 for the high-level outcome, and 0.94 with coverage of 0.37 for the low-level outcome. All configurations exceed the recommended consistency threshold of 0.8, except H1 (consistency = 0.76). The results confirm equifinality and causal asymmetry.

Figure 1. Causal Configurations for High and Low Level of Portfolio Distinctiveness.

High Level of Portfolio Distinctiveness			
	H1	**H2a**	**H2b**
Family Ownership	○	●	●

Family CEO	◯	●	●
CEO Tenure	◯		○
Board Independence	○	○	◯
TMT Familiness	○	○	○
Organizational Slack	○	•	●
Raw coverage	0.21	0.09	0.09
Unique coverage	0.16	0.04	0.04
Consistency	0.76	0.87	0.87
Overall solution coverage: 0.25; Overall solution consistency: 0.78			

Low Level of Portfolio Distinctiveness							
	L1	**L2**	**L3a**	**L3b**	**L4**	**L5**	**L6**
Family Ownership	●	●	◯	○	◯	●	●
Family CEO	•		●	●	◯	○	•
CEO Tenure	●	●	○	◯	○	○	•
Board Independence	●	●	○	○	◯	◯	◯
TMT Familiness	○		◯	○	○	●	●
Organizational Slack	•	•	○	◯	●	•	○
Raw coverage	0.18	0.11	0.06	0.06	0.09	0.07	0.11
Unique coverage	0.08	0.02	0.02	0.02	0.04	0.03	0.06
Consistency	0.94	0.93	1.00	1.00	0.98	0.99	0.97
Overall solution coverage: 0.37; Overall solution consistency: 0.94							

Note: ● = core causal condition (present). • = peripheral causal condition (present). ◯ = core causal condition (absent). ○ = peripheral causal condition (absent). Blank spaces indicate "do not care".

4. Discussion

The findings support a contingent perspective on the legitimacy-distinctiveness relationship [4]. Organizational identity can function as an alternative source of legitimacy buffering, expanding the 'range of acceptability' and mitigating the risks of pursuing distinctiveness [5,6,8]. Configurations H2a and H2b indicate that strong family identity combined with specific attention structures enables distinctive portfolios, while H1 shows that even weak family identity can support high distinctiveness when attention structures are aligned. Comparative analysis of H2b and L4, which share identical attention structures but opposite identity conditions, reveals the contingent buffering role of organizational identity [6]. Attention structures emerge as critical antecedents: CEO succession alters who can place issues on the strategic agenda [7], and newly appointed CEOs can redefine strategic issues, expanding the search space for circular opportunities. Board composition and TMT familiness channel organizational attention through family-centered versus economic commitments. Furthermore, the varying attention structure underscores the configurational and potentially ambivalent role of each condition; its effect on strategic distinctiveness depends on its combination with other conditions rather than being uniformly beneficial or detrimental. The presence of a new CEO contributes to high distinctiveness only when combined with concentrated family ownership; in low-level configurations, even a family successor CEO cannot achieve high distinctiveness without supportive conditions.

5. Conclusions

This research extends critiques of the liability of distinctiveness by relaxing the assumption of static prototypes and homogeneous audiences [5]. We demonstrate that organizational identity functions as an alternative legitimacy buffer, and that such buffering is contingent rather than determinative. The attention-based view provides nuanced insights into how family firms notice, encode, and govern strategic issues [7]. Using fsQCA, we reveal equifinality and causal asymmetry: multiple configurations lead to high distinctiveness, and these are not the inverse of those for low distinctiveness. Managers should deliberately leverage hybrid identity as a strategic resource and align governance-resource configurations to channel attention toward distinctive positions. Future research should directly capture situated attention, extend the framework to other hybrid organizations, and test longitudinal performance effects.

Acknowledges

The author(s) received no financial support for the research, authorship, and/or publication of this article.

References

1. Deephouse DL. Does isomorphism legitimate? Academy of Management Journal. 1996;39(4):1024–1039.
2. Deephouse DL. To be different, or to be the same? It depends. Strategic Management Journal. 1999;20(2):147–166.
3. Phillips D, Edwards BD, Rutherford MW. Conformity or Differentiation: Optimal distinctiveness through mediating channels. Journal of Business Research. 2025;189:115154.
4. McKnight B, Zietsma C. Finding the threshold: A configurational approach to optimal distinctiveness. Journal of Business Venturing. 2018;33(4):493–512.
5. Zhao EY, Fisher G, Lounsbury M, Miller D. Optimal Distinctiveness: Broadening the Interface between Institutional Theory and Strategic Management. Strategic Management Journal. 2017;38(1):93–113.
6. Taeuscher K, Rothe H. Optimal distinctiveness in platform markets: Leveraging complementors as legitimacy buffers. Strategic Management Journal. 2021;42(2):435–461.
7. Ocasio W. Towards an Attention-Based View of the Firm. Strategic Management Journal. 1997;18(S1):187–206.
8. Smith EB. Identities as Lenses: How Organizational Identity Affects Audiences' Evaluation of Organizational Performance. Administrative Science Quarterly. 2011;56(1):61–94.
9. Zhao EY, Glynn MA. Optimal Distinctiveness Revisited. In: Besharov ML, Mitzinneck BC, editors. Organizational Hybridity. Emerald; 2022.
10. Ragin CC. Fuzzy-Set Social Science. Chicago: University of Chicago Press; 2000.
11. Ragin CC, Rihoux B. Qualitative Comparative Analysis (QCA): State of the Art and Prospects. Qualitative Methods. 2004;2(2):3–13.
12. La Porta R, Lopez-de-Silanes F, Shleifer A. Corporate Ownership Around the World. Journal of Finance. 1999;54(2):471–517.
13. Villalonga B, Amit R. How do family ownership, control and management affect firm value? Journal of Financial Economics. 2006;80(2):385–417.
14. Al-Shammari M, Banerjee S, Dadanlar H. Strategic Change and Firms' Optimal Distinctiveness. British Journal of Management. 2025;36(2):810–827.
15. Zhang Y, Wang H, Zhou X. Dare to Be Different? Conformity Versus Differentiation in Corporate Social Activities. Academy of Management Journal. 2020;63(3):717–742.

Entrepreneurship, Teams, and Management

Teampreneurship for Climate Action: An Open Approach to Green Entrepreneurship Education

Lander Jimenez Ocio[1], Jerémy Legardeur[2], Maialen Mendizabal[1], Mar Rubio-Varas[3]

[1]*Mondragon Unibertsitatea, Arrasate-Mondragon, Spain, ljimenez@mondragon.edu ORCID 0000-0003-2446-2819*

[2]*ESTIA, Institute of Technology, Bidart, France, j.legardeur@estia.fr*

[3]*Institute for Advanced Research in Business and Economics (INARBE), Universidad Pública de Navarra, Pamplona, Spain, mar.rubio@unavarra.es*

Corresponding author: ljimenez@mondragon.edu

Abstract

Traditional entrepreneurship education, centred on the individual entrepreneur, is ill-suited to address the systemic nature of the climate crisis. This paper introduces "teampreneurship," a collaborative model grounded in collective intelligence, adaptive leadership, and cooperative values. We present evidence from the first edition of TEAMIT+, an EU-funded programme implemented across four countries (Finland, France, Greece, Spain) in 2024. Using a three-module "learning by creating" methodology, the programme engaged 237 participants. Results show a 99% self-reported improvement in environmental knowledge and a significant shift from individualistic to systemic framings of climate responsibility. Module 3 yielded 10 social-impact business ventures. Findings support the viability of awareness-first, team-based approaches to cultivate the competencies required for green entrepreneurship, though challenges in inter-module connectivity remain.

Keywords: green entrepreneurship; teampreneurship; climate action; experiential learning; collective intelligence; cooperative values; UN SDG 4; UN SDG 13 as well as Inner Development Goals (IDG)s.

1. Introduction

The climate crisis demands a fundamental reorientation of economic value creation, requiring not only technological solutions but profound behavioural and institutional shifts [1]. While green entrepreneurship is recognised as a key driver for this transition, current educational models often fail to cultivate the necessary competencies. Traditional pedagogy centres on the individual entrepreneur and market value, neglecting the systemic complexity and collective action required for sustainability [2], [3]. Literature identifies critical gaps: a lack of interdisciplinary approaches and insufficient focus on collective-action competencies [4], [5].

This paper argues that "teampreneurship" — a collaborative, intercultural model grounded in environmental purpose — offers a viable alternative. We present empirical evidence from TEAMIT+, a European Union-funded programme (Grant Agreement Nr. 101111560) implemented in 2024. Unlike conventional models, TEAMIT+ rests on three pillars: collective intelligence (leveraging diverse knowledge), adaptive leadership (navigating uncertainty without paralysis), and cooperative values (prioritising stakeholder benefit over profit maximisation) [6], [7]. This study evaluates the programme's effectiveness in transforming participants'

environmental understanding and fostering venture creation, addressing the gap between awareness and entrepreneurial action.

2. Materials and Methods

2.1 Programme Design

TEAMIT+ employs a "learning by creating" methodology, synthesising experiential learning [8], team learning [9], dialogue [10], and self-directed learning. The programme comprises three sequential modules:

Module 1 (Awareness): A one-day immersive event ("Ecological and Solidarity's Transitions Day") featuring climate negotiation simulations and workshops on climate justice and circular economy. Implemented simultaneously in four countries (Oct 2024).

Module 2 (Innovation): A 24-hour hackathon ("24 Heures de l'Innovation®") where multidisciplinary teams prototype solutions for real-world industry challenges (Dec 2024).

Module 3 (Venture Creation): A three-month intensive incubation where selected intercultural teams develop social-impact business models with coaching support.

2.2 Participants and Data Collection

Module 1 engaged 237 participants (72.5% higher education students) across Finland, France, Greece, and Spain. Evaluation utilised a pre-post assessment design with structured questionnaires on environmental knowledge and behavioural intentions. Complete matched pairs were obtained for n=160 participants (67.5%). Qualitative data were collected via open-ended reflections. Modules 2 and 284 and 40 participants respectively, with satisfaction surveys administered post-event.

2.3 Analysis

Quantitative data were analysed to measure shifts in self-assessed knowledge and behavioural commitment. Qualitative reflections underwent thematic analysis to identify changes in framing (e.g., individual vs. systemic responsibility) and perceptions of eco-anxiety..

3. Results

3.1 Environmental Awareness and Competency Gains (Module 1)

Module 1 achieved exceptional outcomes, exceeding the 80% target for knowledge improvement. Specifically, 99% of participants reported improved environmental knowledge. The modal self-assessment score shifted from 7/10 pre-intervention to 8/10 post-intervention. Crucially, 64% reported heightened awareness of environmental policy, and 44.6% improved their understanding of the intersection between environmental and solidarity issues.

Qualitative data revealed a cognitive shift: participants moved from viewing climate action through individual consumption choices (e.g., recycling) to recognising systemic interconnections involving policy, economic structures, and social behaviour. Furthermore, 58% expressed a strong commitment to reducing their environmental impact, indicating a successful translation of knowledge into behavioural intention. Satisfaction rates were consistently high across all four national contexts (97% combined "quite" or "very" satisfied).

3.2 Collaborative Innovation and Venture Creation (Modules 2 & 3)

Module 2 achieved a 91% satisfaction rate, with participants valuing the intensive collaborative format. However, recruitment reached only 71% of the target (284 vs. 400), and 45% of participants entered via this module without completing Module 1, creating heterogeneity in foundational knowledge.

Module 3 resulted in the development of 10 business projects across diverse domains: urban food systems, sustainable mobility, indoor environmental health, and circular fashion. Notably, several ventures explicitly addressed eco-anxiety by framing entrepreneurial action as a collective response. The module achieved an 89% satisfaction rate, with participants reporting enhanced professional confidence and intercultural competencies. However, 67% of participants noted insufficient connectivity between Module 3 and the preceding modules, perceiving them as standalone experiences rather than a coherent arc.

4. Discussion

The results validate the core premise that a collective, awareness-first approach can rapidly shift environmental understanding and behavioural intentions. The 99% knowledge gain in Module 1 suggests that immersive, experiential methods (e.g., climate negotiations) are more effective than passive instruction for cultivating the systems-thinking competencies identified as critical for sustainable entrepreneurship [4], [5]. The qualitative shift from individualistic to systemic framing aligns with the theoretical requirement for "normative thinking" in green ventures.

The programme's approach to eco-anxiety—transforming potential paralysis into collective empowerment through actionable pathways—represents a significant pedagogical innovation. By maintaining teams within a "productive zone of disequilibrium" [6], the programme fostered agency rather than guilt. The intercultural dimension further reinforced collective intelligence, as diverse perspectives generated the cognitive dissonance necessary for deep learning [10].

However, limitations exist. The self-reported nature of the data may introduce selection bias. More critically, the perceived disconnect between modules (noted by 67% of Module 3 participants) highlights a structural weakness. The current design risks functioning as a sequence of isolated events rather than a cumulative learning journey. Future iterations must strengthen narrative continuity and ensure that participants entering at Module 2 receive adequate foundational grounding. Additionally, the underrepresentation of VET students and immigrant backgrounds (7.8%) indicates a need for targeted inclusivity strategies to ensure equitable access to green entrepreneurship education.

5. Conclusions

This study demonstrates that "teampreneurship" is a viable and effective model for green entrepreneurship education. By prioritising collective intelligence, adaptive leadership, and cooperative values, the TEAMIT+ programme successfully cultivated systemic thinking and environmental commitment among participants across four European countries. The generation of 10 impact-oriented ventures confirms that awareness can be operationalised into entrepreneurial action within a structured educational framework.

Future research should focus on longitudinal assessment to measure sustained behavioural change and actual venture survival rates. Furthermore, refining the inter-module connectivity and expanding inclusivity strategies will be essential for scaling this model. As the window for climate-resilient development narrows [1],

educational paradigms must evolve from individualistic profit-maximisation to collective, purpose-driven innovation. TEAMIT+ offers a replicable blueprint for this transition.

Acknowledgements

Optional. Funding sources, institutional support, and non-author contributions Funded by the European Union (TEAMIT+ project, Grant Agreement Nr. 101111560). Views expressed are those of the authors only.

References

[1] IPCC. Climate change 2023: Synthesis report. Geneva: IPCC; 2023.

[2] Lourenço F, Jones O, Jayawarna D. Promoting sustainable development: The role of entrepreneurship education. Int Small Bus J. 2013;31(8):841–865.

[3] Gast J, Gundolf K, Cesinger B. Doing business in a green way: A systematic review. J Clean Prod. 2017;147:44–56.

[4] Fichter K, Tiemann I. Factors influencing university support for sustainable entrepreneurship. J Clean Prod. 2018;175:512–524.

[5] Ploum L, Blok V, Lans T, Omta O. Toward a validated competence framework for sustainable entrepreneurship. Organ Environ. 2018;31(2):113–132.

[6] Heifetz RA, Grashow A, Linsky M. The practice of adaptive leadership. Boston: Harvard Business Press; 2009.

[7] ICA. Cooperative identity, values & principles. Geneva: International Co-operative Alliance; n.d.

[8] Kolb DA. Experiential learning. Englewood Cliffs: Prentice-Hall; 1984.

[9] Senge PM. The fifth discipline. New York: Broadway Business; 1994.

[10] Isaacs W. Dialogue: The art of thinking together. New York: Currency; 1999.

[11] Woolley AW, Aggarwal I, Malone TW. Collective intelligence and group performance. Curr Dir Psychol Sci. 2015;24(6):420–424.

[12] TEAMIT+ Evaluation. Year 1 evaluation report. Unpublished internal report; 2024..

Beyond Time, Cost and Scope: Managerial Skills in Achieving Contemporary Dimensions of Project Success

Mirjana Jokanović Đajić[1], Danijela Ćirić Lalić[2], Milica Radovanović[1], Ranka Sudžum[3]

[1] University of East Sarajevo, Production and Management Faculty Trebinje, Trebinje, Bosnia and Herzegovina, mirjana.jokanovic@fpm.ues.rs.ba, 0000-0002-8170-0601, milica.radovanovic@fpm.ues.rs.ba,
[2] Faculty of Technical Sciences, University of Novi Sad, Novi Sad, Serbia, danijela.ciric@uns.ac.rs, 0000-0002-4834-6487,
[3] University of East Sarajevo, The Faculty of Mechanical Engineering , East Sarajevo, Bosnia and Herzegovina, ranka.gojkovic@ues.rs.ba, 0000-0001-5437-2019

Corresponding author: mirjana.jokanovic@fpm.ues.rs.ba

Abstract

Project success has traditionally been evaluated through the "iron triangle" of time, cost, and scope. Contemporary approaches, however, extend this perspective by incorporating additional factors such as user satisfaction, goal achievement, human resource management, productivity, etc. Recent literature increasingly emphasizes that project success largely depends on the project manager and factors associated with their role.

The aim of this paper is to examine how managerial skills of the project manager influence the achievement of contemporary dimensions of project success: project efficiency, impact on the project team, impact on the client, business success, and preparation for the future. The study is based on a review of relevant literature, a conceptual analysis of managerial competencies, and the application of descriptive statistics in data analysis.

The findings indicate that well-developed managerial skills significantly contribute to the achievement of all observed dimensions of project success. It is concluded that a modern understanding of project success requires a holistic approach in which integrated managerial competencies play a central role.

Keywords: project success, managerial skills, project manager, success dimensions, innovative approach

1. Introduction

Identifying critical success factors remains a significant research challenge. Although this area has been widely studied, there is still a noticeable gap in research related to human resources, particularly regarding the role of the project manager and project team members. For this reason, the focus of this paper is on identifying and analyzing factors related to the human aspect of project management that contribute to project success.

A review of relevant literature indicates that successful project execution requires well-developed managerial competencies, including conflict management, risk management, and project portfolio management, as well as skills in planning, coordination, monitoring, and control [1], [2], [3]. Given the key role of the project manager in leading the team, teamwork and collaboration skills are of particular importance [1], [4], [5]. Furthermore, a project manager who clearly defines objectives, manages requirements, and actively involves stakeholders throughout the project lifecycle significantly contributes to project success [5].

Moreover, studies highlight resource management, especially human resource management, as a critical success factor [6]. The specificity of the project environment is reflected in the temporary nature of team engagement and higher turnover compared to functional organizational structures [7], [8], [9]. In modern, particularly multinational projects, additional challenges include managing cultural diversity and building effective teams [10], [11].

The capabilities and skills of the project team as a whole significantly influence project success, with problem-solving, decision-making, commitment, and teamwork identified as crucial factors [12], [13]. Conversely, a lack of adequate competencies may limit the team's ability to make timely and effective decisions [14]. Finally, poor human resource management is recognized as one of the most significant threats to the long-term success of organizations and projects [15], [16].

2. Materials and Methods

The study is based on a review of relevant literature and primary data collected from project managers and project team members across different organizations. This study employed an online survey. The target group consisted of individuals who were either current or former project participants, including those from organizations that periodically carry out projects alongside their primary activities. This approach ensured that respondents had relevant knowledge of project management issues. Geographically, respondents were from Bosnia and Herzegovina, Serbia, and Montenegro. A total of 281 questionnaires were collected, of which 257 were valid and included in the analysis. The sample can be considered reliable, as statistically reliable samples typically include more than 50% valid responses. The sample was diverse in terms of demographics, experience, and organizational representation, providing a comprehensive perspective on project management. Gender distribution was nearly equal, with 129 women (50.2%) and 128 men (49.8%). Respondents' ages ranged from 23 to 70 years. All participants were highly educated, with 49.8% holding a doctorate, 12.8% a master's degree, 30.4% a bachelor's degree, and 7% a secondary school education.

Data were collected using structured questionnaires, focusing on key managerial skills obtained through reviewing secondary data: managing agile processes, teamwork, conflict management, planning, coordination, monitoring and control, resource utilization, and project portfolio management. Participants were selected through purposive sampling to ensure relevance to the examined dimensions of project success.

The study adopts a descriptive approach. Collected data were analyzed using descriptive statistics, to quantify the impact of various managerial skills on achieving project success dimensions: project efficiency, impact on the project team, impact on the client, business success, and capacity building for the future. The analysis was conducted to ensure reproducibility and validity of the results.

3. Results

The results indicate that managerial skills are perceived as highly influential across all project success dimensions and are shown in the following table 1.

Table 1. Impact of Managerial Skills on Project Success Dimensions

Project Success Dimension	Very Low (%)	Low (%)	Medium (%)	High (%)	Very High (%)	High + Very High (%)
Project Efficiency	1.0	0.5	4.5	29.0	65.0	94.0
Team Satisfaction	0.0	1.0	7.0	36.7	55.3	92.0
Client Satisfaction	0.0	3.5	11.1	32.3	53.0	85.3
Business Success	11.6	0.5	1.0	29.1	57.8	86.9
Future Capacity Building	0.0	1.5	11.6	33.2	53.8	87.0

4. Discussion

Managerial skills have been recognized as a critical factor for project success, particularly in the dimensions of user/client satisfaction (53.0% of respondents rated a very high impact) and capacity building for the future (53.8% very high impact). These findings suggest that resource management, planning, and control skills are especially important for the long-term sustainability of project outcomes.

Compared with existing literature, these results support the previously emphasized role of the project manager in team leadership, decision-making, and stakeholder engagement (Durmić, 2020; Creasy & Anantatmula, 2013). However, a critical perspective acknowledges that the impact of managerial skills may be less visible in the early stages of a project but becomes clearer and more significant over the entire project lifecycle.

These insights have practical implications: developing and continuously enhancing managerial competencies can improve project efficiency, client satisfaction, and long-term organizational value. On the other hand, the study's limitations include its descriptive nature and the sample being limited to specific organizations, which may restrict the generalizability of the findings.

5. Conclusions

This study contributes to a deeper understanding of the role of project managers' managerial skills in achieving contemporary dimensions of project success, including project efficiency, impact on the project team, client satisfaction, business success, and capacity building for the future. The results indicate that well-developed managerial competencies, particularly in planning, control, coordination, and resource management, have a critical impact on the long-term sustainability of project outcomes and stakeholder satisfaction.

Although the study provides unique insights into the relationship between managerial skills and project success, it has limitations. Future research should expand this analysis by including diverse organizational contexts, more demographically varied samples, and multiple cultural settings. Additionally, the application of varied

methodologies, such as focus group discussions and personal interviews, is recommended to enrich the empirical evidence. Longitudinal studies examining the effect of targeted training interventions on bridging identified skill gaps could provide further evidence of the long-term effectiveness of training programs. Moreover, investigating the integration of emerging technologies, including artificial intelligence and machine learning, could open innovative avenues for the development and real-time application of managerial competencies.

Overall, the findings emphasize the importance of a holistic approach to developing managerial skills, which is essential for achieving sustainable and multidimensional project success in contemporary business environments.

References

1. Maqbool R, Sudong Y, Manzoor N, Rashid Y. The impact of emotional intelligence, project managers' competencies and transformational leadership on project success: an empirical perspective. Project Management Journal. 2017;48:58–75.
2. Güngör DO, Gözlü S. An analysis of the links between project success factors and project performance. Sigma Journal Engineering and Natural Science. 2016;34:223–239.
3. Belassi W, Tukel OI. A new framework for determining critical success/failure factors in projects. International Journal of Project Management. 1996;14:141–151.
4. Heinz U, Baga T, Gebert D, Kearney E. Leadership and cooperation as success factors in innovative R&D projects on electronic platforms. Team Performance Management. 2006;12:66–76.
5. Durmic N. Factors influencing project success: A qualitative research. TEM Journal. 2020;9:1011–1020.
6. Creasy T, Anantatmula VS. From every direction—How personality traits and dimensions of project managers can conceptually affect project success. Project Management Journal. 2013;44:36–51.
7. Hendriks M, Voeten B, Kroep L. Human resource allocation in a multiproject R&D environment. International Journal of Project Management. 1999;17:181–188.
8. Hueman M, Keegan A, Turner JR. Human resource management in the project-oriented company: A review. International Journal of Project Management. 2007;25:315–323.
9. Belout A, Gauvreau C. Factors influencing project success: the impact of human resource management. International Journal of Project Management. 2004;22:1–11.
10. Chevrier S. Cross-cultural management in multinational project groups. Journal of World Business. 2003;38:141–149.
11. Thamhain HJ. Critical success factors for managing technology-intensive teams in the global enterprise. Engineering Management Journal. 2011;23:30–36.
12. Chen WT, Chen TT, Sheng Lu C, Liu SS. Analyzing relationships among success variables of construction partnering using structural equation modeling: A case study of Taiwan's construction industry. Journal of Civil Engineering and Management. 2012;18:783–794.
13. Choi S, Park KB, Shim SO. Comparing validity of risk measures on newsvendor models in open innovation perspective. Journal of Open Innovation: Technology, Market, and Complexity. 2018;4:783–794.
14. Oh M, Choi S. The competence of project team members and success factors with open innovation. Journal of Open Innovation: Technology, Market and Complexity. 2020;6:51–67.
15. Meyer M, Roodt G, Robbins M. Human resources risk management: Governing people risks for improved performance. SA Journal of Human Resource Management. 2011;9:1–12.
16. Jokanović Đajić M, Cirić Lalić D, Vujičić MD, Stankov U, Petrović M, Đurić Ž. Development and validation of the project manager skills scale (PMSS): An empirical approach. Heliyon. 2024;10:E25055.

Adapting Quality Management Models to Local Organizations: A Literature Review on EFQM and Hybrid Decision-Making Approaches

Tijana Petrovic[1]
[1] *University of Kragujevac, Faculty of engineering, Kragujevac, Serbia, t.cvetic@kg.ac.rs, ORCID 0000-0001-5563-8982,*
Corresponding author: t.cvetic@kg.ac.rs

Abstract
This paper provides a review of recent research focused on the application of the EFQM framework in combination with multi-criteria decision-making (MCDM) methods and advanced analytical approaches. This analysis emphasize studies that integrate methods such as Analytic Hierarchy Process (AHP), Best Worst Method (BWM), and FMOORA, extended with Fuzzy sets and often complemented with optimization and machine learning techniques. The reviewed literature indicates that it is possible to successfully integrate quality management models with hybrid decision-making approaches in order to improve the evaluation of organizational performance. The findings suggest that such approaches provide consistent and reliable results, particularly in the context of complex decision-making environments characterized by uncertainty. Special attention is given to the need for adaptation of quality model frameworks to local businesses operating in the Republic of Serbia. This paper contributes by systematizing existing approaches and demonstrating the potential of hybrid methodologies to support more effective and context-sensitive quality management practices.
Keywords: Quality Models; Business Models; EFQM; Fuzzy sets; Machine learning (UN SDG 3; UN SDG 4; UN SDG 6; UN SDG 7; UN SDG 8; UN SDG 9; UN SDG 10; UN SDG 11; UN SDG 12; UN SDG 13.)

1. Introduction

Integration of quality management frameworks, MCDM methods, and advanced computational techniques can enhance organizational performance, particularly in manufacturing. A central focus is placed on the EFQM excellence model and its relationship with business models as key drivers of sustainable performance. Overall, this research advances methodological and practical understanding of how integrated quality, decision-making, and digital approaches can support continuous improvement and competitiveness in contemporary organizations.

2. Literature review

Recent studies introduce hybrid decision-making approaches, combining fuzzy extensions of the Analytic Hierarchy Process (AHP) with optimization techniques such as constraint programming, enabling more accurate assessment and improvement of business excellence [1-3]. Additionally, multi-stage models integrating methods like FBWM and FMOORA provide robust frameworks for evaluating organizational maturity and performance [1]. The research also addresses quality management practices in the context of Industry 4.0, highlighting the role of digital tools, including real-time nonconformity management systems based on MEAN stack architectures [4]. Furthermore, recent contributions incorporate machine learning techniques to examine the interaction between EFQM criteria and business models, offering predictive insights into quality

performance [3;5]. Most of the analyzed studies are based on the EFQM framework, which is used for defining key evaluation criteria, often in combination with different business models.

Table 1. Comparative overview of the literature

Literature	Method	Quality Model	Application Area	Key Contribution	Note
Petrović et al. 2025 [2]	Machine Learning	EFQM + Business Models	General / Industry	Analysis of the relationship between EFQM and performance using ML	Predictive approach
Petrović et al. 2025 [6]	Fuzzy AHP + Constraint Programming	EFQM	General	Development of a new hybrid model for business excellence assessment	Optimization-based approach
Đorđević et al. 2024 [4]	MEAN Stack Application	Quality Management Systems	SMEs	Real-time nonconformity management system	Digitalization
Petrović et al. 2023 [3]	Statistical Analysis	EFQM + Business Models	Manufacturing	Examination of EFQM–performance relationship	Empirical study
Petrović et al. 2022 [1]	FBWM + FMOORA	EFQM	Manufacturing	Two-stage model for business excellence evaluation	MCDM approach

Table 1 presents a comparative overview of the analyzed studies. A subset of the analyzed studies is closely related to performance measurement, particularly in project-oriented manufacturing companies. In this context, a fuzzy multi-criteria model is used to identify key performance indicators (KPIs) critical to product quality. The model incorporates uncertainty through interval-valued intuitionistic fuzzy numbers and applies an extended TOPSIS method for ranking performance indicators [6]. Based on the results obtained from companies operating in the Republic of Serbia, the highest-ranked KPIs were identified as the most relevant indicators of product quality. These selected KPIs were subsequently used as input variables in further study [3]. In addition, some studies focus on the analysis and structuring of business model components. In one such study, a comprehensive literature review is conducted to identify a broad set of business model elements, which are then reduced using criteria filtering and affinity diagram techniques. The selected elements are further classified into groups through the application of branch and bound algorithm, supported by fuzzy set theory [7]. The outcome of this approach is the development of a new business model framework tailored to organizations operating in the Republic of Serbia. The resulting business model framework from this study also served as input for subsequent research [3].

3. Discussion and further research

Several of the reviewed studies focus on performance measurement and fuzzy MCDM were applied to identify key performance indicators (KPIs) critical for product quality, using interval-valued intuitionistic fuzzy numbers and an extended TOPSIS method for ranking. The highest-ranked KPIs, based on data from companies in the Republic of Serbia, were subsequently used as input in further studies examining the relationship between EFQM criteria, business models, and organizational performance. Other studies analyzed and structured business model components through literature reviews, criteria filtering, and affinity diagrams, followed by classification using a heuristic branch-and-bound algorithm with fuzzy set support. This resulted in a new business model framework adapted to companies operating in Republic of Serbia, which also served as input for the EFQM–performance study. Overall, these studies demonstrate that integrating the EFQM framework with MCDM methods (AHP, BWM), fuzzy logic, FMOORA, constraint programming, and digital tools improves the assessment and prediction of organizational performance. Leadership, process management, and continuous improvement consistently emerge as key factors, while Machine Learning confirms strong links between EFQM criteria, business models, and performance, supporting data-driven decision-making in Industry 4.0 contexts.

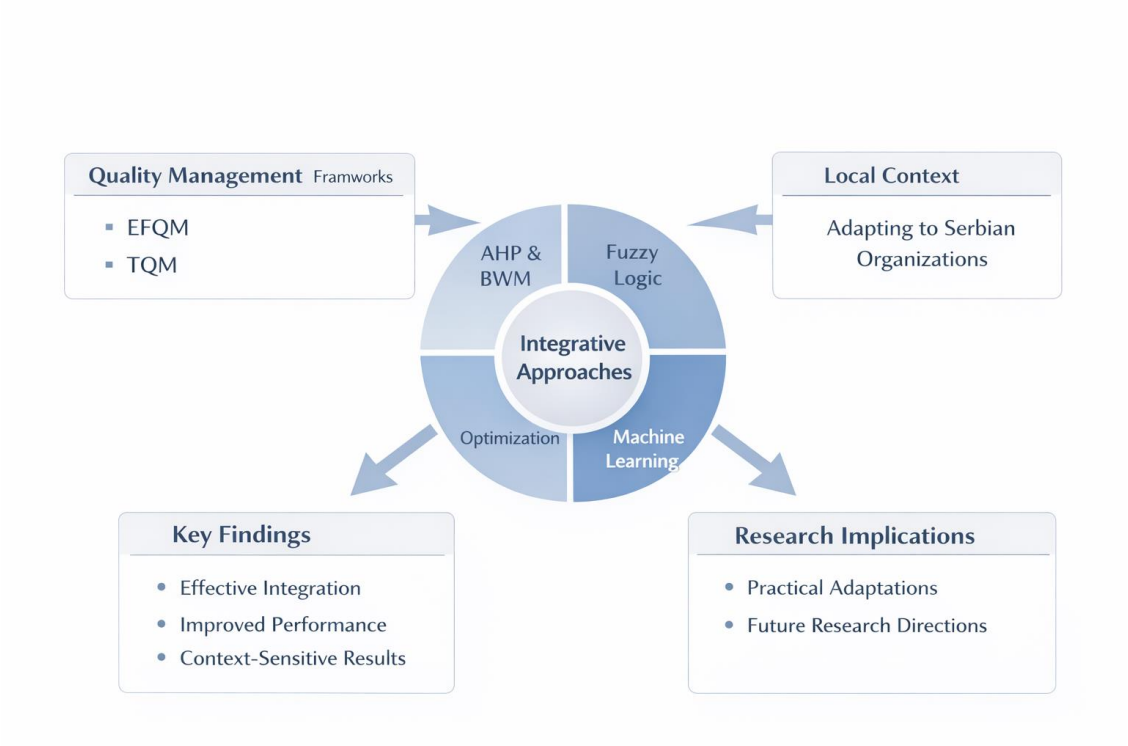


Figure 1. Graphical illustration on literature review

These results indicate a strong potential for predictive analytics in quality management and strategic decision-making. Despite these contributions, certain limitations should be acknowledged: a) the reliance on expert judgment may introduce bias, b) the availability and quality of data can affect the accuracy of machine learning models.

Future research will be directed toward expanding the application of multi-criteria decision-making (MCDM) methods beyond the EFQM framework to other established quality management models. This will enable a comparative analysis of different quality model frameworks and contribute to the identification of the most suitable approaches for various organizational contexts. Future studies will incorporate larger and more diverse datasets in order to enhance the robustness and generalizability of the proposed models. The use of extended datasets is expected to significantly improve the performance of Artificial Neural Networks by enabling more accurate training, validation, and prediction of organizational performance indicators. Overall, these research directions aim to bridge the gap between theoretical quality models and their practical implementation, while simultaneously advancing data-driven and context-aware approaches to business excellence.

References

[1] Petrović T, Vesić Vasović J, Komatina N, Tadić D, Klipa Đ, Đurić G. A Two-Stage Model Based on EFQM, FBWM, and FMOORA for Business Excellence Evaluation in the Process of Manufacturing. Axioms. 2022. 11- 12. 704.
[2] Petrović T, Tadić D, Marinković D, Đurić G, Komatina N. Developing a New Approach for Assessing and Improving Business Excellence: Integrating Fuzzy Analytic Hierarchical Process and Constraint Programming Model. Symmetry. 2025. 17-4. 607.
[3] Petrović T, Paunović V, Komatina N. EFQM and business model relation effect on performance of manufacturing enterprises. International Review. 2023. 1–2. 39–47.
[4] Đorđević A, Stefanovic M, Petrović T, Erić M, Klochkov Y, Mišić M, JavaScript MEAN stack application approach for real-time nonconformity management in SMEs as a quality control aspect within Industry 4.0 concept. International Journal of Computer Integrated Manufacturing. 2024. 37. 630–651.
[5] Petrović T, Đorđević A, Aleksić A, Savković M, Komatina N. Uloga EFQM modela i poslovnih modela u unapređenju performansi kvaliteta: pristup zasnovan na mašinskom učenju. Zbornik Međunarodnog kongresa o procesnoj industriji – Procesing. 2025. 38. 29–38.
[6] Nestić S, Gojković R, Petrović T, Tadić D, Mimović P. Quality Performance Indicators Evaluation and Ranking by Using TOPSIS with the Interval-Intuitionistic Fuzzy Sets in Project-Oriented Manufacturing Companies. Mathematics. 2022. 10. 4174.
[7] Nestić S, Aleksić A, Lafuente J.G, Cvetić T, Đurić G. The Allocation of Business Model Components under Presence of Uncertainties by the Branch-and-Bound Method. Mathematical Problems in Engineering. 2022, 2958519.

Innovation, Education, Skills, and Workforce Development

The Leaky Pipeline in STEM careers: Gender Segregation and the Shift Toward Pedagogical Careers

Sanja Milić[1], Svetlana Pelemiš,

[1]*Faculty of Education, University of East Sarajevo, East Sarajevo, Bosnia and Herzegovina, https://orcid.org/0000-0001-6182-4917*

[2]*Faculty of Technology Zvornik, University of East Sarajevo, East Sarajevo, Bosnia and Herzegovina, https://orcid.org/0000-0001-9682-5899*

Corresponding author: sanja.milic@pfb.ues.rs.ba

Coauthor: svetlana.pelemis@tfzv.ues.rs.ba

Abstract

This paper investigates the phenomenon of horizontal gender segregation within STEM disciplines in Bosnia and Herzegovina by redefining the "Leaky Pipeline" theory. The objective of the research is to identify patterns of internal career redirection of experts from the industrial to the educational sector. The methodology is based on a quantitative analysis of a sample of 228 candidates for pedagogical professional development, classified according to their primary education in natural, technical and medical sciences.
The results indicate an extreme feminization of education in the STEM fields (69,7) despite their lower representation at parent faculties. Such asymmetry confirms the existence of a "soft leak" process, where women with high technical competencies choose education as a "pedagogical refuge" due to a quest for stability and work-life balance. Conversely, male experts perceive education as economically suboptimal, primarily capitalizing on their knowledge in the private sector or abroad. The significance of the paper lies in detecting a systemic gap in which women are pushed into the sphere of knowledge reproduction, while men maintain primacy in technological development and capital accumulation.

Keywords: STEM; gender segregation; soft leak; education; SDG 5 – Gender Equality, Bosnia and Herzegovina.

1. Introduction

For decades, the "Leaky Pipeline" phenomenon has served as a central metaphor in the sociology of education and labor, describing the gradual and continuous loss of female talent from STEM fields (Science, Technology, Engineering, Mathematics) throughout various stages of the career path [1]. The traditional interpretation of this model focuses on the complete abandonment of the scientific sector, suggesting that women drop out of the system due to structural barriers, a lack of mentors, or discrimination [2].
However, contemporary research and empirical data indicate that the "leakage" metaphor requires redefining. Instead of a total exit from STEM, we are witnessing a process that can be termed "internal redirection" or a "soft leak." Women with degrees in natural and technical sciences are not leaving their primary disciplines; rather, they are transitioning from the industrial and research sectors toward education and pedagogy.
Horizontal gender segregation within STEM is not merely a sum of individual preferences but is deeply rooted in the systemic architecture of the modern labor market [3]. While vertical segregation focuses on the barriers preventing women from ascending to

top power positions, horizontal distinction explains why women, even when possessing superior technical competencies, concentrate in sectors that are socially and economically marginalized. In this context, education constitutes a specific space within STEM that absorbs female talent that would otherwise be directed toward industry or pure research.

In modern literature [4], this phenomenon is interpreted as a manifestation of "gender-essentialist beliefs" that permeate educational systems. Even in societies that nominally promote equality, education remains culturally coded as an extension of unpaid labor in the sphere of reproduction and care. When a female engineer or scientist from the natural sciences consciously chooses pedagogical professional development, she enters a sector that offers time sovereignty [5]. This sovereignty is not just a convenience but a necessity in a world where the industrial STEM sector—defined by the concept of "extreme jobs" [6] — demands a total commitment that often excludes any family or private autonomy. This creates a paradox: the educational system utilizes the STEM expertise of women but simultaneously penalizes them economically with lower salaries compared to their male colleagues who remain in the private sector.

The psychological dimension of this process is further illuminated through goal congruity theory. Research by Diekman and colleagues [7] indicates that the STEM industry was historically built around "agentic goals"—power, material gain, and individual success—which are often perceived as incompatible with "communal goals" such as altruism and social contribution. Since women are more frequently socialized toward communality, they find education to be the only available space where their STEM degree can serve a communal purpose. Education thus becomes a "pedagogical refuge," a space where technical knowledge is humanized, but this humanization comes at the cost of losing the economic status and social prestige associated with "hard" engineering work.

Ultimately, this distribution of candidates, where women constitute the absolute majority of those aspiring to education, reinforces the stereotype of science as a field that "belongs" to men in its primary, innovative, and profitable form, while women are assigned the role of those who merely pass that knowledge on. This division of labor within STEM directly contributes to the persistence of the gender pay gap, as educational work is systemically valued less than technological development. In this way, the "leaky pipeline" phenomenon takes on its most subtle form: the pipe does not lose precious fluid but rather redirects it into a reservoir that, while useful to society, remains economically and status-wise undervalued compared to the main stream of technological progress.

In the context of Bosnia and Herzegovina, gender segregation in STEM is fundamentally shaped by post-transitional economic structures and a rigid public sector that continues to operate on traditional professional divisions. The educational system serves as a crucial social security mechanism for women with natural and technical science degrees, offering institutional protection and predictability that are frequently absent in the private sector. Consequently, while male experts are driven by economic rationality toward high-growth industries like IT or emigration to the European Union, female STEM potential is systematically redirected into the sphere of knowledge reproduction and upbringing.

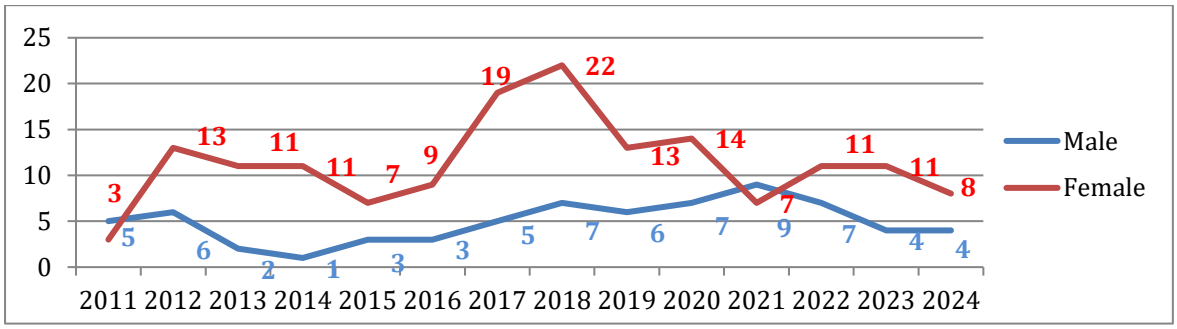
This trend creates a self-reinforcing cycle where the feminization of education leads to its economic devaluation, while industrial sectors remain gender-non-inclusive and fail to integrate female engineering staff. Instead of achieving full economic integration, the labor market facilitates an internal migration of talent where highly qualified women concentrate in sectors with lower budget priorities. Ultimately, this transition into pedagogy represents a strategic yet economically suboptimal choice, as women move toward positions of lower prestige and pay. This internal "leakage" from industry to education functions as a key mechanism that maintains the gender pay gap within scientific and technical disciplines themselves.

2. Materials and Methods

The methodology of this paper is based on a quantitative research approach, focusing on the descriptive and comparative analysis of secondary data. The objective was to identify patterns of gender segregation during the transition from basic STEM education to the teaching sector by analyzing the composition of candidates for pedagogical professional development.
The research sample comprises 228 candidates who graduated from faculties in the fields of STEM sciences and enrolled in the pedagogical group of subjects during the observed period to qualify for work in secondary and primary education.
In the data processing phase, a statistical analysis of frequency distribution and the percentage share of genders within each group was applied. To further investigate the "soft leak" thesis, a comparative method was used to contrast the male-to-female ratios in the technical sector—where a higher presence of men is traditionally expected—against those in the natural sciences.

3. Results

Diagram 1. STEM Graduates Enrolling in Pedagogical Training by Gender (2011–2024).



4. Discussion

Data on candidates for pedagogical professional training indicate a pronounced pattern of professional redirection of STEM graduates toward the educational sector, with women constituting a dominant majority. This finding suggests a redefinition of the “Leaky Pipeline” phenomenon. While the traditional model, as defined by Blickenstaff [1], assumed a linear exit of women from STEM fields, the results show that female STEM potential is not lost but rather redirected from industrial and applied sectors into education. Wang and Degol [8] refer to this process as a “professional detour,” arising from a specific cost–benefit assessment.
Within the observed sample (N=228), women constitute 69.7% of candidates compared to 30.3% men, confirming a pronounced but not absolute gender asymmetry in pedagogical professional orientation within STEM education. The yearly distribution additionally indicates a gradual growth trend between 2015 and 2018, culminating in a peak in 2018, followed by stabilization after 2020. Such dynamics suggest that pedagogical transition is not linear but responsive to structural labor-market conditions.
In the field of natural and technical education pathways, this distribution suggests that the educational sector increasingly functions as a professional stabilization zone. This aligns with the findings of Charles and Bradley [4] regarding the deepening of horizontal segregation within the public sector. The longitudinal pattern indicates that male participation fluctuates across years without a clear growth trajectory, while female participation remains consistently dominant, particularly during the expansion phase between 2016 and 2019. Such asymmetry indicates that men with STEM educational backgrounds are more likely to redirect toward private-sector or international opportunities, while women in Bosnia and Herzegovina more frequently perceive education as a primary destination offering employment stability and temporal predictability.

The paradox observed in technical educational pathways—where women represent the majority despite the traditional male dominance in STEM filds —serves as empirical evidence of internal segregation. This finding can be interpreted through the "gender-equality paradox" framework [9], suggesting that women with technical competencies in economically unstable contexts often choose the security of the public sector over the competitive and structurally exclusive private engineering sector. While men in STEM sciences more frequently pursue agentic career outcomes associated with earnings and advancement [7], women tend to prefer goal congruity through pedagogical engagement and social contribution.

The economic dimension of these movements reveals a significant opportunity cost influencing career decisions, wherein education functions as a form of "pedagogical refuge." The observed gender distribution across years reinforces the structural division between technological production and knowledge reproduction.

The systemic outcome of these processes in Bosnia and Herzegovina is the reinforcement of gendered professional pathways within the educational system itself. The continuous predominance of female candidates across the observed period—particularly during years of higher total enrollment—indicates that structural barriers in technical industries may be indirectly producing internal migration toward education.

5. Conclusions

The data confirm that the "pipeline does not only leak outward" but rather branches toward the educational sector. Women remain within STEM, yet they withdraw from the front lines of high technology into education. This gender segregation is not merely a career choice but a symptom of a system in which the highest-paid positions in industry remain less accessible or less adapted to the needs of women than the educational sector is.

Acknowledgments: This paper is funded through the EIT's Higher Education Initiative A-SIDE project, coordinated by EIT RawMaterials, funded by the European Union

References

1. Blickenstaff, J. C. (2005). Women and science careers: Leaky pipeline or gender filter? *Gender and Education, 17*(4), 369–386.
2. Stefani, A., Minor, R., Leuze, K., et al. (2024). Empirical challenges in assessing the "leaky STEM pipeline": How the research design affects the measurement of women's underrepresentation in STEM. *International Journal of STEM Education, 11*, 54.
3. Makarova, E., Aeschlimann, B., & Herzog, W. (2019). The gender gap in STEM fields: The impact of the gender stereotype of math and science on secondary students' career aspirations. *Frontiers in Education, 4*, 60.
4. Charles, M., & Bradley, K. (2009). Indulging our gendered selves? Sex segregation by field of study in 44 nations. *American Journal of Sociology, 114*(4), 924–976.
5. Blair-Loy, M. (2003). *Competing devotions: Career and family among women executives*. Harvard University Press.
6. Hewlett, S. A., & Luce, C. B. (2006). Extreme jobs: The dangerous allure of the 70-hour workweek. *Harvard Business Review, 84*, 49–59.
7. Diekman, A. B., Brown, E. R., Johnston, A. M., & Clark, E. K. (2010). Seeking congruity between goals and roles: A new look at why women opt out of science, technology, engineering, and mathematics careers. *Psychological Science, 21*(8), 1051–1057.
8. Wang, M.-T., Ye, F., & Degol, J. L. (2017). Who chooses STEM careers? Using a relative cognitive strength and interest model to predict careers in science, technology, engineering, and mathematics. *Journal of Youth and Adolescence, 46*(8), 1805–1820.
9. Stoet, G., & Geary, D. C. (2018). The gender-equality paradox in science, technology, engineering, and mathematics education. *Psychological Science, 29*(4), 581–593.

AI4DLG: Establishing a Joint International Master's Programme in Artificial Intelligence for Digital Learning and Gamification and Developing Its Digital Presence

Jenny Pange[1], Eugenia I. Toki[2]

[1]*Laboratory of New Technologies and Distance Learning, Department of Early Childhood Education, University of Ioannina, Panepistimioupoli, 45100, Ioannina, Greece, jpagge@uoi.gr , ORCID: 0000-0002-1834*

[2]*Department of Speech and Language Therapy, University of Ioannina, Panepistimioupoli B', 45500 Ioannina, Greece, toki@uoi.gr, ORCID: 0000-0001-7995-8745,*

Corresponding author: toki@uoi.gr

Abstract

The AI4DLG initiative reflects a shared effort to develop an innovative and internationally oriented postgraduate programme in a rapidly evolving educational field. Through the academic cooperation of the University of Ioannina and Klaipėda University, the project led to the establishment of the Joint International Master's Programme "Artificial Intelligence for Digital Learning and Gamification." The programme is designed as a three-semester, 90 ECTS, English-medium Joint MSc that combines artificial intelligence in education, digital learning, gamification, pedagogical competence, and research-informed academic practice.

The programme is offered online developed in line with broader European quality principles and with due consideration for the academic and institutional frameworks of both partner universities.

Keywords: AI4DLG; Joint International Master's Programme; artificial intelligence in education; digital learning; gamification; pedagogical competence; higher education innovation; academic dissemination; UN SDG 4.

1. Introduction

Higher education is increasingly challenged to respond to the rapid transformation of teaching and learning shaped by artificial intelligence, digitally mediated learning environments, and new forms of learner engagement. In this context, there is a growing need for postgraduate programmes that combine technological understanding with educational theory, research competence, and pedagogical relevance. The AI4DLG initiative emerged as a response to this need through the academic cooperation of the Department of Early Childhood Education, University of Ioannina, and the Department of Pedagogy, Klaipėda University, leading to the creation of a Joint International Master's Programme focused on AI applications in education, digital learning, and gamification, while also supporting pedagogical competence and ethical awareness.

2. Joint Master Objectives

The main objective of AI4DLG was to establish a future-oriented Joint International MSc with a strong academic identity, a shared curriculum, and a clear international orientation. The project aimed to combine innovation, research, and pedagogy within one coherent postgraduate framework, while also creating a visible and sustainable public presence for the programme. Information of Joint MSc, is offered by the ai4dlg.eu site as its official digital space.

3. The Joint Master AI4DLG

The aim of project is the establishment of the International Joint Master's Programme "Artificial Intelligence for Digital Learning and Gamification." The programme is jointly organised by the Department of Early Childhood Education, School of Education, University of Ioannina, and the Department of Pedagogy, Klaipėda University, with the University of Ioannina serving as the coordinating institution. It is structured as a three-semester, 90 ECTS programme, delivered in English, and leads to a Joint Master's Degree in Educational Sciences. Its curriculum covers key areas such as digital education, research methodology, AI in education, gamification, learning design, learning analytics, internet safety, AI ethics, and human–machine interaction, creating a coherent academic pathway at the intersection of pedagogy, technology, and research.

4. The Development of ai4dlg.eu

The development of the official website ai4dlg.eu offers information of the Joint Master. The site gives the programme a clear digital identity and functions as a dedicated dissemination and communication space for its academic, institutional, and public dimensions. For a joint and internationally oriented programme, such a digital presence is particularly valuable because it supports visibility, accessibility, and outreach.

The website informs about the Joint Master (Figure 1), especially the partner institutions (Figure 2), the academic programme, the quality assurance information, dissemination activities, and contact details, thereby functioning both as an information hub and as a public-facing platform. In this way, ai4dlg.eu strengthens the programme's visibility and supports its long-term sustainability.

5. Conclusions

The **AI4DLG** initiative supports international academic cooperation in higher education. Its main aid is the establishment of the Joint International Master's Programme **"Artificial Intelligence for Digital Learning and Gamification,"**. Information on Joint Master is available on **ai4dlg.eu**, Looking ahead, AI4DLG will offer long-term development of innovative and internationally oriented higher education initiatives.

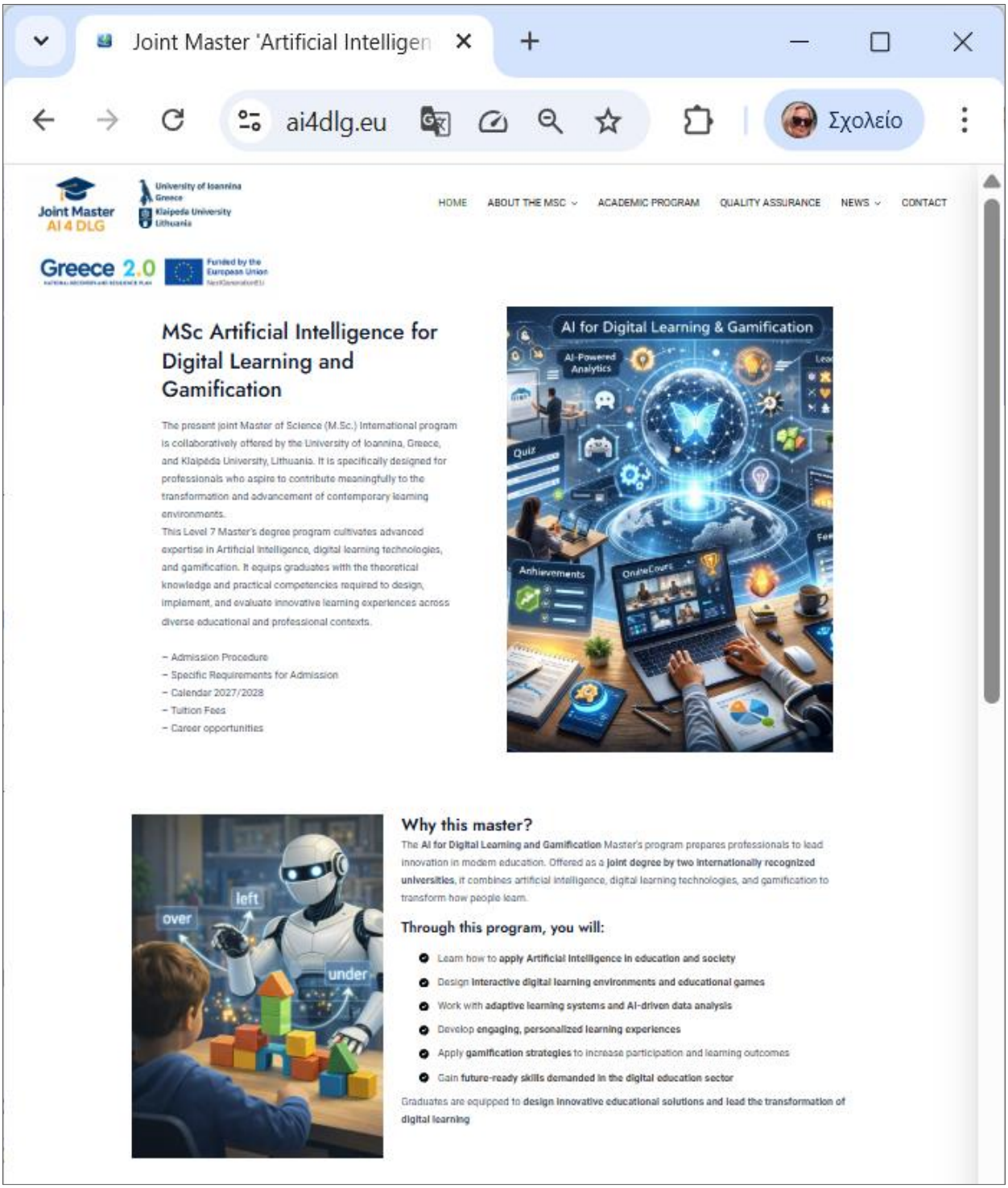


Figure 43: Home page of the Joint Master AI4DLG (ai4dlg.eu)

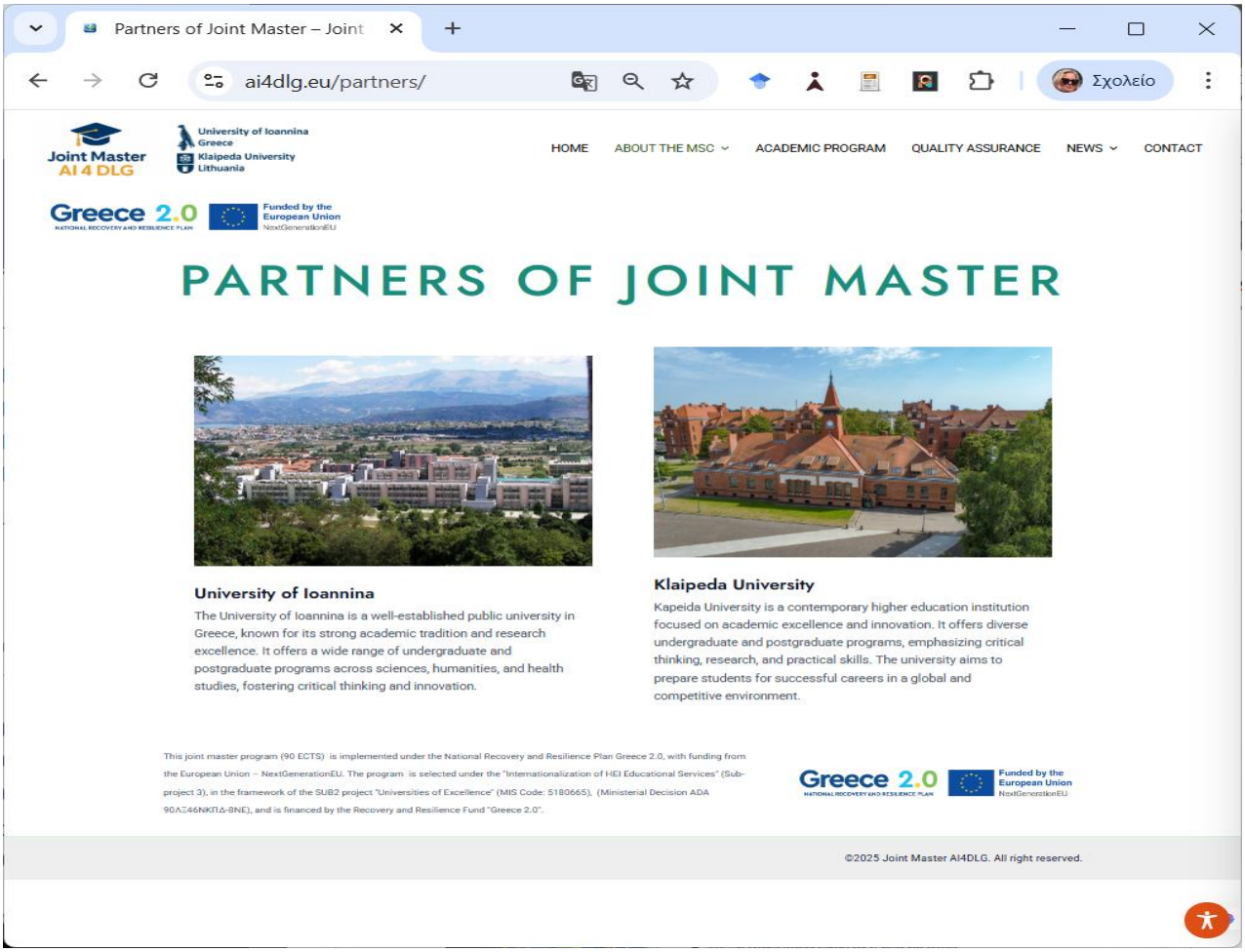


Figure 44. Partners of the Joint Master AI4DLG page (ai4dlg.eu)

Acknowledgements / Funding

This joint international master program (Artificial Intelligence for Digital Learning and Gamification, 90 ECTS) is implemented under the National Recovery and Resilience Plan Greece 2.0, with funding from the European Union – NextGenerationEU and within the framework of Project SUB2: "Universities of Excellence", with OPS Code TA 5180665. The authors also acknowledge the academic cooperation between the University of Ioannina and Klaipėda University, and in particular the contribution of the Department of Early Childhood Education and the Department of Pedagogy to the development of the Joint International Master's Programme "AI for Digital Learning and Gamification".

Integrating Digital and Green Skills in Higher Education

Jenny Pange[1], Dimitrios Panagiotou2, Ioannis Fudos[3]

[1]Laboratory of New Technologies and Distance Learning, University of Ioannina, Greece, Email:jpagge@uoi.gr
[2]Department of Economics, University of Ioannina, Greece, Email: dpanag@uoi.gr (Corresponding Author)
[3]Department of Computer Science & Engineering, University of Ioannina, Greece, Email: fudos@uoi.gr

Abstract

The report focuses on the convergence of the green (environmental sustainability) and digital (technology-driven) transitions, arguing they must be developed synergistically, not in isolation. A significant skills gap exists between what universities teach and what the labor market demands. High youth unemployment (especially in the Mediterranean) and structural weaknesses (e.g., low productivity, skills mismatches) exacerbate the issue. Higher Education Institutions are seen as crucial for driving this transition by revising curricula to foster a "Green Digital Mindset." Economic activity must operate within ecological limits while ensuring social foundations. Education is key to achieving these goals. Divided into *technical* (e.g., renewable energy, waste management) and *transversal/transformative* (e.g., critical thinking, sustainability leadership). Ranging from foundational (office software) to advanced (AI/ML, cybersecurity, cloud computing, data analytics). The key area of convergence, including using AI for energy optimization, IoT for environmental monitoring, GIS for sustainable planning, and digital platforms for the circular economy. The recommendations of the project are: i) Introduce more practical, project-based, interdisciplinary modules that explicitly link digital tools with sustainability challenges, ii) Systematically embed environmental and educational data literacy, iii) Provide continuous staff development in AI, data analytics, and sustainable digital practices.

Keywords: *Twin transition, Green digital innovation, Just transition, Green digital mindset, Sustainable development, Circular economy, Knowledge sharing Digital leadership.*

a-side-project.eu/deeptech-connect-conference-2026

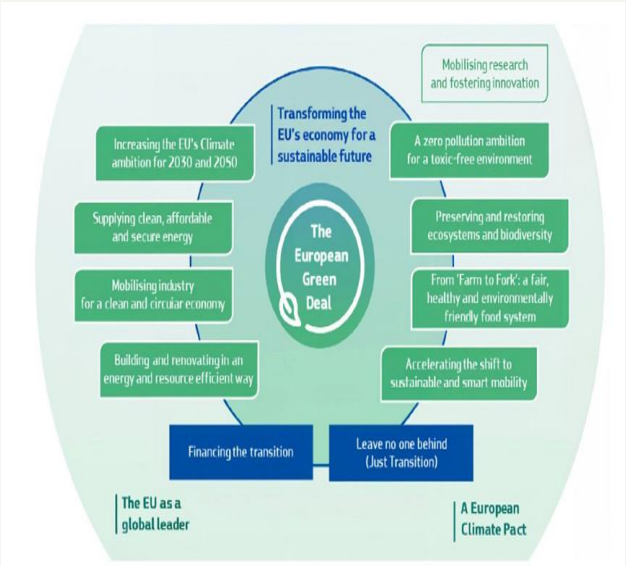
The First DeepTech Connect International Conference 2026

Integrating Digital and Green Skills in Higher Education

Jenny Pange[1], Dimitrios Panagiotou[2], Ioannis Fudos[3]
[1]*Laboratory of New Technologies and Distance Learning, University of Ioannina, Greece*
[2]*Department of Economics, University of Ioannina, Greece*
[3] *Department of Computer Science & Engineering, University of Ioannina, Greece*
contact: dpanag@uoi.gr

DeepTech CONNECT
Co-funded by the European Union
EduHub-360 Innovative Universities for Digital Skills, Green Transition & Inclusion

EUROPEAN GREEN DEAL



MOTIVATION

Contemporary society is at a critical turning point as it faces significant environmental, economic, and social challenges.

Climate change, the depletion of natural resources, social inequalities, political instability affecting access to energy resources and rapid technological development create the need for a new development orientation

In this context, the concept of Just Transition toward a green economy gains particular importance. This transition aims to create a development model that is simultaneously environmentally sustainable, economically stable, and socially just.

MODELS OF GREEN AND DIGITAL SKILLS

The integration of green and digital skills in higher education is based on contemporary theoretical models that connect the economy, society, and the environment.

Institutional	Educational	Societal
Higher education institutions and research centers play a crucial role in this process	Universities can align their curricula with real environmental and social needs.	Contemporary society is at a critical turning point as it faces significant environmental, economic, and social challenges.

KEY FINDINGS AND IMPLICATIONS

Contemporary developments show that digital and green skills do not operate independently but converge into a new field known as Green Digital Innovation.

ACKNOWLEDGMENTS:

The authors gratefully acknowledge the support of the European Union and the contribution of our partners:

1) *Università degli Studi* "G. d'*Annunzio*" Chieti – Pescara, Italy.

2) *ADAM MICKIEWICZ UNIVERSITY, Poznan. Poland*

Co-funded by the European Union
EduHub-360 Innovative Universities for Digital Skills, Green Transition & Inclusion

Acknowledgements / Funding

The authors gratefully acknowledge the support of the European Union and the contribution of our partners:

1) *Università degli Studi* "G. d'*Annunzio*" Chieti – Pescara, Italy.

2) *Adam Mickiewicz University, Poznan. Poland*

Co-funded by the European Union

EduHub-360
Innovative Universities for Digital Skills, Green Transition & Inclusion

1. Cancer statistics, 2022 - Siegel - 2022 - CA: A Cancer Journal for Clinicians - Wiley Online Library [Internet]. [cited 2026 Apr 17]. Available from: https://acsjournals.onlinelibrary.wiley.com/doi/full/10.3322/caac.21708

2. Lyon AR, López-Fernández T, Couch LS, Asteggiano R, Aznar MC, Bergler-Klein J, et al. 2022 ESC Guidelines on cardio-oncology developed in collaboration with the European Hematology Association (EHA), the European Society for Therapeutic Radiology and Oncology (ESTRO) and the International Cardio-Oncology Society (IC-OS). European Heart Journal. 2022 Nov;43(41):4229–361. doi:10.1093/eurheartj/ehac244

3. Chow EJ, Antal Z, Constine LS, Gardner R, Wallace WH, Weil BR, et al. New Agents, Emerging Late Effects, and the Development of Precision Survivorship. J Clin Oncol. 2018 Jul 20;36(21):2231–40. doi:10.1200/JCO.2017.76.4647 PubMed PMID: 29874142; PubMed Central PMCID: PMC6053298.

4. Geiger AM, Castellino SM. Delineating the Age Ranges Used to Define Adolescents and Young Adults. J Clin Oncol. 2011 Jun;29(16):e492–3. doi:10.1200/JCO.2011.35.5602

Developing a European VET Model for Rural Destination Managers- A Competence-Based Approach to Sustainable Tourism

Soultana Demirtzioglou1, Yorgos Goletsis2, Naoum Mylonas3, Luca Reitano4

[1]*Laboratory of Business Economics and Decisions (LABED@UoI), University of Ioannina, Ioannina, Greece, sdemirtzioglou@gmail.com*

[2] *Laboratory of Business Economics and Decisions (LABED@UoI), University of Ioannina, Ioannina, Greece, ORCID id: 0000-0002-6227-0810, goletsis@uoi.gr*

[3] *Department of Tourism, Ionian University, Corfu, Greece, ORCID id: 0000-0002-4286-8022, nmylonas@ionio.gr*

[4]*Department SEAI, Sapienza University of Rome, Rome, Italy, ORCID Id: 0009-0006-0998-0027, luca.reitano@uniroma1.it*

Corresponding author: goletsis@uoi.gr

Abstract

The Eu_VET_RDM4.0 project aims to enhance the competitiveness and sustainability of rural and peripheral tourism destinations in Europe by developing an innovative vocational education and training (VET) model for Rural Destination Managers (RDM 4.0). It focuses on creating a common professional pathway that integrates digital, green, and entrepreneurial skills with sustainable and participatory management approaches.

The project is implemented through international cooperation and a multi-stakeholder methodology, including capacity-building activities, the development of an innovative digital learning environment (RDM-Learning 4.0), and pilot testing in rural and peripheral areas.

Expected results include the creation of a new European professional profile for RDM 4.0, improved collaboration among VET providers, businesses, and rural communities, and increased digital, green, and soft skills across tourism ecosystems. In the long term, the project contributes to more resilient, inclusive, and sustainable tourism development in Europe.

Keywords*: Rural tourism; VET; digital skills; sustainability; capacity building*

1. Project Background and Objectives

The Eu_VET_RDM4.0 project is developed within the Erasmus+ KA220-VET programme, addressing the need to strengthen vocational education and training systems in response to emerging challenges in rural and peripheral tourism areas across Europe. These areas face structural limitations, including low digitalisation, fragmented governance, limited connectivity, and a mismatch between labour market needs and available skills.

The motivation of the project lies in unlocking the potential of rural destinations by equipping stakeholders with the necessary competencies to manage tourism in a sustainable, innovative, and integrated way. In particular, the project responds to the growing demand for professionals capable of combining digital, green, and managerial skills within complex territorial ecosystems. The main objective is to develop a European VET

model for the Rural Destination Manager 4.0, including a common competence framework, training curriculum, and digital learning environment. Expected outcomes include:

- Improved skills among VET providers, SMEs, and rural communities
- Increased collaboration among stakeholders
- Development of a new professional profile aligned with EU priorities
- Strengthened capacity for sustainable and participatory tourism development

2. Methodology and Work Performed

The project adopts a participatory and capacity-building methodology, combining co-design, stakeholder engagement, and practical experimentation. The work is structured into five interconnected work packages, ensuring a logical progression from analysis to implementation and dissemination.

The methodological approach includes:

- Collaborative workshops and stakeholder consultations
- Mapping of territorial needs and skills gaps
- Co-creation of competence frameworks and training models
- Development of digital learning tools and environments
- Pilot testing in real territorial contexts.

3. Key Results

The main results achieved so far derive from the First Training Multilab implemented within WP2, representing the first concrete output of the project.

Through three-day international working groups, stakeholders collaboratively produced a structured analytical framework, identifying:

- Territorial challenges
- Root causes
- Required competencies for RDM 4.0
- Training mechanisms
- Key stakeholders

4. Discussion and Impact

The results obtained so far demonstrate the importance of adopting a multi-stakeholder and competence-based approach to address the complexity of rural tourism development. Compared to traditional VET models, the project introduces a more integrated and flexible framework that combines digital (including AI), entrepreneurial, and governance-related skills. The Multilab findings confirm that challenges are not isolated but shared across regions, reinforcing the need for a common European approach. The co-creation process itself represents an added value, as it ensures that the training model is grounded in real needs and practical experience.

The expected impact includes:

- Strengthening the alignment between VET systems and labour market demands
- Enhancing employability and entrepreneurship in rural areas
- Supporting sustainable and inclusive tourism development
- Improving cooperation between public authorities, education providers, and businesses

5. Conclusions and Outlook

The Eu_VET_RDM4.0 project has successfully completed its initial capacity-building phase, with the First Training Multilab providing a solid foundation for the development of the training model.

The results achieved so far include:

- A shared understanding of key territorial challenges
- A structured competence framework for the RDM 4.0 profile
- Identification of effective training approaches
- These outcomes confirm the relevance of the project and validate its methodological approach.

Future work

The next phases of the project will focus on:

- Developing the **RDM-Learning 4.0 digital environment**
- Designing the full VET curriculum based on identified competencies
- Implementing pilot training activities in rural areas
- Expanding dissemination and stakeholder engagement

In the long term, the project aims to deliver a **replicable and scalable European model**, contributing to the resilience, sustainability, and competitiveness of rural tourism destinations.

Acknowledgements / Funding

This work has been funded by the European Union under the Erasmus+ Programme, Cooperation Partnerships in Vocational Education and Training (KA220-VET), project “European VET Model for the Rural Destination Manager 4.0 (Eu_VET_RDM4.0)”, Project ID: KA220-VET-09486ACC.

The authors would like to acknowledge the contribution of all project partners: FORMA CAMERA (Italy), CNA Roma (Italy), Region of Epirus (Greece), University of Ioannina (Greece), University of Niš (Serbia), Bulgaria Training (Bulgaria), LAG Pomorie (Bulgaria), ITE Network (Spain), and Mancomunidad de la Ribera Alta (Spain). The views and opinions expressed are those of the authors only and do not necessarily reflect those of the European Union or the National Agency (INAPP).

References

1. Eu_VET_RDM4.0. European VET Model for the Rural Destination Manager 4.0. Erasmus+ KA220-VET Project Application Form; 2025.

Green, Social, and Sustainable Innovation

Spontaneous Ecosystems in Rural Areas: A Case Study (*Espacio Comün*, Nalda, Spain)

Sofía Moreno-Domínguez[1]

[1]*Mondragon Team Academy (MTA), Mondragon Unibertsitatea, Spain, smoreno@mondragon.edu, 0000-0002-9164-6514*

Corresponding author: smoreno@mondragon.edu

Abstract

Cultural participation is essential in studying the feeling of belonging among members of communities. In Spain, this rootedness has become known through the dissemination of tangible and intangible heritage in rural areas. The spontaneity of heritage acquires added value when it is connected with local associations and is linked to a geographical area, as in the case of "Espacio Comün" (Nalda, La Rioja, Spain). Espacio Comün aims to create meeting spaces and serve as a reference for other cultural activities that arise from rural development activities in order to establish rural-urban alliances. This initiative involves working side by side with people to promote employment and self-employment, and to support ideas and projects that stimulate the creation and expansion of alternative spaces. The space is available to local artists from Nalda and its surrounding area thanks to a partnership between the "Panal Association" and the "Nuestra Señora de Villavieja" agricultural cooperative. There was a need for a development center where people could become involved in activities that allowed them to make low-risk mistakes, as well as to foster inter-generational exchanges in the rural environment. Social innovation and respect for the environment are crucial elements of this case study, as the project makes a new, alternative use of an old farming building linked to Nalda's past and identity.

Keywords: Rural Development, Cultural Participation, Neo-Rural Movement, Contemporary Rootedness, Arts Communities, 'UN SDG 8', 'UN SDG 10'

1. Introduction: Cultural Participation and Heritage in Rural Areas

When speaking of collective heritage under the umbrella of sustainability and participation (which are closely linked to shared heritage), the focus is on a heritage woven by communities included in a larger, denser society. It can be material, natural or immaterial, and is presented as "a socio-critical reality mediated by the social conditions of production" (Santamarina Campos, 2021:28) [1]. Specifically, for culturally-applied sustainability to be more than sustainable development in the rural environment, a scenario should be created where its presence can be justified beyond the term coined in the Brundtland Commission's report: "Our Common Future" (Soini and Dessein, 2016:2) [2]. Soini and Dessein theorized that sustainability associated with culture should be understood not only as a universal goal, but also as a constantly evolving process centered on imaginary worlds that can project society into the future (Soini and Dessein, 2016:2). In the face of the current environmental degradation, new approaches are emerging that advocate using this collective heritage as a tool for sustainability, including the Sustainable Development Goals of the 2030 Agenda. Here culture is portrayed as an unsubstantial tool or bridge that serves to relate the rest of the goals to each other. A largely normalized way of showcasing the cultural importance of heritage is to disseminate examples of good practices that can be

directly implemented. In recent years, heritage management has moved from the object to the subject. When it comes to persuading communities of the cultural wealth of their assets and customs within an increasingly wider geographical framework, the essential question is, what is the main contribution that cultural heritage can make to economic, social, and environmental progress linked to sustainable development? The responsibility for custody, legacy, and transmission related to new forms of rootedness can be used for creating employment and opportunities for social promotion; or it can be associated with other ethically-based material or spiritual benefits and socially accepted behaviors which can regenerate and/or restore spaces and assets that are essential to the identity matrix of an area, increasing the self-esteem of the local audience.

2. Case Study

In 2018, an experience was launched in the rural ecosystem of Nalda, northern Spain, with the aim of promoting a form of employment that would benefit the quality of life of the local community. It started in the disused part of the local farming cooperative and came together thanks to the spirit of mutual support enacted by cultural agents and local inhabitants. *Espacio Comün* [3] is an innovative project focused on the social economy that allows people from the creative world to develop their projects. The initial aim was to show that it is possible to live and work within the *Red Natura 2000* (2000 Natura Network), a collective project that promotes cooperation between the population in the village of Nalda (La Rioja, Spain) and their surroundings. As part of an attempt to start this initiative in the countryside, *Espacio Comün* is focused on creating action spaces that can serve as incubators and be referent points for cultural activities promoted within the rural ecosystem. It is also aimed at facilitating rural-urban alliances. *Espacio Comün* works hand in hand with local people. In this way, its members are able to identify the needs for promoting employment and self-employment in the area, to support ideas and projects born from areas other than urban areas, and to motivate and assist people who wish to establish themselves in the countryside as part of an initiative linked to neo-rural movements. This approach to entrepreneurship is a nod to the views held by Constance DeVereaux [4], namely, that a strong culture-based and creative educational commitment is needed to support people who may otherwise feel marginalized. An approach that DeVereaux links to indigenous cultures beyond purely economic goals to enjoy a broader sense of freedom of cultural expression. The current building occupied by *Espacio Comün* was the upper floor of the farming cooperative *Nuestra Señora de Villavieja*, a large space where plums used to be left to dry in the past. The experience accumulated by the cooperative *Nuestra Señora de Villavieja* in collaborative work over more than forty years has been essential for the success of this initiative. Their experience has also become reinforced by the 25-year-old connections with the *Panal* [5] and *El Colletero* [6] associations. This background illustrates why this project can be considered to be a pilot project or as an initiative to be followed. This is due to their ability to rethink their context and transform it into something completely new.

3. Results

The former purpose of the *Espacio Comün* building was directly connected to the agricultural tradition that is so important to the highly fertile valley where the village is located. The venue was offered to local creators from Nalda and the surrounding area by the agricultural cooperative itself and the *Panal* and *El Colletero* associations. It began as a development center for people to carry out individual or group projects. A place where people could be supported in their learning, avoiding the feeling of exacerbated risk. It is also a place that promotes inter-generational exchange and transforms the rural world through social innovation and respect for

the ecosystem as a whole. *Espacio Comün* has been working on some pilot experiences within supported creative processes, and producing markets, craft fairs, art exhibitions, workshops, or co-creations. Some of these projects are dedicated to rural activism and most of them go beyond the age-old debate that has always separated craft from art, discarding that boundary altogether. The team of artists and researchers at *Espacio Comün* is made up of ceramic and leather craftspeople, painters, engravers, illustrators, sculptors, and multidisciplinary artists, who have been working on a series of collective processes related to primitive ceramics. This activity also includes gastronomy as a necessary part of this kind of process, which is open to a variety of audiences. The kiln was made collaboratively among the team members, using natural clay and recycled metal and wooden parts. The heat produced by the kiln can be used for cooking and the participants eat together while observing the final ceramic results. The germ of this idea is to open these research processes to more people who are interested in learning about new sustainable values, mutual support, and conducting projects linked to creativity and agroecology in the present with a view to a better future.

4. Discussion

Participation involves taking part and receiving something through action. If this applied to heritage management, there is an inconsistency when it comes to measuring the impact of this type of action at a local, national, or global level, as multiple subjective nuances come into play that are very difficult to measure and evaluate. However, little effort has been made to empower communities, as this involves dealing with complex issues that are outside the realm of heritage projects as such, including bureaucratization, the bunding of actions and services, and the politicization of certain spaces and/or cultural assets for extrinsic purposes. Justice and equality may be the objectives, but these may well be marginalized by other more immediate and profitable priorities. The model of good living Sumak Kawsay [7] shows how heritage is not publicly recognized, which has an impact on its political structure when it comes to making decisions that affect it. It is also not surprising that the official lists of heritage planning such as the World Heritage List (1972) and the Representative List of the Intangible Cultural Heritage attached to neo-capitalism [8]. These lists are also an excuse for state and local discrimination, as they increase territorial inequalities when it comes to stigmatizing certain areas and prioritizing some areas over others. A major challenge would be to shift tourism flows deeply marked by physical and material attractiveness by channeling them through the intangible heritage of customs and issues more centered on the narrative. This approach may impact the direction that interpersonal mobility associated with cultural tourism will take in the coming years. Initiatives as *Espacio Comün,* however much they seek to offer an alternative, must also adhere to an understanding of collective heritage as sustainable action and incorporate the SDGs into their scope of action. In order to do this, an initial step should be to consider the cultural and patrimonial significance of the policies that promote these goals for the coming decades. As these practices depend on a fabric of people and places, related activities are inevitably subject to constant change, and therefore they move further and further away from a closed, specific definition. For this reason, practices such as mediation and social participation are fundamental instruments to ensure their coherence and return them immediately to the society to which they belong, based on respect for a biodiversity beyond speciesism (even more so in rural environments).

5. Conclusions

According to Duxbury, Kangas and De Beukelaer [9], a culture is sustainable when it integrates the social, ecosystemic, and economic dimensions into a whole that is indispensable for full sustainable development. These views are also closely linked to the nature of the rural environment due to its essential characteristics, which entail framing a broad overview of the context to take long-term actions that can be useful and well received by the community (Duxbury, Kangas and De Beukelaer, 2017:221). The approach in this paper is a nudge that goes beyond marketing actions; it is aligned with a current linked to an architecture of joint behavior, with no major incentives or invasions other than the actions that are beneficial to the community (Thaler & Sunstein, 2009) [10]. In order to carry out initiatives that promote community behaviors and try to replicate them while remaining faithful to other ecosystems and their conditions, it is important to have very strong local support. This form of support for the people involved in *Espacio Comün* is provided by the *Panal* and *El Colletero* associations. In this way, the initiatives become rooted in the territories in a natural, non-imposing way. In addition, there is an alliance with another private actor, the agricultural cooperative *Nuestra Señora de Villavieja*. Once these first steps have been taken, it is very important to follow up on them by building a passionate team with a very strong sense of community.

Acknowledgements

I would like to give special thanks to Susana Quintas and Julian Thomas, academic translation and editing services, to my *Espacio Comün* partners, and to the members of the *Panal* and *El Colletero* associations for their support.

References

1. Santamarina Campos, B. 2021. “Collective Heritage. Communities, participation and sustainability”. Andalucía’s Historical Heritage Institute, Cultural and Historical Heritage Council: PH 104 Magazine.
2. Soini, K, and Dessein, J. 2017. “Culture-Sustainability Relation: Towards a Conceptual Framework”. Basel, Switzerland: MDP, Sustainability Journal. https://www.mdpi.com/2071-1050/8/2/167
3. Espacio Comün. 2022. “The project”. Nalda, Spain. http://espaciocomun.es/
4. DeVereaux, C. 2013. “Cultural Education towards Creative Entrepreneurship among Marginalized People”. Arizona, United States: ENCATC Journal of Cultural Management and Policy.
5. PANAL Association. 2022. “What is PANAL?” Nalda, Spain. https://aumentoforestal.wixsite.com/panal
6. El Colletero Association. 2022. “Who we are”. Nalda, Spain. https://www.elcolletero.org/nosotras.html
7. UNESCO. 2007. “The National Plan of Good Living Sumak Kawsay and the Plurinational Plan as the Bases for Cultural Policies”. Paris, France: https://en.unesco.org/creativity/policy-monitoring-platform/national-plan-good-living-sumak
8. UNESCO. 2022. “Browse the Lists of Intangible Cultural Heritage and the Register of good safeguarding practices”. Paris, France. https://ich.unesco.org/en/lists
9. Duxbury, N, Kangas, A, and De Beukelaer, C. 2017. “Cultural policies for sustainable development: four strategic paths”. London, United Kingdom: International Journal of Cultural Policy, Routledge Taylor & Francis Group.
10. Thaler & Sunstein. 2009. “Nudge. Improving decisions about health, wealth and happiness”. London, England: Penguin Books.

Innovative Rotating Staircase System as an Integrated Solution for Improving Accessibility

Student Company

StepShift

Mara Stanojević[1], Jelena Nešić[1], Marta Jovanović[1],
Mentors: Kristina Cvetković, Bojana Đurković

[1] StepShift Student Company, Mechanical and electrical engineering school, Paraćin, Republic of Serbia
Contact email: mes.stepshift@gmail.com | Website: stepshift.squarespace.com

Executive Summary

StepShift represents an innovative technical solution that enables the transformation of conventional staircases into a functional ramp, with the aim of improving accessibility for people with reduced mobility. This paper analyzes the technological characteristics, market potential, and financial sustainability of the system, with a particular focus on its social impact. The system integrates two functions into a single structural solution, eliminating the need for additional space and costly construction interventions. The business model is based on the sale of technical documentation, while production is carried out through partner networks, ensuring high scalability. Financial analysis shows a gross margin of 44% and a low break-even point (below one project per month), indicating a sustainable and profitable business model. In addition to its economic potential, the solution has significant social value in the field of inclusion and accessibility. StepShift has the potential to become a standard in modern architectural design and the implementation of inclusive solutions.

Keywords: accessibility, innovation, inclusion, design, technology, sustainability, UN SDG 10

1. Company Overview

StepShift is an innovative company focused on developing solutions for improving spatial accessibility, specifically through the design and engineering of rotating staircases that slightly rotate and transform into a ramp at the push of a button, enabling easy access for wheelchair users (persons with disabilities). In addition to the primary target group, the ramp can also be used by parents pushing strollers or small children in pushchairs. Our core product is the service of designing these staircases and specifying the basic construction materials based on the given space. Additionally, we can act as an intermediary between clients and manufacturers (companies engaged in staircase production). Our mission is to provide accessibility and independence, primarily for people with disabilities, through practical and innovative solutions that facilitate everyday life, using knowledge, creativity, and teamwork. The vision of our student company is a society in which all spaces are accessible to everyone, without barriers or limitations. Our strategy is to make rotating staircases a widely applicable solution, especially in rehabilitation centers, spa and tourism facilities, as well as in public institutions, schools, and healthcare facilities, contributing to a more inclusive and equitable environment. The company operates through a multidisciplinary team (design, engineering, management, finance) and collaboration with external partners, ensuring a high level of expertise and flexibility.

2. Product Technology Description

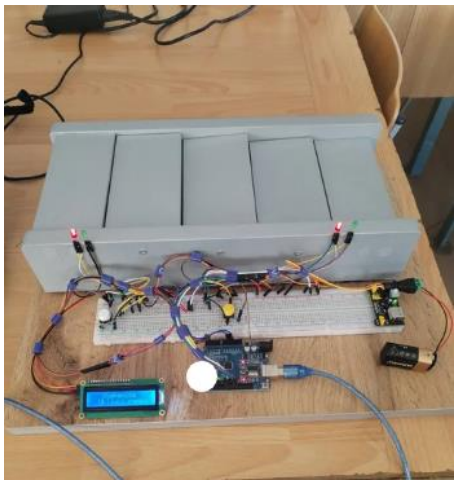


Fig. 1*. Prototype of the rotating staircase system*

The idea originated from observing the everyday challenges faced by people with disabilities when navigating stairs, particularly in locations where ramps are not available. This motivated us to develop a solution that would enable easy and fast access to desired facilities. The development process focused on creating a functional prototype model (Figure 1). The core product is a system of rotating stairs that transform into a ramp at the push of a button.

The technical characteristics are based on the integration of mechanical, electronic, and control components that enable the transformation of stairs into a ramp by rotating each step at a specific angle of inclination. The architecture is modular, allowing adaptation to different facilities and spatial dimensions. The system consists of: servo motors (one per step) (1); Arduino UNO (2), I2C LCD display (2); LEDs (red and green depending on the selected function) (2); two control buttons (2).

The following figure (Figure 2) shows the electrical schematic of the system's operation:

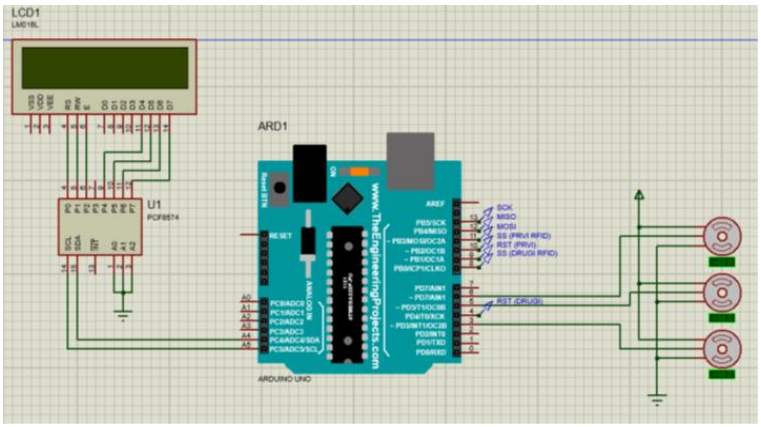


Fig. 2. *Electrical schematic of the rotating staircase system*

The system includes an Arduino Uno development platform (2), LCD display (2), and servo motors (1). The LCD displays (2), information and is connected to the Arduino (1) via analog pins, while the servo motors (1) are connected to digital pins and are activated according to predefined conditions. The user inputs commands via buttons, the Arduino (2) processes them, displays results on the LCD (2), and controls the servo motors (1). This connectivity enables automated control and facilitates easy interaction with the system.

Based on intellectual property analysis, there is potential for protecting the innovation through patenting the technical solution and copyright protection (3) of accompanying documentation, ensuring legal security, market exclusivity, and sustainable competitive advantage.

3. Innovation and Competitive Advantage, Market Application, and Impact

The main innovation lies in integrating two functions into one system—stairs and ramp. Competitive advantages include: space saving, ease of use, lower costs compared to elevators, applicability in existing buildings. The solution represents a significant technological and functional advancement. Target markets include: spa and

rehabilitation centers, healthcare institutions, schools and public buildings. The social impact is reflected in increased inclusion and improved quality of life for people with disabilities.

4. **Business Model**

StepShift's business model is based on selling technical design services (consultation, spatial analysis and development of 3D models, preparation of technical documentation – detailed drawings of all components including dimensions, tolerances, and material specifications), rather than manufacturing physical stair systems.

Project price: The basic package (for a standard ramp of 1.2 m in length) costs 25000 RSD. More complex projects (e.g., lengths over 2 m) cost from 35000 RSD and above. Since StepShift does not manufacture physical components, its production costs relate exclusively to the development and delivery of the project. The average cost per project amounts to 14000 RSD. Our own capital consists of technical equipment owned and used by our school, while the current investment is allocated to marketing and promotion in the amount of 10000 RSD per month. The planned sales volume is two basic packages per month, resulting in revenue of 50000 RSD, with an additional 10% income from production and installation if the client opts for that type of service. The financial overview is as follows (Table 1) (4):

- Project development cost: 14000 RSD
- Project selling price: 25000 RSD
- Marketing cost: 10000 RSD (fixed costs).

Gross profit per project	25000 – 14000 = **11000 RSD**
Gross margin	11000 / 25000 = **44%**
Net profit (example for 1 project per month):	25000-14000 = **1000 RSD**
Net margin	1000 / 25000 = **4%**

Table 1: Financial statement for one sold project

If we sell 2 projects per month, (Table 2 and Table 3) the financial statement and Income Statement (monthly) for 2 projects is:

Gain	50000 – 38000 = 12000
Gross profit	50000 – 28000 = 22000
Gross margin	44%
Net profit	50000 – 38000 = 12000
Net margin	12000 / 50000 = 24%

Price of 2 projects: 50000RSD	Expenditures : Variable costs:28000 RSD+ Fixed costs: 10000 RSD
Gain: 12000 RSD	

Table 2 and Table 3: Financial overview for two sold projects and Income statement for one month

In addition to its core activity, there is an opportunity to generate additional revenue through collaboration with companies engaged in the manufacturing and installation of moving stair systems. In such cases, the company would earn a commission of approximately 10% of the value of each completed project, representing significant potential for future revenue growth. Based on the analysis, the break-even point is 0.91 projects per month. It

can therefore be concluded that completing just one project per month is sufficient to cover all costs, while each additional project contributes to profit generation. It also demonstrates the scalability of the business (4), as revenues increase with completed projects without a significant rise in costs.

5. Market Presentation and Target Segments; Market Strategy

The market for rotating staircases includes facilities where accessibility for people with disabilities is essential, such as spa resorts, rehabilitation centers, and wellness complexes visited by elderly individuals, people with disabilities, and those in recovery. Potential markets also include public institutions, educational institutions, commercial buildings, healthcare facilities, and even private households. The marketing strategy is based on direct collaboration with the management of spa and rehabilitation centers, product presentations, as well as promotion through digital platforms and professional events in the fields of tourism and health tourism, along with participation in various technology and innovation fairs.

6. Social and Environmental Impact (ESG), social value and Regulatory Compliance

The StepShift system contributes to environmental sustainability by optimizing space and reducing the need for additional construction interventions. Unlike traditional ramps and elevators, which require additional materials and structural expansion, StepShift utilizes the existing staircase structure, thereby reducing the consumption of construction resources. The primary social contribution of the StepShift system lies in improving accessibility for people with disabilities and reduced mobility. This solution enables independent and dignified movement of users across various facilities, directly contributing to increased inclusion and equality in society. The system is designed in accordance with applicable standards and regulations, including the Law on Planning and Construction (5) and the Regulation on Technical Standards for Planning, Design and Construction of Facilities (6). The solution is aligned with the principles of sustainable development and the goals of UN SDG 10 – Reduced Inequalities, further confirming its social and global relevance (7). Future product development includes alignment with national and international standards, as well as the possibility of certification, enabling broader application in public and commercial facilities. In the short term (1–2 years), the development of the StepShift system is focused on improving the prototype, testing and optimization of the system, and establishing a network of partners.

Literature:

[1] Warwick A. Smith, „C Programiranje za Arduino” („C Programming for Arduino”)
[2] Marko Tanasković, „Arduino Uno uputstvo za korišćenje sa rešenim primerima” („Arduino Uno User Guide with Solved Examples”)
[3]https://www.zis.gov.rs/edukativno-informativni-centar/prirucnik-za-pronalazace/zastita-vase-ideje/ visited on April 16, 2026
[4] Svetislav Paunović, „ Preduzetništvo” („Entrepreneurship” textbook for the 3rd and 4th grade of secondary vocational school)
[5]https://www.paragraf.rs/propisi/zakon_o_planiranju_i_izgradnji.html visited on March 20, 2026
[6]https://www.paragraf.rs/propisi/pravilnik_o_tehnickim_standardima_planiranja_projektovanja_i_izgradnje_objekata_kojima_se_osigurava_nesmetano_kretanje_i_pristup_osobama_sa_invaliditetom_deci_i_starim_osobama.html visited on March 20, 2026
[7]https://www.undp.org/sr/serbia/ciljevi-odr%C5%BEivog-razvoja visited on April 16, 2026

Multi-Criteria Decision Analysis for ESG measurement: A Systematic and Bibliometric Review

Yorgos Goletsis[1], Vasiliki Spyridonos[2]

[1]*Laboratory of Business Economics and Decisions (LABED@UoI), Dept of Economics, University of Ioannina, Ioannina, Greece, goletsis@uoi.gr, ORCID:0000-0002-6227-0810*

[2]*Dept of Economics, University of Ioannina, Ioannina, Greece, v.spyridonos@uoi.gr,*

ORCID:0009-0006-8140-2029

Corresponding author: v.spyridonos@uoi.gr

Abstract

Environmental, Social, and Governance (ESG) criteria play a critical role in evaluating corporate sustainability and long-term performance. However, ESG assessment remains a complex multidimensional problem, as it requires the integration of heterogeneous, uncertain, and often conflicting criteria. Traditional single-criterion approaches are insufficient to capture this complexity. Multi-Criteria Decision Analysis (MCDA) provides a structured decision-support framework that enables the transparent evaluation of trade-offs among ESG dimensions.

This study investigates the role of MCDA in ESG evaluation, based on a systematic literature review of 165 publications following the PRISMA framework, complemented by bibliometric techniques including co-citation, keyword co-occurrence, and bibliographic coupling analysis.

The findings reveal a strong methodological concentration around widely used techniques such as AHP and TOPSIS, alongside an increasing integration with digital technologies and data-driven decision environments. Emerging application areas include sustainable finance, circular economy, and technology-enabled ESG assessment. Despite this progress, persistent challenges remain, including data quality issues, methodological divergence, and sensitivity to subjective weighting schemes.

The study contributes to the intersection of ESG, decision analytics, and sustainable innovation by demonstrating how MCDA can support robust, transparent, and scalable decision-making in complex technological systems.

Keywords: ESG; MCDA; sustainable innovation; decision support systems; sustainability assessment; ESG evaluation; bibliometric analysis; systematic literature review; UN SDG 9; UN SDG 12

1. Introduction

Environmental, Social, and Governance (ESG) criteria have emerged as a fundamental framework for evaluating corporate sustainability and long-term value creation. A growing body of literature demonstrates that ESG performance is closely linked to financial outcomes, risk mitigation, and long-term competitiveness [1], [2]. In this context, ESG ratings have become widely used tools for assessing sustainability performance; however, significant methodological divergence across rating providers—particularly in terms of indicator selection and weighting schemes—undermines comparability and decision reliability [3], [4]. Despite increasing regulatory efforts to improve transparency, ESG evaluation remains inherently complex, requiring the integration of heterogeneous and often conflicting environmental, social, and governance criteria that cannot be adequately addressed by traditional single-criterion approaches.

Multi-Criteria Decision Analysis (MCDA) provides a structured framework for addressing this complexity by enabling the systematic evaluation and prioritization of alternatives across multiple criteria, while explicitly incorporating trade-offs and stakeholder preferences [3]. The integration of ESG considerations into innovation-driven and data-intensive environments further increases the need for robust decision-support tools. Despite the growing body of ESG–MCDA literature, existing studies remain fragmented, with limited integration of methodological insights and emerging innovation-oriented applications. This study explores the role of MCDA in ESG evaluation and seeks to provide a structured understanding of the field through systematic and bibliometric analysis.

2. Materials and Methods

This study adopts a combined systematic literature review and bibliometric analysis approach to examine the application of Multi-Criteria Decision Analysis (MCDA) within the Environmental, Social, and Governance (ESG) framework. The Scopus database was selected as the primary data source due to its extensive coverage of peer-reviewed publications across multiple disciplines.

A PRISMA-based methodology was employed to ensure a transparent and reproducible study design [4]. The search process was conducted searching for terms relevant multi-criteria analysis or multi-criteria methods and ESG. The final dataset consisted of 165 documents, which were included in the bibliometric analysis.

The analysis was conducted using VOSviewer, a widely used tool for constructing and visualizing bibliometric networks. Three complementary techniques were applied:

(i) keyword co-occurrence analysis to identify dominant research themes,
(ii) co-citation analysis to reveal the intellectual structure of the field, and
(iii) bibliographic coupling to explore emerging research trends and thematic proximity among recent publications.

To enhance the robustness of the results, appropriate normalization settings were applied, including the use of fractional counting, while a thesaurus file was employed to standardize keyword variations. This combined approach enables a comprehensive mapping of the ESG–MCDA research landscape, capturing both its conceptual foundations and evolving research directions.

3. Results

The bibliometric analysis reveals a structured and rapidly evolving research landscape within the ESG–MCDA domain. A strong methodological concentration is observed, with a limited number of MCDA techniques—primarily AHP and TOPSIS—dominating the majority of applications, while other methods remain less frequently applied.

The co-citation analysis identifies four core research streams that shape the intellectual foundation of the field, including the relationship between ESG performance and financial outcomes [1], methodological and technological developments in ESG assessment, ESG rating divergence and governance-related challenges [5], and sustainable investment and portfolio decision-making.

The keyword co-occurrence analysis reveals four major thematic clusters. These include the interaction between economic growth and environmental sustainability, corporate sustainability and circular economy practices, CSR and digital innovation in sustainability-oriented decision-making, and sustainable finance and responsible investment.

The bibliographic coupling analysis highlights emerging research trends, indicating a shift toward advanced and hybrid MCDA methodologies, including fuzzy and data-driven approaches. Recent research increasingly focuses on ESG evaluation frameworks and data-driven sustainability assessment [6], as well as governance-oriented and cross-sector applications.

Overall, the results indicate a clear transition from traditional ESG evaluation approaches toward more sophisticated, multi-criteria and uncertainty-aware decision frameworks, reflecting the increasing need for robust and adaptable tools to support sustainability-related decision-making.

4. Discussion

The findings highlight the increasing role of MCDA as a structured approach for addressing the complexity of ESG evaluation. The dominance of a limited number of methods, such as AHP and TOPSIS, reflects a degree of methodological standardization, while the identified thematic clusters demonstrate the expansion of ESG–MCDA research across diverse domains. These patterns indicate a shift toward more structured and data-driven decision-making processes in sustainability contexts. While these findings demonstrate significant progress, the literature also reveals several persistent methodological and practical challenges. A key limitation concerns the lack of standardized ESG indicators and the significant divergence across ESG rating providers, which undermine data comparability and the robustness of decision outcomes [5], [7]. In parallel, data quality issues—such as incomplete disclosure and inconsistent reporting practices—further affect the reliability of ESG-based evaluations [8]. Additionally, the subjectivity inherent in MCDA weighting processes remains a critical concern, as expert judgments and preference elicitation may introduce bias and sensitivity in final rankings. The context-specific nature of many ESG–MCDA applications further limits the transferability of findings across different institutional and regulatory environments. Stakeholder heterogeneity also complicates decision-making, as different actors emphasize different ESG dimensions [1]. Overall, these challenges underline the need for more transparent and standardized ESG–MCDA approaches to enhance decision relevance and practical applicability.

5. Conclusions

This study provides a systematic and bibliometric overview of the application of Multi-Criteria Decision Analysis (MCDA) within the ESG framework, highlighting a rapidly growing yet methodologically concentrated body of literature. The findings confirm that MCDA offers a structured and transparent approach for integrating heterogeneous environmental, social, and governance criteria, supporting sustainability assessment and decision-making [1]. At the same time, the analysis reveals key challenges that constrain the robustness and comparability of ESG–MCDA applications, including the lack of standardized ESG indicators, rating divergence, data uncertainty, and sensitivity to subjective weighting schemes [5], [7]. These developments are particularly relevant in the context of sustainable innovation, where complex and data-intensive decision environments require advanced analytical support.

References

[1] G. Friede, T. Busch, and A. Bassen, "ESG and financial performance: aggregated evidence from more than 2000 empirical studies," *J. Sustain. Finance Invest.*, vol. 5, no. 4, pp. 210–233, Oct. 2015, doi: 10.1080/20430795.2015.1118917.

[2] R. G. Eccles, I. Ioannou, and G. Serafeim, "The Impact of Corporate Sustainability on Organizational Processes and Performance," *Manag. Sci.*, vol. 60, no. 11, pp. 2835–2857, 2014.

[3] A. Ishizaka and P. Nemery, *Multi-Criteria Decision Analysis: Methods and Software*, 1st ed. Wiley, 2013. doi: 10.1002/9781118644898.

[4] M. J. Page *et al.*, "The PRISMA 2020 statement: an updated guideline for reporting systematic reviews," *BMJ*, vol. 372, p. n71, Mar. 2021, doi: 10.1136/bmj.n71.

[5] F. Berg, J. F. Kölbel, and R. Rigobon, "Aggregate Confusion: The Divergence of ESG Ratings," *Rev. Finance*, vol. 26, no. 6, pp. 1315–1344, Nov. 2022, doi: 10.1093/rof/rfac033.

[6] Y. Liu, J. Osterrieder, B. Hadji Misheva, N. Koenigstein, and L. Baals, "Navigating the Environmental, Social, and Governance (ESG) landscape: constructing a robust and reliable scoring engine - insights into Data Source Selection, Indicator Determination, Weighting and Aggregation Techniques, and Validation Processes for Comprehensive ESG Scoring Systems," *Open Res. Eur.*, vol. 3, p. 119, Jul. 2023, doi: 10.12688/openreseurope.16278.1.

[7] M. Billio, M. Costola, I. Hristova, C. Latino, and L. Pelizzon, "Inside the ESG ratings: (Dis)agreement and performance," *Corp. Soc. Responsib. Environ. Manag.*, vol. 28, pp. 1426–1445, Sep. 2021, doi: 10.1002/csr.2177.

[8] E. Dimson, P. Marsh, and M. Staunton, "Divergent ESG ratings," Nov. 2020, doi: 10.17863/CAM.55949.

Strengthening University Disaster Preparedness: Cross-Country Intervention Strategies from the DRU Project

Konstantinos Plachouras[1], Zoi Nikiforidou[2], Dimitrios Panagiotou[3], Jenny Pange[4]

[1]Department of Speech and Language Therapy, University of Ioannina, 45500 Ioannina, Greece,
kplachouras@uoi.gr, ORCID: 0000-0002-2769-1556,

[2] Department of Early Childhood Learning and Care at the University of Ioannina, 45500 Ioannina,
znikifor@uoi.gr , ORCID: 0000-0003-3371-271X

[3] Department of Economics, University of Ioannina, Ioannina, Greece,

dpanag@uoi.gr , ORCID: 0000-0001-7154-4169

[4]Laboratory of New Technologies and Distance Learning,

Department of Early Childhood Education, University of Ioannina, Ioannina, Greece,

jpagge@uoi.gr , ORCID: 0000-0002-1834

Corresponding author: *kplachouras@uoi.gr*

Abstract

The Disaster-Resilient Universities (DRU) project is an Erasmus+ initiative that aims to strengthen the capacity of higher education institutions to prevent, prepare for, respond to, and recover from natural disasters. Bringing together five partner universities from Albania, Bosnia and Herzegovina, Greece, Italy, and Romania, the project promotes collaborative resilience, exchange of practices, information literacy, and digital readiness in relation to hazards such as fires, floods, and earthquakes.

This paper presents the project through the lens of dissemination and public engagement, with particular emphasis on the dissemination event organized by the University of Ioannina on 16 February 2026. The event addressed key themes such as earthquake protection, the need to inform students about natural disasters, students' perception of disaster risk, and their existing knowledge of natural hazards. In this way, it functioned not only as a presentation of project activities, but also as a space for dialogue, reflection, and awareness-raising within the academic community.

Overall, DRU shows that disaster resilience in higher education depends not only on procedures and planning, but also on education, participation, and shared responsibility. The project offers a valuable model for building more informed, prepared, and resilient university communities.

***Keywords**: Disaster-Resilient Universities (DRU); higher education resilience; disaster preparedness; natural hazard awareness; institutional resilience; student engagement; dissemination; Erasmus+; UN SDG 4; UN SDG 11; UN SDG 13.*

a-side-project.eu/deeptech-connect-conference-2026

The First DeepTech Connect International Conference 2026

Strengthening University Disaster Preparedness: Cross-Country Intervention Strategies from the DRU Project

Konstantinos Plachouras[1], Zoi Nikiforidou[2], Dimitrios Panagiotou[3], Jenny Pange[4]
[1]*Department of Speech and Language Therapy, University of Ioannina, Greece*
[2]*Department of Early Childhood Learning and Care, University of Ioannina, Greece*
[3]*Department of Economics, University of Ioannina, Greece*
[4]*Laboratory of New Technologies and Distance Learning, University of Ioannina, Greece*
contact: kplachouras@uoi.gr

DeepTech CONNECT

Erasmus+ Enriching lives, opening minds. Co-funded by the European Union
DRU
Disaster Resilient Universities
"we collaborate in building disaster resilient communities across Europe"

BACKGROUND & RATIONALE

- Universities face growing risks from natural hazards and disruptions
- These affect infrastructure, teaching, participation, and well-being
- Preparedness should be a shared institutional responsibility
- Resilience means the ability to anticipate, adapt, and recover
- University Resilience depends on: planning, communication, support, and flexibility
- DRU : a more integrated + human-centered approach to preparedness

OBJECTIVES & DEVELOPMENT APPROACH

DRU was developed to **help universities move** beyond fragmented emergency procedures toward more coherent, participatory, and forward-looking preparedness practices. Its goals can be grouped into four interconnected areas:

1. Collaborative resilience
Strengthen cooperation and shared learning among partner universities

2. Awareness & literacy
Improve disaster awareness, information literacy, and risk understanding.

3. Structured preparedness
Support clearer preparedness, response, and continuity-oriented practices

4. Communication in disruption
Enhance the capacity of academic communities to communicate and act effectively.

The project adopts a multi-layered approach that combines institutional cooperation, exchange of practices, contextual understanding of risk, and dissemination within the academic community. Its collaborative and transferable character supports more consistent preparedness models across institutions.

DISSEMINATION ACTIVITY & PUBLIC ENGAGEMENT

In DRU, dissemination is treated not as a secondary promotional task, but as part of resilience-building itself. The dissemination event organized by the University of Ioannina on 16 February 2026 created a structured space for dialogue, reflection, and awareness-raising within the academic community. It connected project ideas with public discussion and highlighted the role of student engagement in translating institutional preparedness into lived awareness.

EVENT FOCUS | UNIVERSITY OF IOANNINA | 16 FEBRUARY 2026

- Earthquake protection and post-event response
- The need to inform students about natural disasters
- Students' perception of disaster risk
- What students should know about natural hazards

DISCUSSION & IMPACT

DRU reframes preparedness from a narrowly technical concern to a broader institutional and educational responsibility. Its impact can be understood at three interconnected levels:

Institutional
Links preparedness with awareness, communication, shared responsibility, and a stronger culture of readiness within universities.

Educational
Brings resilience closer to students and staff by making disaster-related issues discussable, relevant, and participatory.

Societal
Positions universities as multipliers of resilience-oriented knowledge and practice with broader public value.

KEY FINDINGS AND IMPLICATIONS

- Disaster preparedness in higher education is **strengthened** through awareness, participation, and institutional collaboration.
- Dissemination activities can function as educational practices that **connect** project outputs with student-centred engagement.
- *DRU offers a transferable example for **building** safer, more informed, and more responsive university communities.*

ACKNOWLEDGMENTS / FUNDING

Developed within the Erasmus+ project Disaster-Resilient Universities (DRU), KA220-HED – Cooperation partnerships in higher education. Project No. 2024-1-EL01-KA220-HED-000246753.
The authors gratefully acknowledge the support of the European Union and the contribution of all DRU consortium partners.



Figure 1. Dissemination event programme (University of Ioannina, 16 February 2026).

Coordinated by
RawMaterials Connecting matters
ClimateKIC Digital Food Health Manufacturing UrbanMobility Culture & Creativity
eit-hei.eu
@EIT Higher Education Initiative

DeepTech CONNECT
A-SIDE

Acknowledgements / Funding

This work was developed in the framework of the Erasmus+ project Disaster-Resilient Universities (DRU), under KA220-HED – Cooperation partnerships in higher education. The authors gratefully acknowledge the support of the European Union and the contribution of the DRU consortium: the University of Ioannina (coordinator, Greece), the Mediterranean University of Albania (Albania), Javna Ustanova Univerzitet u Zenici / Universitas Studiorum Zeniensis (Bosnia and Herzegovina), Istituto ad Ordinamento Universitario "Scuola Superiore Carolina Albasio" (Italy), and Universitatea Ovidius din Constanța (Romania), Project No. 2024-1-EL01-KA220-HED-000246753.



User-Driven, Digital, and Cultural Innovation

Rethinking Personal Safety Through User-Driven Innovation

SAFER

Ivan Martin[1]

[1]SAFER [2]Mondragon Unibertsitatea, Mondragon, Spain

Contact email: ivan.martina@alumni.mondragon.edu

Executive Summary

SAFER is an emerging venture focused on addressing the growing problem of street violence and personal insecurity in Spain and across Europe. As urban crime rates and public safety concerns continue to rise, particularly among young people and women, SAFER aims to deliver an innovative, user-centered solution tailored to real needs identified through in-depth market research and customer segmentation.

The project is currently in the validation phase, where insights from target users (primarily individuals aged 16 to 40, with a strong emphasis on women) are shaping the development of a dedicated safety solution. While an initial concept involving a physical device has been explored, this approach remains provisional and is currently on hold, as further validation is required to determine its fit with the identified customer segment.

The proposed solution framework focuses on integrating key functionalities such as deterrence of potential aggressors, real-time alerting to emergency services, immediate notification to trusted contacts, and activation of the surrounding environment to increase situational awareness. Additionally, SAFER aims to ensure that any developed solution supports users in acting within legal self-defense boundaries.

SAFER's key innovation lies in its demand-driven design approach, ensuring that the final product is not only technologically effective but also aligned with the expectations, concerns, and behaviors of its users. Unlike conventional safety tools, SAFER seeks to combine prevention, response, and post-incident protection into a cohesive and adaptable system.

Looking forward, the strategic vision of SAFER is to develop a scalable and adaptable safety solution that contributes to safer communities, while positioning itself within a rapidly growing market for personal security. The project also aligns with broader societal goals by promoting safety, well-being, and inclusive access to protection technologies.

Keywords: SAFER; personal safety; street violence prevention; security solution; user-centered design; emergency alert system; innovation; market validation;
UN SDG 3; UN SDG 11; UN SDG 16

1. Company Overview

SAFER is an early-stage venture focused on developing innovative solutions to address the growing challenge of street violence and personal insecurity. The company's mission is to enhance individual safety through accessible, user-centered technologies that empower people to prevent, respond to, and manage risk in everyday environments.

Positioned within the innovation ecosystem, SAFER operates at the intersection of safety technology, user experience design, and data-driven product development. Rather than relying solely on predefined technological

assumptions, the company adopts a research-based approach grounded in extensive market analysis and customer segmentation.
At its current stage, SAFER's core expertise lies in identifying unmet user needs, translating them into actionable product requirements, and designing scalable safety solutions aligned with real-world behaviors and constraints. This positions the company as a demand-driven innovator within the emerging personal security technology space.

2. Technology / Product / Service Description

SAFER is developing a validated, user-driven safety solution framework aimed at reducing the risks associated with street aggression and personal insecurity. The project is currently in the validation phase, where insights from market research and user segmentation are directly informing the design of the solution.
An initial concept involving a physical device has been explored and developed at a conceptual level (including functionality definition and system design), integrating elements such as deterrence mechanisms, real-time emergency alerting, communication with trusted contacts, and environmental awareness activation. However, this approach is currently paused, as the project has shifted towards designing a solution fully tailored to validated user needs.
The underlying foundation of SAFER's approach combines principles of human-centered design, real-time communication systems, and integrated response mechanisms. The goal is to create a cohesive solution capable of operating effectively in high-stress, real-world scenarios while remaining intuitive and legally compliant.

3. Innovation and Competitive Advantage
SAFER's primary differentiator lies in its demand-driven innovation model. Unlike many existing safety solutions that are technology-first, SAFER prioritizes validated user needs as the starting point for product development.
This approach enables the company to design solutions that are more closely aligned with actual user behaviors, increasing both adoption and effectiveness. Additionally, SAFER aims to integrate multiple layers of safety (prevention, real-time response, and post-incident support) into a single unified system, rather than offering fragmented tools.
The project's competitive advantage is further reinforced by its focus on usability, legal compliance, and contextual adaptability (ensuring that users can act confidently and appropriately in critical situations).

4. Market Application and Impact
SAFER targets a rapidly growing market driven by increasing concerns around personal safety in urban environments. The project is supported by extensive market research, including both quantitative surveys and qualitative interviews conducted in person, which consistently indicate a clear and unmet need for more effective and user-adapted safety solutions.
The primary user segment includes individuals aged 16 to 40 (particularly women), while the economic buyer may often be family members seeking safety solutions for their dependents.
The solution is designed to be scalable across multiple contexts (including urban mobility, nightlife environments, and daily commuting scenarios), with the potential to expand into broader safety and security applications.
From a societal perspective, SAFER aims to contribute to safer communities by providing individuals with effective tools to prevent and respond to violence. The project aligns with broader social impact objectives (including improved well-being, increased public safety awareness, and enhanced access to protection technologies).

These findings strongly validate the existence of a clear market gap and reinforce the relevance of SAFER's proposed solution.

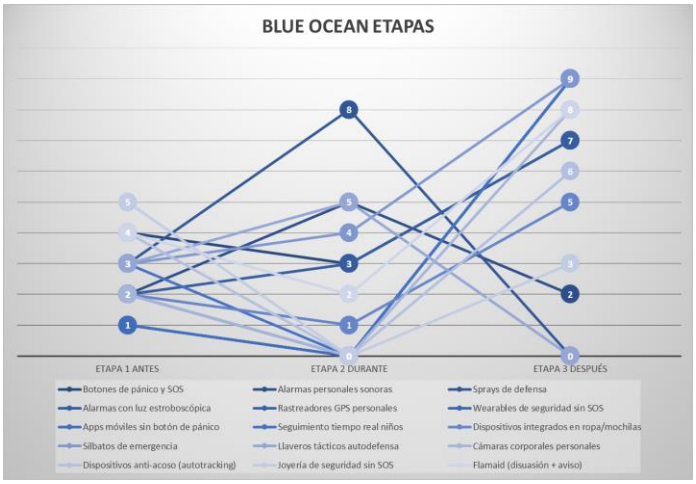


Figure 45 Blue ocean strategy analysis of personal safety solutions across prevention, real-time response, and post-incident phases.

5. Partnerships and Outlook

SAFER is open to establishing collaborations with individuals, organizations, and institutions interested in contributing to the development and growth of the project. This includes potential partners who can provide support through knowledge, technical expertise, or financial resources.

The project actively welcomes opportunities to connect with stakeholders who share an interest in improving personal safety and are willing to contribute in different capacities (whether through investment, research collaboration, or strategic guidance).

In the coming stages, SAFER plans to transition from market validation to prototype development, followed by user testing and iterative refinement. Investment and collaboration will play a key role in enabling this progression, particularly in areas such as product engineering, validation, and go-to-market strategy.

The long-term outlook involves scaling the solution across different markets and establishing SAFER as a relevant player in the personal safety technology sector.

Acknowledgements (Optional)

I would like to express my sincere gratitude to **German Anitua** and **Maider Beitialarrangoitia** for their guidance, support, and valuable insights throughout the development of this project.

1. Ivan Martin. SAFER

The role of Avatar in Business – the case study of a company Priče iz Kanca

Jelena M. Pavlović Jovanović[1], Nataša Spasić[2], Milan Todorović[3]

[1]*Centre for Scientific Research, Faculty of Philology and Arts, University of Kragujevac, Serbia, jelena.pavlovic@filum.kg.ac.rs, 0000-0002-4399-7360*
[2] *natasa.spasic@filum.kg.ac.rs, 0009-0006-7896-3546*

[3] *milan.todorovic@filum.kg.ac.rs, 0000-0001-6699-7956*

Corresponding author: jelena.pavlovic@filum.kg.ac.rs

Abstract

In this paper, we analyzed the possibility of using the avatar concept in the case study of the company *Priče iz Kanca Milice Malešević*. The research was conducted in March 2026. The term avatar is understood in this paper in two ways: avatar as a concept in marketing and avatar as a substitute for a person/company in the digital world. In the first part of the research, we tested the language model ChatGPT-5 for its capabilities to be used in designing the ideal customer avatar. In the second phase of the research, we qualitatively explored the possibility of using 2D avatars and chatbot avatars of the company *Priče iz Kanca* to define concrete objectives. This research, although limited to a single company, demonstrates great potential for the use of artificial intelligence both in defining the ideal customer (theoretical basis, question refinement, persona definition) and in enabling a company to create an avatar of its brand using artificial intelligence capabilities.

Keywords: avatar; marketing; artificial intelligence; consumer journey; design thinking; brand value; UN SDG 8; UN SDG 9

1. Introduction

In the context of online business, the term avatar is mentioned in at least two senses, both of which we will use in this paper. The first equates the notion of an avatar with that of the ideal customer, the persona for whom a particular service or product is intended. This meaning of the term avatar is found, for example, in the training program conducted by Milica Malešević, the founder of the company *Priče iz Kanca*. In her workbook that accompanied the avatar training, Milica Malešević defines the avatar concept as follows: "An avatar is the prototype of a person imagined by you and all your collaborators from the moment of choosing the logo and the color for the website, through creating and designing advertisements, to selecting promotion channels and methods of sale." [1] In design thinking the avatar is equated with the persona, which is defined as a "personalized empathy map." The persona is given a name and human characteristics (needs, desires, fears). In this sense, the concepts of the customer journey and user experience maps are also important. [2] On the other hand, the term avatar is also used in the meaning: "an animated graphical representation of an internet user or a digital game player." [3] A special type of avatar is a virtual agent that companies use to communicate with users, especially in online environments. [4] This type of avatar personifies brand values. [5] With the advent

of artificial intelligence, more and more avatars or virtual assistants (agents) are being used in the form of chatbots. [6] In the context of this paper, the aim is to examine how the concept of the avatar is used in the era of artificial intelligence, focusing on a single company. The company in question is *Priče iz Kanca* from Belgrade, which offers business education services to individuals and companies, and which uses the avatar concept in a twofold manner. The first is the avatar in the sense of the ideal customer, the persona. The company offers this within its entrepreneurship trainings, specifically as part of the Preparations for Entrepreneurship program. The second way the term avatar is used is a chatbot in the form of an avatar of Milica Malešević, which is available on the company's website and allows potential users to try collaborating with Milica Malešević. [7]

2. Materials and Methods

The research was conducted in two stages during March 2026. First, we tested the possibility of defining an avatar via the open large language model GPT-5 by OpenAI. The first stage of the research had two phases: (a) Examination of the artificial intelligence (the free version of the large language model), i.e., the model's knowledge about artificial intelligence; (b) Description of the description of the created avatar based on the questions from Milica Malešević's workbook about the readers of the first researcher's book, as well as creating a persona and a consumer journey map for a possible path to the product. The second stage of the research was conducted on the *Priče iz Kanca* website and included an analysis of the dialogue with the chatbot of Milica Malešević, which is powered by the Pickaxe program. [8] This is the company's avatar, and the terms of use and privacy policy are provided in detail. We used only publicly available materials, without access to the company's internal functioning or the avatar development process. The topic of the conversation was setting goals for selling the first researcher's book in bookstores in the city of Kragujevac. The conversation data were collected and analyzed using qualitative methods: thematic, stylistic, and pragmatic analysis.

3. Results

We present the research results in two separate sections. In Section 3.1, we present the results of the investigation of the avatar as a persona in marketing, using the large language model ChatGPT-5 as an example. In Section 3.2, we present the results obtained from the analysis of the avatar of the company *Priče iz Kanca*.

3.1. Avatar as the ideal customer – possibilities of using large language models

The research showed that large language models can be very useful tools for defining an avatar as the ideal customer. In the first stage of the study, we asked the ChatGPT-5 model about the possibility of defining an avatar in marketing. The artificial intelligence associated the concept of an avatar with a persona or ideal customer and divided its characteristics into several categories: demographics, psychology and interests, problems and needs, and how they conduct themselves during purchase. It provided an example of an avatar for an academic writing course (having recognized that the subject was a researcher, although it assumed the researcher was male) and offered suggestions for what an avatar can be used for. It described the tool as the "imagined ideal customer you address in marketing" (communication with the model, 15.3.2026).

The next prompt was: "Specify how to create an avatar step by step." The response included: definition of the problem; definition of the target group; description of demographics and creation of a basic profile (fictional name, age, place of residence, education, occupation); determination of goals (what is their professional goal and how they define success); uncovering problems and frustrations (what prevents them from achieving the goal); understanding purchase motives; identifying places where they seek information; and writing a short story about the avatar. The model produced the following description at the end: "Milica is 30 years old and an assistant at a university. She is working on her doctoral dissertation and must publish a paper in an international journal. Although she knows her topic well, she is insecure about the structure of a scientific paper in English. She fears that her paper will be rejected, so she is looking for a course that will help her write more confidently and professionally." (conversation with the model, 15.3.2026). The artificial intelligence also offered additional steps when defining an avatar (formulas for copywriting in advertisements, formulas for customer analysis). In the second stage of the study, we asked the artificial intelligence to create an avatar for the first researcher's book. The model designed an avatar based on questions from Milica Malešević's workbook, generated an image of the avatar, provided a description of her daily activities, described a possible consumer journey, and created a map of bookstores in Kragujevac where the book could be sold.

3.2. Results of the descriptive analysis of the avatar of *Priče iz Kanca*

The avatar of the company *Priče iz Kanca* is clearly based on Milica Malešević, who has her own personal brand and who here represents the content, i.e., the signified. The signifier is a 2D photograph of Milica Malešević with a purple background and wearing black glasses, which suggests that the communication takes place in a digital environment. The avatar in this case is a chatbot that imitates Milica Malešević's manner of communication and serves to promote and demonstrate the brand's values and to show potential customers the way the company provides business education; in this role, the avatar clearly functions as a transmitter of brand values. Two functional registers are present. The first is the legal-legislative register, which is tied to detailed descriptions of the terms of use and data retention (with references to laws in Serbia and the European Union). The conversation with the chatbot was conducted on the topic of selling the first author's book in Kragujevac bookstores. The dialogue took place over eight iterations. It unfolds in an intimate, informal style, which is a characteristic of Milica Malešević in the public and social-media communication. Emojis are also used. The exchange consists of chatbot prompts and user responses (in this case, the researcher). In the first part, the bot summarizes and clarifies what the user (the researcher) said and gives a positive evaluation. The second part, opened by discourse markers *Ajde (sad)…* and *E sad…*, which mark the boundaries in segments of communication [9], provides additional explanation for the next step (defining a measurable goal, defining the physical space, defining timeframes). In the third part, concrete questions are reached. The conversation was predefined to respect communication rules, but the model also answers questions unrelated to business ("How are you?"). At the end, the model produces a PDF containing the key points from the conversation and the defined goals that can be used for the company's further work.

4. Discussion and conclusion

The main limitation of this study is the choice of a single case study as the method and the restriction to one company. Nevertheless, these results point to two possible directions for interpreting avatars in marketing with the use of artificial intelligence. The first is the capabilities of artificial intelligence to define the profile of the ideal customer. The second possibility is the creation of avatar models for different companies and the analysis of the language they use. There are numerous implications for further research, both in the area of linguistic analysis of interaction with avatars (stylistic, linguistic, pragmatic) and with regard to the conceptual definition of the avatar. Practically, the study demonstrates many opportunities for applying avatars in day-to-day company tasks, especially within the design-thinking process, both in defining the avatar as the ideal customer and in creating avatars for specific companies.

Acknowledgements

The research presented in this paper was funded by the Ministry of Science, Technological Development and Innovation of the Republic of Serbia (Agreement on the transfer of funds for financing scientific research work of researchers at accredited higher education institutions in 2026, number: 451-03-33/2026-03/200198).

References

1. Malešević, M. Avatar – radna sveska. Beograd, 2025, 1–25, material sa besplatnog treninga, citirano s dozvolom.

2. Jevtić, M., Dekić, M. Design thinking – kako da stvarate proizvode koje ljudi žele. Beograd: Finesa. 2026.

3. AYTAÇ, Z. Avatar based marketing, The Essentials of Today's Marketing, eds. Mehmet BAŞ, İnci ERDOĞAN TARAKÇI, Ramazan ASLAN, Efe Akademik Publishing, Istambul, 2023, 382–399.

4. AYTAÇ, Z. Avatar based marketing, The Essentials of Today's Marketing, eds. Mehmet BAŞ, İnci ERDOĞAN TARAKÇI, Ramazan ASLAN, Efe Akademik Publishing, Istambul, 2023, 382–399.

5. Vadalà, O. The Power of Avatar Marketing: Enhancing Customer Experience, unpublished master thesis, Luiss: Master's Degree in Management, https://tesi.luiss.it/37243/1/745001_VADALA%27_ORNELLA.pdf.

6. Halim N. A. A., Suaib N. M., Fadzli F. E., AI-powered avatar assistants: a systematic literature review of tools, application domains and challenges. Journal of Ambient Intelligence and Humanized Computing. 2026; 17(2):1-38.

7. Avatar available at: https://www.priceizkanca.com/milicai-ciljevi.

8. Program available at: https://pickaxe.co/

9. Schiffrin, D. Discourse Markers. Cambridge: Cambridge University Press. 1987.

InTransparency - Verified Talent Marketplace

A Deep-Tech Platform Architecture for AI-Act-Ready Higher-Education Credentials

Fabio Chefane[1]

[1]*InTransparency, Kilometro Rosso, Bergamo, Italy*

Contact: info@in-transparency.com | in-transparency.com

Executive Summary

InTransparency is a three-sided digital marketplace being built to replace self-declared résumé claims with credentials issued directly by higher-education institutions. The platform targets a structural failure in the Italian and wider European junior labour market, where self-reported skills drive an approximately 30% hiring mismatch rate and an average cost-per-bad-hire exceeding €4,000. By ingesting concrete academic output — theses, examination transcripts, code repositories with commit history, internship deliverables, and faculty endorsements — the platform will produce machine-readable skill credentials that travel with the student across employer systems and, in the medium term, the EU Digital Identity Wallet.

The technology stack is designed around European interoperability standards: W3C Verifiable Credentials with Ed25519 as the reference proof suite; ESCO v1.2.0 skill mapping for cross-border portability; EDCI and Europass v3 JSON-LD exports; Open Badges 3.0 emission. Because the matching component operates in a high-risk use case under Annex III §4 of the EU AI Act, the company is preparing to act as a deployer under Article 26 — whose obligations entered into force on 2 February 2026. The architecture is being developed around the corresponding deployer controls (human oversight, automated-decision logging, DPIA, transparency notices to affected persons), with a staged compliance roadmap targeting full conformity before general availability.

The commercial model is freemium for students and institutional partners, with revenue generated through a pay-per-contact mechanism for employers (€10 per verified contact unlock). The company has been recognised with two prizes at StartCup Bergamo 2025/26, including the Premio Fondazione Pesenti, and operates an active pilot with the Università degli Studi di Bergamo. The 18-month plan targets 5,000 verified student profiles and 120 paying employers across Italy, with European expansion enabled natively by the underlying standards stack once domestic traction is validated.

Keywords: *verified credentials; EU AI Act compliance; W3C Verifiable Credentials; ESCO skill graph; higher-education–industry matching; talent marketplace; Europass; pay-per-contact; UN SDG 4; UN SDG 8; UN SDG 9*

1. Company Overview

InTransparency is an Italian deep-tech start-up building the trust layer between European higher-education institutions and the labour market. The company is headquartered at Kilometro Rosso (Bergamo) and is in the process of incorporation as an SRL Startup Innovativa. The founding mission is to make academic merit verifiable and portable — moving hiring decisions, over time, away from self-declared credentials toward institution-signed evidence of real work.

Founded	2025 — Bergamo, Italy
Legal Form	SRL Startup Innovativa (in formation)
Founders	Fabio Chefane (CEO) + Co-founder
Recognition	2 prizes — StartCup Bergamo 2025/26, incl. Premio Fondazione Pesenti
Pilot	Università Varie e ITS

The problem we verify

European hiring for early-career roles suffers from three compounding inefficiencies: (i) self-declared credentials that cannot be machine-verified; (ii) opaque matching algorithms that neither candidates nor employers can audit; and (iii) fragmented skill taxonomies that block cross-border mobility. The first produces a measured ~30% skill-match error rate; the second is now a regulated risk under the EU AI Act; the third contradicts the EU's own ESCO framework and the Europass Digital Credentials stack.

2. Technology & Product

The platform is being developed around three integrated subsystems: a credential issuance engine, a standards-native skill graph, and an AI matching layer. Each is architected against an explicit European regulatory or standards instrument rather than being retrofitted after the fact, so that conformity obligations are satisfied by design as the corresponding modules reach production.

2.1 Credential issuance pipeline

Student work is ingested in its native form — structured transcripts, GitHub repositories (with commit-history inspection), PDF dissertations, multi-format portfolios and faculty endorsements — and processed through a three-tier pipeline. The tiers combine fully automated extraction for structured sources, semi-automated processing with quality checks for mixed-format material, and a human-in-the-loop review layer for unstructured edge cases. The credential schema is being implemented to the W3C Verifiable Credentials Data Model 1.1, with Ed25519Signature2020 as the reference proof suite and institutional public keys to be published for offline verification as each institution is onboarded.

2.2 Standards-native interoperability roadmap

Layer	Implementation
Verifiable Credentials	W3C VC Data Model 1.1 with Ed25519Signature2020 as the reference proof suite; institutional public keys to be published for third-party verification.
Skill Graph	Mapping against ESCO v1.2.0; API fallback for unmapped terms; design targets cross-border portability across the 27 EU member states.

Layer	Implementation
Digital Credentials	EDCI JSON-LD export schema with EQF level (3–6) and ISCED-F codes, to be enabled as issuing institutions are onboarded.
Profile Export	Europass v3 JSON-LD export and Open Badges 3.0 emission for the Advanced/Expert skill tier (planned).
Competence Frameworks	DigComp 2.2, EntreComp 1.0, GreenComp 1.0 — integration into the unified skill catalogue on roadmap.
Recognition	Bologna Process (ECTS) grade normalisation and Erasmus OLA JSON-LD export for exchange enrolments (roadmap).
Identity	eIDAS 2.0 — SPID/CIE integration under development; EUDI Wallet consumption planned once reference implementations stabilise.

Table 1. European standards the platform architecture is being developed against.

2.3 AI Act deployer posture for the matching layer

The matching functionality integrates a third-party general-purpose AI model; accordingly, the company is preparing to operate as a deployer of a high-risk AI system under Article 26 of Regulation (EU) 2024/1689 (EU AI Act), rather than as a provider. The use case — AI used for candidate evaluation in an employment context — falls within Annex III §4, and deployer obligations entered into force on 2 February 2026. The compliance roadmap is being built around the obligations that apply to a deployer in this posture: human oversight of the matching layer with authority to override and withdraw outputs; logging of automated decisions and their rationale; a Data Protection Impact Assessment consistent with GDPR Article 35; transparency notices to affected students under Article 26(11); and defined procedures for cooperation with national market-surveillance authorities. Data residency is EU-Central (Neon PostgreSQL), and GDPR Articles 15/16/17/20/22 rights are being exposed as self-service actions in the student dashboard. Full deployer conformity is targeted ahead of the public launch of matching features to employers.

3. Innovation & Competitive Advantage

InTransparency is positioned in a market segment no Italian competitor currently addresses: junior white-collar recruiting, verified at source, across every academic discipline. The combination of a zero-upfront-cost model for institutions and employers, a cryptographic verification design, and standards-native interoperability is intended to constitute a compound structural advantage over both incumbent recruitment databases and current AI-powered hiring tools as the architecture reaches production.

Dimension	InTransparency	AlmaLaurea	LinkedIn Recruiter	Agencies
Database access	**Free**	€2,500/yr	€8,000/yr	N/A
Cost per hire	**€100 (≈10 contacts)**	€2,500+	€8,000+	€15,000
Skill verification	**Institution-signed**	Self-declared	Self-declared	Manual

Dimension	InTransparency	AlmaLaurea	LinkedIn Recruiter	Agencies
ESCO / Europass export	**Native**	Partial	No	No
AI Act posture	**Deployer controls (roadmap)**	Not published	Not published	N/A
Cryptographic proof	**W3C VC + Ed25519 (planned)**	None	None	None

Table 2. Competitive comparison across commercial, verification and regulatory dimensions.

Defensible moats

- **Institutional data agreements:** verified academic data sourced directly from issuing institutions, unavailable through any third-party recruitment channel.
- **Cryptographic portability (roadmap):** each credential is designed to be independently verifiable offline via published Ed25519 public keys — a model competitors cannot replicate without reissuing from source.
- **Regulatory posture:** building deployer-side controls (human oversight, logging, DPIA, transparency notices) into the matching layer from day one is a multi-quarter engineering and governance programme that incumbent platforms will have to retrofit into existing systems.
- **Three-sided network effect:** more verified students attract more employers; more paying employers fund more institutional onboarding; more institutions enrich the skill graph.

4. Market Application & Impact

The platform addresses two validated pain points with direct quantitative expression. For employers, each bad hire driven by unverified skill claims carries a documented loss above €4,000; reducing even one in three of these in a 50-hire pipeline recovers more than €60,000 annually. For a 10,000-student university, the manual placement-tracking workload modelled against standard career-service staffing approaches 4,000 hours per year — time reallocable to higher-value advising once verified evidence replaces manual surveys.

€186K Revenue target	**€146K** Net profit (18 mo)	**90%** Gross margin	**5,000** Student profiles

Three-sided commercial model

Segment	Pricing	Role
Students	**Freemium — core free; optional Premium tier**	Primary beneficiary. Zero friction on supply side. Premium adds job-search productivity tools.
Institutions	**Freemium — Core free; Premium (custom quote)**	Source of verified data; Core includes unlimited profiles and analytics; Premium adds enterprise integrations and custom services.

Segment	Pricing	Role
Employers	**€10 per verified contact unlock (credit packs) or subscription**	Sole monetisation engine. ~90% gross margin. Volume packs for 50–1,000+ credits. Optional subscription tiers for higher-volume buyers.

Table 3. Three-sided marketplace structure.

Alignment with the UN Sustainable Development Goals

- **SDG 4 (Quality Education):** the platform validates real academic output as labour-market-relevant formative evidence, strengthening the employment signal of higher-education institutions (target 4.4).
- **SDG 8 (Decent Work and Economic Growth):** by removing résumé-based screening noise and reducing SME recruitment cost barriers, the platform directly addresses youth employment friction (target 8.6).
- **SDG 9 (Industry, Innovation and Infrastructure):** the standards-native verified-credential design and the AI-Act-aware matching architecture are intended to constitute digital infrastructure for the European labour market (target 9.5).

5. Partnerships & Outlook

The platform is in active institutional dialogue with Italian universities and Istituti Tecnici Superiori (ITS). Structured outreach covers more than sixty-five institutions across the five Italian macro-regions, with confirmed meetings at Università Cattolica del Sacro Cuore (Stage & Placement team, Milan campus) and ITS Tech&Food Academy Emilia-Romagna (May 2026). The European roadmap leverages the standards stack — ESCO, Europass, EDCI — to enable zero-rework expansion into further EU member states once domestic validation is complete.

Near-term roadmap

- **Q2–Q3 2026:** expand active pilots from one to five universities; reach 1,500–2,500 verified student profiles; onboard 40–60 paying employers.
- **Q4 2026:** activation of institutional Premium tier and first enterprise employer contracts.
- **2027:** EU multilingual expansion (priority: DE, ES, FR); ISO/IEC 42001 AI-management-system certification; EUDI Wallet consumption once reference implementations reach public beta.

Acknowledgements

The authors acknowledge StartCup Bergamo and Fondazione Pesenti for award recognition; the Università degli Studi di Bergamo (Prof. Campopiano, Dipartimento di Ingegneria Gestionale) for early institutional engagement; and the Kilometro Rosso innovation ecosystem for operational support.

References

1. European Parliament, Council of the European Union. Regulation (EU) 2024/1689 laying down harmonised rules on artificial intelligence (AI Act). Off J Eur Union. 2024;L series. Available from: https://eur-lex.europa.eu/eli/reg/2024/1689/oj

2. European Parliament, Council of the European Union. Regulation (EU) 2016/679 on the protection of natural persons with regard to the processing of personal data (GDPR). Off J Eur Union. 2016;L119:1–88.
3. Sporny M, Longley D, Chadwick D. Verifiable Credentials Data Model v1.1. W3C Recommendation. 2022 Mar 3. Available from: https://www.w3.org/TR/vc-data-model/
4. European Commission, DG Employment, Social Affairs and Inclusion. ESCO — European Skills, Competences, Qualifications and Occupations, version 1.2.0. 2024.
5. European Commission, DG Education, Youth, Sport and Culture; CEDEFOP. Europass Digital Credentials Infrastructure (EDCI). 2024.
6. IMS Global / 1EdTech. Open Badges Specification, version 3.0. 2023.

DeCiTeL (Democratic Citizenship Teaching and Learning)

Jenny Pange[1], Zoi Nikiforidou[2]

[1]*Laboratory of New Technologies and Distance Learning,*

Department of Early Childhood Education, University of Ioannina, Ioannina, Greece,

jpagge@uoi.gr , ORCID: 0000-0002-1834

[2] *Department of Early Childhood Learning and Care at the University of Ioannina, 45500 Ioannina,*
znikifor@uoi.gr , ORCID: 0000-0003-3371-271X

Abstract

DeCiTeL (Democratic Citizenship Teaching and Learning) is an Erasmus+ project under the Teacher Academies, gathering school communities across Europe [Turkey, Greece, France, Belgium, Italy, Romania, Austria] to enhance the teaching of citizenship education at all levels from early childhood to secondary school and equipping educators to empower students to actively contribute to a society grounded in respect, empathy, open-mindedness, and mutual understanding.

Established in 2025, the project aims to strengthen teacher education and to build a sustainable alliance of teacher training institutions that can provide reference models, joint European degrees, learning materials, new curricula elements and innovative training courses for teachers of early childhood, primary and secondary schools involved in the teaching of democratic citizenship education and, more in general, in the development of social, relational and civic competences for children and adolescents.

This paper presents information regarding the aims of the project, core aspects of civic education – citizenship as a discipline in the Greek educational system and the importance of local learning ecosystems in delivering and strengthening knowledge, skills, and values needed to participate actively, responsibly, and critically in democratic society. Special emphasis is given to digital citizenship as civic life now happens online, and everyone needs the skills to engage responsibly, think critically about information, and participate safely in digital communities and democratic processes.

Keywords: DECITEL; Teacher Academies Erasmus+; civic education, digital citizenship

a-side-project.eu/deeptech-connect-conference-2026

The First DeepTech Connect International Conference 2026

DeCiTeL (Democratic Citizenship Teaching and Learning)

Jenny Pange[1], Zoi Nikiforidou[1]
[1]*University of Ioannina*
contact: jpagge@uoi.gr , znikifor@uoi.gr

MOTIVATION & OBJECTIVES

DeCiTeL (Democratic Citizenship Teaching and Learning) is an Erasmus+ project under the Teacher Academies, gathering school communities across Europe to enhance the teaching of citizenship education at all levels from early childhood to secondary school and equipping educators to empower students to actively contribute to a society grounded in respect, empathy, open-mindedness, and mutual understanding.
Established in 2025, the project aims to strengthen teacher education and to build a sustainable alliance of teacher training institutions that can provide reference models, joint European degrees, learning materials, new curricula elements and innovative training courses for teachers of early childhood, primary and secondary schools involved in the teaching of democratic citizenship education and, more in general, in the development of social, relational and civic competences for children and adolescents.

PROJECT DETAILS

The DeCiTeL consortium comprises 13 institutions from 7 countries.



Figure 1. Project details

CITIZENSHIP – CIVIC EDUCATION: THE CASE OF Greece

The development of civic education in Greece reflects broader social and political transformations, with notable progress since the 1980s. However, there are still persistent challenges in teacher training, limited instructional time, and uneven curriculum implementation. While post-1990 European integration influenced a shift toward a more outward-looking perspective, strong ethnocentric traditions that are rooted in historical, cultural, and systemic homogeneity and slow reforms in education have maintained a greater emphasis on national over European and global dimensions. Despite these constraints, research shows that civic education in schools plays a key role in shaping students' democratic attitudes and participation, highlighting its continued importance in fostering active citizenship.
Recently there is growing interest in digital civic education – digital citizenship, as it refers to the skills citizens of all ages need to participate responsibly and critically in civic life through digital platforms and online communities.

Overall

→ a dynamic, inclusive, and value-driven field that blends core principles with national contexts, fosters creativity, and responds to teachers' evolving needs through participatory, peer-based, and whole-school approaches. It promotes innovation, collaboration, and cross-border exchange while remaining open to research and policy developments to better assess and strengthen civic competences.

https://decitel.bogazici.edu.tr/

LOCAL LEARNING ECOSYSTEMS

What is it? A local learning ecosystem (LLE) brings together CSOs, local authorities, universities, schools, teachers, and engaged citizens to co-create inclusive, participatory learning initiatives and contribute to DeCiTeL outputs with local stakeholders involved by the DeCiTeL consortium members and actively supporting the out-of-school dimension of citizenship education.

The role of the LLE includes supporting co-creation exchange of practices, promoting civic engagement, fostering social responsibility, and enhancing local capacity for citizenship education. The desired future impact with LLEs is to create a model that embodies citizenship education in everyday social and institutional life.

Disclaimer

Co-funded by the Erasmus+ programme of the European Union (Erasmus+ Teacher Academy). Views and opinions expressed are, however, those of the author(s) only and do not necessarily reflect those of the European Union or the European Education and Culture Executive Agency (EACEA). Neither the European Union nor EACEA can be held responsible for them.

Acknowledgement

DeCiTeL project (The New Road to a Sustainable Economic Strategy in the Textile Sector; project reference number 2023-1-TR01-KA220-VET-000165791) is co-funded by the European Union.

Co-funded by the European Union

Acknowledgements / Funding

Disclaimer

Co-funded by the Erasmus+ programme of the European Union (Erasmus+ Teacher Academy). Views and opinions expressed are, however, those of the author(s) only and do not necessarily reflect those of the European Union or the European Education and Culture Executive Agency (EACEA). Neither the European Union nor EACEA can be held responsible for them.

Acknowledgement

DeCiTeL project (The New Road to a Sustainable Economic Strategy in the Textile Sector; project reference number 2023-1-TR01-KA220-VET-000165791) is co-funded by the European Union.

Co-funded by the European Union

#DanceMuse: A Phygital Hybrid Museum for the Multisensory and Interdisciplinary Interpretation of Traditional Dance in Epirus

Hybrid Museum of Traditional Dance (#DanceMuse), ID 16289, Greece 2.0 – National Recovery and Resilience Plan (European Union-Next Generation EU), 2025 – 2026

Aikaterini Vasilaki[1], Melina Papadopoulou[1], Christina Nika[2], Dimitrios D. Vergados[2], Stavros Papapanagiotou[3], Apostolos Karalis[3], Christos Papakostas[1]

[1]*Department of Primary Education, University of Ioannina, Greece, a.vasilaki@uoi.gr, 0009-0007-2489-196X*
[2]*Department of Informatics, University of Piraeus, Greece, dcsciot@unipi.gr, 0000-0002-9436-0108*
[3]*Internet Business Hellas, Athens, Greece, sip@ibhellas.gr, 0009-0002-4112-5486*
Corresponding author: a.vasilaki@uoi.gr

Abstract

The #DanceMuse project aims to design and construct an innovative, hybrid-format museum focused on the traditional dance of the Epirus region in Greece. Intangible cultural heritage, particularly dance, often suffers from a lack of haptic and experiential connection when presented through traditional digital screens. This research project utilizes an interdisciplinary approach, combining Folklore, Anthropology, Dance Studies, and Informatics with Museology to create a multisensory cultural model. The methodology leverages state-of-the-art technologies including 3D scanning, motion capture, and Virtual/Augmented Reality (VR/AR) to develop a "phygital" environment for presenting ethnographic research material. The content of this cultural product consists of primary ethnographic research material, which was derived from fieldwork in the region of Epirus, Greece, focusing on traditional music and dance events and ritualistic practices within the communities' settings, combined with the digitization of relevant museum exhibits, the creation of accompanying material, and the utilization of secondary archival sources. Key results include a six-pillar technological ecosystem consisting of 2D/3D models, an interoperable repository, e-book publications, AR applications, a web portal, and a central VR booth that allows for interactive "hand-coupling" with digital dancers. By translating primary ethnographic fieldwork into both physical and digital environment with high-fidelity human kinesiological datasets, the project enables visitors to participate in performances in an embodied manner. The project demonstrates how the convergence of academic disciplines and advanced game engines (Unity) can resolve issues of documentation and interpretation in intangible heritage, ultimately providing a unique museological concept across both physical and digital manifestations.

Keywords: #DanceMuse; Dance Ethnography; Phygital Hybrid Museum; Intangible Cultural Heritage; Virtual Reality; Motion Capture; Epirus; Multisensory Experience; UN SDG 4; UN SDG 11.

1. Project Background and Objectives

The interpretation of intangible cultural heritage (ICH) faces a longstanding limitation: the inherent difficulty in creating an emotional and fully experiential connection between audiences and the heritage resource. The core research question of the #DanceMuse project (ΥΠ3ΤΑ-0561372) is: "How can a visitor truly *feel* the energy and societal impact of a traditional dance beyond the confines of a screen?"

The project focuses on the traditional dance practices in Epirus, Greece, aiming to promote living cultural heritage by presenting performances as holistic experiences with semantic and spatial connotations. Implemented under the Greece 2.0 National Recovery and Resilience Plan and funded by the European Union (Next Generation EU), the project seeks to design a digital and analog cultural model capable of interactively rendering the multisensory experience of traditional dance within a mixed-reality environment.

2. Methodology and Work Performed

To address the experiential gap in ICH, the project adopted an interdisciplinary approach that bridges technology and the humanities, enabling a novel, multisensory experience with dance performance. Our innovative methodology leverages the convergence of state-of-the-art technologies—3D digitisation (3D scanning) of objects, motion capture of human, and Virtual/Augmented Reality (VR/AR)—to design and develop a fully digital environment that allows users to *participate* in the performance in an embodied, immersive experience.

The system architecture follows a three-layer model (Fig. 1). At the first layer, high-resolution audiovisual assets are produced, alongside 3D models generated via photogrammetry and laser scanning, and human-motion datasets captured with motion-capture systems. At the second layer, the digital content is managed and processed within a consolidated repository/server, which supports storage, organisation, and data flows via REST APIs. At the third layer, a responsive web portal with the Digital Museum, complemented by the VR booth and AR applications that together constitute the project's phygital museum, delivering immersive, multisensory experiences to diverse audiences.

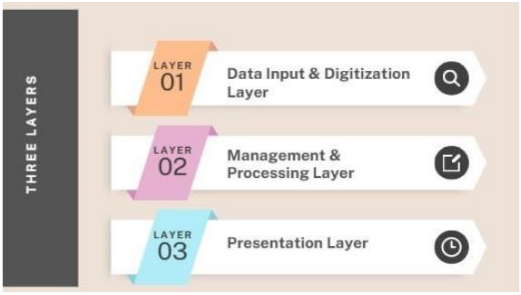


Figure 1: A three-tier structure

The conceptual design followed a three-concentric-ring model, placing the human immersive experience at the center, surrounded by the "cycle of life" and the "cycle of the seasons", following the circular notion of time and space of the traditional communities as opposed to the linear one of the post-modern era with a direct reference to the circular form of the Greek traditional dance. This framework guided the selection and documentation of ethnographic material derived from extensive fieldwork in Epirus as well as the formation of an appropriate environment for interaction and communication with the public [1]. Once the material has been compiled, it was interpreted [2] through the study of the historical, social, economic, and broader cultural context within which the music and dance phenomenon is born, reproduced, and reshaped [3].

The spatial exhibition design translated the conceptual framework into a specific hybrid museological model, comprising both its physical and digital components. For each section, the spatial designer developed the content structure while simultaneously proposing the format in which the ethnographic material would be presented (graphic information, audiovisual information, 3D objects, VR representation). In its final form the overall museological experience is a phygital one, with both physical and digital versions of the same content coexisting and leading one to the other (Fig. 2). The museum's digital version, on the other hand, consists of an autonomous museological environment that translates the circular structure, experiential dimension, and aesthetic code of the physical museum into the digital realm. The key design challenges focus on the transition from a three-dimensional exhibition model to a two-dimensional digital representation, ensuring equivalent experiential quality, and the principles of content distribution based on museological graphic design, as proposed by Pearce [4] for the balance between form and narrative.

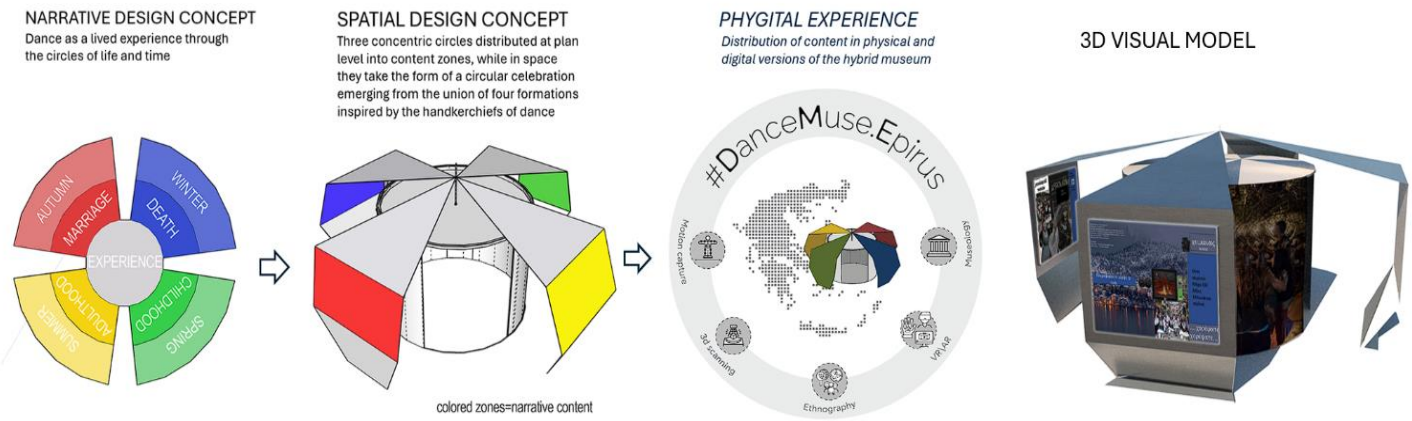


Figure 2: from concept to physical and then to phygital museological form and 3D Visualisations

3. Key Results

The project successfully established six core pillars of the #DanceMuse ecosystem (Fig.3).:

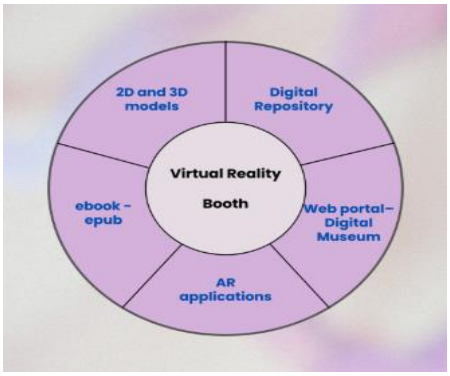


Figure 3: Technological Elements

(i) the creation of 2D and 3D models; (ii) the operation of an interoperable digital repository; (iii) the development of an e-book (ePub) publication stream; (iv) augmented-reality (AR) applications; (v) the implementation of a web portal that hosts the Digital Museum; and (vi) the project's centrepiece: a purpose-built virtual-reality (VR) booth delivering fully immersive interaction. The components are interoperable, enabling end-to-end curation, preservation and re-use of content-pipeline assets across diverse presentation channels—both on site and online.

The VR application delivers head-tracked 360° immersion. Its novelty lies in the "hand-coupling" feature via handheld controllers, allowing users to virtually join hands with digital dancers whose movements are derived

from real-world kinesiological data. Safety mechanisms, such as boundary warnings and time-boxed sessions, were implemented to mitigate VR fatigue [5].

Regarding the underlying software architecture that powers these interactive elements, the digital ecosystem is built upon a modular, MVC-based framework, ensuring a highly responsive user experience across all devices. At its core, an interoperable digital repository securely manages access rights and hosts complex 3D assets in formats such as OBJ and FBX. This secure repository seamlessly feeds the dynamic web portal, which acts as the unified access point for the public to engage with the digital museum's multimedia content, including virtual tours equipped with interactive hotspots and fully rotatable 3D objects. Furthermore, the implementation of the Extended Reality (XR) features relies on advanced game engines, specifically Unity Engine, utilizing custom scripting to manage the virtual environment's logic and flow.

4. Discussion and Impact

The #DanceMuse project demonstrates a shift from ethnography to heritage by creating a sensory space that serves the content rather than its technical surface. The spatial design translates the conceptual whirl of a traditional dance into a physical layout where four outer elements (inspired by dance scarves) converge on the central VR axis. The impact is found in the unified semantic foundation, where the physical museum presents a condensed short version of the content, while the digital portal provides the extended version. This hybridity ensures that the experiential quality remains high across both 2D and 3D interfaces. By moving beyond passive observation to active "embodied" participation, #DanceMuse sets a new standard for the museological presentation of dance and music rituals.

5. Conclusions and Outlook

The #DanceMuse project successfully integrated Folklore, Anthropology, Dance Studies, and Informatics with Museology to solve the challenge of presenting intangible heritage. The main outcome is a functional phygital model that captures the energy of Epirus dance through motion capture and VR. Future work will focus on the exploitation of the repository for educational purposes and the potential expansion of the "hand-coupling" interaction to include haptic feedback suits, further deepening the multisensory experience.

Acknowledgements / Funding

This research project is implemented under the action “SUB1.1: Clusters of Research Excellence” of the sub-action “Strategy for Excellence in Universities & Innovation” (ID 16289), Greece 2.0 – National Recovery and Resilience Fund and funded by European Union Next Generation EU. It was carried out by the University of Ioannina in partnership with the University of Piraeus, Internet Business Hellas, Interoptics, and Toolbox. We acknowledge the support of the local communities in ethnographic research.

References

1. Bronner SJ. American Folk Museums Redux. In: Dewhurst CK, Hall P, Seemann C, editors. Folklife and Museums: Twenty-First Century Perspectives. Rowman & Littlefield; 2016. p.221-244.
2. Dundes A. Who are the Folk? In: Interpreting Folklore. Indiana University Press; 1980.
3. Papakostas Ch, Poulakis N. Dance and Ethnography. In: Papakostas Ch, Loutzaki R, editors. Ethnochorografies. Disigma; 2022. p.1-20.
4. Pearce SM, editor. Interpreting objects and collections. Routledge; 1994.
5. Komianos V, Tsipis A, Kontopanagou K. Introducing Digitized Cultural Heritage to Wider Audiences by Employing Virtual and Augmented Reality Experiences: The Case of the v-Corfu Project. Technologies. 2024;12(10):196.

CIP - Каталогизација у публикацији
Народна библиотека Србије, Београд

001.895(082)(0.034.2)
004.738.5:004.89(082)(0.034.2)
502.131.1(082)(0.034.2)

DEEPTECH Connect International Conference (1 ; 2026 ; Kragujevac)
Conference proceedings [Elektronski izvor] / The First DeepTech Connect International Conference 2026, Deeptech connect 2026, April 24, 2026, Kragujevac ... [etc.] ; editor Fatima Zivic. - Kragujevac : Faculty of Engineering, 2026 (Kragujevac : Faculty of Engineering). - 1 elektronski optički disk (CD-ROM) ; 12 cm

Sistemski zahtevi: Nisu navedeni. - Nasl. sa naslovne strane dokumenta. - Tiraž 100. - Bibliografija uz svaki rad.

ISBN 978-86-6335-134-9

1. Živić, Fatima, 1970- [уредник]
а) Технолошке иновације -- Зборници
б) Машинско учење -- Зборници
в) Одрживи развој -- Зборници

COBISS.SR-ID 205772809